Tofael Ahamed

IoT and AI in Agriculture

Smart Automation Systems for Increasing Agricultural Productivity to Achieve SDGs and Society 5.0

Springer

IoT and AI in Agriculture

Tofael Ahamed

IoT and AI in Agriculture

Smart Automation Systems for increasing Agricultural Productivity to Achieve SDGs and Society 5.0

Springer

Tofael Ahamed
Institute of Life and Environmental Sciences
University of Tsukuba
Tsukuba, Ibaraki, Japan

ISBN 978-981-97-1262-5 ISBN 978-981-97-1263-2 (eBook)
https://doi.org/10.1007/978-981-97-1263-2

Japanese Society of Promotion Science (JSPS)

Agricultural Research Organization (NARO)

© The Editor(s) (if applicable) and The Author(s), under exclusive license to Springer Nature Singapore Pte Ltd. 2024
This work is subject to copyright. All rights are solely and exclusively licensed by the Publisher, whether the whole or part of the material is concerned, specifically the rights of translation, reprinting, reuse of illustrations, recitation, broadcasting, reproduction on microfilms or in any other physical way, and transmission or information storage and retrieval, electronic adaptation, computer software, or by similar or dissimilar methodology now known or hereafter developed.
The use of general descriptive names, registered names, trademarks, service marks, etc. in this publication does not imply, even in the absence of a specific statement, that such names are exempt from the relevant protective laws and regulations and therefore free for general use.
The publisher, the authors, and the editors are safe to assume that the advice and information in this book are believed to be true and accurate at the date of publication. Neither the publisher nor the authors or the editors give a warranty, expressed or implied, with respect to the material contained herein or for any errors or omissions that may have been made. The publisher remains neutral with regard to jurisdictional claims in published maps and institutional affiliations.

This Springer imprint is published by the registered company Springer Nature Singapore Pte Ltd.
The registered company address is: 152 Beach Road, #21-01/04 Gateway East, Singapore 189721, Singapore

If disposing of this product, please recycle the paper.

Preface

Agriculture and food production systems face the common challenge of achieving all 17 sustainable development goals (SDGs). To achieve the SDGs, the Tsukuba Conference (TC) and Tsukuba Global Science Week (TGSW) organize global platforms to determine future policy challenges. This book is the outcome of our yearly efforts to address agricultural challenges, new developments to address climate change, and increased food production to meet global demands. Investing in the agricultural sector can address not only hunger and malnutrition but also other challenges, including poverty, water and energy use, climate change, and unsustainable production and consumption. To increase agricultural productivity, artificial intelligence (AI), machine learning (ML), and deep learning (DL) have led to the development of new prediction strategies for crop production, livestock development, and fisheries from pre-harvest to post-harvest levels. These digital innovations contribute to achieving the SDGs and Society 5.0.

In this book, Chap. 1 reviews the current digital innovations in agri-food systems and aligns them with their contributions toward achieving the SDGs and Society 5.0. Chapter 2 briefly describes current trends and digital innovations in mechanization and automation in smart agriculture. In Chap. 3, the authors present how farmers adopt strategies involving the use of agricultural machines such as combine harvesters for early harvests and the use of postproduction methods to counter fluctuations in crop production due to changing weather conditions. Chapter 4 further explains the appropriate agricultural mechanization scale for Southeast Asian countries. The various agricultural mechanization scales throughout the region and the current trends in agricultural mechanization and automation are also explained in this chapter.

Recent trends in automation include advanced sensors and actuators. The cost and availability of these technologies has made them more attractive for developing navigation platforms using light detection and ranging (LiDAR), global navigation satellite system (GNSS), and vision sensors. The application of sensors with the development of algorithms is described in this book. Some of the key problems and labor shortage areas are highlighted. Among them, the transportation of agricultural products from farms to consumers is particularly challenging. Therefore, Chap. 5 of

this book discusses a small-scale navigation system of mobile robots to carry and deliver agricultural products using a combination of a Kalman filter, fuzzy control, and LiDAR techniques. Furthermore, Chap. 6 reviews the literature that has illustrated the potential of LiDAR for navigation systems in pesticide spraying vehicles in orchards. Since GPS and machine vision are easily influenced and limited by the environment, LiDAR was selected as the only sensor in this study, the planning paths were calculated via the density-based spatial clustering of applications with noise (DBSCAN), K-means, and random sample consensus (RANSAC) algorithms based on tree locations, and the vehicle was guided to follow the path. The feasibility of the system was proven by testing concrete roads and facilitated artificial-tree-based orchards.

With the aging of agricultural drivers worldwide, the safety risks associated with driving agricultural machinery have increased. Therefore, it is necessary to establish a stable, reliable, and effective system to ensure the safety of agricultural drivers. Thus, Chap. 7 elaborates on the application of AI to identify and classify drivers' actions while driving to determine dangerous behaviors and consequently provide an early warning signal to ensure driving safety. This research utilizes deep learning algorithms to determine dangerous driving behaviors to provide early warning signals to prevent accidents. Chapter 8 discusses the development of an autonomous agricultural vehicle based on stereo simultaneous localization and mapping (SLAM) for indoor environment usage. SLAMs are used to integrate the localization function with the construction of the surrounding environment. The environmental parameters that are important for vision SLAM are integrated with camera vision systems. Automation has advanced with the development of sensors ranging from infield plant production to inhouse production systems. Advancements in automations in agronomy are referred to as precision agronomics, which requires plant biophysical information in more detail. In this study, phenotyping plays a significant role in the prediction of growth and yield at the different stages of crop production cycles.

Plant phenotyping is an emerging science for quantifying and analyzing the characteristics of plants. The phenotyping process is particularly important for decision support in agriculture. Chapter 9 briefly describes how the advancement of plant phenotyping can be integrated with artificial intelligence to enhance crop quality resilience for food security under climate change. Chapter 10 is a short strategic note that highlights the application of artificial intelligence techniques in food quality detection. This chapter also discusses the gaps and future research directions that necessitate additional research attention to improve the current performance and applicability of AI-based food quality assessment. Chapter 11 emphasizes high-throughput plant phenotyping (HTPP), which focuses on indoor and controlled environments. Different sensors, techniques, and types of phenotyping are presented in this chapter to provide insight into the potential and development of non-destructive HTPP phenotyping.

In addition to phenotyping, early disease detection can also prevent disease outbreaks. Since plant crops tend to suffer severe impacts due to the fungus, yearlong pesticides are used to prevent foliar disease. However, these pesticides are

concerning for human health and the environment. Furthermore, planting and horticultural crops need additional attention. In this regard, coffee is one of the most widely consumed beverages in the world, and its importance and economic value hold a significant position worldwide. Coffee production is threatened by a devastating disease called coffee leaf rust (*Hemileia vastatrix*), which is recognized as one of the major pests of coffee plantations worldwide. Chapter 12 discusses the need for and potential of modern pest management for coffee leaf rust and how deep learning could control this pest. Horticulture production faces several challenges affecting the yield and productivity of crops worldwide. Among these challenges are increasing labor and land costs, climate change, pest infestations, degrading soil nutrients, and water scarcity. To address these challenges, Chap. 13 discusses the digital transformation of horticultural crop production systems, highlighting the different digital technologies being implemented in pest, nutrient, canopy, and water management as well as in harvesting and post-harvest operations. Furthermore, this chapter also enumerated numerous challenges and opportunities for adopting the showcased digital technologies in horticultural production systems.

Another challenge for plantation crops is weed infestation. Common mechanical practices for weed removal are labor intensive, and new vision systems that use LiDAR and 3D cameras to navigate need to be developed. Chapter 14 describes the challenges of weed control using robotics in complex orchard environments. 3D cameras and LiDAR were subsequently introduced as solutions for navigation systems in orchard environments where the GNSS signal quality is poor due to tree canopy cover. Several advantages and drawbacks of both sensors are also explained. Finally, the chapter also provides examples of how both sensors are utilized in vehicles for weed control, especially for weeds located within rows; this approach is known to be quite difficult and tedious even though weeding is conducted by using a riding mower or by means of a hand grass cutter. The application of unmanned aerial vehicles (UAVs) in pesticide spraying plays an important role in precision agriculture. However, improvements in pesticide application efficiency and cost performance are still under discussion in this field. In Chap. 15, computational fluid dynamics were applied for simulations, and a variable spraying system (VSS) was developed to increase the efficiency of plant protection UAVs based on pulse width modulation reduction and spraying uniformity. In addition to the advancements in sensors and unmanned application development, another challenge is to address the global effects of climate change.

Climate change has a large geospatial dispersion, heterogenous effects across different environments, and unanticipated disturbances in weather and climatic variability. Therefore, climate smart adoption is highly important. Climate agricultural practices, including the adoption of certain crops and technologies, can provide long-term strategic support for agriculture worldwide. In this regard, Chap. 16 highlights the concept of climate smart agriculture (CSA) as an effort to mitigate the challenges of climate change in the agricultural sector. The CSA approach entails the establishment of technical, policy, and investment conditions to achieve sustainable agricultural development for food and nutrition security through climate-resilient and sustainable agriculture. Post-harvest operations are crucial for

preserving agricultural product quality and shelf life. However, the complexity of post-harvest technology and the requirement for expertise in multiple domains make it difficult for companies to manage their operations efficiently. As a result, it is necessary to develop a central provider that provides expert scientific services to companies. Therefore, Chap. 17 briefly introduces the concept of the centralized data processing unit (CDPU) based on the integration of AI and data science to enhance post-harvest operations at the business level. The CDPU system can be integrated with the overall operational management of agricultural production from pre-harvest to post-harvest operations.

Irrigation plays a significant role in the operational management of agricultural fields. Smart water management is important for precise irrigation in agricultural fields as water becomes increasingly scarce. Hence, Chap. 18 explores the potential of smart water management through machine learning to understand plant root zones for irrigation purposes. Tuning the environmental parameters of conventional greenhouses, which need to be controlled manually by farmers, is inconvenient and imprecise. In Chap. 19, AI and IoT technology are presented as alternatives to farmer management of greenhouse systems to reduce the labor force and ensure that the conditions of the greenhouse environment (e.g., temperature, humidity, light intensity) more precisely correspond to the growth stages of lettuce plants. A new feedback control parameter was introduced using the Fuzzy proportional-integral-derivative (PID) controller, which significantly improved the accuracy of the optimization of the environmental control parameters of the greenhouse. Sensors and algorithms help controllers perform precise automated indoor cultivation of mushrooms, which are highly sensitive to weather parameters.

In Chap. 20, the author explores how AI and the IoT can be utilized to address various challenges in the artificial cultivation of mushrooms in tropical and subtropical regions. These technologies have the potential to enhance efficiency and minimize contamination throughout the entire process, from substrate preparation to harvesting. The practical applications discussed in this chapter offer valuable insights and can greatly benefit the local cottage mushroom industry. Furthermore, orchard applications are limited by the challenges of automation and harvesting due to labor shortages. Newly developed orchard architectures with genetic improvements create pathways for harvesting robots to reduce the complexity of the number of degrees of freedom, where complex robots are less adaptable in terms of economy and sustainability. The main challenges of harvesting robots include occlusions from leaves, branches, and fruit clusters for detection and localization. Chapter 21 provides an overview of the methods used to avoid occlusions to increase orchard fruit harvesting efficiency. In Chap. 22, various types of end-effectors commonly used in horticulture, including gripper end-effectors, cutting end-effectors, and spraying end-effectors, are discussed. Sensing and perception technologies, such as computer vision, LiDAR sensing, and thermal imaging, play a crucial role in end-effector automation by providing data about the environment and plants. Actuation and control mechanisms, including electric, pneumatic, and hydraulic technologies, allow for precise manipulation and adaptability of end-effectors. Deep learning algorithms have been applied to end-effector automation, enhancing tasks such as

object classification, yield estimation, pest detection, and weed management. Case studies have demonstrated the design of a three-finger flexible gripper for orchard operations, offering a simple, cost-effective solution for fruit picking. Finally, we discuss the remaining challenges in developing smart automations for end-effectors.

Automations from pre-harvesting to post-harvest stages, including non-destructive quality assessment of foods, have become important criteria for the food industry. In the food industry automation, food quality analysis, imaging, and chemical analysis yield the highest quality assurance. Spectroscopy-based imaging is a non-destructive method that ensures a high-quality assessment of products. Chapter 23 elucidates the current advancements in spectroscopic techniques for food analysis. By exploring the advancements in spectroscopic techniques and their integration with chemometric tools, this chapter provides valuable insights into the potential applications and future directions of these analytical approaches in the food industry. Food diversification has become a food crisis intervention strategy supported by the FAO. Thus, Chap. 24 discusses the potential of endemic fruits to be adapted to local ecosystems.

Food and biomass production has received increased attention worldwide for achieving green energy and energy security. AI and IoT technologies can precisely forecast different stages of biomass production, which can be transformed to energy security to reduce the dependency on fossil fuel to mitigate GHG emissions. Chapter 25 discusses the implementation of the IoT in the agricultural sector, focusing on biomass residue utilization. Biomass residue has several potential applications, including for bioenergy generation. This study proposes the use of the IoT platform to measure the potential environmental impact of oil palm biomass residue for bioenergy. The platform was constructed based on the existing IoT platform on oil palm plantation management combined with a recently underdeveloped tool for calculating the potential impact of oil palm biomass residue utilization for ethanol, electricity generation, and fertilizer. It is expected that farmers, industrial sectors, fuel companies, users, and governments can benefit from the utilization of IoT systems to accelerate GHG mitigation in the future. Chapter 26 provides an integrated method for tracking and tracing agricultural productivity using a web-based IoT monitoring platform. The developed IoT systems visualize real-time environmental data, such as humidity, temperature, soil moisture content, wind speed, and rainfall parameters, acquired via the Dash platform. The insights gained from the system allow farm managers to monitor rainfall patterns and water cycles and make appropriate decisions or control remotely for optimal plant growth.

In addition to plant production, this book also highlights some of the research areas focusing on livestock and aquaculture. Recent advancements in sensors can help increase productivity. There are several IoT-based applications in aquaculture, which is one of the most important sources of animal protein worldwide. Aquaculture is the most economic approach and poses fewer risks as a major source of protein. Smart machine vision can be applied to reduce the need for manual observation in animal farming. Chapter 27 is a short note that demonstrates how smart machine vision can be applied to reduce the need for manual observation in both aquaculture

and husbandry farming, which can contribute to strengthening food security. Chapter 28 introduces a novel, noninvasive method for assessing quail egg freshness using a thermal microcamera and deep learning algorithms. By analyzing thermal images and correlating the air cell area with egg weight, the models predicted freshness with high accuracy. This groundbreaking approach offers promising implications for the food industry and consumers.

Chapter 29 concludes the chapters that have been discussed in this book. This chapter highlights four domains: (1) smart outdoor production, (2) smart indoor production systems, (3) smart orchard management for increasing productivity and post-harvest management, and (4) non-destructive quality measurements. This chapter also outlines the future prospects of intelligence application toward sustainable agri-food systems associated with the SDGs and Society 5.0.

Tsukuba, Ibaraki, Japan Tofael Ahamed

Acknowledgments

The Tsukuba Global Science Week (TGSW) and Tsukuba Conference (TC) created a common platform hosted by the University of Tsukuba for global communication among researchers, universities, and industry. This joint "Agriculture x AI x IoT for Global Food Production" session has consistently contributed to collaboration over the years and has the privilege of hosting experts from diverse countries who generously share their experiences and expertise. Our focus has centered on integrating agriculture with transboundary approaches, including incorporating AI and IoT-based big data schemes to sustain food security. The invaluable knowledge exchange during these conferences has encouraged me to improve the second edition of the book with the goal of offering additional output and information from this TGSW/TC session. These improvements aim to make a substantial contribution toward aligning agriculture with the Sustainable Development Goals (SDGs) and the principles of Society 5.0.

I would like to express my appreciation to Dr. Wanrat Abdullakassim (Kasersart University, Thailand), Dr. Janet P. Pablo (Benguet State University, the Philippines), Dr. Mousona Islam (Bangladesh Council of Scientific and Industrial Research, Bangladesh), Dr. Norhashila Hashim (Universiti Putra Malaysia, Malaysia), Professor Nang Hseng Hom and Professor Nyo Mar Htwe (Yezin Agricultural University, Myanmar), Professor Sanath Amaratunga (University of Peradeniya, Sri Lanka), Dr. Mito Kokawa (University of Tsukuba, Japan), Professor Tatas Brotosudarmo (Universitas Ciputra, Indonesia), and Professor Yan-Fu Kuo (National Taiwan University, Taiwan) for their invaluable contributions to the strategic short note. These strategic short notes played an important role in introducing the concept of each section of the book and fostering interdisciplinary research ideas for readers. Their support during the recent TGSW/TC as our distinguished speakers has been invaluable, and including their insights in this edited version is indeed a significant complement.

In addition to the contributions to our laboratory from the University of Tsukuba, I would like to express sincere gratitude and appreciation to our international contributors, Dr. Samsuzana Abd Aziz and her team at the Universiti Putra Malaysia in Malaysia, and Dr. Shahriar Abdullah Al-Ahmed from the University of

West-Scotland, United Kingdom, for the time that they devoted to preparing and reviewing their chapters at various stages.

This second edition book is composed of 29 chapters. Bringing all the concepts together into one cohesive framework required tremendous effort, and this effort would not have been possible without the exceptional dedication of the team. In this regard, I would like to express special appreciation to my committed team of PhD and master's degree students for their tireless efforts in cross-checking, updating, and formatting the book. I extend my hearty gratitude to Munirah Hayati Hamidon, who demonstrated exceptional leadership by taking the lead in managing the team, efficiently distributing tasks, editing, drawing figures, and overseeing the progress of the book from the initial stage to the final submission stage. Additionally, Bryan Vivas Apacionado, R. M. Rasika D. Abeyrathna, Jiang Ailian, Liu Zifu, Nakaguchi Victor Massaki, Opasatian Ithiphat, Raka Thoriq Araaf, Sampurno Rizky Mulya, Pubudu Kahandage, Sudeshinie Piyathissa, and Arief Ameir Rahman Setiawan provided invaluable support in developing the content, literature review, layout formatting, and cross-checking the references for this book in the last few months. The success and outcome of this book were made possible by the considerable efforts of each team member. I am grateful for their unwavering support, assistance, and patience in the collaborative process, which ultimately led to the succinct production of this second edition. In addition to my dedicated team, I want to express my thanks to Nelundeniyage Sumuduni L. Senevirathne, Parwit Chutichaimaytar, and Arkar Minn, who are PhD students from our graduate school, for their assistance in cross-checking several chapters of this book. I feel incredibly privileged and fortunate to have such an outstanding team, whose contributions were instrumental in ensuring the successful completion of the book.

I would like to acknowledge the support that I have received from the University of Tsukuba in publishing various articles with open access, enabling our researchers to reach other collaborators, which motivated us to further extend our networks by sharing knowledge.

Finally, I would like to thank Springer-Nature for collaborating with me by refereeing our TGSW/TC sessions at the University of Tsukuba and extending our session outcomes as second book.

Tsukuba Tofael Ahamed
Ibaraki, Japan

Contents

1 Digital Innovations in Agrifood Systems to Achieve the SDGs and Society 5.0 1
1.1 Introduction 1
1.2 Digital Innovations in Agrifood Systems 3
1.2.1 Big Data Analytics 3
1.2.2 Internet of Things (IoT) and 5G Wireless Networks 4
1.2.3 Artificial Intelligence in Digital Agrifood Systems 6
1.2.4 Robotics and Drone Technology 8
1.2.5 3D Printing Technology: Changing the Manufacturing in Agriculture 10
1.2.6 Edge Computing 11
1.2.7 Digital Twins and Cross Reality (XR) in Precision Farming 12
1.2.8 Digital-Twin-Driven Smart Supply Chain 14
1.3 Achieving SDGs through Digital Innovations in Agrifood Systems 16
1.4 Achieving Society 5.0 through Digital Innovations in Agrifood Systems 19
1.5 Conclusion 20
References 21

2 Strategic Short Note: Appropriate Integration of Precision Agriculture Technology, IoT, and AI for Enhancing Southeast Asian Agriculture 25
2.1 Introduction 26
2.2 Research and Development for Appropriate Solutions 26
2.3 Conclusions 27
References 27

3 Strategic Short Note: Climate Smart Technology for Corn Production in Rizal, Kalinga, Philippines 29
3.1 Introduction 29

3.2 Biophysical Sensitivity and Technological Adaptations for Yellow Hybrid Corn . . . 30
3.3 Conclusions . . . 31
References . . . 32

4 Appropriate Scale of Mechanization and Automation for Agriculture in Southeast Asia . . . 33
4.1 Introduction . . . 33
4.2 Current Scale of Agricultural Mechanization in Southeast Asia . . . 34
4.3 Transformation of Agricultural Mechanization in Southeast Asia . . . 35
4.4 Level of Automation in Agricultural Machinery . . . 37
4.5 Level of Machinery for Agricultural Practices . . . 39
4.5.1 Tillage Practices . . . 39
4.5.2 Seeding Practices . . . 42
4.5.3 Transplanting . . . 44
4.5.4 Spraying Practices . . . 47
4.5.5 Harvesting Practices . . . 48
4.6 Appropriate Scale of Mechanization in Southeast Asia . . . 51
4.7 Discussion . . . 52
4.8 Conclusion . . . 53
References . . . 53

5 Design of Navigation System for Transportation Mobile Robot for Agricultural Farms . . . 57
5.1 Introduction . . . 58
5.2 Materials and Methods . . . 60
5.2.1 Hardware System . . . 60
5.2.2 Software System . . . 60
5.2.3 Design for Localization System . . . 62
5.2.4 Process for IMU . . . 66
5.2.5 Sensor Fusion for GNSS/IMU . . . 67
5.2.6 Design for Obstacles Avoidance System . . . 72
5.2.7 Design for Navigation System . . . 73
5.2.8 Robot Tracking . . . 74
5.3 Results . . . 76
5.3.1 Experiment for the Automatic Driving . . . 76
5.3.2 Experiment for Obstacles Avoidance . . . 78
5.4 Discussion . . . 82
5.5 Conclusion . . . 82
References . . . 83

6 Automatic Navigation of Pesticide Spraying Vehicle for Orchard Tree Trunk Detection . . . 85
6.1 Introduction . . . 85

6.2 Materials and Methods . . . 87
6.2.1 Experimental Prototype Vehicles . . . 87
6.2.2 Installation of Sensors . . . 87
6.2.3 System Structure . . . 88
6.2.4 Path Planning Algorithm . . . 88
6.2.5 Graphical User Interface (GUI) . . . 90
6.3 Results . . . 91
6.3.1 Planning Path Calibration on a Concrete Road . . . 91
6.3.2 Field Test in a Facilitated Artificial-Tree-Based Orchard . . . 92
6.4 Discussion . . . 94
6.5 Conclusions . . . 95
References . . . 96

7 Driver Safety System for Agricultural Machinery Operations Using Deep Learning Algorithm . . . 99
7.1 Introduction . . . 100
7.2 Materials and Methods . . . 101
7.2.1 The Overall Framework of the Model . . . 101
7.2.2 Dataset Introduction . . . 103
7.2.3 Model Introduction . . . 105
7.3 Results and Discussion . . . 111
7.3.1 Environment for Training and Evaluating . . . 111
7.3.2 Evaluation Metrix . . . 111
7.3.3 Model Results . . . 112
7.3.4 Online Model Realization and Result Display . . . 117
7.3.5 Discussion . . . 120
7.4 Conclusions . . . 121
References . . . 121

8 Navigation System for Autonomous Agricultural Vehicles for Indoor Farms . . . 123
8.1 Introduction . . . 124
8.2 Navigation System . . . 126
8.3 Coordinates Calculation . . . 128
8.3.1 Cloud Map Generation Using ORB_SLAM2 . . . 129
8.3.2 OctoMap . . . 130
8.3.3 CostMap . . . 131
8.3.4 System Data Structure Based on ROS . . . 133
8.4 Path Planning and Path tracking for Tiny Agricultural Vehicles . . . 134
8.4.1 Design of Navigation System Based on move_base Repository . . . 134
8.4.2 Pure-Pursuit Path tracking Algorithm . . . 135
8.4.3 Instruction of DWA . . . 136
8.5 Results and Discussion . . . 138
8.6 Conclusions . . . 146
References . . . 147

9 Strategic Short Note: Integration of Multiomics Approaches for Sustainable Crop Improvement 149
9.1 Introduction 149
9.2 Integrated Multiomics Approaches for Crop Improvement 151
9.3 Concluding Remarks 152
References 152

10 Strategic Short Note: Artificial Intelligence in Food Quality Assessments 155
10.1 Introduction 155
10.2 Application of AI Techniques in Food Quality Detection 156
10.3 Challenges and Future Direction 157
References 158

11 High-Throughput Plant Phenotyping Techniques in Controlled Environments 159
11.1 Introduction 160
11.1.1 Plant Morphological Characteristics 161
11.1.2 Plant Physiology 161
11.2 High-throughput Plant Phenotyping 163
11.2.1 2D Image-Based Phenotyping 164
11.2.2 3D Image-Based Phenotyping 168
11.3 High-throughput Plant Phenotyping Platforms 170
11.3.1 Conveyor-Type 170
11.3.2 Benchtop-Type 171
11.3.3 Gantry-Type 171
11.3.4 Mobile Type 172
11.4 Deep Learning Applications in Plant Phenotyping 173
11.4.1 DL-Based HTPP in the Germination and Early Growth Stages 174
11.4.2 DL-Based HTPP in Vegetative Growth and Development 175
11.4.3 DL-Based HTPP in the Flowering and Reproductive Stages 177
11.4.4 DL-Based HTPP in Harvest and Yield Prediction 177
11.5 Conclusions and Prospects 178
References 180

12 Revolutionizing Agriculture: Embracing Modern Strategies for the Management of Coffee Leaf Rust Disease 183
12.1 Overview of Coffee Leaf Rust 183
12.1.1 Coffee Leaf Rust 183
12.1.2 History of Coffee Leaf Rust 185
12.1.3 Economic and Ecological Consequences of Coffee Leaf Rust 187

12.2 The Need to Shift to Modern Management Methods for Coffee Leaf Rust . . . 188
12.2.1 Why Modern Management? . . . 188
12.2.2 Deep Learning as Modern Approaches for Coffee Leaf Rust . . . 190
12.3 Challenges and Limitations of Using Deep Learning for Coffee Leaf Rust Management . . . 195
12.3.1 Challenges and Limitations . . . 195
12.3.2 Solutions . . . 196
12.4 Conclusion . . . 197
References . . . 197

13 Digital Transformation of Horticultural Crop Production Systems Toward Sustainable Agricultural Productivity . . . 199
13.1 Introduction . . . 200
13.2 Transforming the Horticulture Production System . . . 201
13.3 Digital Technologies in Horticultural Production . . . 202
13.3.1 Digital Transformation of Horticultural Production Environment . . . 203
13.3.2 Digital Transformation of Horticultural Production Operations . . . 208
13.4 Challenges and Opportunities in Digital Horticulture Production and Management . . . 219
13.4.1 Challenges . . . 220
13.4.2 Opportunities . . . 221
13.5 Conclusion . . . 222
References . . . 223

14 Challenges in Orchard Weed Management: Perspectives on the Use of 3D Cameras and LiDAR to Develop a Low-Cost Small-Scale Robotic Weeder . . . 229
14.1 Introduction . . . 229
14.2 Characteristics of Orchard Environments for Robotic Weeding Operations . . . 231
14.3 The Use of 3D Cameras and LiDAR in Robotics-Based W eed Control . . . 233
14.3.1 Machine Vision Using a 3D Camera . . . 234
14.3.2 LiDAR . . . 237
14.4 Weeding Operations Using a 3D Camera and LiDAR for Orchards . . . 240
14.4.1 Current Orchard Weeding Operations Using Autonomous Robots . . . 240
14.4.2 Weed Cutter that Moves Around Tree Trunks for Small-Robot Intrarow Weeding . . . 242
14.4.3 Path Planning and Weed Management Strategy . . . 243
14.5 Conclusions . . . 245
References . . . 246

15 Investigating the Pesticide Spraying Characteristics of Plant Protection UAV and Designing a Variable Spraying System for Improving the Spraying Uniformity 249
15.1 Introduction 249
15.2 Materials and Methods. 251
15.2.1 Analyzing the Effect of Downwash Airflow of Plant Protection UAV Using the Computational Fluid Dynamics (CFD). 251
15.2.2 Development of an Efficient Variable Spraying System (VSS) for Plant Protection UAV Based on Pulse Width Modulation 254
15.3 Results and Discussion 260
15.3.1 Effect of Downwash Airflow of Plant Protection UAV. 260
15.3.2 Variable Spraying System (VSS) for Plant Protection UAV Based on Pulse Width Modulation. 262
15.4 Conclusions 264
References. 265

16 Strategic Short Note: Myanmar Climate-Smart Agriculture. 267
16.1 Introduction 267
16.2 Role of Agricultural Sector in Myanmar 268
16.3 Climate Change Adaptation Option for Agriculture Sector. 268
16.4 Climate Change Mitigation Option for Agriculture Sector 269
16.5 Policy Related to Climate Change from MOALI 269
16.5.1 Collaboration with Others 269
16.6 Summary 270
References. 270

17 Strategic Short Note: Enhancing Postharvest Operations Through Centralized Data Processing and Analysis 271
17.1 Introduction 271

18 Optimization of Soil-Based Irrigation Scheduling Through the Integration of Machine Learning, Remote Sensing, and Soil Moisture Sensor Technology 275
18.1 Introduction 275
18.2 Soil Moisture and Irrigation Management. 277
18.2.1 Significance of Soil Moisture in Agriculture 277
18.2.2 Soil Moisture as a Base for Irrigation Decision-Making 278
18.3 Remote Sensing in Irrigation Scheduling 279
18.3.1 Remote Sensing Technologies 279
18.3.2 Remote Sensing Applications in Irrigation. 280
18.4 Soil Moisture Sensing in Irrigation Scheduling. 283

18.4.1 Types of Soil Moisture Sensors 283
18.4.2 Installation and Calibration of Sensors. 284
18.4.3 Benefits of Soil Moisture Sensor 286
18.5 Machine Learning in Irrigation Scheduling. 287
18.5.1 Introduction to Machine Learning 287
18.5.2 Benefits of Machine Learning 288
18.6 Discussion 289
18.6.1 Irrigation Scheduling Based on Soil Moisture Sensor Data. 289
18.6.2 Irrigation Scheduling Based on Remote Sensing Data. 290
18.6.3 Machine Learning in Soil-Based Irrigation Scheduling 291
18.6.4 Integration of Soil Moisture Sensors, Remote Sensing, and Machine Learning Techniques 291
18.7 Future Directions and Concluding Remarks 293
18.7.1 Emerging Trends in Irrigation Technology. 293
18.7.2 Conclusion and Practical Recommendations 294
References. 294

19 AI-Based IoT Greenhouse Control System for Environmental Parameters. 301
19.1 Introduction 301
19.2 Materials and Methods. 304
19.2.1 IoT-Based Greenhouse System. 304
19.2.2 YOLOv3 Object Detection Model 305
19.2.3 CenterNet Object Detection Model 308
19.2.4 Evaluation Metrics for Object Detection Model 309
19.2.5 Fuzzy PID Control Algorithm 311
19.3 Results 312
19.3.1 System Architecture 312
19.3.2 Monitoring Web Pages of IoT System 314
19.3.3 Object Detection Experiment Results 315
19.3.4 Control Experiment Results 317
19.4 Conclusions 325
References. 326

20 Enhancement of Cottage Mushroom Cultivation in Tropical and Subtropical Regions with IoT and AI Applications 329
20.1 Introduction 330
20.2 Oyster Mushroom Production Process at Cottage Level 331
20.3 Mechanization and Automation of the Substrate Preparation 333
20.3.1 Enabling Seamless Continuity by Integrating the Three Operations 338
20.4 Application of IoT Technology in Disinfection of Substrate. 339
20.4.1 Controlling the Biomass Supply to the Burner. 342

20.5 Controlling the Environment in a Mushroom House/Shed 343
20.5.1 Controlling the Temperature and Humidity of a Mushroom House with IoT 344
20.6 Conclusion 346
References 347

21 Approaches for Improving Fruit Detection and Gripping Mechanisms in Orchard Robotic Fruit Harvesting 349
21.1 Introduction 350
21.2 Occlusions Caused by Plant Parts and Challenges for Robotic Operations 352
21.2.1 Challenges for the Vision System 352
21.2.2 Challenges for Robotic Arm Manipulation 353
21.3 Light Variation, Wind, Shadows, and Vision System Challenges 359
21.4 Recent Trends of Harvesting Robots 361
21.4.1 Kinematic Examples for Basic Robotic Arm Design 363
21.5 Discussion 368
21.6 Conclusion 369
References 370

22 Smart Automation for End-Effectors in the Development of Horticultural Robots 373
22.1 Introduction 373
22.2 Types of End-Effectors for Automation in Horticulture 375
22.2.1 Gripper End-Effectors 375
22.2.2 Cutting End-Effectors 377
22.2.3 Spraying End-Effectors 377
22.3 Sensing and Perception Technologies for End-Effector Automation in Horticulture 378
22.3.1 Computer Vision 378
22.3.2 Lidar Sensing Technology 380
22.3.3 Thermal Imaging Technology 381
22.4 Actuation and Control Mechanisms for Smart End-Effectors 382
22.4.1 Actuation Technologies 382
22.4.2 Control Mechanisms 383
22.5 Applications of Deep Learning for End-Effector Automation in Horticultural Robots 384
22.5.1 Object Classification and Detection 384
22.5.2 Yield Estimation and Quality Assessment 384
22.5.3 Pest and Disease Detection 385
22.5.4 Weed Detection and Management 385
22.6 Case Studies About Design of a Three-Finger Flexible Gripper for Orchard 385
22.6.1 The Three-Finger Flexible Gripper 386
22.6.2 Flexible Finger 387

22.6.3 Connecting Rod Structure 387
22.6.4 Stepper Motor Drive and Lead Screw Transmission 388
22.7 Conclusion 389
References 390

23 Strategic Short Note: Spatially Factorized Spectroscopy—Focusing on a Single Component in a Mixed Sample 393
References 396

24 Strategic Short Note: Reviving Local Resources for Healthier Foods in Indonesia 397
24.1 Introduction 397
24.2 Repositioning Local Food Resources 398
References 399

25 Development of IoT-Based Platform for Biomass Utilization Toward Low-Carbon Economic Society: Case of Oil Palm Residue 401
25.1 Introduction 401
25.1.1 Trend on IoT and Application for Agriculture 401
25.1.2 Potential of Agriculture Residue Utilization to Replace Fossil Fuel 402
25.1.3 Existing IoT Platform for Oil Palm Production System 405
25.2 Methods for Developing the Prototype 406
25.2.1 Identifying Relevant Stakeholders 407
25.2.2 Developing Biomass Utilization Flow 408
25.2.3 Identifying GHG Calculation Methods 409
25.2.4 Constructing the Tool 410
25.2.5 Testing and Validation 412
25.2.6 Writing Guideline 414
25.3 Integrating the Tool Toward IoT Platform of Low-Carbon Economic Society 414
25.4 The Role of AI in Biomass Utilization Platform 416
25.5 Estimating the Cost and Potential Benefits 418
25.6 Conclusion 419
References 419

26 A Web-Based IoT Monitoring and Service System for Agricultural Applications 421
26.1 Introduction 421
26.2 Materials and Methods 422
26.2.1 Web-Based IoT Monitoring System 424
26.3 Hardware Configuration for Sensor Node for an IoT System Prototype in Universiti Putra Malaysia (UPM) 424
26.4 Dash Plotly Framework Design 426
26.4.1 Dash Layout 427

26.4.2 Interactive Dash Components 428
26.4.3 Launch of the Dash Application 428
26.5 Web-Based Dashboard Deployment and Experiment Setup 428
26.5.1 Soil Moisture, Humidity, and Temperature Measurement Test in the Tenth College (K10), UPM . . . 428
26.5.2 Outdoor Environmental Measurement in Taiwan 429
26.6 Assessment of Web-Based IoT Platform 430
26.6.1 Web Application's Overall Performance 431
26.7 Results and Discussion 432
26.7.1 The Overall Performance of the Web Applications 432
26.7.2 Web Application for National Ilan University, Taiwan's Weather Station 436
26.7.3 Impact of the WebBased IoT Monitoring and Service System for Agricultural Applications to Society, Safety, and Health 444
26.8 Conclusions 444
References 445

27 Strategic Short Note: Application of Smart Machine Vision in Aquaculture and Animal Husbandry 447
27.1 Introduction 447
27.2 Overview of Smart Machine Vision in Aquaculture and Animal Husbandry 448
27.3 Examples of Smart Machine Vision in Aquaculture and Animal Husbandry 449
27.4 Conclusion 450
References 450

28 Deep Learning Algorithms for Postharvest Quality Assessment: A New Sensing Methodology for Quail Eggs Freshness Estimation and Shelf-Life Revalidation 453
28.1 Introduction 453
28.2 Materials and Methods 456
28.2.1 Experimental Environment 456
28.2.2 Thermal Imaging 456
28.2.3 Dataset Collection 457
28.2.4 Air Cell Assessment Methodology 458
28.2.5 Deep Learning-Based Object Detection Algorithms 460
28.3 Results 466
28.3.1 Correlation Test 466
28.3.2 Computer Vision Model Prediction 469
28.4 Discussion 475
28.5 Conclusions 477
References 477

29 AI × IoT: Increasing Agricultural Productivity of Crops, Orchards, and Livestock Management Using Smart Agricultural Space for Achieving SDGs 481
29.1 Introduction 481
29.2 Smart Outdoor Systems for Agricultural Production. 482
29.3 Smart Indoor Production Systems 484
29.4 Smart Orchard Management for Increasing Productivity 486
29.5 Smart Management of Poultry and Livestock 487
29.6 Postharvest Management and Nondestructive Quality Measurements 488
29.7 Conclusion 490
References. 490

Index 491

Chapter 1
Digital Innovations in Agrifood Systems to Achieve the SDGs and Society 5.0

Abstract Digital innovation significantly contributes to the transformation of agrifood systems, aiming to achieve the Sustainable Development Goals (SDGs) and the realization of the Society 5.0 vision. The agriculture sector is currently witnessing significant breakthroughs due to the utilization of many technologies, including artificial intelligence (AI), robots, data analytics, mobile apps, blockchain technology, and digital twins. These innovations not only help in productivity enhancement, efficiency, and sustainability but also address societal challenges. These digital innovations contribute to achieving the SDGs by improving food security, reducing poverty, promoting sustainable practices, and fostering inclusive economic growth. Furthermore, these innovations in agrifood systems support the transition toward Society 5.0, in which humans and advanced technologies cooperate for sustainable development. This transition enables precision agriculture, autonomous farming, smart logistics, and intelligent distribution systems, creating more efficient and resilient agrifood systems.

Keywords Agrifood systems · Digital innovation · AI · Blockchain technology · SDG · Society 5.0

1.1 Introduction

Digital innovations in agrifood systems (AFSs) refer to the utilization of digital technologies, such as artificial intelligence (AI), machine learning, big data analytics, blockchain, and the Internet of Things (IoT), to address challenges and improve the efficiency, productivity, and sustainability of agricultural and food production processes (Ancín et al., 2022). These technologies are being used to optimize various aspects of AFSs, including precision agriculture, agricultural machinery and automation, and digital supply chain management. The goal of digital innovations in AFSs is to create a more sustainable, efficient, and resilient food system that can

© The Author(s), under exclusive license to Springer Nature Singapore Pte Ltd. 2024

T. Ahamed, *IoT and AI in Agriculture*,
https://doi.org/10.1007/978-981-97-1263-2_1

meet the growing demand for food for the expanding population while mitigating environmental impact and promoting social equity.

The advancement of digital innovations in AFSs can contribute significantly to achieving the Sustainable Development Goals (SDGs) and realizing the Society 5.0 vision (Fig. 1.1). The SDGs comprise 17 global goals endorsed by the United Nations in 2015, forming a crucial component of the 2030 Agenda aimed at securing an equitable and more sustainable future for the global population (Griggs et al., 2017; Biermann et al., 2017). These goals address various intersecting issues, such as poverty, hunger, health, education, gender equality, climate change, and sustainable economic growth. Notably, the integration of digital innovations in AFSs has

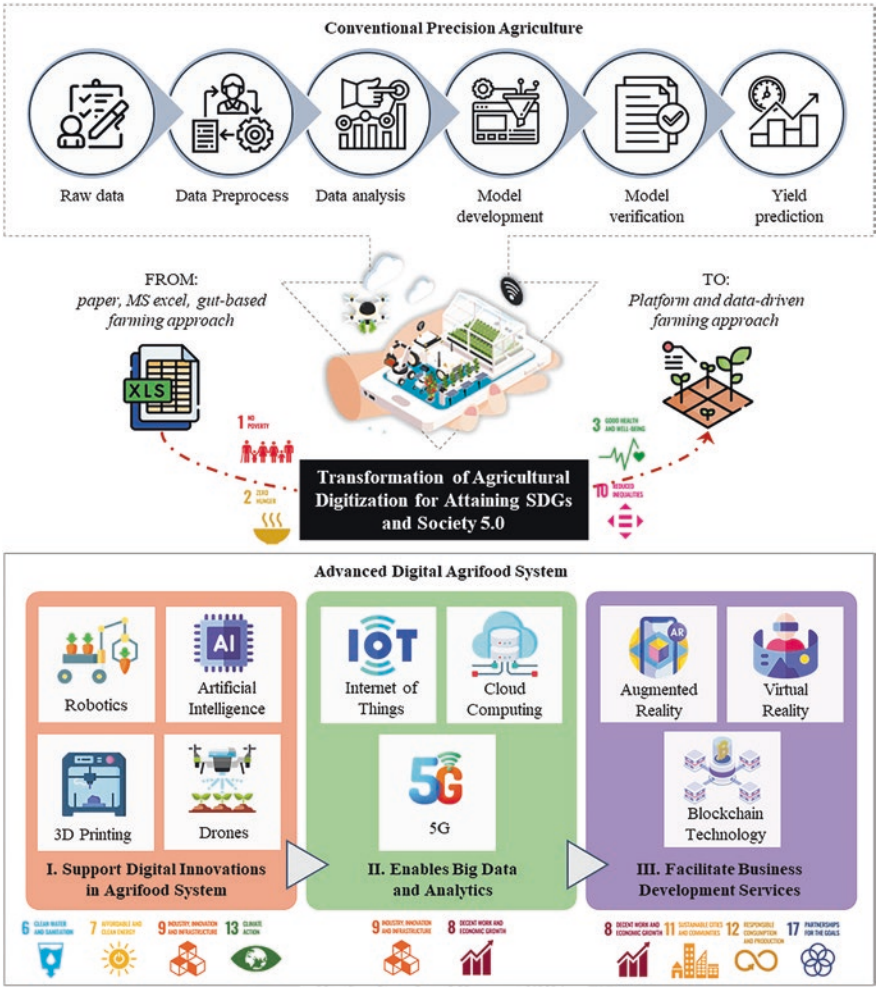

Fig. 1.1 Transformation of agricultural digitalization to achieve the SDGs and realize Society 5.0

the potential to contribute significantly to achieving several SDGs, including the following:

- SDG 2: Zero hunger can be achieved by improving food production, reducing food waste, and boosting food security.
- SDG 8: Decent work and economic growth can be realized by creating new job opportunities and improving productivity in the agriculture sector.
- SDG 9: Industry, innovation, and infrastructure can be realized by promoting innovation in agrifood systems and investing in digital infrastructure.
- SDG 12: Responsible consumption and production can be promoted by advocating for sustainable agricultural practices and mitigating the environmental impact of food production.
- SDG 13: Climate action can be advanced by curbing greenhouse gas emissions from agricultural fields and improving the resilience of food systems to climate change.

Moreover, the transformations of digital innovations in agriculture are aligning with the Society 5.0 concept by promoting the integration of digital technologies into all aspects of society, including the food system. This integration can support the development of a more effective and sustainable food system to better meet the needs of all stakeholders, from producers to consumers, while also promoting social equity and well-being. Society 5.0 is a concept that was initially envisioned by the Japanese government. It envisions a society where people can live harmoniously with technology to address societal challenges (Fukuyama, 2018). This concept recognizes the importance of digital transformation and the integration of new technologies to harmonize economic advancement with equitable social progress and a sustainable future.

Therefore, this chapter aims to elucidate the role of digital innovations, particularly in AFSs, in aligning with the SDGs and Society 5.0. This chapter outlines the different digital technologies being used in agrifood systems, their benefits, and their potential to address social, economic, and environmental challenges. It also discusses the challenges facing digital innovations in agrifood systems and future directions for research and development.

1.2 Digital Innovations in Agrifood Systems

1.2.1 Big Data Analytics

The rapid advancement of technology in various sectors, including the agrifood system, has led to an unprecedented amount of data generation. This exponential data growth has led to the introduction of the term “big data,” referring to vast and complex datasets that are challenging to process using existing database management tools (Rejeb et al., 2021). Big data analytics is the process of accumulating,

managing, and analyzing enormous amounts of data. As outlined by Manyika et al. (2011), the concept of big data encompasses three key components: volume, velocity, and variety. Then, an additional component was introduced by Kunisch (2016), denoted as the fourth V, which pertains to veracity. Notably, Chi et al. (2016) contributed a fifth component, valorization, thereby completing the five fundamental components of big data.

Volume refers to the enormous number of datasets generated daily from various sources, such as sensors and transactions. Velocity relates to the speed of generated datasets and their processing and analysis, often in real time, allowing for timely decision-making. Variety emphasizes the diversity of the datasets, including structured, unstructured, and semistructured information, posing challenges but also offering rich opportunities for analysis. Veracity signifies the accuracy and reliability of the datasets, ensuring that the data collected are trustworthy. Finally, valorization completes the process of transforming raw data into meaningful information and innovative insights, contributing to scientific discoveries and social advancements.

In the context of agrifood systems and the pursuit of the SDGs within the framework of Society 5.0, these five fundamental components of big data play important roles in shaping the future of agriculture and food production. The sheer scale of data (volume) generated by agrifood systems, from crop monitoring sensors to supply chain transactions, presents an opportunity for in-depth analysis. The speed at which these data are generated and processed (velocity) allows for real-time decision-making, enabling farmers to respond swiftly to changing conditions and market demands, thereby contributing to the achievement of SDG 2 (zero hunger) by improving food production and reducing waste. Diverse types of data (variety), ranging from weather patterns to consumer preferences, provide a comprehensive view of the agrifood ecosystem, aiding in sustainable practices aligned with SDG 12 (responsible consumption and production). Ensuring the accuracy and reliability of these data (veracity) is critical for informed decision-making, especially in addressing climate-related challenges (SDG 13: climate action). Additionally, the valorization of these data, through advanced analytics and AI-driven insights, fosters innovation in agrifood systems, creating new economic opportunities and supporting the achievement of SDG 8 (decent work and economic growth). By applying predictive analytics to integrated big data systems, optimization of food quality, safety, and security can be achieved.

1.2.2 Internet of Things (IoT) and 5G Wireless Networks

Big data and the Internet of Things (IoT) are two interconnected technologies that have emerged as a central domain in the global information and communication technology (ICT) industry (ur Rehman et al., 2019). The IoT represents an emerging communication paradigm wherein many devices engage in collaborative data exchange within an integrated structure or function autonomously as separate

entities. Precision agriculture, at the level of farming operations, encompasses the utilization of information and communication technologies to enhance the management of agricultural products, livestock, and natural resources, thereby optimizing farm performance at the economic, social, and environmental scales (Liu et al., 2021). This approach relies on the deployment of various sensors and IoT equipment within agrifood systems. For instance, IoT-enabled sensors are strategically installed on agricultural fields to inspect essential variables such as weather conditions, soil health, crop status, and livestock well-being (Sinha & Dhanalakshmi, 2022). The integration of big data with IoT concepts enables the collection, analysis, and utilization of the large amounts of data generated by IoT devices to derive valuable insights and enhance decision-making processes.

To establish a balance between global demand and supply in the food supply chain, IoT sensors and other information and communication technologies may be implemented to effectively monitor food quality, safety, and security (Lezoche et al., 2020; Abideen et al., 2021). Integrating the IoT in AFSs holds significance for enhancing the flexibility of food supply chains by generating a wealth of real-time data that can be analyzed using advanced predictive analytics. By generating real-time data, which can be analyzed using advanced predictive analytics, the IoT equips AFSs with the ability to determine vulnerabilities in the supply chain promptly. This proactive identification allows for the implementation of necessary measures to maintain the integrity of the food supply. Furthermore, IoT applications in AFSs extend to preserving the quality of fresh produce, ensuring compliance with food safety regulations, and consequently, reducing food waste while bolstering food security (Tagarakis et al., 2021). Nevertheless, there are ongoing issues associated with the use of IoT devices, both at the agricultural level and across the entirety of the food supply chain. Addressing these challenges is necessary to fully unlock the value of the IoT in the food industry.

To facilitate the transition toward Society 5.0 and fulfill the SDGs in the digitalization of AFSs through the IoT, there is a need for a telecommunications network that enhances connectivity and improves the distinction between digital and physical spaces. Most of the current network communication systems, such as 3G/4G, Wi-Fi, long-range wide area networks (LoRaWANs), and the narrowband Internet of Things (NB-IoT), encompass restricted accessibility and bandwidth, leading to latency issues that cause delays in data transfer, hindering efficient data communication (Tang et al., 2021). Addressing this limitation requires the incorporation of greater capacity to support the increasing number of interconnected devices necessary for the advancement of smart agricultural practices. Hence, the emergence of 5G communication networks has the potential to make connectivity more affordable and accessible for a wide range of stakeholders. The fifth generation of wireless networks, referred to as 5G, is the most recent advancement in wireless technology. It aims to provide users or devices with ubiquitous information accessibility and the capability to exchange data in any location and at any time (Andrews et al., 2014).

The remarkable capabilities of 5G networks, including high-speed data transfer and low latency, make these networks suitable for supporting machine-to-machine communications within the agrifood supply chain (van Hilten & Wolfert, 2022). For

example, 5G's efficient connectivity can be advantageous for deploying automated guided transporters in food distribution operations. The emergence of 5G technology in the food industry holds significant promise for transformative advancements in connectivity, data transmission, and operational efficiency, therefore enhancing the degree of communication within the AFS.

Moreover, the integration of 5G and the IoT enables real-time data collection, analysis, and communication, empowering the AFS to make more informed decisions, mitigate risks, and respond promptly to challenges. This increased productivity and flexibility can expedite progress toward the achievement of Society 5.0 and the SDGs, particularly by contributing to addressing food security issues and ensuring the availability of safe and nutritious food for everyone while fostering sustainable practices throughout the food supply chain.

1.2.3 Artificial Intelligence in Digital Agrifood Systems

Artificial intelligence (AI) is a digital technology that is making rapid progress in the agricultural sector. The agricultural sector is projected to experience substantial investments in AI in the coming years, with an anticipated 23.1% compound annual growth rate (CAGR) from 2023 to 2028, indicating the increasing recognition of AI's potential to transform the agriculture market (Market Research Report, 2023). The application of AI is revolutionizing various aspects of farming, and AI has been applied in some key areas in agriculture, such as in robotic farming, crop

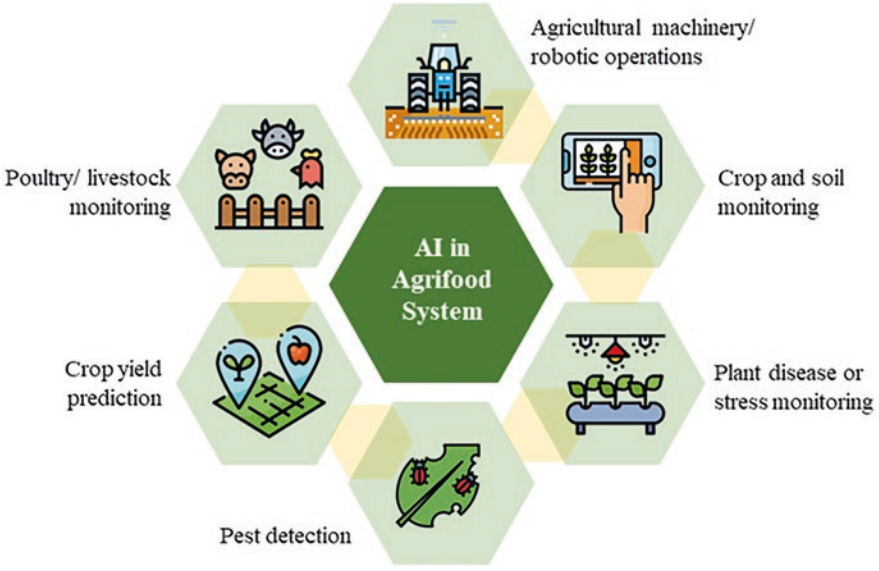

Fig. 1.2 Applications of AI in agrifood system

monitoring and disease detection, crop yield and harvesting prediction, and livestock monitoring (Fig. 1.2).

AI is being used to analyze data obtained from sensors, drones, satellites, and other devices to provide real-time insights into soil conditions, crop health, water usage, and more (Dharmaraj & Vijayanand, 2018). Such insights help farmers optimize the use of resources and apply interventions only where and when necessary, reducing costs and environmental impact. Moreover, AI and machine learning can be employed for monitoring crops and identifying stress or diseases by training on a large dataset of crop images (Fig. 1.3) (Hamidon & Ahamed, 2022). These technologies extract features to facilitate the precise and efficient identification of diseases, pests, and nutrient deficiencies. Such identification enables farmers to implement early interventions to mitigate these issues, minimize crop losses, and improve overall yields.

Furthermore, AI plays a valuable role in yield prediction and harvesting optimization. Algorithms can be used to process historical and real-time weather, soil, and crop growth data to help farmers predict crop yields accurately (Shaikh et al., 2022). This information helps farmers optimize harvesting schedules, plan logistics, and estimate market supply. With the prediction information obtained by AI analysis, farmers are well equipped to strategically plan when to harvest their crops, manage logistical operations more efficiently, and offer more accurate estimates of the supply that they can contribute to the market. All of this leads to better and more precise resource allocation and improved profitability.

The application of AI has also been extended to animal farming and production to help farmers overcome longstanding challenges as well as modern obstacles and limitations (Neethirajan & Kemp, 2021; Bao & Xie, 2022). For example, AI technologies provide poultry farmers with the opportunity to acquire real-time insights into their farming operations (Neethirajan & Kemp, 2021). These insights enable farmers to effectively monitor and regulate crucial environmental conditions such as

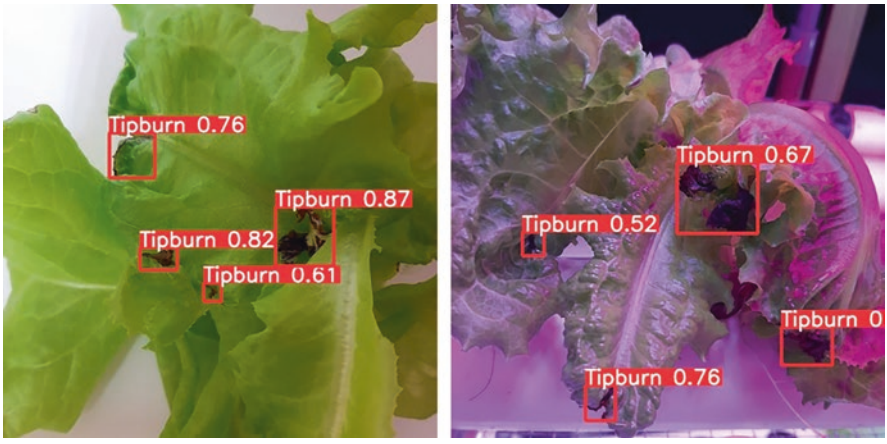

Fig. 1.3 Example of AI being used to detect nutrient deficiency in plants

temperature, light, humidity, and more in their poultry farms. Farmers can assess and monitor their product quality with a rapid and nondestructive approach by using object detection, which is a part of AI methods. By utilizing AI to optimize these conditions, farmers can significantly improve animal health and enhance operational efficiency.

1.2.4 Robotics and Drone Technology

Robotics encompasses a range of essential technologies that have always created new possibilities for automation in AFSs (Mor et al., 2022; Pearson et al., 2022). These technologies provide the foundation for the transition to Society 5.0, a concept that integrates humans and advanced technologies for sustainable development, and the achievement of the SDGs. Through the utilization of robotics, multiple aspects of the agriculture and food industry can be automated, leading to increased efficiency, productivity, and sustainability. This automation includes aspects such as precision farming, autonomous harvesting, robotic food processing, smart logistics, and intelligent distribution systems. The adoption of robotics in the agriculture sector offers opportunities to address challenges related to food security, resource management, labor shortages, waste reduction, and environmental impact. It also enables the creation of new business models and value chains that support sustainable practices and promote social well-being.

The integration of robotics and AI has a crucial role in enhancing flexibility within AFSs, resulting in increased productivity by replacing tasks traditionally reliant on humans with automation. The deployment of robotics and AI enables the agriculture and food systems to operate with greater adaptability and efficiency. Advanced sensors and data analysis capabilities enable robotic systems to accurately inspect and monitor soil or environmental conditions more effectively than

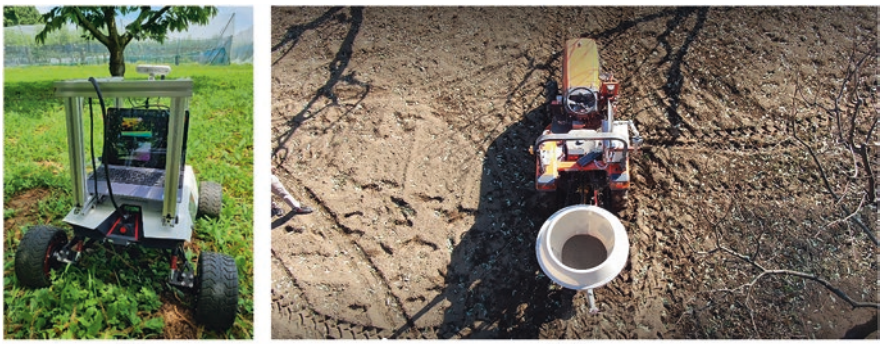

Fig. 1.4 Example of agricultural robots used in an agricultural field: (**a**) mini-scouting vehicle for field monitoring; (**b**) unmanned tractor for fertilizer broadcasting

humans (Fig. 1.4). This valuable information can be utilized to make reliable decisions and optimize cultivation processes, for example, by providing the necessary nutrients, controlling the growth environment, and removing weeds automatically. Furthermore, integrating this innovative and advanced technology into agriculture fields allows for automated harvesting with autonomous vehicles. These vehicles can navigate through fields, identify ripe crops, and perform harvesting tasks without human intervention. Doing so will not only improve efficiency but also address labor issues and reduce the dependence on manual labor.

Alternatively, land-based and aerial drones offer effective substitutes for human labor in labor- and time-intensive agricultural operations such as seeding and weeding, as well as tasks that involve potential health and safety risks associated with fertilizer and chemical spraying (Mogili & Deepak, 2018) (Fig. 1.5). By utilizing the capabilities of drones, these tasks can be automated, increasing efficiency and reducing human involvement. Furthermore, drones are crucial in remote data collection, which can assist farmers in making informed decisions. The collected data serve various purposes, including reducing the risks of disasters, managing crops more effectively and precisely, predicting crop yields, and promoting environmental sustainability. Essentially, drones contribute to a range of agriculture activities by providing data that enable farmers to optimize their practices and address various challenges in their farming operations.

Obtaining timely and reliable data not only benefits individual farmers but also enables stakeholders within AFSs to make more effective policy decisions and implement practical strategies to achieve Society 5.0 and the SDGs. For instance, drones equipped with sensors and imaging technology can monitor crop health,

Fig. 1.5 Drone being used for fertilizer spraying

identify areas of pest infestation or nutrient deficiencies, and provide valuable insights for precision farming practices. This data-driven approach facilitates targeted interventions, optimizing resource utilization, reducing environmental impact, and promoting sustainable agricultural practices. Furthermore, drones can assist in disaster risk reduction by conducting aerial surveys and monitoring areas prone to natural disasters or climate-related events. This information helps in assessing vulnerabilities, developing mitigation strategies, and enhancing overall resilience within agricultural systems.

1.2.5 3D Printing Technology: Changing the Manufacturing in Agriculture

The use of 3D printing, also known as additive manufacturing, is an advanced method of production automation where objects are created by layering materials based on 3D model data using a 3D printer. In contrast to traditional manufacturing methods, such as subtractive manufacturing, where a portion of the material is removed to create a desired product, this technology significantly reduces both waste and lead time (Gache et al., 2022). Although 3D printing technology is not new, its innovative applications hold great relevance and significance for the AFS.

The application of 3D printing in agriculture and food production offers numerous potential benefits. One significant advantage is the ability to create custom-designed tools, equipment, and parts for agriculture and food production processes. This customization allows for precise adaptations to specific needs, improving efficiency and effectiveness in various agricultural activities (Crisostomo & Dizon, 2021). Moreover, 3D printing enables the production of complex geometries and structures that are otherwise difficult to manufacture using traditional methods. This capability offers opportunities for designing innovative farming tools and replacement parts, sensors, and even customized plant structures that can optimize resource utilization, enhance crop yields, and contribute to sustainable farming practices.

Fused deposition modeling (FDM) is a common 3D printing technology used to create a wide range of essential tools and equipment for agriculture. In this field, thermoplastics, particularly PLA and ABS, play significant roles in producing farming tools such as sprinklers and irrigation hose splitters (Pearce, 2015), machine parts such as gears, and even seed broadcasting devices (Fig. 1.6) (Minn et al., 2023). Low-cost materials such as PLA can be used to construct personalized tools such as biodegradable and recyclable fruit pickers and shovels (Pearce, 2015). Despite minor differences in properties such as stiffness and heat resistance, these thermoplastic materials continue to dominate 3D printing due to their affordability and ease of use in the printing process.

3D printing has also been employed for on-site manufacturing, reducing the need for transportation and logistics associated with sourcing parts or equipment from distant locations. This localized production can enhance resilience in the agrifood system, particularly in remote or underserved areas where access to agricultural

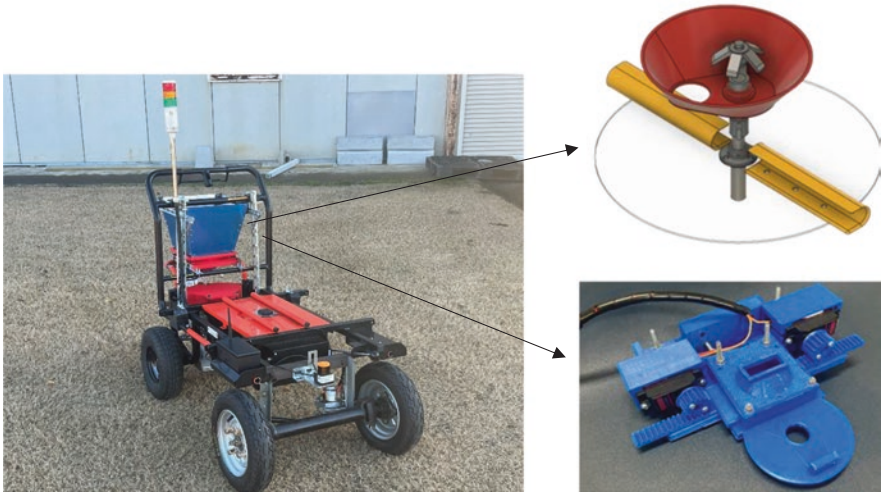

Fig. 1.6 3D-printed seed broadcasting devices

resources may be limited. 3D printing supports sustainable practices by reducing material waste and energy consumption. The technology allows for precise material usage, minimizing excess waste during the manufacturing process. Additionally, the ability to recycle and reuse materials in 3D printing further contributes to a circular economy approach in the agrifood system (Crisostomo & Dizon, 2021).

1.2.6 Edge Computing

Edge computing, also known as decentralized processing, involves the local handling of data near their source or device, which brings enterprise applications in proximity to data sources, including IoT devices or local edge servers. In the context of the AFS, edge computing offers several benefits and opportunities. Edge computing enables real-time data processing and analysis, allowing for faster decision-making and response. In agriculture, data collected from sensors, drones, or other connected devices can be processed locally, minimizing latency and enabling timely actions. For example, real-time analysis of soil fertility data at the edge can facilitate optimal irrigation practices, leading to water conservation while improving crop health (Lavanya et al., 2020). Furthermore, edge computing minimizes the potential threats of unauthorized access or data breaches. Through the local processing of data within the edge computing framework, sensitive information is stored in close proximity to its source, thereby contributing to a more secure and private data and computing paradigm. This aspect is particularly important in the agrifood system, where data related to farm operations, food safety, and supply chain integrity need to be protected (O'Grady et al., 2019).

The integration of edge computing with machine learning and AI offers transformative capabilities within AFSs. With the deployment of ML and AI models at the forefront of edge devices, AFSs can achieve autonomous decision-making at the local level, empowering agricultural devices to analyze data in real time and execute actions without relying on centralized cloud processing. The immediacy of real-time data analysis is particularly advantageous for time-sensitive tasks such as irrigation and pest control, and it enables precision intervention and targeted application of resources, including inputs such as water, fertilizers and pesticides.

In the ever-evolving landscape of agriculture and food systems, the integration of digital twins with edge computing represents a revolutionary leap forward. Digital twins, which are virtual replicas of physical assets, are becoming indispensable tools for optimizing the agrifood sector. They enable real-time monitoring and simulation of everything from crop growth to supply chain logistics. However, the true power of digital twins is unlocked when coupled with edge computing. Edge devices, strategically placed throughout the agricultural ecosystem, process data locally, reducing latency and minimizing the load on central servers. This synergy between digital twins and edge computing empowers farmers, food producers, and distributors with immediate insights, enabling rapid decision-making and fine-tuning of operations. Moving forward, harnessing the potential of digital twins and edge computing will be key in meeting the growing demands of our global population while ensuring the responsible management of our agricultural resources.

1.2.7 Digital Twins and Cross Reality (XR) in Precision Farming

The fundamental approach of digital twins, representing a virtual duplicate of a physical object or system, holds significant potential for future agriculture. The digital twin is a relatively new concept that carries substantial promises to revolutionize smart agriculture to a more advanced level in terms of productivity and sustainability (Verdouw & Kruize, 2017). The digital twin concept includes simulating, planning, analyzing, and improving crop growth to maximize yields and make farming more sustainable. Farmers can monitor and control their farm operations using real-time digital information in a virtual system, thereby reducing the need for manual on-site observation. Nevertheless, a sound basis for progress in the development and implementation of digital twins in agriculture is still in its infancy (Jones et al., 2017; Pylianidis et al., 2021).

A digital twin is necessary to visualize the digital representation of physical farms in the virtual environment. The virtual environment serves as a real-time and remote platform to establish connections with real objects and deliver detailed representations of both the objects and their surroundings in real time. This platform acts as a storage and communication infrastructure that holds a virtual

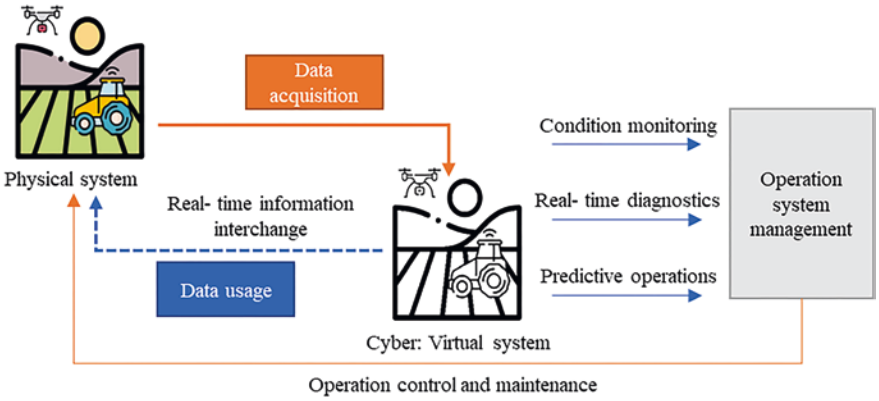

Fig. 1.7 Concept of the digital twin in agriculture

representation of things linking relevant information with the object. As such, a digital twin acts as a central hub of real farm information, continuously combining and updating data from a wide range of sources generated by the virtual farm or operational management system for condition monitoring, real-time diagnostics, and predictive operations (Fig. 1.7).

The implementation of digital twin technology eliminates the inherent constraints related to spatial limitations, temporal factors, and human presence. In contrast to managing agricultural operations through direct physical observation, which necessitates physical proximity, digital twins facilitate the remote control and remote monitoring of farm activities. Doing so allows for the decoupling of physical aspects from the informational components of farm operations. Moreover, a digital twin can be enhanced by data on environmental conditions and farm characteristics acquired through sensors and satellite sensing. As such, this digital platform enables advanced control functionalities for remote farming.

Another forefront technology closely related to the concept of the digital twin and potentially beneficial for remotely monitoring and managing agriculture is cross reality (XR). Cross reality, which includes augmented reality (AR) and virtual reality (VR), serves as an integration platform for visualizing real-world and digital images (Ziker et al., 2021) (Fig. 1.8). It was initially introduced to the technology market with the adoption of smartphones and built-in cameras. Since then, the utilization of XR has expanded across various industries, such as the construction, manufacturing, and automotive industries, education, and surgical procedures. However, compared to other industries, XR technology in agriculture is extremely underexplored (Xi et al., 2018). Farming entrepreneurs are still reluctant to invest in this technology, as they do not simply know the full spectrum of XR possibilities (Yang et al., 2021).

Implementing XR in agriculture creates enormous possibilities for business by automating many processes and interactively showing how agriculture business operations can be conducted. Considering the capabilities of both digital twins and

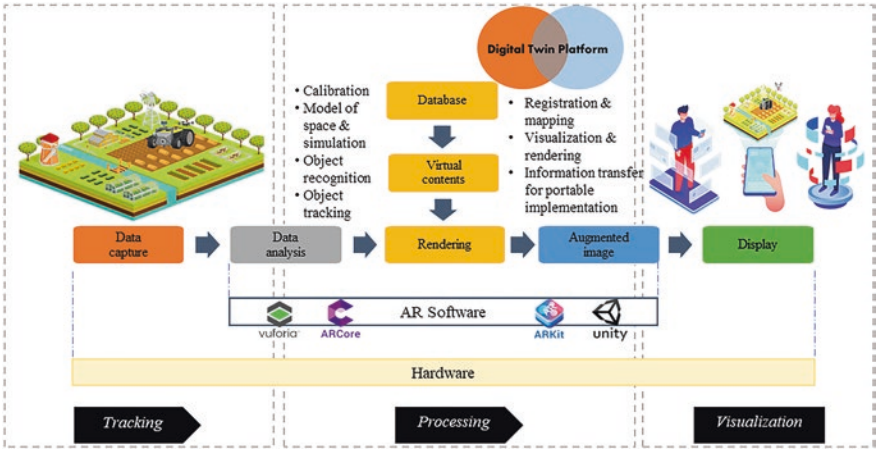

Fig. 1.8 Conceptual overview depicting the integration of the real world with digital images in cross reality

cross-reality applications in agriculture, a comprehensive integration of digital twins and cross-reality platforms could be suggested to support more efficient farm management activities such as farm operation management, remote collaboration, and boardroom discussion to secure a stable source of crop production. The integration of digital twins and cross reality in the agrifood system holds tremendous potential that can contribute to the development of Society 5.0 and the achievement of the SDGs.

1.2.8 Digital-Twin-Driven Smart Supply Chain

Blockchain technology holds transformative potential for evolving AFS supply chains, particularly in fostering transparency and trust among farmers and stakeholders (Tripoli & Schmidhuber, 2018; Menon & Jain, 2021). By implementing blockchain, AFS supply chains can realize a decentralized and secure system for recording and verifying transactions, offering an unaltered recording of every step in the supply chain. Integrating blockchain with the digital twin in AFSs provides a robust foundation for managing and validating the authenticity of digital representations of physical objects and processes. Furthermore, incorporating cross reality into AFSs can amplify the benefits of blockchain and digital twins.

XR refers to the utilization of computer-generated simulations that immerse users in a synthetic environment, facilitated by specialized equipment for user interaction (Rauschnabel et al., 2022). This technology enables direct user engagement with the simulated environment, mimicking natural interactions. The integration of XR in agriculture holds significant potential for farming entrepreneurs, offering

unparalleled opportunities for farm management optimization by both farmers and stakeholders without geographical constraints. A 3D virtual farm, created through simulation technology, allows farm owners to make decisions and manage their farm remotely, eliminating the need for physical presence at the actual farm. The real farm acts as the primary source for collecting sensing and phenotyping data, which are stored in the operational management system. This system enables users to inspect and operate using natural and intuitive perceptions, including visual, auditory, and tactile feedback.

The XR visualization system is fundamentally divided into three layers: the device layer, the network layer, and visualization/application layers (Porcino et al., 2022). Agricultural robotics, employed as the main devices for data acquisition, capture information related to environmental parameters, farm operations, and crop growth progress at the physical farm. The digital twin platform, on the other hand, serves as the core of the XR architecture, comprehending information from specific systems such as irrigation, seedling, and fertilization operations and integrating this

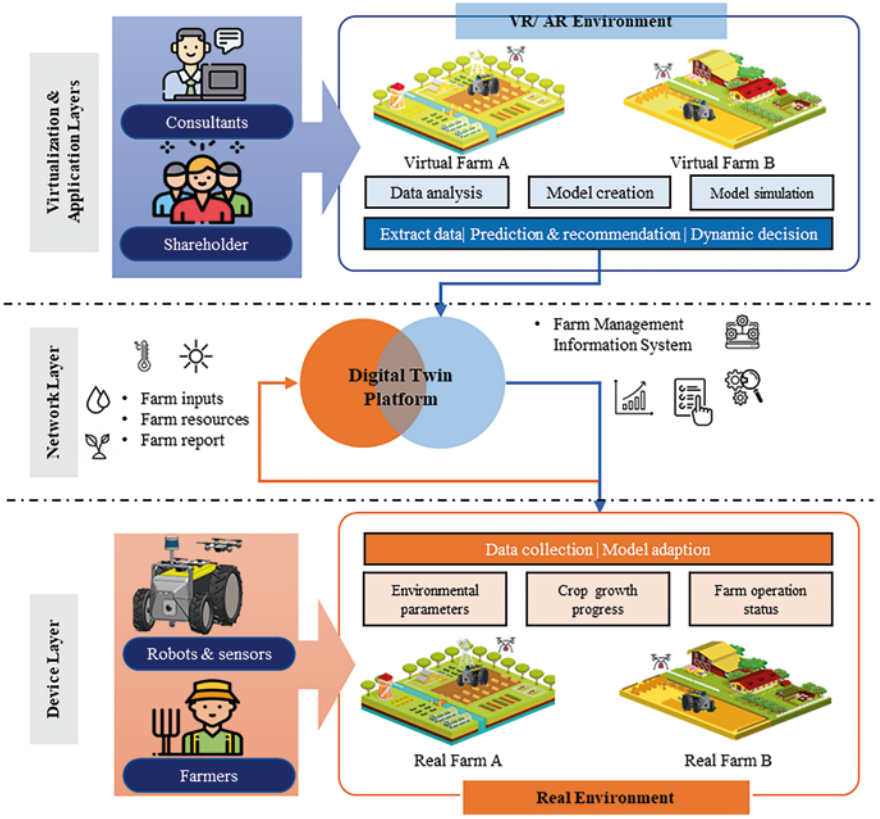

Fig. 1.9 Visualization of the integration of XR and digital twins in a blockchain-enabled agrifood system supply chain

information into a virtual reality fam system (Fig. 1.9). This integration allows users to take control of various systems and enables farm owners and stakeholders to gain a comprehensive understanding of their farm's performance.

1.3 Achieving SDGs through Digital Innovations in Agrifood Systems

The goal of "no poverty" is to eradicate poverty in all its forms and dimensions, as outlined in Sustainable Development Goal 1. This goal aims to ensure that all individuals have access to the basic resources, services, and opportunities necessary to lead a dignified life. In the pursuit of this goal, digital innovations in agrifood systems can contribute significantly to achieving "no poverty" by boosting agricultural productivity, optimizing the food value chain, expanding market access for small-scale farmers, and fostering sustainable and inclusive economic growth.

As part of the United Nations' Sustainable Development Goals, "zero hunger" is SDG 2, which aims to end hunger, achieve food security, improve nutrition, and promote sustainable agriculture. The focus is to ensure everyone's access to safe, nutritious, and sufficient food. The application of digital innovations in agrifood systems can drive the achievement of SDG 2 by enhancing agricultural methods, increasing productivity, streamlining food distribution, minimizing food waste, and empowering both farmers and consumers. "Good health and well-being," SDG 3, aims to ensure the well-being of all individuals across physical, mental, and social dimensions. This goal includes access to quality health care, disease prevention, mental health support, and healthy lifestyles. Digital innovations in agrifood systems can contribute to achieving SDG 3 by enhancing the nutritional value and safety of food, endorsing sustainable farming techniques, and improving access to healthcare information and services. Technologies can optimize farming practices to produce nutrient-rich crops and promote sustainable techniques such as precision agriculture, ultimately leading to healthier food and improved well-being.

Table 1.1 presents several examples that demonstrate the significant progress digital innovations in agrifood systems are making in the direction of achieving the SDGs. Through the strategic use of technology and digital solutions, we have the

Table 1.1 Examples of digital innovation initiatives in agrifood systems aligned with the SDGs

Program	Application	SDGs
Farmcrowdy *Agrictech, Nigeria*	• It connects farmers with investors through crowdfunding • It provides a platform on which individuals can invest in various agricultural projects and earn returns based on the success of those projects • It empowers small-scale farmers	
Esoko	• This is a mobile and web-based platform that provides farmers with real-time market information, weather updates, and farming tips and techniques • It helps small-scale farmers make informed decisions, negotiate better prices, and improve their market competitiveness	
Agri-Wallet *Dodore Kenya Ltd*	• This is a digital financial inclusion platform that provides smallholder farmers with access to credit, insurance, and other financial services	
Plantix *PEAT GmbH, Germany*	• This is a mobile crop advisory application for farmers that deploys image recognition and AI algorithms to diagnose plant diseases • It provides personalized recommendations for treatment	
Building Blocks	• The World Food Programme (WFP) developed Building Blocks, a blockchain-based platform that facilitates secure and transparent transfers of food assistance • This digital innovation ensures efficient and accountable food distribution, reaching those in need more effectively	
Digital Green	• This consists of digital platforms to provide agricultural extension services to smallholder farmers • Farmers gain knowledge about sustainable farming practices through videos and interactive learning	
AgroCenta	• This is an online marketplace that connects small-scale farmers with buyers • It provides digital payment and logistics services • It eliminates intermediaries, ensures fair prices for farmers, and improves access to markets, contributing to reducing hunger and poverty	

(continued)

Table 1.1 (continued)

Program	Application	SDGs
FoodKeeper	• The FoodKeeper app provides users with information on food storage, expiration dates, and safe handling practices • It helps consumers reduce food waste and avoid consuming expired or unsafe food, promoting food safety and health	
E-Nutrifood	• This is an educational platform that serves as a hub for promoting the benefits of consuming nutritious foods commonly grown by local farmers • Its main objective is to disseminate essential information about the production and consumption of these foods, emphasizing their role in maintaining a healthy lifestyle • Users can access valuable knowledge and resources related to nutritional value, cultivation techniques, and recipes of these food items • It raises awareness about the importance of incorporating these nutrient-rich foods into daily diets, thereby contributing to improved health and well-being	

potential to elevate agricultural productivity, optimize food distribution systems, and empower stakeholders at various levels of the agrifood value chain. This concerted effort holds the promise of effectively addressing hunger and realizing sustainable food security.

1.4 Achieving Society 5.0 through Digital Innovations in Agrifood Systems

In Society 4.0, there were numerous issues, such as inefficient information sharing within organizations, the underutilization of knowledge across different fields, and the need to search for relevant information from a large amount of data. Additionally, the challenges of labor shortages, regional depopulation, and limitations encountered by certain individuals due to age or disability were becoming more severe. To overcome these issues, Society 5.0 emphasizes the integration of advanced technologies and the seamless blending of virtual and real spaces (Fukuyama, 2018; Fukuda, 2020). By utilizing technologies such as AI, the IoT, robotics, and big data analytics, Society 5.0 strives to create a human-centered society. This societal model aspires to enable individuals to experience lives that are not only comfortable but also dynamic and characterized by a high standard of living.

Digital innovation within the agrifood system plays a significant role in realizing the principles of Society 5.0. This emerging societal concept envisions integrating technology with human life, creating a balanced ecosystem that addresses challenges and fosters economic growth and social well-being. By adopting digital technologies such as precision agriculture, smart sensors, and data analytics, the agrifood sector aligns itself with the essence of Society 5.0. These tools empower farmers to make informed decisions based on real-time data, optimizing resource allocation, minimizing waste, and enhancing overall productivity. Moreover, the integration of advanced technologies fosters a more sustainable and efficient food value chain, spanning from production to distribution. Through interconnected systems, consumers gain access to transparent information about the origins, safety, and nutritional value of food, empowering them to make informed choices for their well-being. Consequently, digital innovation in the agrifood system not only contributes to economic growth but also embodies the human-centric, technology-driven vision of Society 5.0, where individuals lead enriched lives while addressing pressing societal and environmental concerns (Fig. 1.10).

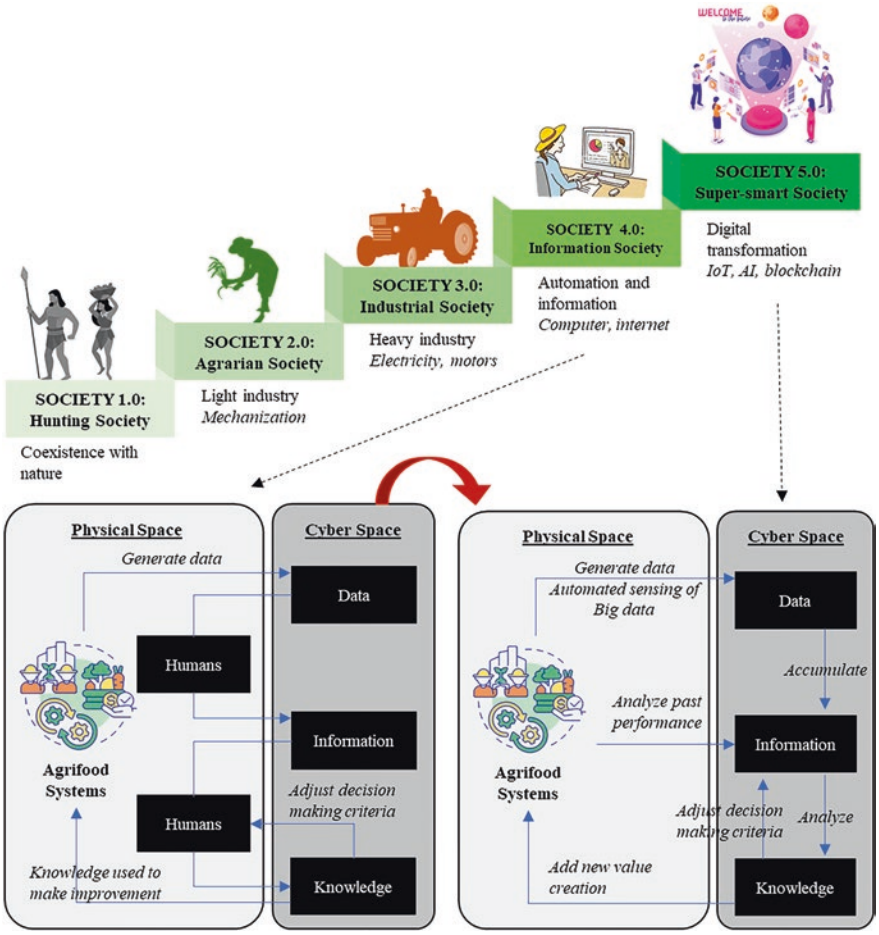

Fig. 1.10 Evolution of the transformation of human society toward Society 5.0 in agrifood systems

1.5 Conclusion

In conclusion, digital innovations in agrifood systems have revolutionized the way we approach agriculture, leading to numerous benefits and opportunities. These innovations have transformed the agriculture industry by improving productivity, efficiency, sustainability, and the overall well-being of farmers and communities. Through technologies such as 5G, AI, robotics, big data analytics, and digital twins in blockchain, farmers can access crucial information, optimize resource allocation, connect with markets, and make informed decisions. All of this has resulted in increased agricultural productivity, enhanced market access, reduced post-harvest losses, and improved livelihoods for farmers.

Furthermore, digital innovations have contributed to addressing key global challenges such as food security, poverty reduction, and environmental sustainability. By adopting precision agriculture practices, optimizing resource use, and implementing climate-smart solutions, more food can be produced while minimizing environmental impact. The use of digital technologies has also enabled the inclusion of small-scale farmers, empowering them with market opportunities and financial services. Continuing to embrace digital innovations in agrifood systems, it is essential to ensure that these technologies are accessible, affordable, and sustainable for all stakeholders. Collaborative efforts among governments, private sector actors, and local communities are vital to leverage the full potential of digital innovations and address the specific needs and challenges of different regions and farming communities. Digital innovation holds tremendous promise for transforming agrifood systems, driving sustainable development, and achieving the United Nations' Sustainable Development Goals and Society 5.0.

References

Abideen, A. Z., Sundram, V. P. K., Pyeman, J., Othman, A. K., & Sorooshian, S. (2021). Food supply chain transformation through technology and future research directions—A systematic review. *Logistics, 5*(4), 83.

Ancín, M., Pindado, E., & Sánchez, M. (2022). New trends in the global digital transformation process of the Agri-food sector: An exploratory study based on Twitter. *Agricultural Systems, 203*, 103520.

Andrews, J. G., Buzzi, S., Choi, W., Hanly, S. V., Lozano, A., Soong, A. C., & Zhang, J. C. (2014). What will 5G be? *IEEE Journal on Selected Areas in Communications, 32*(6), 1065–1082.

Bao, J., & Xie, Q. (2022). Artificial intelligence in animal farming: A systematic literature review. *Journal of Cleaner Production, 331*, 129956.

Biermann, F., Kanie, N., & Kim, R. E. (2017). Global governance by goal setting: The novel approach of the UN sustainable development goals. *Current Opinion in Environmental Sustainability, 26*, 26–31.

Chi, M., Plaza, A., Benediktsson, J. A., Sun, Z., Shen, J., & Zhu, Y. (2016). Big data for remote sensing: Challenges and opportunities. *Proceedings of the IEEE, 104*(11), 2207–2219.

Crisostomo, J. L. B., & Dizon, J. R. C. (2021). 3D printing applications in agriculture, food processing, and environmental protection and monitoring. *Advance Sustainable Science, Engineering and Technology, 3*(2), 372312.

Dharmaraj, V., & Vijayanand, C. (2018). Artificial intelligence (AI) in agriculture. *International Journal of Current Microbiology and Applied Sciences, 7*(12), 2122–2128.

Fukuda, K. (2020). Science, technology and innovation ecosystem transformation toward society 5.0. *International Journal of Production Economics, 220*, 107460.

Gache, C. C. L., Tuazon, B. J., Espino, M. T., Advincula, R. C., & Dizon, J. R. C. (2022). 3D-printed polymeric spare parts for industrial applications: A state-of-the-art review. *SciEnggJ, 15*(2), 128–144.

Griggs, D. J., Nilsson, M., Stevance, A., & McCollum, D. (2017). *A guide to SDG interactions: From science to implementation*. International Council for Science.

Hamidon, M. H., & Ahamed, T. (2022). Detection of tip-burn stress on lettuce grown in an indoor environment using deep learning algorithms. *Sensors, 22*(19), 7251.

Jones, J. W., Antle, J. M., Basso, B., Boote, K. J., Conant, R. T., Foster, I., Godfray, H. C. J., Herrero, M., Howitt, R. E., Janssen, S., Keating, B. A., Munoz-Carpena, R., Porter, C. H.,

Rosenzweig, C., & Wheeler, T. R. (2017). Toward a new generation of agricultural system data, models, and knowledge products: State of agricultural systems science. *Agricultural Systems, 155*, 269–288.

Kunisch, M. (2016). Big data in agriculture—Perspectives for a service organization. *Landtechnik, 71*(1), 1–3.

Lavanya, G., Rani, C., & GaneshKumar, P. (2020). An automated low cost IoT based Fertilizer Intimation System for smart agriculture. *Sustainable Computing: Informatics and Systems, 28*, 100300.

Lezoche, M., Hernandez, J. E., Díaz, M. D. M. E. A., Panetto, H., & Kacprzyk, J. (2020). Agri-food 4.0: A survey of the supply chains and technologies for the future agriculture. *Computers in Industry, 117*, 103187.

Liu, W., Shao, X. F., Wu, C. H., & Qiao, P. (2021). A systematic literature review on applications of information and communication technologies and blockchain technologies for precision agriculture development. *Journal of Cleaner Production, 298*, 126763.

Manyika, J., Chui, M., Brown, B., Bughin, J., Dobbs, R., Roxburgh, C., & Hung Byers, A. (2011). *Big data: The next frontier for innovation, competition, and productivity.* Retrieved October 19, 2023, from https://www.mckinsey.com/business-functions/mckinsey-digital/our-insights/big-data-the-next-frontier-for-innovation.

Market Research Report. (2023). *Google's project mineral in 2023: revolutionizing agriculture with AI.* Retrieved October 4, 2023, from https://www.marketsandmarkets.com/industry-news/Google-Project-Mineral-In-2023-Revolutionizing-Agriculture-With-AI

Menon, S., & Jain, K. (2021). Blockchain technology for transparency in Agri-food supply chain: Use cases, limitations, and future directions. *IEEE Transactions on Engineering Management., 71*, 106.

Minn, A., Abeyrathna, R. R. D., Nakaguchi, V. M., & Ahamed, T. (2023). Development of a 3D Printed New Metering Mechanism for a Multi-Crop Seed Broadcasting System Using an Autonomous Small-Scale Vehicle. *Inventions, 8*(3), 69. https://doi.org/10.3390/inventions8030069

Mogili, U. R., & Deepak, B. B. V. L. (2018). Review on application of drone systems in precision agriculture. *Procedia Computer Science, 133*, 502–509.

Mor, R. S., Kumar, D., Singh, A., & Neethu, K. (2022). Robotics and automation for agri-food 4.0: Innovation and challenges. In *Agri-food 4.0: Innovations, challenges and strategies* (pp. 189–199). Emerald Publishing Limited.

Neethirajan, S., & Kemp, B. (2021). Digital livestock farming. *Sensing and Bio-Sensing Research, 32*, 100408.

O'Grady, M. J., Langton, D., & O'Hare, G. M. P. (2019). Edge computing: A tractable model for smart agriculture? *Artificial Intelligence in Agriculture, 3*, 42–51.

Pearce, J. M. (2015). Applications of open source 3-D printing on small farms. *Organic Farming, 1*, 1.

Pearson, S., Camacho-Villa, T. C., Valluru, R., Gaju, O., Rai, M. C., Gould, I., Brewer, S., & Sklar, E. (2022). Robotics and autonomous systems for net zero agriculture. *Current Robotics Reports, 3*(2), 57–64.

Porcino, T., Ghaeinian, S. A., Franz, J., Malloch, J., & Reilly, D. (2022). Design of an XR Collab. Arch. for mixed immersive and MS interaction. *arXiv preprint arXiv:2208.14842*.

Pylianidis, C., Osinga, S., & Athanasiadis, I. N. (2021). Introducing digital twins to agriculture. *Computers and Electronics in Agriculture, 184*, 105942.

Rauschnabel, P. A., Felix, R., Hinsch, C., Shahab, H., & Alt, F. (2022). What is XR? Towards a framework for augmented and virtual reality. *Computers in Human Behavior, 133*, 107289.

Rejeb, A., Rejeb, K., & Zailani, S. (2021). Big data for sustainable agri-food supply chains: A review and future research perspectives. *Journal of Data, Information and Management, 3*, 167–182.

Shaikh, T. A., Rasool, T., & Lone, F. R. (2022). Towards leveraging the role of machine learning and artificial intelligence in precision agriculture and smart farming. *Computers and Electronics in Agriculture, 198*, 107119.

Sinha, B. B., & Dhanalakshmi, R. (2022). Recent advancements and challenges of internet of things in smart agriculture: A survey. *Future Generation Computer Systems, 126*, 169–184.

Tagarakis, A. C., Benos, L., Kateris, D., Tsotsolas, N., & Bochtis, D. (2021). Bridging the gaps in traceability systems for fresh produce supply chains: Overview and development of an integrated iot-based system. *Applied Sciences, 11*(16), 7596.

Tang, Y., Dananjayan, S., Hou, C., Guo, Q., Luo, S., & He, Y. (2021). A survey on the 5G network and its impact on agriculture: Challenges and opportunities. *Computers and Electronics in Agriculture, 180*, 105895.

Tripoli, M., & Schmidhuber, J. (2018). Emerging opportunities for the application of blockchain in the agri-food industry. *FAO and ICTSD: Rome and Geneva*. Licence: CC BY-NC-SA. 3. https://www.fao.org/documents/card/en?details=CA1335EN

ur Rehman, M. H., Yaqoob, I., Salah, K., Imran, M., Jayaraman, P. P., & Perera, C. (2019). The role of big data analytics in industrial internet of things. *Future Generation Computer Systems, 99*, 247–259.

van Hilten, M., & Wolfert, S. (2022). 5G in agri-food—A review on current status, opportunities and challenges. *Computers and Electronics in Agriculture, 201*, 107291.

Verdouw, C. N., & Kruize, J. W. (2017). Digital twins in farm management: illustrations from the FIWARE accelerators SmartAgriFood and Fractals. In *Proceedings of the 7th Asian-Australasian Conference on Precision Agriculture Digital, Hamilton, New Zealand* (pp. 16–18).

Xi, M., Adcock, M., & McCulloch, J. (2018). Future agriculture farm management using augmented reality. In *2018 IEEE Workshop on Augmented and Virtual Realities for Good (VAR4Good)* (pp. 1–3). IEEE.

Yang, X., Shu, L., Chen, J., Ferrag, M. A., Wu, J., Nurellari, E., & Huang, K. (2021). A survey on smart agriculture: Development modes, technologies, and security and privacy challenges. *IEEE/CAA Journal of Automatica Sinica, 8*(2), 273–302.

Ziker, C., Truman, B., & Dodds, H. (2021). Cross reality (XR): Challenges and opportunities across the spectrum. *Innovative learning environments in STEM higher education: Opportunities, challenges, and looking forward*, 55–77.

Chapter 2
Strategic Short Note: Appropriate Integration of Precision Agriculture Technology, IoT, and AI for Enhancing Southeast Asian Agriculture

Abstract Thailand has delivered a concept of the Bio-Circular-Green (BCG) economy as a growth strategy to achieve self-sufficiency and sustainability for the next society. The roles of agriculture in the future are therefore not only to sustain the food supply but also to provide bio-resources for upcoming activities taking place toward the BCG model. At the same time, the agricultural sector itself is necessarily developed according to the BCG way. Agricultural technology in Thailand and other Southeast Asian countries has been drastically developing during the few past decades. This resulted in the emergence of various innovations, new business models, and the attraction of younger generations to get into the area of agriculture. By targeting to production of high-value crops such as medicinal plants, smart greenhouse and plant factory technology have been widely adopted. The use of IoT in controlling planting conditions inside the greenhouse or plant factory has become common among crop growers. Some private companies in collaboration with researchers have been using Internet of things (IoT) and artificial intelligence (AI) for data analytics. Predictably, the number of start-up businesses or newcomers in this area will continue to increase in the foreseeable future. On the other side, in field crop production, precision agriculture technology has been increasingly adopted. Automatic systems that enhance farm machinery operation have been continuously developed. The use of multispectral imaging unmanned aerial vehicles (UAVs) for crop growth monitoring and yield prediction has become common, especially with rice, sugarcane, cassava, coconut, and oil palm. Likewise, the use of UAVs for spraying and broadcasting has been commonly practiced, which in turn increased the number of service providers. Technology and innovation will compensate for the decline of the farmer and labor population and provide business opportunities. Future challenges include making agricultural production activities more data-driven and making interpretation and management precise while sustaining the environment and resources.

Keywords BCG Economy Model · Precision agriculture · Internet of things · Artificial intelligence · Appropriate solution

© The Author(s), under exclusive license to Springer Nature Singapore Pte Ltd. 2024

T. Ahamed, *IoT and AI in Agriculture*,
https://doi.org/10.1007/978-981-97-1263-2_2

2.1 Introduction

Agricultural mechanization in Southeast Asia is gradually transforming toward a precision agriculture (PA) system since increasing production efficiency becomes crucial to achieving global competitiveness. Environmental issues and subsequent requirements are also influential factors determining changes in agricultural practices. In the case of Thailand, modern agricultural machinery and PA technology received appreciable attention from farmers, agricultural machinery manufacturers, technology providers, and related agro-industries. For example, the Global Navigation Satellite System (GNSS) guidance and auto-steering technology have been demonstrated and increasingly adopted in sugarcane production to facilitate a controlled traffic regime. The use of precision technology resulted in lower soil compaction, more planting rows achieved, less sugarcane damage due to vehicular traffic, and more efficient harvesting operations. Furthermore, the remanufacturing of retired sugarcane harvesters taken place by domestic manufacturers enables sugarcane growers and contractors to afford green harvesting. Changing from burning to baling of sugarcane trash for fueling power plants is concurrently promoting to alleviate air pollution. The redesign of field operation during harvesting and cane transportation systems, associated with GNSS-based vehicle tracking, has been intensively studied to increase the logistic efficiency of harvested sugarcane.

In rice cultivation, laser land leveling (LLL) has been introduced to facilitate alternate wetting and drying (AWD), improve water use efficiency, and reduce greenhouse gas emissions. The LLL technology is also applied to the upland fields since operating a planter on a well-level field can reduce missing errors due to the occasional lift of the planter's ground wheel.

2.2 Research and Development for Appropriate Solutions

PA technology integrated with artificial intelligence (AI) has been applied to find solutions for specific crop systems and regions. Abdullakasim et al. (2022) observed temporal changes in vegetation indices and estimated sugarcane growth using aerial multispectral images. Similarly, Chea et al. (2020) assessed sugarcane yield parameters and fiber using an unmanned aerial system. Singhpoo et al. (2023) applied YOLOv4 and Mask R-CNN to detect cassava stalks for a harvesting robot. Modern technologies, however, may not always apply to the agricultural systems in Southeast Asian countries due to physical and socioeconomic conditions. The causes of limitations involve the costs of commercial-grade technology, the economy of scale, and the relative benefit. Several efforts have been put in to develop affordable technologies to assist local farmers in accessing their crops and field information, e.g., a low-cost chlorophyll sensor for mapping spatial variability of cassava nutrient status (Sookchalearn & Abdullakasim, 2017), or a hot-water treatment equipment for cane setts disinfection in small-scale sugarcane farms (Sukcharoenvipharat et al.,

2023a). Upgrading conventional agricultural machinery to expand its capacity or to attain a higher precision might be an alternative approach for certain circumstances. For example, the development of a low-cost soil strength and subsoiling depth measuring system, which allowed soil mapping (Sukcharoenvipharat et al., 2023b), and a driver assistance system for tractors in sugarcane fields (Thanpattranon et al., 2022).

2.3 Conclusions

Agricultural production systems in Southeast Asian countries have been enhanced, partially, by translating PA concepts and technologies earlier adopted by developed countries, while certain parts of technologies and practices require specific research and reinvention to suit regional conditions. Appropriate integration of PA technology, IoT, and AI, associated with leveraging and upgrading conventional machinery, and remanufacturing of retired machinery, along with a systematic capacity building of stakeholders, can result in practical solutions for the region.

References

Abdullakasim, W., Kasemjit, A., & Satirametekul, T. (2022). Estimation of sugarcane growth using vegetation indices derived from aerial images. *Proceedings of the International Conference "Innovation for Resilience Agriculture",* October 19–21, 2022, Chiang Mai University, Chiang Mai, Thailand, 174–181.

Chea, C., Saengprachatanarug, K., Posom, J., Wongphati, M., & Taira, E. (2020). Sugar yield parameters and fiber prediction in sugarcane fields using a multispectral camera mounted on a small unmanned aerial system (UAS). *Sugar Tech, 22*(4), 605–621.

Singhpoo, T., Saengprachatanarug, K., Wongpichet, S., Posom, J., & Saikaew, K. R. (2023). Cassava stalk detection for a cassava harvesting robot based on YOLOv4 and Mask R-CNN. *Journal of Agricultural Engineering, LIV:1301*.

Sookchalearn, T., & Abdullakasim, W. (2017). A low-cost sensor for measuring and mapping chlorophyll content in cassava leaves. *Chiang Mai University Journal of Natural Sciences, 16*(3), 183–190.

Sukcharoenvipharat, W., Aumarrom, T., Usaborisut, P., Jantra, C., & Abdullakasim, W. (2023a). Design and development of a hot water treatment device for small-scale sugarcane farmers. *Sugar Tech*, *(In Press)*. https://doi.org/10.1007/s12355-023-01330-8

Sukcharoenvipharat, W., Phoonkhwan, R., & Usaborisut, P. (2023b). A low-cost soil strength and subsoiling depth measuring system and soil mapping derived from field tests. *Journal of the Saudi Society of Agricultural Sciences, 22*(3), 139–148.

Thanpattranon, P., Chertkiattipol, S., Chayaprasert, W., Abdullakasim, W., & Usaborisut, P. (2022). Development of a low-cost driver assistance system for tractors in sugarcane fields using a scanning-laser range finder. *Agriculture and Natural Resources, 56*(6), 1183–1190.

Chapter 3
Strategic Short Note: Climate Smart Technology for Corn Production in Rizal, Kalinga, Philippines

Abstract The recorded fluctuating trend in yellow corn production over the years in the municipality of Rizal, Kalinga Province in the Philippines, can be attributed to climatic hazards such as typhoon, monsoon rains, drought, and prolonged dry season affecting the municipality. These phenomena put pressure on the production causing damages and reduction in the yield of corn. For farmers to adapt or mitigate the negative effects of these hazards, several mechanisms and adaptation strategies are practiced coping with the production losses. These include availing of crop insurance, proper selection of yellow corn varieties, use of combine harvester and mechanization to speed up harvesting time, and other appropriate post-production activities. Among the identified adaptation and mitigation practices by the farmers is proper selection of appropriate varieties, which is considered practical and accessible technology that can be readily adapted by the farmers in the area.

Keywords Climate change · Hybrid Yellow Corn · Biophysical sensitivity · Technological adaptations · Varietal evaluation

3.1 Introduction

Corn (*Zea mays* L.) being a high grain producer for food and feed consumption has emerged as one of the leading cash crops in the Philippines. The latest production estimate in the Cordillera Administrative Region (CAR) is 232,351 MT, which contributes 3% to the overall production of the country (PSA, 2019).

Extreme climatic events pose harm to the agricultural production systems, which puts pressures to environmental and food security (IPCC, 2007). In the same way, PSA (2019) recorded a decline in the self-sufficiency ratio of corn in the country from 94.34% in 2017 to 88.43% in 2018 due to the declining production.

The key climate-related hazards affecting Luzon are tropical cyclones (typhoons) and drought that greatly disrupts the activities of farmers (Giles et al., 2019) (Fig. 3.1). In CAR, high production loss was recorded due to the occurrence of Typhoon Storm Ompong (DA-RFO CAR, 2018). A total of 1738 ha yellow corn

© The Author(s), under exclusive license to Springer Nature Singapore Pte Ltd. 2024

T. Ahamed, *IoT and AI in Agriculture*,
https://doi.org/10.1007/978-981-97-1263-2_3

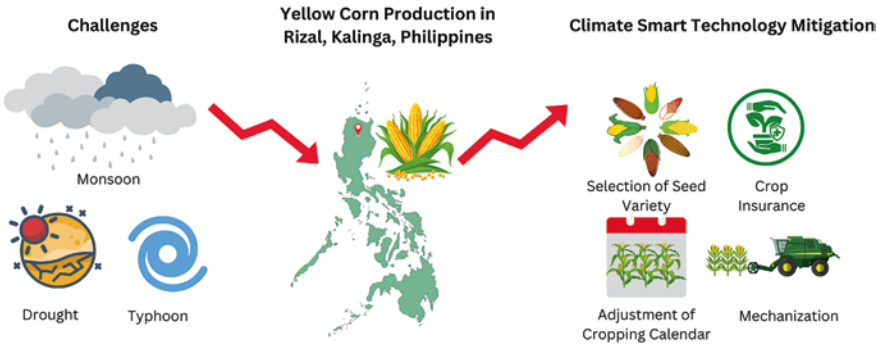

Fig. 3.1 Challenges in yellow corn production in Rizal, Kalinga, Philippines, and Proposed Climate Smart Technology Mitigation

production area was damaged with an estimated value of about Php142 million and affected 1569 farmers in Rizal, Kalinga. While in 2019, as reported by DA- RFO CAR, a total of 2883 hectares of corn production area were damaged in Kalinga Province due to drought. These scenarios may indicate the sensitivity of the province to such adverse climate conditions. The exposure of the corn plant to these climatic hazards differently affects the growth stages of the crop. The stages of corn that are susceptible to water deficit stress include vegetative, flowering, and grain filling stages, where yield loss may be as high as 25%, 50%, and 21%, respectively (Denmead & Shaw, 1960).

Rizal, Kalinga, is one of the site coverages of the Adaptation and Mitigation Initiatives for Agriculture (AMIA) 2 project that is jointly implemented by the Benguet State University (BSU) and Department of Agriculture- Regional Field Office Cordillera Administrative Region (DA-RFO CAR). It is known to be the second highest producing municipality of the province accounting for its 5396.50 ha corn harvested area and 27,733.70 metric tons, which is basically 25% of the total production of the Province (PLGU, 2019).

In addition, the highlands and sloping areas of the Cordillera where corn is intensively grown are exposed to hazards and are amplifying the vulnerability during calamities. Lasco et al. (2016) emphasized the need for more efficient climate-resilient agricultural production system to attain food security (Fig. 3.1).

3.2 Biophysical Sensitivity and Technological Adaptations for Yellow Hybrid Corn

During the growing season (from August to October), severe tropical storms or typhoons and monsoon rains occur at least once to seven times per year causing flooding. During these months, corn plants are already at the reproductive to maturity

stage, which makes them more vulnerable to damages such as lodging leading to low quality of produce.

Corn plants are also affected by drought and prolonged dry season during the second cropping (from March to May) especially during the reproductive to maturity stage of the crop. Effects of the lack of water for irrigation resulted in stunted growth and smaller ears due to damages on silk and tassels resulting to poor pollination, thereby, lowering the yield. As observed by farmers, occurrence of drought is often linked with higher temperature. Corn yield decreases by 13% for every 1 °C increase in growing season temperature (Kucharik & Serbin, 2008), and drought inhibits corn growth, reducing the photosynthetic rate and dry matter accumulation of the plant (Tuan et al., 2011).

Corn growers are vulnerable during heavy rains and floods associated with strong typhoons, especially to soil erosion, landslides, and strong winds while drought has detrimental effects on upland corn and rain-fed production (Giles et al., 2019). These phenomena caused extreme changes in the phase of planting for the dry and wet seasons, hence the evaluation of adapted varieties.

Corn farmers identified availing of crop insurance, proper selection of seed variety, and change or adjustment of cropping calendar as their adaptation/mitigation options.

Varietal evaluation of available corn varieties was conducted in the project site for proper selection of seed variety that can be planted during the time of planting, which is exposed to the natural climate hazards. Result of the trial showed that the six commercial hybrid corn varieties outyielded the farmers' corn variety (*Labus* variety). Hybrid corn NK8840 had a threefold yield increase over the farmers' variety with 6.32 mt/ha compared to 2.36 mt/ha of the *Labus* variety. Also, comparable and greater yield is recorded in varieties NK6410 (5.41 mt/ha) and Healer 101G (4.86 mt/ha).

The effect of water deficit is depending on the genotype (hybrid) ability to tolerate water stress. According to Ion et al. (2013), under limiting water conditions, proper choice of varieties is among the most important possibilities to efficiently use the available water resource. Increasing of yield is achieved by developing new hybrids with high grain yield and better tolerance to biotic and abiotic stresses. That is why farmers would have to often change the cultivated corn variety to new hybrids as a basic condition in order to have higher yield.

3.3 Conclusions

Rizal, Kalinga, is one of the major yellow corn producing areas in the Cordillera where farmers depend on its production as their main source of income, and cropping is twice a year (dry and wet season cropping). In order to mitigate and/or adapt to these damages, farmers have identified several practices to mitigate or adapt to climatic hazards. Proper selection of seed variety is among the prioritized adaptation

of farmers during occurrence of drought and typhoon. Moreover, varietal selection as a technological adaptation option is more feasible, accessible, and practical in the field. The production and economic performance of these available commercial varieties have greater yield than the conventional farmer's choice variety.

References

DA-RFO CAR (Department of Agriculture—Regional Field Office Cordillera Administrative). (2018). Damage assessment for corn caused by Typhoon Ompong.

Denmead, O. T., & Shaw, R. H. (1960). The effects of soil moisture stress at different stages of growth on the development and yield of corn. *Agronomy Journal, 52*, 272–274.

Giles, J., Macandog, P. B., Nowak, A., Pablo, J. P., Sebiano, B., Jr., Palao, L. K., Balanza, J. G., Hildebrand, J., & Grosjean, G. (2019). *Climate-resilient agriculture in The Philippines: Climate risk profile, Luzon* (p. 32). International Center for Tropical Agriculture (CIAT); Department of Agriculture—Adaptation and Mitigation Initiative in Agriculture, Government of the Philippines; The Food and Agriculture Organization of the United Nations (FAO).

Ion, V., Dicu, G., State, D., Fîntîneru, G., Epure, L. J., Basa, A. G., & Toader, M. (2013). Scientific Papers. *Series A. Agronomy, 56*, 276–283.

IPCC (Intergovernmental Panel on Climate Change). (2007). Climate change 2007: Impacts, adaptation and vulnerability. Contribution of Working Group II to the Fourth Assessment Report of the IPCC.

Kucharik, C. J., & Serbin, S. P. (2008). Impacts of recent climate change on Wisconsin corn and soybean yield trends. *Environmental Research Letters, 3*(3), 1–10.

Lasco, R. D., Espaldon, M. L. O., & Habito, C. M. D. (2016). Smallholder farmers' perceptions of climate change and the roles of trees and agroforestry in climate risk adaptation: Evidence from Bohol, Philippines. *Agroforestry Systems, 90*, 521–540. Retrieved July 9, 2020, from. https://doi.org/10.1007/s10457-015-9874-y

PLGU (Provincial Local Government Unit). (2019). Kalinga Province Corn Harvesting Report for 2019 as submitted to the DA- RFO CAR.

PSA (Philippine Statistics Authority). (2019) Corn annual volume of production, area harvested data and corn self-sufficiency ratio. Retrieved April 15, 2020, from openstat.psa.gov.ph portal.

Tuan, N. T., Verdoodt, A., & Ranst, E. V. (2011). Temperature and precipitation suitability evaluation for the winter wheat and summer maize cropping system in the Huang-Huai-hai plain of China. *Agricultural Sciences in China, 10*(2), 275–288.

Chapter 4
Appropriate Scale of Mechanization and Automation for Agriculture in Southeast Asia

Abstract The agricultural industry is critical in Southeast Asian countries. Agricultural mechanization scales vary across the region, depending on farm size and agricultural sector. The small scale gained appeal in Southeast Asia due to increased productivity, less labor usage, and the ability to adapt technology. The Level of Automation is also described in this book chapter. There are five levels of agricultural machinery, and their application in agricultural practices is discussed in this book chapter. The higher level of automation increases the more advanced agricultural machinery technology and less labor-dependent. In Southeast Asia, most countries develop the automation level into three to four stages, which are Conditional Automation and High Automation, and will continue to develop into the fifth stage, which is Full Automation. Automation systems in agricultural machinery are still being developed in various Southeast Asian countries, with the potential to be demonstrated in the future.

Keywords Agricultural mechanization · Automation · Tillage · Spraying · Seeding · Transplanting · Harvesting

4.1 Introduction

Southeast Asian countries have used machines for agricultural jobs for a very long time. Agricultural practices have changed from manual and animal labor to machinery. Examples include tractors, power tillers, and other agricultural machinery (Fig. 4.1). This chapter describes the level of automation from zero to full automation. Recently, Southeast Asian farmers have become interested in automation due to the low birthrate and transitioning demographics and migration patterns of the human population in Southeast Asian countries. Agricultural automation can mitigate the burden on and reduce the labor costs of farmers throughout Southeast Asia, making agriculture more sustainable. This chapter explains the appropriate scale of mechanization and automation for agriculture in Southeast Asia.

© The Author(s), under exclusive license to Springer Nature Singapore Pte Ltd. 2024

T. Ahamed, *IoT and AI in Agriculture*,
https://doi.org/10.1007/978-981-97-1263-2_4

Fig. 4.1 Farmers operate tractors with implements in sugarcane plantations

Fig. 4.2 (**a**) Tractor-powered cassava weeder. (**b**) The Subsoiler and Mold-board plow for Cassava weeding

4.2 Current Scale of Agricultural Mechanization in Southeast Asia

Southeast Asia consists of diverse countries with varied levels of agricultural mechanization. Generally, the level of automation in Southeast Asian countries is lower than that in more developed regions such as North America and Europe. Traditional farming methods and labor-intensive practices persist in many rural areas. According to Chao et al. (2014), manual labor accounts for 48.6% of rice cultivation practices in Cambodia.

Some Southeast Asian countries, such as Thailand and Malaysia, have made significant progress in adopting agricultural mechanization, notably in large-scale commercial farming operations. According to Cramb and Thepent (2020), in the current usage of agricultural machinery in Thailand, 41% of Thai farmers use four-wheel tractors (4WTs), 20% use planters, 30% use small water pumps, 44% use sprayers, 37% use weeders, and 29% use combine harvesters (Fig. 4.2). Countries in Southeast Asia have seen increased mechanization in the cultivation, harvesting,

and processing of rice and other crops, including fruits and vegetables. According to Wijaya and Nurcahyo (2022), the mechanization level refers to the power (hp) of agricultural machinery operations used per unit of agricultural area. The mechanization levels in Indonesia, the Philippines, Vietnam, Thailand, Cambodia, and Malaysia are 1.68, 1.23, 1.5, 2.5, 1.32, and 2.4 hp/ha, respectively. Factors such as fragmented land holdings, limited access to credit, and the prevalence of traditional farming practices have contributed to the slower adoption of agricultural machinery. However, there are ongoing efforts to promote mechanization and improve agricultural productivity in these countries.

4.3 Transformation of Agricultural Mechanization in Southeast Asia

Agricultural mechanization is crucial for the transformation of agriculture in Southeast Asia. With the help of modern machinery and technology, farmers can increase their productivity and efficiency, leading to higher crop yields and better-quality produce. Currently, the level of agricultural mechanization in Southeast Asia varies significantly from country to country. For instance, Thailand and Vietnam have progressed considerably in adopting modern agricultural technologies. At the same time, countries such as Laos and Cambodia still rely heavily on manual labor. Southeast Asia agricultural machinery uses power tillers and simple tractors for farming practices. The prominent examples are power tillers and tractor-drawn rotary tillers (Fig. 4.3).

Fig. 4.3 Farmers operating power tiller in Cassava field

The mechanization-based transformation can be seen in the map of the utilization of farm machinery per unit of agricultural land, which depicts the agricultural mechanization area throughout the region (Fig. 4.4). Based on the map, the Philippines has the highest farm machinery per unit of agricultural area, with 4.39 horsepower per 1000 hectares. Thailand, Vietnam, and Malaysia follow with 1.67, 1.49, and 0.51 hp per 1000 hectares, respectively. Myanmar and Cambodia have farm mechanization values per unit of agricultural land of 0.46 and 0.25 horsepower per 1000 hectares, respectively. Indonesia and Laos have the lowest values, at 0.1 hp/per 1000 hectares (Our World in Data, 2019). All the data from Our World in Data were collected in the year 2019. However, the data from Wijaya and Nurcahyo (2022) on the mechanization levels or farm machinery per unit of agricultural land were collected in the year 2018 for Indonesia, 2015 for Thailand, Vietnam, and Malaysia, 2013 for Cambodia, and 2011 for the Philippines.

Technological advancements in agricultural machinery in this area are still being developed, which was done by research on sensors and actuation technologies, then applying the knowledge of sensors, automation, and GNSS technology to existing agricultural machinery. The following research studies illustrate some of the successful efforts in agricultural automation.

Barawid Jr. et al. (2008) created a system that guides robots in real time in coconut fields using a laser scanner in the Philippines. The goal of this research was to adapt the automated guidance system to enable navigation for coconut fields utilizing a two-dimensional laser scanner as the primary navigational sensor. The focus of this study was on identifying tree rows that could serve as guiding paths for the robot tractor during real-time navigation in coconut fields.

Chunyusen et al. (2021) presented an autonomous agricultural tractor in Thailand. The tractor was outfitted with path planning, local positioning, steering control, and a clutch and gear control system to enable a tractor to be controlled by a computer

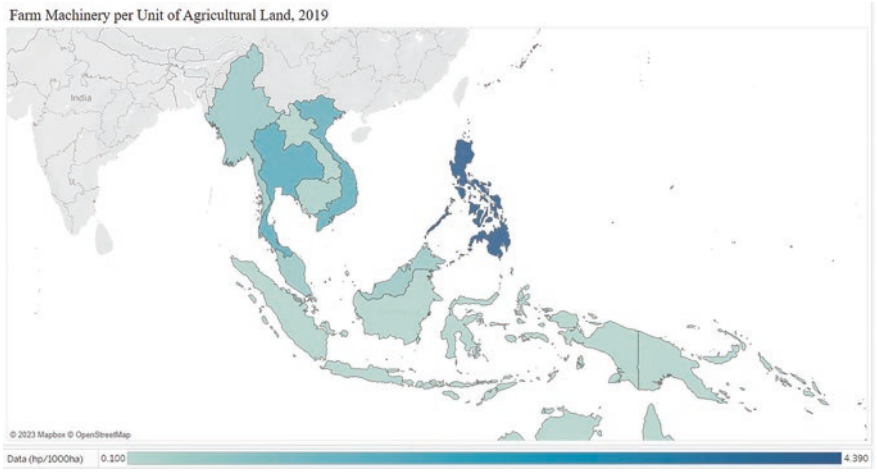

Fig. 4.4 Map of farm machinery per unit of agricultural land in Southeast Asia

for steering and movement. A simulation study was carried out to examine the performance of both open-loop and feedback controllers under disturbed conditions. The steering angle deviation defined the disturbance. The simulation results revealed that the open-loop controller could not correctly direct the tractor along the planned trajectory. However, the feedback controller compensated for positional and heading displacements. The designed steering controller could steer the autonomous tractor on various surfaces. The tractor's position could be accurately determined using the dead reckoning positioning system on concrete and paved surfaces. However, due to the wheel slide, the level of accuracy was reduced while on the soil surface in the field. The experimental results demonstrated that feedback-controller-equipped guidance could successfully steer the autonomous tractor from an initial position to a specific goal position.

Andanaputra et al. (2020) developed a GNSS-based navigation system for an autonomous drone for a pesticide sprayer in agriculture. This research aimed to create drones for implementation in intelligent farming in Indonesia. In the sending process, the drone must be able to detect objects, reach a goal position, and go back safely using the GNSS. The researchers suggested using this ground information for drones to fly by themselves. In their test, the average deviation between the positions they wanted to land at and where they landed was 1.11 m. When using the new course-over-ground algorithm, the average was 2.39 m. The course-over-ground was less reliable than the GNSS and a compass for navigation under 1 m.

Pham et al. (2020) created a computer-vision-based robotic lettuce harvesting system. This study aimed to develop automatic lettuce harvesting methods for hydroponic farms to reduce labor and enable flexible and timely harvesting. A computer-vision-based robotic harvesting system for lettuce in hydroponic farms was described in the paper. Lettuce was cultivated in evenly spaced holes on plastic tubes in these farms. As a result, predicting the location of lettuce stems could be simplified by guessing the location of holes instead. The areas of lettuce-covered spots were approximated using uncovered holes or tube edges identified using Hough transforms. Harvesting was accomplished using a robot manipulator and a servo-controlled gripper. Experimental findings revealed that the system could efficiently conduct harvesting tasks in real-world contexts, with a mean location error of 0.83 mm (typical cases) and a maximum error of 9.62 mm.

4.4 Level of Automation in Agricultural Machinery

In the (Minn & Ahamed, 2023) article, the levels of automation in agricultural machinery were explored with a particular emphasis on creating affordable autonomous equipment for small-scale farms. This falls within the realm of level 0, level 1, and level 2 automation, as illustrated in (Fig. 4.5). Further elaboration on these points is provided in the following sections.

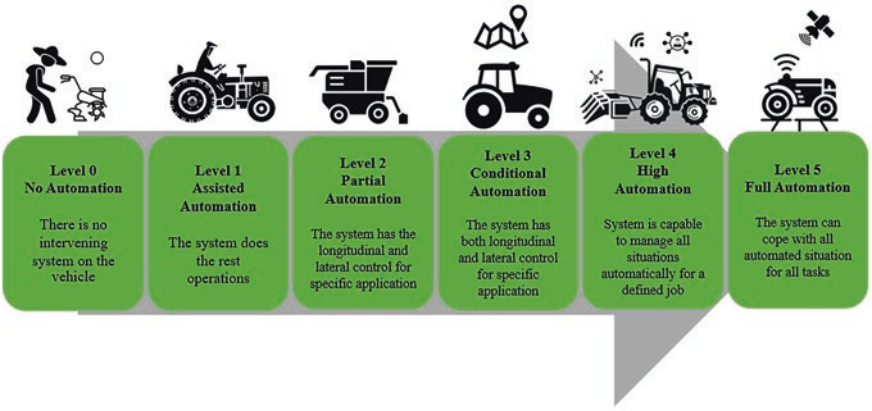

Fig. 4.5 Automation levels refer to machinery control, lateral control, and navigation planning

Level 0 involves human-powered small-scale farm machinery, such as utility tractors, micro tillers, and power tillers.

Level 1 involves assisting automation, including hydraulically controlled utility tractors and seed/fertilizer broadcasting. In level 1, the control system relies on the levering mechanism and linkages. However, these could be substituted with electrical-driven devices, which include a linear actuator, servomotor, stepper motor, and rotary encoder.

Level 2 involves partial automation. Utility tractors equipped with electric control systems are the prime movers. Farmers can operate several implements using a single hydraulic system in agricultural tractors. The proposed hydraulic pump technology will reduce occupational pump fittings but increase implementation control. Hydrostatic Transmission (HST) is a system that uses hydraulic fluid to transfer energy between an engine and a load and then repeats. The system is appropriate only for crawlers, combiners, and multifunctional trailers for farming.

Level 3: Developing the crop production sector and sustainable agriculture depends on conditional automation technology. New sensors are lighter and smaller, offer excellent performance, and have helped in the adoption of digitalization, precise agriculture, and smart farming. Autosteering using sensors and navigation systems has also been created.

Level 4, high automation, involves developing sensing and IoT-based farm machinery, allowing farmers to access their operations through mobile devices. Electric motors have become popular, and farmers are working to address labor shortages and improve their harvesting systems. Electrification is a significant technology in farm machinery, using batteries as a power source. Electric motors are lightweight, robust, reliable, and produce less operating noise. Self-driving primary movers that perform real-time automatic adjustments and reduce soil compaction are being developed. Artificial Intelligence (AI) is used in various farming operations, including soil, crop, plant disease, and weed management.

The topmost level is full automation, in which all farm machinery operations, including remote operations, are automated. This phase concentrates on autonomy in machines and intelligent systems. The development of small-scale autonomous farm implements includes the Fendt Xaver sowing robot and global unmanned spray systems. Japanese farm machinery companies such as Kubota and Yanmar have created autonomous functions for rice transplanters. Yanmar's YR8D model and Kubota's Agri Robo Rice Transplanter still need human supervision. Kubota aims to develop a fully unmanned machine in the future. Yanmar launched the YR8D series rice transplanter in 2019, requiring human guidance. Driverless vehicles equipped with sensory perception technologies lead to greater efficiency by reducing human participation, which are adapted to the Southeast Asian countries.

Moreover, low-cost agricultural equipment automation should be implemented to increase productivity and effectiveness. Level 0 involves no automation, while level 1 involves hydraulic systems, servo motors, and pumps. Level 2 focuses on medium- to large-scale farm machinery automation systems, with recommendations for using low-cost equipment for automation. From level 3 to level 5, technology influences the development of crop production, automation, and sustainable agriculture development. As technology advances, it is essential to coordinate research and development with performance monitoring to ensure the continued success of these technologies in the agricultural sector.

4.5 Level of Machinery for Agricultural Practices

4.5.1 Tillage Practices

In agriculture, tillage refers to soil cultivation after planting and soil preparation for planting, which utilizes tools. The soil is mechanically moved or manipulated into the desired state through tillage (such as pulverization, cutting, or movement). The automation level progresses as technological advancement increases (Fig. 4.6).

The level 0 stage utilizes human resources to perform farm duties. Most poor countries still have this level. Farmers use small utility tractors containing primary hydraulic systems, micro tillers, and power tillers for tilling. The power source consists of farm machinery operating based on small single cylinders.

In the level 1 stage, farmers employ hydraulically controlled utility tractors. Tillers are attached to the differential gear of the tractor and are regulated by the PTO drive shaft. The tiller can be lowered automatically by using a hydraulic mechanism located at the 3-point linkage of the utility tractors. Tractor-powered tillage equipment, namely rotary tillers, disc harrows, and disc plows, is utilized for tillage practices in Southeast Asian countries.

In the level 2 stage, a utility tractor with an electronic control system is the prime mover. Hydraulic systems manipulate the tillage implements equipped in almost all utility tractors. Farmers can operate multiple tools in a single operation with the help of hydraulic systems. Examples include tandem or gang arrangements of

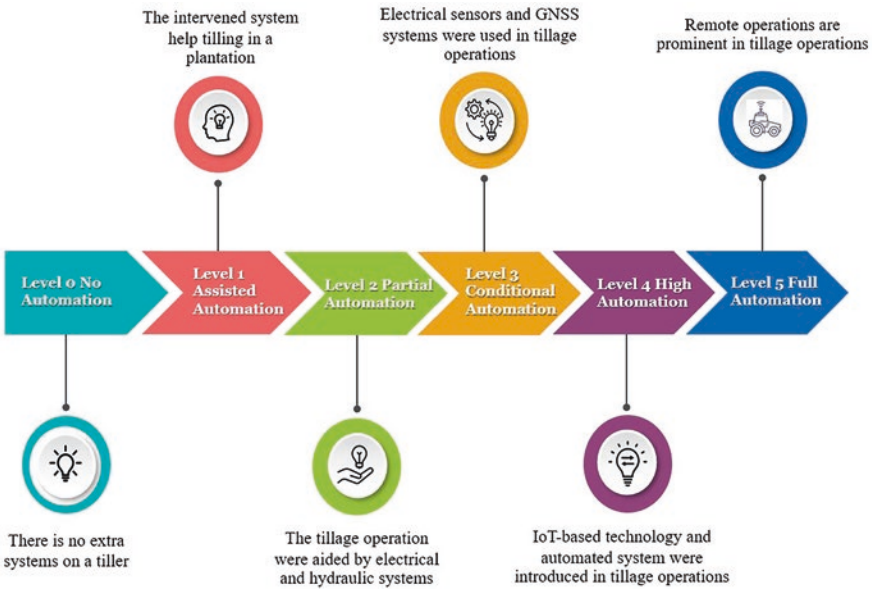

Fig. 4.6 Level of automation in tillage practices

tillage implements. Additionally, farmers can complete a vast extent of tillage. Furthermore, hydraulic pump technology has been created.

4.5.1.1 Transformation of Partial Automation

Agricultural tractors feature modern hydraulic systems. Almost all utility tractors usually have hydraulic lines to control the operated rear appended equipment. Hydraulic systems allow farmers to manage numerous implements simultaneously. Examples include tandem or gang arrangement of tools. Farmers can also acquire diverse types of tillage across this area. Likewise, the advancement in the design of hydraulic pumps reduces the employment level for pump fits and enhances the degree of implementation control.

4.5.1.2 Hydrostatic Transmission (HST)

Hydrostatic transmission allows a vehicle to transform mechanical energy into hydraulic power and repeat (Fig. 4.7). The HST system controls the operations of the engine by turning it, so that it drives the shaft. Charge and axial piston pumps are driven by a drive shaft linked to an input shaft. The charge pump sucks in oil through the oil filter in the transmission case. The oil then fills the case and runs through the closed-circuit oil ducts.

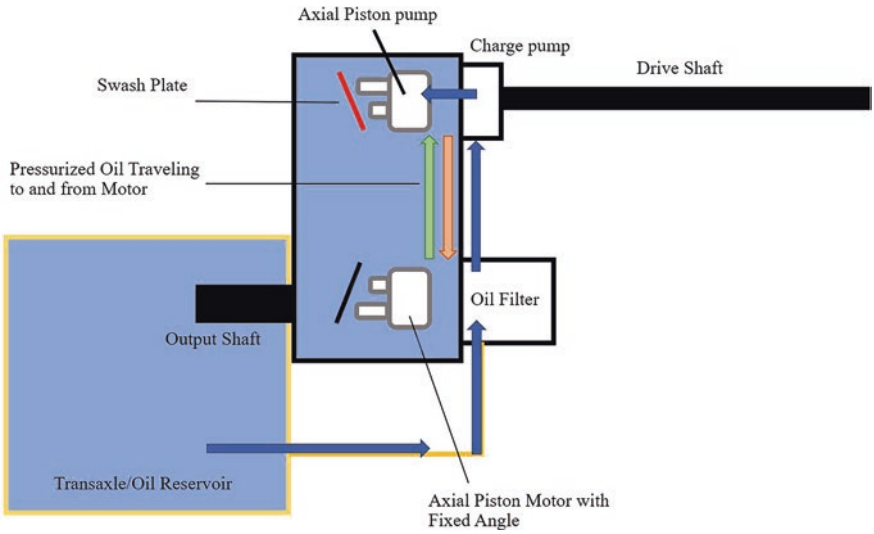

Fig. 4.7 The hydrostatic transmission (HST) diagram

When the user manipulates the transmission control lever, the swash plate causes its angle to change, making the pistons inside the piston cylinder move in and out. The reciprocating pistons allow the oil to pass through the oil passageways and into the axial piston motor. The pushing of oil back to the pump is caused by placing an angle within a fixed engine setting that rotates due to the pistons. The motor is connected to the output shaft that turns a large bull gear in the differential and transfers power to the rear wheels (Tractor Sciences: The Hydrostatic Transmission, n.d.).

HST technology is designed for agricultural machinery where a farmer can work without panic and dig into the soil due to its moving off course. Crawler tractors, as well as combine harvesters, utilize hydrostatic transmission for working at lowlands and multifunction carriers in farmyards.

In the level 3 stage, technology plays a crucial role in the growth of the agricultural production industry, enabling digital transformation, precision agriculture, and smart farming. Sensing technologies and a global positioning system (GPS) have been proposed, enabling the integration of sensors and navigation systems in production systems. Some agricultural machinery firms, such as John Deere, have created the TruSet Active System for tillage operations. This system uses an ultrasonic sensor to measure frame height and tillage depth without affecting crop residue.

4.5.1.3 Transformation of Conditional Automation

A real-time kinematic (RTK) GNSS system has been developed for agricultural machinery navigation, providing precision accuracy of vehicle location, which allows farmers to steer hands-free and perform operations tasks. A low-cost

RTK-GNSS and hybrid navigation systems have also been introduced, enhancing operational performance and precision agriculture.

The development of sensing and IoT-based farm machinery is prevalent in the level 4 stage. Farmers utilize mobile devices for farm operations. Electromechanical drives have gained popularity, but labor shortages and political issues outside the agricultural community control pose challenges. Farmers are working to address these issues by collaborating with technology companies to develop new automated harvesting systems. Future advances in automatic farm machinery include electrification, automation, artificial intelligence, and IoT-based components. BRAIN (Bio-oriented Technology Research Advancement Institute) developed a tillage robot using a 4WD tractor and an AP-L1 station from Topcon. The robot performed well in automatic tracking, position measurement, and data communication at 500 meters, with autonomous operation using XNAV (position detection using an image processor and a laser range sensor) at 0.45 m/s. Tillage work was completed in 2 h and 15 min (Torii, 2000).

In the level 5 stage, which is full automation, all farm machinery operations, including remote operations, are considered at the level 5 stage. The stage's centerpieces are autonomous machines and intelligent systems. The following are some thoughts on small-scale autonomous farming vehicles and equipment. Fendt from the AGCO firm manufactured the Fendt Xaver sowing robot in a small-scale unit. That robot is capable of precision planting and is entirely autonomous. The Xaver firm plans to deploy a sowing robot equipped with sensors for soil moisture, temperature, humidity, and plant waste readings.

4.5.2 Seeding Practices

Sowing practice is the sowing of seeds and planting seedlings to produce agricultural and forestry crops, including placing soil beds for seeds or seedlings on established agricultural land and forestland. The level of automation increases along with the advancement of seeding technology (Fig. 4.8).

Farmers can choose between level 0 (no automation) and level 1 (assisted automation) in seeding. Level 0 involves sowing seeds manually, such as seed broadcasting or manual seeders. Level 1 uses utility tractors with planting systems, while level 2 uses 4-wheel tractors with electronic control systems for seed rate control.

Level 3 involves conditional automation, where technological advancements such as electrical sensors, the GNSS, and a wireless serial port connection are applied to seeding practices. Xie et al. (2021) developed a precision seeding parameter monitoring system using laser sensors and wireless serial port communication. The system had high accuracy, with an average monitoring error of less than 1.2% and a failure rate of 100%. It also had a fast response time and accurate GPS speed measurement. Field tests showed an average monitoring error of less than 1% and a failure rate of less than 1.5%. The system detected missing seeds and achieved online real-time monitoring of precision seeders through test verification.

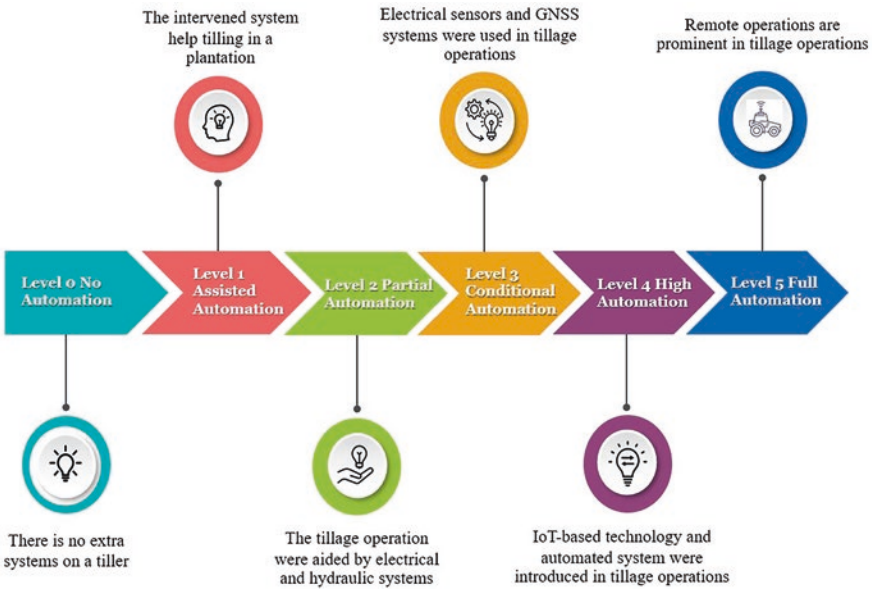

Fig. 4.8 Level of automation in seeding practices

Farmers can access their operations via mobile devices at level 4, sensing, and IoT-based farm machinery development. Electromechanical drives have become widespread, but labor shortages and political considerations beyond the agricultural community's control affect migrant labor availability. Farmers are proactively addressing this issue by cooperating with technology companies to develop new automated harvesting techniques. Four important technologies will drive future breakthroughs in mechanized farm machinery: electrification, automation, artificial intelligence, and IoT-based components. Smart Seeder Max Co. developed an innovative seeder machine that can plant up to five independent crops and six in-ground placement options per row, providing high-resolution prescription input accuracy with the help of finite VR control technologies. Farmers can use a smartphone or tablet to control the VR system, and the intelligent seeder has drill-wide turn compensation.

At level 5, all sorts of farm machinery operations are performed remotely. Asghar Ali et al. (2019) designed an autonomous seeder for maize crops. This robot has a two-dimensional laser and seeding apparatus. A sensor picks up ambient data as a range finding, which manages the operation of the seeder. RANSAC and the line fitting algorithm are used for determining seedbeds with these data. Autonomous navigation utilizes differential drive and PID control. The sowing mechanism ensures the correct and uniform orientation of seeds. The seeder regularly drops seeds at an equal distance while moving. V-Rep generated a simulated field to verify that a seeder functions well in the simulation. The simulation results in (Fig. 4.9) show that the path auto-guided the movements of the seeder and the sowing spot.

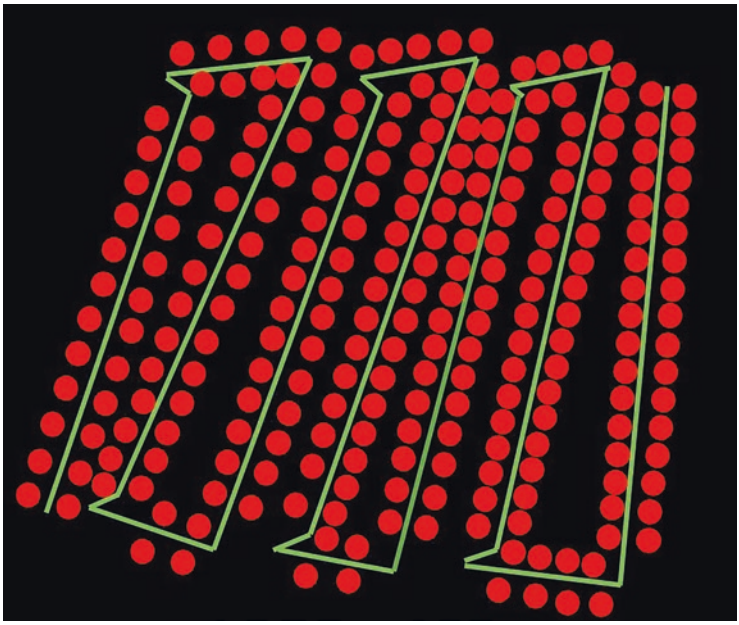

Fig. 4.9 Simulated seed sowing and path planning results, with dropped seed positions in red dots

Currently, this technology is not yet available in Southeast Asia, but it may have the potential to be demonstrated soon.

4.5.3 Transplanting

Transplanting involves moving an actively developing plant from one location to another for continued growth and production. This operation may be undertaken when the seedling height can withstand such shocks and the climatic conditions favor easy establishment in the new area (Agriculturist Musa, 2023). The level of automation increases as transplanting technology develops (Fig. 4.10).

Farmers manually transplant crops at the first automation level using a single-cylinder diesel engine or tractor-mounted transplanter. This method is common among Southeast Asian countries and is suitable for small-scale farmers with surplus labor.

In the second level, partial automation is employed, with a hydraulic pump and fittings for raising and lowering positions and speed control. This level can potentially decrease the burden on farmers, especially small-scale farmers.

Technological improvement occurs in level 3, which is conditional automation. Electrical sensors and a GPS enable precision agriculture, digital

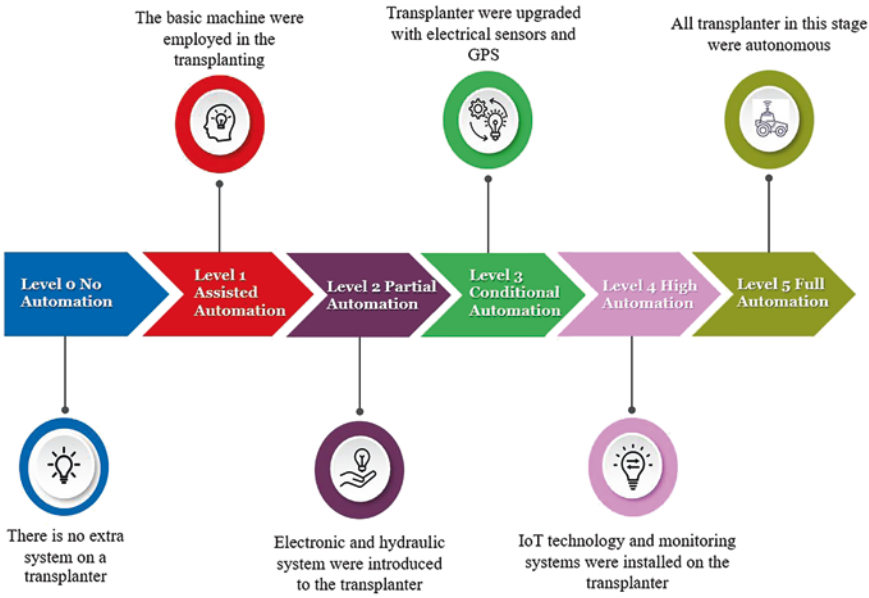

Fig. 4.10 Level of automation in transplanting practices

transformation, smart farming, and sustainable agriculture preservation. Sensors and GPSs have been developed, such as the on-the-go soil sensor for rice transplanters, which uses ultrasonic sensors, electrodes, and platinum resistance thermometers for topsoil depth and apparent electrical conductivity measurements. Smajayu (Shenzhen) Co., Ltd. developed a GPS for rice transplanters that uses satellite signals to manage the depth and spacing of rice plants. GPS technology can boost agricultural production, reduce seed waste, and improve crop management (SMAJAYU, 2023).

In level 4, sensing and IoT-based farm machinery development involves mobile devices for farm operations. Electromechanical drives developed by the Yanmar company utilize an actuator (EPS) to avoid layout changes around the steering mechanism. Additionally, Yanmar Co. developed an automatic rice transplanter that can operate in fully automated mode, including remote operations (Fig. 4.11). Farmers proactively address labor shortages by cooperating with technology companies to develop new automated harvesting techniques. Yanmar demonstrated the operation of this rice transplanter in Thailand (Yanmar, 2022).

In level 5, full automation includes intelligent systems that combine sensors, high-precision navigation, and automation systems. Kubota Co. developed the Robo Rice-Transplanter, a fully autonomous rice transplanter that can work without a driver, including automatic turning operations (Fig. 4.12). This technology enables farmers to plant seedlings more efficiently and effectively. Also, this Robo Rice-Transplanter was demonstrated in Thailand (Kubota, 2023).

Fig. 4.11 (**a**) Automatic rice transplanter developed by Yanmar (**b**) The driver's cabin and GNSS unit of the developed transplanter

Fig. 4.12 GNSS and innovative systems equipped with a robotic rice transplanter from Kubota

4.5.4 *Spraying Practices*

Spraying practices, often known as crop spraying, refer to applying insecticides, pesticides, fungicides, and other prophylactic treatments to crops. Previously called "crop dusting" in agricultural services, the method covers vast regions of crops and protects them from local bugs and pests (AWSM Farming, 2023). (Fig. 4.13) depicts the level of automation in spraying practices ranging from level 0 to level 5. The advancement in technology develops as the level of automation increases.

Farmers have evolved from backpack-type sprayers to 4-wheel-type tractors, utility tractors, and self-propelled types in the automation field. Level 0 involves no automation; farmers use backpack-type sprayers for pesticides or herbicides on the planting field. This method is still prevalent in developing countries, and it is time-consuming and ineffective. Small-scale farmers also use single-cylinder-type dynamic spray tank sprayers for chemical spraying. Level 2 involves partial automation, where farmers use a utility tractor with an electronic control system to manipulate the pump, valve, and spray control unit. Self-propelled sprayers are now widely used and are equipped with electrohydraulic spray pumps and boom controls.

Level 3 involves conditional automation, where electrical sensors and a GPS enable precision agriculture, digital transformation, smart farming, and sustainable agriculture. Sensing technologies and a global positioning system (GPS) have been proposed at level 3, with most tools equipped with sensors to control and monitor activities.

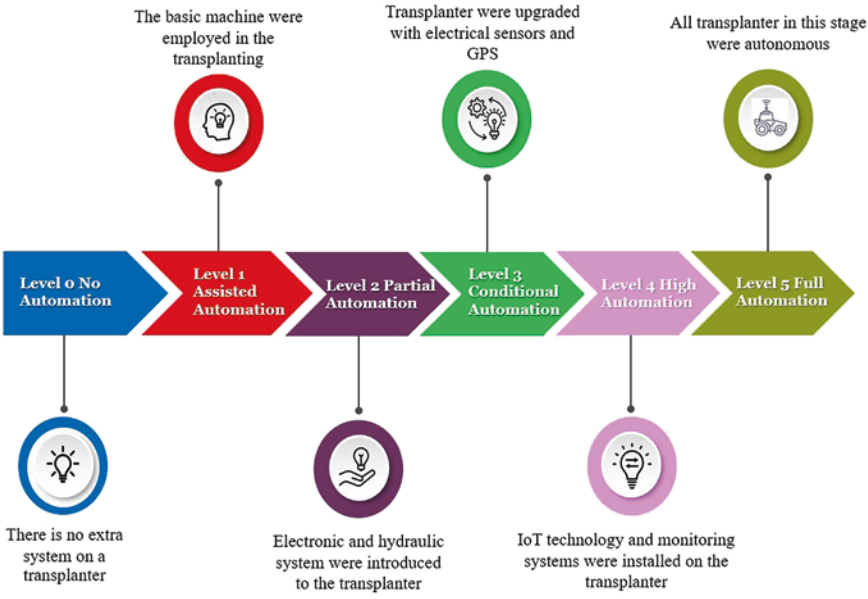

Fig. 4.13 Level of automation in spraying practices

In level 4, farmers may access their operations via mobile devices due to advancements in sensing and IoT-based farm machinery. Electromechanical drives have become popular at this stage. However, labor shortages and political issues outside the agricultural community's control affect farmers' ability to produce and harvest crops. Farmers proactively address these issues by collaborating with technology businesses to develop new automated harvesting systems.

Future advances in automatic farm machinery include electrification, automation, artificial intelligence, and IoT-based components. Chaitanya et al. (2020) developed an intelligent pesticide-spraying robot with machine learning. It can analyze input images and predict remedies. The L293d motor is utilized for movement control of the robot, and Raspberry Pi3 is used to develop the embedded system. Python programming is utilized for machine learning to train the robot with predefined images, allowing it to be controlled remotely without exposure to pesticides. This technology benefits farmers by ensuring that their health remains unaffected by disease.

In level 5, all farm machinery operations are operated autonomously, integrating sensors, high-precision navigation, and automatic systems. The Ecorobotix company developed the Ecorobotix AVO fully autonomous spraying robot. The robot detects a weed and then sprays some herbicide directly on it. Precision spraying requires the robot to carry a significantly smaller volume of liquid than blanket spraying, and the energy needed to generate the smaller spray volume is likewise lower. This technology decreases energy consumption, which is critical when relying on batteries and solar photovoltaics. The AVO reduces herbicide consumption by 90%, carrying only 120 gallons (Nordestgaard, 2020). Currently, this technology is not available in Southeast Asia, but it has a potential to be demonstrated in the future.

4.5.5 Harvesting Practices

Harvesting is the process of obtaining the useful part or sections of a plant when all the nutrients have matured, and the edible parts have reached the right level of maturity. In most cases, the harvest occurs 10–15 days after the grain has reached physiological maturity. Farmers harvested crops by hand with the help of simple tools and engine-powered harvesters. Then, harvesting technology was introduced to farmers, which helped increase harvesting efficiency and reduce labor costs. As harvesting technology developed, the level of automation increased (Fig. 4.14).

Farmers are increasingly adopting automation in their farming practices. Levels 0 and 1 involve manual tools, such as hoes, spades, and shovels, which are still common in developing countries. Small-scale farmers also use single-cylinder diesel-powered hand-push-type harvesters. Level 2 involves assisted automation, where farmers use 4-wheel tractor-mounted or self-propelled harvesters.

Level 3 is conditional automation, where electrical sensors and a GPS are utilized in combined harvesters for precision agriculture, digital transformation, smart

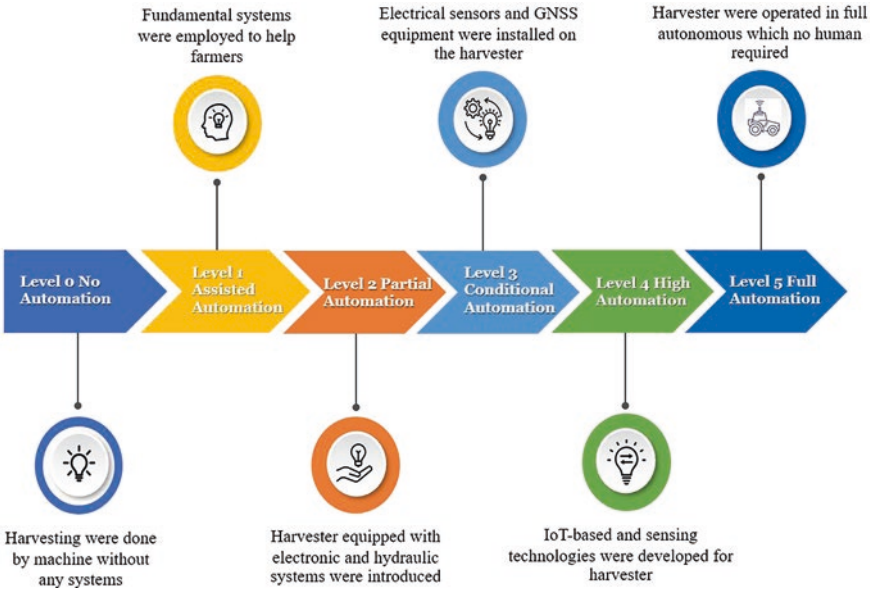

Fig. 4.14 The level of automation for harvesting practices

farming, and sustainable agriculture. Level 3 involves partial automation, where farmers use advanced self-propelled harvesters with electronically controlled systems. Hydraulic systems are widely used in this stage, making machines more productive while operating on the plantation. Sensing technologies and a global positioning system (GPS) have also been developed. Most devices are outfitted with sensors to control and monitor activities (Fig. 4.15), which are adapted to John Deere Sugarcane harvester CH 570 models. Moreover, the John Deere CH570 sugarcane harvester is equipped with high-resolution, stereoscopic optical sensors, and pattern recognition technology to scan the flow of cane as it passes through the elevator, identifying cane volume and differentiating it from trash (John Deere CH570, 2018). This John Deere CH570 sugarcane harvester is demonstrated in Thailand (John Deere Thailand, n.d.)

The new generation-precision farming system for combines and forage harvesters, which includes the CLAAS CEMIS 1200 smart display, GPS pilot steering system, and SAT 900 GNSS receiver, has been developed by CLAAS (Fig. 4.16). Farmers can also opt for a subscription-based correction service called SATCOR from Trimble, which can be precise up to 2.5 cm without having any base station (McNabb, 2022).

Level 4 involves developing sensing and IoT-based farm machinery, allowing farmers to access their operations through mobile devices. Electromechanical drives have gained popularity in this stage, but labor shortages and political issues outside the agricultural community's control affect farmers' capacity to produce and harvest crops.

Fig. 4.15 John Deere's harvester driver's cab shows the monitor and controllers

Fig. 4.16 CLAAS harvester equipped with precision farming system

Yanmar developed an intelligent combine harvester to improve profitability by focusing on harvest volumes and providing real-time information on harvest flow rates and losses during harvesting. The system presents a color-coded display of production per ton, the cumulative harvest quantity, the harvest flow rate, losses

from the threshing cylinder, and losses due to shaking on the monitor. The operator can ascertain the cause of yield loss without reducing yield and efficiency by monitoring the grain flow rate (Kanatani, 2015). This developed intelligent system was applied in the YH1180 combined harvester and demonstrated in Thailand (Yanmar, 2022).

In level 5, harvesters are operated autonomously, integrating sensors, high-precision navigation, and automatic systems. Wang et al. (2017) developed a tomato harvesting robot using a four-wheel independent steering system, 5-DOF harvesting system, navigation system, and binocular stereo vision system for utilization in a greenhouse. The robot's low-speed steering control was based on Ackerman steering geometry, and the laser navigation system used the proportional-integral-derivative (PID) algorithm. The Otsu algorithm and elliptic template method were used for automatic ripe tomato recognition and obstacle avoidance strategies were proposed. The robot's laser navigation system tracked the path with minimal deviation, and the binocular vision system achieved a 99.3% success rate in recognizing ripe tomatoes. The robot's success rate was 86% when identifying and pitching tomatoes.

4.6 Appropriate Scale of Mechanization in Southeast Asia

Southeast Asia has a diverse agricultural landscape, ranging from smallholder farms to more extensive commercial operations. The scale of mechanization and automation should be suitable for the average farm size and structure of the agricultural sector in each country. Crop types and cultivation practices are crucial for determining the scale of mechanization. Southeast Asia is recognized for its diversity of crops, including rice, palm oil, rubber, fruits, and vegetables. Each crop needs specific cultivation practices, and the appropriate scale of mechanization and automation should consider the suitability of technologies for each crop. Labor availability and costs are necessary to determine the appropriate scale of mechanization. Currently, Southeast Asia depends on manual labor in agriculture due to cheap labor costs. However, changing demographics and migration patterns are leading to labor shortages in some parts of Southeast Asia.

Small-scale agricultural mechanization is widely recognized around Southeast Asia due to its potential to address labor shortages, increase productivity, reduce costs, improve quality, and facilitate the adoption of modern farming practices. According to B. DUFF (1986), mechanization increases productivity by increasing crop yields and reducing losses. A mechanized rice field generates more yield than a nonmechanized rice field. Additionally, a mechanized farm requires less labor per hectare than a farm characterized by traditional techniques, saving on labor costs. Small-scale agricultural mechanization can improve crop production quality by performing the functions of leveling, land preparation, deep turning, and deep scarification (Fig. 4.17) (Aslan et al., 2007), which can improve land quality better than traditional manual and livestock operations. Small-scale mechanization can be

Fig. 4.17 Farmers use a tractor-operated cassava rigging machine for cassava planting preparations

adopted quickly. It encourages the use of advanced farming equipment, precision agriculture techniques, and digital tools to enhance productivity, sustainability, and profitability.

4.7 Discussion

Southeast Asia's current agricultural mechanization trends range from traditional farming with manual labor to 4-wheel tractor mechanization. In level 0, farmers utilize micro and power tillers at the no-automation level, meaning that they themselves must control everything. In level 1, farmers use 4-wheel tractors with simple hydraulic systems to carry out farm practices. In level 2, farmers use electronic control systems or combined machines for farm operation. In level 3, farmers utilize electronic sensors and monitors to control the operation of the tractor. Most of the tractor's equipment is manipulated by a joystick in the driver's cab, and farmers can see the process via a monitor. Additionally, RTK GNSS technology is initially implemented in this stage. In level 4, sensing and IoT-based farm machinery development occurs. Farmers must enter their operations through mobile devices. Electromechanical drives are popularized in this stage. In level 5, farmers can remotely control all machines using smartphones.

The level of farm machinery in farm practices, such as tillage, spraying, and harvesting practices, is explained in this chapter. The advancement of practices is increased from level 0 to level 5, ranging from simple tools and machinery to IoT- or innovative technology-based operation—the more advanced the technology is, the lower the labor dependence for agricultural practices. Southeast Asian countries have widely adopted small-scale agricultural mechanization due to its potential to

address labor shortages, increase productivity, reduce costs, improve quality, and facilitate the adoption of modern farming practices. Additionally, mechanization increases productivity by increasing crop yields and reducing losses. This book chapter also introduces agricultural machinery development based on electrical sensors. The development of machinery in Southeast Asia has gradually developed from person-based operation to autonomous operation, for example, autonomous tractors, unmanned aerial vehicle (UAV) sprayers, and robot harvesters. Researchers in Southeast Asian countries have conducted more research to create intelligent agricultural systems for farmers.

4.8 Conclusion

The agricultural sector plays a vital role in Southeast Asian countries. Southeast Asian farmers utilized agricultural machinery for a substantial of time, depending on farm size and industry. Various mechanization scales exist in Southeast Asian countries, from large to small scale, depending on farming operations. The small scale has gained popularity in Southeast Asia due to productivity increases. As time passed by, Southeast Asian farmers gradually adopted the machinery in farm operations, which was explained by using the mechanization level. Also, Southeast Asian researchers progressively developed new agricultural machinery technology. The level of automation in machinery ranges from level 0 to level 5, as discussed in this book chapter. As the level progressed in all practices, it became easier for farmers to carry out farming operations and less dependent on manual labor. Most of the Southeast Asian countries were in the level 3 and 4 stages with the potential to develop into further stages in the future.

References

Agriculturist Musa (2023). *Basic agricultural study a resource hub for young agriculturists: Transplanting method in Agriculture*. Retrieved July 18, 2023, from https://agriculturistmusa.com/transplanting-method-in-agriculture/.

Ali, A., Zohaib, M., & Mehdi, S. A. (2019). An autonomous seeder for maize crop. *ICRAI '19: 2019 5th International Conference on Robotics and Artificial Intelligence*. Retrieved August 24, 2023, from https://doi.org/10.1145/3373724.3373737.

Andanaputra, A. B. T., Ganadhi, E. M., Fakhrezi, M. F., Gunawan, A. A. S., Chowanda, A., Suroso, J. S., et al. (2020). GNSS-based navigation systems of autonomous drone for pesticide sprayer in agriculture. *ICIC Express Letters, Part B: Applications, 11*(12), 1125–1132.

Aslan, S. T. A., Gundogdu, K. S., Yaslioglu, E., Kirmikil, M., & Arici, I. (2007). Personal, physical and socioeconomic factors affecting farmers' adoption of land consolidation. *Spanish Journal of Agricultural Research, 5*, 204–213. https://doi.org/10.5424/sjar/2007052-240

AWSM Farming. (2023). *Crop spraying*. Retrieved July 5, 2023, from https://awsmfarming.co.uk/services/farming/spraying-spreading-injecting/crop-spraying/#:~:text=Crop%20spraying%20is%20the%20process,from%20local%20bugs%20and%20pests.

Barawid, O. C., Jr., Farrokhi Teimourlou, R., Noguchi, N., & Ishii, K. (2008). Automatic guidance system in real-time orchard application (part 1). *Journal of JSAM, 70*(6), 76–84. Retrieved July 18, 2023, from. https://doi.org/10.11357/jsam1937.70.6_76

Chaitanya, P., Kotte, D., Srinath, A., & Kalyan, K. B. (2020). Development of smart pesticide spraying robot. *International Journal of Recent Technology and Engineering (IJRTE), 8*(5), 2193–2202. Retrieved August 24, 2023, from. https://doi.org/10.35940/ijrte.E6343.018520

Chao, Sinh & Chan, Saruth & Lytour, Lor. (2014). Status and prospect of agricultural mechanization in Cambodia. Retrieved April 5, 2024, from https://www.researchgate.net/profile/Sinh-Chao/publication/320305266_Status_and_Prospect_of_Agricultural_Mechanization_in_Cambodia/links/59dcc4fdaca2728e2020ae33/Statusand-Prospect-of-Agricultural-Mechanization-in-Cambodia.pdf

Chunyusen, P., Wathakit, K., Sompong, J., & Kongman, K. (2021). *Development of an autonomous agricultural tractor*. Suranaree University of Technology Intellectual Repository. Retrieved May 24, 2023, from http://sutir.sut.ac.th:8080/jspui/bitstream/123456789/9093/2/Fulltext.pdf

Cramb, R., & Thepent, V. (2020). *Evolution of agricultural mechanization in Thailand*. Retrieved July 18, 2023, from doi:https://doi.org/10.2499/9780896293809_05.

Duff, B. (1986). Some consequences of Agricultural Mechanization in The Philippines, Thailand, and Indonesia. In Small Farm Equipment for Developing Countries: Proceedings of the International Conference on Small Farm Equipment for Developing Countries: Past Experiences and Future Priorities, *Education for inclusion and diversity* (pp. 59–84). Int. Rice Res. Inst. Retrieved July 18, 2023, from http://books.irri.org/971104157X_content.pdf.

John Deere CH570. (2018). John Deere. Retrieved January 7, 2024, from https://www.deere.com/en/harvesting/ch570-sugar-cane-harvester/

John Deere Thailand (n.d.) *John Deere's new sugarcane Harvester Demonstration*. John Deere Thailand. Retrieved January 7, 2024, from https://www.deere.co.th/assets/pdfs/region-1/homepage/thailand/AD-Sugarcane-Demonstration.pdf

Kanatani, K. (2015). *Yanmar technical review: Development of the intelligent combine harvester which contributes to increase in productivity of agriculture*. YANMAR. Retrieved July 19, 2023, from https://www.yanmar.com/global/about/technology/technical_review/2015/1027_3.html.

Kubota (2023) *From Thailand to ASEAN and the World The Demonstration Farm KUBOTA FARM proposes a new future for agriculture*. KUBOTA. Retrieved January 7, 2024, from https://www.kubota.com/kubotastories/kubota-farm/index.html.

McNabb, L. N. (2022). *Trimble and Claas strategic alliance develops next-generation precision farming system for claas agriculture equipment*. Trimble. Retrieved July 19, 2023, from https://investor.trimble.com/news-releases/news-release-details/trimble-and-claas-strategic-alliance-develops-next-generation

Minn, A., & Ahamed, T. (2023). Low-cost automatic machinery development to increase timeliness and efficiency of operation for small-scale farmers to achieve SDGs. In *IoT and AI in Agriculture* (1st ed., Vols. 289–309, pp. 289–309). Retrieved December 27, 2023 https://doi.org/10.1007/978-981-19-8113-5_15.

Nordestgaard, S. (2020). Automation: Autonomous vineyard robots and tractors. *Australian and New Zealand Grapegrower and Winemaker, 680*, 50–67. Retrieved August 24, 2023, from https://www.awri.com.au/wp-content/uploads/2020/09/Nordestgaard2020-AutonomousTractors-GW-September.pdf

Our World in Data. (2019). *Farm machinery per unit of agricultural land, 2019*. Retrieved July 19, 2023, from https://ourworldindata.org/grapher/machinery-per-agricultural-land.

Pham, V. H., Nguyen, H., Doan, T., & Huynh, G. B. (2020). A computer vision based robotic harvesting system for lettuce. *International Journal of Mechanical Engineering and Robotics Research*, 1526–1531. Retrieved July 19, 2023, from. https://doi.org/10.18178/ijmerr.9.11.1526-1531

SMAJAYU. (2023). *How rice transplanter GPS system can improve agricultural efficiency?*. Retrieved July 19, 2023, from https://www.smajayu.com/rice-transplanter-gps-system/.

Torii, T. (2000). Research in autonomous agriculture vehicles in Japan. *Computers and Electronics in Agriculture, 25*(1–2), 133–153. Retrieved August 24, 2023, from. https://doi.org/10.1016/s0168-1699(99)00060-5

Tractor Science: The Hydrostatic transmission. (n.d.). iSaveTractors. https://isavetractors.com/articles-1/tractor-science-the-hydrostatic-transmission/

Wang, L., Zhao, B., Fan, J., Hu, X., Shu, W., Li, Y., Zhou, Q., & Chongfeng, W. (2017). Development of a tomato harvesting robot used in greenhouse. *International Journal of Agricultural and Biological Engineering, 10*(4), 140–149. Retrieved August 24, 2023, from. https://doi.org/10.25165/j.ijabe.20171004.3204

Wijaya, A., & Nurcahyo, R. (2022). *Agricultural mechanization in Indonesia and comparison to Southeast Asia countries*. IEOM Society. Retrieved May 24, 2023, from http://ieomsociety.org/proceedings/2022istanbul/67.pdf

Xie, C., Zhang, D., Li, Y., Cui, T., He, X., & Du, Z. (2021). Precision seeding parameter monitoring system based on laser sensor and wireless serial port communication. *Computers and Electronics in Agriculture, 190*, 106429. Retrieved August 24, 2023, from. https://doi.org/10.1016/j.compag.2021.106429

Yanmar (2022) *Yanmar demonstrates autonomous agricultural machinery at joint Thailand-Japan Project*. YANMAR. Retrieved January 7, 2024, from https://www.yanmar.com/us/news/2022/11/14/116356.html.

Chapter 5
Design of Navigation System for Transportation Mobile Robot for Agricultural Farms

Abstract With the development of precision agriculture, agricultural production now demands higher requirement of automation and automatic navigation systems. In agricultural automatic navigation system, positioning and tracking are the key technologies. Its stability directly affects the reliability and security of agricultural automation equipment. Therefore, this study focused on the research of localization of vehicles and tracking in agricultural automatic navigation systems using an autonomous golf cart. Globally, agricultural farms have been suffering massive labor shortages. Especially, the transportation of agricultural products from the orchard to the packaging facilities, vegetables from farm to packaging center, is always time-consuming and labor-intensive work. Thus, this study aimed to design a navigation system for transportation mobile robot to carry agricultural products in the farms. This research used the golf cart as the research target vehicle to develop the navigation system and designed control system based on robot operating system (ROS), controller area network (CAN) bus was used to operate the communication for the whole vehicle. Kalman filter was used to fuse global navigation satellite (GNSS) and inertial measurement unit (IMU) to acquire the accurate position and navigation of the golf cart. Therefore, the positional error was less than 2 cm. Fuzzy control was employed to realize the tracking for the golf cart. Moreover, light detection and ranging (LiDAR) was utilized to avoid obstacles and finally gained self-automation as the golf cart moved to designated route to carry agricultural products and avoid obstacles. This study also made experiments for automatic driving and obstacles avoidance. The results showed that the navigation system and obstacles avoidance strategies were effective. This research can be used as the working platform of agricultural automation development to provide autonomous mobile function for carrying agricultural products.

Keywords RTK-GNSS · IMU · Kalman filter · Tracking · Agricultural navigation

© The Author(s), under exclusive license to Springer Nature Singapore Pte Ltd. 2024

T. Ahamed, *IoT and AI in Agriculture*,
https://doi.org/10.1007/978-981-97-1263-2_5

5.1 Introduction

With the development of urbanization, more and more labor has flowed into cities; therefore, farmland is facing the problem of labor shortage. During this period, agricultural automation technology has been greatly developed. However, due to the lack of accuracy of manually driven agricultural automation equipment, the following problems have arisen:Excessive use of pesticides and fertilizers leads to environmental degradation and damage to the agricultural ecological environment. Also, the repeated work area and missed work area are large, the production efficiency is low, and the driver's labor intensiveness is also high.

In advancements of agricultural machinery automation, autonomous navigation system is an important technology to improve the accuracy of agricultural machinery performances. Positioning, tracking, and obstacle avoidance are the main research problems of agricultural machinery automatic navigation system. At present, global navigation satellite system (GNSS) positioning technology is mainly used for positioning; however, the GNSS technology is very vulnerable to weather and external environment, resulting in low positioning accuracy. The integrated navigation technology of GNSS and inertial navigation system (INS) can effectively solve this problem and increase the accuracy and stability of positioning.

Therefore, the agricultural navigation system integrated with GNSS, INS, and LiDAR can effectively improve the accuracy of agricultural robots, thus reducing the excessive use of pesticides and fertilizers and improving the agricultural ecological environment. At the same time, it can also reduce repetitive work areas and missed work areas, improve production efficiency, and reduce the labor shortage in farm work.

GPS system is a satellite positioning system with three-dimensional navigation and positioning capabilities, which was developed in the United States in the 1970s and completed in 1994 (Wang, 2010). The system is composed of 24 satellites, and six orbital planes are set to ensure that more than five satellites can be captured at any position on the earth for 3D positioning. GPS navigation has the advantages of all-weather operation, high positioning accuracy, fast speed and has been widely used in various fields (Li, 2015).

Nørremark et al. (2008) of Tokyo University studied and developed the automatic navigation system of combine harvester based on RTK-GPS navigation. The system navigated by tracking the pre-planned path. In the experiment, the navigation errors of the combine at 0.31 m/s and 0.52 m/s were 16 mm and 22 mm, respectively. Noureldin et al. (2009) analyzed the defects of the current agricultural vehicle navigation control system based on artificial intelligence, studied, and developed an automatic navigation system based on the combination of GPS and INS, and proposed an IDNN model for the navigation control method of agricultural vehicles. The comparison test with the traditional Kalman filtering method and the applied artificial intelligence method showed that this method can achieve higher

positioning accuracy, especially in the case of GPS long running interruption, it can show the superiority of its performance. The vehicle robot laboratory of Hokkaido University in Japan has developed a tractor navigation system (Choi et al., 2014) that combined RTK-GPS with inertial measurement unit (IMU). During field tests in the farmland, when the tractor's driving speed was 3 m/s, the tracking error of straight and curved paths was less than 5 cm.

In recent years, laser sensors have been increasingly used in mobile robot navigation control systems (Li & He, 2006) because of their high measurement accuracy, ability to completely liberate labor force, and ability to provide a large amount of distance information at a higher frequency. Chi et al. (2012) used laser sensors as navigation equipment, adapted the advantages of barcode theory and proposed a real-time control algorithm for underground shovel, and obtained the test results with an average error of 15 cm. Lee et al. (2007) of the University of Florida studied and developed an automatic tracking system for citrus harvesting robot based on the status quo of citrus harvesting in the United States. The system navigated based on Lidar and a PID controller and designed to guide the following robot forward. The above studies only focused on the straight path and did not discuss the curved path and headland turning, so the scope of application was limited.

In recent years, research on the navigation system of combine harvester based on laser has been conducted. Teng et al. (2016) took Yanmar AG1100 combine harvester as the research platform. He used laser sensors to obtain wheat field information, used the method of maximum inter class variance to find harvest boundary points, and used the least square method to fit the boundary lines. The test results showed that the average deviation of the detection results of wheat harvesting operation line was 0.12 m under static conditions and 0.24 m under dynamic conditions, which can meet the requirements of wheat harvesting navigation line recognition and was an effective detection algorithm. Xia et al. (2009) proposed a laser-based road surface extraction algorithm for structured and semistructured situations. The experimental results showed that the algorithm had good performance, and road surface information can be extracted from both structured and unstructured roads. Since the agricultural environment was a complex unstructured environment, the algorithm had some reference significance for the extraction of agricultural mobile robot navigation path.

The GPS and laser navigation methods can realize the self-driving of agricultural vehicles, but there are certain limitations. The navigation system of agricultural machinery based on laser can realize real-time detection of obstacles, but it cannot determine the specific position of agricultural machinery in the working environment and cannot detect and ensure the accuracy of the system. On the other hand, GPS navigation can obtain the accurate position of agricultural machinery during operation, but because this navigation method cannot update the surrounding environment information in real time, it is necessary to collect field information and plan the path in advance, and it is impossible to take avoidance measures when encountering obstacles.

5.2 Materials and Methods

5.2.1 Hardware System

This research adopted YAMAHA G30Es golf cart as the research platform; the CAN bus system was used, and sensors were installed on the golf cart to make it automatically carry agricultural products in farms as designated route. The hardware system of this research mainly included GNSS, IMU, LiDAR, CAN USB, PC, and golf cart. GNSS and IMU were connected to PC by USB, LiDAR was connected to PC by ethernet port and powered by battery. CAN USB was a CAN to USB gateway that connected PC's USB port and CAN port, it was used to realize communication between PC and CAN bus system in golf cart. The hardware system is shown in Fig. 5.1.

To make the positioning more accurate and subsequent coordinate transform more convenient, the coordinates of the golf cart, GNSS, and IMU were overlapped, the GNSS antenna and IMU were both installed at the midpoint of the golf cart's front axle, the GNSS antenna was installed at the roof, and the IMU was installed on the platform in front of the steering wheel. Because the golf cart mainly moved forward, it was required to avoid obstacles in front. To sense the environment in front of the golf cart, the LiDAR was installed at front of the golf cart. Sensor's installation is shown in Fig. 5.2.

5.2.2 Software System

This research used C/C++ and Python as the development language, mainly to develop software for positioning and navigation for golf carts. The modules included GNSS, IMU, LiDAR, and CAN USB. All modules were directly connected to ROS,

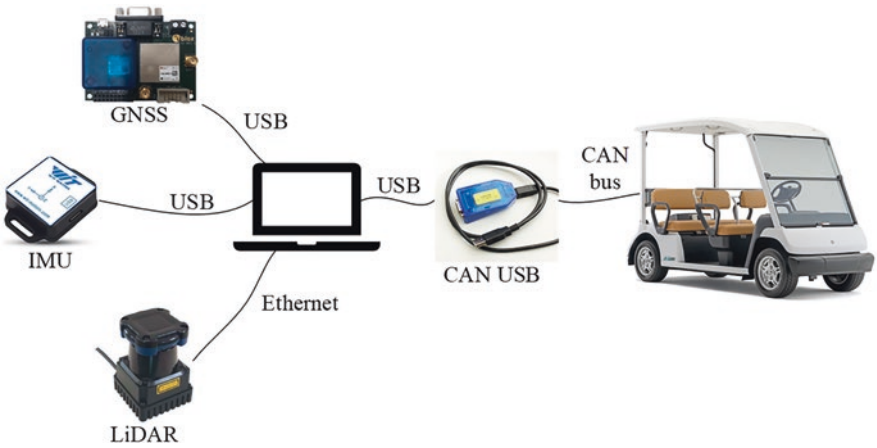

Fig. 5.1 Hardware system for developing navigation system using a golf cart

Fig. 5.2 Sensors installation in the golf cart. (**a**) CAN USB. (**b**) IMU. (**c**) Antenna of RTK-GNSS. (**d**) LiDAR

where GNSS input positioning information, IMU input 9-axis data, and LiDAR input point cloud data. After ROS processed all the information, the programing platform sent the CAN signal to the CAN bus system of the golf cart through CAN USB to control the golf cart.

Therefore, the software system of this research mainly included four parts: data acquisition module, localization module, navigation module, and control module. The data acquisition module mainly included GNSS communication node (urg_node), IMU communication node (wit_node), and LiDAR communication node (urg_node), which were used to obtain sensor information. The localization module mainly included GNSS data transform node (navsat_transform) and Kalman filter fusion node (ekf_localization), which were used to transform and fuse the data of GNSS and IMU to obtain more accurate pose information. The navigation module mainly included map node (map_server), path planning node (move_base), and tracking node (waypoint), which were used to plan the path and use fuzzy control algorithm to obtain the steering angle and speed for golf cart tracking according to target position and current position. When LiDAR sensed there were obstacles in front of golf cart, the navigation module also took actions to avoid it. The control module mainly included golf cart control node (golf_cart), which was mainly used to convert the speed and steering angle into CAN signals and input them to CAN USB to control the golf cart. The overall structure of the software system is shown in Fig. 5.3.

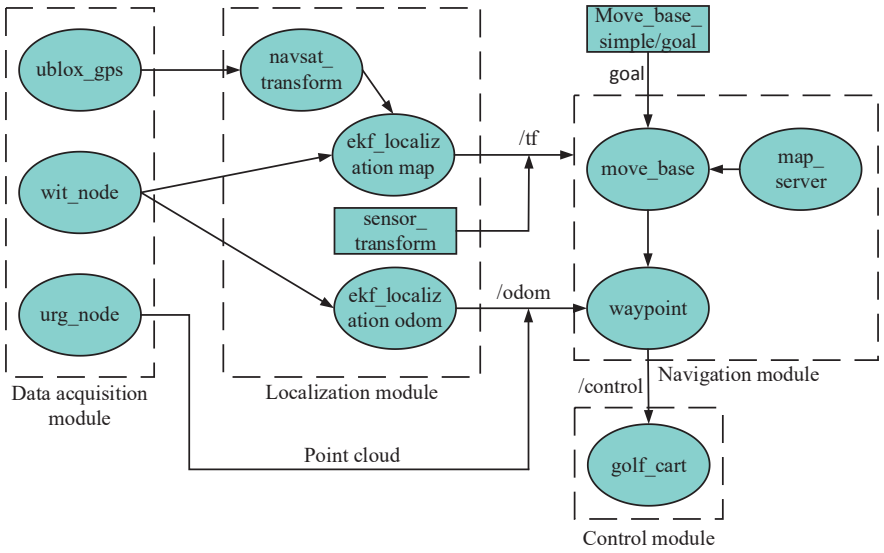

Fig. 5.3 Overall structure for software system

The software process for golf cart navigation system was as follows: First, received the data of GNSS, IMU, and LiDAR, then transformed the GNSS coordinates to obtain the robot coordinate system coordinates. Second, used Kalman filtering algorithm to fuse IMU data and robot coordinate system coordinates to obtain more accurate robot pose information. Third, conducted path planning and set robot path points. Fourth, according to the current position and target position of the golf cart, used the fuzzy control algorithm to get the speed and steering angle information of the golf cart to control the tracking. Avoided obstacles according to the point cloud data of LiDAR. Finally, converted the speed and steering angle of the golf cart into CAN signals and input them into CAN USB to control the golf cart. Software flowchart for golf cart navigation system is shown in Fig. 5.4.

5.2.3 Design for Localization System

5.2.3.1 Setting for Base Station and Rover

u-blox C94-M8P RTK-GNSS introduces the concept of a "Rover" and a "Base Station," base station was used to send correction data stream to rover, rover was installed on the robot to get position with cm-level accuracy. The C94-M8P application board integrates NEO-M8P-2 module with both base station and rover functionality, so each of the boards could be used as base station or rover. The boards can also be configured for either static or moving baseline RTK functionality.

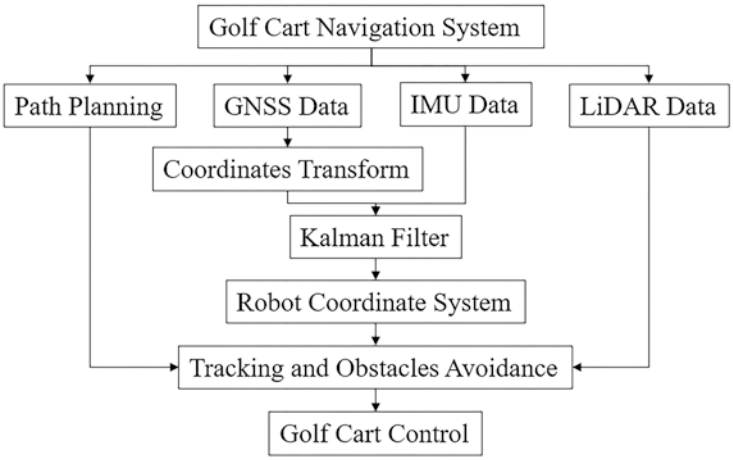

Fig. 5.4 Software flowchart for golf cart navigation system

When the NEO-M8P functioned as a Base Station, the receiver used its measurements from the available satellites to broadcast its position and satellite observation data to the rover. The Base Station must be configured in a fixed position or have completed a survey-in operation before it can output the RTCM reference station position message. In this research, the boards were configured for static baseline RTK functionality, base station was set to self-survey-in its position. Process for configuration for base station was as follows: Step 1 Survey-in configuration, selected TMODE3 (Time Mode 3), set up survey-in mode, select minimum observation time to 300 s and required position accuracy to 3 m. Step 2 Configured base radio link, select PRT (ports), set target to UART1, set "Protocol in" to none to block all the signal from outside at the base station. Then set "Protocol out" to RTCM3 to set the output information to be transmitted to the rover by local communication via UART1, set baud rate to 19,200 bps. Step 3 Set dynamic mode to be stationary. Then, set the minimum elevation angle of acquired satellite to 20°, set minimum threshold of acquired satellite signal to 35 Hz. The base station was installed on the roof of the main building of T-PIRC center as shown in Fig. 5.5.

5.2.3.2 GNSS Data Acquisition

After configuration for the base station and the rover, the position coordinates had output from rover to PC. The data protocol of C94-M8P is NMEA protocol. In this research, $ GNGGA format was used to transmit position coordinates.

Set "Protocol out" of rover to NMEA to output satellite positioning information. After decoding satellite positioning information, the coordinates were obtained. Figure 5.6 is the precision comparison of coordinates before and after RTK.

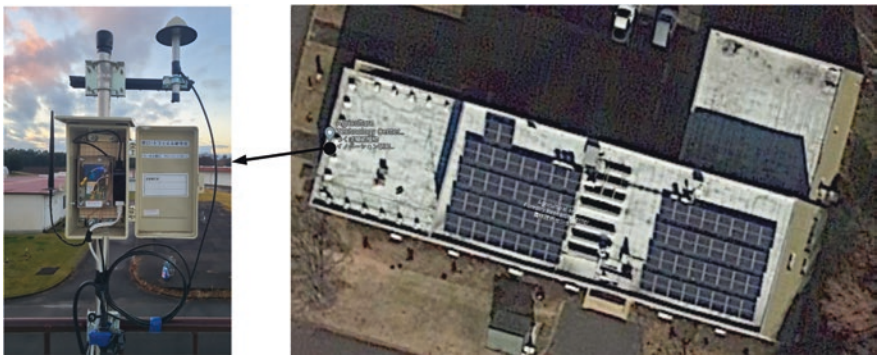

Fig. 5.5 Installation for base station

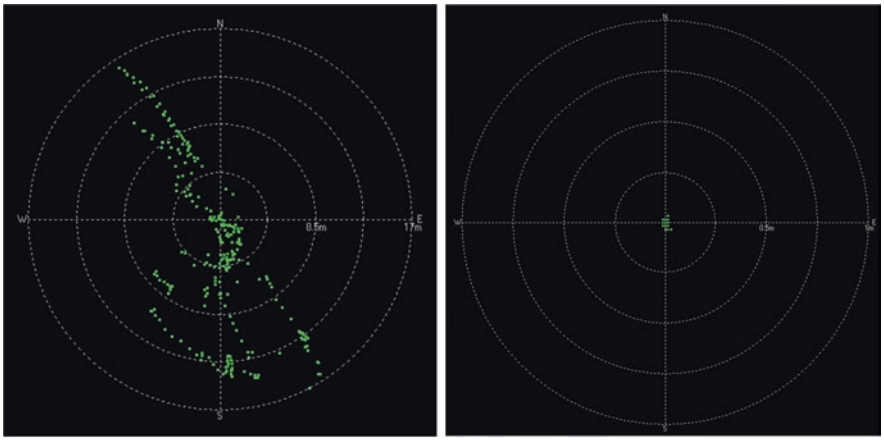

Fig. 5.6 Precision comparison of coordinates before and after RTK

Figure 5.6 shows that the accuracy of GNSS without RTK was very low, the error could reach 17 m. After RTK, the accuracy was much higher, the error was within 2 cm. To further test the positioning accuracy before and after RTK, a positioning accuracy experiment was designed. The experiment was carried out on the road of T-PIRC. The experiment process was to walk along the road, recorded the coordinates with mobile phones and the rover after RTK respectively, then input the coordinates into QGIS, and input Google satellite map into QGIS, so that the recorded coordinates were obtained, as shown in the Fig. 5.7.

The red points were coordinates from RTK-GNSS; the green points were coordinates from mobile phone. In figure, the positioning data of the mobile phone were relatively divergent, and the position accuracy was not high. The positioning data of RTK-GNSS were relatively centralized, and the position accuracy was very high.

Fig. 5.7 Recorded coordinates on the map

5.2.3.3 Coordinates Transform for GNSS

The coordinates from GNSS were in the WGS 84 spatial reference system, which was geographic coordinates, so it can't be used to research directly. Consequently, it's essential to transform geographic coordinates to plane rectangular coordinates. This research used Universal Transverse Mercator (UTM) coordinates system, which is a map projection system for assigning coordinates to locations on the surface of the Earth. It divides earth into 60 zones and projects each to the plane as a basis for its coordinates, so in each zone, there is a plane rectangular coordinates system. Position in UTM coordinates system includes the zone and the x, y coordinate in that plane (Snyder, 1987). As specified, Tsukuba is in the zone of 54 s.

The formulas from latitude, longitude (φ, λ) to UTM coordinates (E, N) are quite complex and not very usable. Here are some simplified formulas with centimetric precision are presented (Formula 5.1–5.6).

The WGS 84 system describes Earth as an ellipsoid along North-South axis with an equatorial radius of $a = 6378.137$ km and an eccentricity of $e = 0.0818192$. Take a point of latitude φ and longitude λ and compute its UTM coordinates using a reference meridian of longitude λ_0. In the following formulas, the angles are in degrees and the distances are in kilometers (Kawase, 2013).

Compute some intermediate values:

$$v(\varphi) = \frac{1}{\sqrt{1 - e^2 \sin^2 \varphi}} \tag{5.1}$$

$$A = (\lambda - \lambda_0)\cos\varphi \tag{5.2}$$

$$\begin{aligned} s(\varphi) = &\left(1 - \frac{e^2}{4} - \frac{3e^4}{64} - \frac{5e^6}{256}\right)\varphi - \left(\frac{3e^2}{8} + \frac{3e^4}{32} + \frac{45e^6}{1024}\right)\sin 2\varphi + \\ &\left(\frac{15e^4}{256} + \frac{45e^6}{3072}\right)\sin 4\varphi - \frac{35e^6}{3072}\sin 6\varphi \end{aligned} \tag{5.3}$$

$$T = \tan^2 \varphi, C = \frac{\mathrm{e}^2}{1 - \mathrm{e}^2}\cos^2 \varphi \tag{5.4}$$

In the northern hemisphere N_0 = 0 km and in the southern hemisphere N_0 = 10000 km. By convention, k_0 = 0.9996 and E_0 = 500 km. The final formulas are:

$$E = E_0 + k_0 a v(\varphi)\left(A + (1 - T + C)\frac{A^3}{6} + (5 - 18T + T^2)\frac{A^5}{120}\right) \tag{5.5}$$

$$N = N_0 + K_0 a\left(s(\varphi) + v(\varphi)\tan\varphi\left(\frac{A^2}{2} + (5 - T + 9C + 4C^2)\frac{A^4}{24} + (61 - 58T + T^2)\frac{A^6}{720}\right)\right) \tag{5.6}$$

In ROS, navsat_transform_node was used to transform latitude and longitude coordinates to UTM coordinates. This node subscribed /gps/fix topic to get latitude, longitude coordinates. After transformation, navsat_transform_node published gps/filtered topic, which includes UTM coordinates.

5.2.4 Process for IMU

This research used BWT901CL which can measure 3-axis angle, angular velocity, acceleration, magnetic field. In this research, it had two functions: one was to get direction based on magnetometer inside, the other one was to design INS to combine with GNSS to get more accurate and reliable position.

In ROS, ran wit_node to get data from IMU, then it published 9-axis data in /imu/data topic, the pose was shown in rviz as shown in Fig. 5.8.

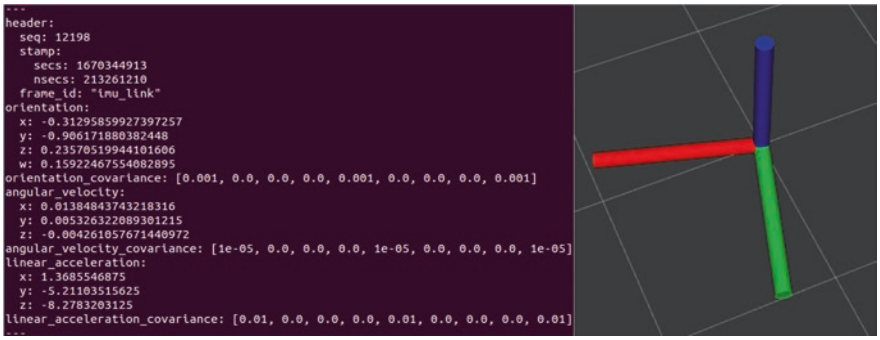

Fig. 5.8 IMU 9-axis data and pose in rviz

5.2.5 Sensor Fusion for GNSS/IMU

5.2.5.1 Coordinate System Specification

Sensor fusion is a method to fuse the data of multiple sensors to obtain more accurate and reliable data. Because this research needed to fuse multiple sensors, it involved multiple coordinate systems (Table 5.1). For localization, three coordinate systems were used: robot system, static coordinate system, and dynamic coordinate system. According to REP-105, the robot coordinate system was fixed on the golf cart. A static coordinate system was built when the system starts to run, the original point was the starting point of golf cart, Y axis was to north, X axis was to east. Dynamic coordinate system was built to express error, which included initial position error and sensor data error, the original point was also the starting point of golf cart. Earth coordinate system was used to provide a common reference coordinate system for multiple map coordinate systems (for example, robots distributed in large areas), the research didn't make use of earth coordinate system.

To make the positioning more accurate and coordinate transform more convenient, the coordinate systems of the Robot, GNSS, and IMU were overlapped, so the frames of gps, imu_link, and base_link were all the same, there is no coordinate transform for these three coordinate systems. According to REP-103, IMU was specified to ENU (East, North, Up) system, it meant when angles for three axes were all zero, forward of IMU was to east, left was to north, up was to sky. The direction specifications for imu_link and map are shown in Fig. 5.9.

Because of the introduction of the odom coordinate system, the problem of positioning was transformed into solving the spatial relationship from odom to base_link or map to odom. Because we only need to know any of the two spatial relationships, we can deduce the exact position and pose of the robot (identified by base_link) on the map.

In Fig. 5.10, the solid arrows between the three coordinate systems indicate that their spatial relationship can be directly determined by the robot_localization

Table 5.1 Coordinate system specification

Name	Frame_id

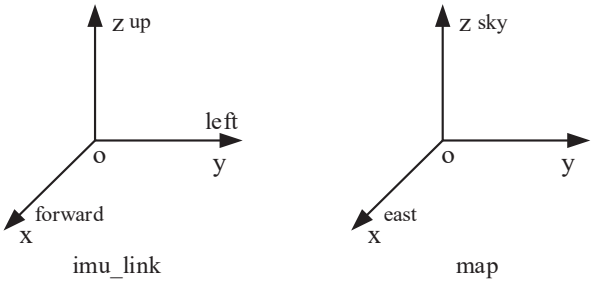

Fig. 5.9 Direction specifications for imu_link and map

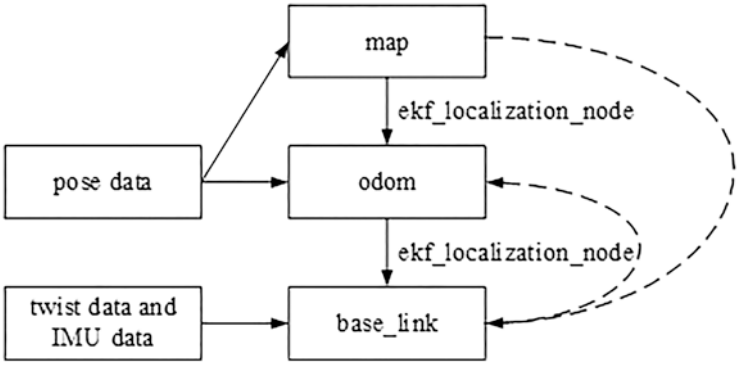

Fig. 5.10 Relationship between coordinate systems

package. The dotted arrows between them indicate that the spatial relationship between them can also be obtained, but it needs to be obtained indirectly through TF transform.

Figure 5.10 also shows the different processing purposes of the input data. The pose data (including odom data) were used to dock the calibration of the map coordinate system and the odom coordinate system, while Twist data and IMU data were used to dock the direction calibration of the base_link. The acceleration on IMU Z-axis was ignored due to the existence of the earth's gravity.

Transform Frame (TF) is a tool commonly used in ROS to realize the transformation of different coordinate systems. It represents the relationship between any two coordinate systems in real time. TF lets the user keep track of multiple coordinate

frames over time. It maintains the relationship between coordinate frames in a tree structure buffered in time, and lets the user transform points, vectors between any two coordinate frames at any desired point in time. TF tree shows all coordinate system relationships of the whole system. Coordinate system relationships of this research can also be shown in TF tree (Fig. 5.11).

5.2.5.2 Kalman Filter for GNSS/INS System

Kalman filter is a recursive filter. This research uses GNSS/INS navigation system to make up for the problems of low output frequency and poor reliability of RTK-GNSS data and large accumulated error of inertial navigation. In this research, the difference between the position values obtained by GNSS and INS was taken as the observation and the measurement variance was established and then processed by Kalman filter. The specific method was to update the estimation of the state quantity by using the estimated value at the previous time and the observed value at the current time to obtain the optimal estimated value at the current time, to improve the accuracy of the navigation system (Hongrun, 2014).

If the system noise and measurement noise were assumed to be Gaussian white noise, the system can be regarded as linear system. Kalman filter was used to filter the data, and the state vector X_k was set as

$$X_k = \left(x_k, y_k, z_k\right) \tag{5.7}$$

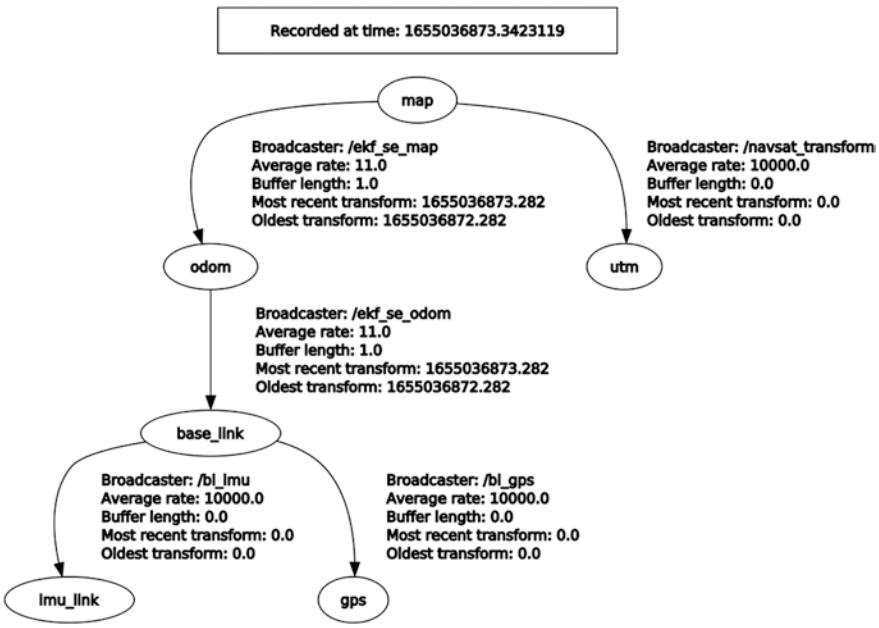

Fig. 5.11 TF tree to show relationships of different coordinate systems

x_k, y_k, and z_k are the displacements of the system in due north, due east, and vertical upward directions.

The state equation of the system after discretization was

$$X_k = FX_{k-1} + \omega_{k-1} \tag{5.8}$$

X_k is the state vector of golf cart at time k, F is the state transition matrix, and $\omega_{(k-1)}$ is the filtering process noise. In this study, it was the zero mean Gaussian white noise of the known covariance matrix.

The observation equation of the system after discretization can be expressed as:

$$Z_k = HX_k + V_k \tag{5.9}$$

Z_K is the system observation value at time k, H is the sensor measurement matrix, and V_k is the measurement noise with normal distribution.

The first step of Kalman filter was to estimate the current state value and error covariance

$$\hat{X}_k = f\left(\hat{X}_{k-1}\right) \tag{5.10}$$

$$\hat{P}_k = FP_{k-1}F^T + Q \tag{5.11}$$

$\hat{X}_k$ is the system state estimate at time k, f is the standard three-dimensional motion model derived from Newtonian mechanics, P is the estimation error covariance, F is the Jacobian matrix of f, and Q is the process noise covariance.

The second step was to use the state observation matrix H, measure the covariance R and error covariance estimate $\hat{P}_k$ to calculate the Kalman gain K, and then use the Kalman gain to update the system state and covariance matrix.

$$K = \hat{P}_k H^T \left(H\hat{P}_k H^T + R\right)^{-1} \tag{5.12}$$

$$X_K = \hat{X}_k + K\left(Z_k - H\hat{X}_k\right) \tag{5.13}$$

$$P_k = \left(I - KH\right)\hat{P}_k \left(I - KH\right)^T + KRK^T \tag{5.14}$$

To take the position and velocity measurement difference obtained by GNSS and INS respectively as the observation and establish the measurement equation, and then deal with it with Kalman filter, the system state model used in this study was the Wiener process model, so F and V_k in the above formula (5.8) and (5.9) can be expressed as:

$$F = \begin{cases} I_3 & TI_3 & \frac{T^2}{2} I^3 \\ O_3 & I_3 & TI_3 \\ O_3 & O_3 & I_3 \end{cases}, V_k = \begin{pmatrix} \frac{T^3}{6} B \\ \frac{T^2}{2} B \\ TB \end{pmatrix} \gamma_k \tag{5.15}$$

γ_k is the white Gaussian noise with the mean value of known covariance being zero.

$$B = \begin{pmatrix} 1 \\ 1 \\ 1 \end{pmatrix}, I_3 = \begin{pmatrix} 1 & 0 & 0 \\ 0 & 1 & 0 \\ 0 & 0 & 1 \end{pmatrix}, O_3 = \begin{pmatrix} 0 & 0 & 0 \\ 0 & 0 & 0 \\ 0 & 0 & 0 \end{pmatrix} \tag{5.16}$$

The state observation values of GNSS and INS are Formula (5.17) and Formula (5.19), respectively.

$$Z_{\text{GNSS}}(k) = H_{\text{GNSS}}(k) X_k + b_{\text{GNSS}}(K) \tag{5.17}$$

$$H_{\text{GNSS}}(k) = \begin{pmatrix} I_3 & O_3 & O_3 \\ O_3 & O_3 & O_3 \\ O_3 & O_3 & O_3 \end{pmatrix} \tag{5.18}$$

$$Z_{\text{IMU}}(k) = H_{IMU}(k) X_k + b_{IMU}(K) \tag{5.19}$$

$$H_{\text{IMU}}(k) = \begin{pmatrix} O_3 & O_3 & O_3 \\ O_3 & O_3 & O_3 \\ O_3 & O_3 & I_3 \end{pmatrix} \tag{5.20}$$

B and m are Gaussian white noise with known mean covariance of zero during GNSS and IMU observation, respectively. The system state estimation formula integrating IMU and GNSS can be expressed as:

$$\begin{aligned} \hat{X}_{\text{GNSS+IMU}}(k) = \hat{X}(k-1) + K_{\text{GNSS+(GNSS+IMU)}}(k)\left(Z_{\text{GNSS}}(k) - H_{\text{GNSS}}\hat{X}(k-1)\right) + \\ K_{\text{IMU+(GNSS+IMU)}}(k)\left(Z_{\text{IMU}}(k) - H_{\text{IMU}}\hat{X}(k-1)\right) \end{aligned} \tag{5.21}$$

5.2.6 *Design for Obstacles Avoidance System*

5.2.6.1 Process for LiDAR

This research used a UTM-30LX-EW Lidar to detect surrounding environment to avoid obstacles, it can get distances from obstacles points to LiDAR. In ROS, ran urg_node to get data from LiDAR, then it published point cloud data in /scan topic, the points are shown in rviz as shown in Fig. 5.12.

The LiDAR was installed at the front of golf cart, and the detection range was 270°. But the range needed to be scanned was 180° from the front, the left 90° left included some part of golf cart, which would affect the results of obstacles detection. Consequently, the left 90° range did not need to be scanned, the research ignored this part as shown in Fig. 5.13 shows the point cloud after setting the scanning range to 180°.

Fig. 5.12 LiDAR point cloud shown in rviz

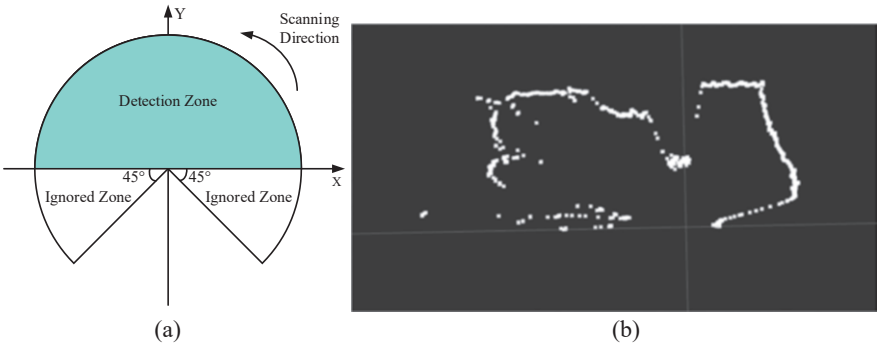

Fig. 5.13 (**a**) Detection zone of LiDAR, (**b**) Point cloud in the scanning range of 180°

5.2.6.2 Obstacles Avoidance Strategy

The obstacle mainly depends on a certain distance from the golf cart. Therefore, the obstacles avoidance strategy was that whether it was a dynamic obstacle or a static obstacle, once it entered the warning zone, the golf cart would stop to avoid it. The safety distance was set to 2 m, so the warning zone was set as the zone 2 m in front of the golf cart (Fig. 5.14a). The process for the strategy was that got distances of all 720 points of detection, then found the shortest one, if the distance was longer than safety distance, the golf cart normally moved, if the distance was shorter than safety distance, the golf cart stopped at once, the process is shown in Fig. 5.14b.

5.2.7 Design for Navigation System

Rviz is a 3D visualization platform in ROS. On the one hand, it can realize the graphical display of external information, on the other hand, it can publish control information to objects through rviz, to realize the monitoring and control of robots. In this research, rviz was used as the upper computer for the golf cart. Path was planned by move_base node in the rviz, then rviz sent the goal to waypoint node to realize navigation for golf cart.

The premise of path planning in rviz was to provide a map for the move_base node, as this research did not need to know the environmental information of the map, only the coordinate information was needed, so an empty map can be used. This research used map_server to provide an empty map to move_base node. Then move_base node was used to plan path in rviz. The path planning steps were as following: First, ran robot_localization node and move_base node, so the static

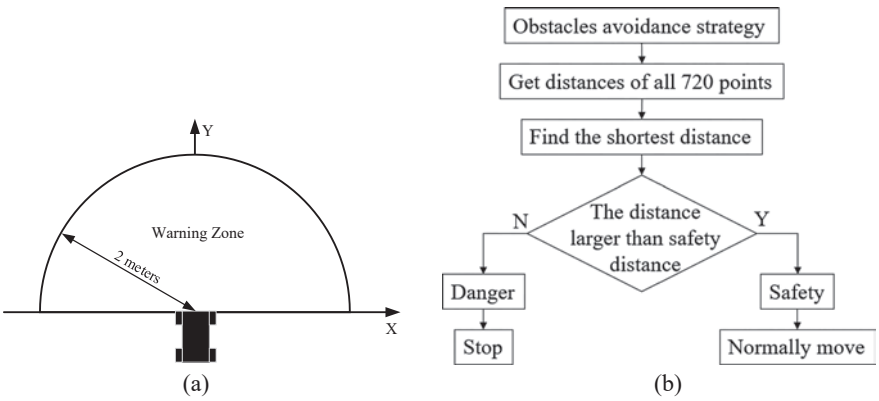

Fig. 5.14 (**a**) Warning zone for obstacles avoidance (**b**) Flowchart for obstacles avoidance strategy

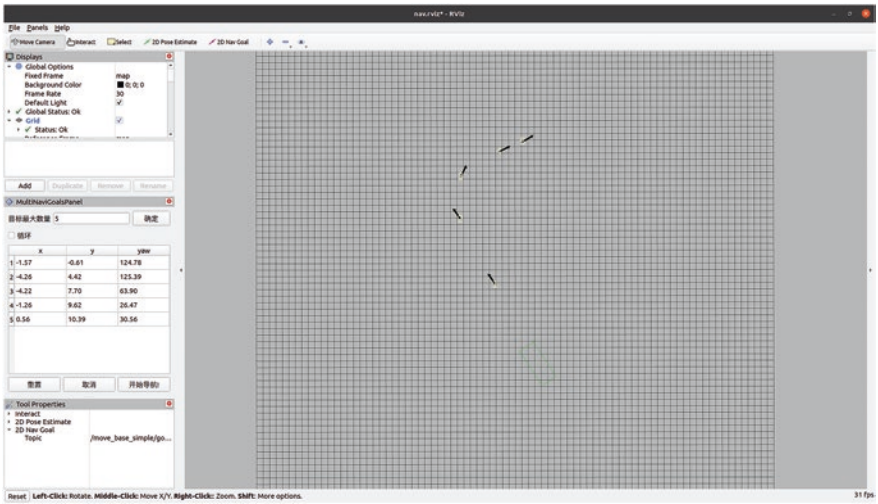

Fig. 5.15 Path planning for golf cart

coordinate system was built, the position of robot was shown in the empty map in rviz. Second, drove the golf cart as designated route to the goal, mark the way point by move_base_simple/goal topic when driving. Finally, positions and poses of all way points were recorded in rviz, so the path planning was complected as shown in Fig. 5.15.

5.2.8 Robot Tracking

5.2.8.1 Fuzzy Control Strategies

Pure purist model described the path of the robot moving at a look_ahead distance based on the kinematics equation and geometric relationship of the robot. Its geometric relationship is shown in Fig. 5.16.

The analysis of geometric relationship between robot and route is shown in the following:

$$L_1 = R\sin\theta \tag{5.22}$$

$$L_2 = R\left(1-\cos\theta\right) \tag{5.23}$$

$$L_1^2 + L_2^2 = L_d^2 \tag{5.24}$$

$$L_2 = m\cos\beta + \sqrt{L_d^2 - m^2}\,\sin\beta \tag{5.25}$$

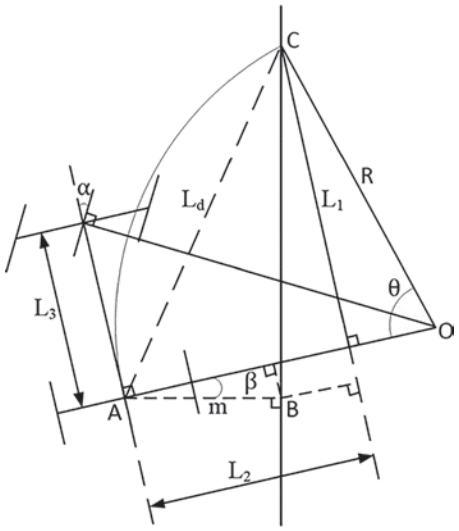

O: Turning center
R: Turning radius
α: Steering angle
β: Yaw angle
m: deviation
BC: specified route
L3: wheelbase

Fig. 5.16 Geometric relationship of pure pursuit model

$$R = \frac{L_3}{\tan\alpha} \tag{5.26}$$

$$2R - L_2 = L_d^2 \tag{5.27}$$

$$\alpha = \tan^{-1}\left(\frac{2L_3\left(m\sin\theta + \sqrt{L_d^2 - m^2} - \cos\theta\right)}{L_d^2}\right) \tag{5.28}$$

According to formula (5.28), α is decided by L_3, m, θ, L_d. Because L_3 is stationary, θ is decided by β, α is decided by m, β, Ld. m, β are decided by the geometric relationship between robot and route, so only the L_d is decided by system. When L_d is large, α is small, the robot moved smoothly, but it would take longer to return to the specified route. When L_d is small, α is large, then the robot can quickly return to the specified route, but it would lead to overshoot. Hence, L_d should be decided by m, β, the basic control rule is that when m, β are large, L_d should be small to eliminate error rapidly; when m, β are small, L_d should be large to avoid overshot. The basic operation is as follows: If m and β are large, the α should be large to avoid overshooting. Also, if m and β are small, the α should be small to make robot return to route quickly. The steering angle was controlled by the deviation and yaw angle, this situation was very suitable to be realized by fuzzy control.

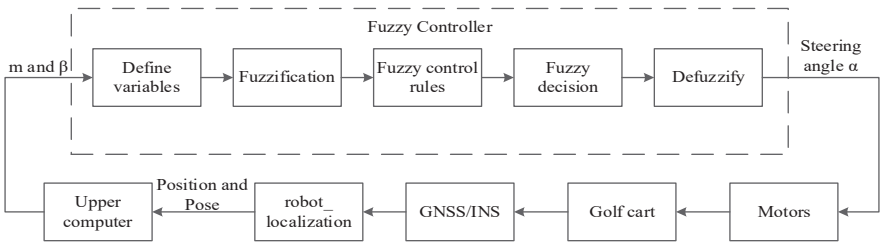

Fig. 5.17 Fuzzy control system for robot tracking

5.2.8.2 Fuzzy Control System Design

The control system was based on fuzzy controller (Fig. 5.17). robot_localization input the position and orientation to the upper computer, then the upper computer calculated m and β and input them to the fuzzy controller. The simulation process of the Fuzzy control included in five steps: first, defined the variables m and β; second, fuzzification that changed the m and β to the language variables. Third, input system for the language variables to the fuzzy control rules, then the decision was made based on the fuzzy rule. Fourth, fuzzy decision was made to get the fuzzy value of α. Fifth, defuzzification was done to change the fuzzy value to exact value of α. Finally, the upper computer controlled the motors according to steering angle so the robot could move back to the specified route.

5.3 Results

5.3.1 Experiment for the Automatic Driving

The navigation system of agricultural machinery can be easily affected by the environment and weather. Therefore, the effectiveness of the navigation system in this study needed to be verified by experiments. This navigation system was designed for agricultural products transportation, so planning a route for transportation was essential. The RTK-GNSS base station was set on the roof of main building, the signal around main building was much better, so planned a route around main building to transport vegetables from warehouse to vegetables selling point near the entrance of T-PIRC (Fig. 5.18), let golf cart automatically move along the route to verify the effectiveness of the system.

The automatic driving experiments were conducted three times, first installed all sensors on golf cart. Then drove golf cart manually along the planned route, recorded positions on rviz when driving. Finally, the golf cart moves along the designated route automatically. The GNSS recorded all coordinates when driving, the QGIS was used to mark all coordinate points as shown in Fig. 5.19, coordinates of observation 1 were marked in white, coordinates of observation 2 were marked in red,

Fig. 5.18 Route for experiment for the automatic driving

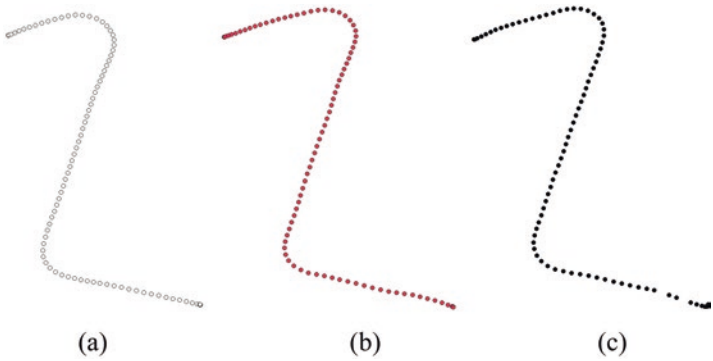

Fig. 5.19 Coordinate points recorded in automatic driving experiments. (**a**) Observation 1, (**b**) Observation 2, (**c**) Observation 3

coordinates of observation 3 were marked in black. To analyze the deviation of routes of different experiments, coordinate points were marked on satellite map as shown in Fig. 5.20.

All three experiments completed the golf cart to automatically transport agricultural products according to the designated route, so the navigation system was effective. However, after measurement, the deviation between different routes was between 0.5 and 2 m, which is far more than the measurement error of GNSS. After analysis, the reason for this result is that the GNSS signal was very fragile and easy to lose. Since the route must be replanned after each experiment, the planned route

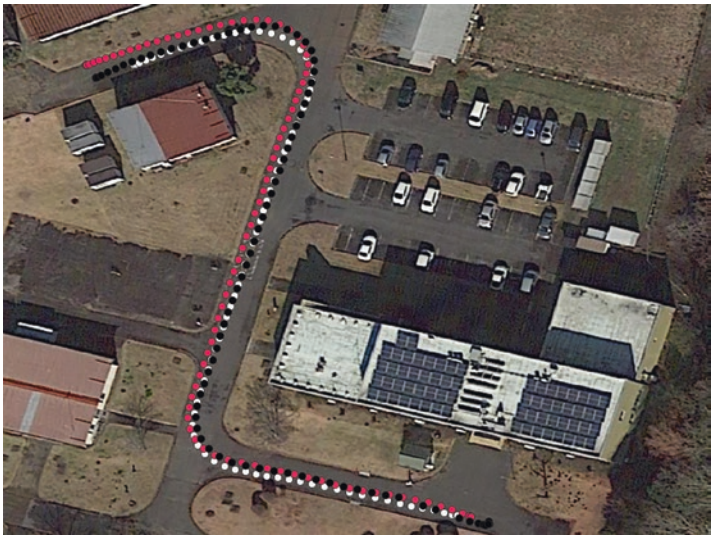

Fig. 5.20 Coordinate points of experiments marked on satellite map

would be different, resulting in a large deviation in the final experimental results. Secondly, the GNSS error in the moving process was more than that in the static state.

5.3.2 Experiment for Obstacles Avoidance

As the experiment route was close to the parking lot, there was a risk of facing the car at the entrance of the parking lot, so obstacle avoidance experiments were conducted at the entrance of the parking lot (Fig. 5.21).

The experiment tested the obstacle avoidance effect of static obstacles and dynamic obstacles respectively, used a roadblock to test static obstacles, people passed by and drove car to test dynamic obstacles (Fig. 5.22a, b, c).

The specific experiment was conducted to let the golf cart move normally, then set different obstacles to test the obstacle avoidance ability of the golf cart and measured the distance from the obstacle to the golf cart with LiDAR after the golf cart stopped to judge the effectiveness of the obstacle avoidance strategy in this research. All experiments were divided into three groups according to the speed of the golf cart, namely 3, 4, and 5 km/h. In each group of experiments, static obstacles, pedestrians from the left, pedestrians from the right, cars entering the parking lot and cars leaving the parking lot were tested respectively. Each group of experiments were repeated five times. The experiment results of golf cart moving in 3 km/h are shown in Table 5.2.

According to the analysis of the data in Table 5.3, although the warning area was set as 2 m, the distance from the golf cart to the obstacle was less than 2 m when the

Fig. 5.21 Obstacle avoidance position

Fig. 5.22 Obstacles avoidance experiment, (**a**) static object, (**b**) pedestrian test, (**c**) dynamic object

Table 5.2 Obstacles distances when golf cart moving at 3 km/h to avoid obstacles

Obstacles	Experiment 1/cm	Experiment 2/cm	Experiment 3/cm	Experiment 4/cm	Experiment 5/cm	Average/cm

golf cart stopped. The main reasons were: first, it took time for the LiDAR to detect obstacles and process data; second, it took time for program processing; third, the golf cart had a braking distance. These three reasons led to the golf cart still moving a short distance after the obstacle has entered the warning area, making the distance between the golf cart and the obstacle less than 2 m.

Table 5.3 Obstacles distances when golf cart moving at 4 km/h to avoid obstacles

Obstacles	Experiment 1/cm	Experiment 2/cm	Experiment 3/cm	Experiment 4/cm	Experiment 5/cm	Average/cm
[illegible]	[illegible]	[illegible]	[illegible]	[illegible]	[illegible]	[illegible]
[illegible]	[illegible]	[illegible]	[illegible]	[illegible]	[illegible]	[illegible]
[illegible]	[illegible]	[illegible]	[illegible]	[illegible]	[illegible]	[illegible]
[illegible]	[illegible]	[illegible]	[illegible]	[illegible]	[illegible]	[illegible]
[illegible]	[illegible]	[illegible]	[illegible]	[illegible]	[illegible]	[illegible]

The distance from pedestrian was slightly less than that from static obstacle because the same obstacle avoidance strategy was adopted for pedestrian and static obstacle, and the detection of dynamic obstacles was slightly slower than that of static obstacles. Also, the pedestrian was walking across the road, neither getting close nor away from the golf cart. The distances from pedestrians from the left and pedestrians from the right were the same.

However, the distances from the car were very different from that of static obstacles. The distance from car entering the parking lot was far less than that of static obstacles, and the distance from car leaving the parking lot was far more than that of static obstacles. This was because car entering the parking lot was getting close to golf cart, while car leaving the parking lot was getting far away from golf cart. The speed of the golf cart was set to 4 km/h and continued to do the experiment and the experiment results are shown in Table 5.3.

The distance listed in Table 5.4 was generally smaller than that in Table 5.3, because the braking distance of the golf cart increased with the speed increased, resulting in a smaller distance to the obstacle.

In experiments 1–3, distances from pedestrians from the left were more than that of pedestrians from the right. On the contrary, in experiment 4 to experiment 5, distances from pedestrians from the left were less than that of pedestrians from the right. After analysis, we found that this was because the golf cart moved in different directions. During experiments 1–3, the right side of the golf cart was facing the sun, so pedestrian from the right side took longer to detect. During experiments 4–5, the left side of the golf cart was facing the sun, so pedestrian from the left side took longer to detect. The effect of the LiDAR would be affected by the sunlight, and the detection time on the side with strong sunlight would be longer. The speed of the golf cart was then set to 5 km/h and the experiment results are shown in Table 5.4.

According to Table 5.4, we found that the distances were smaller than that those in Table 5.3 because the braking distance of the golf cart increased with the increase in speed. However, the reduced value was less than that in Table 5.3 compared with Table 5.2, which showed that the increase rate of braking distance decreased with the increase of speed.

Figure 5.23 shows point clouds of obstacles when golf cart stopped. In the experiments, the golf cart avoided both static obstacles and dynamic obstacles successfully,

Table 5.4 Obstacles distances when golf cart moving at 5 km/h to avoid obstacles

Obstacles	Experiment 1/cm	Experiment 2/cm	Experiment 3/cm	Experiment 4/cm	Experiment 5/cm	Average/cm

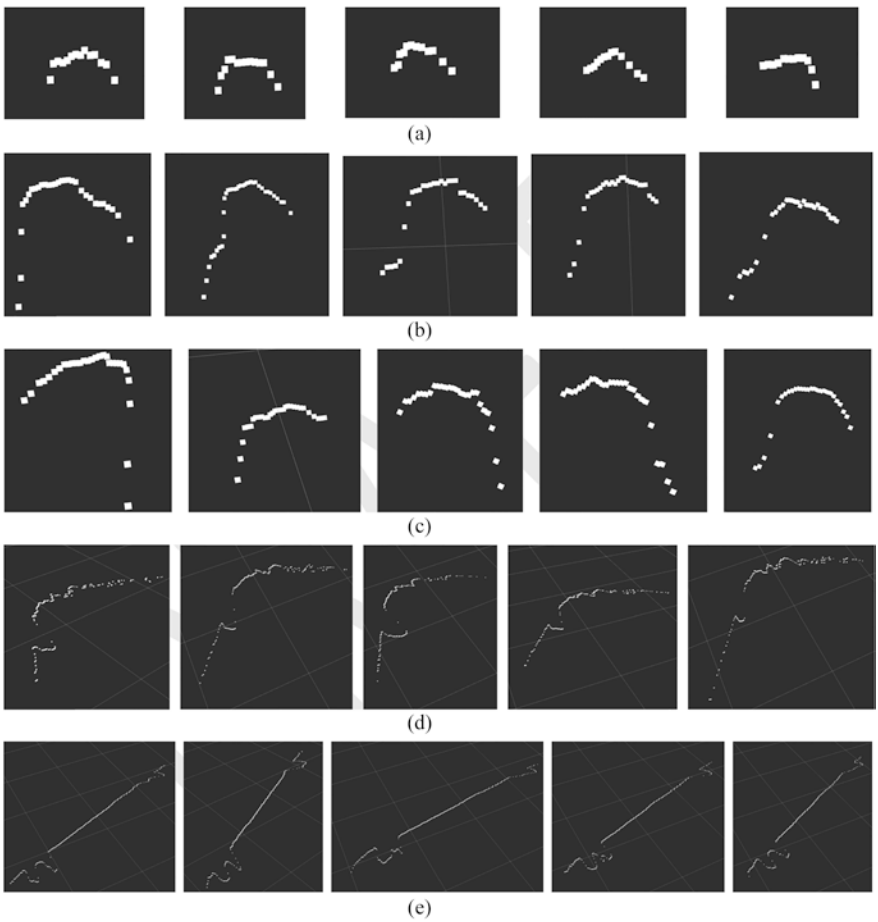

Fig. 5.23 Point clouds for different kinds of obstacles. (**a**) Point clouds for roadblock. (**b**) Point clouds for pedestrian from the left. (**c**) Point clouds for pedestrian from the right. (**d**) Point clouds for car entering the parking lot. (**e**) Point clouds for car leaving the parking lot

although it could not stop immediately when the obstacle entered the warning area, it could stop in time to avoid obstacles. Therefore, the obstacle avoidance strategy in this research was effective.

5.4 Discussion

Positioning, tracking, and obstacle avoidance are the main research fields of agricultural machinery automatic navigation system. This research covered these three research fields. For positioning, it made use of GNSS/INS integrated positioning system to realize accurate position. For tracking, it proposed fuzz control system to realize robot tracking. For obstacles, it used LiDAR to detect obstacles and proposed a simple obstacles avoidance strategy. All these three parts were tested in experiments.

The GNSS/INS system had very high positioning accuracy due to the RTK-GNSS whose error was less than 2 cm. Fuzzy control was used to control robot tracking in the study. LiDAR was used to detect obstacles. The experiment showed that LiDAR was a very reliable sensor and hard to be affected by the environment, also it could sense a large area.

To test the navigation system, an automatic driving experiment and obstacles avoidance experiment were conducted. The experiment results showed that the golf cart can move autonomously along the designated route and avoid obstacles. However, due to the frequent loss of GNSS signals, the route must be replanted after each navigation, resulting in large deviations between different routes. To solve this problem, we can take measures to increase the stability of GNSS or make use of some other more stable sensors to position.

For obstacles avoidance, although golf cart avoided obstacles successfully, golf cart can't stop immediately when obstacles enter warning area because of LiDAR detection time, data processing time, and braking time. What's more, the results also showed the states of obstacles, the sunlight, and the speed of golf cart affected the effectiveness of obstacles avoidance. Consequently, for higher safety, the area of warning area can be increased or make use of more complex obstacles avoidance strategies.

5.5 Conclusion

This research chose the golf cart as research platform, GNSS, IMU, and LiDAR as sensors, and designed navigation system based on ROS. Multisensor fusion technology was used to study the positioning of the golf cart, fuzzy control was used to realize the tracking of the golf cart, and CAN bus was used to control of the vehicle. Finally, the autonomous movement and obstacle avoidance of the golf cart were investigated.

For positioning, this chapter mainly used Kalman filter to fuse RTK-GNSS and IMU data to achieve accurate and reliable positioning. First, RTK-GNSS was studied, and the setting of GNSS base station and rover was studied. Then, the processing method of GNSS data was introduced. Through experiments, it was verified that the error of GNSS data after RTK was less than 2 cm, which had good accuracy. Then the coordinate transformation of GNSS was studied, and the coordinates based on static coordinate system were obtained. After the GNSS processing, the IMU data processing method was introduced. The Kalman filter algorithm was studied based on the data of GNSS and IMU, and robot_localization was used to define each coordinate system and filter the coordinate information.

For obstacle avoidance, this study used LiDAR to detect and avoid the surrounding obstacles.

For tracking, there were three main steps in this study. First, the upper computer recorded the path points to achieve path planning, then the fuzzy control algorithm was used to obtain the control value of the golf cart, including speed and steering angle, and finally, the CAN bus was used to achieve the control of the golf cart. Finally, the positioning system, obstacle avoidance system, and navigation system were integrated to complete the design of the golf cart navigation system. The field experiments of automatic driving and obstacle avoidance were carried out. The experiment results verified the effectiveness of the positioning system, navigation system, and obstacle avoidance system in this study. This chapter also analyzed the problems in the experiments and proposed further research direction. After completing the field experiments of automatic driving and obstacle avoidance, the results showed that the research had certain validity and reliability in practical application. However, the system still had many deficiencies, which needed to be further improved by follow-up research work.

References

Chi, H., Zhan, K., & Shi, B. (2012). Automatic guidance of underground mining vehicles using laser sensors. *Tunnelling and Underground Space Technology, 27*(1), 142–148. https://doi.org/10.1016/j.tust.2011.08.007

Choi, J., Yin, X., Yang, L., & Noguchi, N. (2014). Development of a laser scanner-based navigation system for a combine harvester. *Engineering in Agriculture, Environment and Food, 7*(1), 7–13. https://doi.org/10.1016/j.eaef.2013.12.002

Hongrun, R.. (2014). Research and realization of low cost Beidou/INS integrated navigation system. Master's Thesis, Civil Aviation University of China.

Kawase, K. (2013). Concise derivation of extensive coordinate conversion formulae in the Gauss-Krüger projection. *Bulletin of the Geospatial Information Authority of Japan, 60*, 1–6.

Lee, K. H., Ehsani, R., & Schueller, J. K. (2007). Forward movement synchronization of two vehicles in parallel using a laser scanner. *Applied Engineering in Agriculture, 23*(6), 827–834.

Li, T. (2015). *GPS principle and application* (p. 108). Science Press.

Li, Y., & He, K. (2006). A new obstacle avoidance and navigation method for outdoor mobile robots based on LiDAR. *Robots, 03*, 275–278.

Nørremark, M., Griepentrog, H. W., Nielsen, J., & Søgaard, H. T. (2008). The development and assessment of the accuracy of an autonomous GPS-based system for intra-row mechanical weed control in row crops. *Biosystems Engineering, 101*(4), 396–410. https://doi.org/10.1016/j.biosystemseng.2008.09.007

Noureldin, A., Karamat, T. B., Eberts, M. D., & El-Shafie, A. (2009). Performance enhancement of MEMS-based INS/GPS integration for low-cost navigation applications. *IEEE Transactions on Vehicular Technology, 58*(3), 1077–1096.

Snyder, J. P. (1987). *Map projections—a working manual*. U.S. geological survey professional paper 1395. United States Government Printing Office.

Teng, Z., Noguchi, N., Liangliang, Y., Ishii, K., & Jun, C. (2016). Development of uncut crop edge detection system based on laser rangefinder for combine harvesters. *International Journal of Agricultural & Biological Engineering, 9*(2), 21–28.

Wang, Q. (2010). Principle and application of global positioning system (GPS). *Satellite and Network, 04*, 26–30.

Xia, Y., Chunxia, Z., Debao, C., Yunfei, C., & Guang, H. (2009). A road surface extraction algorithm based on laser radar. *China Journal of Image Graphics, 10*, 2035–2041.

Chapter 6
Automatic Navigation of Pesticide Spraying Vehicle for Orchard Tree Trunk Detection

Abstract Traditional Japanese orchards use nets to limit the height of fruit trees to make it convenient for farmers, but the low and dense branches are not conducive to the operation of large-sized machinery. A small automatic spraying robot can alleviate the problem of labor shortage in orchard. The dense canopy of the orchard not only blocks the GNSS signals. However, the lack of light reduces the accuracy of object recognition by normal RGB camera. In order to overcome these problems, Light Detection and Ranging (LiDAR) was chosen as a single sensor to implement a prototype robot navigation system in this study. In this study, the planning path of the vehicle was obtained by sequentially using various algorithms to process the LiDAR return points. First, density-based spatial clustering of applications with noise (DBSCAN) clusters the LiDAR return points to find the targets, the cones and the tree trunks, after that K-means divided the targets into left and right groups, and finally, random sample consensus (RANSAC) was calculated to get the left and right boundary lines, and the midline of the two boundary lines was the planning path for navigation. In field tests, the results show that the position root mean square error (RMSE) of this vehicle was as 13.8 cm in right turn and 11.4 cm in left turn. The system was able to calculate the path in real time based on the position of the cones and trees and guide the vehicle operate safely.

Keywords LiDAR · Tree trunk detection · Orchard

6.1 Introduction

In response to the aging population and labor shortages, a variety of machines have been developed in agriculture to assist in production. With the continuous development of these machinery and equipment, agriculture is gradually becoming less dependent on human labor. Especially in the case of extensive cultivation and fixed planning areas, advanced automation technology is expected to bring both time and economic benefits to agriculture through timeliness and efficiency of operations. The need for pesticides and herbicides during crop growth may have negative

© The Author(s), under exclusive license to Springer Nature Singapore Pte Ltd. 2024

T. Ahamed, *IoT and AI in Agriculture*,
https://doi.org/10.1007/978-981-97-1263-2_6

impacts on human health, and the use of mechanical equipment becomes a necessary alternative to ensure flexibility and safety in agricultural production (Dang et al., 2022). Although pesticide spraying is an indispensable part of the operation, there is a high risk of chemical contamination associated with the overuse of traditional speed sprayers. Pesticide spraying needs to be repeated several times from crop flowering to fruiting to prevent pest invasion. In some cases, farmers are also required to manually spray pesticides; however, this can lead to pesticides entering the farmer's body through the respiratory system, which can have an impact on their health. Therefore, unmanned agricultural machinery has the potential to solve the manipulation problem through appropriate autonomous guidance systems.

In autonomous agricultural guidance systems, accurate positional information and surrounding environmental data need to be obtained through sensors to ensure that the vehicle follows the designed path. In agricultural automation and robotics applications, outdoor environments are more complex and uncertain compared to indoors, making vehicle navigation particularly important (Bergerman et al., 2016). Orchard navigation systems typically include three main components: environment detection, path planning, and navigation control (Mousazadeh, 2013).

Among the commonly used navigation sensors, Global Navigation Satellite Systems (GNSSs) are well known for the high accuracy they provide in open-field navigation and have further improved the accuracy of localization through the use of Real-Time Kinematic Differential Global Navigation Satellite Systems (RTK-GNSSs) (Sun et al., 2010). However, the performance of GNSS navigation is dependent on signal quality, and orchard navigation suffers from RTK-GNSS signal disruptions due to the high density of canopy often encountered (Li et al., 2009). Due to the use of nets and dense branching in Japanese orchards, GNSS signals may be affected, and many farmland orchards are not equipped with base stations that directly use GNSS.

In contrast, machine vision is widely used in agricultural navigation because of its high flexibility, comprehensive information acquisition, and adaptability to complex environments (Subramanian et al., 2006; Takagaki et al., 2013). However, this method requires a clear contrast between the fruit trees and the background features on the ground, and fruit trees often have a high density of weeds growing at their base, resulting in a tree-ground boundary that may be shifted or even difficult to detect. In addition, environmental lighting has a large impact on machine vision; in the dark or at night, machine vision is less accurate, and even during the day, the shadows of surrounding plants (e.g., weeds) may negatively affect accuracy (Chen et al., 2020).

LiDAR utilizes the time-of-flight principle to scan the surroundings and return accurate distance information in real time. Laser navigation has high accuracy, good resolution, and strong anti- interference capability (Wang et al., 2020). LiDAR is able to overcome the limitations of low light and RTK-GNSS signal interruption. Therefore, the objective of this study is the development of a compact spraying robot utilizing LiDAR for trunk detection in orchards. In order to build a single sensor-based navigation system, a proposal is made to incorporate multiple machine learning algorithms to achieve a navigation system that works stably under different

lighting conditions. LiDAR trunk detection helps to ensure stable navigation of the robot under various lighting conditions.

6.2 Materials and Methods

6.2.1 Experimental Prototype Vehicles

The experimental vehicle used in the study was an EJ20® electric car (Fig. 6.1). The vehicle has a complete motor drive control system but cannot be programmed to control steering. To implement automatic steering, a stepper motor was installed at the rear axle of the steering mechanism. This stepper motor was then driven by a stepper motor driver.

6.2.2 Installation of Sensors

The system collected environmental data by two-dimensional LiDAR SICK LMS511-20100 PRO, passed it to the controller (laptop) to calculate the planning path and get the rotation angle, and then the laptop passed the control signal to Arduino, which controlled the motor rotation as well as the switching of the pump and the signal light (Fig. 6.2). The system was powered by one 110 V portable

Fig. 6.1 Image of the experimental vehicle used in this study. The LiDAR was the only sensor of the system

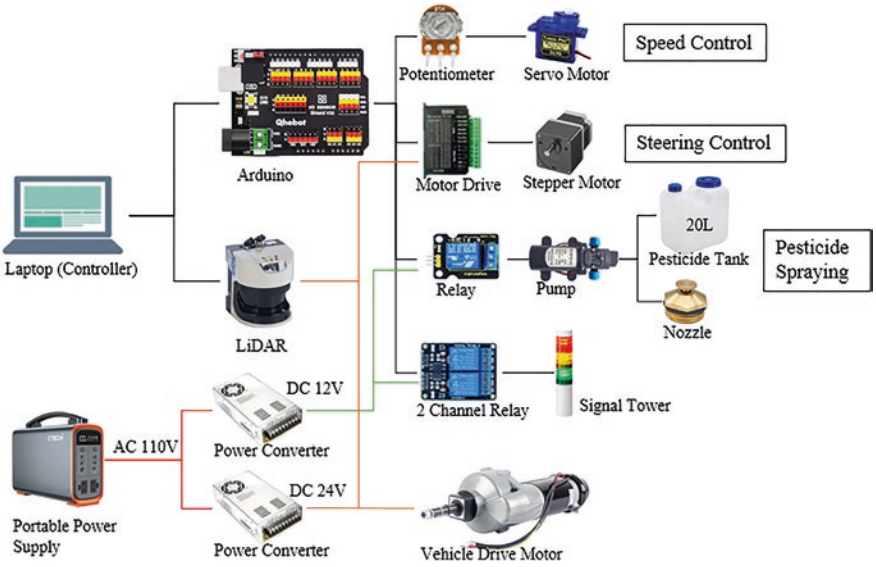

Fig. 6.2 Sensors and connection for the robotic system

power supply, and the voltage was converted to 12 and 24 V by power converters to power different devices.

6.2.3 System Structure

When the system was running, it first sent a start scanning command to LiDAR, if LiDAR scanned an object with a distance of less than 0.1 m, the vehicle will stop or not start, when there was no object within 0.1 m, the laptop will start calculating the route. If the number of objects was sufficient, the system would get the route through multiple algorithms. If there were objects only on one side, the system will consider the vehicle too close to one side and need to steer to the other side. If there was only one object on both sides, the vehicle had run to the end of the road, it would make a U-turn based on the distance to the object. The control commands for the vehicle were sent from the laptop to the Arduino, which would control the running and steering of the vehicle, as well as the switching of the water pump (Fig. 6.3).

6.2.4 Path Planning Algorithm

In this study, three algorithms are used sequentially to obtain the planning path through the LiDAR return data. LiDAR returned distance data of 761 points for each scan, and the position of each point in the coordinate system can be obtained

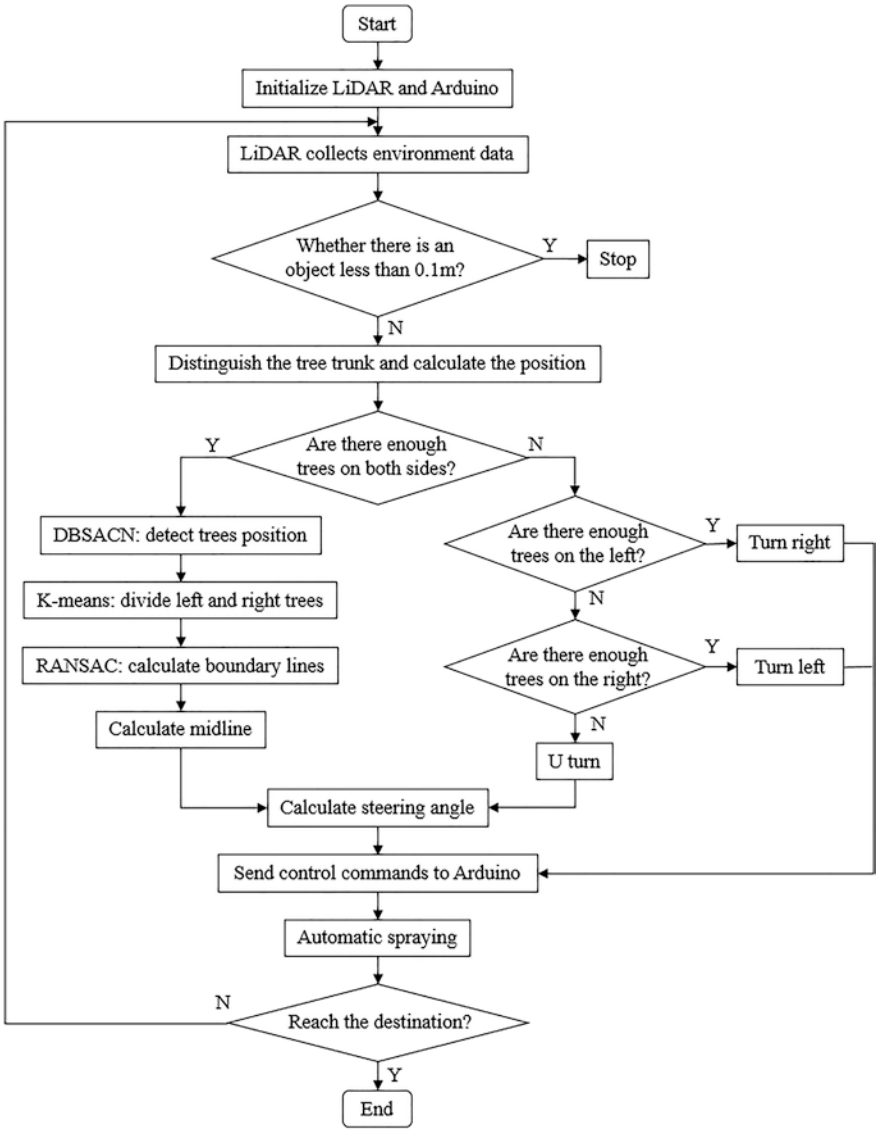

Fig. 6.3 Operational flow of the LiDAR only system

based on the laser light emission angle. Density-based spatial clustering of applications with noise (DBSCAN) can categorize points into different clusters based on the density of the points. Each cluster represented an object. Because the trees in the orchard are planted in straight lines, it provides a good reference for planning the path for autonomous operation. K-means can classify the obtained objects into left and right groups, which are the trees on the left and right, and bring them into random sample consensus (RANSAC) to calculate respectively, which can remove the

noisy points and get the accurate boundary line made up by the position of the trees. The midline calculated from the left and right boundary lines was the planning path of the system (Fig. 6.4). The angle between the planning path and the current direction of the vehicle was the steering angle of the vehicle.

6.2.5 *Graphical User Interface (GUI)*

To visualize the results of the system's planning paths more intuitively, a graphical user interface was constructed in this study using Qt (Fig. 6.5). There were control buttons on the interface to control the on/off of the LiDAR, as well as to control the speed and direction of the vehicle and the switch of the water pump after opening

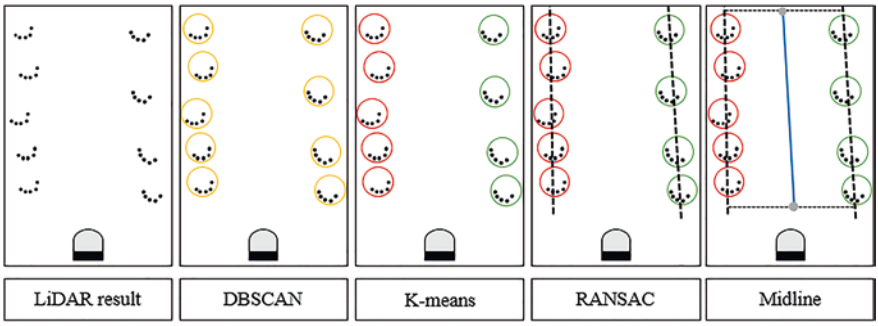

Fig. 6.4 Algorithms for planning path from point clouds

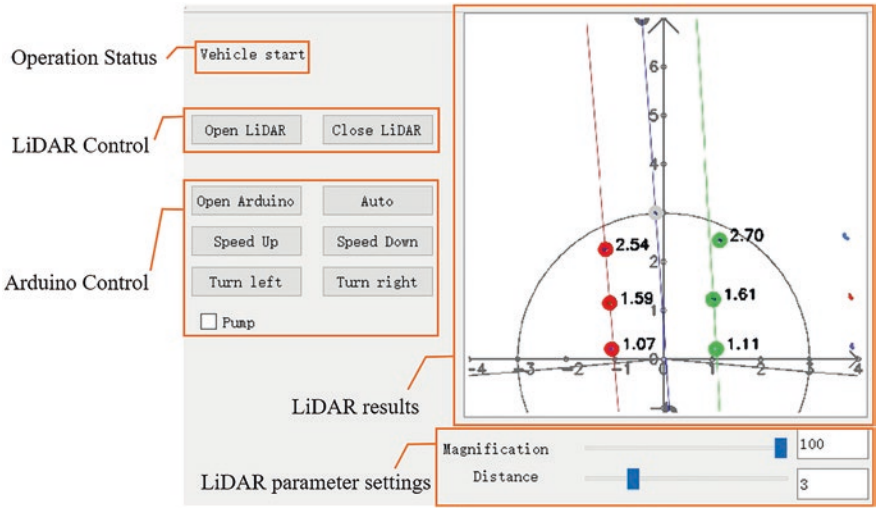

Fig. 6.5 Graphical user interface designed with Qt

the Arduino's communication. The LiDAR's return data and the system's planning paths were displayed in the interface. The black circle in the interface indicated the range of data used in the calculation, and only the points inside the circle were used in the planning path. The radius of the black circle can be adjusted using the slider below, allowing the range to be changed in real time according to the environment. The magnification allows to zoom in and out of the display results to better observe the operation of the system.

6.3 Results

6.3.1 Planning Path Calibration on a Concrete Road

To test the feasibility of the system, it was first tested on a concrete road using cones to simulate the location of orchard trees (Fig. 6.6).

In the calibration, cones were placed in two columns to simulate the position of trees in the orchard (Fig. 6.7a). LiDAR angular resolution of 0.25° was with a range of −5° to 185°, and the scanning distance up to 80 m. To reduce noise points and find targets more accurately, in this study, in LiDAR's scanning range only the target object without others such as the wall nearby, the scanning distance was limited to 5 m. The points returned by LiDAR were calculated by the emission angle with the laser light, and the positions were displayed in the coordinate of the GUI made by Qt (Fig 6.7b). BSCAN divided the points into different clusters according to the density and displayed them in different colors, each cluster represented an object, and the smallest distance value in the cluster was chosen as the distance of the object and displayed on the GUI (Fig 6.7c). The trees in the orchard were arranged linearly and could be clearly divided into left and right rows using K-means (Fig 6.7d); red was the left side of the tree, and green was the right side. The points on the left and right sides were brought into the RANSAC algorithm to obtain the boundary lines on both sides (Fig. 6.7e). RANSAC can determine which cones are on a straight line based on their

Fig. 6.6 Testing of the experimental system on a concrete road using cones instead of trees

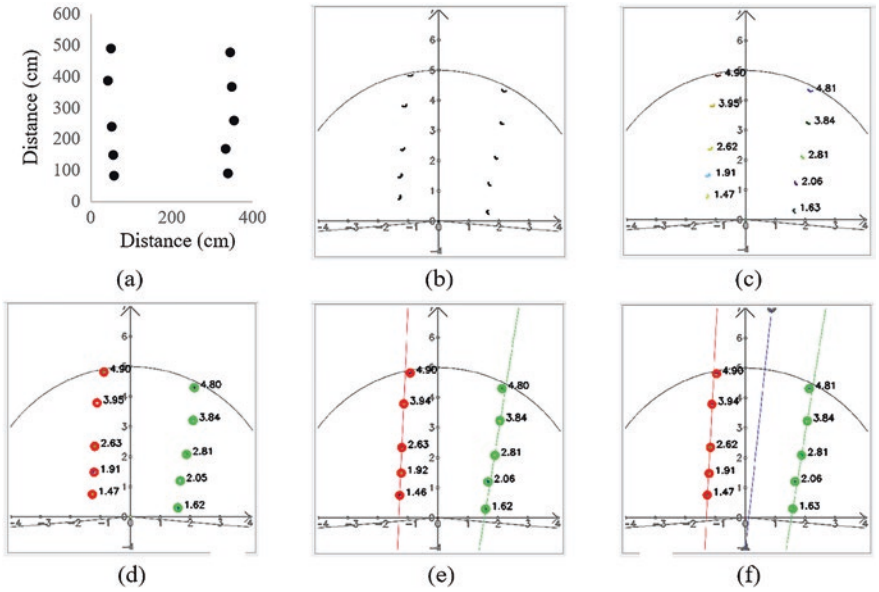

Fig. 6.7 Path planning results: (**a**) cones positions; (**b**) data returned by LiDAR; (**c**) DBSCAN; (**d**) K-means; (**e**) RANSAC; (**f**) Midline

location, and these cones can be used to calculate paths, while those cones outside the straight line will be considered noise points and will not be included in the calculation. Finally, the midline of the two boundary lines was the planning path (Fig 6.7f).

6.3.2 Field Test in a Facilitated Artificial-Tree-Based Orchard

The test was conducted in the Tsukuba Plant Innovation Research Center (T-PIRC), University of Tsukuba. In the orchard, trees are planted in a straight line, but there will be some lack of trees in some positions. This situation was taken into consideration in the experiment, so the third column had only four trees to simulate the lack of trees. From the experimental results, this system was still able to find the path accurately (Figs. 6.8 and 6.9). The experimental vehicle first found a planning path based on the trees on both sides and followed the path. If there were trees on only one side during the run, the vehicle would turn toward the other side. Until there were only one tree on the left and one on the right in front, the vehicle would approach the midpoint of the last tree on the left and right, and when it reached the end of the road, it would make a U-turn with the distance of the tree on the left or right as the radius, and when it detected that there were trees on both sides again, the vehicle would enter into the planning of the path according to the trees on both sides

Fig. 6.8 Images of vehicle turning right at artificial-tree-based orchard

Fig. 6.9 Images of vehicle turning left at artificial-tree-based orchard

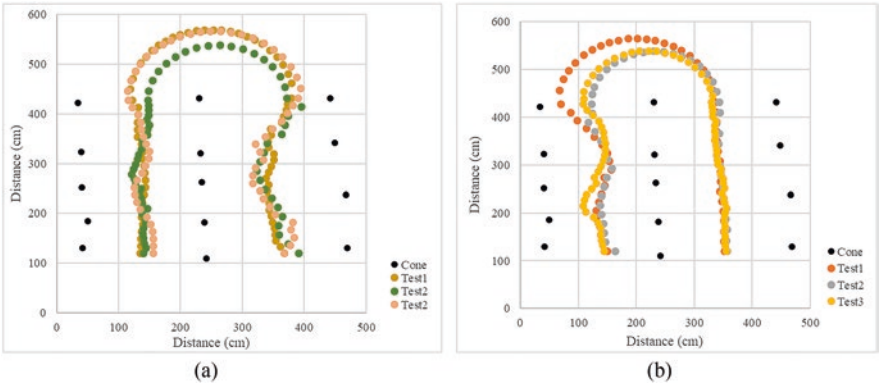

Fig. 6.10 Vehicle tracks in artificial-tree-based orchards: (**a**) right turn; (**b**) left turn

again. By analyzing the vehicle tracks, the root-mean-square deviation (RMSEs) values for the three tests were 11.4, 14.5, and 15.5 cm for the right turn with a mean value of 13.8 cm, and for the left turn they were 18.6, 6.7, and 8.8 cm with a mean value of 11.4 cm (Fig. 6.10).

6.4 Discussion

In contrast to RGB camera and GNSS navigation system, this study achieved a stable navigation system in an orchard by using LiDAR as the only sensor. The lighting conditions in the orchard affect the RGB images, making it impossible to accurately recognize objects in low light; meanwhile, the dense canopy of the trees can cause interruptions in the GNSS signals. In contrast, LiDAR is unaffected by these factors, providing the basis for automatic navigation by using DBSCAN, K-means, and RANSAC algorithms. In this study, by combining DBSCAN, K-means, and RANSAC algorithms, the results of 761 points returned by LiDAR were firstly based on density clustering to find the object location, then divided into left and right groups, and eliminated the noise points to get the accurate boundary lines, and got the steering angle based on the middle line of two boundary lines with the present direction of the vehicle, in order to control the vehicle to move safely in the orchard.

But LiDAR as the only sensor has many limitations. In this study, since LiDAR cannot recognize the target object, the accuracy of the system was increased by limiting the scanning distance of LiDAR to control only the target object within the scanning range of LiDAR. For smarter navigation systems, sensors can be added for wider use. For example, thermal camera is less affected by lighting conditions and can be used with LiDAR to enable target recognition in different lighting conditions (Jiang et al., 2022).

The fusion of LiDAR and thermal camera vision has now been realized in this study. Due to the special imaging principle of the thermal camera, this study calibrated the thermal camera using a specific calibration plate. The calibration plate was made of acrylic with circular holes (Fig. 6.11a), and when the calibration images were taken, the plate was heated by a heat gun to extract more accurate images by utilizing the thermal camera's characteristics (Fig. 6.11b). After capturing several images from different orientations, the camera was calibrated using MATLAB R2021b® to obtain the intrinsic parameters.

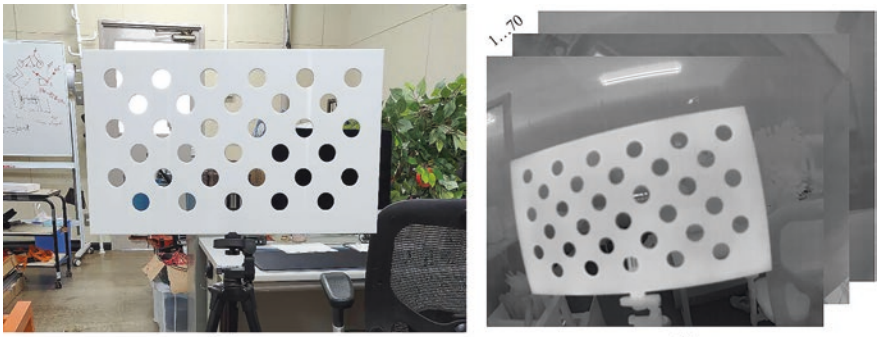

Fig. 6.11 Calibration of thermal camera. (**a**) Special acrylic calibration plate used in this study. (**b**) 70 calibration images taken after heating the acrylic calibration plate

The Perspective-N-Point (PNP) algorithm can estimate the camera pose by calculating the projection between N feature points in the world and N image points in the image. In this study, the world coordinates and pixel coordinates of 16 points were used to calculate the camera's extrinsic parameters. Through Eq. (6.1), the LiDAR data points can be converted into pixel coordinates and displayed in the camera image (Fig. 6.12).

$$s\begin{bmatrix} u \\ v \\ 1 \end{bmatrix} = \begin{bmatrix} f_x & 0 & c_x & 0 \\ 0 & f_y & c_y & 0 \\ 0 & 0 & 1 & 0 \end{bmatrix} \begin{bmatrix} R & t \\ 0 & 1 \end{bmatrix} \begin{bmatrix} X_w \\ Y_w \\ Z_w \\ 1 \end{bmatrix} \tag{6.1}$$

where (u, v) is the image pixel coordinate, (f_x, f_y) is thermal camera focal length, (c_x, c_y) is camera optical center, these parameters were obtained from the camera's intrinsic parameter calibration. R is a 3 × 3 rotation matrix, t is a 3 × 1 transformation matrix, these parameters were obtained from the camera's extrinsic parameter calibration. (X_w, Y_w, Z_w) is world coordinate measured by LiDAR.

In our further research, we will incorporate deep learning algorithms that will enable this project to recognize the types of target objects, overcoming the limitations of LiDAR for positional estimation in vehicle navigation.

6.5 Conclusions

Real-time automated navigation is a challenging task due to the complex environmental conditions in orchards. In order to overcome the problems of low light and signal occlusion, a 2D LiDAR was selected as the only sensor and combined with

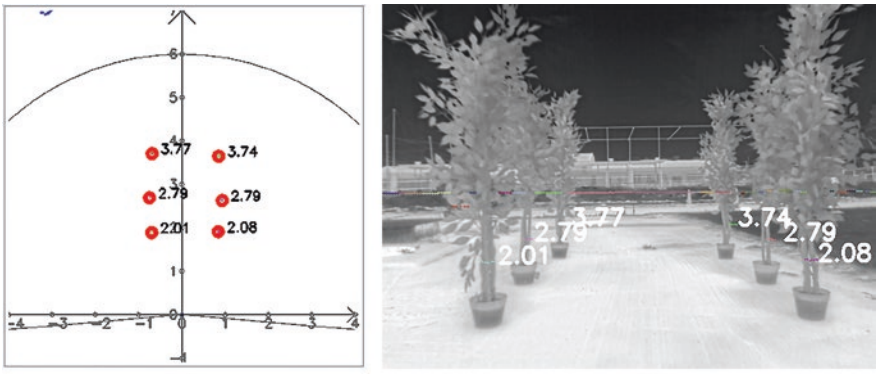

Fig. 6.12 Fusion of LiDAR data and thermal camera image: (**a**) LiDAR returned data, (**b**) LiDAR data in thermal image

DBSCAN, K-means, and RANSAC algorithms to realize a real-time navigation system in an orchard in this study. The experiments were first calibrated on concrete road and later tested in an artificial-tree-based orchard. The experimental results showed that this system can plan to get an accurate path in the orchard and lead the vehicle to operate safely. Because this system has only one sensor, the algorithm complexity is low and does not need to rely on computers with powerful computing capabilities.

This experiment demonstrated that LiDAR can be utilized as the only sensor for real-time navigation system. However, LiDAR can only detect the distance of the object and cannot distinguish the category of the object, so it is necessary to make sure that there are no other obstacles in the scanning range, otherwise it will reduce the accuracy of the system. However, limiting the range of scanning reduces the number of objects and k-means may make errors in clustering. Densely planted fruit tree joint orchards can provide LiDAR with higher-density point clouds compared to conventional orchards, and in the algorithm for planning path, the number of objects on the left and right sides increases, which improves the accuracy of clustering and leads to higher accuracy results. In order to achieve a smarter real-time navigation system, this study plans to break the limitations of LiDAR by combining thermal cameras with LiDAR results to identify targets through deep learning, providing a solution for automated pesticide spraying robots in orchards to improve orchard productivity and alleviate the labor shortage problem.

Acknowledgments Thanks to Open-Access Publishers Land from MDPI to have their policy to support the authors for reusing of the published article. In this regard, we would like to extend our gratitude to Sensors Journal to publish this article (Ailian Jiang, Tofael Ahamed. Navigation of an Autonomous Spraying Robot for Orchard Operations Using LiDAR for Tree Trunk Detection, Sensors, 23(10), 4808; https://doi.org/10.3390/s23104808, 2023). Some modifications have been conducted in this book chapter. This study was supported by grants from the Japanese Society of Promotion Science JSPS Kiban C (Grant Number 21 K05844) and JST SPRING, grant number JPMJSP2124. The authors would like to thank the Tsukuba Plant Innovation Research Center (T-PIRC), University of Tsukuba, for providing facilities for conducting this research in its orchards.

References

Bergerman, M., Billingsley, J., Reid, J., & van Henten, E. (2016). Robotics in agriculture and forestry. In *Springer handbook of robotics* (pp. 1463–1492). Springer.

Chen, J., Qiang, H., Wu, J., Xu, G., Wang, Z., Liu, X. J. C., & Agriculture, E. I. (2020). Extracting the navigation path of a tomato-cucumber greenhouse robot based on a median point Hough transform. *Computers and Electronics in Agriculture, 174*, 105472

Dang, N. T., & Luy, N. T. (2022). LiDAR-based online navigation algorithm for an autonomous agricultural robot. Journal of Control Engineering and Applied Informatics, 24(2), 90–100.

Jiang, A., Noguchi, R., & Ahamed, T. (2022). Tree trunk recognition in orchard autonomous operations under different light conditions using a thermal camera and faster R-CNN. *Sensors, 22*(5), 2065.

Li, M., Imou, K., Wakabayashi, K., & Yokoyama, S. (2009). Review of research on agricultural vehicle autonomous guidance. *International Journal of Agricultural and Biological Engineering, 2*(3), 1–16.

Mousazadeh, H. (2013). A technical review on navigation systems of agricultural autonomous off-road vehicles. *Journal of Terramechanics, 50*(3), 211–232.

Subramanian, V., Burks, T. F., & Arroyo, A. A. (2006). Development of machine vision and laser radar based autonomous vehicle guidance systems for citrus grove navigation. *Computers and Electronics in Agriculture, 53*(2), 130–143. https://doi.org/10.1016/j.compag.2006.06.001

Sun, H., Slaughter, D. C., Ruiz, M. P., Gliever, C., Upadhyaya, S. K., & Smith, R. F. (2010). RTK GPS mapping of transplanted row crops. *Computers and Electronics in Agriculture, 71*(1), 32–37. https://doi.org/10.1016/j.compag.2009.11.006

Takagaki, A., Masuda, R., Iida, M., & Suguri, M. (2013). Image processing for ridge/furrow discrimination for autonomous agricultural vehicles navigation. *IFAC Proceedings Volumes, 46*(18), 47–51. https://doi.org/10.3182/20130828-2-SF-3019.00045

Wang, X., Pan, H., Guo, K., Yang, X., & Luo, S. (2020). *The evolution of LiDAR and its application in high precision measurement.* Paper presented at the IOP Conference Series: Earth and Environmental Science.

Chapter 7
Driver Safety System for Agricultural Machinery Operations Using Deep Learning Algorithm

Abstract One of the most critical aspects of ensuring the safety of agricultural machinery drivers is the timely recognition and detection of dangerous actions of the driver for subsequent safe handling. This research aims to identify and classify the driver's actions while driving to determine whether the driver is in dangerous behavior and thus be able to raise an early warning. Considering that there are few studies and datasets in agricultural driving security systems, a dataset on agricultural driving is needed to assist people in this area of research. The driver action dataset collected in this research includes five categories: looking around, talking, playing on the phone, drowsiness, and normal driving. In this research, offline and online training validation methods were designed to evaluate the classification performance of video classification algorithms by a modified MoViNet model. Considering that the safety system requires very high real-time performance, this research replaced all 3D convolutions of the model with depth-separable convolutions to obtain the contextual semantic information of the temporal layer and spatial dimensional information, and CGAP obtained the temporal layer. The SE block obtained spatial dimensional information. The model had 70% offline classification accuracy, 70% regression, 70% accuracy, 0.70 F1 scores, and 0.90 AUC scores on the validation set. The offline classification accuracy of the model on the test set was 80%, the recall rate was 79%, the prediction was 81%, the F1 score was 0.79, and the AUC score was 0.93. At the same time, the model could achieve 10 fps when inferring online, and the recognition effect did not decrease, basically realizing real-time online processing. In conclusion, this research contributed to developing agricultural driving safety systems and facilitated the researchers' study in the same field.

Keywords Agricultural driving safety system · Deep learning · Video classification

© The Author(s), under exclusive license to Springer Nature Singapore Pte Ltd. 2024

T. Ahamed, *IoT and AI in Agriculture*,
https://doi.org/10.1007/978-981-97-1263-2_7

7.1 Introduction

Between 2016 and 2020, there were 333 known accidents of agricultural machinery, most of which were caused by improper operation, distracting action, or uncertain safety (National Police Agency Traffic Accident Analysis Data, 2022). As age increases, drivers are more likely to have traffic accidents. It shows that there will be more risk in agricultural driving in the future. Therefore, it is essential to build a safe and stable driver safety system to protect the drivers' security.

Jan et al. found that the use of cell phones by drivers, regardless of the driving environment, reduced their ability to respond in emergencies and increased the risk of traffic accidents (Jan & Anne, 2006). Owens et al. found that messaging while driving disturbs the driver's attention and thus increases the chance of traffic accidents (Owens et al., 2011). In 2007, the U.S. Department of Transportation concluded that fatigue was the most common cause of road safety accidents (Nordbakke & Sagberg, 2007). These data show that distracted action and fatigue are essential in driving safety systems, and how to quickly and accurately identify and alert drivers to dangerous actions is one of the most critical issues to address.

Various technologies have been developed to detect driver actions, and these technologies can be broadly classified into three classes. First, data analysis using on-board sensors; second, direct access and analysis of the driver's body information through physical devices; and third, computer vision and machine learning techniques for driver action detection.

The first method is a recognition algorithm based on vehicle driving information and state (such as speed, acceleration, steering wheel rotation, and other information). For example, through on-board sensors, the steering wheel rotation is monitored to obtain the steering wheel operation characteristics in the fatigue driving states, such as slow route drift and fast corrective counter-steering; subsequently, machine learning classification algorithms such as support vector machine (SVM) and K-Nearest Neighbor are used to classify the driver's driving behavior characteristics to identify whether the driver is fatigued or not (Krajewski et al., 2009). However, relying solely on steering wheel rotation information increases the risk of error. Das et al. applied steering wheel rotation data to the judgment of drunk driving and found that accurate judgment could not be made simply by combining this type of data with machine learning methods (Das et al., 2012). It was also proposed to combine control data such as throttle and brake data, Driving Under the Influence (DUI) history, and others. Combining control data such as throttle and brake data, DUI history, and other data for judgment may be the solution.

The second method is the recognition algorithm based on driver bioelectrical signals and physiological information. Among them, bioelectrical signals mainly include electroencephalogram (EEG), electrocardiogram (ECG), and electrooculogram (EOG) signals, while physiological information includes blood pressure and pulse. Applying the above information, related studies (MARDI et al., 2011) achieved a great result. However, this method requires many sophisticated instruments to monitor the driver's physical condition in real time, which could be more

conducive to normal driving. In contrast, this type of technology is generally applied to specific driving scenarios and is not robust in the natural environment. The measurement instruments are expensive and cannot be integrated into the car, and these drawbacks also seriously limit the development and popularity of this method.

The third method is a computer-vision-based recognition algorithm, which is also an important method for commercial use. This method does not require sensors on the human body and is relatively inexpensive and straightforward to set up; at the same time, compared to the first method, it has better adaptability and can be analyzed for a variety of behaviors. Compared to sensor data, image data are more intuitive and contain more information. Combining these advantages, this computer-vision-based recognition method has become increasingly popular and is our research's primary method. Reddy et al. used the Multi-Task Cascaded Convolutional Networks (MTCNN) model to obtain the bounding boxes of the eyes, mouth, and face. Then, they used these bounding boxes as the input of the Driver Drowsiness Detection Network (DDDN) model to obtain the classification results (Reddy et al., 2017). Zhang used the Kernel Mutual Subspace Method (KMSM) machine learning model to cluster and classify the collected data (Zhang et al., 2018). To summarize, the existing methods based on computer vision generally have the following three drawbacks: first, most of the datasets studied are from laboratory environments, which are less noisy and have less interference than natural environments; second, most of the studies are still limited to the recognition of a single action or state and most of them are limited to the recognition of fatigue driving; The third is that most methods are based on image processing and do not make good use of the temporal information of the video, while there are many categories such as looking around actually cannot fully express by using pictures and need videos to respond to the situation ideally.

This research focused on a deep learning method based on a driver behavior recognition algorithm, mainly for driver behavior recognition in in-vehicle monitoring system scenarios. The five driver behaviors were recognized, including playing with the cell phone, fatigue, talking, looking around, and normal driving.

7.2 Materials and Methods

7.2.1 The Overall Framework of the Model

With the development of AI technology, more and more research has been conducted to use machine learning in various fields of computer vision, including image classification, object detection, and pose estimation. In this research, deep learning techniques were used in driver action recognition modeling method, mainly for driver action recognition in agricultural machinery vehicle monitoring system scenarios. Considering that many actions cannot be represented by a single image (e.g., looking left and talking right) or the actions cannot be fully represented by a single

image (e.g., fatigue), combined with the increasing data processing power of processors nowadays. Therefore, this research intends to recognize the driver's actions by means of video classification. The overall framework flow of the algorithm is shown in Fig. 7.1. Firstly, we obtained single frame RGB data, depth data, and infrared data through the real-sense camera, superimposed these data in the third dimension (color space dimension) to obtain more data-rich information, then kept these frame data into the buffer, and when the number of data frames in the buffer reached 8, we input this video clip into the deep learning and then added the last four frames in the buffer. The video segment was input to the deep learning model to obtain the action classification category to which the video segment belongs, and then the action category was displayed on the monitor in real time. If the current video category belonged to the dangerous action, the system sent out the alert message of the corresponding category.

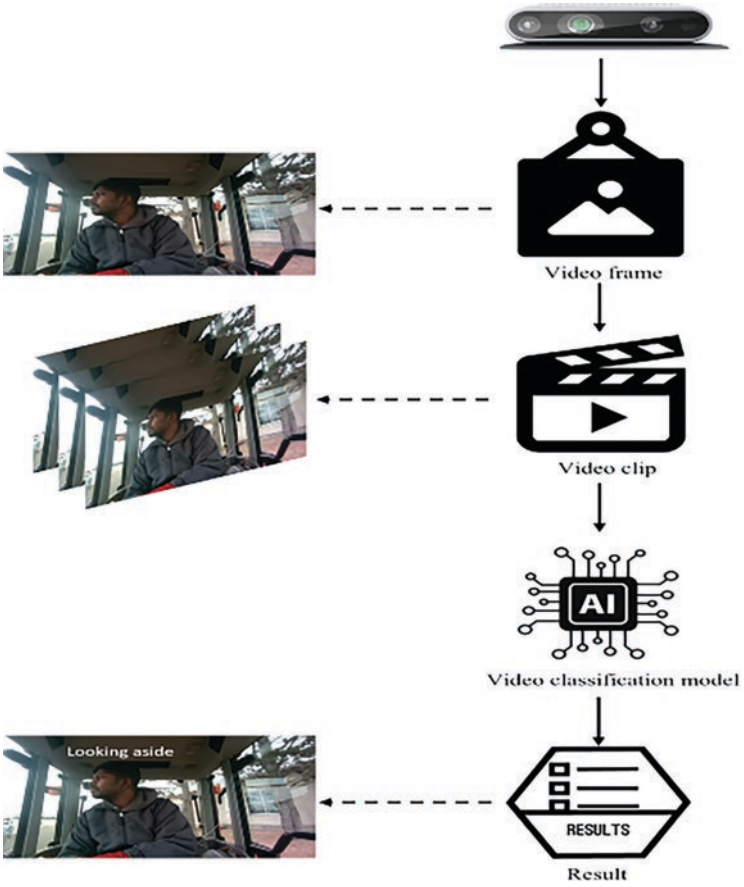

Fig. 7.1 The overall model framework of this research

7.2.2 Dataset Introduction

7.2.2.1 Data Collection Part

In contrast, the category of fatigue belongs to fatigue driving. Among the danger classes defined, distracted actions are dangerous actions that need to be alerted. At the same time, fatigue driving is a very dangerous action in the current situation and needs to be handled quickly. This research also includes normal driving because most driving situations are normal, which can make the model work in practice.

This research then explains how these dangerous actions are performed. When data are collected for each experiment, drivers are informed of the individual maneuvers and the corresponding templates before the start. They are also asked to expand on these dangerous maneuvers as they see fit. Play the phone class used the phone to send messages, read the content on the phone, and use the phone to call. In most cases, the phone's location was captured by the camera. Suppose there was an overlap between playing with the phone and other categories (e.g., looking around, talking). The classification defaulted to playing with the phone. Looking around was defined as the driver's attention is drawn to people, events, scenery, etc., outside the car, and generally, this action lasts more than 3 s or changes very frequently. Talking was defined as talking to other people in the cockpit of the agricultural machinery or outside the agricultural machinery. Fatigue was the driver's action when fatigued, usually yawning, nodding, drooping, and rubbing eyes.

The camera used in this research was the Intel real-sense D455 camera, which can acquire high resolution and high FPS RGB, depth, and infrared data compared to other ordinary RGB cameras. It also had an integrated IMU sensor inside. A series of APIs (e.g., viewer API) and the python library pyrealsense2 were provided to facilitate researchers to make better use of the camera. The main data used in the current research were RGB video data for subsequent processing. In the future, considering the wide range of utilization, infrared data were used, and the data were superimposed to four dimensions using the dimensional superposition method to further improve the effectiveness of the model input. The camera was placed in the front area of the driver, and the angle control enabled it to capture most of the driver's actions to ensure the implementation ability of the system. The layout of the sensor system was configurated as Fig. 7.2.

In real time, the driving agricultural machinery included a tractor and an agricultural golf car. The placement of the camera was basically the same as the one mentioned above, and an extra bracket was added to the camera on the golf car for better data collection. From the experiment, a total of 10 drivers of agricultural machinery operators were collected as volunteers, of whom nine were male and one was female. The video data collected focused on one person driving a tractor, and the remaining nine were driving a golf cart. The driving time was from 1:00 p.m. to 5:00 p.m. The outdoor conditions at the time of data collection included rain, clouds, sunshine, and sunlight, which almost covered the driving conditions of agricultural machinery under realistic conditions. The driving location was in T-PIRC, and the route was the T-PIRC connector road, free route was chosen according to the

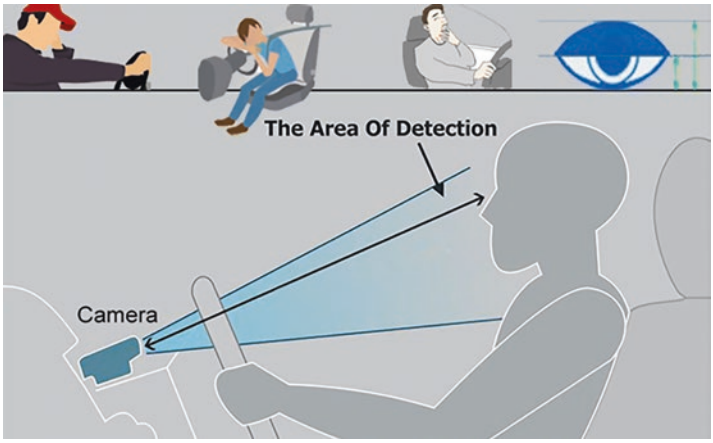

Fig. 7.2 The layout of the sensor system

Fig. 7.3 Presentation of video action dataset in five categories

driver's random choices from the connections. The driver completed the actions continuously and all actions were guaranteed to last more than 10 s to facilitate the generation of the data set (Fig. 7.3).

7.2.2.2 Data Processing

At first, the data were collected by connecting the real-sense camera to the PC via USB 3.1, and then collected the video data via the official API Intel real-sense viewer v2.44.0. The collected video data consisted of depth data and RGB data, where the

Table 7.1 Training dataset demonstration

Data class	Videos number	Input numbers
Looking aside	60	570
Playing with phone	117	1156
Drowsiness	71	661
Normal driving	122	1183
Talking	88	661

Table 7.2 Validation dataset demonstration

Data class	Videos number	Input numbers
Looking aside	18	165
Playing with phone	28	280
Drowsiness	20	188
Normal driving	27	262
Talking	19	181

parameters of depth video were 848 × 480 resolution, 30FPS frame rate, and Z16 data type, and the parameters of RGB video were 1280 × 720 resolution, 30FPS frame rate, and RGB8 data type. The video data collected through the viewer API was a bag file, which contains a lot of related data for storing ROS messages. Then the bag file was converted into a corresponding RGB video file, depth video file, RGB image, and depth image by using bag2video code, which could facilitate the subsequent processing. After that, the video editing software was used to filter out the video clips that meet the requirements of the driver's action, each video clip lasts 10 s, and these video clips were always the driver's continuous action. However, it was found that the bag file occupied too much hard disk memory; a 20-minute RGB and depth video would occupy 98G. Considering the problem of limited hard disk capacity, a later study directly obtained the original data of the frames through pyrealsense2 and OpenCV library and then saved them to the corresponding video. The video files collected by this method only took up 3G in total, which could meet the current requirements.

Considering the need to divide the dataset during training, this research divided the dataset into a training set and a validation set with a ratio of 8:2. The data of both the training set and the validation set were randomly selected after the shuffle (Table 7.1). The number of videos was the number in the dataset, each video size is 1920 × 1080 × 3 with a duration of 10 s, and the fps was 30 or 25. Meanwhile, in the actual training, the model's input data were 24 frames of video, so the input data of the model in the table were more than the number of videos. Tables 7.1 and 7.2 below show the specific distribution of the data in the training and test sets of this research.

7.2.3 Model Introduction

This section describes the deep learning models used in this study, all of which were video classification models. Compared to traditional image classification models, these models can better handle semantic information in the temporal dimension to

ensure more reliable model performance, and the dataset was also based on video. Therefore, this type of model was particularly suitable for the research.

7.2.3.1 MoViNet

Considering the current 3D convolutional detection results, although accurate but memory consumption and the number of parameters were relatively large and could not be used in a real-time environment. Therefore, Google in 2021 proposed the MoViNet model, a better model with better accuracy and computing efficiency. In comparison of the Kinetics 600 dataset, MoViNets were both more precise and more effective than 2D and 3D networks. While MoViNet-A6 achieved state-of-the-art 83.5% accuracy while being 5.1xfaster than X3D-XL Streaming, MoViNet-A2 achieved 6% higher accuracy than MobileNetV3 at the same FLOPs. MoViNets sacrificed 1% accuracy for ten times less memory usage. The network model adopted a total of three optimization strategies: (1) Using MoViNet search space, (2) Using Stream Buffers, and (3) Temporal Ensembles.

Neural Architecture Search (NAS) is a method for automating and optimizing the network architecture design process. TuNAS (Bender et al., 2020) was used to manage input data dimensions such as depth, resolution, height, and weight as parameters for the search to get a better model. In order to get the desired results for each model, the authors optimize the search in the search space for the parameters of each model. The authors expanded the search space by referring to the mobilenet-v3 model and the EfficientNet model, and instead of searching for a single model and scaling it, they searched for all six models from A0 to A5, ensuring that each model has good adaptability.

A multi-clip evaluation method is typically utilized as the input of the model in previous research to better utilize the spatial information of videos. To make better use of the semantic relationships between videos, while allowing the existence of overlapping parts of consecutive video clips. This approach had two problems: (1) the overlapping part of short video clips could only improve short semantic association, but not long-distance semantic association, which reduced the accuracy of the model; (2) this approach recalculated some video clips and thus wasted the resources and affected the efficiency.

To solve this problem, this research used the stream buffer module to replace the previous multi-clip evaluation method. The Stream buffer method no longer required overlapped consecutive video clips; each input was a different video clip from the previous one, and the use of buffers allows the model to better use the long-distance semantic association (Fig. 7.4).

Considering the unidirectionality in the video time dimension, the casual convolution had better support for unidirectionality compared to the bidirectionality of normal convolution. This research substituted all temporal convolutions with Causal Convolution (Oord et al., 2016), making them effectively unidirectional along the temporal dimension by taking advantage of the translation equivariant aspect of convolution. Because the input part used the stream buffer method, no additional

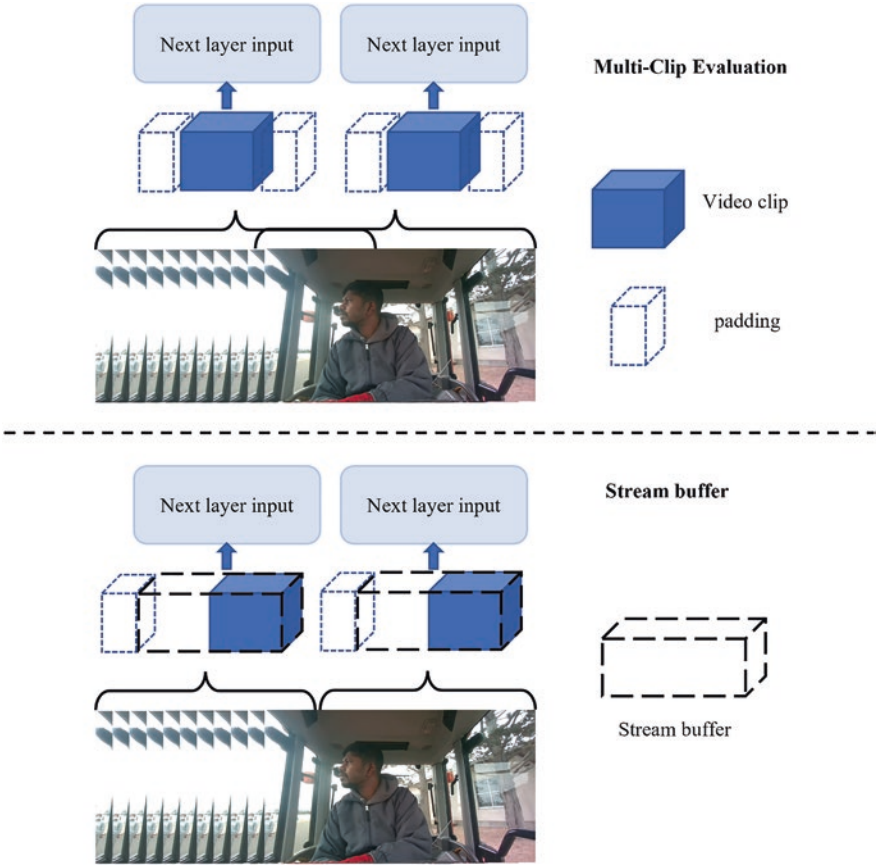

Fig. 7.4 Multi-clip evaluation(up) vs stream buffer(down)

padding was needed, and the data inside the last stream buffer could be directly used as the padding part. In this case, it is necessary to ensure that the temporal kernel size k of the cascaded convolution was equal to the size of the stream buffer plus one. The comparison of these normal Convolution and Causal Convolution is shown in Fig. 7.5.

In order to better utilize the performance of the model without increasing the flops of the model, this research used an ensemble method by averaging the prediction results of two small models to obtain more accurate results. This research trained two MoViNets separately using the same architecture but with a frame rate cut in half and training time kept constant (leading to a 50% decrease in the overall number of input frames). In this research, the video was input into both networks, one network's frames were offset by one frame, and the unweighted logits were given an arithmetic average before being subjected to SoftMax. Before half the frame rate, this method generated a bi-model integration with the same FLOP as the single model, yielding a prediction with a rich representation.

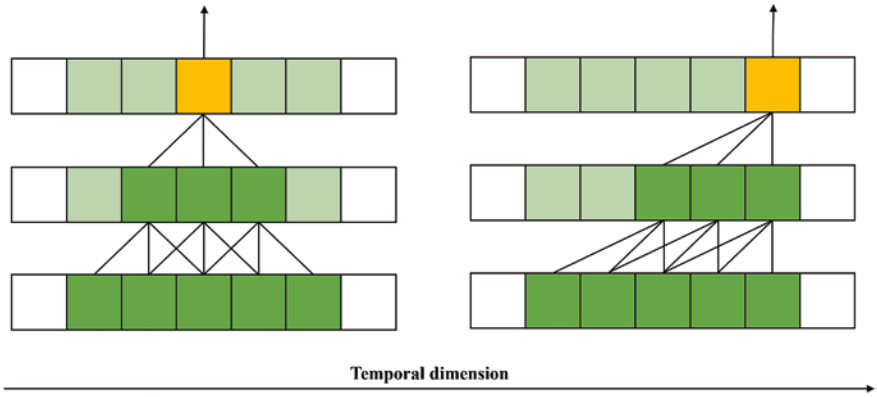

Fig. 7.5 Convolution(left) vs Causal Convolution(right)

7.2.3.2 Model Module

In addition to the methods employed above, this study also employed a modified SE block. The Squeeze-and-Excitation Network (SENet) was the ILSVRC 2017 competition's winning architecture (Hu et al., 2018), and the SE block is an important component of SENnet, which greatly improves the accuracy rate with only less than 2% improvement in consumption, reaching a good result of 2.25% top-five error rate in the 2017 competition. The SE block had three main components. First, each two-dimensional feature channel was converted into an actual number by the Squeeze operation, which compressed features according to the spatial dimension. This number had a global perceptual field, and the output dimension was the same as the number of input feature channels. It describes how results are distributed globally throughout the feature channels. Additionally, it enables layers near the input to have a global field of vision, which is quite helpful for various tasks. Next is the excitation operation, similar to the gating in recurrent neural networks. A parameter w is used to generate weights for each feature channel, where the learning of parameter w explicitly simulates the correlation between feature channels. Finally, the reweight operation was conducted. We attached importance to the output weight of the exception as the importance of each feature channel after feature selection and then completed the rescaling of the original feature on the channel dimension by multiplying the weight one by one with the previous feature channel. The input of the SE block was the concat of the current spatial dimension information and the spatial-temporal cumulative information on the special diagnosis map by using the spatial 3D pooling and Cumulative Global Average Pooling (CGAP) methods and the specific display (Fig. 7.6).

MobileNet v1 (Andrew & Menglong, 2017) is an efficient deep convolutional network proposed by Google in 2017, while depth-wise separable convolution is a convolutional module proposed in MobileNet v1. ReZero (Bachlechner et al.,

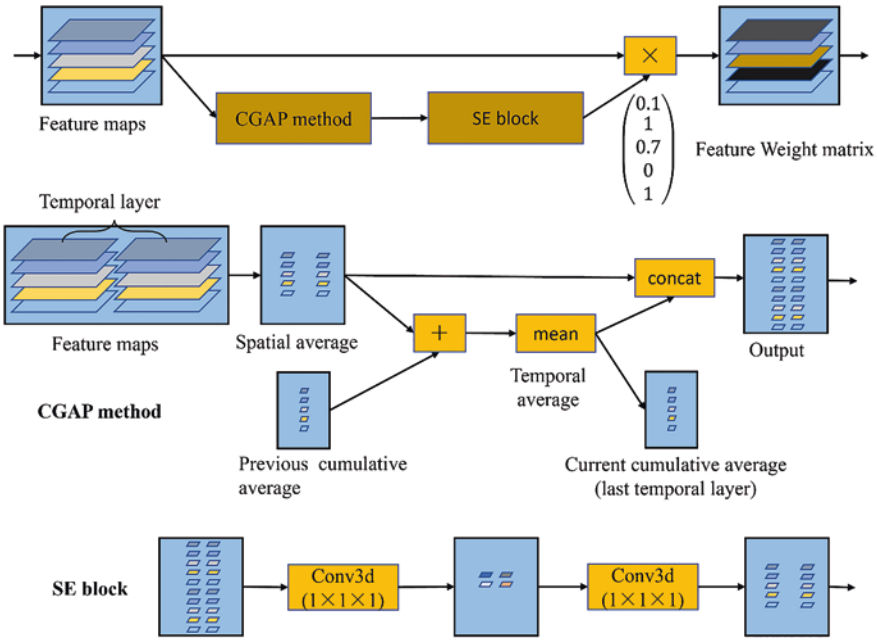

Fig. 7.6 Revised SE block (CGAP module added)

2021) initialized all network layers as constant mappings. In each layer, the researchers introduce a residual connection with respect to the input signal x and a trainable parameter α that regulates the output $F(x)$ of the current network layer. α is set to zero at the beginning of the training. As a result, all gradients related to the parameters making up the transform F vanish at the start of neural network training. These parameters are then dynamically produced with the proper values during the training process. ReZero brings two main benefits: (1) the ability to train deeper neural networks and (2) faster convergence. Therefore, the ReZero method is used for each residual connection block in this study. The specific formula is shown below:

$$x_{i+1} = x_i + \alpha_i F\left(x_i\right) \tag{7.1}$$

By combining some of the above methods, a basic block can be formed. These basic block blocks remain basically the same throughout the model architecture, and the overall structure is the same except for some parameters that need to be changed or the entry convolutional layers, ensuring that the overall structure of the model is not very difficult to code. The base model layer consists of an expansion layer, a depth separation layer, a modified SE-BLOCK layer, and a point-wise layer, and this base model layer appears in large numbers as the base module of the overall model.

7.2.3.3 Loss Function

The loss function utilized in this work is the cross-entropy loss function, which aims to reduce the difference between the prediction function distribution and the actual distribution of the model. This chapter will detail the cross-entropy loss function and how to use it for training.

According to Shannon, the founder of information, "information is something that is used to eliminate random uncertainty," which means that the size of information is measured by the degree to which the information eliminates uncertainty. The probability of the information happening is negatively correlated with the amount of information. The amount of information decreases as the likelihood increases, and the number of information increases as the likelihood decreases. Let the probability of an event occurring be $P(x)$, quantities of information $I(x)$ is expressed as: $I(x) = -\ log\ (P(x))$. Information entropy, also known as entropy, is used to express the expectation of all information quantities. The expectation is the sum of the probabilities of each possible outcome in the experiment multiplied by its outcome. Therefore, the entropy of the information quantity can be expressed as follows: (here X is a discrete random variable)

$$\mathrm{H}(X) = -\sum_{i=1}^{n} P(x_i)\log\left(P(x_i)\right) \quad \left(X = x_1, x_2, x_3 \ldots, x_n\right) \tag{7.2}$$

The Kullback-Leibler divergence can be used to quantify the difference between two probability distributions $P(x)$ and $Q(x)$, which are two different probability distributions for the same random variable X. In machine learning, we frequently use $P(x)$ to represent the sample's actual distribution and $Q(x)$ to represent the distribution that the model predicts. The smaller the Kullback–Leibler divergence, the closer the distributions of $P(x)$ and $Q(x)$, and the meaning of training is to make the distribution of $Q(x)$ close to $P(x)$ by repeatedly training $Q(x)$ to obtain the best model parameters.

$$D_{KL}(P \quad Q) = \sum_{i=1}^{n} p(x)\log\frac{p(x)}{q(x)} \tag{7.3}$$

$$= \sum_{i=1}^{n} p(x)\log\frac{1}{q(x)} - \sum_{i=1}^{n} p(x)\log\frac{1}{p(x)}$$

$$= H(P,Q) - H(P)$$

In machine learning training networks, the actual probability distribution $P(x)$ is determined after the input data and labels, so the information entropy *(H(P))* in this case is constant. The smaller the value, the better the prediction, as Kullback-Leibler divergence measures the difference between the true probability distribution $P(x)$ and the anticipated probability distribution $Q(x)$. So the Kullback–Leibler divergence needs to be minimized, and the cross-entropy is equal to the Kullback–Leibler

divergence plus a constant (information entropy), and the formula is easier to calculate than the Kullback–Leibler divergence, so the cross-entropy loss function *(H(P,Q))* is often used in machine learning to calculate the loss.

$$H(P,Q) = -\sum_{i=0}^{n} p(x) \log q(x) = -\log q_m \tag{7.4}$$

Therefore, the cross-entropy function can be optimized by simply taking the log-softmax value of the correct label and then taking the negative sign that is the cross-entropy loss, and the implementation in pytorch is through Logsoftmax layer and NLLLoss layer.

7.3 Results and Discussion

7.3.1 Environment for Training and Evaluating

The model training lasted for a total of 50 epochs and nearly 70 h. The training environment was on a local laptop with Intel(R) Core (TM) i7-9750H CPU @ 2.60GHz, Nvidia GeForce GTX2070 GPU, Windows 10 Home Edition, and Cuda version v11.6.124. The software environment was Python 3.8.15, PyTorch 1.13.0, TensorBoard 2.9.0, torchvision 0.14.0, OpenCV-Python 4.6.0.66, pyrealsense2 2.47.0.3313.

7.3.2 Evaluation Metrix

The main evaluation metrics utilized in this research are loss, precision, recall, accuracy, F1 score, PR curve, ROC curve, and confusion matrix. The other evaluation metrics will be explained in detail later. Precision is the proportion of positive samples that the model correctly predicts to be positive samples. The proportion of positive samples that were expected to be positive is known as recall. The precision and recall rates are combined to provide the F1 score, an evaluation index. The formula is described in the following part. The Receiver Operating Characteristic (ROC) curve, which has the axes FPR (the false positive rate) and TPR (or recall), is mainly used to assess the overall effectiveness of the examined classifier. The area measures the area under the ROC curve under curve (AUC), and the bigger the AUC, the more influential the model is. A standard format for expressing accurate evaluation in the form of an n-row and n-column matrix is the confusion matrix, often known as the error matrix. For simplicity of description, Fig. 7.7 shows a simple confusion matrix in binary classification.

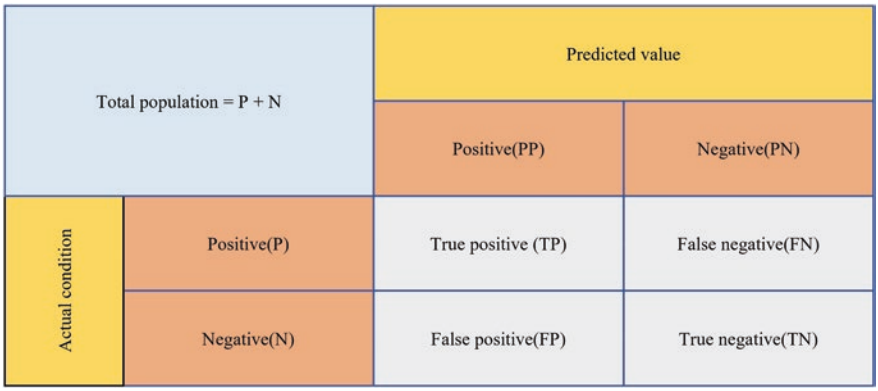

Fig. 7.7 Binary classification confusion matrix example

$$\text{Precision} = \text{PPV} = \frac{TP}{TP + FP} \tag{7.5}$$

$$\text{Recall} = \text{TPR} = \frac{TP}{P} = \frac{TP}{TP + FN} \tag{7.6}$$

$$\text{Accuracy} = \text{ACC} = \frac{TP + TN}{P + N} = \frac{TP + TN}{TP + TN + FP + FN} \tag{7.7}$$

$$\text{FPR} = \frac{FP}{N} = \frac{FP}{FP + TN} \tag{7.8}$$

$$F_1\text{score} = \frac{2}{\frac{1}{Precision} + \frac{1}{Recall}} = \frac{2TP}{2TP + FP + FN} \tag{7.9}$$

7.3.3 Model Results

The model training lasted for a total of 50 epochs and nearly 70 h, and the training method was performed. The batch at training time was four, and the rest of the hyperparameters were described. The loss plot during training is shown in Fig. 7.8, and the cross-entropy loss of the final model slowly decreased until it was equal to about 0.08, which showed that the model was learned and improved. However, because the loss was accumulated in training using multi-loss, there was a threefold loss accumulation compared to other models, so the loss's value was higher than the other models.

The loss collection method for the validation set differed from the training one. The loss was generated once per epoch, while the training one was recorded once per iteration. From Fig. 7.9, the loss was unchanged. However, the actual model was

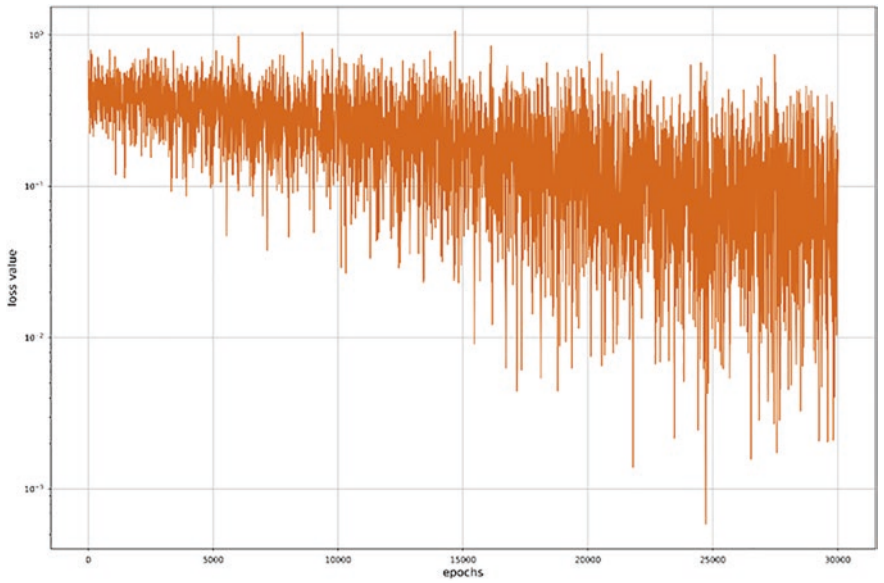

Fig. 7.8 Losses for each iteration during the training dataset

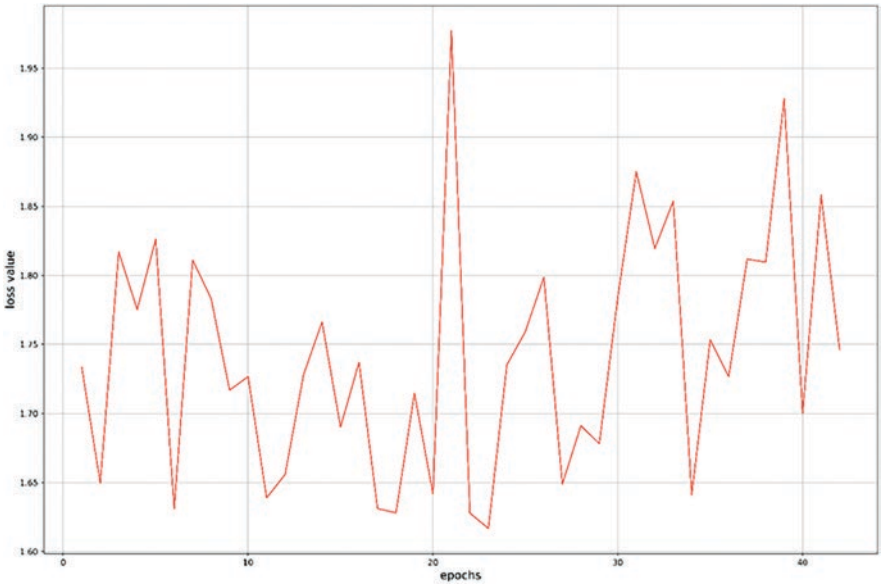

Fig. 7.9 Average losses for each epoch during the validate dataset

learned and improved because this research used gradient cropping during training. Therefore, the high gradients were removed from the model, and the overall average was hardly any change.

The recall rate curves of different categories and total accuracy curves during the training process are shown in Fig. 7.10. As for the precision curves during training, because the corresponding precision values were not saved in the first 21 epochs of training, the corresponding precision curves were only kept for the subsequent epochs. The graph of precision is shown in Fig. 7.11. As seen from this series of plots, the model could learn the pattern information for the play phone fatigue

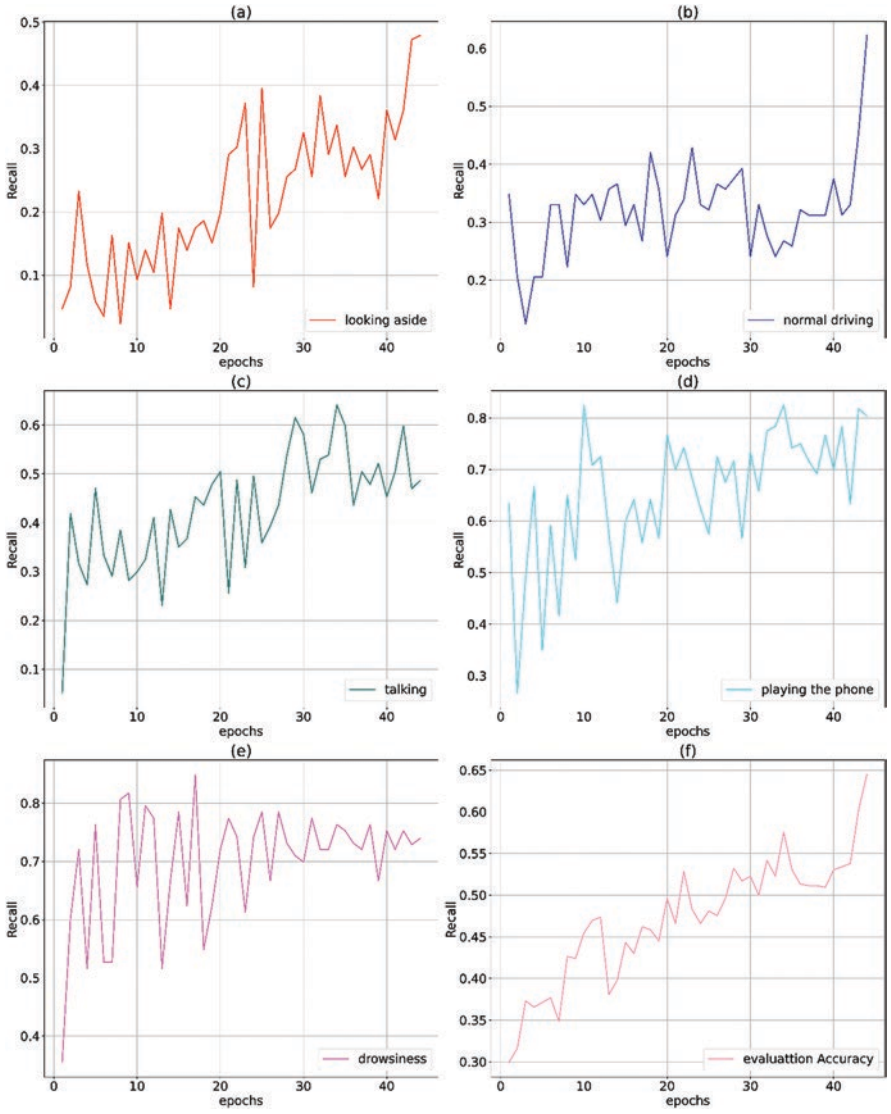

Fig. 7.10 Five classes recall rate curves and evaluation accuracy curves (**a**) looking aside recall rate curve (**b**) normal driving recall rate curve (**c**) talking recall rate curve (**d**) playing the phone recall rate curve (**e**) drowsiness recall rate curve (**f**) evaluation accuracy curve

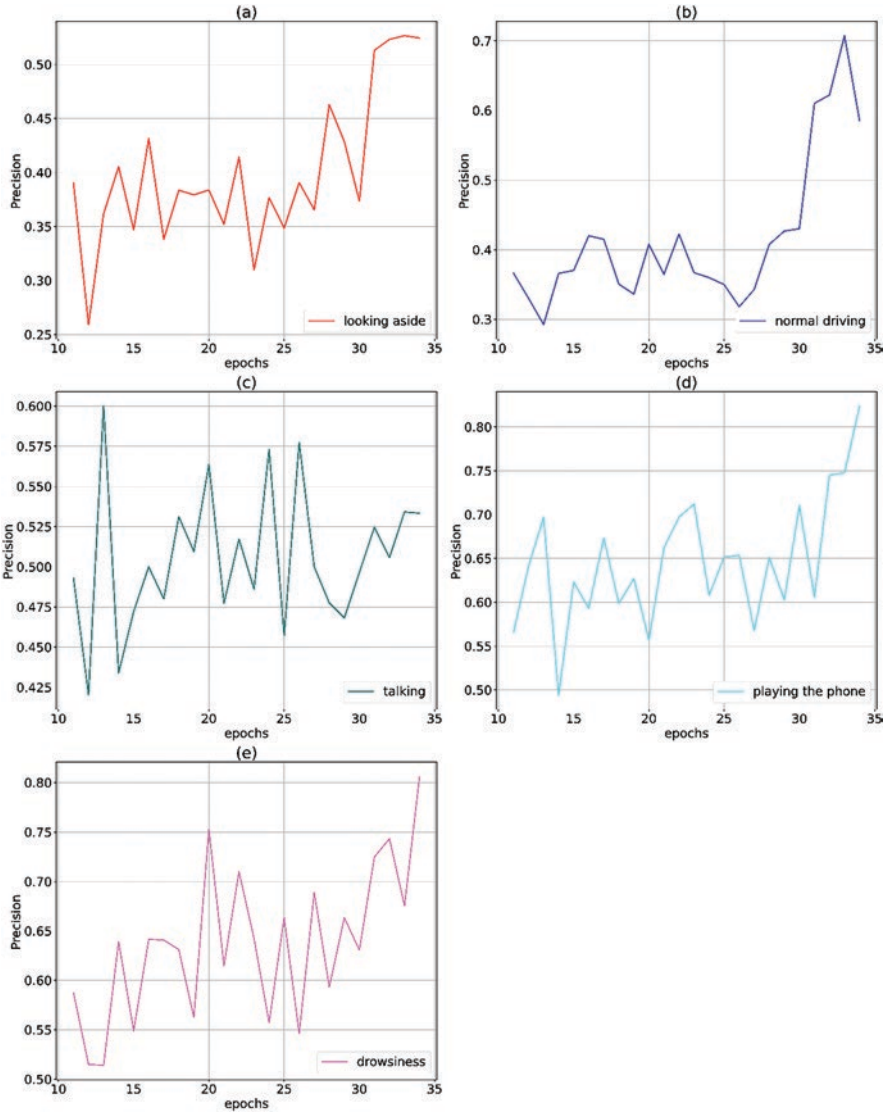

Fig. 7.11 Five classes precision rate curves (**a**) looking aside precision rate curve. (**b**) normal driving precision rate curve. (**c**) talking precision rate curve. (**d**) playing the phone precision rate curve. (**e**) drowsiness precision rate curve

category within a few epochs. In contrast, the categories of normal driving, talking, and looking to the left and right are slowly improved and accompanied by some degree of oscillation. This is consistent with the hypothesis of this study that these three categories were linked. Also, as seen from the graphs, the curves still tend to improve, indicating that the model needs to be trained to perfection.

It was considered that probabilities are easier to see the model prediction categories and the difficult part of the model. The probability confusion matrix for the five categories is shown in Fig. 7.12. It was clear from the figure that the probability of predicting both playing with the phone and fatigue was over 80%, which achieved an excellent result. However, the classification of looking aside, talking, and normal driving was not particularly good. The confusion matrix showed that the model had a 17% probability of predicting the looking aside label as talking, which was consistent with our hypothesis at the beginning, because much of the collected data did appear to be talking when looking around. Similarly, the talking category could easily overlap with the looking around and talking categories, so it was easy to predict both categories as well. As for normal driving, sometimes drivers faced forward and said one or two words, which this research thought either normal driving or talking was ok, so it could be easy to understand why the prediction was wrong. As for why a large part of normal driving was predicted as playing with cell phones and drowsiness, this needs further analysis. Then, in order to eliminate the classification errors caused by the overlap of these categories, this research adjusted the model prediction results to three categories: distracted action (looking aside, playing the phone, talking), normal driving, and drowsiness, resulting in Fig. 7.13, which showed that the classification probabilities of distracted action and fatigue action were quite good, reaching more than 80%, achieving a perfect classification effect.

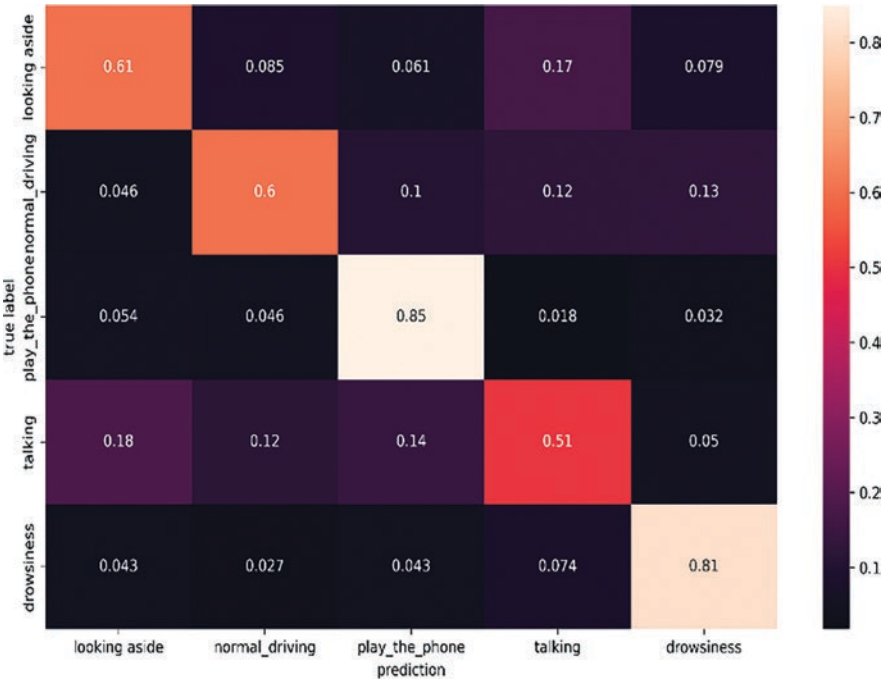

Fig. 7.12 Confusion matrix of actual five categories

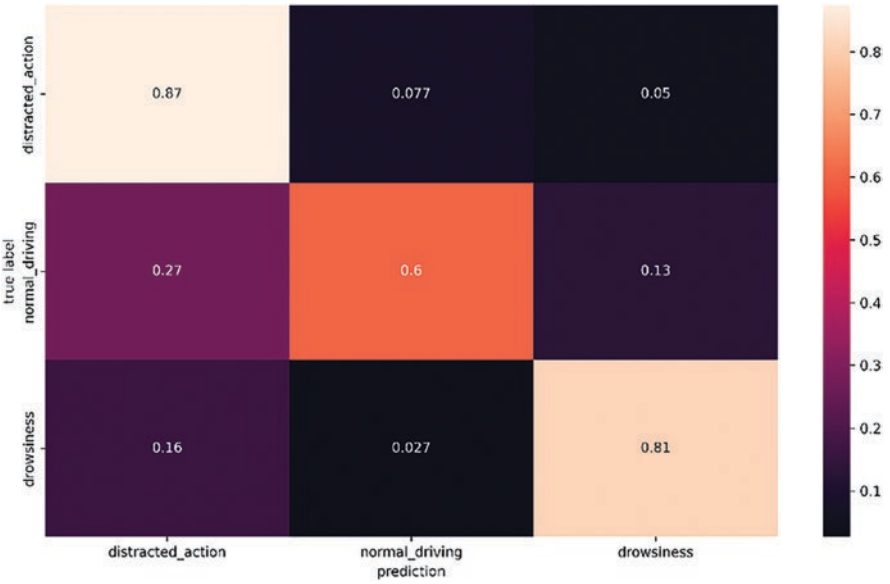

Fig. 7.13 Confusion matrix of revised three categories (distracted action, normal driving, and drowsiness)

Figure 7.14 shows the Receiver Operating Characteristic (ROC) curves for each of the five categories and the macro-average ROC curve. The ROC is a curve describing the ability of the model. It showed that the model had good classification ability for talking and fatigue but could have better classification ability for talking, normal driving, and looking around. This is the area that needs to be focused on in the future.

Table 7.3 presents all the metrics for each category and the overall model. The accuracy, recall rate, F1 score, and AUC score for each category are included, as well as the accuracy, recall rate, F1 score, accuracy, and AUC score for all categories.

7.3.4 Online Model Realization and Result Display

Previously, the model was verified offline by training. Although the model's results were satisfactory, they were not verified to the real-time core aspect; therefore, the purpose of this section was to demonstrate the model's results in a practical setting. The actual online demonstration environment was implemented through the laptop as well as the training, and the online demonstration steps and data acquisition methods were almost the same. Considering that the model was an action video classification model, this study did not pass the image frames into the model frame by frame but cumulatively. A predefined container buffer was used to store the

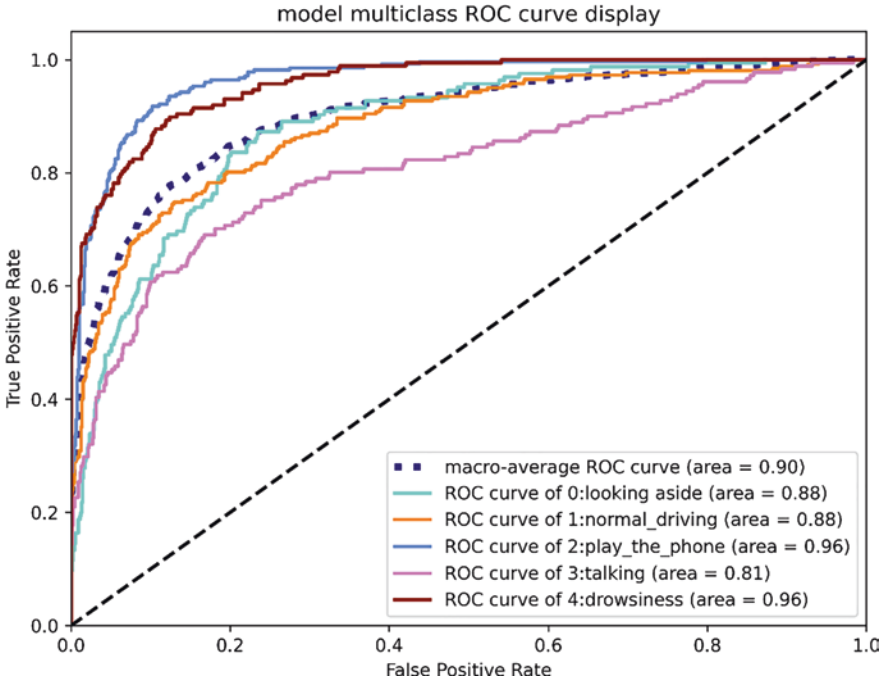

Fig. 7.14 Presentation of ROC curves for all categories and category macro-average ROC curves

Table 7.3 Final model results for each evaluation metrics

Class	Precision	Recall	Accuracy	F_1 score	AUC score
Looking aside	59%	61%		0.60	0.88
Normal driving	76%	60%		0.67	0.88
Play phone	80%	85%		0.82	0.96
Talking	55%	51%		0.53	0.81
Drowsiness	73%	81%		0.77	0.96
Oval all	70%	69%	70%	0.69	0.90

frames, and when the number of container frames reached 8, all the data frames in the container were passed to the model to produce a classification result. Then the first four frames in the container were discarded, and new frames accumulated. The detailed presentation is shown in the figure below (Fig. 7.15).

This research then showed the results of the online model implementation. Putting a video file in the paper was impossible, so the result graphs were presented through images with category prediction probability timelines (Fig. 7.16).

As shown by the above probabilities over time, the categories had good understanding of the actual semantic information, and the categories of the current video

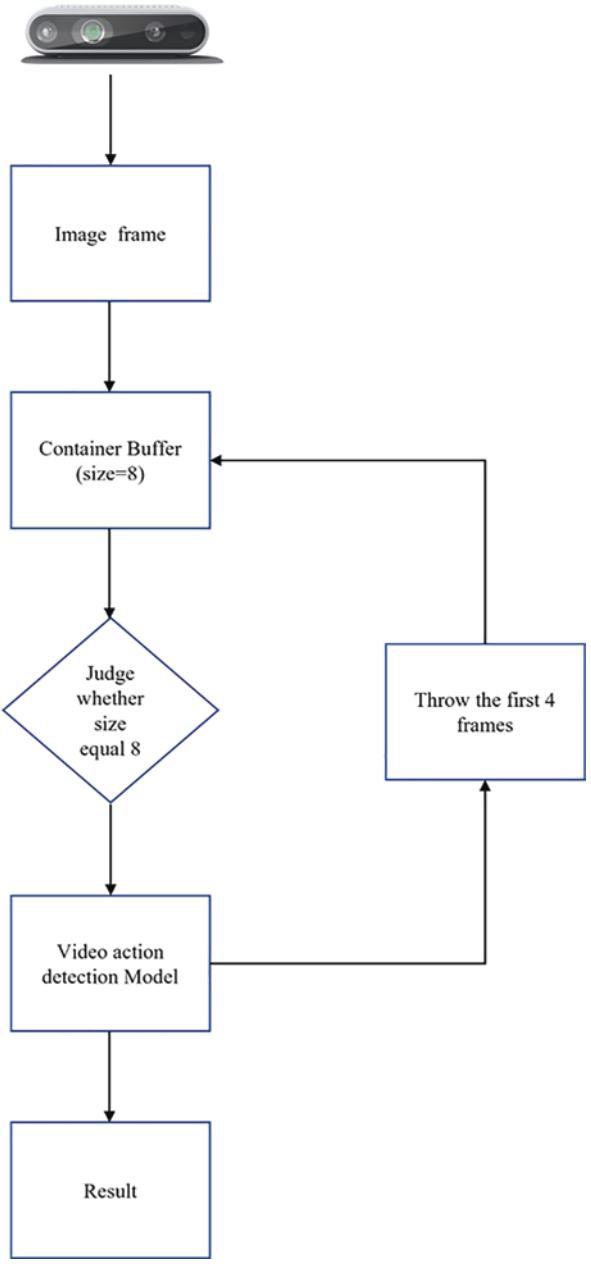

Fig. 7.15 Model online implementation methodology

clips could be obtained by judging certain clips of certain videos. However, the model has had a high bias for talking class, and it was easy to judge other categories as talking category causing misjudgment; hence, we need to focus on this aspect in the future.

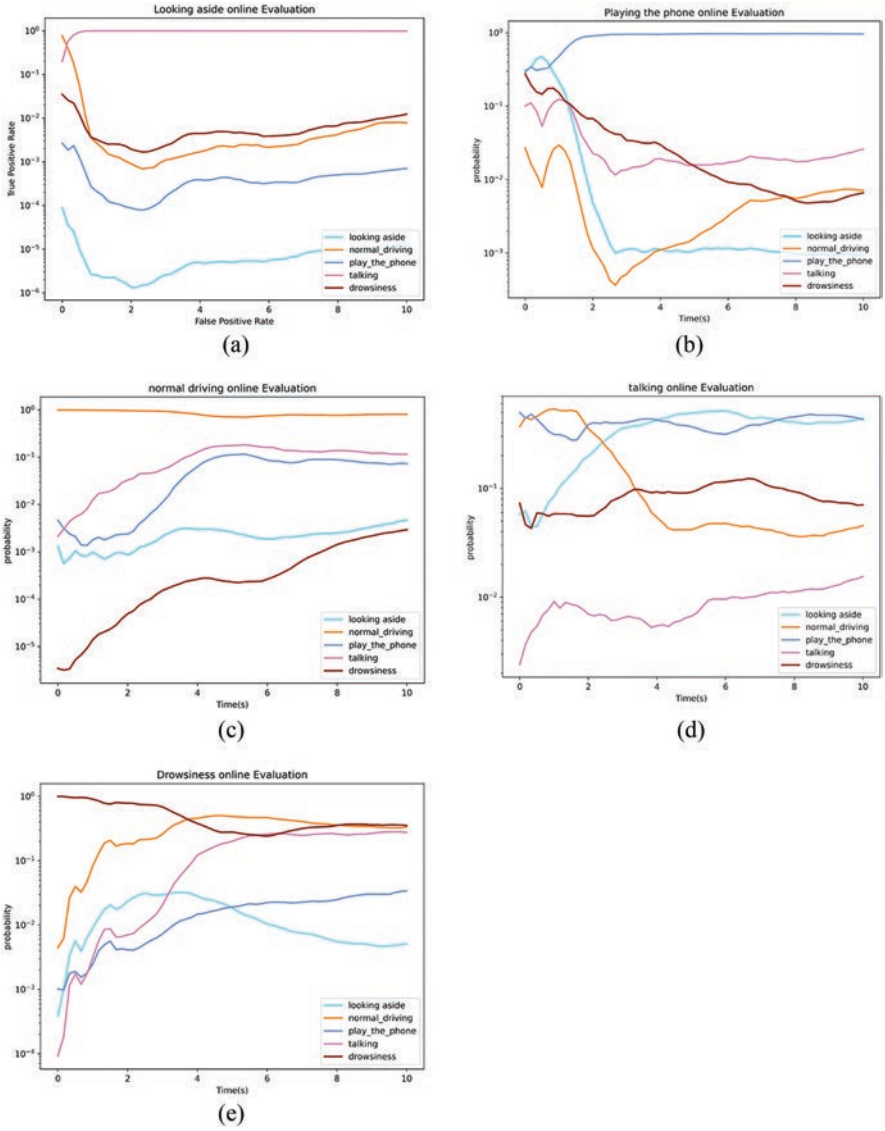

Fig. 7.16 (**a**) Looking aside online action prediction probability graphs over time; (**b**) Playing the phone online action prediction probability graphs over time; (**c**) Normal driving online action prediction probability graphs over time; (**d**) Talking online action prediction probability graphs over time; (**e**) Drowsiness action prediction probability graphs over time

7.3.5 Discussion

This research has experimentally validated the feasibility and effectiveness of the model by substituting video classification models and deep learning algorithms into agricultural driving safety systems. The above result graph showed that the model

has robust classification and real-time prediction capabilities, and these advantages indicated that the model could be applied in practice. However, as described in the introduction of the figure results, the model was prone to misclassification for semantically overlapping actions, which required further support for the data component. There is room for improvement in the model's accuracy, so subsequent research will focus on this aspect.

7.4 Conclusions

This research aimed to develop a driving safety system for agricultural machinery to ensure the safety of the driver and the vehicle's occupants. Several works have been completed in this research, including system and model architecture design, development of video action classification algorithms for driver distracted and fatigue actions, the creation of driver action dataset, and experimental validation of the model in the field. The main contributions and future work of this research are summarized below. Three categories of distracted action behaviors and one category of fatigue action behaviors were defined, while an additional category of normal driving was added to give the model realistic usability. At the same time, for the context semantic information of video and the spatial structure information of the image frame, this research used the MoViNet v0 model to classify video actions. The model had 70% offline classification accuracy, 70% recall rate, 70% precision, 0.69 F1 scores, 0.90 AUC score on the validation set, and the offline classification accuracy of the model on the test set was 80%. The recall rate was 79%, the prediction was 81%, the F1 score was 0.79, and the AUC score was 0.93. At the same time, the model could achieve 10fps when inferring online and the recognition effect did not decrease, basically realizing real-time online processing. To improve this research, further attempts will be made to complete the driving safety system for agricultural driving, presenting the shortcomings of existing research and the parts that deserve further research in the future in the extend driver action datasets and model improvements.

References

Andrew, G., Menglong, Z. (2017). Efficient convolutional neural networks for mobile vision applications[J]. Mobilenets.

Bachlechner, T., Majumder, B. P., Mao, H., et al. (2021). Rezero is all you need: Fast convergence at large depth[C]//Uncertainty in Artificial Intelligence. PMLR: 1352–1361.

Bender, G, Liu, H, Chen, B, et al. (2020). Can weight sharing outperform random architecture search? an investigation with tunas[C]//Proceedings of the IEEE/CVF Conference on Computer Vision and Pattern Recognition: 14323–14332.

Das, D., Zhou, S., & Lee, J. D. (2012). Differentiating alcohol-induced driving behavior using steering wheel signals. *IEEE Transactions on Intelligent TransportationSystems, 13*(3), 1355–1368.

Hu, J., Shen, L., Sun, G. (2018). Squeeze-and-excitation networks[C]//Proceedings of the IEEE conference on computer vision and pattern recognition: 7132–7141.

Jan, T., & Anne, B. (2006). Mobile phone use-effects of conversation on mental workload and driving speed in rural and urban environments. *Transportation Research Part F: Psychology and Behaviour, 9*(4), 298–306.

Krajewski, J., Sommer, D., Trutschel, U., Edwards, D., & Golz, M. (2009, June). Steering wheel behavior based estimation of fatigue. In Driving assessment conference (Vol. 5, No. 2009). University of Iowa

Mardi, Z., Ashtiani, S. N. M., & Mikaili, M. (2011). EEG-based drowsiness detection for safe driving using chaotic features and statistical tests. *Journal of Medical Signals and Sensors, 1*(2), 130.

National Police Agency Traffic Accident Analysis Data (2022). *Traffic accident analysis information.* https://www.npa.go.jp/bureau/traffic/bunseki/sonota/290317koureiunten.pdfNordbakke, S., & Sagberg, F. (2007). Sleepy at the wheel: Knowledge, symptoms and behaviour among car drivers. *Transportation Research Part F Traffic Psychology & Behaviour, 10*(1), 1–10.

Oord, A., Dieleman, S., Zen, H., et al. (2016). Wavenet: A generative model for raw audio. *arXiv*. preprint arXiv:1609.03499.

Owens, J. M., Mclaughlin, S. B., & Sudweeks, J. (2011). Driver performance while text messaging using handheld and in vehicle systems. *Accident Analysis and Prevention, 43*(3), 939–947.

Reddy, B., Kim, Y.-H., Yun, S., Seo, C., Jang, J. (2017). Real-time driver drowsiness detection for embedded system using model compression of deep neural networks. In: 2017 IEEE Conference on Computer Vision and Pattern Recognition Workshops (CVPRW). 2017 IEEE Conference on Computer Vision and Pattern Recognition Workshops (CVPRW). Honolulu, HI, USA, 2017/07/21–2017/07/26: IEEE, pp. 438–445.

Zhang, Y., Gao, P., & Ahamed, T. (2018). Development of a rescue system for agricultural machinery operators using machine vision. *In Biosystems Engineering, 169*, 149–164. https://doi.org/10.1016/j.biosystemseng.2018.02.009

Chapter 8
Navigation System for Autonomous Agricultural Vehicles for Indoor Farms

Abstract Simultaneous Localization and Mapping (SLAM) is a fundamental technology in autonomous driving and refers to realizing autonomation and intelligent navigation functions. The SLAM is used to integrate localization function with the construction of the surrounding environment. When the robot vehicle moves, the system builds a consistent map using sensing of the environment according to its pose estimation. This research aims to design an autonomous agriculture vehicle for scouting based on stereo visual SLAM in the indoor environment. This research utilized a stereo camera as the primary sensor to perceive surrounding environment information. The system extracted image features between each continuous frame and then regards these features as natural landmarks. As a result, the system could estimate the pose and movement between these frames and updated the global map, which was also a whole process of SLAM. This research outcomes reported image local invariant features extracting algorithm, global localization, environment mapping based on the image frames, path planning, and path tracking. The ORB_SLAM was used, which is one of the SLAM repositories that oriented FAST and Rotated BRIEF to describe features. Our research used the ORB method to realize the SLAM function and compared the SIFT and ORB methods in different environments. The result shows that when these two methods analyze the same images, the ORB method exhibited excellent performance and satisfied the need for real-time operation with higher accuracy. The fast library for approximate nearest neighbors (FLANN) matching algorithm had excellent matching results and ensured that the estimated pose was right for generating accurate global maps. Robot Operation System (ROS) is an open-source meta-operating system for robots that was used to construct the whole navigation system part. The objective of the navigation section was to navigate the vehicle to the designated destination. This research's path planning and tracking algorithm used Dynamic-Window Approach (DWA) and pure-pursuit, which updated the map in real time. According to the dynamic map, the system demonstrated a no-collision path to the destination.

Keywords Visual-SLAM · Robot Operation System · Dynamic Window Appraoch · Path planning

© The Author(s), under exclusive license to Springer Nature Singapore Pte Ltd. 2024

T. Ahamed, *IoT and AI in Agriculture*,
https://doi.org/10.1007/978-981-97-1263-2_8

8.1 Introduction

With the development of computers, automatic control, and artificial intelligence technology, people have turned their attention to intelligent agricultural robots. Innovative agricultural machinery plays an essential role in modern agricultural production. The world population is rapidly increasing, which puts farmers under tremendous pressure to become more productive to feed a rapidly growing population. Furthermore, younger people lack the experience and passion for crop growing. Also, the labor shortage has been a severe problem in the world. In farming, agricultural robots have dedicated much manual work. This situation is prevalent in indoor growing environments such as greenhouses. The farmers can adjust the temperature, pH, EC, and humidity, such environmental parameters in the greenhouse.

Pest control is significant in modern greenhouse tomato production, and scientific pest control profoundly affects tomato plants' growth, development, yield, quality, and taste. There are three methods to prevent and treat pests and diseases in greenhouses—spray, smoke, and dust. For example, Miridae always appears during the whole production of tomatoes. Miridae are small, terrestrial insects, usually oval-shaped or elongated, measuring less than 12 millimeters. The usual pest control method for this tiny pest is to expose the bugs to the smoke. Smoke in each plant when the agricultural vehicle moves into the greenhouse. The XAG chinese company has developed an autonomous agricultural vehicle with a spraying system XAG R150 (Fig. 8.1).

Farm operations, such as planting, cultivation, spraying, and harvesting, require a vehicle that can autonomously drive to the designated position. It is a challenging task because the operator needs to pay attention to many operations while operating agricultural machinery. The development of autonomous farm vehicles can significantly reduce this stress, which requires agricultural vehicles to have the ability to

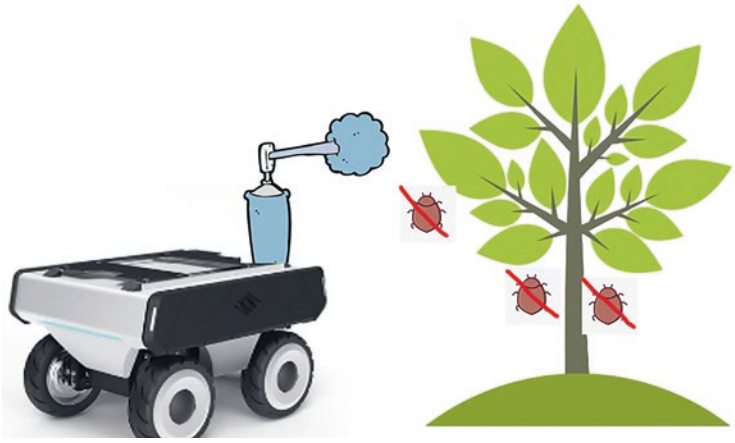

Fig. 8.1 Farmers applied agricultural machinery in plant protection and pest prevention

arrive at a designated position when the operator sets up a destination. As a result, equipment installed in the vehicle can adequately treat each plant grown in the goal.

Some techniques, which include mechanical and optical sensors for precepting existing features (rows) and a wide range of navigation methods such as GPS, radios, and LiDAR, have been used in agricultural navigation. However, no previous systems and techniques were advanced and suitable for agricultural field production. With the application of GPS in the 1990s, the drawbacks of previous approaches do not show in GPS. As a result, much research utilized GPS to conduct their research. However, the GPS signal is sometimes fragile in forests, orchards, and indoor growing environments. Traditional agricultural vehicles use GPS, LiDAR, and RTK-GPS in their navigation system. However, the GPS and LiDAR signals are sometimes unreliable in the orchard and greenhouse. As a result, researchers decided to use the camera instead of GPS. The camera can detect dynamic obstacles when operating in the field. It is possible to use low-cost sensors for obstacle detection and localization. The researchers find that SLAM has been a better solution to realize the function of localization and mapping than GPS. Birrell et al. (2019) created "vegebot," a unique robot that relies on computer vision to achieve high accuracy when harvesting food. Blackmore et al. (2002) proposed a robotic plan that increases productivity while reducing environmental impact. This solution uses small, lightweight robots, like a giant human workforce that treats plants individually. Various research studies have been done on autonomous driving for agricultural vehicles during the last two decades. This article mainly discusses developments in vision-based navigation areas. The required technologies for autonomous vehicles are categorized into vehicle localization, environment perception, and motion control.

With the development of indoor growing, more and more farmers use autonomous vehicles to smoke pesticides. It requires agricultural vehicles to have the ability to drive to the designated destination. It needs to perceive the surrounding environment and localize itself in the background. In the traditional navigation system, other researchers prefer GPS and LiDAR. However, GPS and LiDAR are not practical for indoor growing environments. Because the signal of GPS is inferior in indoor environments, LiDAR cannot provide sufficient environmental information. As a result, there has been a massive demand for a new indoor growing navigation system. The visual SLAM algorithm can achieve localization in some scenes. However, due to the work frequency of the camera, which is usually around 30 frames/second, it isn't easy to extract effective feature points due to the blurring of the image during fast motion. In addition, when tracking feature points, too quick movement can cause feature points to be untracked, which leads to localization failure. In a greenhouse environment, the camera is also susceptible to leaf shading or uneven illumination, making it impossible to locate the robot. In addition, the sparse point cloud map built by the feature point-based vision SLAM can only be used for localization but not navigation, so there are limitations in using it for greenhouse autonomous mobile robots.

This research aimed to develop a new vision-based navigation system for an indoor agricultural vehicle for pest control. The reason for using the camera as the

primary sensor is that the camera can provide rich images and information about the environment. The environment perception section is based on ORB_SLAM2. To overcome the disadvantage of creating a sparse map by the original SLAM, the ORB_SLAM2 must be improved to generate dense point cloud maps.

8.2 Navigation System

Mobile robots involve control theory, artificial intelligence technology, multi-sensor fusion (MSF) technology, electronic information, and computer technology and are widely used in many fields. Mobile robots usually operate in unknown environments with no global positioning information. One of its main challenges is using the sensors in an unfamiliar environment to complete autonomous navigation by sensing its state and surrounding environment. Synchronous localization and map construction technology can obtain accurate position and map environment information, which becomes an important tool to solve the above challenges and a current research hotspot in robotics.

Since the application environment of the agricultural robots is mostly outdoors, the Global Navigation Satellite System (GNSS) can provide absolute positioning information in outdoor unobstructed conditions. Therefore, GNSS-based autonomous navigation solutions are widely used in machinery for field production. Perez-Ruiz et al. (2013) used Real-Time Extended (RTX) GNSS with signal correction using dedicated reference stations. RTK-GNSS dynamic test positioning accuracy reached 1.43 cm, and RTX-GNSS positioning accuracy reached 2.55 cm. They placed the GNSS navigation system on agricultural tractors, which benefits precision agriculture and agricultural automation. However, using GNSS navigation in dense orchard environments has some limitations, such as satellite signal occlusion, inherent time delay, and RF interference, and the current high-precision GNSS navigation system is costly. Since the orchard robot needs to work under the dense tree canopy for a long time, the blocking problem can reduce the receive satellite signals. The positioning accuracy of GNSS decreases significantly in an indoor environment, which cannot meet the needs of autonomous navigation.

Vision sensors are also a better choice for autonomous navigation of agricultural robots due to advantages such as increasing maturity of image processing technology and lower economic cost. Navigation by vision sensors detecting the edges of crop rows and soil planes is the most used vision navigation method. David et al. (2016) proposed a vision-based navigation method for agricultural robots. This navigation method installs the camera and IMU on top of the robot and uses the attitude information measured by the IMU to process the raw camera image to generate a top view of the farm ground. Then, make the crop rows as parallel textures and estimate the robot's heading information by extracting similar surfaces in the top view, which is corrected with the heading information.

Sharifi and Chen (2015) propose a vision navigation method for orchard robots. The technique uses a clustering algorithm to transform the image into a feature space for modeling. Then, it uses a graph partitioning algorithm to classify the feature space into three main categories: sky, trees, and ground. Then, utilizing Hough Transform to extract the boundary lines between the land and the trees for the classification image, and the distance from the robot to the boundary lines on both sides is used for localization and navigation. The result of this method is shown in Fig. 8.2. Gai et al. (2021) proposed a vision-based system for under-canopy navigation using a Time-of-Flight camera. They used a new algorithm to detect parallel crop rows from depth images taken under crop canopies. First, they generated crop field maps as occupancy grids when reliable robot locations were available. The sources were GPS and IMU. The system can provide inter-row vehicle positioning data. The test result showed that the system can map the crop rows with mean errors of 3.4 and 3.6 cm.

In simultaneous positioning and map-building technology, there are two types—radar and visual acquisition devices. A series of RGB D cameras such as Microsoft Kinect, Intel RealSense, and Asus XtionProLive can obtain RGB images and matching depth images at the same time, saving a lot of computation time and better meeting the requirements of real-time simultaneous localization and map construction for mobile robot vision. Zhao et al. (2020) proposed a ground-level mapping and navigating system based on the Mesh Simultaneous Localization and Mapping algorithm, a computer-vision algorithm, and the Internet of Things. It has created a 3D farm map on both the edge and the cloud. They only use a monocular camera to collect frames in the ground-level robot vehicle's layer. Implement the Agricultural system robot navigation system by path planning on maps created that monitor terrain, crops, and other objects. The IoT technology in the research makes the system more flexible and convenient.

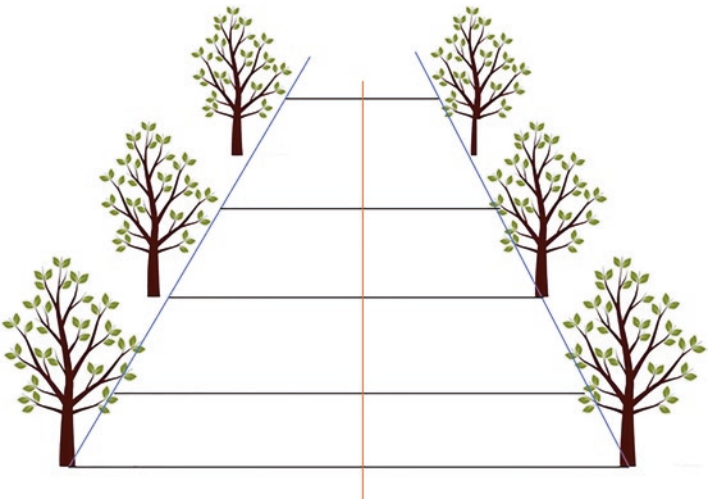

Fig. 8.2 The fruit tree row detection based on the image clustering algorithm method

8.3 Coordinates Calculation

A geometric model can describe the process of the camera projecting 3D coordinates to a 2D image plane. The simplest geometric model is the pinhole camera model. The pinhole camera model describes the relationship between the coordinates of a point in a 3D space while it projects onto the image plane of a camera. The pinhole camera mode is used in computer vision. It is simple and accurate enough to explain the basic imaging principle. Light passes through a single hole in the pinhole camera model, the camera center, O. Then the image is projected onto an image plane. The diagram is shown in Fig. 8.3. The image plane is placed in front of the camera center. In the image plane, the image plane is upside down behind the camera center. After analyzing the relationship, it can be described by the following equation.

$$\begin{cases} u = f_x \dfrac{X}{Z} + c_X \\ v = f_y \dfrac{Y}{Z} + c_y \end{cases} \tag{8.1}$$

If we use matrix form to revise it, we can obtain

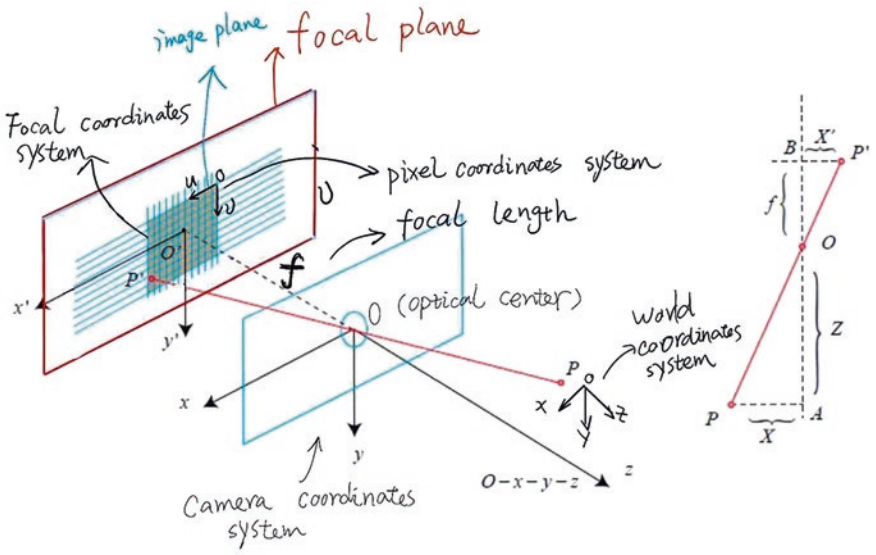

Fig. 8.3 This diagram shows a pinhole camera model. O-x-y-z is camera coordinates. O is the optical center of the camera. Point P is the real point in the real world. The point P is projected to the focal plane through optical center O. We assume P=$[X, Y, Z]^T$, the projected $P' = [X', Y', Z']^T$, the length from the focal plane to the optical center is f (focal length). The coordinate of P' In the image, the plane is $[u, v]^T$

$$\begin{pmatrix} u \\ v \\ 1 \end{pmatrix} = \frac{1}{Z} \begin{pmatrix} f_x & 0 & c_x \\ 0 & f_y & c_y \\ 0 & 0 & 1 \end{pmatrix} \begin{pmatrix} X \\ Y \\ Z \end{pmatrix} \Rightarrow \mathrm{K}\left(\mathrm{R}P_w + t\right) \tag{8.2}$$

The camera pose can be described by rotation matrix R and translation vector t. K is camera intrinsic. The R and t are camera extrinsic. Through this equation, we can determine the coordinates of each pixel. It provides essential data information for the next section.

8.3.1 Cloud Map Generation Using ORB_SLAM2

The previous section introduced the methodology of using the stereo camera to get the coordinates of each pixel in world coordinates. This research aims to deal with the localization problems in an indoor growing environment and simultaneously construct the surrounding environment. In the classic Visual SLAM model, the map consists of all features. The system must map the surrounding environment and plants to navigate agricultural vehicles. This section focuses on constructing dense point cloud maps with RGBD cameras. Then, the system stitches the 3D point clouds based on the calculated camera poses. Thus, humans can directly recognize the cloud map of the surrounding environment established by SLAM. In addition, the dense point cloud map is speeded up and filtered to build an octree map (OctoMap), which reduces the storage space of the dense map and creates a CostMap to provide the basis for the following robot navigation. Mur-Artal et al. (2015) from Zaragoza University published the ORBSLAM2, which is a reliable and accurate SLAM solution for Monocular, Stereo, and RGB-D cameras. It can run in real-time projects while estimating the camera trajectory and reconstructing the precepted environment's sparse 3D cloud map. The current ORBSLAM system is the most convenient and excellent one globally.

The original ORB_SLAM2 can only output a sparse map because this research is about agricultural scout vehicle navigation. The sparse map can only be used for tracking and recognition. It is not suitable for precision navigation projects. A real-time construction method was used to construct dense maps, and a dense map-building thread is built in addition to the original lines of ORB_SLAM2. The RGBD image received by the system has nearly 300,000 pixel points each time. As a result, only critical frames from it are selected and stored in the keyframe queue. Since a robot moving in a greenhouse could not quickly produce a sizeable positional transformation, two adjacent frames captured by the camera had many duplicate pixel points and generate many redundant points. Therefore, keyframes are selected instead of some locally similar images when constructing dense point cloud maps.

In this research, the PCL library established the code for generating a cloud map and was depicted in RVIZ. The Point Cloud Library (PCL) is a standalone, large-scale, open project for 2D/3D image and point cloud processing, which is widely

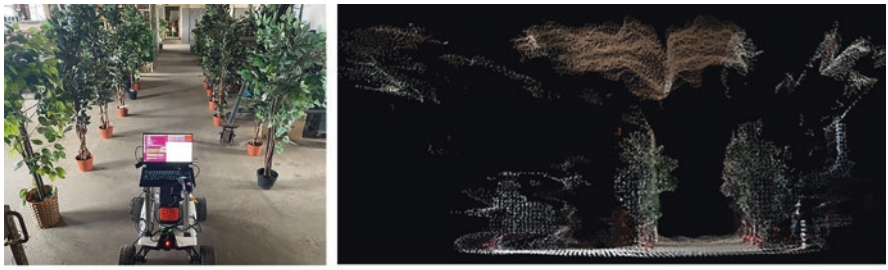

Fig. 8.4 (**a**) and (**b**) show the indoor the cloud map inside a workshop under 0.05 resolution

used in environmental reconstruction. RVIZ is a 3D visualizer for the Robot Operating System framework. It provides rich interfaces for robotics projects. The following designs are also based on RVIZ as the central platform (Fig. 8.4).

8.3.2 OctoMap

The OctoMap is a map that is commonly used in navigation and offers better compression performance. Point cloud maps are based on a three-dimensional structure, and we can adjust the map's resolution. However, point cloud maps have several drawbacks. They are usually large in size. For example, a 640 × 480 image, which generates 300,000 spatial points, requires a significant amount of storage space, even after filtering. Additionally, point cloud maps provide excessive details. Due to the large size of these spaces, we cannot model a larger environment within limited memory unless we reduce the resolution. However, reducing the resolution leads to a degradation in map quality. In contrast, the OctoMap can compress the point cloud map and can be updated in real time. This map significantly reduces the computational effort of the navigation system. The space in the OctoMap is depicted in (Fig. 8.5).

In the OctoMap, the 3D space is modeled as many small squares. If each face of a small square is cut into two equal pieces, the small square becomes eight small squares of the same size. The cutting process is repeated until the final square size is the most accurate. The initial space is regarded as a father node. This parent node expands into eight child nodes. Then, the process is repeated to form an octree. The nodes of the octree store information about occupancy. At the point cloud stage, zero indicates an unoccupied square space, and one indicates an occupied space. This algorithm chooses to express node occupancy in Log-odds form because sometimes there are nodes with unknown states. For example, a floating-point number can be used. The initial value of x is 0.5, which increases if it is constantly observed to be occupied or decreases if continuously monitored to be unoccupied. In this way, the obstacle information can

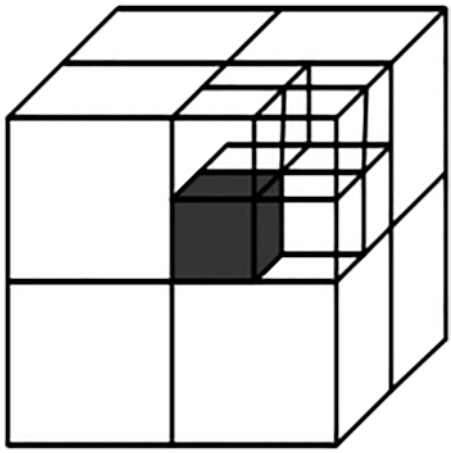

Fig. 8.5 The space in OctoMap is divided into eight-cell rooms every time

be marked on the map. The algorithm uses the following equation to describe node occupancy.

$$y = logit(x) = \log\left(\frac{x}{1-x}\right) \tag{8.3}$$

At this point, the entire octree map can be updated based on the RGBD data. When a pixel with a depth value is observed in the RGBD image, occupancy data are kept at that spatial point, and the line from the camera's optical center to this point is unobstructed by objects. The OctoMap example of an indoor environment is shown in (Fig. 8.6).

8.3.3 CostMap

The OctoMap already helped to compress the point cloud map. The system could generate and update the map in real time. However, OctoMap could not use indirectly in navigation because it was hard for vehicles to determine the location of each obstacle. As a result, OctoMap was converted into CostMap. In the CostMap, the three-dimensional map can be projected into the two-dimensional map. Because a ground vehicle only drives on the ground, the two-dimensional map was more than enough for the navigation in the indoor environments.

CostMap was built by the costmap_2d function package in ROS1. It's a multi-layer structure map. A layer of CostMap was updated with only one kind of data. For example, the SLAM algorithm generates the static map at the bottom layer. The obstacles layer was a CostMap layer updated by sensor data. It is even possible to customize a CostMap layer for some particular purposes so that the generated paths avoid certain areas.

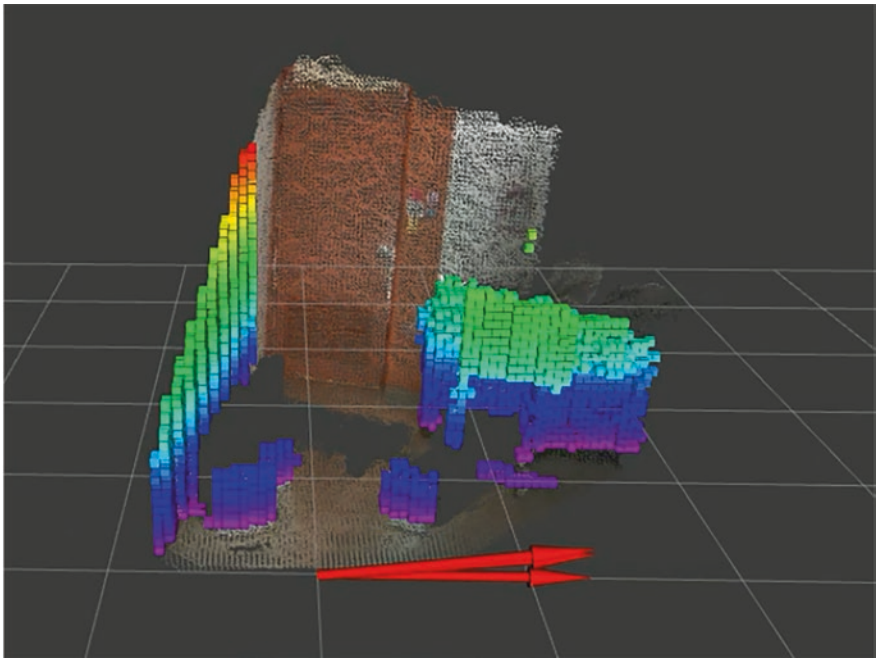

Fig. 8.6 OctoMap of an indoor environment

The Yaml file for this research was written in the program by calling the costmap_2d function package. Yaml file is used to set the parameters necessary to generate the CostMap. CostMap mainly has a static layer, obstacle layer, voxel layer, and inflation layer. The inflation layer uses InflationLayer type data, the fixed layer uses StaticLayer type data, and the obstacle layer can choose either VoxelLayer data or ObstacleLayer data. The specific configuration of the plug-in is in the global_costmap_params.yaml file and local_costmap_params.yaml file. The red area indicates the area of obstacles, and the blue area shows the location of inflated barriers. The radius of the robot's inner tangent circle determines the blue area. As we all know, different vehicles have different safe spaces from themselves to obstacles. This step allows us to customize CostMap for each particular vehicle. The main interface provided to the user is Costmap2DROS, and the factual map information is stored in the individual Layers. The following diagram briefly illustrates the relationship between the various interfaces of Costmap. The Structure of CostMap is shown in Fig. 8.7.

In the navigation section, the primary node was "move_base." The two-dimensional CostMap was constructed in this node. The "planner_costmap_ros" was a global navigation map. The "controller_costmap_ros" was a local navigation map. When the system converted OctoMap to CostMap, the safe and dangerous areas are distributed, provide good information essential for the next path planning and tracking section. The whole flowchart of environment construction is shown in Fig. 8.8.

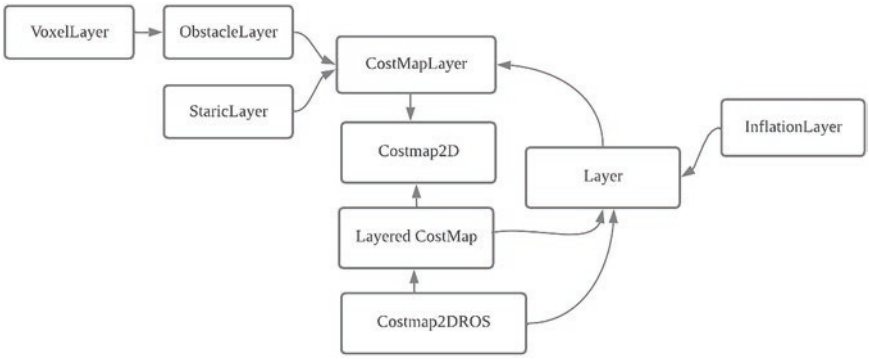

Fig. 8.7 Structure of CostMap

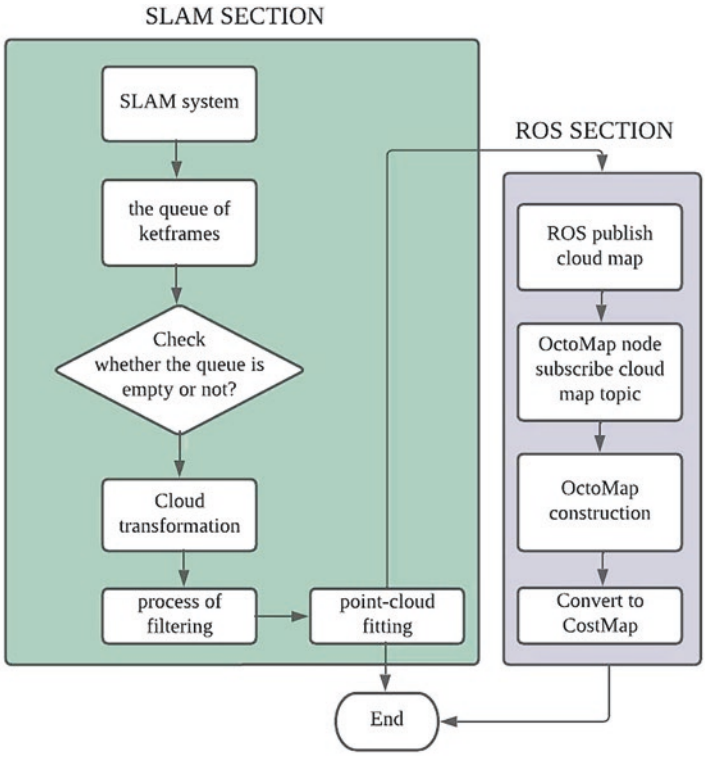

Fig. 8.8 Flowchart of system construction

8.3.4 System Data Structure Based on ROS

ROS is an open-source program library designed for building robots. It offers exit tools and a repository for users to create their robotics systems. ROS aims to improve software reuse and simplify system construction. It uses a point-to-point distributed

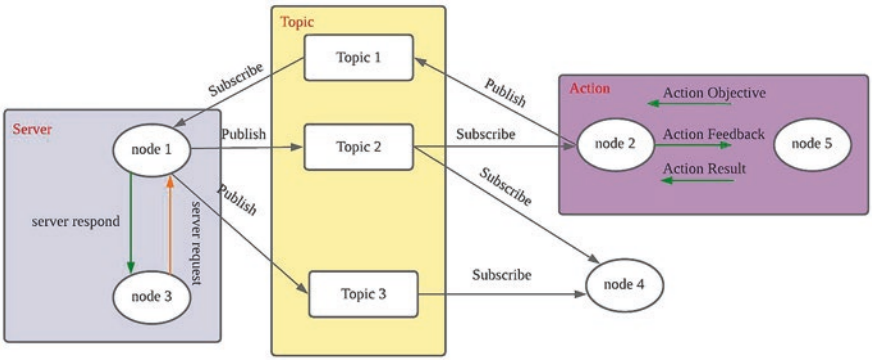

Fig. 8.9 ROS communication structure

communication mechanism, providing multi-node communication services. The three core communication mechanisms are Topic, Service, and Parameter management. Nodes, executable programs, communicate among themselves through sending and receiving messages and dividing data transmission into topics, services, and actions. Primary nodes can publish topics, restore data, and subscribe to receive information. Figure 8.9 depicts the visual representation of the communication structure.

8.4 Path Planning and Path tracking for Tiny Agricultural Vehicles

8.4.1 Design of Navigation System Based on move_base Repository

Path planning is the most core and essential function in the navigation system. The structure was built based on the Robot Operation System (ROS). The move_base repository was used to achieve the navigation function. Figure 8.10 depicts the structure of move_base. The move_base storage provides algorithms based on action. Users can set up a designated destination, and then the system can control the vehicle's chassis to move to this destination. In contrast, the vehicle continuously feeds its pose and state information to the upper system. As a result, the move_base repository consists of global path planning and local path planning.

In the program, the primary system had the libraies: "move_base/goal," "move_base/cancel (actionlib_msgs/GoalID)," "move_base/feedback," "move_base/status," and "cmd_vel." Because ROS platform was to activate the SCOUT MINI through CANBUS communication, the SCOUT MINI reffered a node named "cmd_vel" to subscribe to the control command from the move_base node.

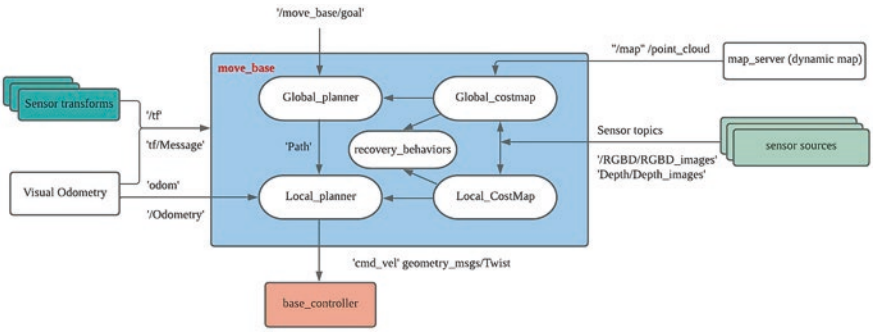

Fig. 8.10 Structure of move_base. The move_base is consisted of global_planner, global_costmap, recovery_behaviors, local_planner, local_costmap

8.4.2 Pure-Pursuit Path tracking Algorithm

Pure-pursuit is a path-tracking algorithm. It computes the angular velocity command that moves the robot from its current position to reach some look-ahead point in front of the robot. In these paths following problems, we can use bicycle models to replace accurate models. The bicycle model is a common simplification of an Ackermann-steered vehicle used for geometric path tracking. This algorithm helps us to control the front wheel angle δ, such that the car follows a given path, which is known as lateral vehicle control. In the pure-pursuit method, choose a target point in the desired direction, which is a look-ahead distance l_d away from the vehicle. The look-ahead distance is a fixed distance on the reference path ahead of the vehicles. The look-ahead distance is a vital parameter that affects the performance of tracking. Calculate the angle δ by this algorithm such that the car reach the target point according to the kinematic bicycle model. L is the distance between the front axle and the rear axle. R is the radius of the circle that the rear axle will travel along at the given steering angle. The illustrated geometric of the algorithm is shown in Fig. 8.11.

Through this geometric graph, we can see that

$$\tan\delta = \frac{L}{R} \tag{8.4}$$

The rear axle follows the orange curvature of a circular arc to the target point—the angle α between the vehicle's heading vector and the look-ahead vector. As a result, we can get the following equations.

$$\frac{l_d}{\sin(2\alpha)} = \frac{R}{\sin\left(\frac{\pi}{2}-\alpha\right)} \Rightarrow \frac{l_d}{2\sin(\alpha)\cos(\alpha)} = \frac{R}{\cos\alpha} \Rightarrow \frac{l_d}{\sin(\alpha)} = 2R \tag{8.5}$$

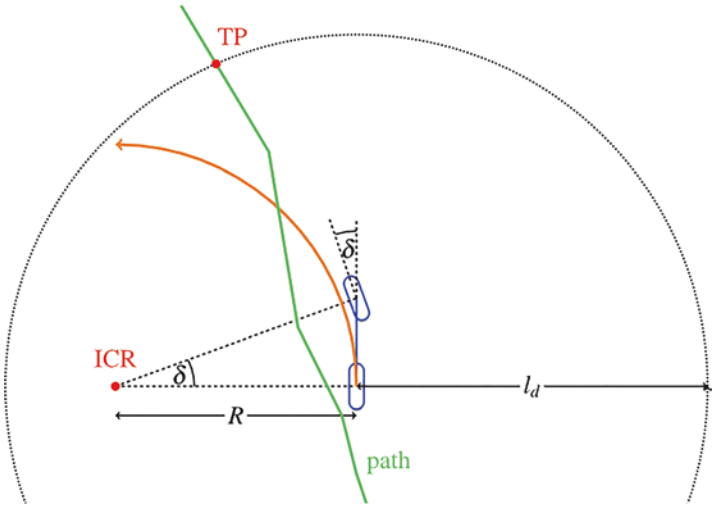

Fig. 8.11 The illustration of Pure pursuit

$$\begin{cases} \dfrac{1}{R} = \dfrac{2\sin(\alpha)}{l_d} \\ \tan\delta = \dfrac{L}{R} \Rightarrow \tan^{-1}\dfrac{L}{R} \end{cases} \Rightarrow \delta(t) = \tan^{-1}\left(\frac{2L\sin(\alpha(t))}{l_d}\right) \tag{8.6}$$

$$\sin(\alpha) = \frac{e_{ld}}{l_d} \Rightarrow \delta(t) = \tan^{-1}\left(\frac{2L\sin(\alpha(t))}{l_d}\right) \tag{8.7}$$

The steering angle can be calculated and changes with time and reference path through these equations. Pure-pursuit is a proportional controller of the steering angle operating on a cross-track error. This model approximates the motion of a vehicle reasonably well at low speeds and moderate steering angles. A short look-ahead distance provides more accurate tracking, while a longer length offers smoother tracking. This research implements the experiments under a 0.5 m look-ahead distance.

8.4.3 Instruction of DWA

The dynamic window approach (DWA) is an online collision avoidance strategy for mobile robots in robotics motion planning. After the robot obtains the destination information, the global path planning plans a rough route according to this route and reports CostMap. The local path planner is designed a specific action strategy for the robot, mainly using the DWA algorithm in ROS. When move_base is in the

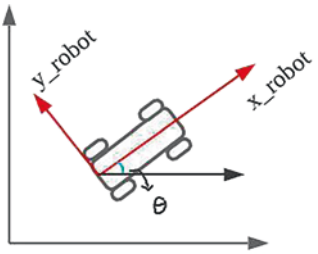

Fig. 8.12 Motion model of differential vehicle

planning stage, the DWA algorithm calculates an optimal speed command and sends it to the robot motion chassis for execution.

DWA algorithm is a typical action sampling algorithm. In this method, we use speed and angular velocity. The principle of this algorithm is to assume a vehicle's speed and then estimate where this vehicle moves according to this assumed speed and angular velocity. As a result, we need to build a vehicle motion model. In this research, the vehicle is differential contro and need to consider the x-axis's speed and the axis's angular velocity. Because the time interval is extremely short, we can assume the trajectory of this period is a straight line. We can use the following equation to describe the motion of the vehicle. The motion model of the differential vehicle is displayed in Fig. 8.12.

$$\Delta s = v * \Delta t \tag{8.8}$$

$$\Delta x = v\Delta t \cos\left(\theta_t\right) \tag{8.9}$$

$$\Delta y = v\Delta t \sin\left(\theta_t\right) \tag{8.10}$$

$$\begin{cases} x = x + v\Delta t \cos\left(\theta_t\right) \\ y = y + v\Delta t \sin\left(\theta_t\right) \\ \theta = \theta_t + w\Delta t \end{cases} \tag{8.11}$$

The program's maximum and minimum speed and angular velocity were set. The speed and velocity change according to the selected optimal trajectory. If the speed and angular velocity of the vehicle are too big, it has the problem of losing correspondent figures in the feature matching section. The RealSense camera was used, which had 30 frames in 1 s. As a result, if the speed and angular velocity are too fast, there is a risk of blurring the image. The domain of acceleration and angular velocity in this research is shown in the following equation.

$$V_s = \{(v,\omega) | v \in [v_{\min}, v_{\max}] \omega \in [\omega_{\min}, \omega_{\max}]\} \tag{8.12}$$

Because acceleration has a domain determined by an electronic motor, the maximum and minimum speed, and angular velocity, the vehicle can accelerate and decrease in a specific time interval also have a domain.

$$V' = \{(v,\omega)|v \in \left[v_{current} - \dot{v}_{brake}\,\Delta t, v_{current} + \dot{v}_{acceleration}\,\Delta t \right] \tag{8.13}$$

$$\omega \in \left[\omega_{current} - \dot{\omega}_{brake}\,\Delta t, \omega_{current} + \dot{\omega}_{acceleration}\,\Delta t \right]\}\}$$

When there is an obstacle in front of the vehicle, the speed and angular velocity should meet the following conditions to stop the vehicle with maximum deceleration. The dist(v,ω) is the closest distance from the obstacle to the car.

$$V'' = \{(v,\omega)|v \le \sqrt{2dist(v,\omega)\dot{v}_{brake}} \quad \omega \le \sqrt{2dist(v,\omega)\dot{\omega}_{brake}}\} \tag{8.14}$$

According to these motion equations, we can estimate the trajectory of the next time interval. The system selected the most optimal course. This function evaluates the trajectory. The α, β, τ are the coefficients of the correspondent evaluation function.

$$G(v,w) = \sigma\left(\alpha \bullet heading(v,w) + \beta \bullet dist(v,w) + \tau \bullet velocity(v,w)\right) \tag{8.15}$$

8.5 Results and Discussion

The GPS and LiDAR are widely used in outdoor navigation systems. However, for an indoor growing environment, localization has always been a difficult situation. In this research, the ORB_SLAM2 was proposed to solve this indoor environments. ORB-SLAM2 is a versatile and accurate SLAM solution for Monocular, Stereo, and RGB-D cameras. The primary sensor in this research is RealSense D455, a stereo camera. It can provide 30 frames per second. The system in this research needs to select different keyframes from the camera, which are used for generating a cloud map. The main difference between ORB_SLAM and other SLAM systems is that the methods used to extract features differ. Such as SIFT (Scale-Invariant feature transform), Oriented FAST, and Rotated BRIEF (ORB).

These two feature extraction methods are widely used in computer vision. However, we can see when using these two methods to process the same picture, the result of the SIFT algorithm extracted more than 368 feature points. The experiment result is shown in Figs. 8.13 and 8.14. However, the ORB algorithm only needs to extract 123 feature points. Afterward, FLANN was used for feature-matching algorithm to match these extracted features. The number of mismatching features is very few in both methods. These extracted features can all be compared and calculated in the next trajectory estimation section. The result shows that SIFT required 5.23 s to remove components and 0.00132856 s to match features. The ORB resuired cost of 0.201622 s to extract features and 0.0010285 s to compare features. The comparison

Fig. 8.13 (**a**) Processed results of ORB. (**b**) Extracted features by SIFT

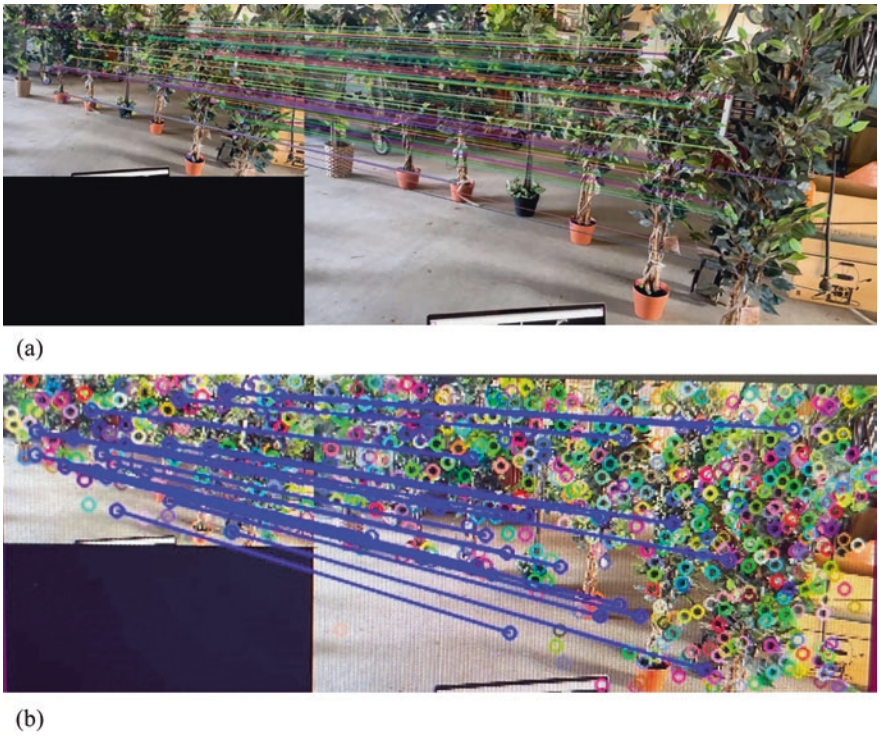

Fig. 8.14 (**a**) Matching result in ORB. (**b**) Matching result in SIFT

result is shown in Figs. 8.15 and 8.16. If we need to use these methods in navigation projects, the algorithm must meet the need for real-time operation. The ORB algorithm had great running speed when compared with the SIFT algorithm. As a result, ORB was a more suitable algorithm for this research.

The original ORB_SLAM2 system could generate only the sparse map. However, the sparse map could not meet the need for navigation. The original ORB_SLAM2

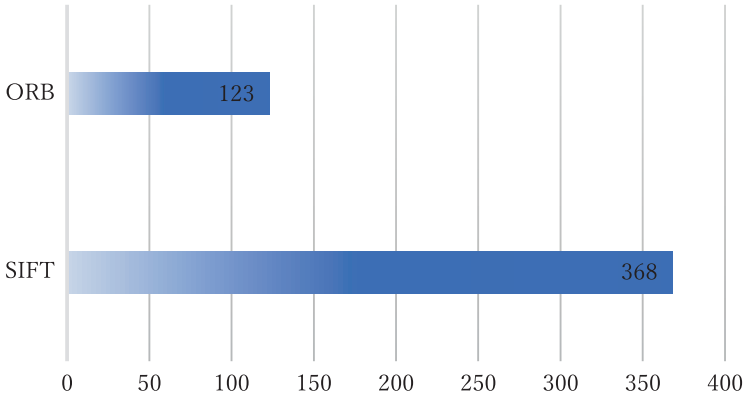

Fig. 8.15 Comparison between the extracted features of ORB and SIFT

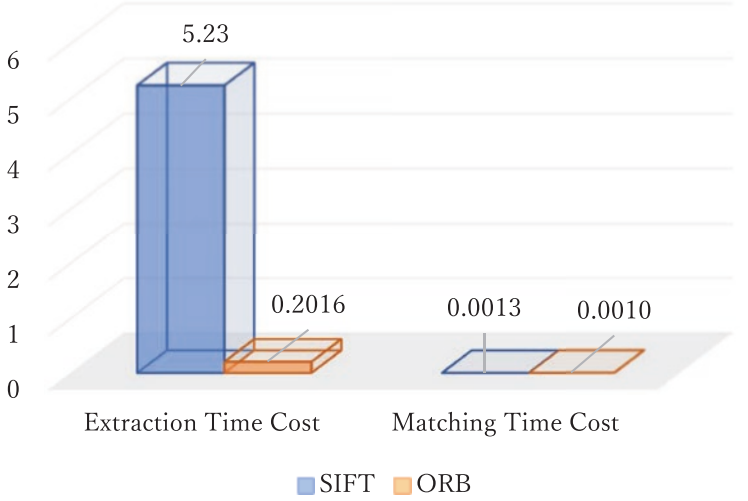

Fig. 8.16 Time comparison between ORB and SIFT

was used to trace past trajectories. To fit the need for navigation, ORB_SLAM2 was revised to make it generate the dense map. In the dense map, the operator could recognize the surrounding environment. It provides a good foundation for the next path-planning section. In this research, the resolution of three-dimensional maps matters a lot in navigation systems. The reliability and accuracy of a three-dimensional map at four different resolutions were checked and selected the 0.04 resolution. The cloud map under different resolutions is shown in Fig. 8.17. The accuracy of the point cloud map is related to the accuracy of navigation and the ability of obstacle avoidance. The dense map was converted to OctoMap (Fig. 8.18). The OctoMap could compress the three-dimensional cloud map to save more space and time when processing and updating maps. The area of objects was inflated. It

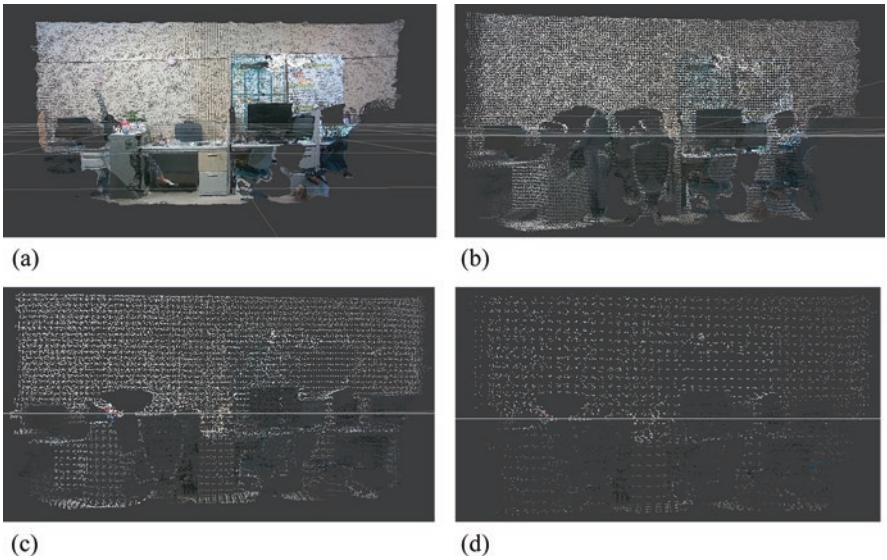

Fig. 8.17 Mapping Examples (**a**) 0.01 resolution. (**b**) 0.04 resolution. (**c**) 0.08 resolution. (**d**) 0.12 resolution

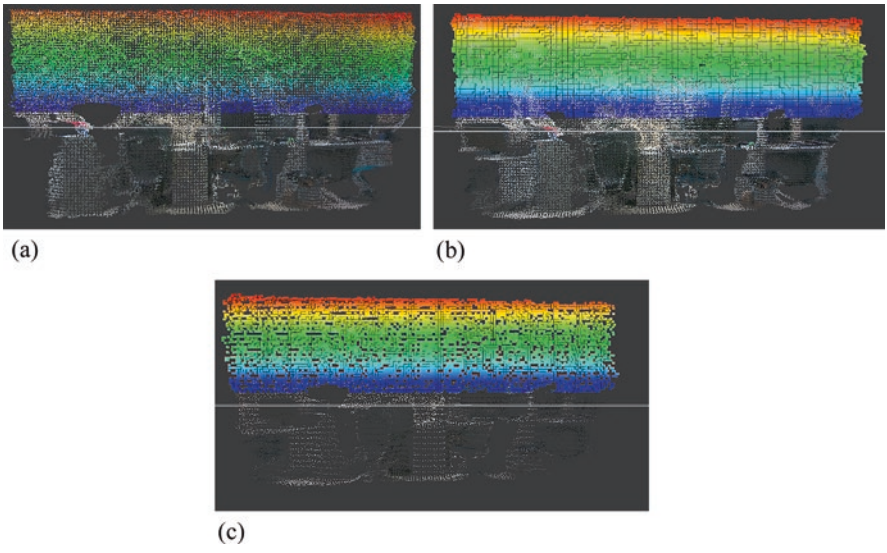

Fig. 8.18 OctoMap result (**a**) 0.01 resolution. (**b**) 0.04 resolution. (**c**) 0.08 resolution

may cause a problem that the agricultural vehicle cannot reach plants as close as possible. However, if we choose, the resolution of OctoMap is too low (Fig. 8.18), there was chance of losing the advantage of using OctoMap. Therefore, the most

appropriate resolution for this study was determined by comparing OctoMap at three resolutions was 0.04.

The EVO package was used in this research to evaluate the estimated trajectory and localization. This package provides executables and a small library for handling, evaluating, and comparing the trajectory output of odometry and SLAM algorithms. First, observed the accuracy of the estimated trajectory against the actual course. The tape was used to make a reference path on the ground. The experiment result is shown in Fig. 8.19. The mini scout vehicle follows this reference path and ensures that the camera is always on the track. The result is shown in Fig. 8.20. When the system estimates the vehicle's trajectory, there is a problem of accumulating drift. Adding the loop closure function to my research can fix this problem. Loop closure detection detects whether an agent has returned to a previously visited location. When the vehicle returns to the starting point, the trajectory looped was closed (Fig. 8.21). This step could improve the accuracy of the established three-dimensional map and estimated trajectory. The correction result is shown in Fig. 8.22.

To simulate the pest control, a humidifier was installed on the scouting vehicle. It could produce the smoke of pesticides continuously at the indoor environment. The artificial trees are used to build a simulation environment of an indoor environment. The equipment and environment are shown in Figs. 8.23 and 8.24. In this experiment, set up a designated destination in the three-dimensional cloud map, and then the system designs a no-collision path. The roboy vehicle used the smokes on the trees alongside this path. The trajectory of this time experiment is shown in Fig. 8.25. In this experiment, when the system had a destination set up by users, the vehicle could always design a safe path without collision. It can prove that this system's

Fig. 8.19 The experimental environment for evaluating the accuracy of estimated trajectory

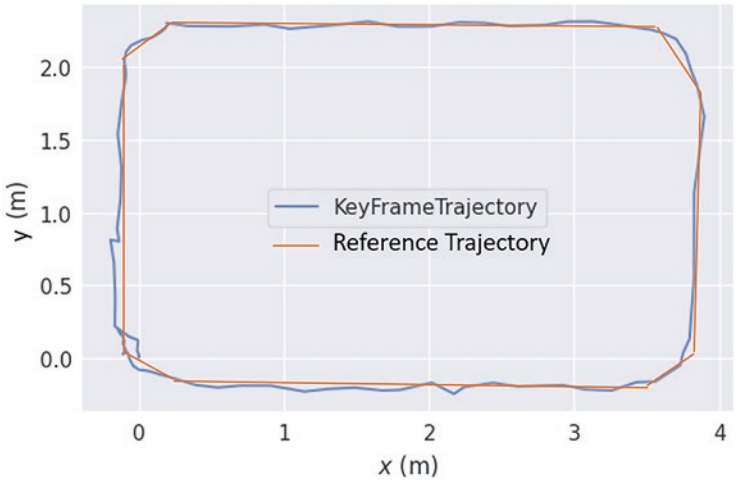

Fig. 8.20 Comparing two trajectories. The orange line is the reference trajectory. The blue line is the estimated trajectory

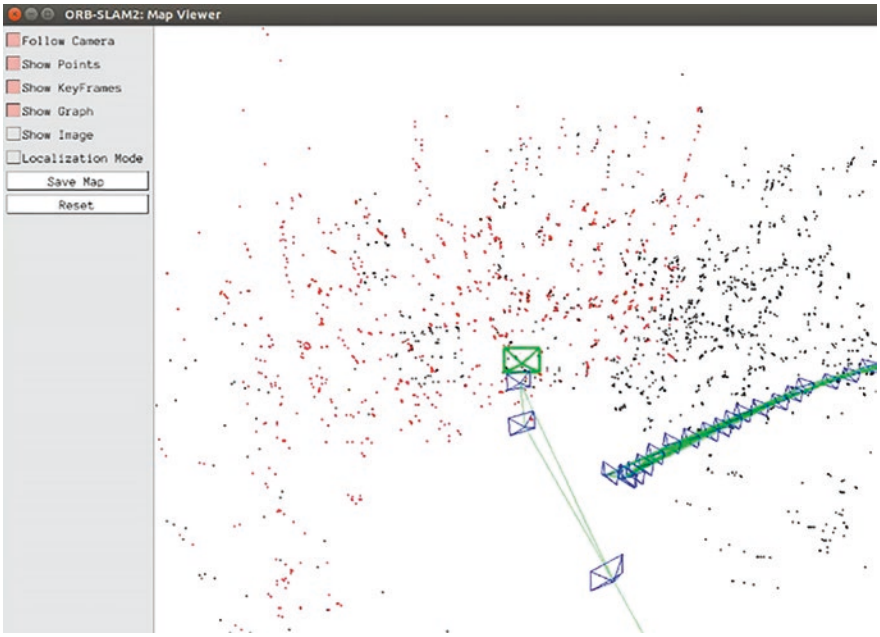

Fig. 8.21 Accumulating drift while the camera returns to the starting point

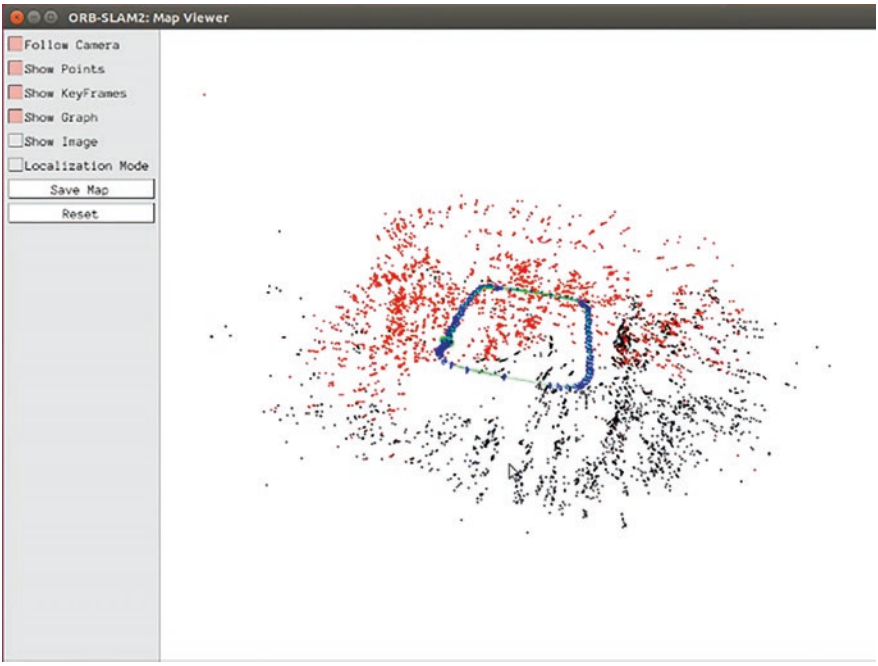

Fig. 8.22 Corrected trajectory is revised by the loop closing function

Fig. 8.23 Smoking system and navigation experiment using SCOUT_MINI vehcile

Fig. 8.24 Artificial trees in the workshop creates an indoor environment

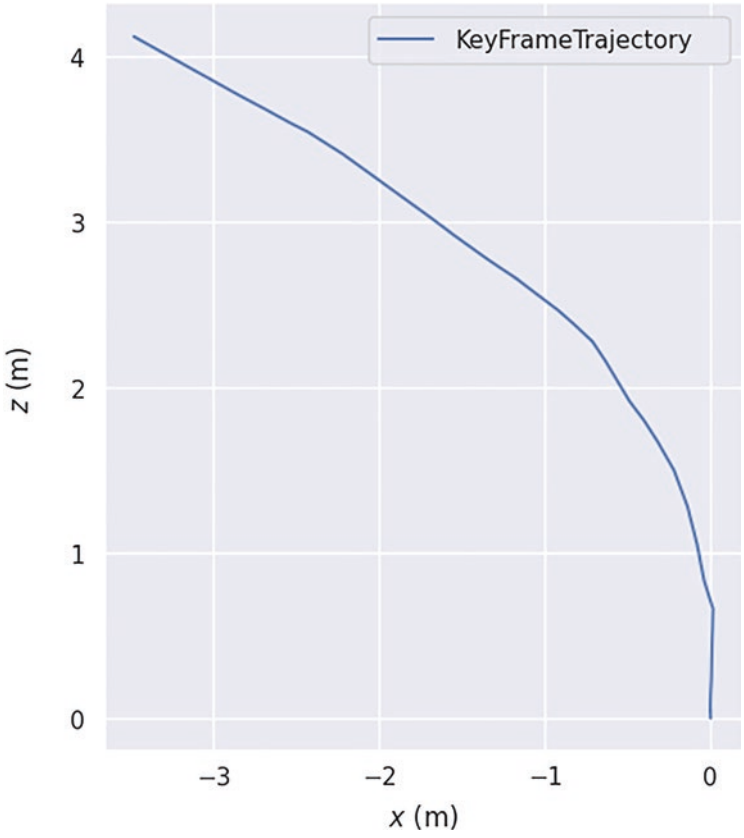

Fig. 8.25 Estimated trajectory of the spray and navigation experiment

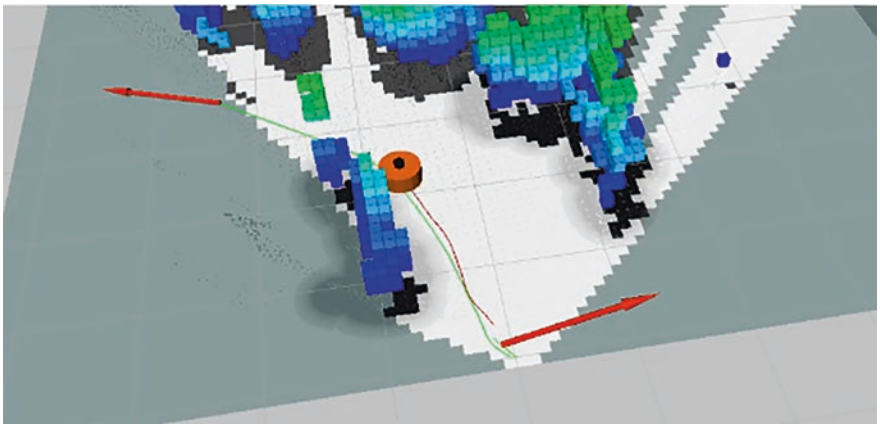

Fig. 8.26 Path planning experiment result in RVIZ simulation software. The red line shows the development of local path planning. The green line shows the outcome of global path planning

localization and navigation ability was above average level. Therefore, we can successfully apply the system in navigation systems and indoor growing environments.

The operation screen is in the path planning section (Fig. 8.26). The right arrow is the starting point, and the left is the destination. The location of obstacles was converted in OctoMap to CostMap as the gray black area around obstacles. When the goal was set, the system first designed a global path to the destination. Because when the vehicle was moved, the map was also updated. As a result, the planned route updated when the vehicle moved.. The DWA path planning algorithm can be designed more smoothly than other path planning algorithms. It can always find the fastest route to reach the destination (Fig. 8.26).

8.6 Conclusions

According to the result of this research, it has proved that this innovative ORB_SLAM2 could achieve the function of localization and environment mapping. The vehicle built on the system based on this system could adapt well to the indoor navigation environment. Even though, the accumulating drift problem sometimes affects the accuracy of localization. Boosting the inflated area of obstacles could avoid this problem. The dynamic windows approach (DWA) could design a smooth one according to the surrounding environment. The error of the estimated trajectory is only 3–4 cm away from the reference path. As a result, the navigation system in this research solved the localization and navigation problem of indoor agricultural vehicles. The drift and slip problems were the main factors affecting navigation accuracy. The loop-closing function could reduce this problem to some extent. However, slip problems may still influence the accuracy of localization, which was the main problem while using the visual-based navigation system only for autonomous

driving. A possible solution to this problem is integrating IMU and LiDAR with this navigation system. On the other hand, when we set up a designated destination in the system, the system could design a collision-free path by DWA. It can avoid dynamic or statistical obstacles. However, the planned route was sometimes far from the plants, resulting in improper smoking, which was away from artificial tree. Further research needs to carriy out for effective smoking and can be pentrated to tree canopy with extended fumigation process.

References

Birrell, S., Hughes, J., Cai, J. Y., & Iida, F. (2019). A field-tested robotic harvesting system for iceberg lettuce. *Journal of Field Robotics, 37*, 225–245. https://doi.org/10.1002/rob.21888

Blackmore, S., Have, H., & Fountas, S. (2002). Specification of behavioural requirements for an autonomous tractor. In *Automation Technology for off-Road Equipment Proceedings of the 2002 Conference* (p. 33). American Society of Agricultural and Biological Engineers.

David, B., Upcroft, B., Wyeth, G., Corke, P., English, A., Ross, P., Patten, T., Fitch, R., Sukkarieh, S., & Bate, A. (2016). Vision-based obstacle detection and navigation for an agricultural robot. *Journal of Field Robotics, 33*(8), 1107–1130. https://doi.org/10.1002/rob.21644

Gai, J., Xiang, L., & Tang, L. (2021). Using a depth camera for crop row detection and mapping for under-canopy navigation of agricultural robotic vehicles. *Computers and Electronics in Agriculture., 188*, 106301.

Mur-Artal, R., Jose, M. M. M., & Juan, D. T. (2015). ORB-SLAM: A versatile and accurate monocular SLAM system. *IEEE Transactions on Robotics, 31*(5), 1147–1163.

Perez-Ruiz, M., Carballido, J., Agüera, J., & Rodríguez-Lizana, A. (2013). Development and evaluation of a combined cultivator and band sprayer with a Row-Centering RTK-GPS guidance system. *Sensors, 13*, 3313–3330. https://doi.org/10.3390/s130303313

Sharifi, M., & Chen, X. (2015) A novel vision based row guidance approach for navigation of agricultural mobile robots in orchards. In 2015 6th International Conference on Automation, Robotics and Applications (ICARA) (pp. 251–255). IEEE.

Zhao, W., Wang, X., & Qi, B. (2020). Ground-level mapping and navigating for agriculture based on IoT and computer vision. *IEEE Access, 8*, 221975–221985. https://doi.org/10.1109/ACCESS.2020.3043662

Chapter 9
Strategic Short Note: Integration of Multiomics Approaches for Sustainable Crop Improvement

Abstract Optimizing climate-change adaptation is required to bring the new solutions to increase agricultural productivity, ensuring that food security and environmental protection become the anbitious challenges confronting by the scientists in this twenty-first century**.** In this regard, responses to the biotic and abiotc stress determination of crops and analyzing signal pathways have been recognized the most efficient way for the elucidation of growth, senescence, yield, and the responses to the variety of crops that have benefited greatly from the use of multiomics approaches and high-throughput techniques for climate adaptation. These omics approaches have been implemented in some important crops including wheat (Triticum aestivum L.), soybean (Glycine max), tomato (Solanum lycopersicum), barley (Hordeum vulgare L.), maize (Zea mays L.), millet (Setaria italica L.), cotton (Gossypium hirsutum L.), Medicago truncatula, and rice (Oryza sativa L.). This multiomics would provide insights into the functional mechanisms of genes and their networks to improve crop science, genetics, growth, yield, and resistance in response to physiological and environmental stress. The recent developments of bioinformatics and artifical intelleligence (AI) opened the opportunity for interconnected approach and supported with informations for creating climate resilient, higher nutritive crops to ensure food security. In this regard, phenotype-to- genotype and genotype-to-phenotype approach based on integration of multiomics with systems biology and biorinformatics in response to environmental stress has been proposed here, which may also be useful to improve crop breeding.

Keywords Genomics · Transcriptomics · Proteomics · Bioinformatics · Genotypes · Phenotypes · System biology · Bioinformatics · Artificial intelligence

9.1 Introduction

Plants live in conditions that are continuously changing and frequently unfavorable or stressful for growth and development. These unfavorable environmental factors include biotic stressors like pathogen, contamination, and herbivore attacks, as well

© The Author(s), under exclusive license to Springer Nature Singapore Pte Ltd. 2024

T. Ahamed, *IoT and AI in Agriculture*,
https://doi.org/10.1007/978-981-97-1263-2_9

as abiotic stressors like drought, heat, cold, nutrient shortage, an excess of salt, or toxic metals like aluminum, arsenate, and cadmium in the soil. Drought, salt, and temperature stresses are major environmental factors that reduce plant productivity in agriculture and threaten food security. Furthermore, enhancing plant stress tolerance is essential for agricultural productivity as well as environmental sustainability because crops with poor stress tolerance use excessive amounts of water and fertilizer.

Agricultural systems around the world are becoming increasingly vulnerable due to the impacts of a growing global population, which is predicted to reach 10 billion in the next 30 years. Rapid urbanization and extreme weather events such as floods, prolonged periods of drought, extreme heat and salinity are becoming more and more prevalent in both tropical and temperate regions. These factors severely affect plant growth, development, and productivity and significantly impact global food security. Breeders are confronted with new obstacles in these conditions. Basically, they must develop traits that can ensure high(er) and stable yields, resistance (or resilience) to a variety of biotic and abiotic hazards, as well as satisfaction of consumer demands for safer and more nutritious foods.

In addition to conventional breeding and gene editing technology, omics-approaches are widely used to produce climate smart cultivars with desired qualities including increased productivity, abiotic and biotic stress tolerance, and nutritive quality. In modern molecular biology, the suffix "-omics" specially refers to a collection of technologies applied to the analysis of a huge and complete dataset of a particular class or type of biological molecule in a cell, tissue, organ, or whole organism.

Several omics approaches, such as genomics, mutagenomics, transcriptomics, proteomics, metabolomics, phenomics, and ionomics, have revealed each corresponding molecular biological facet integrated with plant systems (Fig. 9.1).

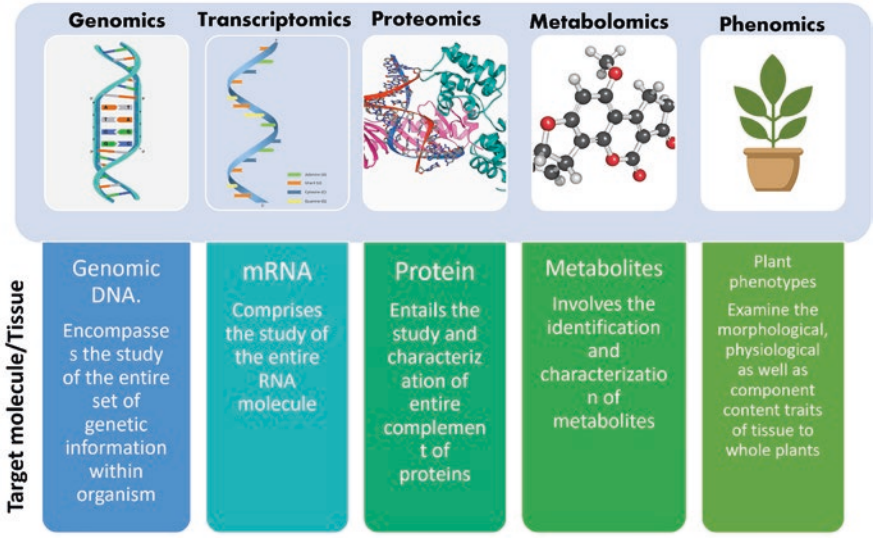

Fig. 9.1 Overview of main omics approaches

9.2 Integrated Multiomics Approaches for Crop Improvement

Genomics, proteomics, and metabolomics are the three core omics technologies, which respectively deal with the analysis of genome, proteome, and metabolome of cells and tissues of an organism (Hasin et al., 2017; Khalid et al., 2019). Phenomics is the characterization of phenotypes through the acquisition of high-dimensional phenotypic data on an organism-wide scale. Phenotyping techniques play a crucial role for analyzing field grown crops in comparison to plants in either the laboratory or greenhouse. How the genotype is connected to the phenotype and subsequent plant responses to environmental challenges could be predicated through multiomics integration (Mohanta et al., 2017; Kumar et al., 2021a, b; Wang et al., 2019).

The integration of multiomics approaches with other crop improvement strategies such as speed breeding and gene editing technologies is now frequently referred to as systems biology. Systems biology is a field of interdisciplinary research that integrates multiomics datasets, biological concepts, mathematical models, and machine-learning technologies to understand complex biological networks or systems (Pinu et al., 2019; Zenda et al., 2021).

Machine learning is a subset of the broader field of artificial intelligence (AI). It gives computers the ability to independently learn from data and carry out tasks for which they were not specifically built. Its objective is to let machines to carry out operations that call for human intellect, such as diagnosing, planning, and predicting. However, using machine learning for bioinformatics, researchers can specify the design of gene editing experiments and predict their outcomes and also able to identify genes that are likely to be involved in particular diseases. In this way, implementation of ML approach reduced the screening burden by around 95%.

Therefore, multiomics approaches integrated with other modern plant breeding, data analysis, and gene editing technologies and ML could be indispensable strategies to achieve abiotic and biotic stress tolerance, higher nutritional quality, and other key agronomic traits to fulfill global food and nutrition security (Fig. 9.2).

Integration of multiomics generated data and ML approach with plant breeding and gene editing technologies will provide a comprehensive, time- and cost-effective strategy for the creation of climate-resilient and nutrition-rich crops.

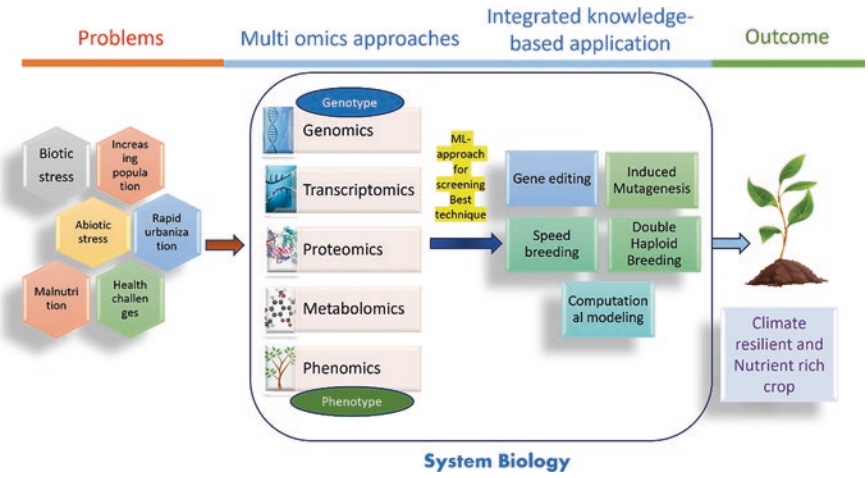

Fig. 9.2 Overview of multiomics approaches for crop improvements

9.3 Concluding Remarks

The combination of several omics approaches plays an indispensable role to identify potential candidate genes and their pathways. More importantly, the integration of systems biology with complex omics datasets has improved our understanding of molecular regulator networks for crop improvement. The "genotype to phenotype"as well as "phenotype to genotype"strategies enable quality crop phenotypic traits. From this perspective, the integration of multiomics with systems biology through ML approach is proposed that can be helpful to develop quality agronomic traits for crop improvements under different environmental stress conditions.

References

Hasin, Y., Seldin, M., & Lusis, A. (2017). Multi-omics approaches to disease. *Genome Biology, 18*(1), 1–5. https://doi.org/10.1186/s13059-017-1215-1

Khalid, N., Aqeel, M., & Noman, A. (2019). System biology of metal tolerance in plants: An integrated view of genomics, transcriptomics, metabolomics, and phenomics. *Plant Metallomics and Functional Omics: A System-Wide Perspective*, 107–144. https://doi.org/10.1007/978-3-030-19103-0_6

Kumar, J., Sen Gupta, D., Baum, M., Varshney, R. K., & Kumar, S. (2021a). Genomics-assisted lentil breeding: Current status and future strategies. *Legume Science, 3*(3), e71. https://doi.org/10.1003/leg3.71

Kumar, N., Soren, K. R., Bharadwaj, C., Sneha Priya, P. R., Shrivastava, A. K., Pal, M., Roorkiwal, M., Kumar, K., Patil, B. S., Soni, A., & Nimmy, M. S. (2021b). Genome-wide transcriptome analysis and physiological variation modulates gene regulatory networks acclimating salinity tolerance in chickpea. *Environmental and Experimental Botany, 187*, 104478. https://doi.org/10.1016/j.envexpbot.2021.104478

Mohanta, T. K., Bashir, T., Hashem, A., & Abd-Allah, E. F. (2017). Systems biology approach in plant abiotic stresses. *Plant Physiology and Biochemistry, 121*, 58–73. https://doi.org/10.1016/j.plaphy.2017.10.019

Pinu, F. R., Beale, D. J., Paten, A. M., Kouremenos, K., Swarup, S., Schirra, H. J., & Wishart, D. (2019). Systems biology and multi-omics integration: Viewpoints from the metabolomics research community. *Metabolites, 9*(4), 76. https://doi.org/10.3390/metabo9040076

Wang, Z., Shi, H., Yu, S., Zhou, W., Li, J., Liu, S., Deng, M., Ma, J., Wei, Y., Zheng, Y., & Liu, Y. (2019). Comprehensive transcriptomics, proteomics, and metabolomics analyses of the mechanisms regulating tiller production in low-tillering wheat. *Theoretical and Applied Genetics, 132*, 2181–2193. https://doi.org/10.1007/s00122-019-03345-w

Zenda, T., Liu, S., Dong, A., Li, J., Wang, Y., Liu, X., Wang, N., & Duan, H. (2021). Omics-facilitated crop improvement for climate resilience and superior nutritive value. *Frontiers in Plant Science, 12*, 774994. https://doi.org/10.3389/fpls.2021.774994

Chapter 10
Strategic Short Note: Artificial Intelligence in Food Quality Assessments

Abstract This paper explores the role of Artificial Intelligence (AI) in revolutionizing food quality assessments. As food products become increasingly complex and diverse, traditional quality assessment methods encounter limitations in accuracy, efficiency, and scalability. AI technologies present promising solutions by harnessing advanced algorithms, machine learning techniques, and data analytics to augment the accuracy and speed of food quality assessments. This chapter offers an overview of state-of-the-art AI applications across various aspects of food quality assessment. Furthermore, it addresses the challenges and opportunities inherent in integrating AI into the food industry. Through a thorough exploration of key concepts and advancements, this chapter aims to provide valuable insights to researchers, industry professionals, and policymakers regarding the transformative potential of AI in ensuring food safety, integrity, and consumer satisfaction.

10.1 Introduction

The agricultural and food industries have witnessed significant transformation in recent decades due to the rapid growth of science and technology. Technological innovations have improved and increased the efficiency of food production to meet the continuously growing demand due to the increasing population. Food loss and spoilage, low-quality food items supply, manufacturing contamination, unauthorized addition of preservatives and additives, food fraud, and adulteration are just a few of the threats faced by food security (Hu et al., 2019; Tan & Xu, 2020). Poor monitoring techniques of food quality contribute to the threat received by food safety, which leads to high spoilage and wastage. Food deterioration is detrimental to people's health and the nation's economy (Arshad et al., 2023). To abate the health complications and hazards due to food quality deterioration, the rapid

© The Author(s), under exclusive license to Springer Nature Singapore Pte Ltd. 2024

T. Ahamed, *IoT and AI in Agriculture*,
https://doi.org/10.1007/978-981-97-1263-2_10

assessment of food quality is brought into the limelight and developed into a major area of interest for researchers and industrial food producers. This sets Artificial intelligence (AI) on the right track in promoting rapid food quality assessment by integrating it with high-capacity sensors, vast databases, and computing techniques such as soft computing, internet computing, and the Internet of Things (IoT). AI is essential to expedite the advancement of reliable and improved food quality assessment with hastened response capability and delivers results with high precision and repeatability during the process (Addanki et al., 2022). AI does not only improve time efficiency but also serves as the benchmark for state-of-the art noninvasive food quality assessment techniques.

10.2 Application of AI Techniques in Food Quality Detection

AI is the term given to the area of computer science that focuses on intelligent computational methods. The technique imitates the intellectual potential of humans when tackling problems involving comprehension, logic, learning, and decision-making. In the application of AI in food quality assessment, it uses machine learning for prediction and classification, computer vision for visual appraisal of food quality, and deep learning for complex pattern identification. AI has recently emerged due to a variety of sensors for the collection of large data and its high computational capacity to quantify, qualify, and analyze complex data patterns. Some of the commonly utilized AI algorithms include artificial neural networks (ANNs), support vector machines (SVM), fuzzy logic (FL), and random forest (RF). The development of the AI system involves the training of the algorithm with existing information, which includes variables from sensors as input features and targeted variables as output features. The performance of the AI can be tested and validated using a new set of input features to forecast the output target (Lutz & Coradi, 2022). Over the past few years, they have become incredibly popular, and they are being employed to address difficult and technical problems. Today, several food quality evaluation techniques are increasingly developed with the help of AI. The application includes the integration of AI with laser scanner for diseases detection in milk (Khoroshailo & Kozub, 2020), computer vision to detect gas hole formation in cheese (Dias et al., 2021), e-nose to test for volatile compounds in coffee (Cui et al., 2020), e-tongues to classify beverages (Tan & Xu, 2020), hyperspectral camera to classify fruit and vegetable (Steinbrener et al., 2019), visible/near-infrared camera to detect freeze damage in orange (Tian et al., 2022), and near-infrared spectroscopy for coffee adulteration (Chakravartula et al., 2022).

AI is highly beneficial as an important section of integrated systems or an alternative method to traditional food assessment techniques. The conventional analytical method such as liquid chromatography, gas chromatography, mass spectroscopy, physiochemical analysis, and physical inspection by experts are time-consuming, laborious, prone to human error, and not eco-friendly (Anwar et al., 2023;

Wakchaure et al., 2023). The introduction of AI into the assessment system can deal with noisy and missing data as it can learn from examples and capable of performing at high speed of prediction and generalization once trained. They have also been employed for complex detection systems to model, control, optimize, identify, predict, and classify the target. The implementation of AI into food quality assessment techniques offers several benefits from high accuracy and efficiency, reduce human error and subjectivity, rapid response and detection, real-time monitoring and early verification of quality issues, and enhanced quality control and assurance process.

10.3 Challenges and Future Direction

The positive outcome achieved by AI in the assessment of food quality paves the way for more exploration and the creation of reliable instruments, Nonetheless, there are some gaps and future trends that demand research attention to improve the performance, applicability, and acceptability of AI-based food quality assessment devices in the food and food-related industries. The sensor‘s performance is of great concern in some components such as optical and acoustic sensors that are sensitive to environmental factors. The information required for the training of AI is mostly captured under a controlled environment, and the performance of the AI algorithm is directly related to that of the sensors. Therefore, future research should be focused on improving the stability of the sensor by taking advantage of new materials such as hybrid or nanomaterial with enhanced sensitivity and resistance to environmental factors. Another main challenge of food quality assessment with the help of AI is the adoption of new technology into the production system by native and some food industries that are highly accustomed to the traditional techniques. This problem has kept several hundreds of the developed AI models in the laboratory. To move the techniques from lab to field and boost the acceptability of the assessment techniques, future research should make an effort to develop user-friendly devices for the AI-based food quality assessment or create a user application that could be integrated into the user’s existing gadget such as a smartphone. Making more opportunities for the hybridization of AI with varieties of appropriate high-quality sensors is encouraged to effectively evaluate food quality and upholds the goals of food safety.

Acknowledgments The author would like to acknowledge the Ministry of Higher Education, Malaysia, through the Transdisciplinary Research Grant Scheme Project (TRGS/1/2020/UPM/02/7) for the support given to this study.

References

Addanki, M., Patra, P., & Kandra, P. (2022). Recent advances and applications of artificial intelligence and related technologies in the food industry. *Applied Food Research, 2*(2), 100126. https://doi.org/10.1016/j.afres.2022.100126

Anwar, H., Anwar, T., & Murtaza, S. (2023). Review on food quality assessment using machine learning and electronic nose system. *Biosensors and Bioelectronics: X, 14*(May), 100365. https://doi.org/10.1016/j.biosx.2023.100365

Arshad, F., Deliorman, M., Sukumar, P., Qasaimeh, M. A., Olarve, J. S., Santos, G. N., Bansal, V., & Ahmed, M. U. (2023). Recent developments and applications of nanomaterial-based lab-on-a-chip devices for sustainable agri-food industries. *Trends in Food Science and Technology, 136*(April), 145–158. https://doi.org/10.1016/j.tifs.2023.04.010

Chakravartula, S. S. N., Moscetti, R., Bedini, G., Nardella, M., & Massantini, R. (2022). Use of convolutional neural network (CNN) combined with FT-NIR spectroscopy to predict food adulteration: A case study on coffee. *Food Control, 135*(December 2021), 108816. https://doi.org/10.1016/j.foodcont.2022.108816

Cui, D. D., Liu, Y., Chen, Y. P., Feng, X., Lu, Y., & Yu, B. (2020). Application of SPME-GC-TOFMS, E-nose, and sensory evaluation to investigate the flavor characteristics of Chinese Yunnan coffee at three different conditions (beans, ground powder, and brewed coffee). *Flavour and Fragrance Journal, 35*(5), 541–560. https://doi.org/10.1002/ffj.3597

Dias, J., Lage, P., Garrido, A., Machado, E., Conceição, C., Gomes, S., Martins, A., Paulino, A., Duarte, M. F., & Alvarenga, N. (2021). Evaluation of gas holes in "queijo de Nisa" PDO cheese using computer vision. *Journal of Food Science and Technology, 58*(3), 1072–1080. https://doi.org/10.1007/s13197-020-04621-0

Hu, K., Liu, J., Li, B., Liu, L., Gharibzahedi, S. M. T., Su, Y., Jiang, Y., Tan, J., Wang, Y., & Guo, Y. (2019). Global research trends in food safety in agriculture and industry from 1991 to 2018: A data-driven analysis. *Trends in Food Science and Technology, 85*(January), 262–276. https://doi.org/10.1016/j.tifs.2019.01.011

Khoroshailo, T. A., & Kozub, Y. A. (2020). Robotization in the production of dairy, meat and fish products. *Journal of Physics: Conference Series, 1515*, 2. https://doi.org/10.1088/1742-6596/1515/2/022007

Lutz, É., & Coradi, P. C. (2022). Applications of new technologies for monitoring and predicting grains quality stored: Sensors, internet of things, and artificial intelligence. *Measurement: Journal of the International Measurement Confederation, 188*(December 2021). https://doi.org/10.1016/j.measurement.2021.110609

Steinbrener, J., Posch, K., & Leitner, R. (2019). Hyperspectral fruit and vegetable classification using convolutional neural networks. *Computers and Electronics in Agriculture, 162*(October 2018), 364–372. https://doi.org/10.1016/j.compag.2019.04.019

Tan, J., & Xu, J. (2020). Applications of electronic nose (e-nose) and electronic tongue (e-tongue) in food quality-related properties determination: A review. *Artificial Intelligence in Agriculture, 4*, 104–115. https://doi.org/10.1016/j.aiia.2020.06.003

Tian, S., Wang, S., & Xu, H. (2022). Early detection of freezing damage in oranges by online Vis/NIR transmission coupled with diameter correction method and deep 1D-CNN. *Computers and Electronics in Agriculture, 193*(December 2021), 106638. https://doi.org/10.1016/j.compag.2021.106638

Wakchaure, M., Patle, B. K., & Mahindrakar, A. K. (2023). Application of AI techniques and robotics in agriculture: A review. *Artificial Intelligence in the Life Sciences, 3*(January), 100057. https://doi.org/10.1016/j.ailsci.2023.100057

Chapter 11
High-Throughput Plant Phenotyping Techniques in Controlled Environments

Abstract Advancements in plant phenotyping techniques have become critical to solving the complex relationships between genotypes and their corresponding phenotypes. Controlled environments provide researchers with an opportunity to manipulate various growth conditions, thus enabling a deeper understanding of plant responses. This chapter reviews the recent developments in high-throughput plant phenotyping techniques tailored for controlled environments. An inclusive discussion of the spectrum of imaging methods is presented, elucidating the capacity of these methods for efficient and accurate data acquisition and encompassing traits related to growth, morphology, physiology, and stress responses. Furthermore, the integration of automation, robotics, and data analytics-based deep learning (DL) has propelled the field forward, enabling the conducting of large-scale, reproducible experiments. Challenges such as data management, standardization, and the extraction of meaningful biological insights are addressed. By highlighting the advantages and limitations of these techniques, a comprehensive overview is provided for researchers aiming to employ high-throughput phenotyping in controlled environments. As plant phenotyping continues to significantly contribute to crop improvement, climate adaptation, and fundamental plant biology, the consolidation of innovative technologies with controlled environment experimentation is opening new avenues for accelerating scientific discoveries and enhancing agricultural sustainability.

Keywords Plant phenotyping · Controlled environment · High-throughput · Plant morphology · Plant physiology · Deep learning

11.1 Introduction

The impacts of climate change, including the decline in pollinators and water levels, have introduced significant challenges for crop growers in meeting the food demands of a world population that is projected to reach 9.1 billion by 2030. To address the need for food security and sustainability, growers must optimize their resource

© The Author(s), under exclusive license to Springer Nature Singapore Pte Ltd. 2024

T. Ahamed, *IoT and AI in Agriculture*,
https://doi.org/10.1007/978-981-97-1263-2_11

utilization and maximize their crop yield and quality, which has made plant growth monitoring a fundamental aspect of modern precision farming. The growth and development of plants represent the outcomes of complex interactions between their genetic makeup and their surrounding environment. Therefore, a comprehensive understanding of specific plants is crucial for effective plantation management, and such an understanding can enable informed decisions in regard to fertilization, harvesting, and the early prevention of pests and diseases. Thus, plant phenotyping has been introduced as a process for acquiring and providing relevant information for quality plant growth development.

By monitoring plant growth, valuable information can be obtained to establish connections between plant genes and the observable traits of plants. Consequently, this information serves as a valuable reference or indicator in plant breeding programs. Growers and researchers can gain insights into the relationship between a plant's genetic traits and its responses to environmental factors. These insights can enable growers to make more informed decisions, optimize their cultivation practices, and develop new crop varieties with greater resilience to changing conditions, thus ensuring sustainable agricultural production in the face of climate change.

Plant phenotyping involves analyzing the different observable characteristics or traits of plants to indicate their growth stage and overall health. These traits might include morphological features, such as plant height, leaf area and root architecture, and physiological or biochemical properties, such as photosynthetic activity, chlorophyll content, and nutrient uptake. Phenotyping plays an important role in plant research, breeding, and agricultural practices. By accurately characterizing plant traits, scientists and breeders can better understand how plants respond to environmental factors, stress conditions, and genetic variations to develop improved crop varieties that are more productive, more resilient to diseases and pests, and better adapted to specific growing conditions.

Traditionally, plant phenotyping involves manual measurements and expert field observations. The conventional phenotyping process is heavily reliant on manual labor, thus necessitating the involvement of many experts to manually measure and evaluate plant samples and meticulously document those traits. Moreover, the traditional process frequently involves the collection of plant samples for subsequent laboratory investigation, which unfortunately requires destructive methods that can result in the loss of the plant specimens under study. This labor-intensive phenotyping method suffers from limitations in throughput, leading to compromised data accuracy and a restricted number of extractable plant traits. Additionally, this manual approach results in a limited analysis of the extractable plant traits. As a result, researchers have recognized the need for innovative and automated techniques in plant phenotyping to enhance both the efficiency and accuracy of data acquisition, thus facilitating a more comprehensive understanding of plant characteristics and behaviors.

Currently, technological advancements have led to the development of nondestructive high-throughput methods (Das Choudhury et al., 2019). These methods enable the rapid and automated collection of data on plant phenotypes, allowing researchers to analyze large populations of plants more efficiently. Specifically, machine vision can be used to collect plant information in a noninvasive way compared to the chemical and physical methods traditionally used, and machine vision does not damage plants. It also provides continuous feedback with high efficiency and low cost. Machine vision technology has been employed in various areas, such as plant phenotype analysis, pest and disease detection, and nutrient stress identification.

11.1.1 Plant Morphological Characteristics

Plant morphology encompasses various characteristics of external plant structures, such as color, size, texture, and shape, which can be identified in regard to the different parts of plants, including their flowers, leaves, stems, fruits, or canopies. This information serves as an indicator of plant growth state and health status, providing valuable in-depth information for decision-making and management in horticulture or farming operations (Fig. 11.1). For instance, the height of a plant can provide information about its growth rate or annual growth cycle, depending on the weather or nutrient specifications. The quality of fall foliage can also serve as an indicator of plant health. Furthermore, the top canopy area may correlate with the plant's fresh and dry weight (Tian et al., 2022).

11.1.2 Plant Physiology

Plant physiology is an aspect of plant phenotyping that involves studying and measuring different internal traits of plants. The focus of plant physiology is on understanding how plants function internally, including such aspects as how they absorb water, nutrients, and sunlight and how these processes affect plant growth and health. Information on plant physiology in the context of plant phenotyping can help scientists or growers link the internal activities of plants to their observable morphological characteristics, such as size, shape, and color. For example, knowing how a plant internally regulates water usage can help researchers measure its drought tolerance through the observation of traits such as leaf wilting or root depth. By linking plant physiology with phenotyping, scientists can identify the best traits for specific conditions, which can help breeders develop more resilient and productive plant varieties for agriculture and other applications.

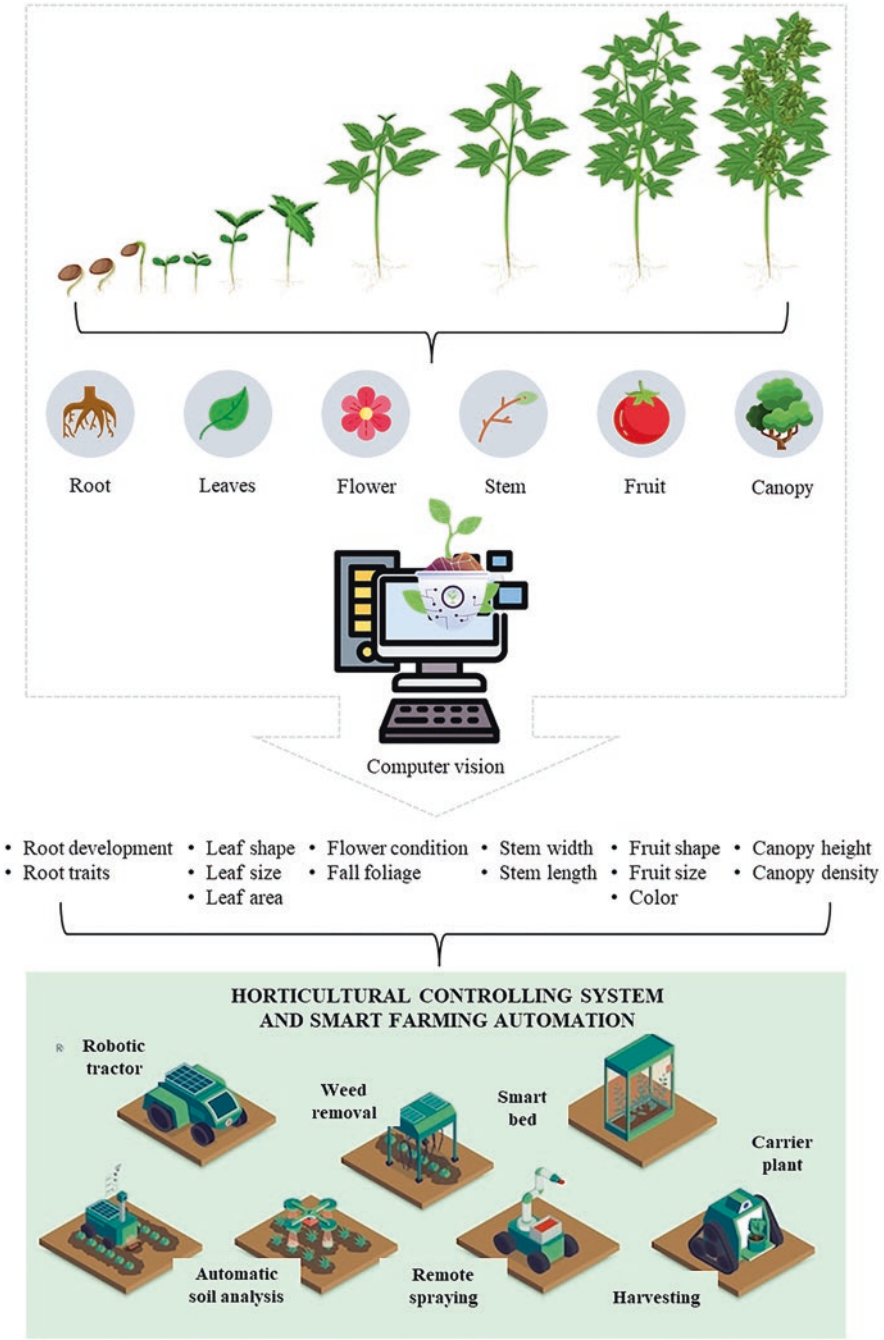

Fig. 11.1 Plant morphology identified through machine vision phenotyping, using an integrated control system and automation

11.2 High-throughput Plant Phenotyping

A comprehensive grasp of both plant morphology and physiology provides a crucial foundation for the groundbreaking field of high-throughput plant phenotyping (HTPP). In HTPP, the integration of a plant's physical appearance (morphology) with its internal processes (physiology) is important. HTPP is an advanced scientific approach that involves the rapid and automated measurement of various plant traits on a large scale. This cutting-edge method is particularly valuable in agricultural research and plant breeding and enables researchers to simultaneously characterize numerous plants, thus providing large amounts of data for analysis. These data enable researchers and scientists to identify or modify desirable plant traits, monitor plant responses to abiotic and biotic environments, and accelerate the development of improved crop varieties.

Image-based approaches have been a prominent subject in contemporary plant phenotyping due to the increasing availability of low-cost optical sensors such as digital RGB cameras. This technology shift highlights the evolution of HTPP, emphasizing the importance of visual data in gaining a better understanding of plant traits and behavior. In high-throughput plant phenotyping, researchers commonly apply two main approaches based on imaging techniques: (1) 2D image-based phenotyping and (2) 3D image-based phenotyping. 2D phenotyping involves capturing and analyzing two-dimensional images or data. These images are typically taken from a single viewpoint, such as the top view or side view of plants, and provide information about the size, shape, color, and visible features of plants. In 2D phenotyping, measurements and analyses are limited to the length and width of the objects being studied, and the depth and volume aspects are ignored. 2D image-based phenotyping is diverse and varied, ranging from basic color capture using RGB cameras to more advanced methods such as fluorescence, infrared, and multispectral or hyperspectral imaging. In contrast, 3D image-based phenotyping involves capturing three-dimensional data about plant structures. This method provides more comprehensive information than simply length and width, enabling the creation of detailed 3D models of plants. Techniques such as light detection and ranging (LiDAR), structured light scanning, and depth sensors are used in 3D image-based phenotyping.

Both 2D and 3D image-based phenotyping methods are valuable for plant research and agriculture, and each offers unique perspectives and insights into plant attributes and behaviors. Plant phenotyping has made use of these image sensing systems to capture pixelated representations using visible light, infrared, fluorescent response, and temperature and then to transform the captured information into estimations of various plant traits related to morphology, physiology, and component content (Table 11.1) (Li et al., 2021). Researchers choose these methods based on the specific attributes of interest and the level of detail needed for analysis.

11.2.1 2D Image-Based Phenotyping

11.2.1.1 RGB Imaging System

RGB imaging is extensively used in plant phenotyping as a nondestructive and cost-effective means of examining numerous plant features and characteristics. RGB imaging indicates the capture of digital images using red, green, and blue light channels that share similarities with the human vision system. These photos can be processed and analyzed to derive a basic visual analysis of plant characteristics. In addition, RGB images can also be used to assess a variety of traits, including the number of agronomical yield components, relevant phenological stages, crop development monitoring, growth measurements of individual plants, and foliar symptom identification in relation to a variety of biotic and abiotic stresses.

Through image analysis software and algorithms, including machine learning and deep learning (DL), researchers can accurately quantify plant characteristics. For example, the green color intensity in an RGB image can be used to measure plant vigor, while changes in leaf color can indicate stress or nutrient deficiencies (Kolhar & Jagtap, 2023). Additionally, RGB imaging aids in monitoring plant responses to environmental factors such as light, water, and temperature through visual symptom analysis, thus enabling scientists to gain insights into how plants adapt to their surroundings. RGB technology enables nondestructive and high-throughput phenotyping to efficiently investigate large numbers of plants. This method is particularly beneficial in breeding initiatives, where the detection of desired features in large numbers of plants is necessary for producing new crop varieties that are resilient and ideally suited to their environments.

Table 11.1 Sensors currently available for monitoring, quantifying, and estimating key morphological, physiological, and component content traits

	Morphological traits			Physiological traits			Component content traits		
Sensors/cameras	**Plant height**	**Biomass**	**Canopy coverage**	**Senescence**	**Light use efficiency**	**Disease/ pests**	**Chlorophyll content**	**Nitrogen content**	**Water content**
RGB camera	■	■	■	■		■	■	■	■
Hyperspectral camera	■	■	■	■		■	■	■	■
Thermal camera			■			■			■
Fluorescence sensor		■			■	■			
Stereo/3D camera	■	■	■						
LiDAR	■	■	■						

11.2.1.2 Fluorescence Imaging System

Another type of phenotyping technique is the fluorescence imaging system. Fluorescence imaging methods in HTPP have transformed the ways that plant biologists analyze plant biology and plant reactions to environmental variables. Fluorescence imaging serves as a potent method for exploring photosynthetic activity across cellular, leaf, and whole-plant levels, thus facilitating the phenotyping of plants (Pérez-Bueno et al., 2019). Fluorescence imaging involves capturing fluorescence signals or parameters and commonly utilizes charge-coupled device (CCD) cameras that are sensitive to fluorescence signals. This sensitivity is achieved by illuminating samples with visible or UV light through pulsed lasers, pulsed flashlight lamps, or LEDs (Fig. 11.2). The resulting pixel value images of fluorescence parameters are visualized using a false color code, spanning from black (0.00) through red, yellow, green, and blue to pink (culminating at 1.000) (Li et al., 2014).

However, fluorescence imaging systems have certain limitations. One major constraint is their requirement for a dark-adapted reference, which means that plants need to be acclimated to darkness before accurate fluorescence measurements can be taken. This dark adaptation is necessary to establish a baseline fluorescence level, enabling researchers to accurately assess any changes in fluorescence under different conditions. Additionally, the proximity of the imaging system to the plant canopy is crucial for obtaining reliable and detailed data. In practical terms, this means that the imaging system must be placed close enough to the plants to capture accurate fluorescence signals. Achieving this proximity can be challenging, especially in the case of large or dense plant populations.

Despite these limitations, fluorescence imaging remains a useful tool in plant phenotyping, particularly in controlled environments such as research greenhouses or growth chambers where the lighting conditions can be precisely controlled. In these settings, researchers can optimize the fluorescence imaging setup to mitigate the challenges related to dark adaptation and proximity, enabling the in-depth studies of plant responses to various stresses.

11.2.1.3 Hyperspectral Imaging System

Apart from RGB and fluorescence cameras, one of the most advanced HTPP imaging systems is the hyperspectral system. Compared to RGB cameras, which operate over a relatively wide range of the electromagnetic spectrum by combining red, green, and blue channels, hyperspectral cameras are designed to capture images at more discrete spectral wavelengths (Fig. 11.3). This allows the hyperspectral data to capture detailed spectral information across a broader range of the electromagnetic spectrum, ranging from ultraviolet (UV) to shortwave infrared (SW-IR) wavelengths in the range of 350 nm and 2500 nm (Kashyap & Kumar, 2021). These systems enable an analysis of traits that are not detectable by human eyes, pushing

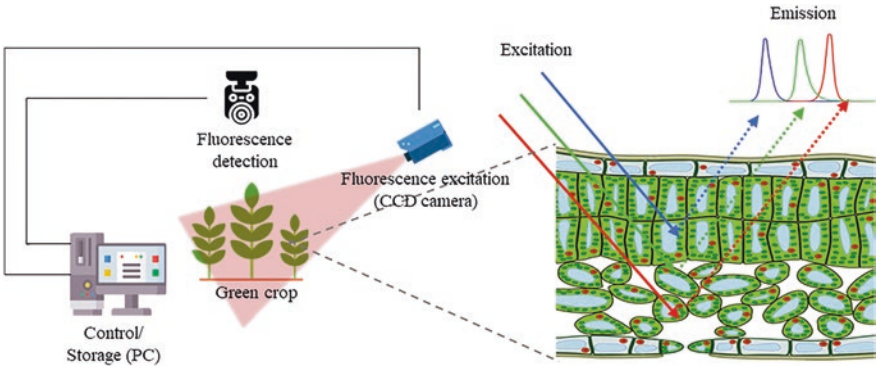

Fig. 11.2 Working principle of fluorescence imaging

the limits of knowledge beyond that achieved through visual perception. This ability makes hyperspectral imaging a powerful HTPP tool for quantifying the complex biological processes of plants, such as photosynthesis and nutrient uptake, as well as detecting stress factors, such as abiotic stress, biotic stress, and biochemical parameters (Sarić et al., 2022). Various wavelength ranges can provide distinct information; healthy plants commonly exhibit a strong absorption of visible light (VIS 400–700 nm) due to pigments related to chlorophyll and photosynthesis. In contrast, the near-infrared (NIR 700–1000 nm) light that becomes scattered is primarily dependent on leaf cell structure, and the reflectance of leaves in the SW-IR (1000–2500 nm) is influenced by water and chemical content (Kashyap & Kumar, 2021).

However, there are certain challenges associated with hyperspectral imaging in HTPP. One significant drawback is the complexity of processing and analyzing the large amount of data generated by hyperspectral cameras. To manage and evaluate these data, advanced computational tools and expertise are needed, making the process both time-consuming and resource-intensive. Additionally, hyperspectral imaging equipment can be costly to acquire and maintain, limiting its accessibility to researchers under limited budgets. Furthermore, environmental factors such as lighting conditions and atmospheric interference can affect the quality of hyperspectral images, which could potentially lead to analytical inaccuracies.

Nevertheless, these limitations can be overcome through the use of advanced data processing techniques, such as machine learning or DL algorithms and data mining, to effectively manage and extract useful patterns from the enormous datasets involved. In addition, collaboration among experts from various domains, including plant biology, computer science, and engineering, can facilitate the development of novel data analysis solutions and algorithms. Furthermore, continual advancements in sensor technology and image processing algorithms can lead to more economical and user-friendly hyperspectral imaging systems and increase their availability to a broader range of researchers and practitioners in the HTPP field. The calibration and standardization of equipment on a regular basis can also

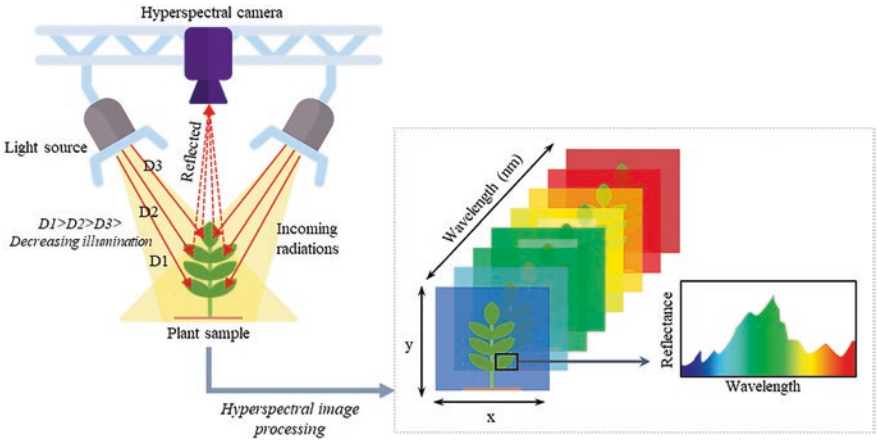

Fig. 11.3 Overview of hyperspectral imaging working principles in plant phenotyping

assist in eliminating errors caused by environmental factors, thus assuring the authenticity of the extracted data. By proactively addressing these challenges, the benefits of hyperspectral imaging in HTPP can be optimized, leading to more comprehensive and insightful plant phenotype analyses.

11.2.1.4 Thermal Imaging System

Thermal imaging systems have led to further remarkable HTPP progress in assessing plant health, stress responses, and physiological activities. Unlike visible light mechanisms, thermal cameras capture the infrared radiation (heat) emitted by plants (Vadivambal & Jayas, 2011). The camera then converts the infrared radiation from the plants into temperature variation, thus providing useful information for monitoring plant activities such as stomatal conductance, plant transpiration, and photosynthesis. This method allows for the determination of the temperature distribution through quick and noninvasive techniques that do not involve direct contact or cause any damage to the plants (Ali et al., 2019). Infrared radiation includes near-infrared (0.75–1.3 μm), shortwave infrared (1.3–3 μm), mid-wave infrared (3–8 μm), far-infrared (8–14 μm), and extreme infrared (14–1000 μm) wavelengths. Longwave infrared radiation, which is particularly sensitive to low temperatures such as indoor settings, is particularly advantageous for plant phenotyping (Wen et al., 2023).

Thermal imaging in HTPP offers multiple advantages. For instance, a thermal imaging system can be deployed to identify water stress in plants by detecting the higher temperatures in stressed or dehydrated plants resulting from their reduced transpiration rate, thus enabling efficient irrigation management and improved crop yield. In addition, disease and pest detection can also be facilitated by revealing distinct thermal patterns in infected plants to enable early identification and timely

interventions such as targeted treatments or quarantine, thus minimizing crop loss. Additionally, thermal imaging provides valuable insights into plant responses to environmental stressors such as heatwaves or extreme cold conditions. This technology enables the assessment of thermal tolerance in different plant varieties, facilitating the selection and breeding of more resilient crops in the face of changing climates. Its capacity for detecting stress in its early stages, prior to the manifestation of visible signs, makes thermal imaging a valuable tool for understanding and enhancing plant health across diverse agricultural settings.

The effectiveness of thermal imaging in capturing accurate temperature data on plants can be influenced by several radiometric attributes, including transmittance (τ), emissivity (ε), and reflectance (Fig. 11.4) (Wen et al., 2023). These factors characterize the properties of the plants being observed as well as those of their surrounding environment. Transmittance refers to the ability of materials to transmit infrared radiation, emissivity represents the efficiency an object displays in emitting thermal radiation, and reflectance accounts for the radiation that is reflected off the surface of the object and its environment. These attributes can affect the accuracy and reliability of thermal data, and they are important considerations when using thermal imaging for plant analysis in different settings and conditions.

11.2.2 3D Image-Based Phenotyping

11.2.2.1 LiDAR

In phenotyping studies, especially in the context of plantations, distinguishing between plant organ expansion and movement in 2D images can be challenging, particularly when the plant images are captured under different lighting conditions. To address this challenge, the third dimension (3D) needs to be considered to enable more precise growth quantification. Light detection and ranging (LiDAR) is one of the 3D imaging techniques used in HTPP. In the context of phenotyping, LiDAR technology leveraging laser beams is used to measure distances and create detailed 3D models of objects, such as plant canopies, thereby enabling researchers to obtain precise measurements of plant height, canopy architecture, volume, and biomass (Fig. 11.5). By scanning plants with laser beams and measuring the time it takes for the light to bounce back, LiDAR systems generate point clouds that represent the spatial distribution of objects in the scanned area. These point clouds can be processed to create detailed 3D models, which can provide valuable information about the plant's physical structure. LiDAR is less sensitive to lighting conditions and performs well in various environments, including low-light settings.

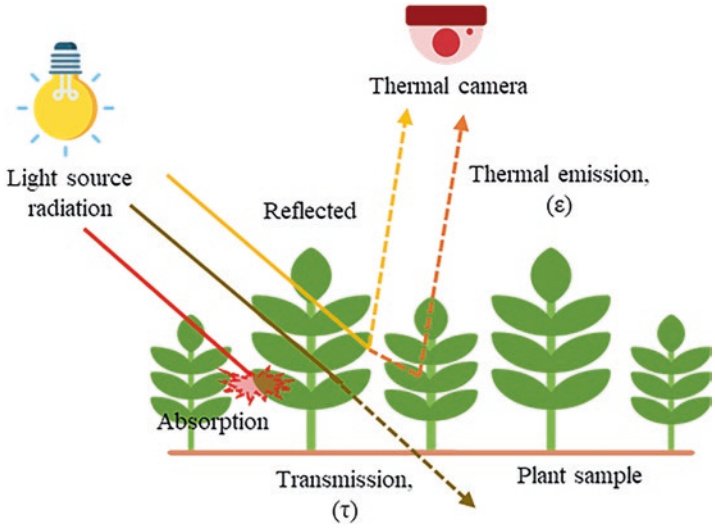

Fig. 11.4 Thermal imaging principles based on transmittance (τ), emissivity (ε), and reflectance

11.2.2.2 Depth Camera

While LiDAR stands out as a powerful tool for 3D-image-based phenotyping that can provide detailed spatial information using laser beams, an alternative approach involves the utilization of depth cameras. In plant phenotyping, depth cameras employ technologies such as stereo vision, structured light, or time-of-flight. Depth cameras can capture rich surface details with high spatial resolution than LiDAR, and they are more often cost-effective and compact. This makes them particularly valuable in scenarios where precision at close ranges is needed. In addition to capturing the color and intensity of the plants, the depth camera also captures the information regarding the distance to each point in the scenes to provide the three-dimensional architecture of plants. This information offers detailed insights into plant morphology and growth dynamics.

One notable advantage of the use of depth cameras in plant phenotyping is their high spatial resolution, allowing for the meticulous capture of surface details. This key feature enables researchers to analyze the intricate structures of leaves, stems, and other plant components. Additionally, depth cameras are more cost-effective and compact than LiDAR, making them more accessible under budget constraints and space considerations. In practice, depth cameras are usually deployed in agricultural settings and are mounted on phenotyping platforms or drones to scan crops and generate highly detailed three-dimensional point clouds. These point clouds have become invaluable resources for researchers and farmers for their precise measurements of parameters such as plant height, canopy structure, and leaf distribution.

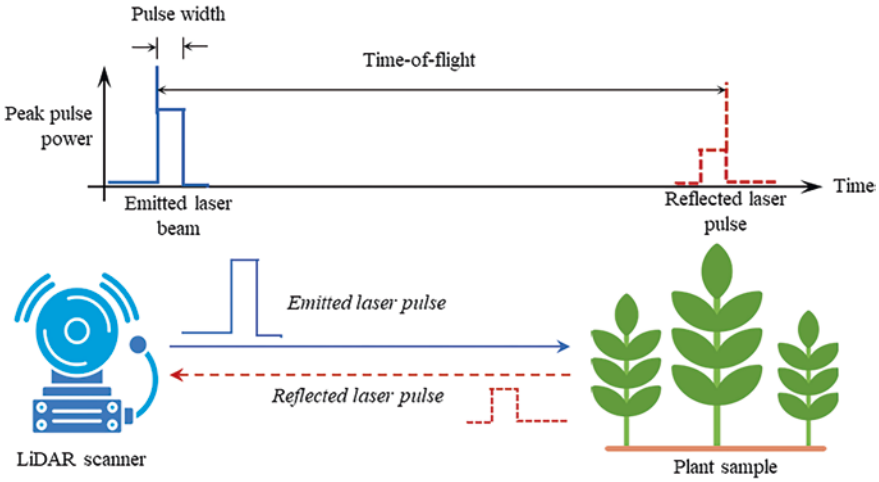

Fig. 11.5 The working principle of LiDAR

11.3 High-throughput Plant Phenotyping Platforms

Exploring the complexities of image-based phenotyping reveals that the choices and capabilities of sensors and cameras significantly shape the depth of insight obtained in phenotyping processes. These technologies, which range from high-resolution cameras to sophisticated depth sensors, act as sensory components in the phenotyping process by capturing data on plant morphology and environmental conditions. However, the full potential of these imaging sensors to rapidly and efficiently capture and measure various plant traits on a large scale can be leveraged by incorporating these sensors into HTPP platforms.

11.3.1 Conveyor-Type

Conveyor-type phenotyping is an HTPP approach that applies the plant-to-sensor concept and is operated in a controlled environment. The plants are systematically moved on a conveyor belt to acquire plant data and physical properties. This approach is especially helpful for large-scale research and breeding programs since it allows for the rapid and automated measurement of plant traits (Li et al., 2021).

Typically, conveyor-type phenotyping consists of a conveyor belt that moves plants along a set path, with sensors and imaging devices strategically placed along this path to capture plant traits. Real-time data, including plant growth, morphology, stress responses, and disease symptoms, are collected via these sensors. This method allows for high-throughput analysis and enables the screening of thousands of plants for the identification of specific traits, the study of environmental responses, or in the technological enhancement of breeding programs. The collected data are then processed and analyzed for meaningful insights.

11.3.2 Benchtop-Type

Benchtop phenotyping platforms have become essential instruments in the field of controlled environment agriculture, as they offer researchers precise control and in-depth analysis capabilities within compact spaces. In the context of controlled environments, such as plant factories, these benchtop systems are particularly valuable for their adaptability and versatility. Designed to be placed on laboratory benches or workstations, these platforms facilitate detailed studies of individual plants or small groups within a controlled indoor environment. One of the key advantages of benchtop phenotyping platforms lies in their ability to provide controlled, stable conditions for plants, including consistent lighting, temperature, humidity, and nutrient levels. This controlled environment ensures that the experiments are not influenced by external factors, thus allowing researchers to focus solely on the impact of specific variables on plant growth and development.

Benchtop systems are particularly well suited for monitoring various plant traits, including leaf morphology, color intensity, growth patterns, and plant responses to different stress factors. Researchers can conduct experiments through precise replication, enabling the study of plants under specific treatments or genetic modifications. This controlled approach is essential for understanding how different factors influence plant phenotypes, which is crucial for crop improvement efforts and the development of resilient plant varieties. Furthermore, these platforms facilitate rapid data acquisition and analysis. High-throughput imaging technologies integrated into benchtop systems enable the efficient screening of numerous plant samples. Advanced image analysis software is used to process the data and extract valuable insights into plant characteristics and growth dynamics. This automation not only saves time but also enhances the accuracy and reliability of the results.

11.3.3 Gantry-Type

Gantry-type phenotyping platforms represent a significant advancement in the domain of controlled environment agriculture, particularly for large-scale operations. These platforms are equipped with a variety of sensors, cameras, and robotic arms, are mounted on sturdy frameworks, and can be designed to move both horizontally and vertically to monitor plants at different heights and angles. The primary advantage of gantry-type platforms is their scalability. Unlike smaller benchtop systems, gantry platforms can cover vast sections of indoor agricultural spaces, enabling researchers to conduct large-scale experiments with precision by capturing data from multiple points within the environment. This scalability is especially crucial for commercial operations and research facilities that aim to optimize crop production on a substantial scale.

Additionally, gantry platforms offer flexibility in positioning sensors and cameras at different heights and angles. This adaptability allows researchers to capture

plant data from various perspectives, ensuring a thorough examination of traits such as plant height, canopy structure, and leaf morphology. The ability to adjust sensor configurations according to specific research needs enhances platform versatility and makes them suitable for a wide range of plant species and experimental setups. Moreover, gantry platforms contribute to the efficiency of data collection. By automating the movement of sensors and cameras, these platforms can systematically scan large plant populations, enabling high-throughput phenotyping. The data collected are then processed through the use of advanced algorithms to provide valuable insights into plant growth patterns, stress responses, and other phenotypic characteristics. This efficient data collection and analysis method streamlines research efforts, allowing scientists to identify valuable traits and accelerate breeding programs or optimize cultivation techniques for commercial production.

11.3.4 Mobile Type

The mobile HTPP is designed to traverse fields and efficiently gather crop phenotypic traits either in semiautomatic or fully automatic mode. This system can be integrated into various agricultural platforms, including refitted machinery, such as tractors, sprayers or harvesters, and self-developed mechanical platforms, such as carts, buggies, or commercially available automatic platforms.

Typically, a mobile HTPP comprises four key subsystems: the sensing system, data acquisition system, mechanical platform, and driving system. The sensing system incorporates a range of sensors, including GPS for location tracking, environmental sensors for monitoring factors such as light and wind speed, and phenotypic sensors such as RGB, multispectral, hyperspectral, and thermal sensors. The data acquisition system involves specialized software on an onboard computer for managing and processing the gathered data. The mechanical platform is responsible for bearing loads and providing mobility to the system, while the driving system can be categorized into electricity-driven, engine-powered, or manually operated.

One key aspect of mobile HTPP that should be highlighted is the real-time monitoring capability and capacity of this system, which provides immediate feedback on crop conditions. The continuous and dynamic nature of data collection continuously leads to deeper understandings of plant growth patterns, enabling farmers to respond more promptly to environmental conditions. The adaptability of the mobile HTPP extends beyond its physical integration with different agricultural platforms. It also possesses the flexibility to incorporate additional sensors or upgrade existing sensors, ensuring that the system remains current with technological advancement. This adaptation is vital in addressing emerging challenges and incorporating new scientific discoveries into the plant phenotyping process.

As HTPP platforms evolve into core tools for phenotyping, their integration with state-of-the-art technologies is propelling the field into a new era of

sophisticated agriculture. These platforms, whether standalone mechanical systems or systems mounted on refitted machinery, offer an unparalleled ability to capture intricate details of plant growth and environmental conditions. However, their potential emerges more fully when combined with the advanced capabilities of DL applications in the analysis of the gathered information or data. Incorporating DL into plant phenotyping processes leverages the wealth of data collected by HTPP platforms.

11.4 Deep Learning Applications in Plant Phenotyping

Extensive research has been conducted to develop image analysis models specifically designed to enable efficient HTPP (Arya et al., 2022). The automation levels and their capacity for measuring certain phenotypic traits or statistics differ across these models. According to their complexity, image-based phenotypes can be categorized into two main classes, namely the linear functions of plant pixels and nonlinear functions of plant pixels (Fig. 11.6). Linear phenotypes in image processing phenotyping refers to plant traits that can be quantified through straightforward, linear relationships through the use of pixel intensities in the acquired digital images (Ubbens & Stavness, 2017). Features such as leaf area, color intensity, chlorophyll content, NDVI, and stem diameter can be derived from pixel values through the use of simple calculations based on basic mathematics or algorithms. While these features provide valuable quantitative information, more complex nonlinear phenotypic features can also be extracted from images using sophisticated image processing techniques, thus allowing for a more detailed and comprehensive analysis of plant traits and characteristics.

Nonlinear phenotyping in image processing, on the other hand, is a method of quantifying more complex plant traits that cannot be directly measured through pixel intensities. Some instances of nonlinear phenotypic features in image processing include plant organs, plant age or maturity, growth rate, and yield. More advanced algorithms are needed to extract meaningful information regarding those features from an image, and that information cannot be calculated solely on the basis of pixel values. The importance of nonlinear phenotypic traits lies in the way that they capture intricate patterns, shapes, and relationships within plant materials, enabling a more detailed analysis of plant phenotypes. Hence, to extract nonlinear phenotypic features, advanced image processing techniques such as computer vision, machine learning, and deep learning (DL) are employed (Fig. 11.7). These methods allow researchers to explore deeper into the complexity of plant structure and aid in the development of more comprehensive solutions for plant disease detection, the breeding of new plant varieties, and the development of resilient plant traits that facilitate resilience to various biotic or abiotic stresses (Ubbens & Stavness, 2017).

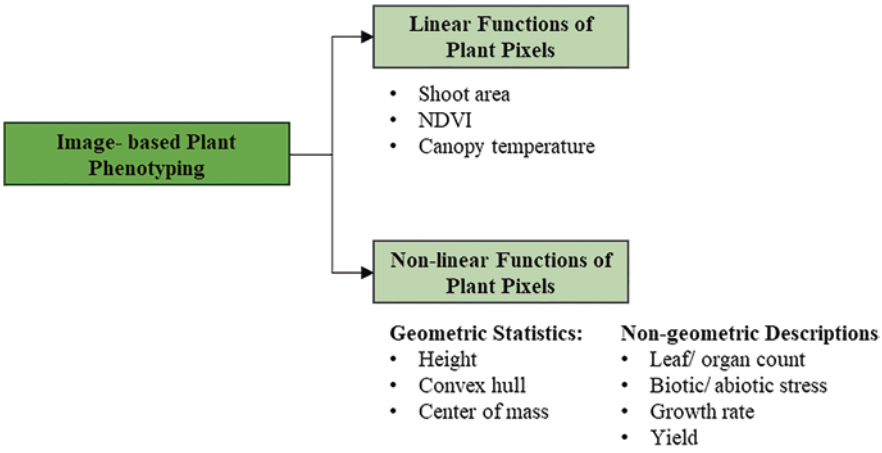

Fig. 11.6 Image-based phenotype classifications

11.4.1 DL-Based HTPP in the Germination and Early Growth Stages

At the germination and early growth stages of plant development, DL models are employed to analyze seed germination patterns, monitor seedling emergence, and assess plant vigor. Convolutional neural networks (CNNs) enable the extraction of meaningful information from images to aid in the detection of emergence rates, seedling uniformity, and potential stress factors. These models can provide insights into the effects of different environmental conditions on germination success and early plant growth. For instance, Nehoshtan et al. developed a universal seed germination prediction tool based on DL and RGB imaging (Nehoshtan et al., 2021). Samiei et al. implemented a deep neural network followed by a long short-term memory cell to classify three stages of plant growth for red clover and alfalfa (Samiei et al., 2020). Han et al. introduced a novel framework for accurate leaf area measurement in melon seedlings using point cloud data from an Azure Kinect camera to measure leaf area (Han et al., 2022). Li et al. developed an improved object-detection model based on Faster R-CNN for high-precision detection of hydroponic lettuce seedlings in a greenhouse (Li et al., 2021). Zhang and Li developed ESPA based on the YOLOv5 attention mechanism to determine the survival rate of canola seedlings at different growth stages (Zhang & Li, 2022). Hamidon and Ahamed addressed the labor-intensive task of manually identifying defective lettuce seedlings in indoor farming, which is particularly challenging under the varying lighting conditions when using DL algorithms (Fig. 11.8) (Hamidon & Ahamed, 2023).

The utilization of DL enhances researchers' ability to efficiently process and interpret large volumes of image data. This improves our understanding of the

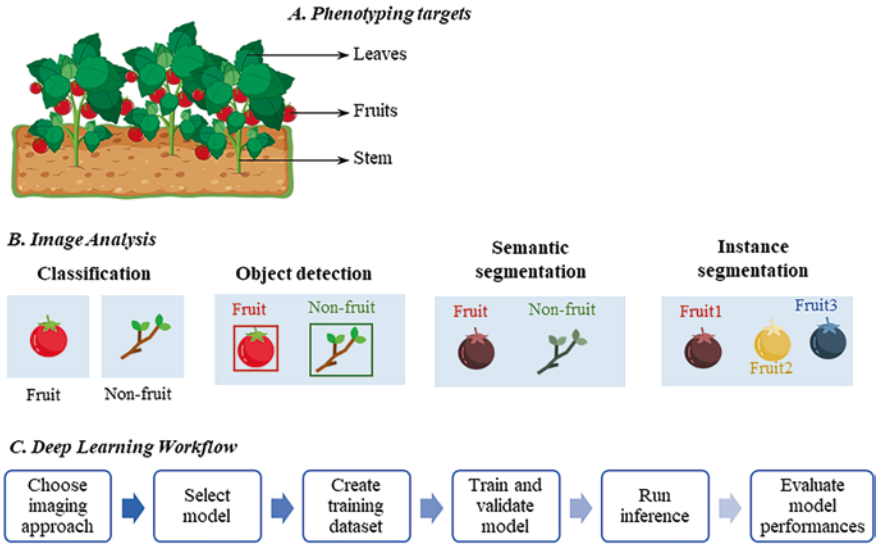

Fig. 11.7 Overview of the deep learning framework in plant phenotyping

uncertainty processes that occur during germination and early growth, enabling more informed decision-making in agriculture and plant breeding. Moreover, the insights derived from these models can inform the design of experiments and guide the development of interventions to improve germination rates, seedling uniformity, and overall plant health.

11.4.2 DL-Based HTPP in Vegetative Growth and Development

During the vegetative growth phase, DL techniques play a crucial role in monitoring plant architecture, leaf area, canopy cover, and biomass accumulation. Advanced algorithms, such as recurrent neural networks (RNNs) and long short-term memory (LSTM) networks, which are designed to capture temporal dependencies, prove particularly advantageous in tracking plant growth over extended time periods. This application allows for a comprehensive analysis of substantial datasets comprising images and sensor-derived information. Franchetti et al. (2019) proposed a method for measuring basil plant growth in closed vertical farming under an artificial lighting environment. The method includes 3D reconstruction, leaf segmentation, geometric surface modeling, and deep network estimation for weight prediction and is focused on three important phenotype features: height, weight, and leaf area. Hwang et al. (2022) introduced "pseudo crop mixing," which is an artificial intelligence method for monitoring lettuce crop growth in vertical farms. This method is used to

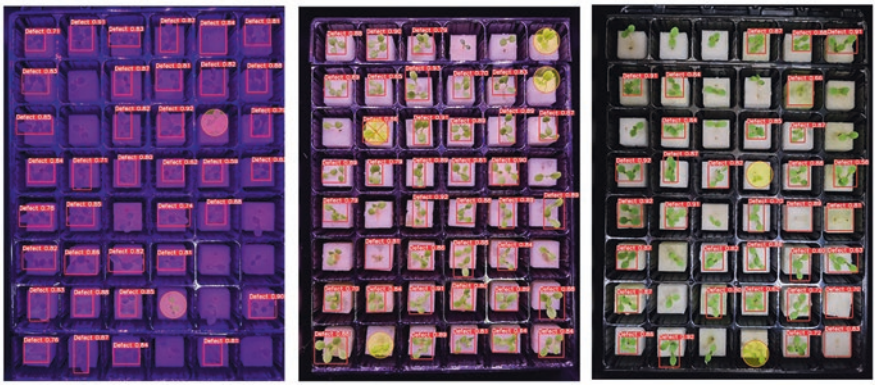

Fig. 11.8 Potential DL use in detecting seedling status under complex indoor lighting conditions

predict crop area in images, providing size quantification and offering cost-efficient and robust solutions for diverse environments. Kim et al. (2022) developed a spatial transformation approach inspired by the spatial transformer network (STN) to predict plant growth by generating an image at a later time for quantitative measuring growth progression. Buxbaum et al. (2022) introduced an end-to-end DL method for predicting lettuce plant biomass directly from color and depth image data acquired from a low-cost sensor. Gang et al. (2022) showcased a two-CNN model utilizing RGB and depth images to predict various attributes of greenhouse-grown lettuce, including fresh weight, dry weight, height, diameter, and leaf area in a hydroponics system.

Collectively, these studies contribute novel insights and methodologies for advancing the efficiency and accuracy of plant growth prediction and monitoring techniques through the use of DL. By integrating large datasets of images from diverse sources and employing DL architectures, researchers can uncover comprehensive insights into the dynamics of plant development, thereby optimizing crop production and strengthening agricultural resilience.

11.4.3 DL-Based HTPP in the Flowering and Reproductive Stages

Moreover, the application of DL also significantly contributes to understanding the flowering and reproductive stages of plants. Through the deployment of DL algorithms in processing images and time-lapse videos, the processes of pollination, flower development, and fruit production can be automatically tracked. Chang et al. (2021) demonstrated a novel method using HTPP data and advanced DL techniques, U-Net and SE-ResXt101. In their research, they identified a specific developmental timeframe that is crucial for predicting the different stages of Arabidopsis growth,

presenting potential applications in forecasting the growth and yield of leafy plants such as lettuce. Another study by Zhang et al. (2023) addressed the challenges of greenhouse environments, introducing the YOLOXPC model, which is an improved version of YOLOX, for the accurate detection of small targets such as tomato flowers and fruits. Additionally, Xu et al. (2022) introduced FlowerYolov5, which is a method based on Yolov5s, to enhance the detection of tomato flowering stages in pollination robots within smart greenhouses. In another study, Mu et al. (2023) developed a detection method of apple flower and king flower based on Mask R-CNN for precision pollination.

These innovative tools play crucial roles in evaluating the process of pollination events, analyzing the presence of any anomalies within flowers, and even predicting potential yield outputs, particularly in controlled environments. The temporal analysis capabilities of DL techniques empower researchers to thoroughly examine the evolving patterns during the flowering and reproductive stages of plants. This analytical capacity leads to valuable insights into the specific timing and duration of these essential developmental phases, contributes to making informed decisions regarding crop management strategies, optimizes pollination processes, and ultimately enhances agricultural productivity.

11.4.4 DL-Based HTPP in Harvest and Yield Prediction

As plants approach maturity, the capabilities of DL techniques hold promise in enhancing yield prediction accuracy. By training DL through a rich repository of growth parameters, historical data, and real-time weather conditions, the models can provide precise estimations of crop yield. Notably, the integration of DL methodologies with autonomous harvest robots presents an innovative approach for detecting maturity stages. Additionally, by equipping these robotic systems with advanced visual sensors such as depth cameras and deploying DL algorithms, robots can not only differentiate between and track targets but also analyze visual characteristics that indicate maturity, such as color changes and size dimensions. Several studies have proven how DL can be utilized in monitoring and indicating the maturity of crops. As an example, Zhou et al. (2020) proposed an improved faster RCNN to detect strawberries and assess their plumpness from an analysis of RGB images captured by a self-developed "large scene camera system." Seo et al. (2021) developed a real-time robotic system for monitoring the growth of tomato fruits in hydroponic conditions. The robotic system was equipped with an RGB camera with DL to detect and classify the maturity of the fruits into six levels. Wei et al. (2022) predicted the ripeness of greenhouse grapes by analyzing the color values of grape skin using a back-propagation neural network algorithm (BPNN). These examples showcase the potential of DL in HTPP automation, particularly in accurately predicting and monitoring crop maturity in controlled environments.

This fusion of technologies of DL-based HTPP can empower robots to make informed decisions regarding the optimal harvesting timing, ensuring that crops are

collected when they reach their peak ripeness. Combining deep learning with autonomous harvest robots transforms precision agriculture by maximizing labor utilization and minimizing waste. This approach can be used to efficiently harvest crops at the precise time when they reach their prime state of maturity.

11.5 Conclusions and Prospects

Advancements in HTPP techniques for controlled environments have revolutionized our ability to understand and manipulate plant traits with unprecedented precision. These techniques, which encompass various aspects, such as phenotyping, computation, breeding enhancement, and insight analysis, have collectively propelled plant science into a new era of innovation and discovery (Fig. 11.9). Phenotyping technologies have evolved from traditional labor-intensive and subjective methods to automated, noninvasive, and high-resolution approaches. This shift has enabled researchers to capture intricate details of plant growth, physiology, and environmental responses, thus providing a deeper understanding of plant biology. As a complement to these advancements, computational tools have emerged as essential system enhancements for managing the enormous volumes of data generated and extracting previously inaccessible meaningful patterns. Through the integration of deep learning, data analytics, and modeling, researchers can now identify the complex relationships between genotype and phenotype and predict plant behavior under various conditions.

The impact of these advancements on breeding enhancement is profound. High-throughput phenotyping allows breeders to rapidly screen and select plants with desired traits, which considerably accelerates the breeding process. This not only improves crop yield and quality but also contributes to addressing global food security challenges. Additionally, the newfound insights into plant responses to stressors and environmental changes provide opportunities to develop resilient crop varieties that can thrive in changing climates and challenging conditions. As we look to the future, the prospects of high-throughput plant phenotyping techniques continue to expand. The integration of multiomics data (genomics, transcriptomics, proteomics, and metabolomics) with phenotypic information holds promise for a holistic understanding of plant biology and the enabling of a systems-level approach to unravel intricate regulatory networks. Furthermore, future advancements in imaging technologies, robotics, and sensor networks will likely lead to even higher levels of automation and scalability, which can enable researchers to conduct large-scale experiments and gather data from diverse plant populations. However, challenges such as data management, protocol standardization, and cost-effectiveness still need to be addressed. Collaborations between researchers, engineers, and industry partners will be essential in overcoming these hurdles and ensuring the practical implementation of these techniques on a larger scale.

In conclusion, advancements in high-throughput plant phenotyping techniques under controlled environments have ushered in a new era of transformative research.

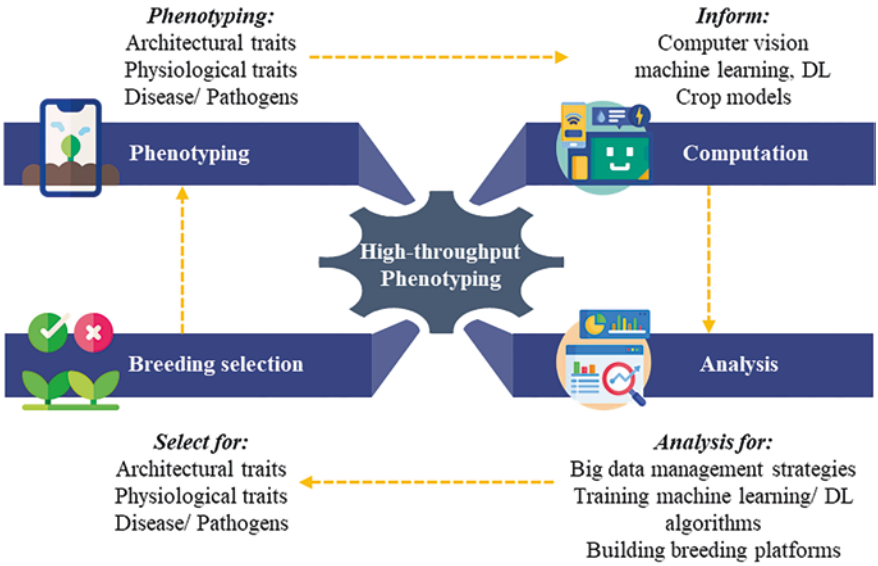

Fig. 11.9 High-throughput phenotyping encompasses phenotyping, computation, analysis, and breeding selection

The convergence of phenotyping, computation, breeding enhancement, and insight analysis has positioned plant scientists and breeders to make unprecedented breakthroughs in crop improvement and agricultural sustainability. With ongoing technological innovations and collaborative efforts across disciplines, the potential to unlock the secrets of plant biology and address global challenges remains vast and inspiring.

References

Ali, M. M., Bachik, N. A., Muhadi, N. A., Yusof, T. N. T., & Gomes, C. (2019). Non-destructive techniques of detecting plant diseases: A review. *Physiological and Molecular Plant Pathology, 108*, 101426.

Arya, S., Sandhu, K. S., Singh, J., & Kumar, S. (2022). Deep learning: As the new frontier in high-throughput plant phenotyping. *Euphytica, 218*(4), 47.

Buxbaum, N., Lieth, J. H., & Earles, M. (2022). Non-destructive plant biomass monitoring with high spatio-temporal resolution via proximal RGB-d imagery and end-to-end deep learning. *Frontiers in Plant Science, 13*, 758818.

Chang, S., Lee, U., Hong, M. J., Jo, Y. D., & Kim, J. B. (2021). Time-series growth prediction model based on U-net and machine learning in Arabidopsis. *Frontiers in Plant Science, 12*, 721512.

Das Choudhury, S., Samal, A., & Awada, T. (2019). Leveraging image analysis for high-throughput plant phenotyping. *Frontiers in Plant Science, 10*, 508. https://doi.org/10.3389/fpls.2019.00508

Franchetti, B., Ntouskos, V., Giuliani, P., Herman, T., Barnes, L., & Pirri, F. (2019). Vision based modeling of plants phenotyping in vertical farming under artificial lighting. *Sensors, 19*(20), 4378.

Gang, M. S., Kim, H. J., & Kim, D. W. (2022). Estimation of greenhouse lettuce growth indices based on a two-stage CNN using RGB-D images. *Sensors, 22*(15), 5499.

Hamidon, M. H., & Ahamed, T. (2023). Detection of defective lettuce seedlings grown in an indoor environment under different lighting conditions using deep learning algorithms. *Sensors, 23*(13), 5790.

Han, B., Li, Y., Bie, Z., Peng, C., Huang, Y., & Xu, S. (2022). MIX-NET: Deep learning-based point cloud processing method for segmentation and occlusion leaf restoration of seedlings. *Plants, 11*(23), 3342.

Hwang, Y., Lee, S., Kim, T., Baik, K., & Choi, Y. (2022). Crop growth monitoring system in vertical farms based on region-of-interest prediction. *Agriculture, 12*(5), 656.

Kashyap, B., & Kumar, R. (2021). Sensing methodologies in agriculture for monitoring biotic stress in plants due to pathogens and pests. *Inventions, 6*(2), 29.

Kim, T., Lee, S. H., & Kim, J. O. (2022). A novel shape-based plant growth prediction algorithm using deep learning and spatial transformation. *IEEE Access, 10*, 37731–37742.

Kolhar, S., & Jagtap, J. (2023). Plant trait estimation and classification studies in plant phenotyping using machine vision–a review. *Information Processing in Agriculture, 10*(1), 114–135.

Li, D., Quan, C., Song, Z., Li, X., Yu, G., Li, C., & Muhammad, A. (2021). High-throughput plant phenotyping platform (HT3P) as a novel tool for estimating agronomic traits from the lab to the field. *Frontiers in Bioengineering and Biotechnology, 8*, 623705.

Li, L., Zhang, Q., & Huang, D. (2014). A review of imaging techniques for plant phenotyping. *Sensors, 14*(11), 20078–20111.

Mu, X., He, L., Heinemann, P., Schupp, J., & Karkee, M. (2023). Mask R-CNN based apple flower detection and king flower identification for precision pollination. *Smart Agricultural Technology, 4*, 100151.

Nehoshtan, Y., Carmon, E., Yaniv, O., Ayal, S., & Rotem, O. (2021). Robust seed germination prediction using deep learning and RGB image data. *Scientific Reports, 11*(1), 22030.

Pérez-Bueno, M. L., Pineda, M., & Barón, M. (2019). Phenotyping plant responses to biotic stress by chlorophyll fluorescence imaging. *Frontiers in Plant Science, 10*, 1135.

Samiei, S., Rasti, P., Ly Vu, J., Buitink, J., & Rousseau, D. (2020). Deep learning-based detection of seedling development. *Plant Methods, 16*(1), 1–11.

Sarić, R., Nguyen, V. D., Burge, T., Berkowitz, O., Trtílek, M., Whelan, J., Lewsey, M. G., & Čustović, E. (2022). Applications of hyperspectral imaging in plant phenotyping. *Trends in Plant Science, 27*, 301.

Seo, D., Cho, B. H., & Kim, K. C. (2021). Development of monitoring robot system for tomato fruits in hydroponic greenhouses. *Agronomy, 11*(11), 2211.

Tian, Z., Ma, W., Yang, Q., & Duan, F. (2022). Application status and challenges of machine vision in plant factory—A review. *Information Processing in Agriculture, 9*(2), 195–211.

Ubbens, J. R., & Stavness, I. (2017). Deep plant phenomics: A deep learning platform for complex plant phenotyping tasks. *Frontiers in Plant Science, 8*, 1190.

Vadivambal, R., & Jayas, D. S. (2011). Applications of thermal imaging in agriculture and food industry—A review. *Food and Bioprocess Technology, 4*, 186–199.

Wei, X., Wu, L., Ge, D., Yao, M., & Bai, Y. (2022). Prediction of the maturity of greenhouse grapes based on imaging technology. *Plant Phenomics, 2022*, 9753427.

Wen, T., Li, J. H., Wang, Q., Gao, Y. Y., Hao, G. F., & Song, B. A. (2023). Thermal imaging: The digital eye facilitates high-throughput phenotyping traits of plant growth and stress responses. *Science of the Total Environment, 165626*, 165626.

Xu, T., Qi, X., Lin, S., Zhang, Y., Ge, Y., Li, Z., Dong, J., & Yang, X. (2022). A neural network structure with attention mechanism and additional feature fusion layer for tomato flowering phase detection in pollination robots. *Machines, 10*(11), 1076.

Zhang, P., & Li, D. (2022). EPSA-YOLO-V5s: A novel method for detecting the survival rate of rapeseed in a plant factory based on multiple guarantee mechanisms. *Computers and Electronics in Agriculture, 193*, 106714.

Zhang, F., Lv, Z., Zhang, H., Guo, J., Wang, J., Lu, T., & Zhangzhong, L. (2023). Verification of improved YOLOX model in detection of greenhouse crop organs: Considering tomato as example. *Computers and Electronics in Agriculture, 205*, 107582.

Zhou, C., Hu, J., Xu, Z., Yue, J., Ye, H., & Yang, G. (2020). A novel greenhouse-based system for the detection and plumpness assessment of strawberry using an improved deep learning technique. *Frontiers in Plant Science, 11*, 559.

Chapter 12
Revolutionizing Agriculture: Embracing Modern Strategies for the Management of Coffee Leaf Rust Disease

Abstract Millions of people throughout the world enjoy coffee every day, and coffee-growing regions rely on this product for their economic growth. Coffee is one of the most valuable commodities in the world. Unfortunately, the sustainability of this popular drink is threatened by a disease called coffee leaf rust. Coffee leaf rust is a devasting disease caused by fungus that can damage coffee plantations and affect coffee production globally. Due to the persistence and adaptability of coffee leaf rust, coffee farmers are forced to address this disease on a continual basis. Thus, the use of modern pest and disease management methods to ensure the continued production of coffee and protect the livelihoods of those who depend on this crop is essential. This chapter highlights the transformative potential of deep learning in detecting coffee leaf rust in the fight against coffee leaf rust disease, which can offer a ray of hope for the advanced management of coffee leaf rust in the future.

Keywords Coffee Leaf Rust · Deep Learning · Plant Disease

12.1 Overview of Coffee Leaf Rust

12.1.1 Coffee Leaf Rust

Coffee is one of the most widely consumed beverages in the world. The aroma and distinct flavors of coffee have made people all over the world fall in love with this drink and even include coffee drinking as part of their daily routine. However, coffee production is indeed under threat due to the effects of climate change. The coffee plant is highly sensitive to climatic conditions, and even small changes in temperature and rainfall patterns can have significant impacts on its growth, yield, and quality. One plant-disturbing organism that attacks the organs of the coffee plant is coffee leaf rust (*Hemileia vastatrix*). *H. vastatrix* can cause severe damage and death to coffee plants. This can lead to decreasing production results and a decrease in production cause losses. Such losses can be either direct or indirect losses. Direct losses are the losses suffered by farmers due to disease. In Arabica

© The Author(s), under exclusive license to Springer Nature Singapore Pte Ltd. 2024

T. Ahamed, *IoT and AI in Agriculture*,
https://doi.org/10.1007/978-981-97-1263-2_12

coffee, direct losses are still a major problem. Disease causes the leaves of the Arabica coffee plant to fall, the plant to become bare, the shoots on the branches to die, and eventually, the plant to die.

Leaf rust disease commonly attacks coffee plants and is caused by the fungus *H. vastatrix*. This fungus is an obligatory parasite with no other host that reproduces through light spores that are easily carried by the wind. The fungus spreads very quickly through spores either with the help of wind or rain splashes, so that when one of the plants is attacked, the surrounding plants easily become infected as well (Bowden et al., 1971).

Attacks generally occur on the underside of the leaf. This starts with symptoms of yellow wounds covered with powder or stains appearing on the lower surface of the leaves (Fig. 12.1). On young wounds, pale yellow stains appear with clear sporulation that can cause the leaves to dry and fall, eventually causing the plant to become bare. This decreases coffee bean production, which results in economic losses to farmers.

Diseased plants are marked by the presence of light-yellow spots on the underside of the leaves, which then turn dark yellow, blacken, and dry. An orange powder forms on the underside of the leaves, in severe cases the leaves fall off, so the plant gradually becomes bare. Such plants run out of starch reserves in their roots and branches, which results in plant death. In Arabica coffee, this disease is a major problem (Cerda et al., 2017).

Coffee leaf rust (*H. vastatrix*) follows a distinct life cycle. It begins when fungal spores, called uredospores, land on coffee leaves. These spores germinate and penetrate the leaf's surface either through stomata or directly through cells (Keith et al., 2022). Once inside, the fungus develops infection through the hyphae that spread

Fig. 12.1 Coffee leaf rust

within the leaf. During the development stage, the fungus forms specialized structures called appressoria, which help penetrate the plant's cells. Haustoria is then formed, allowing the fungus to extract nutrients from the coffee plant. The spore production stage involves the formation of pustules called uredia on the underside of infected leaves. These uredia release vast quantities of uredospores, which are easily carried by wind to infect other plants. The cycle continues as uredospores infect additional susceptible plants.

In some cases, coffee leaf rust can enter a sexual stage. Dark-colored structures called telia develop on infected leaves and produce basidiospores during this stage. These spores can also be wind-dispersed and contribute to the spread of the disease. Coffee leaf rust is primarily transmitted through wind dispersal (Bowden et al., 1971). Uredospores, being lightweight, can travel long distances through the air. Similarly, basidiospores, if present, are carried by wind currents. Additionally, human factors such as contaminated tools and the movement of infected plant material can contribute to the transmission of coffee leaf rust. Insects and animals, although not the primary means of transmission, can mechanically carry rust spores on their bodies.

12.1.2 History of Coffee Leaf Rust

According to some reports, the most recent coffee leaf rust epidemic in Mesoamerica, which started in 2012, decreased production by as much as 90% in some regions, according to Ivette Perfecto in Tsing et al., 2021. The cause of the epidemic is still a mystery. Experts were baffled about why coffee rust suddenly spread to that extent over the entire area at that time. Why did this outbreak have more vigor than earlier outbreaks? Why, decades after the disease's first introduction to the area, was it relatively unproblematic until the 2012 outbreak? According to Ivette Perfecto in Tsing et al., 2021, the answer to these questions is closely tied to both the ecology of the illness and the monocultural plantation model that now dominates the coffee-producing landscapes.

In Fig. 12.2, the fungus *H. vastatrix*, which causes coffee leaf rust, most likely coevolved with plants of the genus Coffea in eastern Africa. McCook claims that the first case of the illness appeared in the British province of Ceylon (now Sri Lanka) in 1869 (McCook, 2019). The destruction was so severe that by 1880, the majority of the Arabica coffee plants had to be abandoned, as noted by Ivette Perfecto in Anna et al., 2021. As a result, tea finally supplanted coffee as Sri Lanka's primary export crop.

Ceylon offered the best environment for the growth of the fungus, which was due to its two monsoon seasons and its absence of a lengthy dry season. As a result, as noted by Ivette Perfecto, the British had adopted an industrial system strategy and constructed a sizable quantity of roads and trains solely for the purpose of removing coffee from the island.

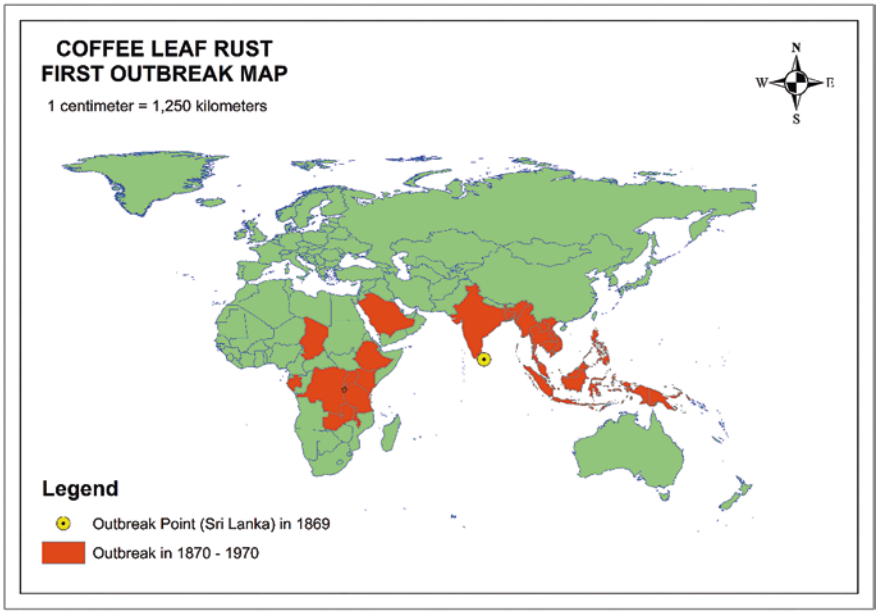

Fig. 12.2 Initial coffee leaf rust outbreak

It is possible that the massive monocultures of coffee plants that were established to justify the infrastructure facilitated the initial spread of coffee leaf rust (Tsing et al., 2021). The disease originated in Ceylon and quickly spread to other coffee producing regions in Asia, Africa, and the Pacific. Ivette also mentioned that by applying copper and other fungicides or switching to *Coffea canefora var.,* or Robusta, which was resistant to the rust but produced a lower-quality beverage, farmers were able to limit the occurrence of the disease in some areas that exhibited a noticeable dry season.

As a result of the destruction of Arabica coffee production in Asia, the Americas became a major producer of higher-quality Arabica coffee (Talhinhas et al., 2017). Producers in the Americas, meanwhile, were always concerned that the catastrophe that struck Asia might someday spread to their lands.

When rust was discovered in the coffee farms of Brazil's Bahia state in 1970, these concerns were validated (see Fig. 12.3). According to several studies, the rust traveled over the Atlantic Ocean carried by winds from the Ivory Coast or Angola in the so-called “celestial river of dust” that connects the two continents (Bowden et al., 1971). From this perspective, this species' spores have an extremely high potential for long-distance dissemination.

Robusta coffee, which is resistant to rust and is primarily produced in Brazil, may have averted an epidemic of the illness at that time. However, a few years later, in 1976, rust was found in Carazo, Nicaragua, which sparked a panic among the mostly Arabica-producing coffee growers in Central America and Mexico (Fig. 12.3). Nevertheless, according to Ivette Perfecto in Anna et al., 2021, for at

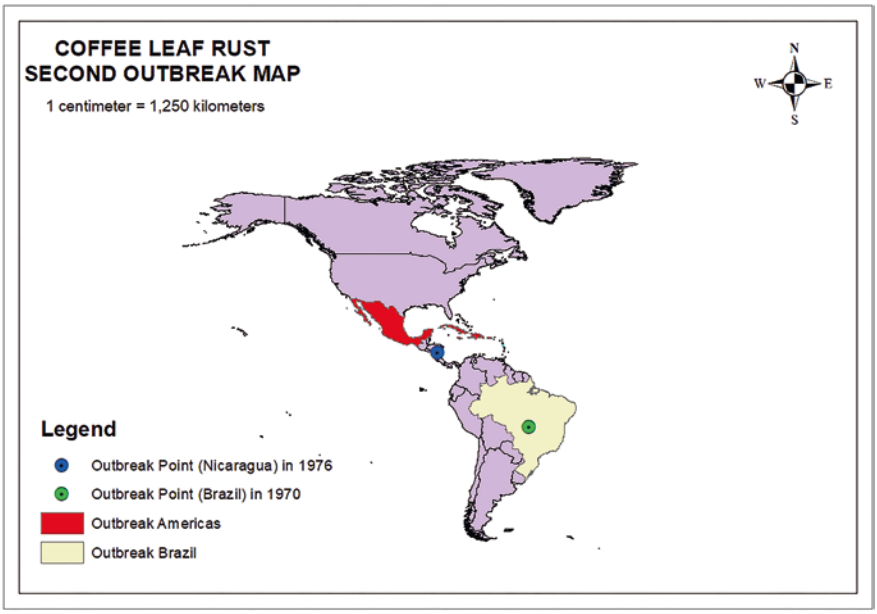

Fig. 12.3 Coffee Leaf Rust: Second Outbreak

least the following 36 years at least, the plague never reached the catastrophic proportions in Mesoamerica that it had in Ceylon.

12.1.3 Economic and Ecological Consequences of Coffee Leaf Rust

Coffee leaf rust (*H. vastatrix*) poses significant economic and ecological consequences for the coffee industry. On the economic front, the disease leads to a notable reduction in crop yield, leading to substantial financial losses for coffee farmers (Gichuru et al., 2021). Decreased productivity translates into lower revenues and diminished incomes, which affects the livelihoods of those dependent on coffee cultivation. Moreover, coffee leaf rust outbreaks introduce market instability, causing price fluctuations and supply shortages. The reduced production levels and lower-quality coffee that result from the disease can create uncertainty in the coffee market, which affects both producers and consumers. The employment sector also suffers as reduced crop yields and financial losses lead to job cuts throughout the coffee value chain, impacting the workers involved in harvesting, processing, and exporting coffee.

Ecologically, coffee leaf rust exerts a detrimental effect on the biodiversity of coffee plantations. In an effort to control the disease, farmers often resort to widespread fungicide use (McCook, 2006). However, these chemicals can have unintended consequences, negatively impacting nontarget organisms such as beneficial

insects, birds, and soil microorganisms. This disruption of the ecological balance within coffee ecosystems can result in biodiversity loss and the degradation of ecosystem services provided by these organisms.

The implications of coffee leaf rust not only concern money but also ecology. When outbreaks occur, changes in land use practices are inevitably result, as farmers seek to mitigate the negative impact of the disease. This may involve replacing susceptible coffee varieties with more resistant varieties or diversifying crops (Tadesse et al., 2021). While these actions are aimed at enhancing resilience, they can also help to diversify the landscape and enhance the natural environment in coffee-growing regions. Furthermore, coffee leaf rust outbreaks can contribute to deforestation problems since farmers face financial problems due to the outbreak and proceed to cut down trees and clear land for alternative agricultural activities or even stop growing coffee altogether, which leads to a decrease in production. Deforestation disrupts local ecosystems, leading to habitat destruction, and making environmental issues worse.

Furthermore, it is important to consider how the disease impacts soil health and fertility. When coffee plants are repeatedly affected by the coffee leaf rust, it increases their susceptibility to other pests and diseases. As a result, farmers may use more types of fungicides and increase their rate of application, which can negatively impact soil health. This excessive use of fungicides can harm beneficial microorganisms in soil, reduce organic matter content, and endanger long-term soil health.

To address the economic and ecological consequences of coffee leaf rust, adopting holistic and sustainable approaches is crucial. Such approaches include promoting disease-resistant coffee varieties, implementing integrated pest management strategies, and adopting agroforestry systems to enhance the resilience of coffee ecosystems (Villarreyna-Acuña et al., 2020). Additionally, investing in the research and development of innovative solutions, such as breeding resistant coffee varieties and implementing sustainable disease management practices, is vital for the long-term viability of the coffee industry and the conservation of coffee-growing ecosystems. Addressing these challenges can mitigate the adverse effects of coffee leaf rust and build a more sustainable and resilient coffee sector. Thus, it is important to note that with the development of technology and research, the transition to modern pest and disease management methods of controlling coffee leaf rust is deemed necessary to protecting the coffee industry.

12.2 The Need to Shift to Modern Management Methods for Coffee Leaf Rust

12.2.1 Why Modern Management?

Currently, most coffee producing countries still use conventional management methods to overcome coffee leaf disease. Fungicides and physical labor have been the mainstays of traditional CLR control techniques. These methods have

drawbacks in terms of efficacy, cost, and environmental impact, even though they offer some relief. One of the most common practices is the manual application of pesticides by humans (Fig. 12.4). Pesticide applications play an important role in managing and controlling coffee leaf rust disease.

However, the conventional management of coffee leaf rust has several limitations and drawbacks that make it less desirable than modern management approaches. Some of the reasons why conventional disease management might not be considered ideal for coffee leaf rust management follow:

1. Environmental Impact: Conventional management depends on chemical fungicides, which can have antagonistic effects on the environment (de Mário et al., 2021). These fungicides lead to the contamination of soil, water sources, and surrounding ecosystems and threaten beneficial organisms in the soil.
2. Fungicide Resistance: Frequent and continuous use of chemical fungicides in conventional management can lead to the emergence of fungicide-resistant strains of coffee leaf rust (de Mário et al., 2021). Fungicide resistance decreases the effectiveness of control measures and can result in the need for stronger and more frequent applications and higher doses of chemicals and pesticides, which can harm the environment.
3. Short-Term Solutions: Conventional management is often focused on reactive approaches, where fungicide is applied only after the symptoms of coffee leaf rust appear. This reactive strategy provides temporary relief but does not solve the underlying causes or even provide long-term solutions to the problem (Tadesse et al., 2021). It can lead to a cycle of dependence on fungicides and tends to increase the overall fungicide application rate.
4. Economic Burden: The cost of purchasing and applying chemical fungicides in conventional management can pose significant financial problems for coffee farmers (Villareyna. et al., 2020). Continued reliance on fungicides can increase

Fig. 12.4 Pesticide application on coffee leaf rust

production costs and reduce profit margins, particularly for small-scale farmers who may struggle to afford the necessary resources and inputs.
5. Public Health Concerns: The use of chemical fungicides in conventional management raises concerns regarding human health. Farmers who handle and apply these chemicals may be exposed to health risks, including skin irritation, respiratory problems, and numerous long-term health problems associated with pesticide exposure.
6. Consumer Preferences for Sustainability: With the increasing global demand for sustainably produced products, consumers are currently seeking coffee that is grown with environmentally friendly and responsible social practices. Thus, conventional management, which still depends on a high level of chemical fungicide use, may not suit consumer preference for the sustainable and eco-friendly management of coffee production.

These limitations and concerns regarding conventional management highlight a need to shift to modern and eco-friendly management approaches to controlling coffee leaf rust. Modern approaches such as integrated pest management, resistant variety usage, proactive monitoring, and sustainable practices can provide more environmentally friendly, economically viable, and sustainable alternatives for managing coffee leaf rust, which can help to reduce excessive usage of chemical pesticides. Shifting from conventional to modern management approaches to controlling coffee leaf rust is necessary to the promotion of sustainable practices, ensuring long-term effectiveness, maintaining economic viability, the enhancement of climate change resilience, and the satisfaction of consumer demands for sustainable products. By embracing these modern approaches, coffee producers can effectively overcome coffee leaf rust while also protecting the environment, optimizing productivity, and thriving in a changing industry landscape. Currently, the advanced application of technology is also in facilitating the management of pest disease in plants, including those affecting coffee plantations. One example is the detection of coffee leaf rust through image detection performed via deep learning algorithms. An overview of the utilization of deep learning in disease detection using image datasets is discussed in the following section.

12.2.2 Deep Learning as Modern Approaches for Coffee Leaf Rust

Deep learning is a branch of artificial intelligence that is focused on developing algorithms and computer models with the capacity to independently learn and understand data. It is based on artificial neural networks that can absorb, analyze, and retrieve information from highly complex data (Novtahaning et al., 2022). Deep learning is known for its advantages in a variety of fields, including speech recognition, automatic spelling, and even facial recognition, which are common today. One interesting application of deep learning is in plant disease detection. Conventionally,

plant disease detection relies on direct human visual observations, which can be inaccurate, time-consuming, and inconvenient due to the limited availability of farmers. With the existence of deep learning, computer systems can be trained to recognize and detect diseases in plants more accurately and effectively.

With deep learning applications, the early detection of plant diseases, including coffee leaf rust, is possible. To develop a model from the data to train deep learning algorithms to recognize the patterns and distinctive features that differentiate healthy and infected plants, a dataset is required that includes images of healthy leaves and infected leaves, ranging from initial symptoms to full infection. A deep learning model can learn to identify this pattern with high accuracy. The model allows us to predict whether the plant is infected or not based on a given dataset, which makes early-stage disease identification possible. Furthermore, preventing symptoms from appearing could lead to the reduced use of chemical pesticides (Carmo et al., 2022; Soares et al., 2022). With this early detection, disease control measures can be taken quickly to prevent further spread.

Previous studies (Soares et al., 2022; Trujillo & Perez-Ruiz, 2023) have shown that early detection or the simple detection of coffee leaf rust is the first process in achieving effective crop protection. The detection of coffee leaf rust provides opportunities for advanced technology implementation for fighting this rust disease. Research by Soares et al., 2022 demonstrated how to conduct early detection of coffee leaf rust using modern technologies. This research was carried out by testing the effectiveness of multispectral images using an unmanned aerial vehicle (UAV) to distinguish coffee leaf rust. The results implied that the detection accuracy was 80%.

In practice, coffee leaf rust detection using a deep learning algorithm begins with image processing, as shown in Fig. 12.5. The coffee leaf rust detection process proceeds through several steps until the final detection results are obtained. Data acquisition and preparation are important for the subsequent detection processes. The deep learning model's performance is directly impacted by the quality and variety of the data (Morbekar et al., 2020). A carefully selected dataset containing representative photos enables the algorithm to accurately learn the traits of coffee leaf rust. The model remains unable to identify the disease without a high-quality image dataset. As a case study, coffee leaf rust detection using a deep learning algorithm was performed in Majalengka Regency, Indonesia, which is one of the major coffee-producing countries in the world. As shown in Fig. 12.6, data collection was carefully performed using a high-resolution camera to obtain high-quality data to obtain a high-quality detection result. Advance methods in data collection have been implemented in several studies on coffee leaf rust, including the use of UAVs and high-tech cameras among other methods, depending on the detection scale and research objectives. In addition, data augmentation is aimed at increasing the number of images in the dataset by editing the images through such functions as cropping, rotating, and adjusting colors and exposures with appropriate software, such as Adobe Lightroom, or through the use of environments, such as MATLAB. In deep learning, “data annotation” refers to the act of labeling or marking data to offer important and relevant information for machine learning and deep

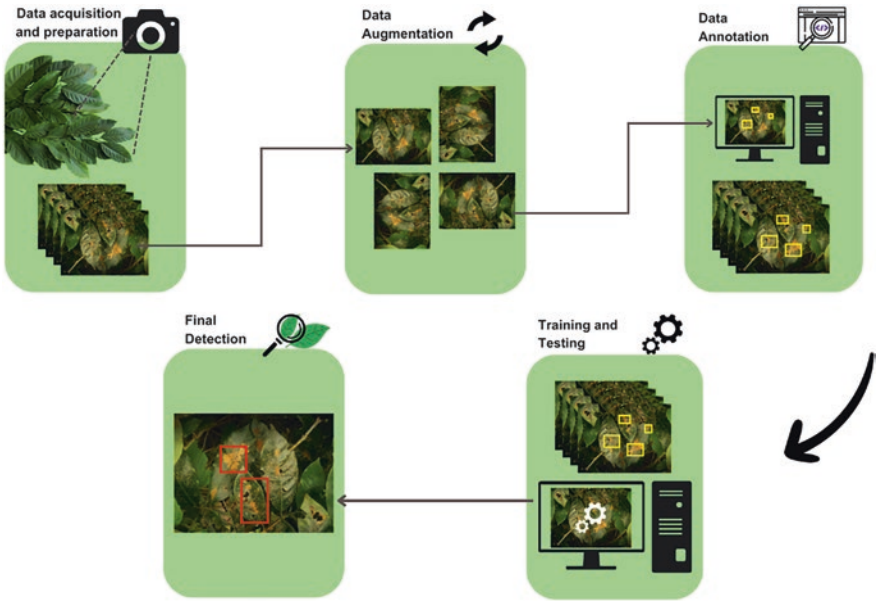

Fig. 12.5 Image detection framework using Deep Learning

Fig. 12.6 Image data collection of coffee leaf rust in Majalengka Regency, Indonesia

learning model training (Rasmussen et al., 2022). When learning to make predictions from labeled instances, supervised learning relies on this annotation. In this study, images were annotated using LabelImg software and labeled "CLR." Only the images with clear and visible coffee leaf rust were selected. A total of 1025 images were used for training and validation. The dataset was divided into two sets

of images with a ratio of 70% used for training (718 images) and 30% used for validation (307 images).

When using deep learning for image identification tasks, several pretrained models are often used. These models can be adjusted or utilized as feature extractors for certain image recognition tasks because they have already been pretrained on sizable datasets, generally consisting of millions of photos. In this study, a pretrained model from You Only Look Once (YOLO) was used. All 1025 labeled images were trained with the YOLOv5 algorithm through a Convolutional Neural Network (CNN) using the PyTorch framework and analyzed using the TensorFlow package in TensorBoard, which was developed by Google. The training took 1 h and 10 min with 50 epochs, the image size was 416, and the batch size was 16. The trained model was tested with different images from the dataset containing the desired object for coffee leaf rust detection.

As shown in Fig. 12.7, coffee leaf rust is detected with some degree of precision. This is due to several factors that can influence the detection results, such as an imbalanced dataset. An imbalanced dataset occurs when the number of samples in one of the classes is insufficient (Wang et al., 2016). This can cause the model to struggle to correctly identify instances of coffee leaf rust, thus leading to a higher number of false positives. Insufficient training data can cause issues and deep learning models require a diverse and representative training dataset to accurately learn the patterns and features of the target class. If the dataset used for training is small or lacks variability, the model may not generalize well to unseen data, which results in low detection precision. Increasing the size of the training dataset or using data

Fig. 12.7 Coffee leaf rust detection using Deep Learning

augmentation techniques can help mitigate this issue. Complex or ambiguous class boundaries and some detection tasks, such as distinguishing between various stages or severities of coffee leaf rust, contain complex or ambiguous class boundaries (Morbekar et al., 2020). Deep learning models can struggle with accurate classification in such instances, resulting in lower precision. In such cases, it may be necessary to refine the dataset, provide clearer labels or annotations, or explore alternative approaches such as multiclass classification or object detection. The choice of model architecture and hyperparameters can greatly impact precision (Kalliola et al., 2021). If the model architecture is ill suited for the detection task or incapable of capturing the relevant features, it can result in low precision. Additionally, hyperparameters such as the learning rate, regularization techniques, or optimizer selection can influence the model's ability to generalize and discriminate between classes. Experimenting with different architectures and hyperparameter settings can help improve precision.

After the trained model was tested, it successfully detected coffee leaf rust in each frame. The trained model has a mean average precision (mAP) of 59.8% and a recall of 53.2%. The mean average precision was significantly low due to the small number of epochs. The dataset was trained with only 50 epochs. As can be seen in the metrics of mAP displayed in Fig. 12.8, the obj_loss for validation is increasing, which is possibly due to overfitting in the dataset. This indicates that the model only results in accurate predictions for training data and for the new data predictions, as Li mentioned in Li et al., 2019. The matrix describes the results in detail, and several parameters are used, such as precision, loss, and mean average precision (mAP). Overfitting occurs when a model becomes too specialized in the training data and fails to generalize well to unseen data. Overfitted models tend to have high precision on the training set but perform poorly on new data. This can lead to low detection precision (Ying, 2019). Regularization techniques such as dropout, early stopping, or weight decay can help reduce overfitting and improve generalization performance. Low-quality or noisy data, such as images with low resolution, improper

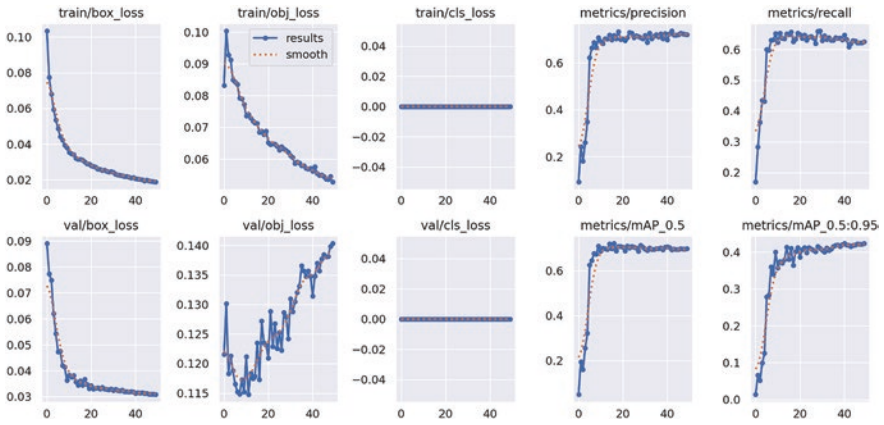

Fig. 12.8 YOLO detection results in detecting coffee leaf rust

lighting, or occlusions, can negatively impact the precision of a deep learning model. Such data can introduce ambiguity or confusion, making it difficult for the model to accurately detect coffee leaf rust. Preprocessing techniques such as noise reduction, image enhancement, or data filtering can help mitigate the impact of poor quality or noisy data (Ying, 2019). Insufficient model training requires an adequate number of training iterations or epochs for optimizing model performance. If the model is trained over too few iterations, it may not have converged to an optimal solution, resulting in suboptimal precision. Increasing the number of training iterations or employing techniques such as learning rate scheduling can help improve model precision (A. Morbekar et al., 2020). Addressing these factors and iteratively refining the model, dataset, and training process can help improve the precision of a deep learning model in detecting coffee leaf rust. Carefully analyzing the specific challenges and limitations of the problem and experimenting with different approaches to achieving the desired precision is important.

As a future direction, the detection model for coffee leaf rust has a high potential before being implemented in advanced agricultural management practices, especially for the monitoring and managing of coffee leaf rust disease. Implementation, such as the use of apps for farmers and their usage in smart, automatic, or even unmanned sprayers, can make this pest disease management even more convenient.

12.3 Challenges and Limitations of Using Deep Learning for Coffee Leaf Rust Management

12.3.1 Challenges and Limitations

The use of deep learning to deal with coffee leaf rust also has challenges and limitations that merit consideration. One of these is data limitations; deep learning requires large amounts of high-quality data for the training of accurate models. However, specific data on coffee leaf rust and its related factors can be difficult to obtain. Sufficient amounts of weather data, information on coffee varietal resistance, and other field data must be available to build an effective model. Data limitations can hinder deep learning's ability to provide accurate predictions. As with most high-level computing tools, deep learning requires considerable computational power for training and running the model. Sources such as graphics processing units (GPUs) are required for this, which obviously involves high costs, which can be a barrier for small-scale farmers or coffee farms with limited access to the necessary computing infrastructure. The process of developing an effective model requires intensive and iterative research, as well as the capability for interpreting the results. This might be a problem for coffee farmers, particularly because most coffee farmers in coffee-producing countries have a limited understanding of such technologies.

It is important to know whether the actual farmers are ready to accept these changes and innovations. Most of the farmers are not fully aware of this new technology and the novel methods it enables, and its implementation may impose an additional financial burden for farmers, as well as intensive theoretical and practical training.

To face these challenges and limitations, it is important to continue research and development into deep learning as a solution for coffee leaf rust management. With increasing data availability and advanced computing technology, it is possible that deep learning can be more effective in future management, but it is also important for stakeholders, such as government, farmers, and the related sectors to work together to address any social challenges that may rise and to construct decent policies for its applications.

12.3.2 Solutions

There are ways to be considered as a solution for deep learning application for overcoming coffee leaf rust disease, such as proper and better data collection, that should be considered since obtaining high-quality data on coffee leaf rust is necessary to achieve decent detection capabilities. The exchange of knowledge and experience can help in understanding the problems faced by farmers, identifying specific data needs, and developing more relevant solutions. This collaboration can also assist in validating and improving developed deep-learning models. The improvement of computing infrastructure is seen as a means of addressing the high computing needs in those areas affected by coffee leaf rust. This might involve building a data center or accessing cloud computing to facilitate intensive data processing. Governments, nonprofit organizations, and the private sector can collaborate in providing more affordable computing resources for farmers and researchers. To deal with environmental changes, deep learning models need to be developed and, in turn, adapted to new conditions. This might involve updating and retraining the model using updated data. Further research is also needed to identify important indicators that influence the spread of coffee leaf rust for adjusting and improving the model. The provision of interpretability tools and the development of methods and tools that enable the interpretability of deep learning models is also an important step. This can involve data visualization, model explanation, and other techniques that help farmers and other stakeholders understand the basis for the predictive results and recommendations provided by the model, which increase the confidence with which such recommendations are acted on. These solutions aims to make the use of deep learning in the overcoming of coffee leaf rust more effective, relevant, and widely adopted by farmers and stakeholders in the coffee industry. Additionally, well-planned training, monitoring, and research programs from the collaboration of stakeholders are necessary to continuously realize these solutions.

12.4 Conclusion

The coffee plant is highly sensitive to climatic conditions, and even small changes in temperature and rainfall patterns can have significant impacts on its growth, yield, and quality. One of the plant-disturbing organisms that attacks the organs of the coffee plant is coffee leaf rust (*H. vastatrix*). Coffee leaf rust can cause damage and death to coffee plants, which can decrease production and increase losses worldwide. Such losses can occur as either direct or indirect losses. Direct losses are losses suffered by farmers due to the disease. Shifting from conventional to modern management approaches to controlling coffee leaf rust is necessary for the promotion of sustainable practices, ensuring long-term effectiveness, maintaining economic viability, the enhancement of climate change resilience, and meeting consumer demands for sustainable products. By embracing these modern approaches, coffee producers can effectively combat coffee leaf rust while safeguarding the environment, optimizing productivity, and thriving in a changing industry landscape. Currently, the advanced application of technology is also assisting in the management of pest disease in plants, including that on coffee plantations. One example is the detection of coffee leaf rust through the use of an image detection method that is performed with deep learning algorithms. Deep learning has potential as a new opportunity in plant disease management, not excluding coffee plant disease. Through accurate detection and proper control, the usage of deep learning technology can help farmers overcome plant disease threats. Further research and development are needed to achieve better detection and obtain satisfying results regarding this technology. Collaboration between the stakeholders is important to ensure that the farmers are ready to accept such innovations and to ensure that it is run in compliance with designated policy for the safety and efficiency of this management.

Disease detection is only a single aspect of holistic modern plant disease management. As mentioned before, this detection can be used for advanced agricultural management practices, especially for monitoring and managing coffee leaf rust disease. However, training and support for end users, such as farmers or agricultural extension officers, should be provided to effectively utilize disease detection systems and advance agricultural practices.

References

Bowden, J., Gregory, P. H., & Johnson, C. G. (1971). Possible wind transport of coffee leaf rust across the Atlantic Ocean. *Nature, 229*, 500–501. https://doi.org/10.1038/229500b0

Carmo, G. J. S., Castoldi, R., Martins, G. D., Jacinto, A. C. P., Tebaldi, N. D., Charlo, H. C. O., & Zampiroli, R. (2022). Detection of lesion lettuce caused by pectobacterium carotovorum sbsp. Carotovorum by supervised classification using multispectral images. *Canadian Journel of Remote Sensing, 48*, 144–157.

Cerda, R., Avelino, J., Gary, C., et al. (2017). Primary and secondary yield losses caused by pests and diseases: Assessment and modeling in coffee. *PLoS One, 12*, e0169133. https://doi.org/10.1371/journal.pone.0169133

de Mário, R. L. V., Pozza, E. A., Reichel, T., & Botelho, D. M. S. (2021). Strategies for coffee leaf rust management in organic crop systems. *Agronomy, 11*(9), 1865. https://doi.org/10.3390/agronomy11091865

Gichuru, E., Alwora, G., Gimase, J., & Kathurima, C. (2021). Coffee leaf rust (Hemileia vastatrix) in Kenya—A review. *Agronomy, 11*(12), 2590. https://doi.org/10.3390/agronomy11122590

Kalliola, J., Kapočiūtė-Dzikienė, J., & Damaševičius, R. (2021). Neural network hyperparameter optimization for prediction of real estate prices in Helsinki. *Peer Journel of Computer Science, 7*, e444. https://doi.org/10.7717/peerj-cs.444

Keith, L. M., Sugiyama, L. S., Brill, E., et al. (2022). First report of coffee leaf rust caused by Hemileia vastatrix on coffee (Coffea arabica) in Hawaii. *Plant Disease, 106*, 761. https://doi.org/10.1094/PDIS-05-21-1072-PDN

Li, H., Li, J., Guan, X., Liang, B., Lai, Y., & Luo, X. (2019). Research on overfitting of deep learning. In *2019 15th international conference on computational intelligence and security (CIS). Macao, China* (pp. 78–81). IEEE. https://doi.org/10.1109/CIS.2019.00025

McCook, S. (2006). Global rust belt: Hemileia vastatrix and the ecological integration of world coffee production since 1850. *J Global History, 1*, 177–195. https://doi.org/10.1017/S174002280600012X

McCook, S. (2019). *Coffee is not forever: A global history of the coffee leaf rust* (1st ed.). Ohio University Press. https://doi.org/10.2307/j.ctv224ttm0

Morbekar, A., Parihar, A., & Jadhav, R. (2020). Crop disease detection using YOLO. In *2020 international conference for emerging technology (INCET), 2020* (pp. 1–5). IEEE.

Novtahaning, D., Shah, H. A., & Kang, J.-M. (2022). Deep learning ensemble-based automated and high-performing recognition of coffee leaf disease. *Agriculture, 12*(11), 1909.

Rasmussen, C. B., Kirk, K., & Moeslund, T. B. (2022). The challenge of data annotation in deep learning—A case study on whole plant corn silage. *Sensors, 22*(4), 1596. https://doi.org/10.3390/s22041596

Soares, T. A., Martins, G. D., & Siquieroli, A. C. S. (2022). Early detection of coffee leaf rust caused by Hemileia vastatrix using multispectral images. *Agronomy, 12*, 2911. https://doi.org/10.3390/agronomy12122911

Tadesse, Y., Gebeyehu, D., & Kesho, A. (2021). Coffee leaf rust disease and climate change. *World Journal of Agricultural Sciences, 17*, 418–429. https://doi.org/10.5829/idosi.wjas.2021.418.429

Talhinhas, P., Batista, D., Diniz, I., Vieira, A., Silva, D. N., Loureiro, A., Tavares, S., Pereira, A. P., Azinheira, H. G., Guerra-Guimarães, L., Várzea, V., & Silva, M. D. C. (2017). The coffee leaf rust pathogen Hemileia vastatrix: One and a half centuries around the tropics. *Molecular Plant Pathology, 18*(8), 1039–1051. https://doi.org/10.1111/mpp.12512

Trujillo, J. L. A., & Perez-Ruiz, A. (2023). Technologies applied in the field of early detection of coffee lead rust fungus diseases: A review. *Transactions of the Chinese Society of Agricultural Machinary., 54*(5), 163–179.

Tsing, A. L., Deger, J., Saxena, A. K., & Zhou, F. (2021). *(2021). Feral atlas: The more-than-human Anthropocene*. Stanford University Press. https://doi.org/10.21627/2020fa

Villarreyna-Acuña, R., Barrios, M., Sergio, V. M., Cerda, R., Vignola, R., & Avelino, J. (2020). Economic constraints as drivers of coffee rust epidemics in Nicaragua. *Crop Protection, 127*, 104980. https://doi.org/10.1016/j.cropro.2019.104980

Wang, S., Liu, W., Wu, J., Cao, L., Meng, Q., & Kennedy, P. J. (2016). Training deep neural networks on imbalanced data sets. In *International joint conference on neural networks* (pp. 4368–4374). IJCNN. https://doi.org/10.1109/IJCNN.2016.7727770

Ying, X. (2019). An overview of overfitting and its solutions. *Journal of Physics Conference Series, 1168*, 022022. https://doi.org/10.1088/1742-6596/1168/2/022022

Chapter 13
Digital Transformation of Horticultural Crop Production Systems Toward Sustainable Agricultural Productivity

Abstract The rising global population puts pressure on the production of horticultural crops worldwide, creating soaring demand on horticultural products.To meet this demand, conventional horticultural crop production should be transformed into a more efficient and productive system with a better ability to face current challenges, such as increasing labor and land costs, climate change, pest infestations, the degradation of soil nutrients, and water scarcity. This chapter reviews the recent developments in digital horticultural crop production systems that created an opportunity to address the aforementioned challenges. Different technologies, such as the Internet of Things (IoT), artificial intelligence (AI), and big data, usher the digital transformation of horticultural production that aimed at making the system more efficient and effective. These technologies are now being used in greenhouses and plant factories and are being integrated in different crop production operations, such as pest and disease monitoring and detection, nutrient and water management as well as in harvesting and postharvest operations. The digital transformation of horticultural crop production systems is exciting and optimistic; however, there are still challenges that need to be addressed to fully utilize these technologies at the farm level. The lack of infrastructure, high costs, and some social and behavioral constraints hinder the adoption, particularly in developing countries and rural areas. On the other hand, the digital transformation of horticulture can create new opportunities for socioeconomic growth, digital literacy, SDG attainment, and environmental and health benefits towards a more sustainable agricultural productivity.

Keywords Horticulture · Digital technology · IoT · AI · Production · Deep learning

© The Author(s), under exclusive license to Springer Nature Singapore Pte Ltd. 2024

T. Ahamed, *IoT and AI in Agriculture*,
https://doi.org/10.1007/978-981-97-1263-2_13

13.1 Introduction

Horticulture is a branch of agriculture that deals with the production of fruits, vegetables, and ornamental plants. It plays an important role in providing nutritious foods containing the essential vitamins and minerals that humans need. The demand for horticultural products is expected to increase as the global population rose to 8 billion in November of 2022 (UN, 2022). However, increasing production can be a challenging task for the horticulture industry, as it cannot apply a one-size-fits-all solution to the pressing problems it currently facing due to the highly diversified crops under its domain. The crops require different and specific inputs, production techniques, and postharvest operations (Xu, 2022). Moreover, escalating expenses related to labor and land are posing challenges to horticultural production in many countries around the world.

In addition to the complexity of horticulture production practices, high input, labor and land costs, climate change also poses a major production challenge that has exacerbated the problems presented by pests, water scarcity and soil fertility decline. According to Gora et al. (2019), fluctuations in temperature and rainfall patterns contribute to increased occurrences of pests and diseases, which particularly affect the flowering and fruiting stages of plants. For example, a 10 °C rise in temperature can double the metabolic rate of insect pests, accelerating their development, consumption, and capacity to damage crops (Bale et al., 2002; Dukes et al., 2009). Khan et al. (2018) estimated that approximately 20% of apple yield loss that occurred in India was due to pests. In Brazil, citrus diseases such as huanglongbing (HLB), black spot, leprosis, and citrus canker pose a potential yield loss of up to 80% (Moreira et al., 2022), while in West Africa, fruit flies are a major concern in mango production due to possible yield losses of 17–73% (Vayssières et al., 2009). Other important horticultural crops are also negatively affected by pests. For instance, in tomato production, pests can reduce tomato yield up to 34.4% under the current practices, and this number rises to 77.7% without any crop protection intervention (Zalom, 2003). Likewise, there is a 40% potential yield loss in global potato crops due to pests (Oerke, 2006).

Moreover, climate change also causes extreme droughts and floods, which affect agricultural production. For instance, severe droughts and floods in Asia resulted in an economic loss of up to USD 49 billion (FAO, 2021) and affected 13.1 M ha of croplands in Southeast Asia. Water stress is a major concern in horticulture production, as it affects crop physiological processes, such as photosynthesis and transpiration, nutrient uptake, germination, and flowering, resulting in a significant decrease in potential yield (Bhardwaj, 2012). For example, water stress in banana production can result in small-sized fingers and a low-quality bunch. The banana plant requires sufficient water, especially during the flowering stage, to fill and produce high-quality fingers (Gora et al., 2019).

With the increasing pressure to increase production, despite worsening environmental conditions, many researchers are finding solutions to combat these challenges through the use of emerging technologies in digital agriculture. Currently,

horticultural production employs various digital technologies to lessen the effects of climate change and counter the negative impacts of pests, drought, and soil fertility decline. Digital technologies and automation can now be found in horticulture greenhouse production and plant factories. Robotics, sensor-driven solutions, data management, the Internet of Things (IoT), and artificial intelligence (AI) have the potential to take on supervisory roles and optimize production systems, thereby enhancing the competitiveness and sustainability of horticultural production (Shamshiri et al., 2018). Some horticultural practices employ a combination of digital technologies to perform specific tasks, such as irrigation, pest and disease detection, nutrient application, and even harvesting and postharvest operations. Although their progress and utilization are still in the initial phases of development (Ludwig-Ohm et al., 2023), the application of digital technologies in horticulture can still increase the efficiency of the system by addressing its various operational and environmental shortcomings.

13.2 Transforming the Horticulture Production System

Agriculture has been highly dependent on manual labor for a very long time. The production of vegetables, fruits, and even ornamental plants requires human and/or animal labor. It was only around the 1900s that machinery began to supplement agriculture and horticulture operations for soil tillage, irrigation, and harvesting (Liu et al., 2021). This period is known as Agriculture 1.0 in general and Horticulture 1.0 in regard to crop production, where the introduction of tractors increased the operation efficiency of the industry. Further development was observed in agriculture and horticulture around the 1950s when synthetic fertilizers and chemical pesticides were introduced in the production system and tremendously increased the yield of different crops (Zambon et al., 2019). This is dubbed the "Green Revolution" and/or Agriculture/Horticulture 2.0, which revolutionized the agriculture and horticulture industry in the dimensions of production and yield. Although this period brought a remarkable increase in the yield of many horticultural crops, it also came with challenges, as the overuse of chemical pesticides and synthetic fertilizers caused environmental and health concerns. Thus, around 1990, the concept of precision agriculture/horticulture was initiated. Agriculture/horticulture 3.0 boasts the utilization of precision technologies and automation that reduce the use of chemicals in the field and save on energy and water usage (Ahmad & Nabi, 2021). According to the International Society of Precision Agriculture (ISPA) in 2019, "Precision Agriculture (PA) is a management strategy that gathers, processes, and analyses temporal, spatial, and individual data and combines it with other information to guide site, plant, or animal-specific management decisions to improve resource efficiency, productivity, quality, profitability and sustainability of agricultural production." This has been the guiding principle of Horticulture 3.0 in the era of precision agriculture for ensuring prosperity and to the transition into a new

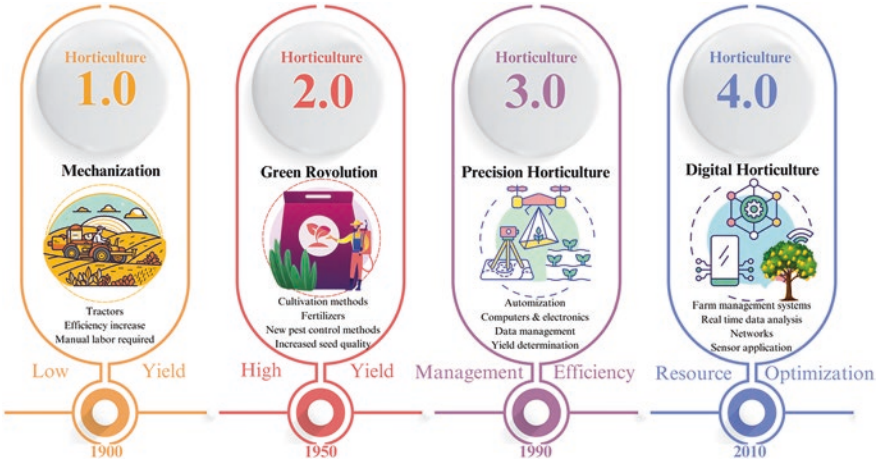

Fig. 13.1 Transformation of the horticulture production system

revolution in agriculture and horticulture, which is the digital age of production dubbed as Agriculture/Horticulture 4.0.

Taking its roots from the PA, digital agriculture/horticulture began around 2010 and involves revolutionary farm management systems, real-time data analysis, networks, and sensor applications. Big data collection and analysis are the major components of digital horticulture and serve to provide valuable information on soil conditions, weather patterns, plant health, and pest populations (Heege, 2018). Digital horticulture holds enormous potential to solve many horticultural production problems; for instance, pests and disease outbreaks can be prevented through early disease monitoring and detection provided by the combined insect monitoring data, crop development, and meteorological data of the digital system. The current level of development also defies conventional pest control methods by utilizing specialized robotic sprayers and drones to treat only the specific crop that requires treatment rather than spraying the entire field with chemical pesticides that can also kill beneficial organisms and affect the overall diversity of the area (Iost Filho et al., 2022). This new revolution can improve farm profitability by increasing production efficiency, reducing wasteful input consumption, and minimizing both waste and environmental harm (Khanna, 2021). Figure 13.1 summarizes the important milestones and transformation of horticulture production that have occurred over time.

13.3 Digital Technologies in Horticultural Production

The emergence of different technologies, such as the Internet of Things (IoT), artificial intelligence (AI), and big data, ushers horticulture production toward digital transformation in an attempt to make production more efficient and

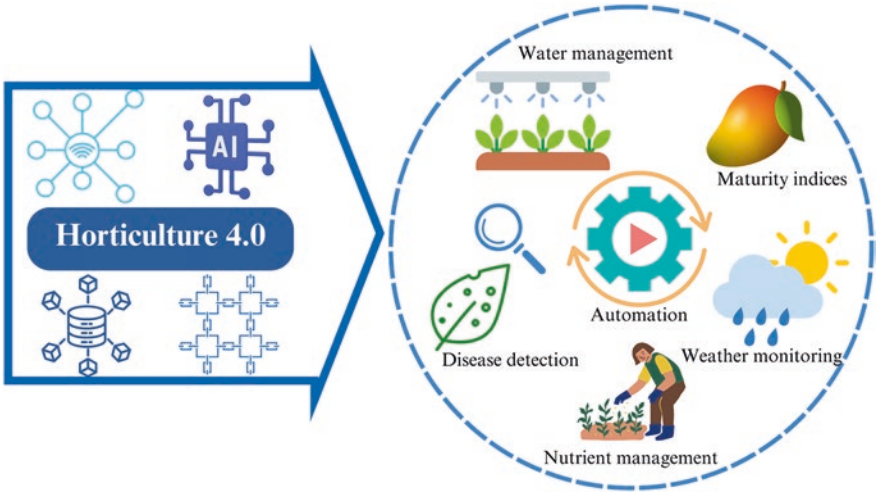

Fig. 13.2 Different technologies comprising digital horticulture and its application in horticulture crop production systems

effective. These technologies can be used in automating several operations in the field, greenhouses, and plant factories as well as in managing irrigation, detecting diseases, monitoring soil fertility, scheduling harvesting, and observing weather patterns (Fig. 13.2).

13.3.1 Digital Transformation of Horticultural Production Environment

13.3.1.1 Smart Greenhouse Production

Greenhouses have been a main fixture in modern horticulture production. These structures were designed to increase the productivity and efficiency of production by providing an appropriate environment for plant growth year-round (Nemali, 2022). Temperature, lighting, and irrigation systems are the main components of greenhouse management that provide optimum conditions for plant growth. Modern greenhouses feature artificial heating and cooling systems to balance the extreme field environment, especially during cold winters and hot summers. Artificial lighting systems using light-emitting diodes (LEDs) have recently gained popularity due to their high energy efficiency and low cost. LEDs are also a safer choice for lighting compared to traditional lamps since they lack glass covers, have lower surface temperatures, and do not contain mercury (Morrow, 2008). They can also change to different colors using a phosphor conversion technique (Kong et al., 2019), which

has been significant in influencing plant morphology and growth (Heo et al., 2002). On the other hand, drip and sprinkler irrigation has been the standard for water management in greenhouse production due to its high-water efficiency compared to the conventional surface irrigation systems (Incrocci et al., 2020). Recently, soilless and hydroponic systems have also gained popularity for the water and nutrient management of crops inside greenhouses (Nemali, 2022).

With the pressure to increase production while increasing the efficiency of resource use, greenhouse production is also evolving and transitioning into a smarter production system. Smart greenhouse production is expanding worldwide with the help of AI and IoT technologies, which enable production with less reliance on human intervention. Temperature, light, soil moisture, and humidity can now be monitored 24/7 and automatically controlled to provide optimum growth conditions for crops (Dayioğlu & Turker, 2021).

A smart greenhouse monitoring system using an adaptive neuro-fuzzy inference system (ANFIS) and IoT technology has been developed to enhance greenhouse crop production (Soheli et al., 2022). Data on temperature, light, and soil moisture are collected in real time through different sensors. These data are utilized in a fuzzy control system that processes the information, while ANFIS is used to make predictions regarding optimal weather parameters. This enables the growers to monitor and adjust the temperature and humidity inside greenhouse. The system was designed for winter crop cultivation, where the ideal conditions are a temperature of 24° C and humidity of 76%. Soheli et al. also developed a mobile app that allowed farmers to access all the relevant data through their phones with data transfer facilitated by global system for mobile communications (GSM) or transmission control protocol/internet protocol (TCP/IP) networks. To ensure data security, potential IoT perception layer attacks were analyzed for their likelihood using a confusion matrix, and necessary security measures were implemented. The system exhibits a high capability of 93.62% in detecting attacks or security breaches at the perception layer, with a precision value of 0.83, recall of 0.78, and an F1 score of 0.81. This work stands out in its integration of IoT technology to identify data threats in conjunction with fuzzy set principles, which sets it apart from other existing systems.

In another study by Tripathy et al., 2021, the authors developed MyGreen, an IoT-based smart greenhouse for sustainable agriculture, by harnessing the potential of sensors and IoT technologies in rose greenhouse farming. They monitored various parameters, such as humidity, nutrient levels, pH, EC value, temperature, UV light intensity, Co_2 levels, and the quantity of insecticides or pesticides, using different sensors to provide valuable data to inform the early detection and diagnosis of abnormal growth and diseases. To manage and coordinate all greenhouse operations, they also introduced a decision support system (DSS) as the central control system. Figure 13.3 shows the modified framework of the study of Tripathy et al. (2021).

In 2017, Liao and colleagues devised an IoT system for the greenhouse production of orchids comprising of three key components: an environmental monitoring system, a wireless imaging platform, and a host analysis platform, as illustrated in Fig. 13.4. They employed environmental sensors to gauge temperature, relative

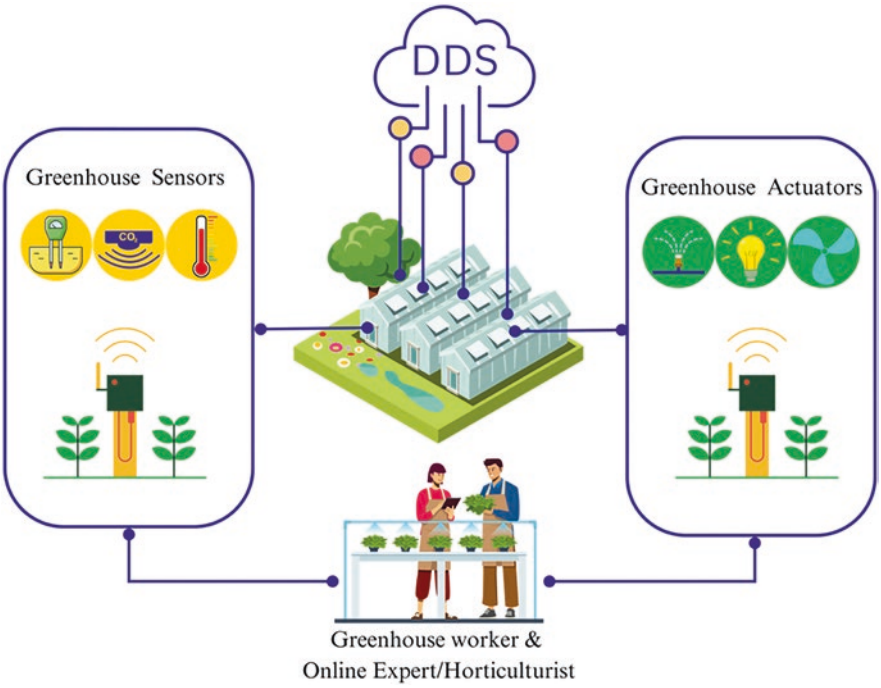

Fig. 13.3 MyGreen, IoT-based Smart Greenhouse Framework developed by Tripathy et al. (2021)

humidity (RH), and light, and cameras to capture images of the orchids. The IoT-based environmental monitoring system was composed of 12 wireless sensor networks (WSNs) in conjunction with a ZigBee-based gateway. The role of WSNs was to collect data on environmental conditions, while the gateway served to organize and transmit the sensor readings to the host platform via Wi-Fi. Simultaneously, the IoT-based wireless imaging platform was constructed using a Raspberry Pi single-board computer equipped with cameras. Both sensor data and camera images were stored on the host platform for further analysis (Liao et al., 2017).

In recent years, the integration of different digital technologies into greenhouse production has been evident in various greenhouse operations, such as irrigation, pest management, and lighting. As the technology continues to be developed, future development is expected to harness the potential of digital technologies in greenhouse production.

13.3.1.2 Plant Factory Revolution

The constant pursuit of efficient production systems to meet the demands and environmental concerns of the increasing global population has led the horticulture industry to develop plant factories. This production system revolutionizes the way

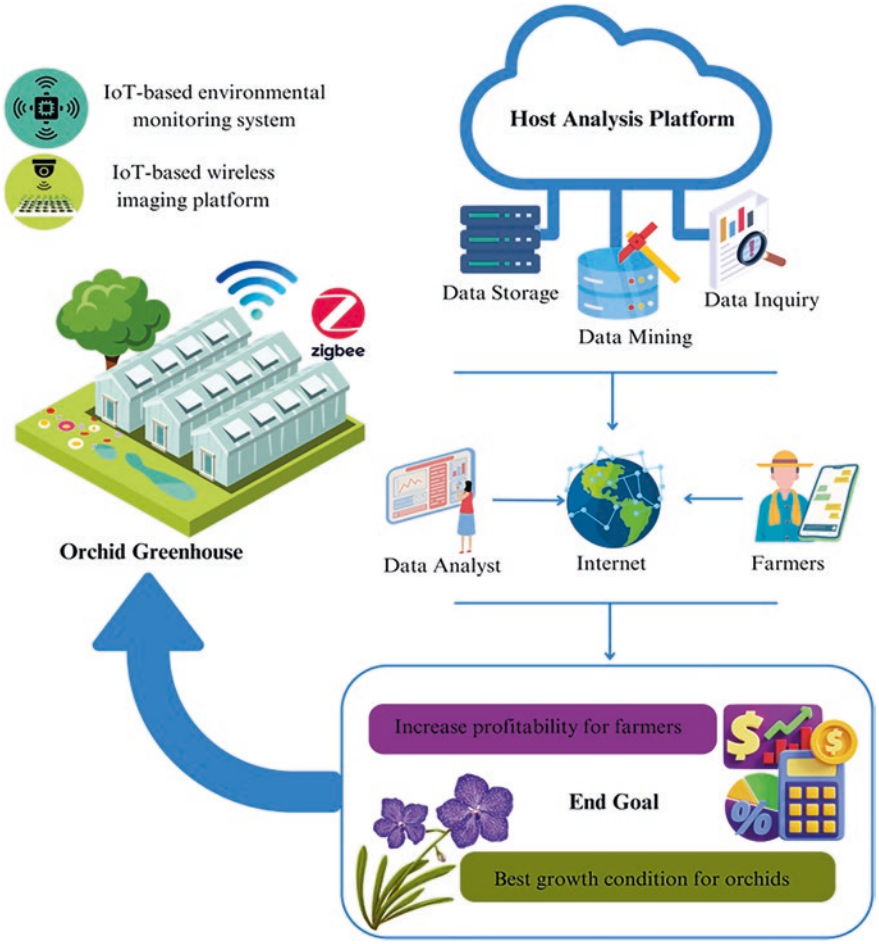

Fig. 13.4 Modified conceptual diagram of the IoT-based monitoring system for greenhouses based on Liao et al. (2017)

we cultivate crops by enhancing the level of productivity per unit area and by utilizing vertical spaces to produce high-quality crops. Plant factories, unlike conventional crop production, do not require a vast area of land to produce the common vegetables we need. They can be established in limited spaces within or nearby urban areas to support the demand of urban consumers. This also reduces transportation costs by bringing the production site near to or within urban areas. In addition, with the advancement of AI technology, research involving AI in plant factories is gaining momentum. In a study conducted by Hyunjin and Sainan (2021), a plant factory production design was implemented using AI in Korea. These authors installed different sensors and integrated IoT technology to remotely control and monitor temperature, humidity, and oxygen level inside the growing area, as well as

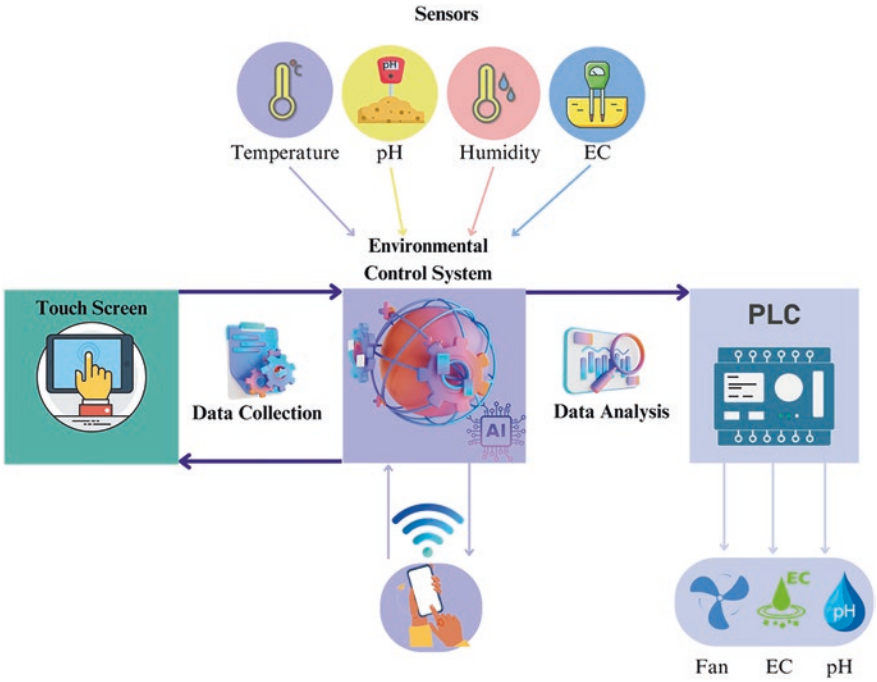

Fig. 13.5 Modified plant factory design using AI technologies based on Hyunjin and Sainan (2021)

regulate the operation of LEDs and cooling fans using a smartphone. The data regarding temperature, humidity, pH, and EC sensors were transmitted to the environmental control system, which can then adjust factors such as EC, pH, and temperature via a PLC (programmable logic controller) control program. Figure 13.5 shows the modified plant factory design by Hyunjin and Sainan.

Aside from IoT technologies and sensors, plant factory production now employs different AI technologies to efficiently monitor crop growth. Moon et al. (2022) analyzed the growth of lettuce in plant factories using deep networks based on automated feature extraction. In addition, Hamidon and Ahamed (2023) used deep learning algorithms to detect defective lettuce seedlings grown in an indoor environment. These authors used different deep learning algorithms, such as CenterNet, YOLOv5, YOLOv7, and faster R-CNN, among them, YOLOv7 showed the highest detection accuracy of defective lettuce seedlings at 97.2%.

Moreover, machine learning and optical flow analysis helped Nagano et al. (2019) to predict the growth of lettuce by tracking leaf movements. They focused on tracking the time-series movements of lettuce leaves by employing optical flow (OF) analysis. OF analysis is an image processing technique that captures the differences between consecutive frames caused by the subject's motion. They developed a growth prediction model with a correlation coefficient of 0.743.

Plant factory production systems may be the best model for the digital transformation of horticulture production, as they can be easily adapted to the available digital technologies to increase production efficiency in a controlled environment. Based on its regulation of the temperature, light, and RH, the plant factory sets the best environment for utilizing new technologies to make production, from seedlings to harvesting, more efficient and productive.

13.3.2 Digital Transformation of Horticultural Production Operations

13.3.2.1 Pest Management

Crop pests are classified into four main categories: (1) vertebrate pests (birds, rodents, and other mammals); (2) invertebrate pests (ticks, insects, slugs, and spiders); (3) weeds (grasses, sedges, and broadleaf plants); and (4) diseases (fungi, bacteria, viruses, and other microorganisms) (Extension.psu.edu, 2022). According to Boote et al. (1983), pests attack and affect crops in several ways, causing a decrease in crop productivity by competing for light and essential soil nutrients, reducing photosynthesis, accelerating leaf senescence, consuming tissue and plant parts, or reducing crop stands and sap assimilates. These damages can cause an annual global crop production loss between 20% and 40%, as reported by the Food and Agriculture Organization (FAO) in 2019, where insect damage cost approximately $70 billion USD and crop disease infections amounted to 220 billion USD per year.

The conventional method for pest and disease monitoring relies heavily on human expertise for visual identification of pests, a process that is both subjective and labor-intensive, making it unsuitable for large-scale use (Li et al., 2021). Favorably, the increasing prevalence of embedded devices equipped with cameras and internet connectivity has opened new possibilities for automated pest

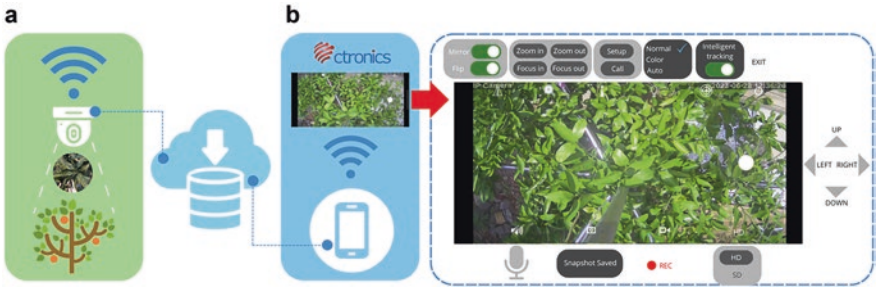

Fig. 13.6 (**a**) Collection of images remotely through the CTRONICS mobile application, (**b**) CTRONICS mobile application interface for data collection

monitoring in horticulture production with the potential to greatly enhance the monitoring efficiency of farms (Preti et al., 2020).

For instance, a system was developed that uses a camera sensor and deep learning algorithms to detect the presence of sooty mold in citrus canopy at night (Apacionado & Ahamed, 2023). The system utilizes an affordable home surveillance camera with night vision capability to capture and monitor the condition of the citrus tree. It uses IoT technology to remotely capture and collect images from the field using the CTRONICS mobile application (Fig. 13.6).

The collected images underwent several images processing steps, including slicing, cleaning, splitting, labeling, augmentation, and file conversion, before being subjected to deep learning algorithms (Fig. 13.7). The study collected and used 4200 images for training, 200 images for validation and 100 images for testing via YOLOv5m, YOLOv7, and CenterNet. The results revealed that, among them, YOLOv7 had the most accurate detection at 74.4% mAP.

Numerous studies have also been conducted by other researchers on the digitalization of pest identification and monitoring of horticultural crops. In a study by Uğuz et al. (2023), YOLOv5 was successfully employed to achieve a 99% average precision (AP) in the detection of *Alternaria alternata* and thrips in citrus. Similarly, Soeb et al. (2023) demonstrated the superior performance of YOLOv7 in detecting tea leaf diseases in natural settings using a Canon EOS 80D Single-Lens Reflex (SLR) camera, outperforming previous detection models such as CNN, DNN, and AX-Retina. They attained a detection accuracy of 97.3% with a precision of 96.7%, a recall of 96.4%, and a mean average precision (mAP) of 98.2%. Moreover, Syed Ab Rahman et al. (2022) utilized a two-stage deep convolutional neural network (CNN) approach using Faster R-CNN to identify citrus diseases. Their model achieved a detection accuracy of 95.37% for citrus black spot, citrus canker, and citrus greening disease.

In addition, several studies have harnessed unmanned aerial vehicle (UAV) technology for the surveillance and identification of crop diseases. Abdulridha et al. (2019) employed UAV-based remote sensing to identify citrus canker by utilizing a Resonon Pika l 2.4 hyperspectral camera mounted on a DJI Matrice 600 Pro Hexacopter, and they achieved a remarkable 100% accuracy in the classification of citrus canker in the orchard. Similarly, DadrasJavan et al. (2019) successfully detected citrus greening in low-altitude multispectral images by employing a Micasense RedEdge multispectral camera attached to a UAV. Their classification results reached 81.75%, underscoring the potential of low-altitude multispectral imagery for the swift detection of citrus greening disease.

In recent years, deep learning has proven to be a formidable tool in disease management in the area of horticulture production. It is used to monitor and detect various pests and diseases affecting numerous horticultural crops. With recent developments, the usage trajectory of this technology in coming years will extend beyond early detection and forecasting. Its significance will become even more pronounced in the realm of horticulture production in the near future.

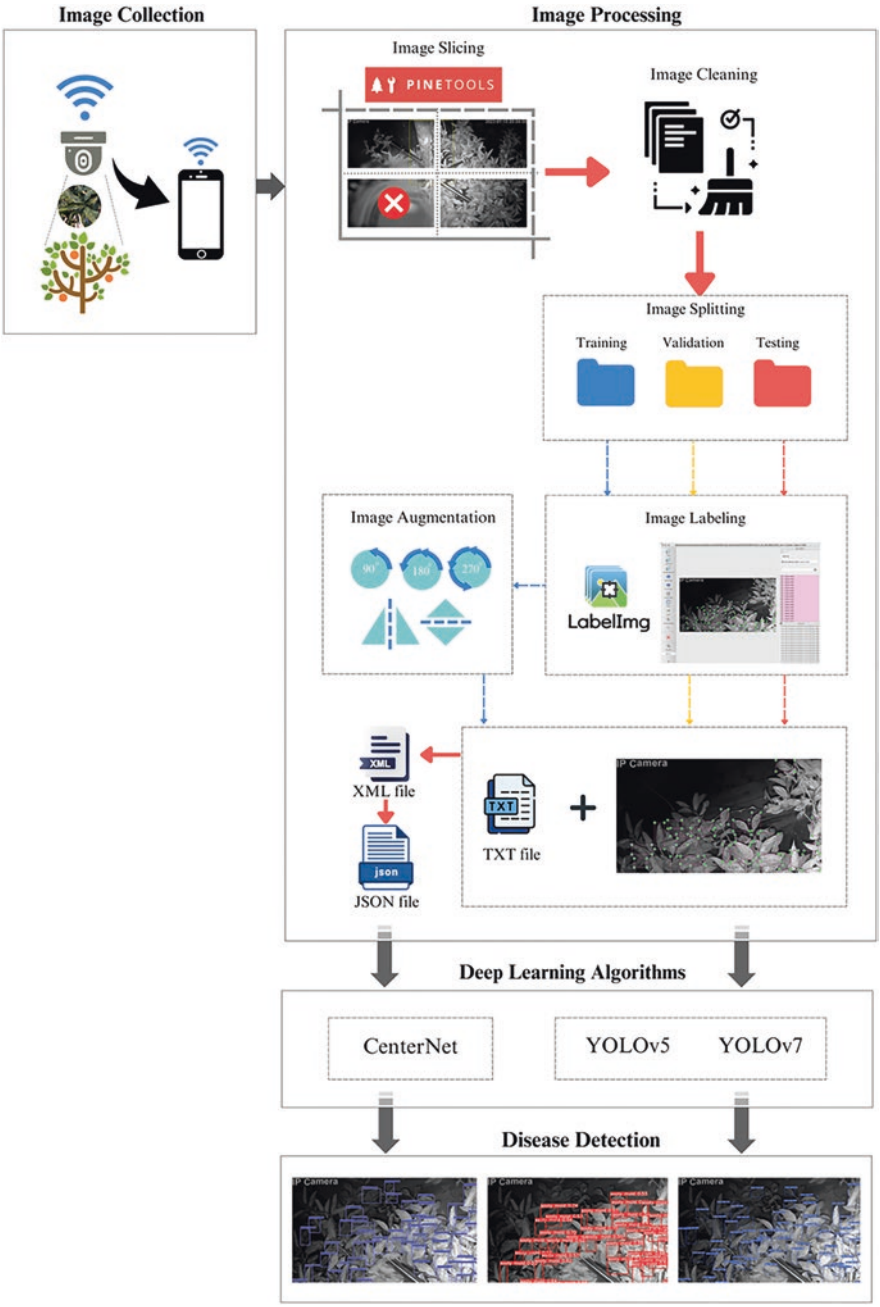

Fig. 13.7 Conceptual framework for detecting sooty mold in citrus canopy using deep learning algorithms

13.3.2.2 Water Management

Water management is one of the most important components of horticulture production. Water is a main input in production and heavily dictates the quality of plant growth. For these reasons, water application must be carefully managed, especially in the context of climate change, which can severely affect the supply of water around the world. Many studies have examined the use of precision and smart irrigation methods to increase the efficiency of water use.

An IoT-based irrigation system called "AgriSens", which is tailored for dynamic irrigation scheduling in irrigated crop fields, was developed by Roy and his team (Roy et al., 2021). AgriSens offers real-time automatic irrigation, as well as the option for remote manual irrigation at different growth stages of crops. This IoT system not only improves irrigation process efficiency but also minimizes water wastage. To accurately determine water requirements, the system relies on sensors measuring various parameters, such as RH, soil moisture, temperature, and light intensity. The use of IoT-based smart irrigation systems with such capabilities can significantly enhance irrigation efficiency.

In a related study, Benyezza et al. (2021) presented a block diagram for an illustrative irrigation system comprising three main components: data processing, cloud infrastructure, and communication (Fig. 13.8).

Another revolutionary advancement in the digital era of horticulture is the development of the digital twin. Digital twins (DTs) are virtual duplicates of real-world physical systems, both living entities and inanimate objects. They seamlessly

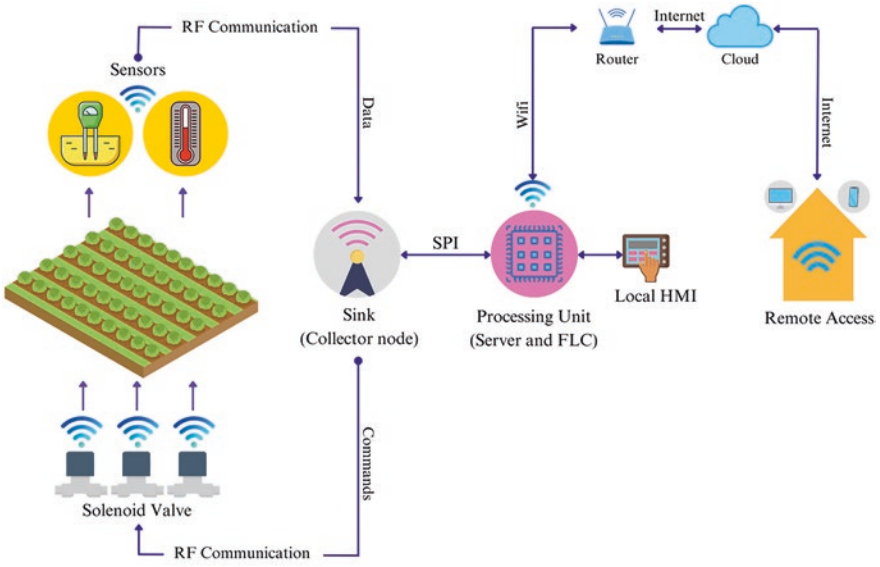

Fig. 13.8 Block diagram of the example irrigation system based on Benyezza et al. (2021)

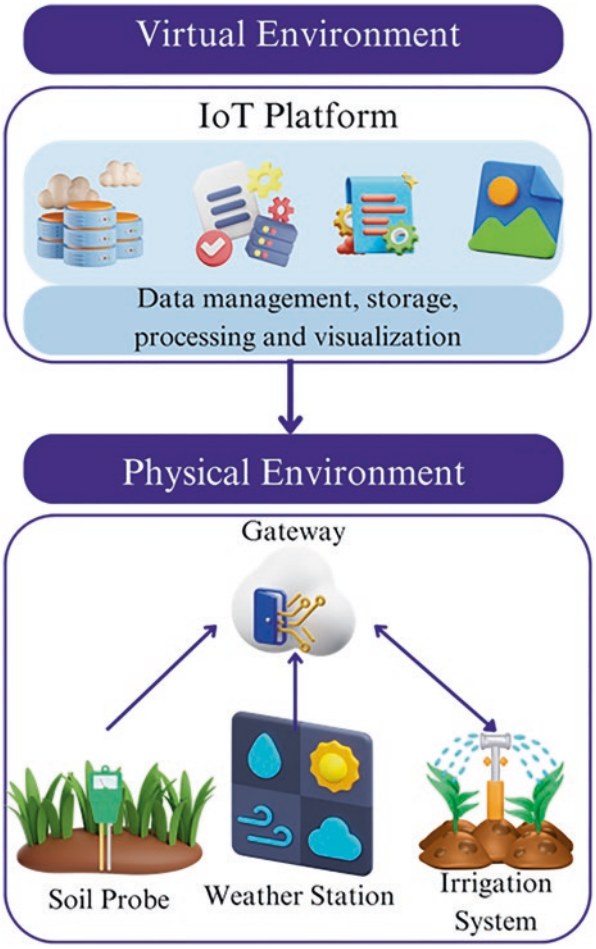

Fig. 13.9 System Design of a Digital Twin for Smart Irrigation based on Alves et al. (2023)

combine solutions for intricate systems analysis, decision support, and technology integration (Pylianidis et al., 2021). Recently, this technology has slowly been integrated into agriculture and horticulture. For instance, Alves and his team (Alves et al., 2023) developed a digital twin for smart irrigation systems (Fig. 13.9). Their system replicates an irrigation system where physical components such as sensors and actuators are interconnected with their virtual counterparts. The system is a combination of an IoT platform based on FIWARE and a discrete event simulation model in Siemens Plant Simulation software. The IoT platform collects, consolidates, and processes data related to soil conditions, weather, and crop status to generate daily irrigation recommendations. The simulation model was employed to replicate the behavior of an irrigation system under a specific application scenario. Real-time communication between the platform and the simulation model was

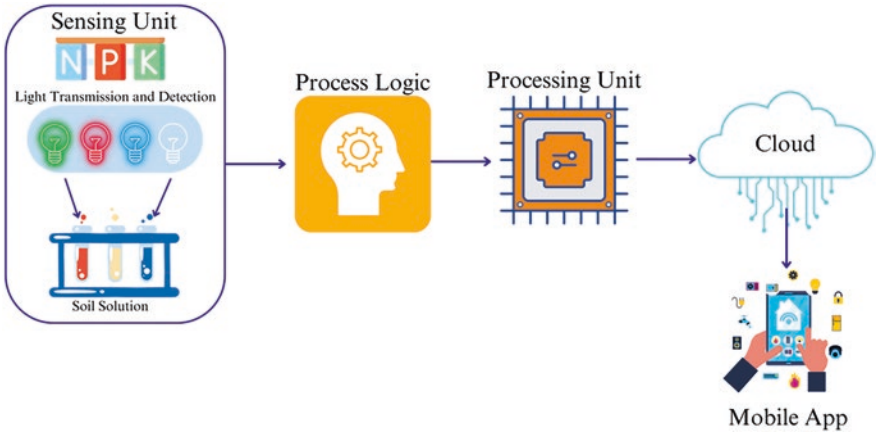

Fig. 13.10 Proposed IoT-based system for NPK detection based on Madhumathi et al. (2022)

facilitated by an open-platform communications united architecture (OPC UA) server.

13.3.2.3 Nutrient Management

In crop production, one of the critical aspects affecting optimal crop growth is balanced nutrient application. Thus, effective nutrient management and precise fertilizer application are essential for enhancing crop productivity and soil fertility. With the recent development in digital production, new technologies are also being introduced in nutrient management to enhance its efficiency. Researchers in this field, such as Madhumathi et al. (2022), have proposed soil nutrient detection and recommendation using IoT and Fuzzy Logic. They developed an IoT-based system to identify nutrient deficiencies in the soil and recommend the appropriate fertilizer quantities (Fig. 13.10). Their system employs colorimetry principles for assessing soil nutrient levels. It also incorporates a fuzzy expert system designed to provide fertilizer recommendations. The system utilizes a set of 27 IF-THEN rules established through the Mamdani influence system, which connects input and output membership functions based on linguistic variables for fertilizer guidance. Experiments were conducted using MATLAB to cover various nitrogen, phosphorous, and potassium ranges. The NPK data generated by the system were transmitted to the ThingSpeak cloud and made accessible through a mobile application, thus enabling farmers to access nutrient information specific to their fields. This system serves as a valuable resource for farmers, ultimately leading to more efficient and sustainable farming practices.

In addition, Suchithra and Pai (2020) designed a system that uses soil test data to effectively categorize and forecast soil fertility indices and pH levels based on a range of soil attributes. They employed the extreme learning machine (ELM)

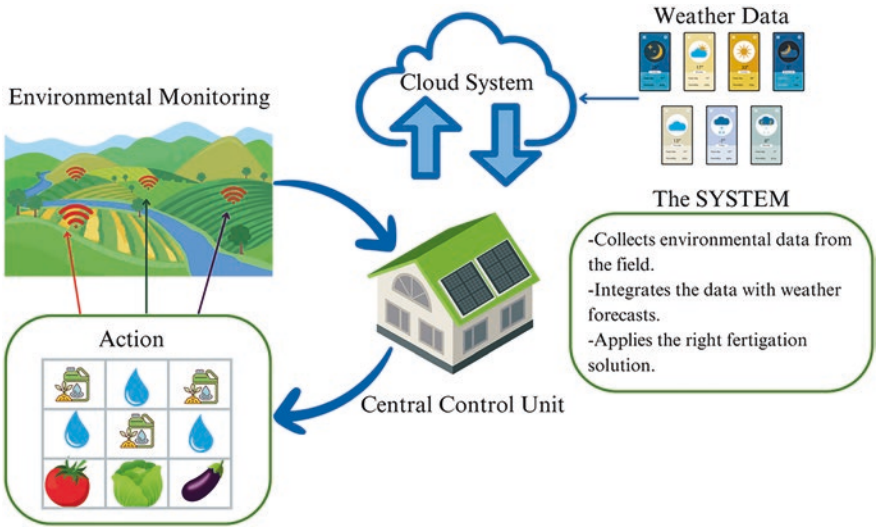

Fig. 13.11 Solar Fertigation architecture based on Ahmad et al. (2022)

algorithm and implemented a neural network (NN) structure with a single hidden layer. Impressively, their research yielded significant results, achieving accuracy rates of up to 78% in the prediction of potassium fertility indices and up to 89% in the classification of pH values.

In a separate study by Ahmad et al. (2022), the authors integrated agronomic models into an intelligent system for scheduling irrigation and fertilization based on plant requirements (Fig. 13.11). The system also monitors and manages the soil moisture content through automating watering. Referred as "solar fertigation," their system relies on photovoltaic solar power and IoT infrastructure to enable precise irrigation. The IoT system continuously tracks various parameters, such as temperature, radiation, humidity, and soil moisture. The study also introduced a decision support system (DSS) platform that combines soil, weather, and plant data through the use of sensors.

13.3.2.4 Harvesting

Harvesting is one of the most important operations in horticultural production. According to Erkan and Dogan (2019), harvesting plays a crucial role in determining the quality of produce. Fruits and vegetables should be harvested at the correct stage of maturity to preserve their nutritional value and freshness. It is also important to handle the operation carefully to avoid damaging the crops to maintain the market quality. However, due to the diversity of horticultural products, each crop involves a specific harvesting technique and is highly reliant on manual labor. Thus,

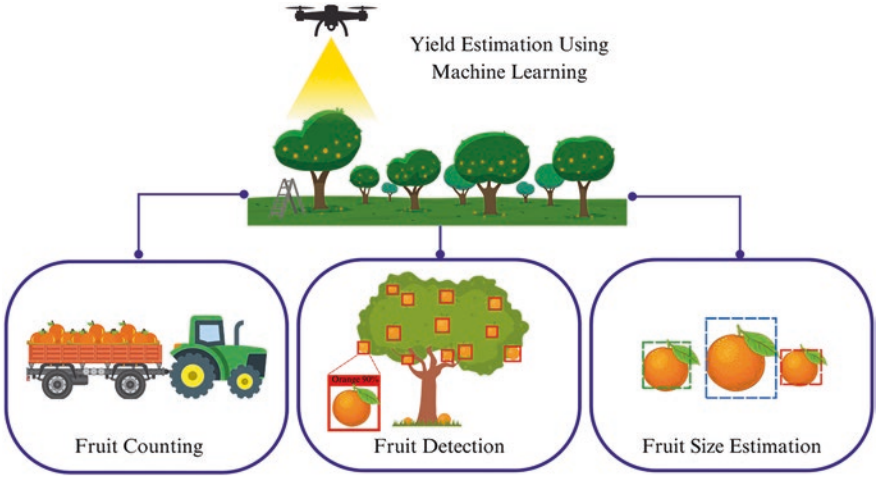

Fig. 13.12 Yield and size estimation of citrus using UAV and deep learning algorithms based on Apolo-Apolo et al. (2020)

the digitalization and automation of harvesting have been an efficient tool for increasing the productivity of many horticultural farms.

New technologies are being incorporated into different aspects of harvesting operations, ranging from yield estimation through maturity index determination and fruit picking. In a study conducted by Apolo-Apolo et al. (2020), UAV and deep learning techniques were utilized to estimate the yield and size of citrus fruits (Fig. 13.12). These authors introduced a new method that utilized long short-term memory (LSTM) networks to estimate yields for both individual trees and entire commercial orchards. The method involves the use of color ranges and artificial reference objects to gauge fruit size and ultimately determine the average fruit yield in the orchard. Apolo-Apolo et al. used Faster R-CNN for fruit counting and obtained an average standard error (SE) of 6.59%. In addition, individual yield estimation using LSTM was conducted in the study, and an appropriate error of SE = 4.53% and SD = 0.97 kg were obtained from actual and estimated yields per tree, respectively. Moreover, a comparison was also conducted among the real overall yield, the estimated total yield, and the yield as estimated by a technician. The technician's estimation had an error rate of 13.74%, whereas the model exhibited errors of 7.22% (as standard error) and 4083.58 kg (as standard deviation).

In another study by Koirala et al. (2019), real-time fruit detection and estimation were conducted on a mango orchard using YOLO algorithms. These authors built a new architecture based on YOLOv3 and YOLOv2-tiny, called "MangoYOLO." The model successfully determined an estimated fruit load between 4.6% and 15.2% from the mango orchard. In a separate study, the detection and counting of tomato fruits inside a greenhouse using Mask R-CNN were performed by Manya et al. (2020).

Aside from yield estimation and fruit counting, modern technology can assist in determining the maturity indices of horticultural crops to determine the optimal

time for harvesting the crops. The assessment of fruit and vegetable ripeness plays a pivotal role in optimizing field operations and achieving the desired product quality during harvesting. The conventional method of maturity identification of horticultural crops requires expertise and in-depth experience to predict the optimal time of harvest. The conventional method also entails numerous manual sampling and subsequent chemical analyses prior to harvest. With the advancement in technology, it is now possible to estimate fruit maturity using computer vision and machine learning (Vrochidou et al., 2021). Machine vision technology has revolutionized agricultural automation by providing faster, cost-efficient, and nondestructive approaches to ripeness estimation. For instance, in a study conducted by Garillos-Manliguez and Chiang (2021) on the fruit maturity estimation of papaya using multimodal deep learning (DL) and visible light and hyperspectral imaging, the authors were able to classify six maturity stages of papaya fruit. In a similar study on dates, the Intelligent Harvesting Decision System (IHDS) using DL and computer vision was successfully used to detect the seven maturity stages of date fruit with 99.4% accuracy, 99.7% recall, and 99.7% precision (Faisal et al., 2020).

Another exciting development in harvesting operations is the development of robots for the harvesting of different horticultural crops. A robotic harvesting system for tomatoes was proposed by Kim et al. (2022). These authors developed a deep learning network called Deep-ToMaToS, which can simultaneously perform three-level maturity classification and estimate the 6D pose (3D translation +3D rotation) of the target tomato. The robotic harvesting system incorporates a harvesting motion control algorithm that relies on the results of the 6D pose estimation. The system exhibits a 96% estimation accuracy based on the ADD_S metric and an average harvesting success rate of 84.5% based on the proposed harvesting motion algorithm.

Arad et al. (2020) introduced SWEEPER, a robot designed to harvest sweet pepper in greenhouses. The robotic system consists of a six-degree-of-freedom industrial arm equipped with a specially designed end effector, an RGB-D camera, a high-performance computer with a graphics processing unit, programmable logic controllers, various electronic components, and a small container for storing the harvested sweet pepper. The SWEEPER robot has a harvest success rate of 61% in optimal crop conditions.

Zhang et al. (2021) developed a robotic apple harvesting prototype with mechatronic design and a motion control approach. The robot includes a fruit detection component and localization system based on deep learning, which utilizes RGB-D camera. A three-degree-of-freedom manipulator was designed with a unique combination of pneumatic and motor-based actuation mechanisms to enable precise and sharp movements. The end effector uses a vacuum-based mechanism for detaching apples. These three components are integrated into a compact, simple, and robust apple harvesting prototype.

13.3.2.5 Postharvest

The responsibilities of a farmer extend beyond harvesting their crops, as they must engage in thorough postharvest management practices to guarantee the quality of their produce. Once the fruits and/or vegetables are detached from the tree or mother plant, deterioration accelerates; thus, farmers should provide an appropriate environment to slow down this process through proper postharvest management practices. Postharvest management is aimed at preserving the quality and safety of horticultural crops while reducing losses during the journey from the point of production to consumption (Kader, 2003). However, this is not an easy job, as postharvest losses and wastes (PHLW) still account for 60% of the total production, which

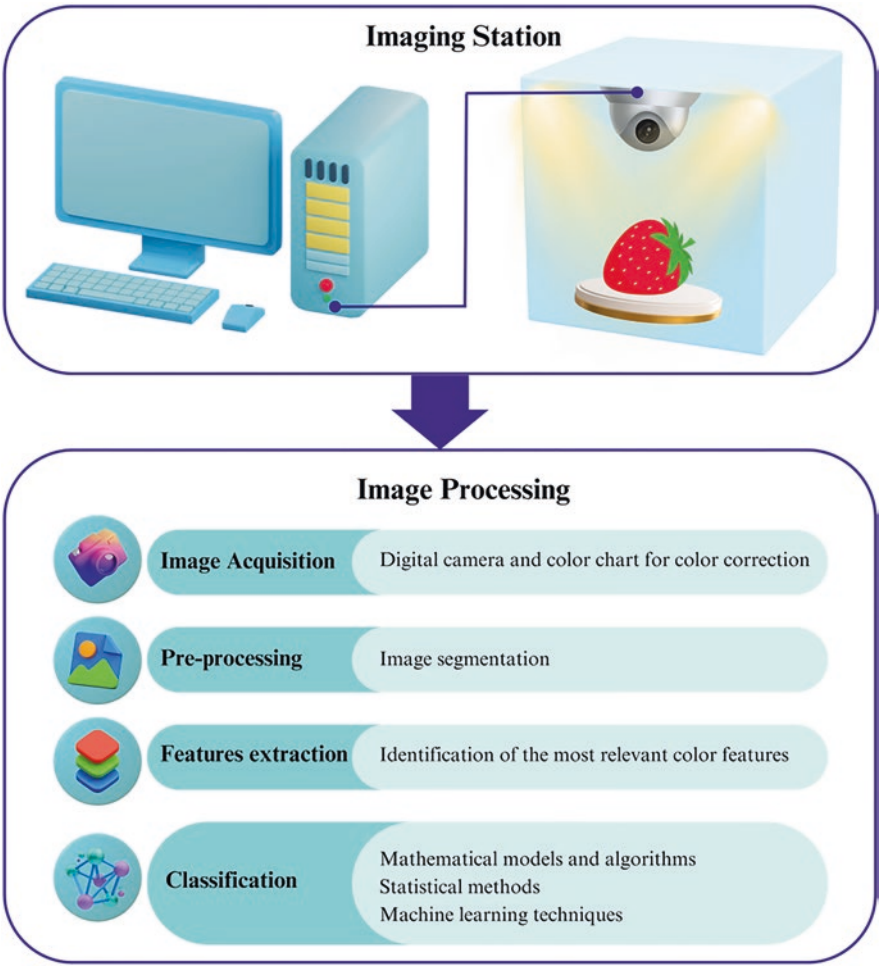

Fig. 13.13 General workflow of an image-processing system in postharvest operations based on Palumbo et al. (2022)

varies by the type of commodity, season, and region (Yahia et al., 2019). Mitigating PHLW is therefore a serious concern that needs to be addressed to ensure the provision of food for the expanding global population.

In recent years, with the advancement of agriculture and computer technologies, postharvest operations have also been digitalized to cope with the demands of the new era. DL is now being used in the postharvest management of apples, strawberries, banana, etc. A general workflow of the image processing system using DL in postharvest is shown in Fig. 13.13.

Stasenko et al. (2021) used DL to predict decay in apples. They employed U-Net, DeepLab, and Mask R-CNN models to identify and predict areas of postharvest decay in stored apple fruits. Their approach involves the separate segmentation and prediction of postharvest decay and nondecay areas in apples. They captured images using a custom testbed comprising a digital camera, a steeper driver pallet for apples, and a PC. Mask R-CNN outperformed the other models, achieving a mean average precision (mAP) of 98.81% for apples and 43.60% for postharvest decay zones.

In a similar study, Zhou et al. (2022) provided a quick and affordable approach for strawberry bruise inspection with DL using UV light. Strawberries are very susceptible to bruising, which causes flattening and discoloration that can reduce its shelf life. In this study, the authors utilized Mask R-CNN to detect four bruise categories: minor, light, moderate, and severe. They achieved an F1 score of 0.99 for detecting strawberry bruises and the highest F1 score of 0.92 for classifying minor bruises under UV light. Using this method, farmers can identify bruised strawberries during processing and harvesting, thus enhancing the quality of strawberries sent to the market and extending the shelf life of fresh strawberries.

A study conducted by Ucat and Dela Cruz (2019) on grading banana also used DL technology. Currently, banana classification in the Philippines relies solely on the visual assessment of a quality inspector, which may lead to errors and inconsistent grading results. They proposed a methodology that used Python OpenCV and TensorFlow to grade banana based on size. Using this method, they achieved higher than 90% classification accuracy rate, which can assist in the automation of a postharvest classification system for grading Cavendish bananas in the field, thereby improving the consistency and efficiency of the process.

In contrast to visual assessment, other studies have focused on the development of electronic noses (E-noses) for examining the quality of crops. Over the past few years, the E-nose has gained popularity as a preferred sensing technology, serving as an alternative to the traditional headspace solid-phase microextraction/gas chromatography–mass spectrometry (HS-SPME/GC-MS) method (Palumbo et al., 2022). It is equipped with a range of both partially specific and wide-spectrum electronic chemical sensors that mimic the human sense of smell. It generates a digital volatile organic compound (VOC) fingerprint that can be analyzed using appropriate statistical techniques. Typically, these electronic devices consist of three main components: a sample-handling mechanism, a detector, and a data collection system.

Huang et al. (2019) utilized the combination of an E-nose and machine vision technologies to assess spinach freshness during storage. Machine vision was employed to capture image data, while E-nose technology recorded odor information from the spinach samples. Freshness prediction was carried out using a back-propagation artificial neural network (BPNN) model that fused multisensory data from machine vision and the E-nose. This approach achieved a spinach freshness detection accuracy of 93.75%, which demonstrated that by combining machine vision and E-nose data through multisensory data fusion, we can smartly and rapidly assess the freshness of postharvest spinach during storage without the need for chemical pretreatments and destructive freshness assessment methods.

13.4 Challenges and Opportunities in Digital Horticulture Production and Management

Digital horticulture holds promise for numerous benefits in horticulture production and management. It boasts an increase in efficiency and productivity through the help of technological advancements in IoT, AI, and big data. However, there are still some challenges that need to be addressed to fully transition horticulture production into its digital age. The following presents some of the challenges that digital horticulture is currently facing, along with opportunities that can bring success and benefits to the horticulture industry (Fig. 13.14).

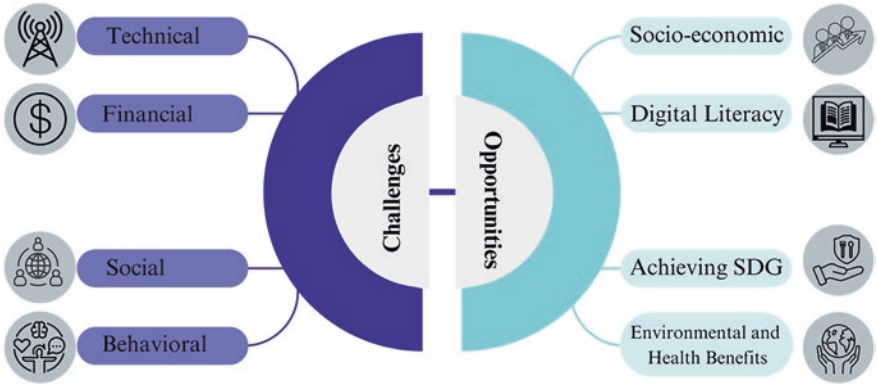

Fig. 13.14 Challenges and opportunities facing digital horticulture

13.4.1 Challenges

13.4.1.1 Technical Challenge

Connectivity is a primary component of digital horticulture, where internet connection and wireless data transmission play critical roles in digital operations. However, most production sites still lack the network infrastructures needed for steady internet connections. According to the World Bank (2022), in developing countries, only 35% of the total population has access to the internet compared to 80% in developed countries. Another important scenario, the rural and urban digital divide, is also a major concern. The rural areas where most of the production sites are located have limited access to the internet compared to urban areas. For instance, in Brazil, approximately 70% of rural establishments do not have internet access (IBGE, 2017). The disparity of internet access between developed and developing countries and urban and rural areas should be addressed to catalyze the global spread of digital technology in horticultural production. This is a major challenge in driving digital horticulture production that works with heavy reliance on internet connectivity.

13.4.1.2 Financial Challenge

Another challenge facing digital horticulture is the high initial cost or investment needed to transition from conventional to digital operations. The cost hinders the transition, as approximately 63% of the world's most impoverished individuals are employed in the agricultural sector, predominantly in small rural areas (IFAD, 2020).

13.4.1.3 Social Challenges

Aging Farmers. Farmers around the world are aging, the average age of farmers in Peru, Mexico, and Nigeria is 53 years old, 58 years old in the United States, and 67 years old in Japan. One-third of the farmers in Europe are above 65 years old (Arslan, 2019; Jöhr, 2012). This scenario makes it difficult for the farmers to adapt to new technologies that is particularly true of the digital technology, which can be a considerable burden to them.

Educational Attainment. Most farmers, especially in developing countries, have lower educational attainment and are fearful about new technologies, as education plays a significant role in adapting to new technologies, specifically in agriculture modernization (Lockheed et al., 1980).

13.4.1.4 Behavioral Challenges

Attitude to adopt. Farmers tend to be traditional and conservative in adopting new technologies. They embrace technology based on its practical utility rather than its technological premise (Dayioğlu & Turker, 2021). Farmers normally want proof of success before they use new practices or technology.

Fear of Labor Replacement. The introduction of autonomous and digital systems in horticulture production, or in any sector, has the potential to replace human labor, leading to concerns about unemployment, particularly in developing countries where the majority of the population works in agriculture (Kansake et al., 2019).

13.4.2 Opportunities

13.4.2.1 Socioeconomic Opportunities

New Job Opportunities. The advent of digital horticulture holds promise not only for efficient production and increased productivity but also for substantial socioeconomic transformations. The adoption of digitalization is anticipated to result in the creation of new job opportunities, foster innovation in the ecosystem, and reduce the social barriers to hiring, particularly those associated with age and gender inequality (Sadjadi & Fernández, 2023).

Attracts Younger Generations. The aging of farmers and lack of family succession are major concerns for agricultural farms around the world. Younger generations are no longer interested in farming and view agriculture as a traditional and not very lucrative profession. However, the integration of digital technologies in the production system enhances the appeal of farming to younger generations (Dayioğlu & Turker, 2021).

13.4.2.2 Digital Literacy

With the proliferation of different digital technologies on different platforms, such as social media and e-commerce, the digital anxiety of farmers and growers is decreasing due to their familiarity with these common digital platforms. However, proper capacity building on horticulture digital technologies is still necessary for farmers to fully understand and utilize these new technologies.

13.4.2.3 Achieving the Sustainable Development Goals

Digitalization is considered a crucial mechanism for realizing more sustainable agriculture and strategically confronting the challenges noted in the UNs SDGs (UN, 2018). Through digitalization, there is the potential to enhance the real-time monitoring of crops, enabling the early detection of pest and disease outbreaks.

Additionally, digitalization can contribute to optimizing yields and resources to help end food hunger and promote food security.

13.4.2.4 Environmental and Health Benefits

Embracing digital production practices can lessen the burden of the farmers and minimize both the physical and chemical risks (European Agency for Safety and Health at Work, 2021). In addition, digital horticulture also promotes more environmentally sound practices that can protect the environment.

13.5 Conclusion

In conclusion, the integration of digital technologies in horticultural production leads to enhanced efficiency through the quantification of crucial ground information such as soil moisture, soil nutrients, temperature, and humidity. These data facilitate more precise cultural operations, such as pest management, irrigation, and fertilization. In addition, digital transformation can be extended to provide a comprehensive monitoring system, thus ensuring crop quality from planting to harvesting. Recent technologies such as the IoT, AI, and big data improve the efficiency of horticultural production, thereby mitigating the impact of climate change, pests, diseases, high labor and land costs, as well as depleting water and soil nutrients.

Digital technologies are now being integrated into various aspects of horticultural operations, including automating greenhouse production and smart plant factories, and assisting in cultural operations, such as pest and disease monitoring, water and nutrient management, and harvesting and postharvest operations. The system incorporates different sensors to measure environmental parameters and analyzes them to provide the proper environment for plant growth and development.

While the digital transformation of horticultural crop production systems is exciting, optimistic, and holds outstanding promise, acknowledging the existing challenges that must be addressed for widespread implementation of the technology at the ground level is crucial to benefit farmers in the field.

For the digital transformation to thrive and prosper, it must be inclusive and accommodate diverse stakeholders. The path involves not only embracing digital technologies but also ensuring sustainable resource use and inclusivity in application. Despite the significant role of digital technologies throughout horticulture production systems, it is essential to emphasize that success still depends on the responsible minds of the farmers, sustainable practices and clean energy and water usage from farms to consumers. This emphasizes the importance of clean inputs and proper utilization of technology in horticultural production, as digital technologies are simply data after all. Farmers still have the final decision for their farms. These technologies are only offered as a guide for making the production more efficient and productive toward sustainable agricultural productivity. Transformation may

takes time, but as long as it addresses the challenges and continuously answers the gaps, especially in terms of connectivity in developing countries and rural areas, and be able to capacitate the farmers, reduce the cost, and constantly pursue sustainability, the digital transformation of horticulture production will succeed.

References

Abdulridha, J., Batuman, O., & Ampatzidis, Y. (2019). UAV-based remote sensing technique to detect citrus canker disease utilizing hyperspectral imaging and machine learning. *Remote Sensing, 11*(11), 1373. https://doi.org/10.3390/rs11111373

Ahmad, L., & Nabi, F. (2021). Agriculture 5.0: Artificial Intelligence. In *IoT and machine learning* (1st ed.). CRC Press. https://doi.org/10.1201/9781003125433

Ahmad, U., Alvino, A., & Marino, S. (2022). Solar fertigation: A sustainable and smart IoT-based irrigation and fertilization system for efficient water and nutrient management. *Agronomy, 12*, 1012. https://doi.org/10.3390/agronomy12051012

Alves, R. G., Maia, R. F., & Lima, F. (2023). Development of a digital twin for smart farming: Irrigation management system for water saving. *Journal of Cleaner Production, 388*, 135920. https://doi.org/10.1016/j.jclepro.2023.135920

Apacionado, B. V., & Ahamed, T. (2023). Sooty Mold detection on citrus tree canopy using deep learning algorithms. *Sensors, 23*(20), 8519. https://doi.org/10.3390/s23208519

Apolo-Apolo, O. E., Martínez-Guanter, J., Egea, G., Raja, P., & Pérez-Ruiz, M. (2020). Deep learning techniques for estimation of the yield and size of citrus fruits using a UAV. *European Journal of Agronomy, 115*, 126030. https://doi.org/10.1016/j.eja.2020.126030

Arad, B., Balendonck, J., Barth, R., Ben-Shahar, O., Edan, Y., Hellström, T., & Van Tuijl, B. (2020). Development of a sweet pepper harvesting robot. *Journel of Field Robotics, 37*(6), 1027–1039. https://doi.org/10.1002/rob.21937

Arslan, A. (2019). *How old is the average farmer in today's developing world?* Retrieved November 10, 2023, from https://www.ifad.org/en/web/latest/-/blog/how-old-is-the-average-farmer-in-today-s-developing-world

Bale, J. S., Masters, G. J., Hodkinson, I. D., Awmack, C., Bezemer, T. M., Brown, V. K., Butterfield, J., Buse, A., Coulson, J. C., Farrar, J., Good, J. E. G., Harrington, R., Hartley, S., Jones, T. H., Lindroth, R. L., Press, M. C., Smyrnioudis, I., Watt, A. D., & Whittaker, J. B. (2002). Herbivory in global climate change research: Direct effects of rising temperature on insect herbivores. *Global Change Biology, 8*, 1–16. https://doi.org/10.1046/j.1365-2486.2002.00451.x

Benyezza, H., Bouhedda, M., & Rebouh, S. (2021). Zoning irrigation smart system based on fuzzy control technology and IoT for water and energy saving. *Journal of Cleaner Production, 302*, 127001. https://doi.org/10.1016/j.jclepro.2021.127001

Bhardwaj, M. L. (2012). *Challenges and opportunities of vegetable cultivation under changing climate scenario. A training manual on vegetable production under changing climate scenario* (pp. 13–18). Springer.

Boote, K. J., Jones, J. W., Mishoe, J. W., & Berger, R. D. (1983). Coupling pests to crop growth simulators to predict yield reductions. *Phytopathology, 73*(11), 1581–1587. https://doi.org/10.1094/Phyto-73-1581

DadrasJavan, F., Samadzadegan, F., & Seyed Pourazar, S. H. (2019). UAV-based multispectral imagery for fast citrus greening detection. *Journal of Plant Diseases and Protection, 126*, 307–318. https://doi.org/10.1007/s41348-019-00234-8

Dayioğlu, A. M., & Turker, U. (2021). Digital transformation for sustainable future-agriculture 4.0: A review. *The Journal of Agricultural Science, 27*, 373–399. https://doi.org/10.15832/ankutbd.986431

Dukes, J. S., Theoharides, K. A., Pontius, J., Orwig, D., Stinson, K., Garnas, J. R., Stange, E. E., Ayres, M., Rodgers, V. L., Brazee, N., Cooke, B., Harrington, R., Ehrenfield, J., Gurevitch, J., Lerdau, M., & Wick, R. (2009). Responses of insect pests, pathogens, and invasive plant species to climate change in the forests of northeastern North America: What can we predict? *Canadian Journal of Forest Research, 39*(2), 231–248. https://doi.org/10.1139/X08-171

Erkan, M., & Dogan, A. (2019). Harvesting of horticultural commodities. In E. M. Yahia (Ed.), *Postharvest technology of perishable horticultural commodities* (pp. 129–159). Woodhead Publishing. https://doi.org/10.1016/B978-0-12-813276-0.00005-5

European Agency for Safety and Health at Work. (2021). *Cobots, robots and drones: The impact of digital technology on OSH in agriculture and forestry*. Policy Brief. Retrieved 10 November 2023, from https://osha.europa.eu/en/publications/cobots-robots-and-drones-impact-digital-technology-osh-agriculture-and-forestry

Extension.psu.edu. (2022). *Pests and pesticides in agriculture*. Retrieved 10 November 2023, from https://extension.psu.edu/pests-and-pesticides-in-agriculture. Accessed on: 10 November, 2023.

Faisal, M., Alsulaiman, M., Arafah, M., & Mekhtiche, M. A. (2020). IHDS: Intelligent harvesting decision system for date fruit based on maturity stage using deep learning and computer vision. *IEEE Access, 8*, 167985–167997. https://doi.org/10.1109/ACCESS.2020.3023894

Food and Agriculture Organization of the United Nations (FAO). (2019). *New standards to curb the global spread of plant pests and diseases*. Retrieved 26 June 2023, from http://www.fao.org/news/story/en/item/1187738/icode/

Food and Agriculture Organization of the United Nations (FAO). (2021). *The impact of disasters and crises on agriculture and food security: 2021*. FAO. https://doi.org/10.4060/cb3673en

Garillos-Manliguez, C. A., & Chiang, J. Y. (2021). Multimodal deep learning and visible-light and hyperspectral imaging for fruit maturity estimation. *Sensors, 21*, 1288. https://doi.org/10.3390/s21041288

Gora, J. S., Verma, A. K., Singh, J., & Choudhary, D. J. (2019). *Climate change and production of horticultural crops from: Agricultural impacts of climate change*. CRC Press. https://doi.org/10.1201/9780429326349-3

Hamidon, M. H., & Ahamed, T. (2023). Detection of defective lettuce seedlings grown in an indoor environment under different lighting conditions using deep learning algorithms. *Sensors, 23*(13), 5790. https://doi.org/10.3390/s23135790

Heege, H. J. (2018). *Precision in crop farming: Site specific concepts and sensing methods applications and results*. Springer.

Heo, J., Lee, C., Chakrabarty, D., & Paek, K. (2002). Growth responses of marigold and salvia bedding plants as affected by monochromic or mixture radiation provided by a light-emitting diode (LED). *Plant Growth Regulatory, 38*, 225–230. https://doi.org/10.1023/A:1021523832488

Huang, X., Yu, S., Xu, H., Aheto, J. H., Bonah, E., Ma, M., Wu, M., & Zhang, X. (2019). Rapid and nondestructive detection of freshness quality of postharvest spinaches based on machine vision and electronic nose. *Journal of Food Safety, 39*(6), e12708. https://doi.org/10.1111/jfs.12708

Hyunjin, C., & Sainan, H. (2021). A study on the design and operation method of plant factory using artificial intelligence. *Nanotechnology For Environmental Engineering, 6*, 41. https://doi.org/10.1007/s41204-021-00136-x

IBGE. (2017). *Censo agropecuário*. Retrieved November 10, 2023, from https://censos.ibge.gov.br/agro/2017

Incrocci, L., Thompson, R. B., Fernandez-Fernandez, M. D., De Pascale, S., Pardossi, A., Stanghellini, C., Rouphael, Y., & Gallardo, M. (2020). Irrigation management of European greenhouse vegetable crops. *Agricultural Water Management, 242*, 106393. https://doi.org/10.1016/j.agwat.2020.106393

International Fund for Agricultural Development (IFAD). (2020). *Covid-19*. Retrieved November 10, 2023, from https://www.ifad.org/en/covid19

International Society of Precision Agriculture (ISPA). (2019). *Precision Ag definition*. Retrieved November 10, 2023, from https://link.springer.com/journal/11119/updates/17240272

Iost Filho, F. H., Pazini, J. B., Alves, T. M., Koch, R. L., & Yamamoto, P. T. (2022). How does the digital transformation of agriculture affect the implementation of integrated Pest management? *Frontiers in Sustainable Food Systems, 6*, 972213. https://doi.org/10.3389/fsufs.2022.972213

Jöhr, H. (2012). Where are the future farmers to grow our food? *International Food and Agribusiness Management Review, 15*(A), 9.

Kader, A. A. (2003). A perspective on postharvest horticulture (1978-2003). *HortScience, 38*(5), 1004–1008. https://doi.org/10.21273/HORTSCI.38.5.1004

Kansake, B. A., Kaba, F. A., Dumakor-Dupey, N. K., & Arthur, C. K. (2019). The future of mining in Ghana: Are stakeholders prepared for the adoption of autonomous mining systems? *Resources Policy, 63*, 101411. https://doi.org/10.1016/j.resourpol.2019.101411

Khan, A. A., Wani, A. R., Zaki, F. A., Nehru, R. K., & Pathania, S. S. (2018). Pests of apple. In Omkar (Ed.), *Pests and their management*. Springer. https://doi.org/10.1007/978-981-10-8687-8_14

Khanna, M. (2021). Digital transformation of the agricultural sector: Pathways, drivers and policy implications. *Applied Economic Perspectives and Policy, 43*(4), 1221–1242. https://doi.org/10.1002/aepp.131031221

Kim, J., Pyo, H., Jang, I., Kang, J., Ju, B., & Ko, K. (2022). Tomato harvesting robotic system based on deep-ToMaToS: Deep learning network using transformation loss for 6D pose estimation of maturity classified tomatoes with side-stem. *Computers and Electronics in Agriculture, 201*, 107300. https://doi.org/10.1016/j.compag.2022.107300

Koirala, A., Walsh, K. B., Wang, Z., & McCarthy, C. (2019). Deep learning for real-time fruit detection and orchard fruit load estimation: Benchmarking of 'MangoYOLO'. *Precision Agriculture, 20*, 1107–1135. https://doi.org/10.1007/s11119-019-09642-0

Kong, Y., Nemali, A., Mitchell, C. A., & Nemali, K. (2019). Spectral quality of light can affect energy consumption and energy-use efficiency of electrical lighting in indoor lettuce farming. *HortScience, 54*, 865–872. https://doi.org/10.21273/HORTSCI13834-18

Li, L., Zhang, S., & Wang, B. (2021). Plant disease detection and classification by deep learning—A review. *IEEE Access, 9*, 56683–56698. https://doi.org/10.1109/ACCESS.2021.3069646

Liao, M. S., Chen, S. F., Chou, C. Y., Chen, H. Y., Yeh, S. H., Chang, Y. C., & Jiang, J. A. (2017). On precisely relating the growth of Phalaenopsis leaves to greenhouse environmental factors by using an IoT-based monitoring system. *Computers and Electronics in Agriculture, 136*, 125–139. https://doi.org/10.1016/j.compag.2017.03.003

Liu, Y., Ma, X., Shu, L., Hancke, G. P., & Abu-Mahfouz, A. M. (2021). From industry 4.0 to agriculture 4.0: Current status, enabling technologies, and research challenges. *IEEE Transactions on Industrial Informatics, 17*(6), 4322–4334. https://doi.org/10.1109/TII.2020.3003910

Lockheed, M. E., Jamison, T., & Lau, L. J. (1980). Farmer education and farm efficiency: A survey. *Economic Development and Cultural Change, 29*(1), 37–76.

Ludwig-Ohm, S., Hildner, P., Isaak, M., Dirksmeyer, W., & Schattenberg, J. (2023). The contribution of horticulture 4.0 innovations to more sustainable horticulture. *Procedia Computer Science, 217*, 465–477. https://doi.org/10.1016/j.procs.2022.12.242

Madhumathi, R., Arumuganathan, T., & Shruthi, R. (2022). Soil nutrient detection and recommendation using IoT and fuzzy logic. *Computer Systems Science and Engineering, 43*(2), 455–469. https://doi.org/10.32604/csse.2022.023792

Manya, A., Hubert, F., Schadeck, F. F., Dick, L., Marcel, M., Nanne, F., Gerrit, P., & Ron, W. (2020). Tomato fruit detection and counting in greenhouses using deep learning. *Frontiers in Plant Science, 11*, 571299. https://doi.org/10.3389/fpls.2020.571299

Moon, T., Choi, W. J., Jang, S. H., Choi, D. S., & Oh, M. M. (2022). Growth analysis of plant factory-grown lettuce by deep neural networks based on automated feature extraction. *Horticulturae, 8*, 1124. https://doi.org/10.3390/horticulturae8121124

Moreira, R. R., Machado, F. J., Lanza, F. E., Trombin, V. G., Bassanezi, R. B., de Miranda, M. P., Barbosa, J. C., da Silva Junior, G. J., & Behlau, F. (2022). Impact of diseases and pests on premature fruit drop in sweet orange orchards in São Paulo state citrus belt, Brazil. *Pest Management Science, 78*, 2643–2656. https://doi.org/10.1002/ps.6894

Morrow, R. C. (2008). LED lighting in horticulture. *HortScience, 43*(7), 1947–1950. https://doi.org/10.21273/HORTSCI.43.7.1947

Nagano, S., Moriyuki, S., Wakamori, K., Mineno, H., & Fukuda, H. (2019). Leaf-movement-based growth prediction model using optical flow analysis and machine learning in plant factory. *Frontiers in Plant Science, 10*, 227. https://doi.org/10.3389/fpls.2019.00227

Nemali, K. (2022). History of controlled environment horticulture: Greenhouses. *HortScience, 57*(2), 239–246. https://doi.org/10.21273/HORTSCI16160-21

Oerke, E. (2006). Crop losses to pests. *The Journal of Agricultural Science, 144*(1), 31–43. https://doi.org/10.1017/s0021859605005708

Palumbo, M., Attolico, G., Capozzi, V., Cozzolino, R., Corvino, A., de Chiara, M. L. V., Pace, B., Pelosi, S., Ricci, I., & Romaniello, R. (2022). Emerging postharvest technologies to enhance the shelf-life of fruit and vegetables: An overview. *Food, 11*(23), 3925. https://doi.org/10.3390/foods11233925

Preti, M., Verheggen, F., & Angeli, S. (2020). Insect pest monitoring with camera-equipped traps: Strengths and limitations. *Journal of Pest Science, 94*, 203–217. https://doi.org/10.1007/s10340-020-01309-4

Pylianidis, C., Osinga, S., & Athanasiadis, I. N. (2021). Introducing digital twins to agriculture. *Computers and Electronics in Agriculture, 184*, 105942. https://doi.org/10.1016/j.compag.2020.105942

Roy, S. K., Misra, S., Raghuwanshi, N. S., & Das, S. K. (2021). AgriSens: IoT-based dynamic irrigation scheduling system for water management of irrigated crops. *IEEE Internet of Things Journal, 8*(6), 5023–5030. https://doi.org/10.1109/JIOT.2020.3036126

Sadjadi, E. N., & Fernández, R. (2023). Challenges and opportunities of agriculture digitalization in Spain. *Agronomy, 13*(1), 259. https://doi.org/10.3390/agronomy13010259

Shamshiri, R. R., Kalantari, F., Ting, K. C., Thorp, K. R., Hameed, I. A., Weltzien, C., Ahmad, D., & Zahra, M. S. (2018). Advances in greenhouse automation and controlled environment agriculture: A transition to plant factories and urban agriculture. *International Journal of Agricultural and Biological Engineering, 11*(1), 1–22. https://doi.org/10.25165/j.ijabe.20181101.3210

Soeb, M. J. A., Jubayer, M. F., & Tarin, T. A. (2023). Tea leaf disease detection and identification based on YOLOv7 (YOLO-T). *Scientific Reports, 13*, 6078. https://doi.org/10.1038/s41598-023-33270-4

Soheli, S. J., Jahan, N., Hossain, M. B., Adhikary, A., Khan, A. R., & Wahiduzzaman, M. (2022). Smart greenhouse monitoring system using internet of things and artificial intelligence. *Wireless Personal Communications, 124*, 3603–3634. https://doi.org/10.1007/s11277-022-09528-x

Stasenko, N., Savinov, M., Burlutskiy, V., Pukalchik, M., & Somov, A. (2021). Deep learning for Postharvest decay prediction in apples. In *IECON 2021—47th Annual Conference of the IEEE Industrial Electronics Society* (pp. 1–6). IEEE. https://doi.org/10.1109/IECON48115.2021.9589498

Suchithra, M., & Pai, M. L. (2020). Improving the prediction accuracy of soil nutrient classification by optimizing extreme learning machine parameters. *Information Processing in Agriculture, 7*(1), 72–82. https://doi.org/10.1016/j.inpa.2019.05.003

Syed-Ab-Rahman, S. F., Hesamian, M. H., & Prasad, M. (2022). Citrus disease detection and classification using end-to-end anchor-based deep learning model. *Applied Intelligence, 52*, 927–938. https://doi.org/10.1007/s10489-021-02452-w

Tripathy, P. K., Tripathy, A. K., Agarwal, A., & Mohanty, S. P. (2021). MyGreen: An IoT-enabled smart greenhouse for sustainable agriculture. *IEEE Consumer Electronics Magazine, 10*(4), 57–62. https://doi.org/10.1109/MCE.2021.3055930

Ucat, R. C., & Dela Cruz, J. C. (2019). Postharvest grading classification of Cavendish Banana using deep learning and Tensorflow. In *International symposium on multimedia and communication technology (ISMAC), Quezon City, Philippines* (pp. 1–6). IEEE. https://doi.org/10.1109/ISMAC.2019.8836129

Uğuz, S., Şikaroğlu, G., & Yağız, A. (2023). Disease detection and physical disorders classification for citrus fruit images using convolutional neural network. *Journal of Food Measurement and Characterization, 17*, 2353–2362. https://doi.org/10.1007/s11694-022-01795-3

United Nations. (2018). *Sustainable development goals*. Retrieved November 10, 2023, from https://sustainabledevelopment.un.org/sdg6

United Nations. (2022). *Department of Economic and Social Affairs*. World population to reach 8 billion on 15 November 2022. Retrieved November 10, 2023, from https://www.un.org/en/desa/world-population-reach-8-billion-15-november-2022

Vayssières, J. F., Korie, S., & Ayegnon, D. (2009). Correlation of fruit fly (*Diptera tephritidae*) infestation of major mango cultivars in Borgou (Benin) with abiotic and biotic factors and assessment of damage. *Crop Protection, 28*(6), 477–488. https://doi.org/10.1016/j.cropro.2009.01.010

Vrochidou, E., Bazinas, C., Manios, M., Papakostas, G. A., Pachidis, T. P., & Kaburlasos, V. G. (2021). Machine vision for ripeness estimation in viticulture automation. *Horticulturae, 7*, 282. https://doi.org/10.3390/horticulturae7090282

World Bank. (2022). Retrieved November 10, 2023, from https://www.worldbank.org/en/topic/digitaldevelopment/brief/connecting-for-inclusion-broadband-access-for-all

Xu, X. (2022). Major challenges facing the commercial horticulture. *Frontiers in Horticulture, 1*, 980159. https://doi.org/10.3389/fhort.2022.980159

Yahia, E. M., Fonseca, J. M., & Kitinoja, L. (2019). Postharvest losses and waste. In E. M. Yahia (Ed.), *Postharvest technology of perishable horticultural commodities* (pp. 43–69). Woodhead Publishing. https://doi.org/10.1016/B978-0-12-813276-0.00002-X

Zalom, F. G. (2003). Pests, endangered pesticides and processing tomatoes. *Acta Horticulturae, 613*, 223–233. https://doi.org/10.17660/ActaHortic.2003.613.35

Zambon, I., Cecchini, M., Egidi, G., Saporito, M. G., & Colantoni, A. (2019). Revolution 4.0: Industry vs. agriculture in a future development for SMEs. *PRO, 7*(1), 36. https://doi.org/10.3390/pr7010036

Zhang, K., Lammers, K., Chu, P., Li, Z., & Lu, R. (2021). System design and control of an apple harvesting robot. *Mechatronics, 79*, 102644. https://doi.org/10.1016/j.mechatronics.2021.102644

Zhou, X., Ampatzidis, Y., Lee, W. S., Zhou, C., Agehara, S., & Schueller, J. K. (2022). Deep learning-based postharvest strawberry bruise detection under UV and incandescent light. *Computers and Electronics in Agriculture, 202*, 107389. https://doi.org/10.1016/j.compag.2022.107389

Chapter 14
Challenges in Orchard Weed Management: Perspectives on the Use of 3D Cameras and LiDAR to Develop a Low-Cost Small-Scale Robotic Weeder

Abstract In orchard weed management, accurate information about the orchard environment, such as tree positions and diameters, weed locations, and obstacles, is essential for robotic weeders to enable autonomous navigation. Three-dimensional (3D) cameras and light detection and ranging (LiDAR) sensors have the potential to provide good perception for a weeding robot, as GNSS cannot provide consistent point cloud data due to canopy coverage in dense-canopy areas. However, the success of robotic weed control comes not only from navigation but also from the proper use of weeding tools. This chapter describes the potential of 3D cameras and LiDAR to support the development of low-cost small-scale robotic weeders for orchard operations. First, we discuss the complexity of the environment in an orchard, where a robot may have difficulty navigating under the canopy of fruit trees while avoiding surrounding obstacles. After that, the advantages and disadvantages of various perception sensors are detailed based on the literature. Finally, we introduce a weed control strategy for orchard weeding operations in terms of the navigation strategy and weed cutting mechanisms of small robots. The robotic weeder can be used for interrow and intrarow weeding, utilizing 3D cameras and LiDAR as the main sensors with the support of perception sensors other than those using satellite-based navigation.

Keywords Orchard · Weed management · 3D camera · LiDAR

14.1 Introduction

Management of undesirable plants in orchards is crucial, as it determines the quality of yield. Orchard weeds can aggressively compete with trees for nutrients and water from the soil, provide habitats for pests and shade, and stunt young trees (Riczu et al., 2015). Weeds also interrupt irrigation and chemical spraying operations, causing water, herbicides, and pesticides to go to nontarget areas (Brunharo et al., 2020; Liu et al., 2022). Farmers may need to perform repetitive work using mechanical or chemical means, as weeds can regrow quickly after being eradicated. Therefore,

© The Author(s), under exclusive license to Springer Nature Singapore Pte Ltd. 2024

T. Ahamed, *IoT and AI in Agriculture*,
https://doi.org/10.1007/978-981-97-1263-2_14

mowing grass is one of the most difficult tasks in agriculture, especially in larger and semimountainous areas.

As the number of agricultural workers has decreased and the population has aged (Magaki, 2023), robotic and automated machines have been extensively implemented in orchard operations, including weed control (Zhang et al., 2019). Therefore, the use of autonomous weeders has the potential to support weeding operations and address the shortage of human labor. However, there are two main issues in the development of autonomous weeders for orchards: one is to determine how weed control can be performed efficiently, and the other is to determine how a vehicle can move autonomously both between tree rows (interrow) and within tree rows (intrarow) in an orchard (Wang et al., 2022).

Weed control in orchards can be performed mechanically by using tillage implements, riding mowers (RMs), walking mowers (WMs), and brush cutters (BCs) (Hossain & Komatsuzaki, 2021). Although tillage has been a common method of weed control since ancient times (Peruzzi et al., 2017), the use of tillage in orchards can damage the root system between tree rows due to the gradual compaction of soil, inhibiting plants from taking up water and nutrients from the ground. Moreover, mechanical mower operations are costly since the orchard floor needs to be clear of weeds, so mowing needs to be performed frequently. Therefore, many researchers have dedicated their efforts to improving the efficiency of weed eradication in the form of robotics-based methods and tools. In a robotic platform, one of the challenges that needs to be overcome is accurate autonomous navigation system development.

In autonomous navigation, a key point is related to the ability of a vehicle to determine a specific destination and then plan a path to reach it without human intervention. While the location corresponds to the position of the robot obtained by sensors, planning a path for the robot to move along necessitates a controlling algorithm and obstacle avoidance strategies. Wang and Noguchi (2019) developed a robotic tractor that can operate autonomously without human intervention through a real-time kinematic global navigation satellite system (RTK-GNSS) positioned with a quasizenith satellite system (QZSS). Kaizu et al. (2018) proposed a control system for a robotic mower to run autonomously in a specified area using RTK-GNSS information. However, due to the high and dense canopy of trees, RTK-GNSS signals may occasionally be unable to establish the accurate location of the vehicle, making autonomous navigation difficult for orchard operations (Li et al., 2009).

The development of autonomous navigation is certainly not only dependent on the GNSS; methods of determining a robot's position, such as simultaneous localization and mapping (SLAM), are also worth considering. SLAM uses external sensors, such as cameras, LiDAR, inertial measurement units (IMUs), and wheel encoders, to calculate odometry and enable sequential self-estimation of the robot's position. Although it is recognized that the self-estimated position may drift, the drift inaccuracy can be reduced by introducing limitations such as loop closure (Inoue et al., 2022). Orchard navigation is the most complex scenario, and

interruption of RTK-GNSS signals can occur because of high and dense canopies (Li et al., 2009).

In addition to navigation issues, the weed control methods and tools used are important factors that determine the success of effective and efficient robotic-based weed control. Since sustainable fruit has become a concern of the global community, the use of pesticide spraying in weed control is slowly being abandoned and replaced with mechanical methods. Selecting a lawn mower that can be attached to an autonomous robot must take into account orchard conditions such as terrain, tree space, and landmarks. The use of RLM has proven to be effective in weed control, although it is limited to small orchards (0–0.33 ha) (Hossain & Komatsuzaki, 2021). Furthermore, the navigation capabilities of RLMs in intrarow areas within orchards are still limited and require further study. Therefore, this chapter focuses on the difficulty of managing weeds in orchard systems and outlines the possibilities of robotic systems that enable weeding in orchards using 3D cameras and LiDAR. Then, we introduce a navigation strategy and propose a weed-cutting mechanism based on 3D cameras and LiDAR that does not injure the orchard-distributed root system near the main tree trunks.

14.2 Characteristics of Orchard Environments for Robotic Weeding Operations

Autonomous steering system schemes that can be applied to weed control have been widely studied for decades. An integrated system scheme for the components of autonomous driving known as "perception – decision-making – control" has been established (Wang et al., 2022; Jones et al., 2019). In the perception step, sensors are the main components used to obtain data about the orchard environment, such as the locations of trees, weeds, fixed poles, garden edges, and fences, which are used in the decision-making step. The decision-making step is performed based on the environmental data obtained on the path to be traveled by the vehicle, which provides information regarding any obstacles on the path. Finally, the controller step is related to regulating the steering of the vehicle to move along the trajectory.

Orchards have a wide range of invasive plant species, each exhibiting growth patterns, characteristics, and responses to control methods. Weed-removing robots must be versatile enough to handle different types of weeds effectively. Furthermore, accurate weed detection and identification are crucial for targeted removal. Robotic systems must employ advanced sensors and algorithms to accurately identify and differentiate noxious herbs from crops. Another challenge is that some fruit crops are also sensitive to mechanical disturbances and herbicide application. Weed-removing robots need to operate with precision and selectivity to avoid damaging fruit trees while effectively removing weeds. This requires sophisticated robotic control and sensing capabilities.

Orchard field layouts frequently have complex designs with rows of trees spaced at different distances. Robots that remove weeds find it difficult to navigate and correctly identify weeds due to this environmental condition. The difficulty is further increased by the existence of barriers such as dead branches, stones, and uneven terrain. In this study, we consider the application of sensing for two types of orchards when using robotic weed management: a conventional orchard and a joint-tree orchard (Fig. 14.1). As shown in the image, the trees are arranged with a uniform row spacing, and there are many iron poles near the trees that help the trunks grow upright (Fig. 14.1a). In addition, the iron poles are interconnected with vertical poles, allowing the trees to be connected to each other (Fig. 14.1b). The two types of orchard layouts greatly support the robot in navigating smoothly both within and between rows of trees.

Some orchards have dense canopies and many branches connected with tree stacking systems (such as poles and wires) (Fig. 14.1b), which affects the quality of GNSS signals received by rovers. Thus, orchards generally do not have dedicated base stations for satellite data transmission. Structured and known orchard road path locations can be obtained through GNSS systems; however, obstacle avoidance with GNSS is quite difficult to achieve. Therefore, the performance of navigation systems based on GNSS is highly dependent on the quality of the GNSS signal (Ailian et al., 2022).

Another issue is that some weed plants have to be left alive because they are in positions that cannot be reached by either a lawn mower or a robotic weeder, as shown in Fig. 14.2. These weeds can be eradicated by hand pulling or hand mowers. Therefore, in addition to the usual weed eradication carried out in rows, a special weed control strategy is needed for weeding in such positions. Even though riding mowers and some medium-size weeder machines can be controlled remotely, special skills are needed by laborers to operate the mower.

Fig. 14.1 (**a**) Conventional pear orchard and (**b**) joint-tree kiwi orchard at the Tsukuba-Plant Innovation Research Center (T-PIRC), University of Tsukuba, Tsukuba, Ibaraki, Japan

Fig. 14.2 Remaining weeds after weed control using a conventional weeder

14.3 The Use of 3D Cameras and LiDAR in Robotics-Based Weed Control

In recent decades, significant improvements in robotic systems have been reported due to advances in computer technology and sensors. Additionally, more affordable technology has facilitated advances in this area worldwide. There are at least three subsystems of autonomous vehicles that combine several sensors: perception, decision, and control. At the perception level, sensors are primarily used to obtain environmental data about the surroundings of the orchard, such as information about fruit trees, poles, weeds, soil, and the road, which are used to make the decisions at the next stage; at the decision level, the obtained environmental information is further processed, and then the travel path is extracted to account for obstacles. Finally, the controller is designed to drive the system to follow the chosen path. Table 14.1 shows the advantages and shortcomings of three kinds of sensors that are generally used in the perception step.

Distance estimation is an important part of autonomous driving. Camera and LiDAR technology can play a role in synchronously transmitting the 3D points of the surrounding environment and obtaining the distance information needed for navigation. However, in practice, cameras outperform LiDAR in capturing rich depth information (Simon et al., 2018). The challenge in estimating the distances of objects in real 3D environments with 2D images includes inferring depth information from 2D image objects, which is considered quite difficult due to the lack of explicit depth cues in the images. This is known as depth ambiguity and is caused by lighting, texture, and occlusion (Zhang et al., 2022). In addition, the estimated distances of objects in the image can be affected by the internal and external constraints of the camera used, such as focal length, lens distortion, and sensor size (Usmankhujaev et al., 2023). Therefore, object distance estimation methods for autonomous vehicles should fulfill criteria such as a low error magnitude and a high reaction rate.

Table 14.1 Classification of unmanned perception methods in orchards

	Advantages	Shortcomings
GNSS Guevara et al. (2020)	Operates throughout the entire day; with global coverage, GNSS is capable of providing location and time information at almost any location on earth.	Loss of signal in the orchard caused by canopy occlusion, multipath effects, radio frequency interference, etc., causes significant inaccuracies in GNSS navigation and even incorrect navigation
Visual sensor Vrochidou et al. (2022)	Provides rich visual information about the orchard environment, including red-green-blue (RGB) maps and depth maps.	The performance of vision cameras may be affected by poor lighting conditions, such as low light or excessive bright light. Requires significant computational power and longer processing time
LiDAR Bergerman et al. (2015)	LiDAR can produce highly accurate and detailed 3D mapping of the orchard environment. It has consistent performance in various lighting conditions, both during the day and at night.	The cost is high, and the system is greatly affected by bad weather

Fusion sensors and combined sensors are commonly used in the field for increased detection accuracy and capacity. For example, using a combination of cameras and LiDAR with appropriate algorithms can produce an accuracy of detection of tree and nontree objects in orchards of up to 96.64% (Shalal et al., 2015). LiDAR can detect edge points and widths and recognize tree and nontree objects, and the camera can help verify the color and parallel boundaries of the edges of tree and nontree objects. Another example is the combination of multiple sensors used in an automated fruit harvesting design. The combination of 3D LiDAR, image, GNSS, and IMU sensors is used to recognize the surrounding environment in the garden, avoid obstacles, and obtain the shortest distances to objects (Lee et al., 2022). Another fusion sensor uses a combination of ultrasonic radar and LiDAR to improve obstacle perception. Some LiDARs have a weakness in perceiving ground obstacles because of their longitudinal sensitivity range. An ultrasonic sensor that is placed under the robot can overcome the weakness of LiDAR and better identify ground obstacles (Wang et al., 2022).

14.3.1 Machine Vision Using a 3D Camera

Although traditional 2D imaging methods for mapping orchard environments can be limited in the field by factors such as shadows and distance, 3D imaging mitigates this challenge by using depth data to create accurate imaging models. However, for the navigation system, the powerful capabilities of the 3D camera cannot work alone in perceiving the orchard environment. The key aspect of visual navigation is

its accurate and reliable extraction of the navigation baseline through image processing technology (Zhou et al., 2022).

For the autonomous navigation problem, the research ideas are generally focused on two aspects: road- or sky-based navigation line generation and crop detection–based fitting of navigation lines. Crop detection–based navigation methods require accurate identification of crop trunks and are highly robust to complex road environments, thus requiring high adaptability. In simple terms, the tree objects captured by the camera are used as a reference to determine the steering angle of the vehicle. A line can be created to guide the movement of the robot. Machine learning algorithms such as k-means and random sample consensus (RANSAC) are used in this regard (Ailian & Ahamed, 2023). Real objects in the orchard environment in 3D are transformed into 2D objects to determine the vehicle path. Moreover, the steering angle and direction can also be determined based on tree objects or other objects seen by the camera so that the robot can move away from the objects.

Three-dimensional imaging employs sensor data to create models of objects based on point clouds, which consist of large datasets of points in 3D space. Some photogrammetric techniques, such as stereo vision and structure from motions (SfM), are well known as low-cost and efficient methods for generating 3D point clouds of objects. SfM, using a single camera that captures several 2D images of the object from different viewpoint distances with a specific amount of overlap among the images (Fig. 14.3), can be applied to objects such as trees, fruits, fixed poles, and fences that are present in orchards. Subsequently, the 3D point cloud is created based on features that are matched from different images (i.e., views) of the object. The point cloud represents a 3D model of the orchard layout, which can be used to gather tree positions based on depth data (distance). In stereo vision, a binocular camera captures two images of the object simultaneously and utilizes triangulation to generate a depth map (Dobbs et al., 2022).

The model of a 3D camera for use either indoors or outdoors depends on the camera model and manufacturer. For example, the Intel Realsense D455 has an optimal distance of 6 m outdoors. Figure 14.4 shows orchard trees captured by both an RGB camera and a depth sensor. With the depth sensor, users can determine the distances of objects in front of them. However, the specifications and limitations of the camera's capabilities, such as light sensitivity, may vary depending on the camera's model. In Fig. 14.4, the RGB image clearly shows a purple color in the lower right corner; this is caused by the recording time during the day and the heat of the sun, which is quite hot near young fruit trees that do not have large canopies.

The accuracy of both SfM and stereo vision may be affected by wind in the field, which causes the leaves of the trees to move and overlap (Dobbs et al., 2022). However, poles or crossed poles to support trees to grow straight can also be used to avoid the influence of wind. In addition, the accuracy of localization can be affected by lighting. Therefore, when a 3D camera is combined with deep learning object detection, the level of accuracy depends on how many images are used for training and capturing image data at various times of day (morning, afternoon, and evening) and under varying lighting can be beneficial. Furthermore, in the case of object detection under trees, such as detection of weeds or shrubs, achieving high

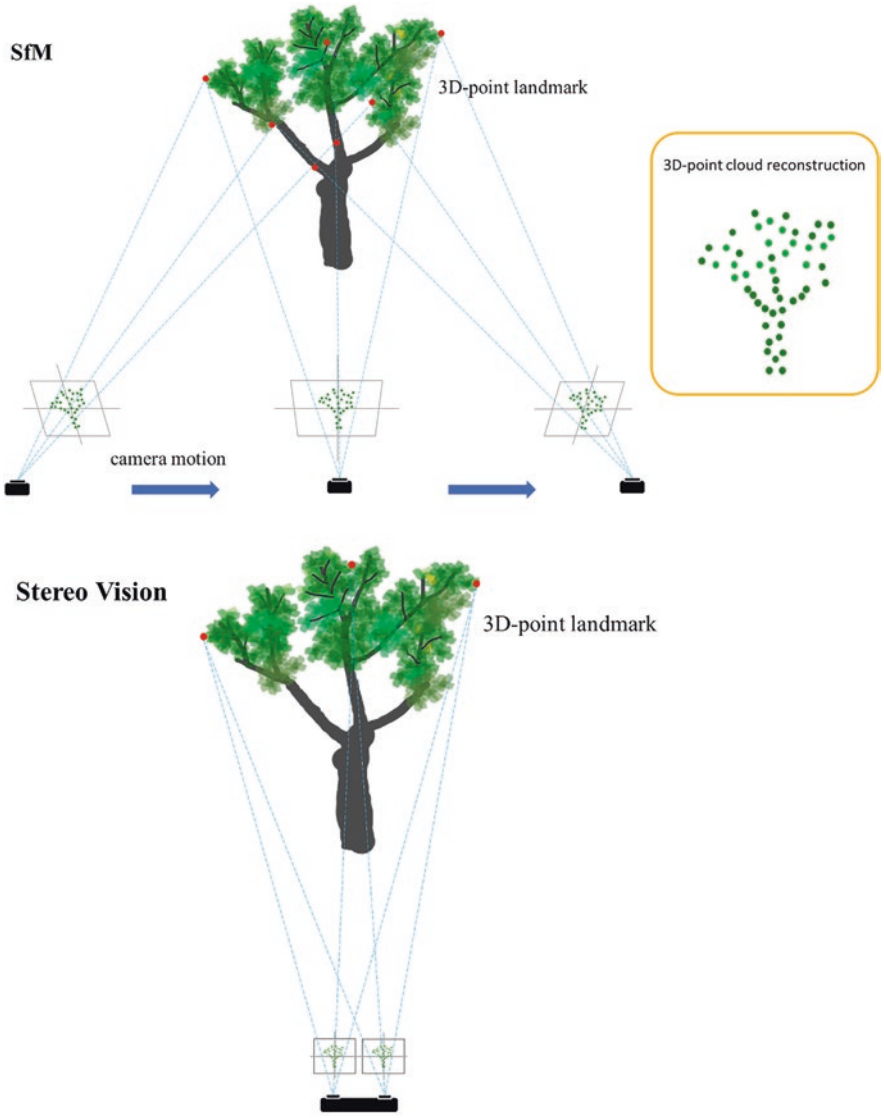

Fig. 14.3 The difference between 3D reconstructions of images from SfM and stereo vision

accuracy is a possible challenge when the information generated from the RGB sensor is out of sync with the depth sensor due to objects being obscured by uneven tree shading.

Currently, the utilization of deep learning methods has become very common to improve the accuracy of perception sensors. For example, an autonomous navigation system for a robotic lawn mower for orchards using 3D cameras and an inertial measurement unit (IMU) without the global navigation satellite system (GNSS),

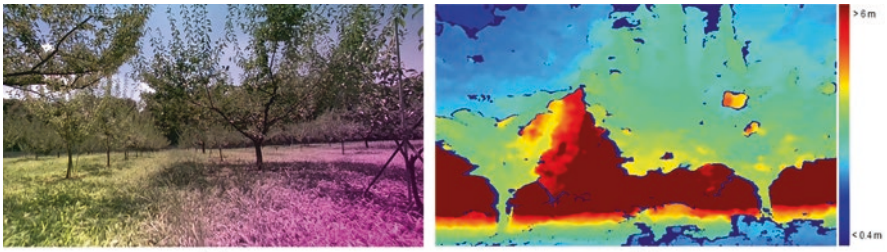

Fig. 14.4 (**a**) RGB image and (**b**) depth image captured by a Realsense D455 depth camera

proposed by Inoue et al. (2022), uses deep learning. A convolutional neural network (CNN) that was trained on many images was used to recognize the obstacles around a robot, and visual simultaneous localization and mapping (VSLAM) was used to estimate the position of the robot. With the incorporation of deep learning, a known tree location is transformed into XY coordinates for robot motion direction determination and obstacle avoidance.

14.3.2 LiDAR

Zhou and Hu (2015) proposed a method to calculate tree center points, where LiDAR is used to detect tree trunks in the tree rows to the left and right of the sensor. Point clusters whose shape resembles a circular arc can be identified. The coordinate position of the center and diameter of the tree trunk can be obtained through geometric derivation. As the robot moves, its position and posture are adjusted in real time by matching the coordinates of the detected rod center point with those obtained earlier. Blok et al. (2019) conducted further research on robot self-positioning. This study proved the applicability of two probabilistic localization algorithms using a single 2D LiDAR sensor for robot navigation of tree rows in an orchard. The first localization algorithm was a particle filter (PF) model that used a laser beam, and the other was a Kalman filter (KF) with a line detection algorithm. Experiments were designed to evaluate the accuracy of navigation and strength of both methods, and the results showed that PF was preferable to KF for interrow navigation.

Ailian and Ahamed (2023) succeeded in using LiDAR as a single sensor in a robot sprayer navigation system in an orchard. This system can address the limitations of GNSS signals for robots under a tree canopy and overcome the effect of lighting on the camera sensor. In the study, trees captured by LiDAR in the form of point clouds were grouped using the k-means algorithm, and RANSAC was used to plot the robot's navigation path in the orchard system. Pure pursuit tracking and an additional proportional-integral-derivative (PID) strategy were used to estimate the vehicle's steering angle.

There are various types of LiDAR that can be used in robotics applications in agriculture, such as 2D LiDAR. Figure 14.5 shows the RPLiDAR S2 TOF 360°, an 18 m range indoor/outdoor sensor. This is included in single-line LiDAR. Single-line LiDAR refers to a single-line laser beam produced by the laser source. In LiDAR, there are four main components: the laser, receiver, signal processing unit, and rotating mechanism. The laser-emitting mechanism lights up in pulses. After the emitted laser hits an obstacle, the reflected light converges on the receiver through the lens group. Then, the signal processing unit is responsible for controlling the emission of the laser and processing the signal received by the receiver. Based on that information, the distance from the target object is calculated. Finally, the rotating mechanism is responsible for rotating the three mentioned core components at a stable speed. It enables the surrounding objects to be scanned and generates real-time information regarding distance (d) (Fig. 14.6).

Figure 14.7 illustrates the objects read by RPLiDAR, which are presented in a point cloud (red). Each point that is read can provide information such as the angle, distance, and quality of light reflected by the object. Additionally, the location of the LiDAR position when reading obstacles is the center of the Cartesian coordinates. Information from this point cloud can then be processed to estimate the distances of objects to the LiDAR sensor. For example, LiDAR can be installed on ground vehicles to avoid collisions. A driving motor that moves forward can be instructed to stop temporarily if there is an object within a distance of 5 m. Then, if the vehicle stops for more than 5 s, it can turn to the right to move around the obstacle.

In an orchard environment where fruit trees are planted at regular intervals, the point cloud resulting from LiDAR data is illustrated in Fig. 14.8. From this image, we can estimate the position of the LiDAR, which is in the center, reading the locations of the trees surrounding it. The current position of the LiDAR is between rows

Fig. 14.5 RPLiDAR S2L 360° laser range scanner

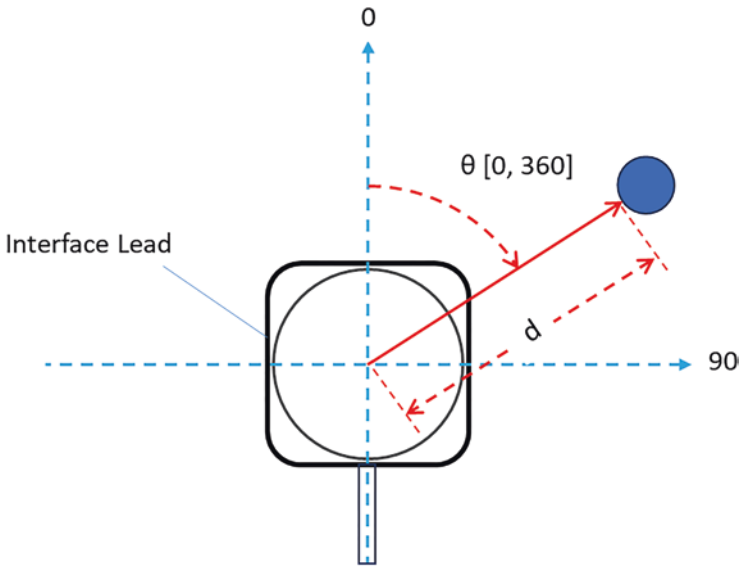

Fig. 14.6 Angle (θ) and distance (d) geometric value definitions for 360° LiDAR

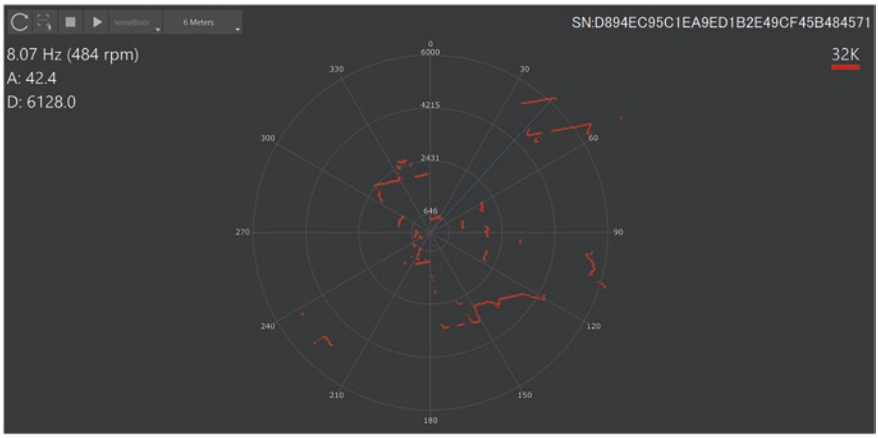

Fig. 14.7 Example of a 2D point cloud scanned by RPLiDAR S2

of trees. The distance between the rows of trees is approximately 6 m, and the distance between trees within rows is 3 m. For regular tree positions such as this, machine learning algorithms can help a robot walk between tree rows (Ailian & Ahamed, 2023). However, the weeding strategy and cutter also need significant attention to avoid injuries to the main tree trunks. In the next section, we highlight weeding operations that can be developed using a robotic platform with the main support of a depth camera and LiDAR.

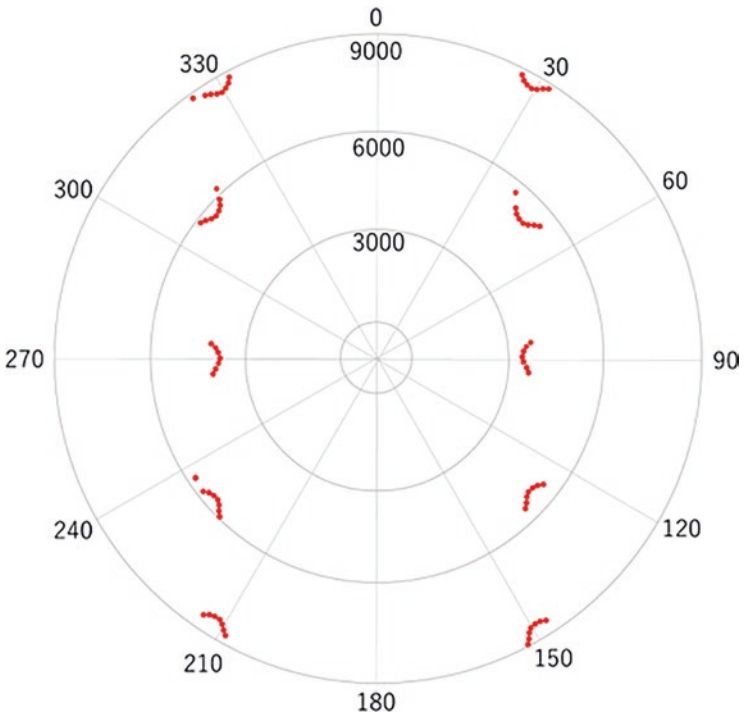

Fig. 14.8 Point clouds of trees scanned from the inter row positions

14.4 Weeding Operations Using a 3D Camera and LiDAR for Orchards

In this part, we introduce the weeding strategy for autonomous weeding in orchard operations that utilizes the potential of a 3D camera and LiDAR for orchard environmental perception as well as an adaptive weed cutter for small robots around a tree trunk. As previously described regarding the advantages of these sensors in subchapter 14.3, in the weed cutter robot, LiDAR can be used to detect the positions of trees, and then the RANSAC algorithm can determine the direction of the robot in traveling close to or between trees. The 3D camera can be used to detect the position and estimate the diameter of the tree to determine the steering angle for intrarow weeding or grass cutting around the circumference of the tree stem.

14.4.1 Current Orchard Weeding Operations Using Autonomous Robots

Effective weed control in an orchard successfully clears weeds throughout the orchard floor. In complex orchards, fruit trees are planted regularly and support the implementation of autonomous weed control robots. However, the robot's

navigation strategy during weed eradication needs to be adjusted to the architecture of the orchard. Weeds in the interrow area are easier to cut than weeds in the intrarow area using only the LiDAR sensor for navigation. LiDAR provides information on the positions of fruit trees in the interrow area, which are also considered obstacles that must be avoided. By using LiDAR, the robot can also estimate when to turn based on information about the rows of trees at the edge of the orchard. However, weeds located in the intrarow area and weeds around a tree trunk ring are quite difficult to eradicate using mechanical methods. In this case, the 3D camera is expected to be able to help improve weed control in the intrarow area.

Reiser et al. (2019) proposed a weeding system for an autonomous electrical robot that performed intrarow weeding in vineyards, called a side-shift rotary weeder. The autonomous robot used was a medium-size caterpillar robot (Reiser et al., 2017). The rotary weeder installed on the side of the robot can cut weeds between rows. Interestingly, this rotary weeder is equipped with a sonar sensor so that when there are trees nearby, an electric actuator moves the rotary weeder away from the tree row (Fig. 14.9). This system allows weeds that are close to the tree to be cleared without injuring the tree while the robots keep moving. After finishing one side row, the robot performs a U-turn to the other side of the tree row and completes one intrarow weeding operation.

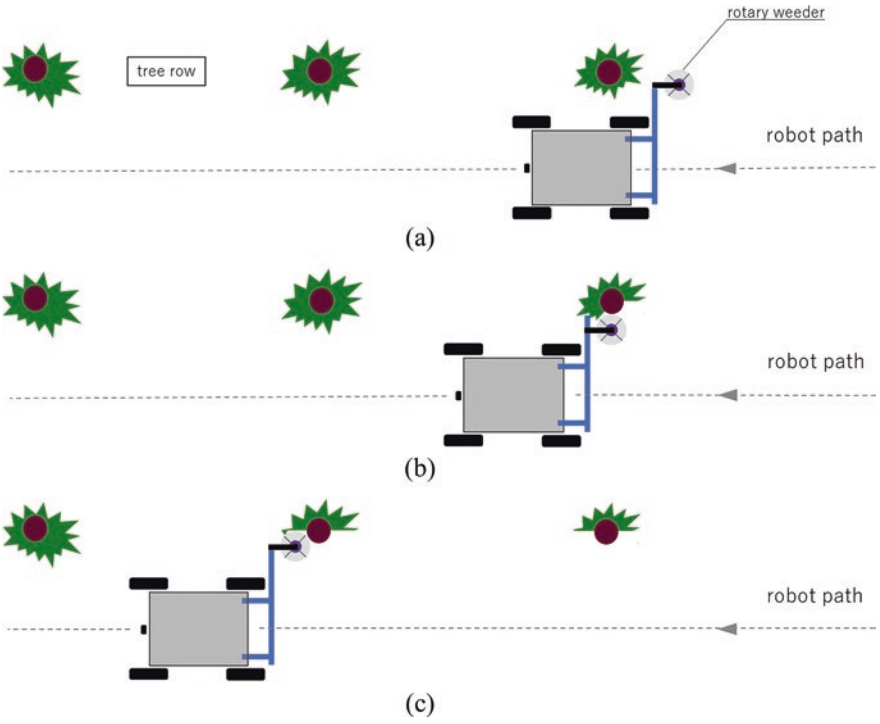

Fig. 14.9 Top view of the side-shift rotary weeder for intrarow weeding. (**a**) Rotary weeder in the initial condition; (**b**) the rotary weeder is shifted out from the tree row to cut the weeds, then (**c**) is shifted back to the tree row when passing the tree trunk

RLM can also be applied to an orchard weeding system. The RLM has better performance than conventional mowers for small orchards (Hossain & Komatsuzaki, 2021). RLMs have appropriate blades for grass cutters that chop weeds to a small size, so they easily decompose in the soil. However, intrarow navigation is very challenging. Another problem in obstacle avoidance is fallen fruit or broken tree branches, which cause RLMs to change their navigation direction. Therefore, a small robot is needed that is similar to the RLM but has navigation capabilities in both intrarow and interrow areas.

14.4.2 Weed Cutter that Moves Around Tree Trunks for Small-Robot Intrarow Weeding

Another interesting option is to develop a new cutter design utilizing a 3D printer and brushless DC motor attached to an autonomous vehicle for intrarow weeding, including weeding around tree trunks. The weed cutter can be used with a lightweight knife or nylon cord. The knife-type cutter is used to cut weeds between rows (intrarow), while the rope is used to cut grass within rows. Compared to the knife cutter (Fig. 14.10), the rope or brush cutter (Fig. 14.11) is less prone to breakage when cutting weeds around tree trunk rings. In addition, in orchards that are on hilly land, the nylon cord is strong, resisting breakage when the cutter blade hits rocks and uneven ground (Nishimura & Yamaguchi, 2023). At high RPMs, the nylon cord can cut any weeds or grass encountered.

Compared to ordinary DC motors, brushless DC motors have advantages including quieter operation, high torque and RPM, and lightweight. This lightweight allows the design of a grass cutter that can be carried by a drone.

A proposed adaptive lightweight cutting mechanism for areas near trees is given using a brushless DC motor, the MT2204 (2300 KV, 25 g, 32.2 mm in length, 27.9 mm in diameter; Fig. 14.12). This motor is generally used for small drones; however, it has the potential for low-cost and effective weed cutter research. Despite its lightweight and small size, this motor can rotate the grass cutter and cut grass by

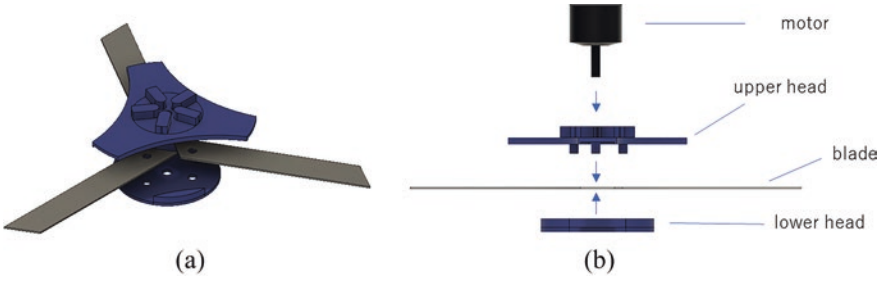

Fig. 14.10 (**a**) 3D design of a lightweight grass cutter; (**b**) assembly of the grass cutter

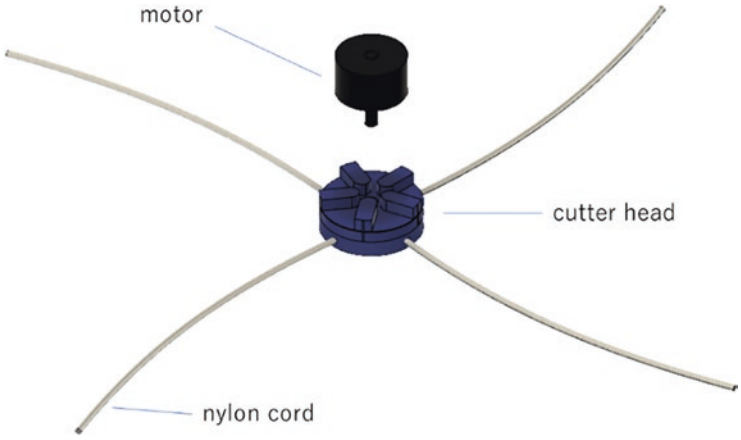

Fig. 14.11 3D design of a nylon cord grass cutter

Fig. 14.12 BLDC motor for lightweight grass cutters

first connecting with an ESC 40A, a special motor driver for brushless DC motors. The higher the voltage applied, the higher the RPMs and torque of the motor, giving it the potential for utilization in a robotic platform.

14.4.3 Path Planning and Weed Management Strategy

In weed management, path planning significantly influences the productivity of weeding operations. Figure 14.13 is an illustration of the movement of an autonomous weeder during weed control based on LiDAR as the main navigation tool. In this case, only the tree object is used for orientation. LiDAR can be employed to

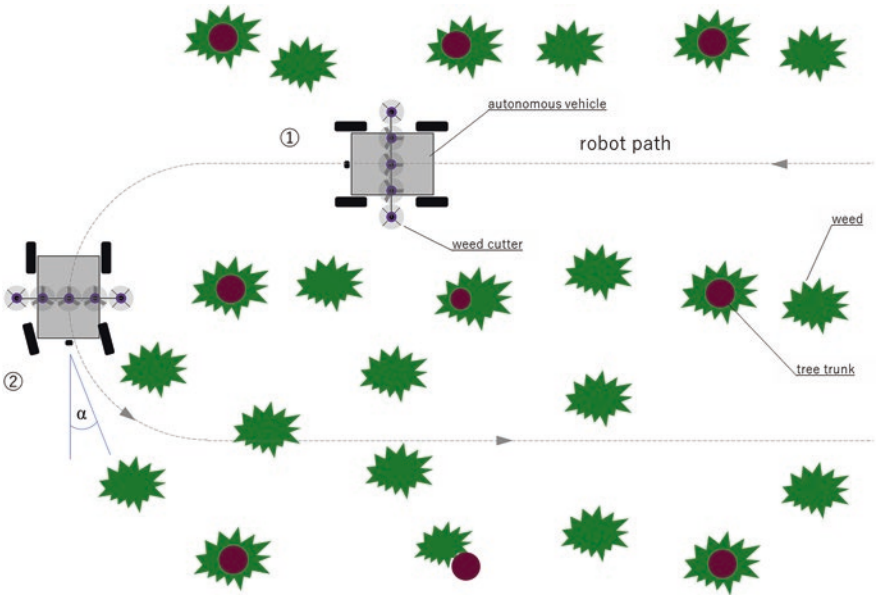

Fig. 14.13 Top view of inter row weeding based on LiDAR perception and the vehicle turn position

find surrounding objects, and the DBSCAN and K-means algorithms can group tree objects, for example, trees to the right and left of the robot. Then, after the groups of tree objects are obtained, a straight line can be proposed using RANSAC, and if there are two straight lines, then the robot will be instructed to move between the two straight lines. Moreover, a more advanced algorithm is needed for the robot to perform a U-turn to increase the robot's degree of autonomy.

LiDAR sensors are used for path planning through local map construction. Research conducted by Wang et al. (2022) also used a centerline tree detection navigation system for two rows of trees recognized by the sensor. The centerline becomes the robot's track when walking between two trees (interrow). Then, when the robot has reached the edge of a row of trees, it can turn at a certain angle (α) toward another row of trees (Fig. 14.13).

Very complex intrarow weed control can also be achieved by moving the robot in a circle around a tree. As illustrated in Fig. 14.14, a robot can be equipped with a 3D camera sensor. 3D cameras can be combined with deep learning methods such as the You Only Look Once (YOLO) algorithm for easily detection of tree objects. Depth sensors are also used to determine the distances and diameters of trees. Then, the robot can approach the tree according to the detected distance, and the steering angle can be adjusted according to the tree diameter information to move the robot to circle a trunk at a certain distance.

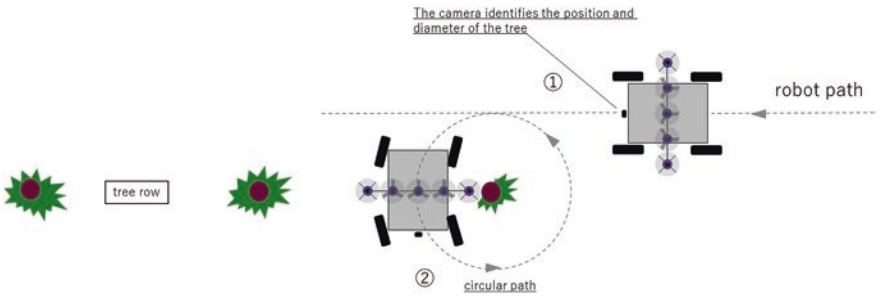

Fig. 14.14 Top view of intrarow weeding based on 3D depth camera perception

The circular path concept is also used by Lee et al. (2022) in the design of autonomous driving for fruit harvesting in orchards. When harvesting is performed, the robot moves around one tree and then moves to another tree to continue the harvesting process. The system works under two main principles: distinguishing which trees are ready for harvest, and which are not based on maps that have been made through SLAM (Simultaneous Localization and Mapping) and creating efficient routes for harvesting. We can also apply this method to address our problem in intrarow weeding operations with the support of LiDAR for obstacle avoidance, and we can combine it with a 3D camera that can locate and distinguish objects around trees. The camera can also help acquire information about tree diameters for estimating the steering angle needed to move in a circular path (Fig. 14.14).

14.5 Conclusions

The use of robotics in orchard weed control has gained importance due to labor shortages and the need for efficient operation, which is vital for maintaining yield quality. In this chapter, autonomous weeding methods are discussed, with a focus on the challenges of navigation and weed management. The development of autonomous weeding in orchards by using 3D cameras and LiDAR offers a solution for efficient weed control and navigation when GNSS signals are interrupted by tree canopies. In this regard, machine learning techniques can enhance sensor performance with the fusion of data from multiple sensors. To address weed cutting, a strategy for managing weeds and minimizing tree trunk injury in the case of round tree trunks is also described. In the integrated sensing system, LiDAR is proposed in this chapter for interrow weeding with a BLDC-type cutting mechanism with a nylon cord and a 3D camera to navigate around trees and cut weeds. Therefore, combining LiDAR and depth cameras with a deep learning approach for suitable weed cutter robotic systems can effectively manage orchard weeds, promoting better yield quality to enable precise agricultural practices.

References

Ailian, J., & Ahamed, T. (2023). Navigation of an autonomous spraying robot for orchard operations using LiDAR for tree trunk detection. *Sensors, 23*(10), 4808. https://doi.org/10.3390/s23104808

Ailian, J., Noguchi, R., & Ahamed, T. (2022). Tree trunk recognition in orchard autonomous operations under different light conditions using a thermal camera and faster R-CNN. *Sensors, 22*(5), 2065. https://doi.org/10.3390/s22052065

Bergerman, M., Maeta, S. M., Zhang, J., Freitas, G. M., Hamner, B., Singh, S., et al. (2015). Robot farmers: Autonomous orchard vehicles help tree fruit production. *IEEE Robotics and Automation Magazine, 22*, 54–63. https://doi.org/10.1109/MRA.2014.2369292

Blok, P. M., van Boheemen, K., van Evert, F. K., IJsselmuiden, J., & Kim, G. H. (2019). Robot navigation in orchards with localization based on particle filter and Kalman filter. *Computers and Electronics in Agriculture, 157*, 261–269. https://doi.org/10.1016/j.compag.2018.12.046

Brunharo, C. A. C. G., Watkins, S., & Hanson, B. D. (2020). Season-long weed control with sequential herbicide programs in California tree nut crops. *Weed Technology, 34*, 834–842. https://doi.org/10.1017/wet.2020.70

Dobbs, A., Ginn, D., Skovsen, S., Bagavathiannan, M., Mirsky, S., Reberg-Horton, C., & Leon, R. (2022). New directions in weed management and research using 3D imaging. *Weed Science, 70*(6), 641–647. https://doi.org/10.1017/wsc.2022.56

Guevara, J., Cheein, F. A. A., Gené-Mola, J., Rosell-Polo, J. R., & Gregorio, E. (2020). Analyzing and overcoming the effects of GNSS error on LiDAR based orchard parameters estimation. *Computers and Electronics in Agriculture, 170*, 105255. https://doi.org/10.1016/j.compag.2020.105255

Hossain, M. Z., & Komatsuzaki, M. (2021). Weed Management and economic analysis of a robotic lawnmower: A case study in a Japanese pear orchard. *Agriculture, 11*, 113. https://doi.org/10.3390/agriculture11020113

Inoue, K., Kaizu, Y., Igarashi, S., Furuhashi, K., & Imou, K. (2022). Autonomous navigation and obstacle avoidance in an orchard using machine vision techniques for a robotic mower. *Engineering in Agriculture, Environment and Food, 15*(4), 87–99. https://doi.org/10.37221/eaef.15.4_87

Jones, M. H., Bell, J., Dredge, D., Seabright, M., Scarfe, A., Duke, M., & MacDonald, B. (2019). Design and testing of a heavyduty platform for autonomous navigation in kiwifruit orchards. *Biosystems Engineering, 187*, 129–146. https://doi.org/10.1016/j.biosystemseng.2019.08.019

Kaizu, Y., Tsutsumi, T., & Igarashi, S. (2018). Development of an autonomous driving control system for a robot mower using a low-cost single-frequency GNSS and a low-cost IMU. *Journal of the Japanese Society of Agricultural Machinery and Food Engineers, 80*(5), 271–279. https://doi.org/10.11357/jsamfe.80.5271

Lee, H. M., Noh, D. H., Kang, H. G., Byum, S. W., & Choi, J. H. (2022). *Design of autonomous driving algorithms for fruit harvesting in orchards* (pp. 497–499). IEEE. https://ieeexplore.ieee.org/document/9829690

Li, M., Imou, K., Wakabayashi, K., & Yokoyama, S. (2009). Review of research on agricultural vehicle autonomous guidance. *International Journal of Agricultural and Biological Engineering, 2*, 1–16.

Liu, S., Wang, X., Li, S., Chen, X., & Zhang, X. (2022). Obstacle avoidance for orchard vehicle trinocular vision system based on coupling of geometric constraint and virtual force field method. *Expert Systems with Applications, 190*, 116216.

Magaki, W. (2023). Development of temporary and seasonal agricultural labor forces in Japan. *JARQ Japan Agricultural Research Quarterly, 57*(1), 9–12. https://doi.org/10.6090/jarq.57.9

Nishimura, Y., & Yamaguchi, T. (2023). Grass cutting robot for inclined surfaces in hilly and mountainous areas. *Sensors, 23*, 528. https://doi.org/10.3390/s23010528

Peruzzi, A., Martelloni, L., Frasconi, C., Fontanelli, M., Pirchio, M., & Raffaelli, M. (2017). Machines for non-chemical intra-row weed control in narrow and wide-row crops: A review. *Journal of Agricultural Engineering, 48*, 57–70.

Reiser, D., Martin-Lopez, J., Memic, E., Vazquez-Arellano, M., Brandner, S., & Griepentorg, H. (2017). 3D imaging with a sonar sensor and an automated 3-axes frame for selective spraying in controlled conditions. *Journal of Imaging, 3*(1), 9.

Reiser, D., Sehsah, E.-S., Bumann, O., Morhard, J., & Griepentrog, H. (2019). Development of an autonomous electric robot implement for intra-row weeding in vineyards. *Agriculture, 9*(1), 18. https://doi.org/10.3390/agriculture9010018

Riczu, P., Nagy, A., & Lehoczky, T. J. (2015). Precision weed detection using terrestrial laser scanning techniques. *Communications in Soil Science and Plant Analysis, 46*(S1), 309–316.

Shalal, N., Low, T., McCharty, C., & Hancock, N. (2015). Orchard mapping and Mobile robot localisation using on-board camera and laser scanner data fusion-part a' tree detection. *Computer and Electronics in Agriculture, 119*, 254–266. https://doi.org/10.1016/j.compag.2015.09.025

Simon, M., Milz, S., Amende, K., Gross, H.M. (2018) Complex-YOLO: Real-time 3D object detection on point clouds. arXiv 2018, arXiv:1803.06199v2.

Usmankhujaev, S., Baydadaev, S., & Kwon, J. W. (2023). Accurate 3D to 2D object distance estimation from the mapped point cloud data. *Sensors (Basel, Switzerland), 23*(4), 2103. https://doi.org/10.3390/s23042103

Vrochidou, E., Oustadakis, D., Kefalas, A., & Papakostas, G. A. (2022). Computer vision in self-steering tractors. *Machines, 10*, 129. https://doi.org/10.3390/machines10020129

Wang, H., & Noguchi, N. (2019). Navigation of a robot tractor using the centimeter level augmentation information via quasi-zenith satellite system. *Engineering in Agriculture, Environment and Food, 12*(4), 414–419. https://doi.org/10.1016/j.eaef.2019.06.003

Wang, S., Song, J., Qi, P., Yuan, C., Wu, H., Zhang, L., Liu, W., Liu, Y., & He, X. (2022). Design and development of orchard autonomous navigation spray system. *Frontiers in Plant Science, 13*, 960686. https://doi.org/10.3389/fpls.2022.960686

Zhang, Q., Karkee, M., & Tabb, A. (2019). The use of agricultural robots in orchard management. ArXiv, abs/1907.13114.

Zhang, S., Wang, C., Dong, W., & Fan, B. (2022). A survey on depth ambiguity of 3D human pose estimation. *Applied Sciences, 12*(20), 10591. https://doi.org/10.3390/app122010591

Zhou, J., Geng, S., Qiu, Q., Shao, Y., & Zhang, M. (2022). A deep-learning extraction method for orchard visual navigation lines. *Agriculture, 12*(10), 1650. https://doi.org/10.3390/agriculture12101650

Zhou, J. J., & Hu, C. (2015). Inter-row localization method for agricultural robot working in close planting orchard. *Transactions of the Chinese Society of Agricultural Machinery, 46*, 22–28. https://doi.org/10.6041/j.issn.1000-1298.2015.11.004

Chapter 15
Investigating the Pesticide Spraying Characteristics of Plant Protection UAV and Designing a Variable Spraying System for Improving the Spraying Uniformity

Abstract Application of pesticide has become an essential management practice in modern agriculture. However, due to the limitations in available pesticide application technologies, control of some pests has become challenging. Recently, multirotor unmanned aerial vehicle (UAV) has become a popular tool in pesticide spraying due to the ability of creating downwash airflow by the rotation speed of the rotor. In this study, the effect of downwash airflow of plant protection UAV was simulated using the computational fluid dynamics (CFD) method in ANSYS software under different spraying conditions. As the second step of the study, a variable spraying system (VSS) was developed to increase the efficiency of plant protection UAV based on pulse width modulation. According to the CFD simulations, at the position of 0.3 m and 2 m below the UAV, the velocity of downwash airflow decreased by 24.6% and 22%, respectively, from full load state to no-load state, which indicated that the intensity of the downwash airflow is reduced and can affect the penetration ability. The 100 μm droplets in position hysteresis state will decrease its velocity to 0 after transverse movement of 0.103 s and fall at a velocity of 0.307 m/s in the vertical direction, which will not significantly affect the spraying width. The newly designed VSS showed a 48% of pesticide usage reduction from conventional pesticide application, and this system also maintained the spraying uniformity throughout the total operational time.

Keywords Plant protection UAV · Spraying uniformity · Pulse width modulation

15.1 Introduction

The latest world population projections indicate that the world population will reach 9 billion people in the year 2050 (FAO, 2009). The United Nations World Food Program's live Hunger Map reported that 811 million of world population suffer from malnutrition due to the inadequate food availability in different areas of the world (UN, 2021). Current food habits of mankind have also deviated from quantity of food to the quality of food based on the recent discussions of healthy lifestyle in

© The Author(s), under exclusive license to Springer Nature Singapore Pte Ltd. 2024

T. Ahamed, *IoT and AI in Agriculture*,
https://doi.org/10.1007/978-981-97-1263-2_15

both developing and developed economies. Innovations for high-yielding crop varieties and technological developments for reducing crop losses are the two main paths for increasing the quantity and quality of crop production (Anderson et al., 2019). Pathogens, arthropods, and weeds are cumulatively responsible for crop losses. According to statistics, the total annual loss of agricultural production accounts for 45% (Abouziena & Haggag, 2016). The application of pesticides for crop protection is the most widely practiced, efficient, and convenient method compared to the conventional methods. Since the mass production of pesticides initiated in the 1940s, the use of pesticides showed a rapid increase yearly with the green revolution (Goldman, 2007). Currently, the consumption of pesticides has reached more than 2.7 million tons per year (FAO, 2020). Application of pesticide is considered as a major crop management practice in modern agriculture.

At the same time, technological improvements in pesticide application for efficient pest management have become a common topic with sustainable development discussions worldwide. Even though hand or backpack sprayers are the common technologies for spraying pesticide under small-scale applications due to the less efficiency and difficulty of application for large-scale farms, more advanced mechanisms were developed. At present, the use of mechanized spraying vehicles has become the major plant protection mechanism in large-scale crop cultivations such as orchards. However, the automation of mechanized spraying has become a requirement based on the possible health problems caused by pesticides during the spraying operation. Therefore, with the advancement of the aviation industry, Unmanned Aerial Vehicles (UAVs) were designed for performing pesticide spraying tasks in large-scale farms (Mogili & Deepak, 2018).

Yamaha developed the first UAV applied in agriculture in 1997, and as of 2014, over 2600 Yamaha UAVs are operating for agricultural purposes worldwide (Del et al., 2021). With the development of UAV technology, multirotor UAV have become the popular tool used for plant protection. High efficiency and safety of the operator are the most important features associated with plant protection UAV. Additionally, the rotation of the rotor of UAV can create downwash airflow, which makes the droplets more penetrating. However, there are several problems of plant protection UAV that have been identified related to the droplet dispersion and spraying uniformity (Wang et al., 2017, 2018). The strength of the downwash airflow can easily affect the movement of the droplets due to the small droplet size of the pesticide sprayed by the plant protection UAV (usually available for spraying with a size of 50–300 μm). Therefore, the dispersion of the pesticide inside the crop canopy area is unpredictable (Chen & Lan, 2017; Qiu et al., 2013; Zhang et al., 2012). At the same time, the dynamic changes of flight altitude of the UAV can cause uneven droplet movement and spraying, which is usually followed by the changes of the strength of the downwash airflow (Wang et al., 2018; Qin et al., 2016). Considering the abovementioned problems, analysis of the droplet dispersion and spraying uniformity is required for developing an efficient system for application of pesticide using plant protection UAV. Therefore, the objective of this study was to investigate the pesticide spraying characteristics

and design a variable spraying system for maintaining the spraying uniformity for improving the efficiency of the pesticide application by plant protection UAV.

15.2 Materials and Methods

In this research, the methodology was divided into two sections: analyzing the effect of downwash airflow of plant protection UAV using the computational fluid dynamics (CFD) simulations in ANSYS software and development of an efficient variable spraying system (VSS) for plant protection UAV based on pulse width modulation.

15.2.1 Analyzing the Effect of Downwash Airflow of Plant Protection UAV Using the Computational Fluid Dynamics (CFD)

15.2.1.1 Calculation of the Change State of Rotation Speed

Primary parameters of FLIGHTS-AG UAV were used for corresponding calculations as the reference UAV for this study (Table 15.1). The speed and altitude of the UAV were considered as constant during the spraying process for the following calculations. As the density of the liquid varies based on the type of the pesticide, density was considered as similar to that of water.

The gravity change of the UAV from the full load state to the end of spraying can be expressed as follows:

$$G = g\left(W - N\,\mathrm{Vs}\,T\right)\left(0 \le T \le \frac{10}{Vs}\right) \tag{15.1}$$

where, G is gravity of entire drone (N), W is the weight of drone (kg), Vs is spraying flow rate per nozzle (0.8 L/min for this study), T is spraying time (min), N is number of nozzle, and g is gravitational acceleration (9.81 m/s^2).

Table 15.1 Primary parameters of FLIGHTS-AG UAV

Parameter	Value	Other
Flight speed (km/h)	15	Spraying performance
Body weight (kg)	14.8	
Max payload capacity (L)	10	
Rotor diameter (inch)	30	
Number of rotors	4	
Spray flow rate (L/min)	0.8 ~ 1.6	
Number of nozzles	4	

The movements of UAV (taking off, flying, and landing) are powered by the thrust generated by rotor rotation. In practical situations, the thrust produced by rotor is dynamic, which is affected by external factors. According to the aerodynamic characteristics of propellers, rotor can be described in terms of thrust coefficient, torque coefficient, advance ratio, and rotor efficiency (Brandt & Selig, 2011), which can be defined as:

$$C_t = \frac{T}{\rho n^2 D^4} \tag{15.2}$$

where, C_t is thrust coefficient, T is thrust (N), n is revolutions per second (rev/s), D is rotor diameter (m), and ρ is density of air (kg/m^3). (According to the international standard atmosphere states, the density of air was considered as 1.225 kg/m^3 at sea level and 15 °C)

$$C_Q = \frac{Q}{\rho n^3 D^5} \tag{15.3}$$

where, C_Q is torque coefficient, Q is torque (Nm).

$$J = \frac{v}{nD} \tag{15.4}$$

where, J is advance ratio, v is velocity.

$$\eta = \frac{J}{2\pi} \cdot \frac{C_t}{C_Q} \tag{15.5}$$

where, η is rotor efficiency.

Usually, efficiency of the UAV rotor is considered as 70–80% for static thrust calculations of the rotor. Due to the interference effect of multirotor UAV, the rotor efficiency was considered as 70% in this study. The flight of UAV was considered as constant speed maintaining the same altitude. Therefore, the fluctuations of the flight altitude were neglected in hovering status. The thrust generated by the rotor was considered to be balanced by the gravity of the drone itself. The change of rotor rotation speed according to the operating time can be calculated using the corresponding data.

15.2.1.2 3D Modeling

The 3D model diagram of FLIGHTS-AG UAV was developed based on the relevant parameters using the SolidWorks software (Fig. 15.1). Downwash airflow of a UAV categorized into low-speed compressible turbulence and most of turbulence models are vulgar incompressible. However, according to previous studies, the

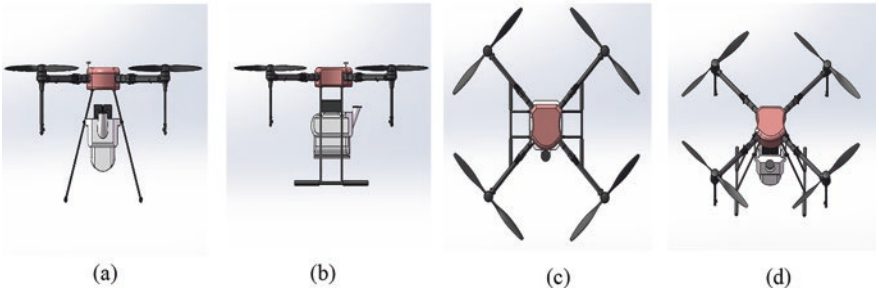

Fig. 15.1 3D model diagram of FLIGHTS-AG UAV: (**a**) front view, (**b**) side view, (**c**) top view, and (**d**) isometric view

incompressible turbulence model can be approximately replaced with the compressible turbulence model (Gao, 2015). Therefore, the flow mode of complete turbulence was set for CFD simulation of this study model. The rotation region of the rotor was designed, and appropriate computing domain and the corresponding mesh were generated. Finally, the pressure, average velocity, and overall thrust were set as the objective, and the simulations were carried out.

15.2.1.3 Downwash Airflow Simulation

The model was simulated by Computational Fluid Dynamic (CFD), and ANSYS software was used for downwash airflow simulation. From the full load state to no-load state, different rotor rotation speeds were set (62 rev/s, 55 rev/s, 47 rev/s) for simulation. It is considered that the downwash airflow of UAV causes the small size droplets to volatilize more easily, and the big size droplets easily bounce away before contacting the plant surface. Based on this assumption, the droplet size was considered as 100 μm, and the influence of natural wind was not considered.

15.2.1.4 Data Analysis

Initial pressure and high-speed downward airflow cause the deposition of droplets rapidly along the direction of airflow. However, due to the rapid motion of UAV, some droplets at the edge of downwash airflow considered to be in the position hysteresis state. These droplets can be subjected to move under horizontal and vertical forces. In the horizontal direction, the lagged droplets can be moved by inertia, and their velocity decays to 0 under the influence of air resistance (if the droplets do not evaporate). Eq. 15.6 shows the air resistance of droplets, and Eq. 15.7 shows the time of droplets velocity decay to 0 in horizontal direction. In the vertical direction, the droplets fall in the air. Assuming that the droplets are uniform spheres, the downward movement can be mainly affected by viscous forces. The terminal

velocity was considered to be stable when gravity and viscous forces are in balance according to Stokes's law (Eq. 15.8).

$$F_r = \frac{1}{2} C \rho S v_h^2 \quad (15.6)$$

$$t_h = \frac{m v_h}{F_r} \quad (15.7)$$

$$F_d = 6\pi \eta_v v_d R \quad (15.8)$$

where, F_r is the air resistance (N), S is the windward area (m^2), v_h is the velocity of droplet motion in horizontal direction (m/s), C is the resistance coefficient, t_h is the time of droplets velocity decay to 0 (s), m is mess of droplet (g), F_d is the resistance of droplets in vertical direction (N), v_d is the final speed of droplets (m/s), R is the droplets radius (m), and η_v is the air viscosity.

15.2.2 Development of an Efficient Variable Spraying System (VSS) for Plant Protection UAV Based on Pulse Width Modulation

15.2.2.1 PWM Modulation Principle

Pulse width modulation (PWM) system regulates the width of a series of pulses, equivalent to the required waveform (including shape and amplitude), and digitally encodes the analog signal level as shown in (Fig. 15.2), the PWM oscillogram at different duty cycles. The output signal is controlled by adjusting the duty cycle, and then the amplified signal is used to control the device to be operated (Jiang et al., 2016; Wen et al., 2018; Zhai et al., 2012).

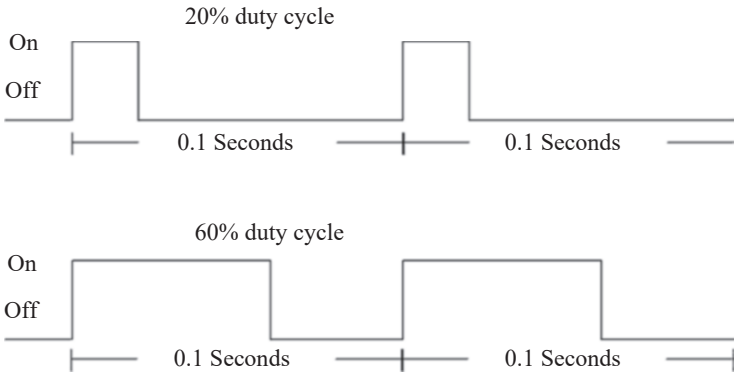

Fig. 15.2 The PWM oscillogram under different duty cycle

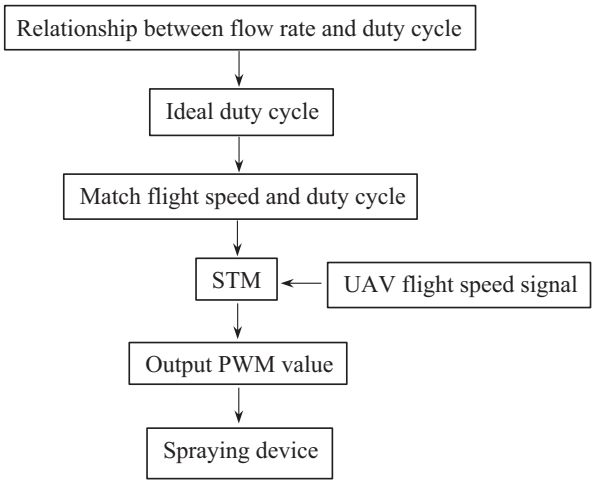

Fig. 15.3 The block diagram of the variable spraying system control

15.2.2.2 Variable Spraying System (VSS) Control Principle

Variable spraying system (VSS) is mainly combined with the PWM modulation principle, by accepting the real-time flight speed of the UAV to adjust the duty cycle value to control the switch of the solenoid valve in the spraying equipment and finally, achieve variable spraying. As shown in the block diagram of the variable system control (Fig. 15.3), the corresponding reference and the data to be executed need to be recorded in the system. Therefore, the experiment should be conducted to find out the relationship between the spraying flow. After that, the duty cycle and corresponding flight speeds should be calculated before the whole system is built. In this design, response time of data transmission needs to be reduced so that the correct instructions for subsequent spraying control can be provided more efficiently (Xu et al., 2014).

15.2.2.3 The Main Program of Variable Spraying Control System Based on PWM

The main program of the variable spraying system was designed along the following steps: starting of the system, initializing the UAV internal system, sending the UAV flight speed data to STM from the speed sensor, performing the scanning analysis under successful data collection, or continuing to wait until the finalizing of the scanning analysis. As the final step, the spray flow rate was decided by the system according to the corresponding PWM value (Fig. 15.4). The information of flight speed, spray flow rate, and output PWM value was recorded into the control chip in advance to reduce the calculation time of the chip.

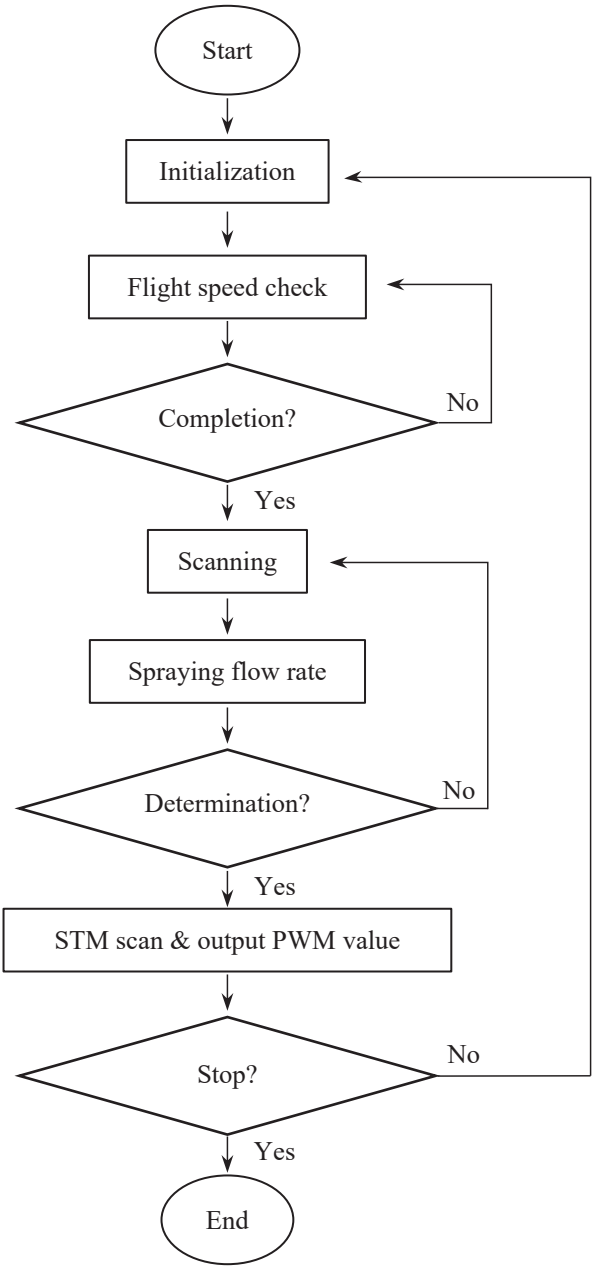

Fig. 15.4 The main program of variable spraying control system

15.2.2.4 System Composition

The VSS consisted of an STM32 control chip, relay, power supply, LCD display, diaphragm pump, pesticide tank, solenoid valve, pressure nozzle, and flow

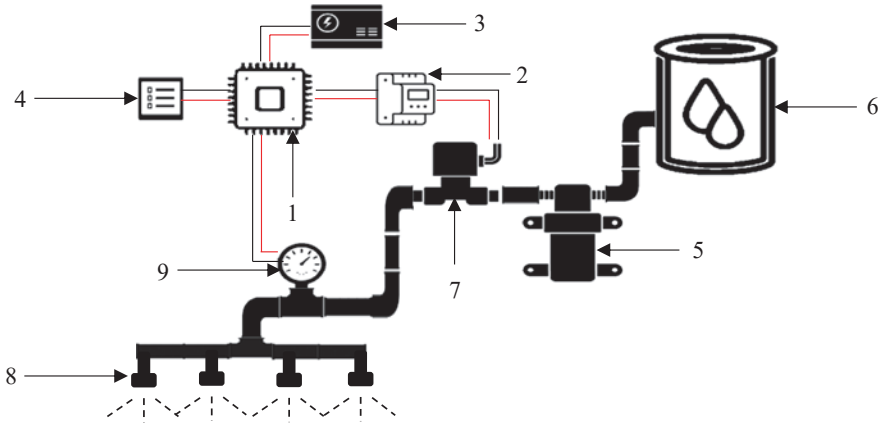

Fig. 15.5 Structure diagram of the newly designed variable spraying system (VSS). (1. STM32 control chip; 2. relay; 3. power supply; 4. LCD display; 5. diaphragm pump; 6. pesticide tank; 7. solenoid valve; 8. pressure nozzle; 9. flow sensor)

sensor (Fig. 15.5). The STM32 control chip was programmed to receive real-time flight status data, integrate the flight status data information, and then transmit the command to the spraying system. Power output by the control chip was amplified by a relay and then transmitted to the solenoid valve, which controlled the spraying flow rate of the diaphragm pump. The flow sensor was designed to monitor the output flow and send the feedback data to the STM32 control chip. An LCD display was included in the system to display all the required information.

15.2.2.5 Calculating the Relationship Between the Spray Flow Rate and Duty Cycle

A simple spraying system with diaphragm pump model Ling Ao HY-521 was set up for measuring the flow rate. The system consisted of an AC/DC converter, speed controller, diaphragm pump, water flow sensor, nozzle, Arduino Uno, and PC. The output flow rate was measured by adjusting the duty cycle value from 0 to 100%. The water flow sensor was used as a measuring tool to transmit the obtained flow value data to record the data in the PC. The experiments were repeated until obtaining reliable data values for PWM output duty cycle and the corresponding spraying flow rate (Fig. 15.6). According to the experimental results, when the duty cycle was at the range of 0–5%, the motor was in the electrified and dead state. Therefore, the corresponding spray flow rate was recorded as 0. When the duty cycle is 90–100%, the spray flow rate tends to be stable and reaches the maximum value.

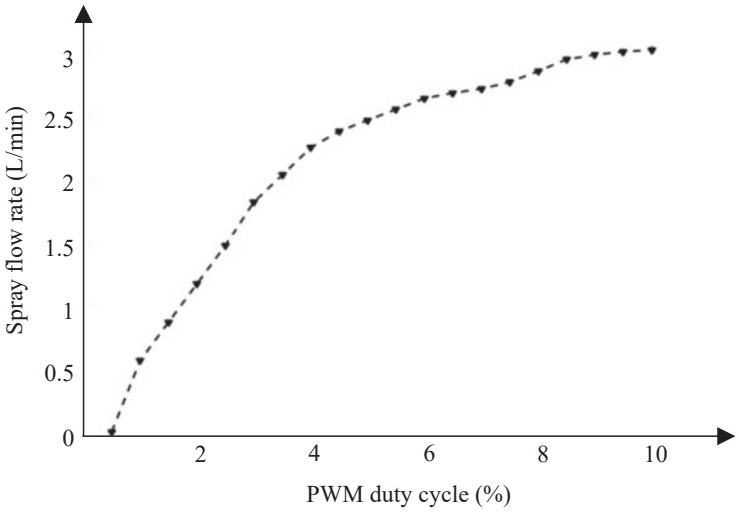

Fig. 15.6 Diagram of pulse width modulation (PWM) duty cycle and spray flow rate

15.2.2.6 Comparison of Theoretical Pesticide Consumption Between Variable Spraying System and Non-variable Spraying System

The VSS can improve the spraying uniformity, and at the same time, it also reduces the waste of pesticides. This study was conducted to compare the theoretical pesticide consumption between VSS and non-VSS. External effects from the environment were not considered in both systems in this study. Analysis of flight speed (the main factor considered in the calculations) in the spraying process was emphasized. The flight and spraying reference parameters were considered as; flight area: 28 m × 28 m, maximum spray flow rate: 3 L/min, spray width: 4 m, flight acceleration of UAV: 3 m/s^2 and stable flight speed of UAV in spraying state: 6 m/s (Fig. 15.7a).

The changes in flight state of UAV due to hovering, acceleration, uniform speed, and deceleration were considered for theoretical flow consumption of VSS (Fig. 15.7b). Change in flight status of a constant flow spraying system can lead to overspray or missed spraying during the spraying process. Unnecessary spraying during the turning movement of UAV also leads to the waste of pesticides. The flight speed variation of the UAV in the reference field was considered as initiated from a hovering state of 0 m/s with an acceleration of 3 m/s^2. The UAV was considered to fly at a constant speed after reaching the maximum flight speed of 6 m/s. Deceleration considered as −3 m/s^2 until reaching the end of the field for the turning movement. The turning movement of the UAV was considered as uniform flight with a constant speed due to the short distance. Flight speed variations during the overall flight task (except in turning movement) in the reference field were considered for the theoretical calculations (Fig. 15.8a). The required spray flow rates under different flight speeds were calculated in order to obtain uniformity in spraying considering a linear

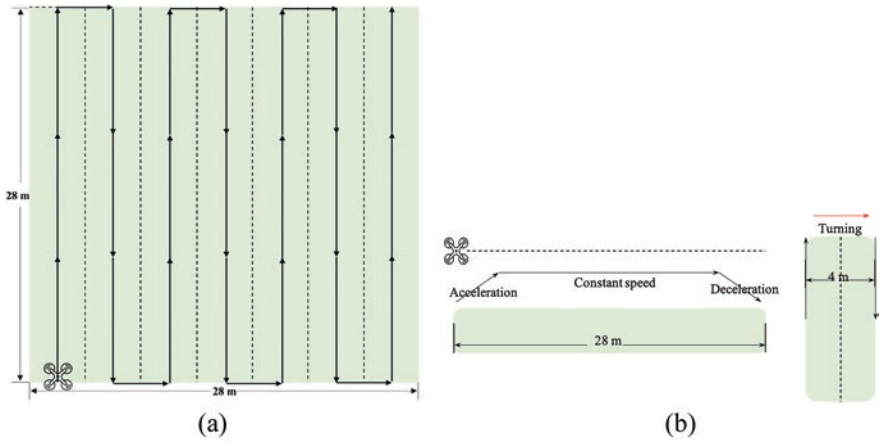

Fig. 15.7 (**a**) Sketch map of UAV flight area (**b**) schematic diagram of UAV flight status

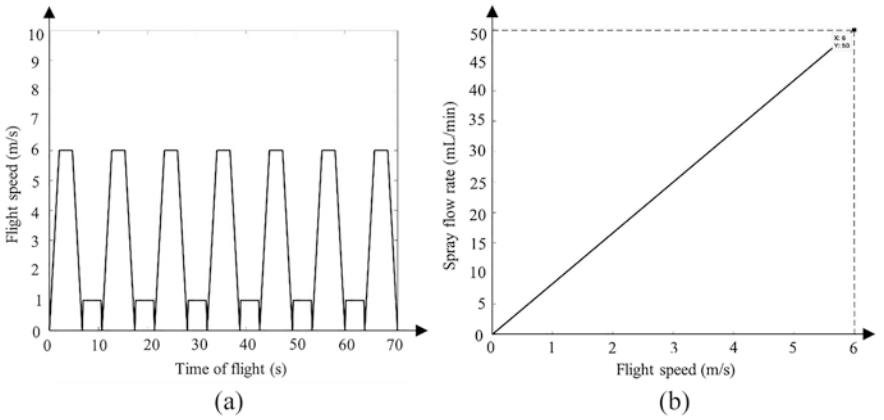

Fig. 15.8 (**a**) Speed variations for the overall flight and (**b**) ideal linear relationship between flight speed and flow rate

relationship between two parameters as given Eq. 15.2, the ideal linear diagram shown as Fig. 15.8b.

Based on the relationships obtained between time of flight-flight speed (Fig. 15.8a) and flight speed-spray flow rate (Fig. 15.8b), the theoretical flow consumptions were calculated for non-VSS and VSS.

Considering the constant spray flow rate (FR) and total operational time (t) in the non-VSS, the total amount of pesticide consumption (V_T without VSS) was calculated by the following equation.

$$V_T \text{ without } VSS\left(L\right) = FR\left(\text{L / s}\right) \times t\left(s\right) \tag{15.9}$$

The required spray flow rates under different flight speeds were calculated considering a linear relationship using the following equation.

$$\text{Spray flow rate}\left(\text{L}/\text{s}\right)=\frac{25}{3}\times\text{Flight speed}\left(\text{m}/\text{s}\right) \tag{15.10}$$

The total amount of pesticide consumption with VSS (V_T with VSS) was calculated considering the different spray flow rates obtained during four different movement patterns using the following equation (Eq. 15.11).

$$V_T \text{with} VSS = 7\left(FR_a \times t_a\right)+7\left(FR_c \times t_c\right)+7\left(FR_d \times t_d\right)+6\left(FR_t \times t_t\right) \tag{15.11}$$

Different spray flow rates were considered as spray flow rate under acceleration movement (FR_a), spray flow rate under constant speed movement (FR_c), spray flow rate under deceleration movement (FR_d), and spray flow rate under turning movement (FR_t). Flight speed differences at turning were not considered and considered as a constant speed (FR_t) as the time taken for turning movement is very short and the effect of speed variation can be negligible. Time taken for each movement pattern at one step was considered as time taken for acceleration movement (t_a), time taken for constant speed movement (t_c), time taken for deceleration movement (t_d), and time taken for turning movement (t_t).

The relationship between the variable system flow and the duty cycle of the PWM square wave signal can be obtained by fitting the actual flow and duty cycle curves with a quadratic polynomial as:

$$y=\left(0.00226\times x^4-0.0189\times x^3+0.0546\times x^2+0.01\times x+0.0481\right)\times 100\% \tag{15.12}$$

where x is the flight speed in m/s, and y is the duty cycle of the PWM square wave signal as a percentage (%).

15.3 Results and Discussion

15.3.1 Effect of Downwash Airflow of Plant Protection UAV

15.3.1.1 Change of Rotor Rotation Speed in Hover

The total time taken for continuous spraying from full load state to no-load state was resulted as 188 s. Rotor rotation speed showed a 22.7% reduction as the weight of UAV decreased as a result of maintaining the same flight speed and altitude in hover (Fig. 15.9). Reduction of rotor speed during this scenario weakened the downwash airflow intensity.

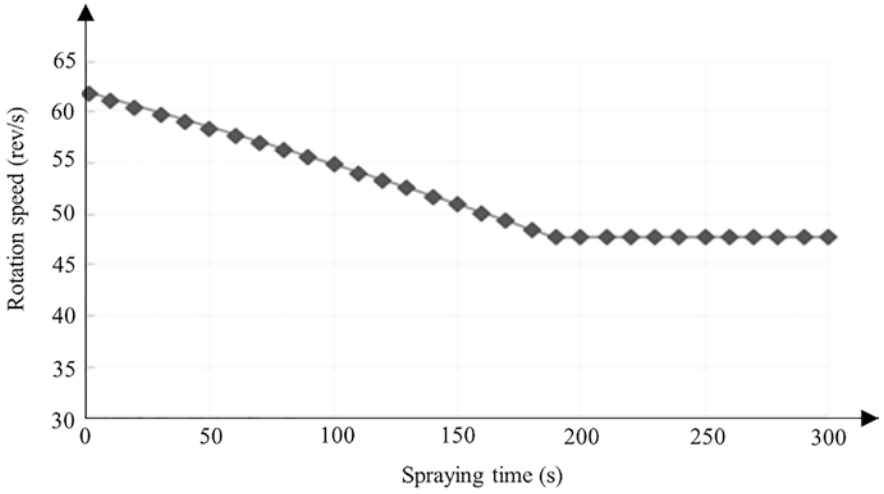

Fig. 15.9 Change of rotor rotation speed in hover

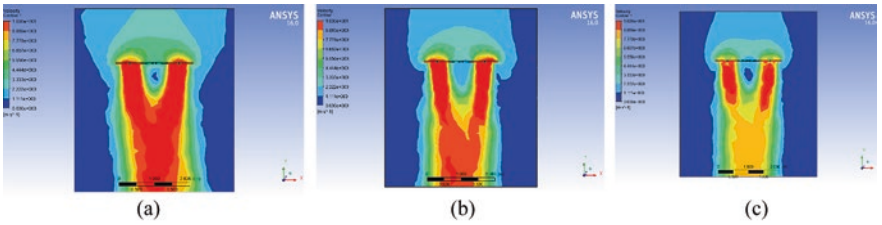

Fig. 15.10 CFD simulations in ANSYS software. (**a**) The cut plot of airflow field with rotation speed of 62 rev/s. (**b**) The cut plot of airflow field with rotation speed of 55 rev/s. (**c**) The cut plot of airflow field with rotation speed of 47 rev/s

15.3.1.2 Analysis of the Movement of Droplets

According to the CFD simulations at the rotor rotation speed of 47 rev/s under no load, there is a clear reduction of rotation speed, which affected the variation of airflow velocity at different heights of the pesticide spray by UAV (Fig. 15.10c). According to the CFD simulations, the airflow fields at different rotor speeds showed a significant change in the vertical airflow intensity at the center of the UAV (Fig. 15.10a–c).

The vertical downward movement of the droplet was mainly affected by the downwash airflow near the center of the rotor and the initial pressure given by the pressure nozzle. A 0.3 m long spray boom of UAV was used as a reference to measure the initial wind pressure on droplets. Vertical airflow velocity at the position of 0.3 m below the center of UAV was observed as reduced by nearly 24.6% from full load state to no-load state (Fig. 15.11a). The airflow velocity at position of 2 m below the UAV was considered as the effective altitude, which influenced the

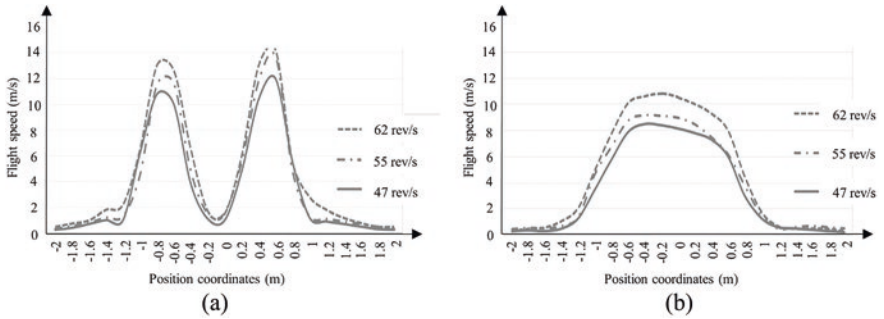

Fig. 15.11 The velocity of airflow (**a**) at position of 0.3 m below the rotor and (**b**) at position of 2 m below the rotor

penetration of pesticide droplets into the canopy. The velocity of airflow at this point resulted in a reduction of around 22% (Fig. 15.11b).

Therefore, the weakening of airflow in the vertical direction will obviously affect the downward penetration ability of droplets, and it also affects the spraying uniformity. The droplets in position hysteresis state, the movement in the horizontal direction only affected by the air resistance. In this state, the time taken for velocity decay to 0 m/s was resulted as 0.103 s. Therefore, the effect of the horizontal movement of the droplets on the spraying width was negligible. In this study, the vertical direction speed was resulted as 0.307 m/s when the gravity of droplet and resistance were balanced.

15.3.2 Variable Spraying System (VSS) for Plant Protection UAV Based on Pulse Width Modulation

15.3.2.1 The Relationship Between Flight Speed and Pulse Width Modulation (PWM) Duty Cycle

Experimental results demonstrated that when the duty cycle was 90–100%, the spray flow rate tended to be stable and reached the maximum value. The relationship between flight speed and the PWM duty cycle was derived based on the results obtained by combining the relationship between spraying flow rate and duty cycle (based on experimental results) and the flight speed and spraying flow rate (based on simulation results) (Fig. 15.12). However, at the turning movement of the UAV, flight speed showed values less than 1 m/s, which was considered as non-spraying area for this study. Therefore, the actual effective duty cycle output range was 10–90%.

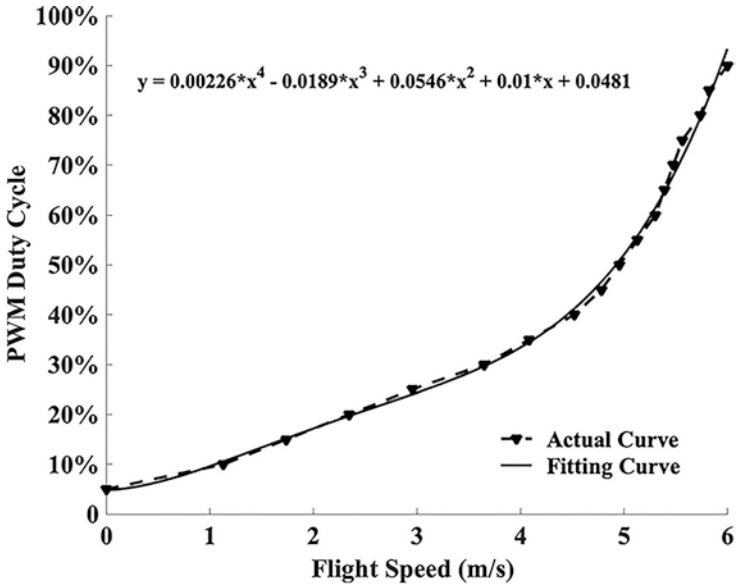

Fig. 15.12 Relationship between flight speed and PWM duty cycle

15.3.2.2 Amount of Spraying for Reference Area by Variable Spraying System and Non-variable Spraying System

In the non-VSS, the spray flow rate remained constant throughout the operational time of the UAV sprayer even though it consisted of different movement patterns. The required amount of pesticide for reference operation area in the non-VSS was resulted as 3537 mL (regardless of error loss). However, under VSS, where the different spray flow rates under different movement patterns were considered, only 1838 mL of pesticide was needed while maintaining the spraying uniformity throughout the total operational time (Fig. 15.13). According to the results, the variable spraying system can be applied to overcome problems such as uneven spraying and pesticide waste.

Additionally, the simple structure and low weight of this newly designed spraying system (VSS) made it suitable for use in a drone. At the same time, the low power consumption of the control system of VSS did not show any effect on the power consumption of the UAV. Therefore, spraying function of the UAV can be executed smoothly using the newly designed VSS for plant protection UAV.

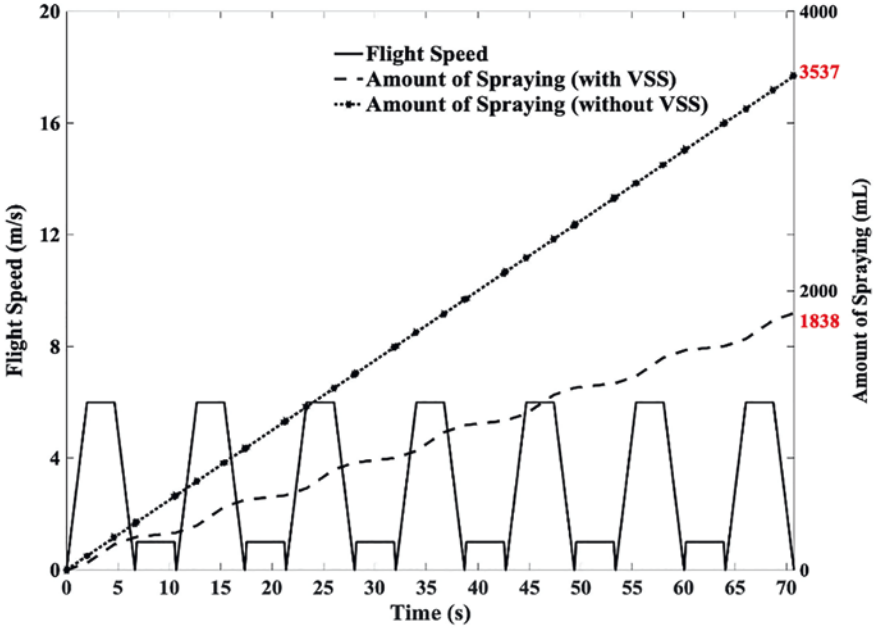

Fig. 15.13 Amount of spraying for reference area by variable spraying system and non-variable spraying system

15.4 Conclusions

This study analyzed the change in the intensity of the downwash airflow with the reduction of the UAV's weight while maintaining a constant flight altitude. A combination of experimental and data modeling methods was applied to analyze the movement of the pesticide droplets under the action of the downwash airflow through dynamic forces. In the second stage, a variable spraying system based on PWM control was designed for plant protection UAV for obtaining uniform pesticide spraying in agricultural fields.

1. The rotor rotation speed decreased by 22.7% as the weight of the UAV decreased during the spraying process, resulting in a reduction in the intensity of the downwash airflow.
2. The intensity of the downwash airflow decreased by 22% at 2 m below the UAV (at the crop canopy level), which directly led to the reduction of the penetration ability of the droplets and thus affected the deposition of the droplets.
3. The newly designed VSS is simple in structure and has the possibility to cooperate with UAV. At the same time, it also resulted in a reduction in pesticide consumption by approximately 48% compared to the non-VSS.
4. By taking the change of flight speed as the signal source of the variable system, it can effectively control the amount of spraying under different flight speeds to improve the uniformity of pesticide spraying using plant protection UAV.

In summary, the plant protection UAV applications still need to be improved considering downwash air flow effect on spraying uniformity. Newly designed variable spraying system can be applied for plant protection UAV in order to achieve precision agriculture considering effectiveness of spraying operation, economic performance, and environmental impacts.

References

Abouziena, H. F., & Haggag, W. M. (2016). Weed control in clean agriculture: A Review1. *Planta Daninha, 34*(2), 377. https://doi.org/10.1590/S0100-83582016340200019

Anderson, J. A., Ellsworth, P. C., Faria, J. C., Head, G. P., Owen, M. D. K., Pilcher, C. D., Shelton, A. M., & Michael, M. (2019). Genetically engineered crops: Importance of diversified integrated pest management for agricultural sustainability. *Frontiers in Bioengineering and Biotechnology, 7*, 24.

Brandt, J., & Selig, M. (2011). *Propeller performance data at low Reynolds numbers. 49th AIAA Aerospace Sciences Meeting including the New Horizons Forum and Aerospace Exposition, 04 January 2011–07 January 2011, Orlando, Florida*. AIAA. https://doi.org/10.2514/6.2011-1255

Chen, S. E., & Lan, Y. (2017). Effects of spraying parameters of small plant protection UAV on droplets deposition distribution in citrus canopy. *Journal of South China Agricultural University, 38*(5), 97–102.

Del, C. J., Cruz, U. C., Barrientos, A., & De León, R. J. (2021). Unmanned aerial vehicles in agriculture: A survey. *Agronomy, 11*, 203. https://doi.org/10.3390/agronomy11020203

FAO. (2009). *Proceedings of the expert meeting on how to feed the world in 2050*. FAO Headquarters.

FAO. (2020). *Pesticide use, pesticides trade and pesticides indicators, FAO stat analytical brief*. https://www.fao.org/faostat/en/#data/

Gao, C. (2015). *Autonomous soaring and surveillance in wind fields with an unmanned aerial vehicle*. University of Toronto, Canada.

Goldman, L. R. (2007). Managing pesticide chronic health risks: U.S. policies. *Journal of Agromedicine, 12*(1), 67–75. https://doi.org/10.1300/J096v12n02_08. PMID 18032337. S2CID 216149465.

Jiang, H., Zhang, L., & Shi, W. (2016). Effects of operating parameters for dynamic PWM variable spray system on spray distribution uniformity. *IFAC-Papers Online, 49*(16), 216–220.

Mogili, U. M. R., & Deepak, B. B. L. (2018). Review on application of drone systems in precision agriculture. *Procedia Computer Science, 133*, 502–509. https://doi.org/10.1016/j.procs.2018.07.063. ISSN 1877-0509.

Qin, W. C., Qiu, B. J., Xue, X. Y., et al. (2016). Droplet deposition and control effect of insecticides sprayed with an unmanned aerial vehicle against plant hoppers. *Crop Protection, 85*, 79–88.

Qiu, B. J., Wang, L. W., Cai, D. L., et al. (2013). Effect of flight altitude and speed of unmanned helicopter on spray deposition uniform. *Transactions of the CSAE, 29*(24), 25–32.

UN. (2021). *Department of Economic and Social Affairs*. Sustainable Development Goal 2, Zero Hunger. https://sustainabledevelopment.un.org/sdg2

Wang, C. L., He, X. K., Wang, X. N., Wang, Z. C., Wang, S. L., Li, L. L., et al. (2018). Testing method and distribution characteristics of spatial pesticide spraying deposition quality balance for unmanned aerial vehicle. *International Journal of Agricultural and Biological Engineering, 11*(2), 18–26.

Wang, D. S., Zhang, J. X., Li, W., Xiong, B., & Zhang, S. L. (2017). Design and test of the dynamic variable spraying system of plant protection UAV. *Transactions of the Chinese Society of Agricultural Machinery, 48*, 86–93.

Wang, X. N., He, X. K., Song, J. L., Wang, Z. C., Wang, C. L., Wang, S. L., et al. (2018). Drift potential of UAV with adjuvants in aerial applications. *International Journal of Agricultural and Biological Engineering, 11*(5), 54–58.

Wen, S., Zhang, Q., Deng, J., et al. (2018). Design and experiment of a variable spray system for unmanned aerial vehicles based on PID and PWM control. *Applied Sciences, 8*(12), 2482.

Xu, X., Xu, S., Liu, Y. X., et al. (2014). Variable pesticide spraying system design based on small UAV. *Guangdong Agricultural Sciences, 9*, 207–210.

Zhai, C. Y., Wang, X., Liu, D. Y., et al. (2012). *Nozzle flow model of high-pressure variable-rate spraying based on PWM technology* (Vol. 422, pp. 208–217). Advanced Materials Research.

Zhang, J., He, X. K., Song, J. L., et al. (2012). Influence of spraying parameters of unmanned aircraft on droplets deposition. *Transactions of the Chinese Society for Agricultural Machinery, 43*(12), 94–96.

Chapter 16
Strategic Short Note: Myanmar Climate-Smart Agriculture

Abstract Agriculture is playing a crucial role in the country's food security and serving as the primary source of income for its people in Myanmar. Myanmar's vast agroecological range allows for the cultivation of many diverse crop species. However, the country is suffering from the negative impacts of climate change, such as inconsistent and scarce rainfall, heat stress, droughts, floods, seawater intrusion, land degradation, deforestation, and other natural calamities. In the face of climate change, ensuring the nation's food supply will necessitate a steady and substantial increase in agricultural output. Efforts to adapt to and mitigate climate change in the agricultural sector must be undertaken with food and nutrition security. The adoption of climate-resilient agricultural practices that can endure climatic shifts and aid in reducing greenhouse gas emissions will necessitate the introduction of new technologies, alterations to existing ones, and amendments to pertinent laws and policies.

Keywords Climate smart agriculture · Adaptation · Mitigation · Food security

16.1 Introduction

Climate-smart agriculture (CSA) is a strategic approach to sustainable agricultural development that addresses the dual challenges of ensuring food security and mitigating climate change. Myanmar is a country with diverse agroecological conditions and a large population that depends on agriculture for their livelihoods and nutrition. However, Myanmar is notably vulnerable to the impacts of climate change due to its geographical location and reliance on agriculture. Myanmar is prone to various natural hazards, including extreme temperatures, drought, cyclones, flooding and storm surge, and heavy rainfall events (World bank group, 2021). Drought is considered the most severe natural hazard in the country. These challenges pose serious threats to the food security, agricultural productivity, and rural livelihoods in the country. CSA primarily aims to attain sustainable agricultural development, promoting food security and nutrition by implementing agriculture approaches resilient

© The Author(s), under exclusive license to Springer Nature Singapore Pte Ltd. 2024

T. Ahamed, *IoT and AI in Agriculture*,
https://doi.org/10.1007/978-981-97-1263-2_16

to climate change and low in emissions. CSA encompasses the development of technical, policy, and investment conditions to support the adoption of innovative farming practices, technologies, and policies that can enhance the adaptation and mitigation capacities of the agricultural sector in Myanmar (Hom et al., 2015; Htwe et al., 2019).

16.2 Role of Agricultural Sector in Myanmar

The agricultural sector plays a vital role in Myanmar's economy and society. Agriculture sector contributes to about 23.7% of the country's GDP, accounts for 35.1% of total export earnings in 2020–2021 (MOALI, 2021). The sector is also the main source of livelihood and income for the majority of the population in Myanmar. Agriculture sector faces challenges on climate change such as increasing incidence of droughts and floods, erratic weather patterns threaten productivity and food security. Moreover, lack of proper irrigation, storage facilities, and access to markets hinder development. Limited adoption of modern technologies and practices also hinders adaptation to changing conditions and improving yields. The economic landscape in Myanmar heavily relies on the agricultural sector, given its key role in ensuring national food security and serving as a primary livelihood source for the populace. The sector also has great potential to contribute to the country's economic growth, poverty reduction, and environmental sustainability, if the challenges and opportunities are effectively addressed.

16.3 Climate Change Adaptation Option for Agriculture Sector

Climate change has emerged as a paramount concern on the Myanmar government's agenda. The adverse impacts of climate change in agriculture sector of Myanmar are caused by high temperature, erratic rainfall, droughts, salinity, and floods. The action plans are to produce climate-resilient varieties such as tolerant to drought, heat, salinity, and flood; crop diversification such as integrated farming system; conservation agriculture practices like minimum tillage, mulching, and cover cropping to improve soil health, water retention; integrated pest management. Moreover, efficient utilization of irrigation water such as utilization of drip irrigation, sprinklers, and precision agriculture techniques to conserve water and increase water use efficiency are practicing in some area of Myanmar. Rainwater harvesting is also practicing in the central dry zone area of Myanmar. Furthermore, capacity building program for farmers on climate-smart techniques is also done by the extension staff in collaboration with NGOs.

16.4 Climate Change Mitigation Option for Agriculture Sector

Myanmar's agriculture sector is vulnerable to climate change, which can lead to crop failures, food insecurity, and economic losses. For the mitigation option in the context of climate change, the practices that can reduce greenhouse gas emissions are start practicing in the country. These practices include nutrient management; use of alternate wetting and drying techniques in rice production; soil carbon sequestration practices like conservation agriculture, cover cropping, and biochar application to enhance soil carbon storage. Sustainable land management practices such as conservation agriculture and integrated pest management are also performing in the country for long-term climate resilience and mitigation. Moreover, investing in research and development on innovative mitigation technologies and practices adapted to Myanmar's context is essential. Adopting climate-smart agricultural practices are also important to reduce GHG emissions.

16.5 Policy Related to Climate Change from MOALI

The Ministry of Agriculture, Livestock, and Irrigation (MOALI) has established polices, objectives and strategies to advance the agriculture sector, with a particular emphasis on prioritizing food security and reducing rate of rural poverty (MOALI, 2019). Myanmar Agriculture Development Strategy and Investment plan (2018–2023), Myanmar Climate Change Policy (2019), and Climate Change Strategy and Action Plan (2016–2030) are several examples of the policies related to climate change formulated collaboratively by MOALI and MOREC. The Myanmar Climate Change Policy (2019) aims to sustain the growth and productivity of food systems through low-carbon, climate-resilient, and gender-responsive actions. It also encourages to adopt innovative approaches and the use of advance technologies for practicing resource-efficient and low-carbon methods in agriculture. The Climate Change Strategy and Action Plan (2016–2030) focuses on enhancing climate-resilient productivity and implementing climate-smart responses in the agriculture sector. The plan includes measures to adapt to the impacts of climate change and mitigate greenhouse gas emissions, and also outlines specific actions and targets for the agriculture sector to address the challenges posed by climate change.

16.5.1 Collaboration with Others

To reduce impact of climate change, Myanmar needs to collaborate with others institution to get technology and information related to climate change. Collaboration with agribusinesses can enhance technology access, market opportunities, and value

addition for farmers. Community engagement is also important to empower the framer's groups and local communities to access climate-smart agriculture technologies and sharing knowledge. Facilitating partnerships and collaboration between government agencies, research institutions, private sector actors, and farmers are important to ensure a coordinated and inclusive approach to CSA implementation.

16.6 Summary

Myanmar, being rich in natural resources and biodiversity, has the capacity to foster climate resilience in agriculture. Despite the significant challenges it faces, Myanmar possesses remarkable prospects and potential that can be harnessed to achieve climate resilience and food security. The government needs to support the prioritization on investments in capacity building, research and development on CSA technologies, and ensuring sustainable support. By actively supporting these priorities, the government can enable Myanmar to harness its potential and become a leader in climate-smart agriculture, achieving food security, climate resilience, and regional green leadership.

References

Hom, N. H., Htwe, N. M., Hein, Y., Than, S. M., Kywe, M., & Htut, T. (2015). *Myanmar climate-smart agriculture strategy*. CGIAR Research Program on Climate Change, Agriculture and Food Security (CCAFS), International Rice Research Institute (IRRI).

Htwe, N. M., The, N. E. M., Naing, N. N. Z., & Hein, Y. (2019). Documenting the application of the Myanmar climate-smart agriculture strategy. In *CCAFS working paper* (Vol. No. 292). CGIAR Research Program on Climate Change, Agriculture and Food Security (CCAFS).

MOALI. (2019). *Myanmar agriculture in brief*. Ministry of Agriculture, Livestock and Irrigation.

MOALI. (2021). *Myanmar agriculture in brief*. Ministry of Agriculture, Livestock and Irrigation.

World Bank Group. (2021). *Climate Change Knowledge Portal* (worldbank.org). https://climateknowledgeportal.worldbank.org/country/myanmar/vulnerability

Chapter 17
Strategic Short Note: Enhancing Postharvest Operations Through Centralized Data Processing and Analysis

Abstract Post-harvest operations play a major role in the agricultural industry through different expertise from multiple disciplines. Postharvest industries are scattered over the country or the region depending on many factors to increase the efficiency of production and profitability. The main drawback is the expertise and knowledge to address the different issues in postharvest operations. Bringing the data from different post-harvest operations to a central location could make decision-making easier and more reliable for the industry as well. The recent development in Artificial Intelligence (AI) and the Internet of Things (IoT) can bring data into a central location in real-time by dint of cloud-based systems. The expert can use this data to understand the trends of post-harvest operations while improving the operation in real-time guiding the process operations.

Keywords Post-harvest operations · Production · Profitability · Central location · Artificial Intelligence (AI) · Internet of Things (IoT) cloud-based systems

17.1 Introduction

The science of postharvest technology has become increasingly complex, requiring expertise in various aspects to carry out operations efficiently. Postharvest operations play a critical role in maintaining the quality and shelf life of agricultural products. However, the complexity of postharvest science and the need for expertise in multiple areas pose challenges for companies in effectively managing their operations. Therefore, as Fig. 17.1 illustrates, it is advantageous to establish a central service provider for serving companies for their expert scientific services using the recent developments of information technology. Cloud computing provides a great opportunity in this context and the recent developments of Artificial Intelligence

© The Author(s), under exclusive license to Springer Nature Singapore Pte Ltd. 2024

T. Ahamed, *IoT and AI in Agriculture*,
https://doi.org/10.1007/978-981-97-1263-2_17

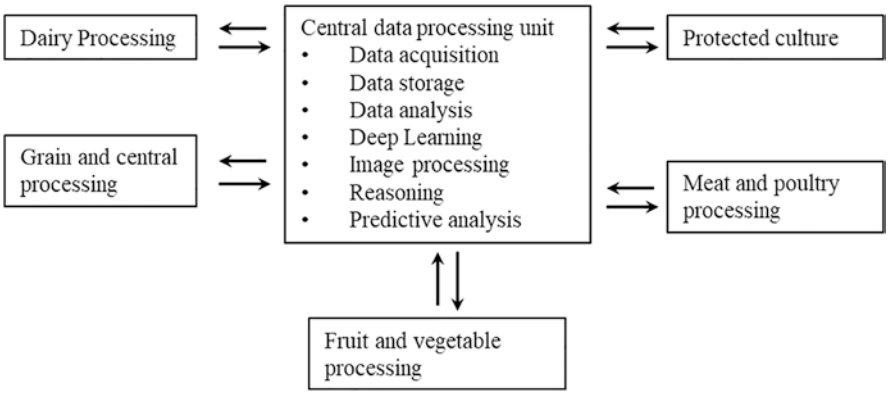

Fig. 17.1 Schematic diagram of the central service provider

(AI), and Data Science will help in taking appropriate decisions without much involvement of humans.

Evolving symbiosis between Artificial Intelligence (AI) and the Internet of Things (IoT) can be used to collect real-time data from postharvest facilities, to monitor various physical and chemical parameters such as temperature, humidity, air quality, pressure, different gas concentrations, light intensity, sound levels, images of objects and this data can be used to identify potential issues before they become significant problems. Innovation and growth of the field of postharvest operations would be one of the dominant features of the convergence of AI and IoT in this Fourth Industrial Revolution (4IR) if used efficiently. This requires rigorous research and strategic foresight in minimizing the unique challenges inevitably those would encounter.

The data collected from IoT devices installed in processing facilities of different companies should be stored in a centralized location where it is aggregated, analyzed, and processed and the expert services will be provided. The data will be used for fault finding, error correction, and predictive analysis. Data science techniques can be used to analyze data to identify patterns and trends and can be used to predict potential issues before they occur, enabling companies to take proactive measures to prevent losses and improve postharvest operations. Data science can also be used to optimize postharvest operations, reducing waste, and improving efficiency. For example, data analytics can be used to identify the optimal transportation routes and storage conditions for perishable products, reducing losses and improving product quality. Advanced algorithms can extract meaningful insights that help optimize postharvest processes for different crops and commodities. In addition to optimizing current postharvest practices, the centralized data processing unit (CDPU)'s rich dataset also offers a unique opportunity for research and development. Further the centralized data storage enables benchmarking of postharvest operations across companies. This facilitates performance evaluation and identification of areas for

improvements. Companies can benefit from shared knowledge and experiences through the centralized data storage system. Lessons learned from one company's postharvest challenges can be applied to the others, leading to collective improvements.

Future of the CDPU concept will be determined by the competitive expert services that the institute would provide acquiring the latest technologies available, not only the information technologies but also the subject matter specialties. AI is a tool that should be used with carefully supervised manner in getting reliable services to the processing industry.

Chapter 18
Optimization of Soil-Based Irrigation Scheduling Through the Integration of Machine Learning, Remote Sensing, and Soil Moisture Sensor Technology

Abstract This review book chapter delves into the transformative landscape of soil-based irrigation scheduling, with a focus on integrating cutting-edge technologies. The chapter begins by elucidating active and passive remote sensing techniques, emphasizing their role in estimating soil moisture levels. It further explores the benefits of soil moisture sensors in irrigation management, including improved water-use efficiency, water conservation, and data-driven decision-making. Subsequently, the narrative shifts to machine learning (ML) in irrigation scheduling, delineating fundamental ML concepts, and their applications in optimizing water usage and crop yield. The abstract highlights how ML supports real-time decision-making, risk mitigation, precision irrigation, and optimization under uncertainty. The discussion section engages in a comprehensive exploration of the implications, challenges, and opportunities associated with these technologies. In particular, it underscores the potential benefits and the challenges involved in utilizing soil moisture sensors, remote sensing data, and ML techniques in synergy. The section emphasizes the importance of data quality assurance, interdisciplinary collaboration, continuous learning, and technology investment in practical irrigation recommendations. The chapter concludes by underscoring the transformative potential of integrated irrigation management systems, offering a greener and more productive future for agriculture.

Keywords Artificial intelligence · Irrigation scheduling · Soil moisture content · Remote sensing · Sensors

18.1 Introduction

In light of population growth, climate change, and shifts in dietary habits toward water-intensive products due to increased incomes, experts predict that agricultural production will need to expand by approximately 70% by the year 2050 (Tilman & Clark, 2015). Among the existing challenges, the impact of climate change leads to more frequent and intense droughts (Ragab & Prudhomme, 2002), requiring serious

© The Author(s), under exclusive license to Springer Nature Singapore Pte Ltd. 2024

T. Ahamed, *IoT and AI in Agriculture*,
https://doi.org/10.1007/978-981-97-1263-2_18

attention for ensuring sustainable agriculture, over the coming years. Sustaining agriculture is mainly achieved through employing irrigation (Jägermeyr et al., 2015a, b), which is the largest global freshwater consumer (Döll & Siebert, 2002). However, the planetary threshold for freshwater withdrawal is rapidly nearing its limit or in some parts of the world, it has already been surpassed. Additionally, it is also expected that 25–40% of the water currently allocated to irrigated agriculture will be redirected to higher-productivity sectors (World Bank, 2022). Consequently, the imperative to seek and adapt water-efficient irrigation approaches becomes essential. To this end, proper irrigation scheduling is crucial which not only saves water but also increases crop production. There are three types of irrigation scheduling that are commonly practiced, known as soil-based, climate-based, and plant-based. From these approaches, soil-based has been widely used due to its accuracy and easy implementation (Henggeler et al., 2011). However, the measurement of soil moisture in the plant root zone has become a challenge. This challenge can be addressed by employing soil moisture sensors, remote sensing, and machine learning techniques, which provide valuable insights into crop root zone soil moisture.

Soil moisture is a critical component of the Earth's water cycle and plays a vital role in various environmental processes, including plant water availability, nutrient transport, and ecosystem health (Tuller et al., 2004). Accurate estimation of soil moisture content, particularly in the plant root zone, is essential for effective irrigation management (Cheng et al., 2020; Gago et al., 2015), optimizing crop productivity, and mitigating water stress. Traditional methods for measuring soil moisture, such as soil moisture sensors, tensiometers, and pressure plates, are limited in spatial coverage, labor-intensive, and time-consuming (Hedley & Yule, 2009a, b; Migliaccio et al., 2010; Thompson et al., 2007). However, recent advancements in soil moisture sensors and remote sensing technologies have provided new opportunities for nondestructive and continuous monitoring of soil moisture content, enabling more efficient estimation of soil moisture including both soil moisture content and soil matric potential. Of these techniques, soil moisture sensors provide direct measurements of soil moisture content at specific locations and depths. These sensors, such as time domain reflectometry (TDR), capacitance-based sensors, and neutron probes, offer high temporal resolution and can capture fine-scale spatial variations in soil moisture (Robinson et al., 2008). They provide valuable in situ data for calibration and validation of remote sensing-based soil moisture estimation techniques, improving the accuracy and reliability of soil moisture content estimates. Nevertheless, soil moisture sensors provide point-source measurements, and usually require considerable financial resources (Blasch et al., 2022; Cahn & Johnson, 2017), which make them challenging for growers to use. This problem can be addressed through employing remote sensing techniques.

Remote sensing, through its ability to capture data over large spatial extents, offers a valuable tool for indirect estimation of soil moisture. Remote sensing platforms, including satellites, aircraft, and drones, equipped with optical, thermal, and microwave sensors, can capture various surface properties related to soil moisture dynamics (Pereira et al., 2015; Pôças et al., 2020). By utilizing empirical, semi-empirical, and physically based models, remote sensing data can be processed to

retrieve soil moisture information. These models exploit the interactions between electromagnetic radiation and the soil-vegetation system, providing estimates of soil moisture content at different depths and resolutions (Jackson et al., 2010). However, in seasons and regions where there is frequent cloud or daily monitoring is required, this technique may not be feasible to accurately predict the soil moisture in the plant root zone. In such scenarios, machine learning techniques can help as it learns from the past days' soil moisture trend and predicts future soil moisture change or depletion level.

Machine learning algorithms have demonstrated their effectiveness in handling complex and large-scale datasets, making them promising tools for estimating soil moisture using remote sensing and soil moisture sensor data. These algorithms can learn patterns and relationships from input data and generate predictive models that estimate soil moisture based on various environmental and soil moisture-related parameters (Ge et al., 2018). Supervised learning algorithms, including Random Forest, Support Vector Machines, and Artificial Neural Networks, have been widely employed to develop predictive models by leveraging historical data and associated soil moisture measurements (Rani et al., 2022). Recently, the use of machine learning algorithms based on remote sensing and soil moisture sensor data which offer significant opportunities for estimating soil moisture in the plant root zone is being recommended. These approaches provide a nondestructive and continuous monitoring solution, allowing for better water resource management, improved agricultural practices, and enhanced ecosystem sustainability (Maia et al., 2022). By harnessing the power of machine learning, we can advance our understanding of soil moisture dynamics and improve decision-making processes in water and agricultural management.

Therefore, the objective of this review chapter is to provide a comprehensive overview of the current state-of-the-art techniques and methodologies used for estimating soil moisture and soil matric potential in the plant root zone using machine learning approaches, with a focus on remote sensing and soil moisture sensor data. We will explore the integration of remote sensing and soil moisture sensor data, the application of different machine learning algorithms, and the performance evaluation techniques employed in soil moisture estimation. Additionally, we will discuss the challenges, limitations, and future directions in this field, aiming to provide insights and guidance for researchers and practitioners interested in employing machine learning for soil moisture estimation.

18.2 Soil Moisture and Irrigation Management

18.2.1 Significance of Soil Moisture in Agriculture

Soil moisture, the water content present in the soil matrix, is a fundamental determinant of agricultural productivity and sustainability. Its significance arises from its direct influence on plant health, growth, and overall crop yield. As a primary source

of water for plants, soil moisture acts as a conduit for nutrient uptake, facilitating the transport of essential elements required for various physiological processes. Adequate soil moisture levels are pivotal for sustaining metabolic reactions, photosynthesis, and transpiration, which collectively contribute to the vitality and vigor of crops. The intricate relationship between soil moisture and plant performance is exemplified by its impact on stomatal conductance. Stomata, the microscopic pores on the surface of leaves, regulate water vapor exchange and carbon dioxide uptake. Optimal soil moisture levels maintain turgidity within plant cells, ensuring efficient stomatal function. In situations of inadequate soil moisture, stomata close to conserving water, resulting in reduced photosynthetic rates or even metabolic processes, and decreased crop growth. Ors et al., 2021 found that water stress conditions can permanently damage plant growth by disrupting root and stem development and by reducing the width and number of leaves. Moreover, presence of limited moisture in the root zone, plants undergo a chemical environmental change in their roots, which impacts the rate of photosynthesis (He et al., 2021). Conversely, excess soil moisture can lead to anaerobic conditions and root suffocation, impairing nutrient absorption, affecting the active oxygen metabolism of plants, photosynthetic proportion, developmental stages of plants, and crop production (Elkelish et al., 2020).

Furthermore, soil moisture extends its influence on soil structure and microbial activity. Proper moisture content supports favorable soil structure, enabling root penetration and nutrient diffusion. In addition, soil moisture influences microbial communities that contribute to nutrient cycling and organic matter decomposition. Water availability affects microbial diversity and activity, impacting nutrient availability and overall soil health. Precise knowledge about the state of soil moisture and its dynamic is crucial for agricultural water management to not only avoid plant water stress but also to sustainably manage water and reduce environmental footprint, which is a pressing issue in water scares regions of the world (Tuller et al., 2019).

18.2.2 Soil Moisture as a Base for Irrigation Decision-Making

Irrigation decisions are usually carried out based on monitoring soil moisture content in the plant root zone, plant water status, and the amount of water lost by evapotranspiration. This chapter focuses on irrigation based on soil moisture which is perhaps the most widely used approach (Hedley & Yule, 2009a, b). For detailed information about each of the methods refer to (Gu et al., 2020; Jones, 2004; Seyar & Ahamed, 2023). Soil moisture is crucial when it comes to irrigation decision since it represents the proportion of moisture present in the plant root zone. Understanding the temporal and spatial variability of soil moisture is essential for optimizing irrigation practices. Failure to account for soil moisture fluctuations can result in inefficient water application, leading to either water wastage or inadequate crop hydration. Soil moisture can be measured using methods like gravimetric, sensor, and remote sensing techniques.

Advancements in technology, particularly the integration of soil moisture sensors and data-driven approaches, offer the means to enhance irrigation decision-making. Soil moisture sensors provide real-time measurements, enabling the quantification of moisture levels at different soil depths and locations within a field. This spatial granularity empowers farmers to tailor irrigation schedules to match the specific needs of different crop zones. Data-driven models further amplify the potential for optimizing irrigation. Machine learning algorithms can assimilate soil moisture data alongside meteorological and crop-specific information to generate predictive models. These models can forecast soil moisture dynamics, enabling proactive adjustments to irrigation schedules. The integration of historical data and machine learning techniques empowers the identification of patterns and correlations, allowing for precise irrigation strategies aligned with plant growth stages. Incorporating soil moisture sensors and data-driven models into irrigation management represents a paradigm shift from reactive to proactive decision-making. The ability to monitor, analyze, and predict soil moisture variations facilitates the implementation of irrigation strategies that conserve water, enhance crop productivity, and mitigate the ecological footprint of agriculture. As soil moisture's intricate role in plant health becomes increasingly evident, harnessing technology to inform irrigation practices emerges as a transformative approach to sustainable agricultural water management.

18.3 Remote Sensing in Irrigation Scheduling

18.3.1 Remote Sensing Technologies

Remote sensing technologies have emerged as powerful tools for enhancing irrigation scheduling by providing comprehensive and nearly real-time insights into the spatial and temporal dynamics of agricultural landscapes. These technologies encompass a range of methods and platforms that capture electromagnetic radiation emitted or reflected by Earth's surface. From satellites orbiting the planet to drones soaring above fields, remote sensing technologies enable the acquisition of critical data that can inform irrigation decisions.

Satellites equipped with multispectral and hyperspectral sensors offer a macroscopic view of land surfaces, providing information on land cover, vegetation health, and soil moisture distribution over large geographic areas. High-resolution satellite imagery, such as that from Sentinel-2, Sentinel-1, and Landsat satellites including landsat7, landsat8, and landsat9, enables the monitoring of crop growth patterns, stress indicators, and soil moisture fluctuations. These data aid in identifying areas requiring targeted irrigation intervention.

Aerial photography, facilitated by UAVs (Aerial Photography and Unmanned Aerial Vehicles) or drones, offers a flexible and detailed perspective on agricultural fields. UAVs equipped with specialized cameras can capture high-resolution images and multispectral data, enabling precise assessments of crop health and water stress.

These platforms allow for frequent and on-demand monitoring, making them valuable tools for detecting irrigation needs and optimizing water distribution. Remote monitoring is usually performed to observe crop physiology (Duchemin et al., 2006), water stress, and crop water requirements (Er-Raki et al., 2010; Gontia & Tiwari, 2008; Simonneaux et al., 2009).

In the case of predicting evapotranspiration through remote sensing technology, direct measurement of crop evapotranspiration is not possible. However, two common methods have been employed to calculate the cropland evapotranspiration. These methods include (a) crop coefficient and reference evapotranspiration in which the crop coefficient is inferred from crop reflectance measurement, and (b) surface temperatures and remotely sensed reflectance coupled with ground-based metrological data to calculate crop evapotranspiration (ET_c) from the surface energy balance equation (Neale et al., 2003). Moreover, to predict soil moisture using remote sensing technologies, various authors have developed several techniques based on land surface temperature (LST) and soil reflectance (El-Zeiny & Effat, 2017; Haas, 2010; Wang et al., 2008). Normalized Difference Vegetation Index (NDVI), LST, and/or the linear relationship of LST/NDVI with SMC have also been used to estimate surface soil moisture content (SMC) (Petropoulos et al., 2009).

18.3.2 Remote Sensing Applications in Irrigation

Remote sensing technologies have been widely used to predict surface soil moisture. The application may increase due to the low cost and accessibility of real-time and high-quality image data. This is crucial, particularly in regions where limited data are available. Remote sensing predicts soil moisture from the reflectance of surface soil and land surface temperature. Application of remote sensing is not an exception of challenges; since these technologies including passive microwave remote sensing produce large-scale images in order of tens of kilometers, which are difficult to be implement at a finer scale. However, recent research proposed the use of downscaling algorithms as a solution to this problem (Merlin et al., 2015; Peng et al., 2017; Sabaghy et al., 2018). The downscaling algorithms can be broadly categorized into three main groups: (a) using data from satellite observation, for instance, some of the proposed methods have downscaled coarse resolution passive microwave SM retrievals which rely on use of higher resolution radar observations (Fang et al., 2019; Zhan et al., 2017), (b) using other related land surface information including vegetation and soil properties (Mishra et al., 2018; Tagesson et al., 2018), and (c) model-based or statistical-based like land surface model (LSM) that uses originated geophysical variables at high spatial resolution (Sánchez-Ruiz et al., 2014; Zhao et al., 2018).

Additionally, prediction can be challenging whenever there is water, snow, vegetation, and other surface material that expose various characteristics including light absorption quantity and reflectance and significant topographical changes exist in the area (Lakhankar et al., 2009a, b; Sandells et al., 2008). On the other hand, in

areas where there is no or low soil cover with flat features, the estimation of soil moisture is easy while accurate results can also be achieved. The main reason behind the fact that the topography and land cover as the major challenges that cause problems with soil moisture estimation, refers to the electromagnetic radiation in the case of passive remote sensing while in active remote sensing reflected microwave radiation from the soil surface to the sensor represents the soil properties of the specific area. In such condition where land is covered, the reflection may not accurately represent the true value due to the land cover (Du et al., 2000) or roughness of the land surface which may also lead to overestimation or underestimation of the value (Dubois et al., 1995). Additionally, the depth of soil moisture is another key challenge for remote sensing technologies. Nonetheless, these technologies have been successful in retrieving soil moisture data to a depth of 5 cm in bare soil or soil with low vegetation (Chauhan et al., 2003; Dunne et al., 2007; Jackson et al., 1996). However, accurately estimating soil moisture in the majority of the plant's active root zone, which extends beyond 5 cm, poses a challenge for remote sensing.

To this end, researchers have used several clustering techniques including ISODATA, *k*-mean, and Gaussian Mixture based on different data sources, to delineate the heterogeneity of soil profile by categorizing into different areas that share homogeneous properties (Galambošová et al., 2014; Martinez-Casasnovas et al., 2012; Schepers et al., 2004). Yield maps, topography, remote sensing data, soil apparent electrical conductivity are the most widely used to delineate plant root zone (Bellvert et al., 2012; Liu et al., 2018; Ohana-levi et al., 2019; Scudiero et al., 2018). Recently employing remote sensing has increased due to the accessibility to low-cost remote sensing data to obtain biophysical parameters of vegetations (Fontanet et al., 2018). Below is given the general illustration of retrieving soil moisture using remote sensing techniques (Fig. 18.1).

18.3.2.1 Active Remote Sensing Techniques

Soil properties including soil moisture estimation via active remote sensing rely on electromagnetic microwave radiation with wavelengths ranging from 0.5 to 100 cm. The utilization of synthetic aperture radar (SAR) sensors has been widespread in predicting soil moisture levels because they produce high-quality images by capturing spatial variations in surface soil moisture. To carry out this retrieval process, both sensor and soil parameters are considered (Baghdadi et al., 2008). The sensor parameter factor is characterized by the variation in signal backscatter, which depends on factors such as wavelength, incidence angle, and polarization. Meanwhile, the soil-parameter factor encompasses aspects such as the soil surface, signal attenuation through vegetation cover (Batlivala & Ulaby, 1997), and the backscatter of radiation from vegetation volume. It is important to note that as surface soil moisture content decreases, the radar backscatter value becomes stronger.

The term "backscatter signal (σo)" refers to the radiation reflected from an object's surface area and measured per unit area in radar cross section. SAR has the potential to penetrate the subsoil layer (Prost, 2001) and provides high-resolution

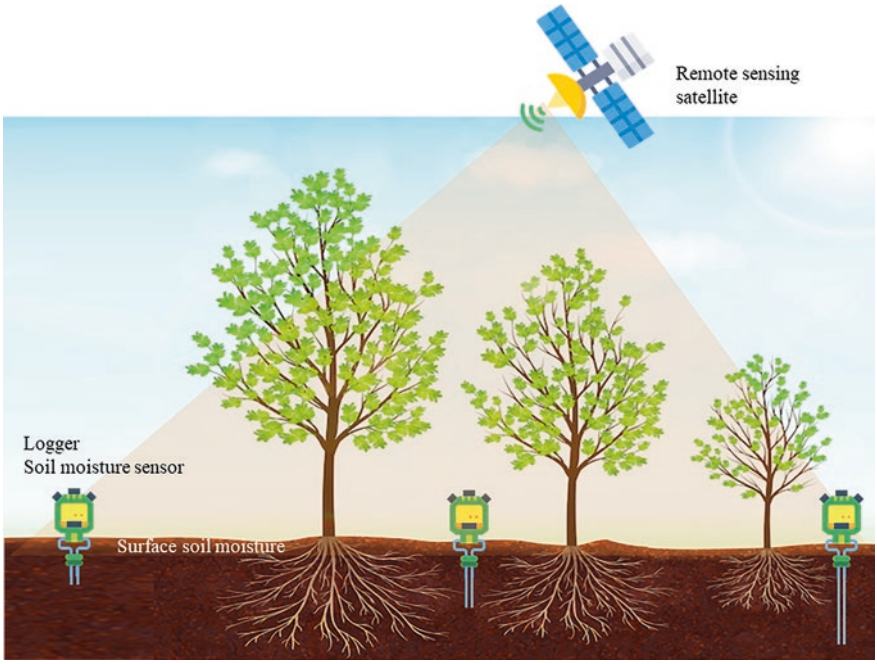

Fig. 18.1 Illustration of retrieving soil moisture through remote sensing

images, typically at scales of tens of meters. However, SAR is less affected by weather conditions but more sensitive to factors like soil topography and vegetation due to its low revisit frequency (Wang & Qu, 2009). Various methods, including backscattering models, statistical analysis techniques, and neural networks, make use of active remote sensing data. However, discussing all these methods in detail is beyond the scope of this chapter. For more comprehensive information, please refer to (Ahmed et al., 2011).

18.3.2.2 Passive Remote Sensing Techniques

Passive remote sensing has been widely employed as an effective method for depicting the global distribution of soil moisture (Walker & Houser, 2001). This approach possesses the capability to independently retrieve soil moisture levels, even when vegetation is present (Jackson & Schmugge, 1991). Additionally, it furnishes valuable information regarding land characteristics, encompassing soil surface temperature and NDVI. Unlike active remote sensing, passive remote sensing covers a relatively large surface area but typically offers a lower spatial resolution, usually spanning tens of kilometers. Thermal infrared remote sensing, operating within the electromagnetic wavelength range of 3–14 μm, is instrumental in predicting various land properties. The inception of passive remote sensing in soil estimation dates to its proposal by Walker et al., 1997. Subsequently, its applications expanded, making

use of the interplay between land parameters, vegetation indices, and surface radiation temperature measurements (Choudhury et al., 1995; Owen et al., 1998).

Various approaches exist within passive remote sensing for estimating soil moisture, including brightness models, the universal triangular relationship method, statistical analysis techniques, and the application of neural networks. However, in this chapter, we won't delve into the specifics of each approach. Detailed information about each of these methods can be found in the work of Ahmed et al. (2011).

18.3.2.3 Combination of Passive and Active Remote Sensing Techniques

The integration of passive and active remote sensing techniques offers a complementary approach to soil moisture estimation. Passive sensors excel at providing information on surface properties and can penetrate through vegetation to some extent. Active sensors, on the other hand, offer depth-specific information about soil moisture but may be affected by surface conditions. By combining these techniques, researchers can harness the strengths of both to improve the accuracy and spatial resolution of soil moisture maps. Additionally, advancement in spacecrafts with multisensor capability facilitated the integration of both remote sensing techniques in a single system including ALOS-PALSAR and Soil Moisture Active and Passive (SMAP). For the first time, the integrated approach is implemented by O'Neil (1996). The result was promising compared to individual remote sensing method application. Combined applications of passive and active remote sensing including SAR and radiometer have shown to reduce soil moisture prediction error to ±30% (Ulbay et al., 1983). Microwave combined algorithms, statistical analysis technique, and neural networks approaches are the most common methods that use integration of active and passive remote sensing techniques (Ahmed et al., 2011).

18.4 Soil Moisture Sensing in Irrigation Scheduling

Advancements in soil moisture sensing have ushered in a new era of precision agriculture, providing farmers with unprecedented insights into the moisture dynamics of their fields. These innovations have the potential to revolutionize irrigation management by enabling data-driven decisions that optimize water usage, enhance crop yield, and promote sustainable resource stewardship.

18.4.1 Types of Soil Moisture Sensors

Modern agriculture benefits from a diverse array of soil moisture sensors, each designed to capture moisture content with varying levels of accuracy, depth penetration, and spatial coverage. These sensors can be broadly categorized into two main groups; soil water content or volumetric, and soil water tension sensors

(Peters et al., 2013). The soil water content sensor measures the proportion of water present in a plant root zone while the soil tension sensor represents the amount of water that is available to the plant. In other words, volumetric soil moisture sensors estimate soil moisture by determining the volume of water within a known soil volume and soil tension sensors measure the tension among the soil particles that let the water be consumed by plants. Employing each of them associated with specific limitations and advantages. However, volumetric sensors offer more precise information on the total amount of water present in the plant root zone and the amount of water that needs to be applied to refill the plant root zone soil moisture to the predefined threshold. Volumetric water content is measured as a percentage of water per volume (%) or inches of water per foot of root zone soil depth (inch/ft). Soil tension, on the other hand, is how hard a dry soil is pulling or sucking on soil water and is measured using vacuum or pressure units including pounds per square inch (psi) but is often given in centibar (cbar). The Time Domain Reflectometry (TDR) sensor, Neutron probes, and capacitive soil moisture sensors are the most widely sensors of this group. They offer high accuracy, wide measurement ranges, and minimal sensitivity to soil salinity. Capacitance-based sensors, are versatile and provide real-time data, enabling dynamic irrigation adjustments. These sensors have been employed in different studies (Seyar et al., 2023). Tensiometers and granular matrix sensors fall under the category of soil water tension sensors.

18.4.2 Installation and Calibration of Sensors

The effectiveness of soil moisture sensors hinges on proper installation and accurate data collection. Sensor placement and calibration are critical to obtaining reliable measurements that reflect actual soil moisture conditions. The sensor should be placed in the area where the majority of the plant's active roots exist, and it should represent the moisture percentage of the plant root zone. The distance from the plant root should be carefully considered if it is placed too close to the roots, it may damage the plant's growth while placing too far away is not going to represent the moisture of the plant root zone. Moreover, sensor depth is another crucial factor that needs to be considered while installing the sensors. This is extremely important whenever there is a field with variable soils that the water holding capacity of soil may vary with depth; the top layer may run out of water first or vice versa. In such scenarios, the placement of the sensor is of crucial importance to avoid water stress and maximize production. Installing sensors at representative soil depths is essential to capture meaningful data. Normally, sensors should be positioned near plant root zones to ensure alignment with crop water requirements. The sensor which is placed nearer to the surface of the soil will represent when to carry out the irrigation procedure while the sensor which is deployed in the deeper part of the soil will show when to stop the irrigation. Additionally, factors such as soil type, texture, and topography should be considered when

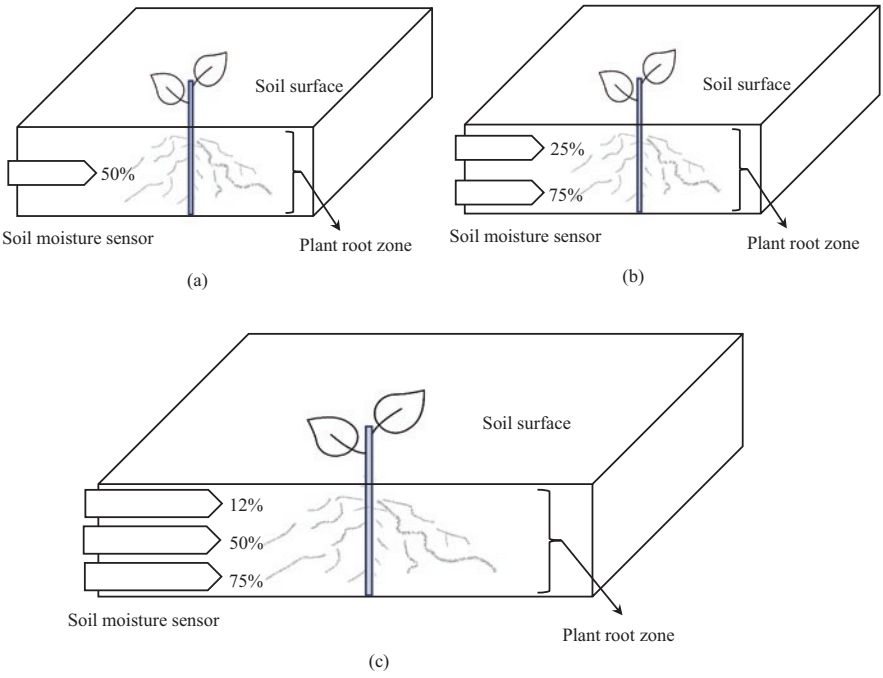

Fig. 18.2 Different scenarios of soil moisture sensor placement in the field (**a**–**c**)

determining sensor placement. Another important factor is the number of sensors that should be employed, which highly depend on the availability and type of sensors, and several soil properties such as soil texture, structure, presence of organic matter, and salinity level. In Fig. 18.2, different scenarios of soil moisture sensor placement are presented. However, before installing, the sensor calibration procedure should be performed to increase the sensor reading accuracy and turn it into meaningful data.

Calibration ensures that sensor readings accurately correspond to actual soil moisture levels. This process involves comparing sensor measurements to ground-truth data obtained through gravimetric sampling or other reference methods including other high-accuracy sensors. From the correlation between the two methods, a linear regression will be created that can be used in programming or traditional calculation during the interpretation of sensor data. Calibrating sensors at different moisture levels and soil conditions enhances accuracy across varying environmental conditions. It is usually recommended to provide several soil samples with different moisture percentages from dry to saturated proportions. However, in cases where the measurements including field capacity are determined by the same sensor, calibration is not required. This is because we need to find out the soil moisture deficit—the maximum amount of water that can be applied without wasting water to deep percolation past the bottom of the root zone, which can be calculated from the field capacity of soil and current sensor readings, we just compare the same sensor

reading with itself. On the other hand, in cases where the field capacity—which is the amount of water that is held by the soil after 12–48 (sandy to clay soil) hours of drainage or downward pulling, is determined by gravimetric or other sensor, calibration is usually recommended to increase the accuracy of soil moisture sensor reading. Soil moisture sensors generate continuous data streams, offering real-time insights into soil moisture dynamics. Sensor data can be collected manually or transmitted wirelessly to data loggers, which record and store the measurements. Advanced systems enable remote data access through mobile applications or cloud-based platforms, enhancing convenience and accessibility for farmers (Seyar & Ahamed, 2023).

18.4.3 Benefits of Soil Moisture Sensor

Advancements in soil moisture sensing technology yield a multitude of benefits and innovations that transform irrigation management and agricultural practices. Soil moisture sensors facilitate precise irrigation by providing accurate, localized measurements. This precision minimizes water wastage, prevents over-irrigation, and ensures that crops receive optimal moisture levels. A study by Gupta et al. (2022) highlights the significant water savings achieved through sensor-based precision irrigation, leading to improved water use efficiency and reduced environmental impact. Additionally, the integration of soil moisture sensors with data analytics and automation systems enables real-time decision-making. Automated irrigation systems can adjust water application based on sensor data, weather forecasts, and crop water demand, optimizing irrigation schedules without human intervention. This automation conserves labor, reduces operational costs, and maximizes resource utilization.

Finally, soil moisture sensors contribute to the implementation of variable rate irrigation (VRI), a technique that adjusts water application rates based on spatial variability within fields. VRI systems use sensor data to modulate irrigation equipment, delivering water precisely where and when it is needed. This approach mitigates under- and over-irrigation issues, promoting uniform crop growth and minimizing yield disparities.

Soil moisture sensor data, when combined with other agricultural data sources, provide holistic insights into crop health, yield potential, and irrigation efficiency. Integrating sensor data with geographic information systems (GIS) and remote sensing data enhances the characterization of soil moisture trends and variability. This comprehensive understanding supports informed decision-making and fosters sustainable farming practices. Ongoing research and development have led to innovations in sensor technology. Wireless sensor networks, Internet of Things (IoT) integration, and miniaturization have expanded sensor capabilities and ease of use. Sensors can now monitor multiple soil parameters beyond moisture, such as temperature, salinity, and nutrient levels, enabling comprehensive soil health assessments.

18.5 Machine Learning in Irrigation Scheduling

Machine learning (ML), a subset of artificial intelligence, has emerged as a transformative force in various industries, including agriculture. By leveraging data-driven algorithms and computational models, ML has the potential to revolutionize irrigation scheduling, optimize water usage, and maximize crop yield. This section delves into the application of machine learning in irrigation scheduling, elucidating its fundamental concepts, data utilization strategies, and its role in enhancing irrigation decisions.

18.5.1 Introduction to Machine Learning

Machine learning encompasses a broad array of algorithms and methodologies that empower computers to acquire knowledge from data and enhance their performance over time. In simpler terms, machine learning constitutes the study of computer algorithms designed to facilitate the automatic improvement of computer programs through accumulated experience (Mitchell, 1997). The field of machine learning (ML) encompasses a diverse range of algorithms, all aimed at addressing real-world challenges in a heuristic manner. Prior to applying specific ML algorithms, users must gather data and conduct rigorous quality checks and enhancements. These algorithms are then employed on training data, which serves as the foundation for constructing a representative model. Subsequently, the model's performance and accuracy are assessed using testing data. If the model fails to meet acceptable standards, adjustments may include selecting alternative algorithms, acquiring more data, or enhancing data quality. Once the model demonstrates satisfactory performance, it can be deployed for its intended task.

In the context of irrigation scheduling, ML algorithms process historical and real-time data to detect patterns, correlations, and trends that inform optimal irrigation strategies (Fig. 18.3). The iterative nature of machine learning permits algorithms to adapt and enhance their predictions with new information. Machine learning encompasses three primary categories of algorithms: supervised learning, unsupervised learning, and reinforcement learning.

Supervised learning, a prominent ML approach, revolves around training models using labeled data with known outputs, enabling them to make predictions or classifications. Model training continues until satisfactory performance levels are achieved. This type of learning is commonly employed for tasks such as classification and regression. Within the domain of irrigation scheduling, regression algorithms, a subset of supervised learning, hold particular relevance. These algorithms predict continuous outcomes, such as soil moisture levels, based on input variables like weather data, crop type, and soil characteristics. Decision trees, support vector machines (SVMs), linear regression, logistic regression, Naïve Bayes, neural networks, and random forest (RF) are the prevalent regression algorithms employed in irrigation ML models (Rani et al., 2022).

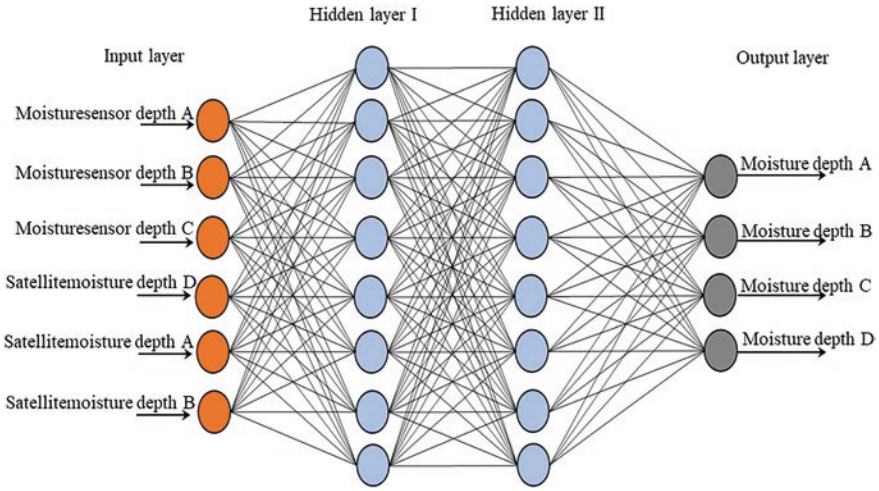

Fig. 18.3 Illustration of predicting soil moisture through machine learning

Unsupervised learning, on the other hand, involves algorithms learning from unlabeled data and drawing inferences without external guidance. This category of learning is utilized to uncover hidden patterns, group similar data, perform exploratory data analysis, and reduce dimensionality. It primarily focuses on tasks such as clustering and association. Common categories of unsupervised learning include K-means, Apriori algorithm, hierarchical clustering, expectation-maximization algorithm, and principal component analysis (Rani et al., 2022).

Reinforcement learning, the third category, features algorithms navigating through uncertain environments by acting. Feedback in the form of rewards or penalties guides the algorithm to maximize its performance. In this type of learning, predefined data are not provided; rather, the algorithm generates data through interactions with its environment, and decisions are made sequentially. Prominent algorithms in this group encompass Q-learning, deep deterministic policy gradient (DDPG), and state-action-reward-state-action (SARSA). On occasion, reinforcement learning is employed in conjunction with deep learning techniques (Rani et al., 2022).

18.5.2 Benefits of Machine Learning

Machine learning (ML) augments irrigation decisions through dynamic and data-driven strategies that adapt to changing environmental conditions. The predictive nature of ML models empowers farmers to anticipate soil moisture trends and optimize irrigation schedules, thereby reducing water wastage and promoting efficient water utilization. The application of machine learning can enhance irrigation decisions in various ways. Machine learning can support real-time decisions. ML models equipped with real-time data integration facilitate timely irrigation decisions. By assimilating current weather forecasts, soil moisture measurements, and crop water

demand, the model generates recommendations for optimal irrigation timing and volume. The study by Lee et al. (2019) exemplifies this concept by employing ML to forecast soil moisture levels, aiding in adaptive irrigation scheduling that aligns with changing environmental conditions.

Moreover, it can help in risk mitigation. Machine learning algorithms aid in mitigating risks associated with improper irrigation practices. By considering historical data and predicting soil moisture variations, models can identify potential water stress conditions and trigger irrigation interventions. This proactive approach safeguards crops against drought-induced damage and contributes to resilient agricultural systems. Additionally, machine learning provides the opportunity for precision irrigation: The precision achieved through machine learning-driven irrigation scheduling enhances water use efficiency and minimizes resource wastage. ML models can create irrigation prescriptions tailored to specific soil types, crop varieties, and growth stages. The work of Singh et al. (2019) demonstrates the benefits of ML-guided precision irrigation, showcasing significant water savings and yield improvements in maize cultivation.

Lastly, machine learning possibly brings optimization under uncertainty: Machine learning addresses uncertainties inherent in agricultural environments, such as varying climate patterns and soil characteristics. By integrating probabilistic models and uncertainty quantification techniques, ML algorithms provide irrigation strategies that account for potential variability. This approach, as highlighted by Mishra et al. (2018), aids in risk-informed decision-making, and optimizing irrigation under changing conditions.

18.6 Discussion

Irrigation scheduling lies at the heart of sustainable agriculture, ensuring optimal water use and crop productivity. The integration of soil moisture sensor technology, remote sensing techniques, and machine learning, presents a promising avenue for advancing irrigation practices. This section engages in a comprehensive discussion of the implications, challenges, and opportunities associated with irrigation scheduling based on soil moisture sensor data, remote sensing data, machine learning, and the integration of these technologies.

18.6.1 Irrigation Scheduling Based on Soil Moisture Sensor Data

Maximizing irrigation is crucial considering climate change not only for saving water but also for meeting the demands of increasing food. Soil moisture sensors have emerged as invaluable tools for irrigation management, offering real-time insights into soil water content and enabling precise water application. The use of soil moisture sensor data for irrigation scheduling holds the promise of reducing

water wastage, optimizing water distribution, and enhancing crop yield. Blonquist Jr et al. (2006) used a time domain transmission (TDT) soil moisture sensor and compared it with ET-based irrigation recommendations in sprinkler irrigation systems. As a result, they found that TDT soil moisture sensor-based irrigation used 16% less water as opposed to the ET-based and 53% less water to a fixed irrigation (50 mm week^{-1}) system. Moreover, Domínguez-Niño et al. (2020) employed a capacitive soil moisture sensor in a drip-irrigated garden as a complementary to the soil water balance method and found that the sensor has the potential not only to save water but also to make the irrigation system automatic. The ability to monitor moisture levels at different depths and locations within fields empowers farmers to tailor irrigation schedules to specific crop needs. Deploying several capacitive sensors at different locations and depths have shown great potential in real-time monitoring soil moisture (Jabro et al., 2020).

While the benefits of soil moisture sensors are evident, challenges remain. Sensor accuracy, calibration, and maintenance require attention to ensure reliable measurements. Addressing these challenges through sensor innovation, improved calibration techniques, and simplified maintenance protocols can enhance the effectiveness of irrigation scheduling based on soil moisture sensor data. The work of Soulis et al. (2015) emphasizes the significance of sensor accuracy in guiding irrigation decisions and highlights the potential for improved irrigation scheduling when a sensor is positioned and calibrated effectively.

18.6.2 Irrigation Scheduling Based on Remote Sensing Data

Irrigation scheduling based on monitoring soil moisture has been widely used due to the advancement in soil moisture measurement technologies including remote sensing. The application of remote sensing data for irrigation scheduling introduces the potential to assess crop conditions from a macroscopic viewpoint. Olivera-Guerra et al. (2020) incorporated optical and thermal Landsat-7/8 data into a crop model to predict the timing and amount of irrigation and have achieved promising results. Moreover, Garrido-Rubio et al. (2020) used a remote sensing-based soil water balance (RS-SWB) to get remote sensing-based irrigation water accounting (RS-IWA) with input data including time series of basal crop coefficient and fractional vegetation cover and found a root square mean error of 12% at the plot level for maize and wheat and 15% at water user association management scale for spring crops, summer crops, and double harvest, alfalfa, and vineyard based on RS-IWA result. Remote sensing techniques when combined with ground data measurement including soil moisture sensors can help to indirectly estimate soil moisture even at higher depths. Santos et al. (2014) used remote sensing-based plant vigor and compared it with capacitive soil moisture sensors that were deployed at different depths up to 100 cm and found that placing soil moisture sensors at a depth of 60 cm is the most ideal option. The studies highlight the potential of remote sensing applications in irrigation scheduling, especially in retrieving surface soil moisture data that is central to providing plants with the right amount of water at the appropriate time.

Yet, challenges persist in translating remote sensing data into actionable irrigation strategies. Cloud cover, atmospheric interference, and sensor limitations can affect data availability and accuracy. Overcoming these challenges involves advancements in sensor technology, data fusion techniques, and improved processing algorithms.

18.6.3 Machine Learning in Soil-Based Irrigation Scheduling

Machine learning has the potential to revolutionize soil-based irrigation scheduling in agriculture. By leveraging data-driven insights and adapting to real-time conditions, machine learning algorithms can optimize water use, increase crop yield, and promote sustainable farming practices. Machine learning techniques have been used to predict pedotransfer functions (PTFs) which are the equations or algorithms that indicate the relationship between different soil properties. These soil properties are not easily available or are tough to measure. In such conditions, using machine learning can help to easily predict the soil properties including soil moisture content while saving cost. Additionally, machine learning is used to model the soil water retention curve which depicts the correlation between soil water content and soil matric potential. A study by Gorthi and Dou (2011) used precipitation, air, soil temperature, and soil-adjusted vegetation index to predict soil moisture content to 6 cm depth. Another researcher Pekel (2020) used temperature, relative humidity, time, and soil temperature as input variables into decision tree regression to estimate soil moisture. Deep learning regression networks with big data have also been used to predict soil moisture considering soil moisture, temperature, humidity, temperature, and pressure as input data (Cai et al., 2019). The studies indicate the potential of machine learning in soil-based irrigation scheduling. However, addressing challenges related to data quality, model interpretability, and implementation costs is essential for the widespread adoption of these technologies. As we move forward, collaboration among farmers, researchers, and policymakers will be crucial in harnessing the full potential of machine learning for irrigation scheduling and ensuring a more resilient and sustainable agricultural future.

18.6.4 Integration of Soil Moisture Sensors, Remote Sensing, and Machine Learning Techniques

The integration of soil moisture sensors, remote sensing, and machine learning techniques presents a powerful synergy that addresses the limitations of each technology while capitalizing on their respective strengths. By fusing real-time soil moisture data with remote sensing-derived information and incorporating it into a machine learning model, a comprehensive understanding of soil moisture dynamics and crop water needs emerges. This integration enables site-specific and timely

irrigation decisions that optimize water use efficiency and crop yield. However, integration demands harmonizing data from disparate sources and addressing interoperability challenges. These data mainly come from ground-based measurements, satellite data, and environmental parameters measurements (Fig. 18.4).

Several studies have been conducted globally to predict soil moisture by employing machine learning algorithms based on ground-based measurements and satellite data. In one study, it was reported that artificial neural networks showed better results as opposed to multiple linear regression (MLR) in predicting soil moisture

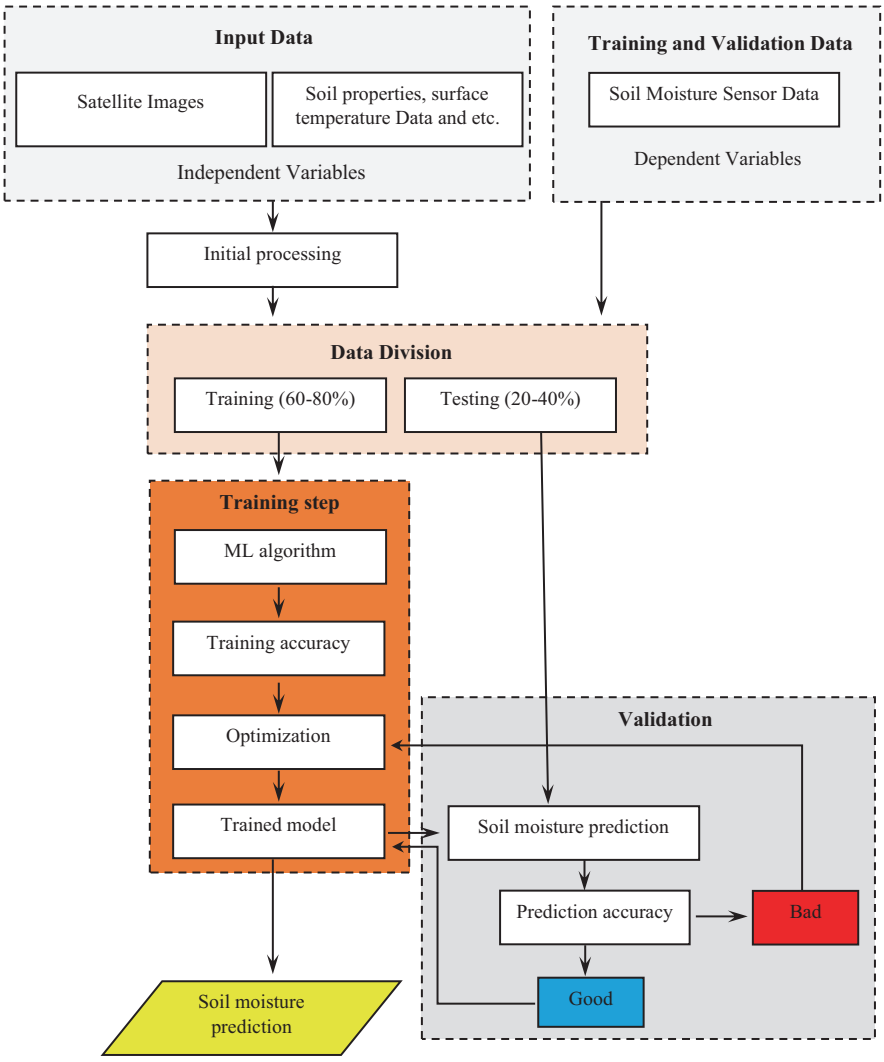

Fig. 18.4 General flowchart for predicting soil moisture using data from soil moisture sensors and remote sensing, employing machine learning techniques

information from C-band backscatter data and RADARSAT-1 and NDVI (Lakhankar et al., 2009a, b). In another study by Torres-Rua et al. (2016), using satellite images and energy balance products in vector regression, the estimation of soil moisture was carried out. Moreover, Sentinel-1 backscatter data, along with ancillary data including digital elevation model, soil property, and land cover maps, were used as inputs into Cubist, random forest, and machine learning algorithms, concluding that the Cubist algorithm and root mean square error (RMSE) performed better compared to random forest and machine learning at predicting soil moisture (Chatterjee et al., 2020). Grillakis et al. (2021) used data from the European Space Agency (ESA) through the Climate Change Initiative (CCI), along with in situ observations, physical soil, climate, and vegetation descriptors, to assess root zone soil moisture between 2001 and 2018. They achieved good agreements with the European Center for Medium-Range Weather Forecasts, ERA5 Land, and the Farming Early Warning Systems Network Land Data Assimilation System reanalyzes of soil moisture datasets.

Additionally, Peng et al. (2021) used a combination of datasets from JULES-CHESS simulated soil moisture and satellite soil moisture, mainly from SMAP L3E, SMAP L4, SMOS L4, Sentinel 1, ASCAT, and Sentinel 1/SMAP, which were first validated against observed soil moisture from COSMOS-UK, a network of in situ cosmic-ray-based sensors. These data were then input into a model, and the conclusion was that the model developed based on the merged soil moisture datasets performed better by improving the temporal variability of the JULES-CHESS simulation. These studies exemplify the potential of sensor-remote sensing-machine learning fusion in enhancing irrigation management and emphasize the need for integrated platforms that facilitate data synthesis and analysis.

18.7 Future Directions and Concluding Remarks

18.7.1 Emerging Trends in Irrigation Technology

The trajectory of irrigation technology is poised for continued advancement, driven by emerging trends that hold transformative potential. These trends encompass the evolution of sensors, data analytics, and decision support systems, all contributing to more intelligent and efficient irrigation practices.

Sensor Miniaturization and Connectivity: Advances in sensor miniaturization and wireless connectivity are making sensors more accessible and scalable. Miniaturized sensors can be deployed densely across fields, capturing high-resolution soil moisture data. The proliferation of Internet of Things (IoT) networks further enhances data collection and real-time monitoring.

Data-Driven Decision Support: Machine learning's role in irrigation scheduling is expected to expand, fueled by improvements in algorithms and computational power. Models will become more sophisticated, integrating diverse data sources for robust predictions. Real-time decision support systems will harness machine

learning's capabilities, offering farmers actionable insights through user-friendly interfaces.

18.7.2 Conclusion and Practical Recommendations

The integration of soil moisture sensing, remote sensing, and machine learning holds immense potential for optimizing irrigation scheduling and promoting sustainable agriculture. This interdisciplinary approach offers precision, efficiency, and resilience in irrigation management, mitigating water scarcity challenges and enhancing crop yield.

Practical recommendations:

1. **Data Quality Assurance:** Ensure accurate and reliable data from soil moisture sensors and remote sensing platforms through proper calibration, validation, and maintenance protocols.
2. **Interdisciplinary Collaboration:** Foster collaboration between agronomists, data scientists, and technology experts to leverage diverse expertise in designing and implementing integrated irrigation strategies.
3. **Continuous Learning and Adaptation:** Embrace a continuous learning approach to machine learning models, allowing algorithms to adapt to changing environmental conditions and optimize irrigation schedules over time.
4. **Investment in Technology:** Invest in the latest sensor technologies, remote sensing platforms, and machine learning tools to stay at the forefront of irrigation innovation.

In conclusion, the integration of soil moisture sensing, remote sensing, and machine learning represents a transformative paradigm for irrigation scheduling. This holistic approach offers the potential to revolutionize agriculture, ensuring efficient water utilization, sustainable crop production, and resilience in the face of changing climate and environmental dynamics. As technology continues to evolve, the journey toward optimized irrigation practices holds promise for a greener and more productive agricultural future.

References

Ahmed, A., Zhang, Y., & Nichols, S. (2011). Review and evaluation of remote sensing methods for soil-moisture estimation. *SPIE Reviews, 2*(1), 028001.

Baghdadi, N., Zribi, M., Loumagne, C., Ansart, P., & Anguela, T. P. (2008). Analysis of Terra SAR-X data and their sensitivity to soil surface parameters over bare agricultural fields. *Remote sensing of environment, 112*, 4370–4379.

Batlivala, P. P., & Ulaby, F. T. (1997). *Feasibility of monitoring soil moisture using active microwave remote sensing,"University of Kansa Center for Research, Inc., Remote Sensing Laboratory Technical Report No. 264–12*. University of Kansas Space Technology Center, Center for Research.

Bellvert, J., Marsal, J., Mata, M., & Girona, J. (2012). Identifying irrigation zones across a 7.5-ha "pinot noir" vineyard based on the variability of vine water status and multispectral images. *Irrigation Science, 30*, 499–509. https://doi.org/10.1007/s00271-012-0380-y

Blasch, J., Van Der Kroon, B., Van Beukering, P., Munster, R., Fabiani, S., Nino, P., et al. (2022). Farmer preferences for adopting precision farming technologies: A case study from Italy. *European Review of Agricultural Economics, 49*, 33–81. https://doi.org/10.1093/erae/jbaa031

Blonquist, J. M., Jr., Jones, S. B., & Robinson, D. A. (2006). Precise irrigation scheduling for turfgrass using a subsurface electromagnetic soil moisture sensor. *Agricultural Water Management, 84*(1–2), 153–165.

Cahn, M. D., & Johnson, L. F. (2017). New approaches to irrigation scheduling of vegetables. *Horticulturae, 3*, 28. https://doi.org/10.3390/horticulturae3020028

Cai, Y., Zheng, W., Zhang, X., Zhangzhong, L., & Xue, X. (2019). Research on soil moisture prediction model based on deep learning. *PLoS One, 14*(4), e0214508.

Chatterjee, S., Huang, J., & Hartemink, A. E. (2020). Establishing an empirical model for surface soil moisture retrieval at the US climate reference network using sentinel-1 backscatter and ancillary data. *Remote Sensing, 12*(8), 1242.

Chauhan, N. S., Miller, S., & Ardanuy, P. (2003). Spaceborne soil moisture estimation at high resolution: A microwave optical/IR synergistic method. *International Journal of Remote Sensing, 24*(22), 4599–4622.

Cheng, M., Jiao, X., Guo, W., Wang, S., & Sang, H. (2020). Temporal and spatial distribution characteristics of irrigation water requirement for main crops in the plain area of Hebei Province. *Irrigation and Drainage, 9*, 1051. https://doi.org/10.1002/ird.2489

Choudhury, B. J., Kerr, Y. H., Njoku, E. G., & Pampaloni, P. (1995). *Passive microwave remote sensing of land-atmosphere interactions*. VSP.

Döll, P., & Siebert, S. (2002). Global modeling of irrigation water requirements. *Water Resources Research, 38*(4), 8–10. https://doi.org/10.1029/2001WR000355

Domínguez-Niño, J. M., Oliver-Manera, J., Girona, J., & Casadesús, J. (2020). Differential irrigation scheduling by an automated algorithm of water balance tuned by capacitance-type soil moisture sensors. *Agricultural Water Management, 228*, 105880.

Du, Y., Ulaby, F. T., & Dobson, M. C. (2000). Sensitivity to soil moisture by active and passive microwave sensors. *IEEE Transactions on Geoscience and Remote Sensing, 38*(1), 105–113.

Dubois, P. C., Zyl, J., & Engman, T. (1995). Measuring soil moisture with imaging radars. *IEEE Transactions on Geoscience and Remote Sensing, 33*(4), 915–926.

Duchemin, B., Hadria, R., Erraki, S., Boulet, G., Maisongrande, P., Chehbouni, A., Escadafal, R., Ezzahar, J., Hoedjes, J. C. B., Kharrou, M. H., Khabba, S., Mougenot, B., Olioso, A., Rodriguez, J.-C., & Simonneaux, V. (2006). Monitoring wheat phenology and irrigation in Central Morocco: On the use of relationships between evapotranspiration, crops coefficients, leaf area index and remotely-sensed vegetation indices. *Agricultural Water Management, 97*(1), 1–27.

Dunne, S. C., Entekhabi, D., & Njoku, E. G. (2007). Impact of multiresolution active and passive microwave measurements on soil moisture estimation using the ensemble Kalman smoother. *IEEE Transactions on Geoscience and Remote Sensing, 45*(4), 1016–1028.

Elkelish, A. A., Alhaithloul, H. A. S., Qari, S. H., Soliman, M. H., & Hasanuzzaman, M. (2020). Pretreatment with Trichoderma harzianum alleviates waterlogging-induced growth alterations in tomato seedlings by modulating physiological, biochemical, and molecular mechanisms. *Environmental and Experimental Botany, 171*, 103946.

El-Zeiny, A. M., & Effat, H. A. (2017). Environmental monitoring of spatiotemporal change in land use/land cover and its impact on land surface temperature in El-Fayoum governorate. *Egypt. Remote Sensing Applications: Society and Environment, 8*, 266–277.

Er-Raki, S., Chehbouni, A., & Duchemin, B. (2010). Combining satellite remote sensing data with the FAO-56 dual approach for water use mapping in irrigated wheat fields of a semi-arid region. *Remote Sensing, 2*(1), 375–387.

Fang, B., Lakshmi, V., Jackson, T., Bindlish, R., & Colliander, A. (2019). Passive/active microwave soil moisture change disaggregation using SMAPVEX12 data. *Journal of Hydrology, 574*, 1085–1098.

Fontanet, M., Fernàndez-garcia, D., & Ferrer, F. (2018). The value of satellite remote sensing soil moisture data and the DISPATCH algorithm in irrigation fields. *Hydrology and Earth System Sciences, 22*, 5889–5900.

Gago, J., Douthe, C., Coopman, R. E., Gallego, P. P., Ribas-Carbo, M., Flexas, J., Escalona, J., & Medrano, H. (2015). UAVs challenge to assess water stress for sustainable agriculture. *Agricultural Water Management, 153*, 9–19. https://doi.org/10.1016/j.agwat.2015.01.020

Galambošová, J., Rataj, V., Prokeinová, R., & Prešinská, J. (2014). Determining the management zones with hierarchic and non-hierarchic clustering methods. *Research in Agricultural Engineering, 60*, 60.

Garrido-Rubio, J., Gonzalez-Piqueras, J., Campos, I., Osann, A., Gonzalez-Gomez, L., & Calera, A. (2020). Remote sensing–based soil water balance for irrigation water accounting at plot and water user association management scale. *Agricultural Water Management, 238*, 106236.

Ge, L., Hang, R., Liu, Y., & Liu, Q. (2018). Comparing the performance of neural network and deep convolutional neural network in estimating soil moisture from satellite observations. *Remote Sensing, 10*(9), 1327.

Gontia, N. K., & Tiwari, K. N. (2008). Development of crop water stress index of wheat crop for scheduling irrigation using infrared thermometry. *Agricultural Water Management, 95*(10), 1144–1152.

Gorthi, S., & Dou, H. (2011). *Prediction models for the estimation of soil moisture content. In international design engineering technical conferences and computers and information in engineering conference* (Vol. 54808, pp. 945–953). Design Engineering Division and Computers and Information in Engineering Division.

Grillakis, M. G., Koutroulis, A. G., Alexakis, D. D., Polykretis, C., & Daliakopoulos, I. N. (2021). Regionalizing root-zone soil moisture estimates from ESA CCI soil water index using machine learning and information on soil, vegetation, and climate. *Water Resources Research, 57*(5), e2020WR029249.

Gu, Z., Qi, Z., Burghate, R., Yuan, S., Jiao, X., & Xu, J. (2020). Irrigation scheduling approaches and applications: A review. *Journal of Irrigation and Drainage Engineering, 146*(6), 04020007.

Gupta, D., Gujre, N., Singha, S., & Mitra, S. (2022). Role of existing and emerging technologies in advancing climate-smart agriculture through modeling: A review. *Ecological Informatics, 71*, 101805.

Haas, J. (2010). *Soil moisture modelling using TWI and satellite imagery in the Stockholm region. M.Sc dissertation, School of Architecture and the built environment*. Royal Institute of Technology (KTH).

He, Z. H., Li, M. N., Cai, Z. L., Zhao, R. S., Hong, T. T., Yang, Z., & Zhang, Z. (2021). Optimal irrigation and fertilizer amounts based on multi-level fuzzy comprehensive evaluation of yield, growth and fruit quality on cherry tomato. *Agricultural Water Management, 243*, 106360.

Hedley, C., & Yule, I. (2009b). A method for spatial prediction of daily soil water status for precise irrigation scheduling. *Agricultural Water Management, 96*(12), 1737–1745. https://doi.org/10.1016/j.agwat.2009.07.009

Hedley, C. B., & Yule, I. J. (2009a). A method for spatial prediction of daily soil water status for precise irrigation scheduling. *Agricultural Water Management, 96*(12), 1737–1745.

Henggeler, J. C., Dukes, M. D., & Mecham, B. Q. (2011). Irrigation scheduling. In L. E. Stetson & B. Q. Mecham (Eds.), *Irrigation* (p. 495). Irrigation Association.

Jabro, J. D., Stevens, W. B., Iversen, W. M., Allen, B. L., & Sainju, U. M. (2020). Irrigation scheduling based on wireless sensors output and soil-water characteristic curve in two soils. *Sensors, 20*(5), 1336.

Jackson, T. J., Cosh, M. H., Bindlish, R., Starks, P. J., Bosch, D. D., Seyfried, M., & Du, J. (2010). Validation of advanced microwave scanning radiometer soil moisture products. *IEEE Transactions on Geoscience and Remote Sensing, 48*(12), 4256–4272.

Jackson, T. J., Schmugge, J., & Engman, E. T. (1996). Remote sensing applications to hydrology: Soil moisture. *Journal of Hydrological Sciences, 41*(4), 517–529.

Jackson, T. J., & Schmugge, T. J. (1991). Vegetation effects on the of soils microwave emission. *Remote Sensing of Environment, 36*, 203–212.

Jägermeyr, J., Gerten, D., Heinke, J., Schaphoff, S., Kummu, M., & Lucht, W. (2015a). Water savings potentials of irrigation systems: global simulation of processes and linkages. *Hydrology and Earth System Sciences, 19*(7), 3073–3091. https://doi.org/10.5194/hess-

Jägermeyr, J., Gerten, D., Heinke, J., Schaphoff, S., Kummu, M., & Lucht, W. (2015b). Water.

Jones, H. G. (2004). Irrigation scheduling: Advantages and pitfalls of plant-based methods. *Journal of Experimental Botany, 55*(407), 2427–2436.

Lakhankar, T., Ghedira, H., Temimi, M., Azar, A. E., & Khanbilvardi, R. (2009b). Effect of land cover heterogeneity on soil moisture retrieval using activemicrowave remote sensing data. *Journal of Remote Sensing, 1*, 80–91.

Lakhankar, T., Ghedira, H., Temimi, M., Sengupta, M., Khanbilvardi, R., & Blake, R. (2009a). Nonparametric methods for soil moisture retrieval from satellite remote sensing data. *Remote Sensing, 1*(1), 3–21.

Lee, Y., Jung, C., & Kim, S. (2019). Spatial distribution of soil moisture estimates using a multiple linear regression model and Korean geostationary satellite (COMS) data. *Agricultural Water Management, 213*(March), 580–593. https://doi.org/10.1016/j.agwat.2018.09.004

Liu, H., Whiting, M. L., Ustin, S. L., Zarco-Tejada, P. J., Huffman, T., & Zhang, X. (2018). Maximizing the relationship of yield to site-specific management zones with objectori-ented segmentation of hyperspectral images. *Precision Agriculture, 19*, 348–364. https://doi.org/10.1007/s11119-017-9521-x

Maia, R. F., Lurbe, C. B., & Hornbuckle, J. (2022). Machine learning approach to estimate soil matric potential in the plant root zone based on remote sensing data. *Frontiers in Plant Science, 13*, 931491.

Martinez-Casasnovas, J. A., Agelet-Fernandez, J., Arno, J., & Ramos, M. C. (2012). Analysis of vineyard differential management zones and relation to vine development, grape maturity and quality. *Spanish Journal of Agricultural Research, 10*, 326–337.

Merlin, O., Malbéteau, Y., Notfi, Y., Bacon, S., Khabba, S., & Jarlan, L. (2015). Performance metrics for soil moisture downscaling methods: Application to DISPATCH data in Central Morocco. *Remote Sensing, 7*(4), 3783–3807.

Migliaccio, K. W., Schaffer, B., Crane, J. H., & Davies, F. S. (2010). Plant response to evapo-transpiration and soil water sensor irrigation scheduling methods for papaya production in South Florida. *Agricultural Water Management, 97*(10), 1452–1460. https://doi.org/10.1016/j.agwat.2010.04.012

Mishra, V., Ellenburg, W. L., Griffin, R. E., Mecikalski, J. R., Cruise, J. F., Hain, C. R., & Anderson, M. C. (2018). An initial assessment of a SMAP soil moisture disaggregation scheme using TIR surface evaporation data over the continental United States. *International Journal of Applied Earth Observation and Geoinformation, 68*, 92–104.

Mitchell, T. M. (1997). *Machine learning* (Vol. 45, pp. 870–877). McGraw Hill.

Neale, C. M. U., Jayanthi, H., & Wright, J. L. (2003). Crop and irrigation water management using high-resolution airborne remote sensing. In *Proc. ICID workshop remote sensing of ET for large regions, CD-ROM*. International Commission on Irrigation and Drainage.

O'Neil, P. E. (1996). Use of active and passive microwave remote sensing for soil moisture estimation through corn. *International Journal of Remote Sensing, 17*(10), 1851–1865.

Ohana-levi, N., Bahat, I., Peeters, A., Shtein, A., Netzer, Y., & Ben-gal, A. (2019). Original papers a weighted multivariate spatial clustering model to determine irrigation management zones. *Computers and Electronics in Agriculture, 162*, 719–731. https://doi.org/10.1016/j.compag.2019.05.012

Olivera-Guerra, L., Merlin, O., & Er-Raki, S. (2020). Irrigation retrieval from Landsat optical/thermal data integrated into a crop water balance model: A case study over winter wheat fields in a semi-arid region. *Remote Sensing of Environment, 239*, 111627.

Ors, S., Ekinci, M., Yildirim, E., Sahin, U., Turan, M., & Dursun, A. (2021). Interactive effects of salinity and drought stress on photosynthetic characteristics and physiology of tomato (Lycopersicon esculentum L.) seedlings. *South African Journal of Botany, 137*, 335–339.

Owen, T. W., Carlson, T. N., & Gillies, R. R. (1998). An assessing soil moisture of satellite remotely-sensed land cover parameters in quantitatively describing the climatic effect of urbanization. *International Journal of Remote Sensing, 19*(9), 1663–1681.

Pekel, E. (2020). Estimation of soil moisture using decision tree regression. *Theoretical and Applied Climatology, 139*(3), 1111–1119.

Peng, J., Loew, A., Merlin, O., & Verhoest, N. E. (2017). A review of spatial downscaling of satellite remotely sensed soil moisture. *Reviews of Geophysics, 55*(2), 341–366.

Peng, J., Tanguy, M., Robinson, E. L., Pinnington, E., Evans, J., Ellis, R., & Dadson, S. (2021). Estimation and evaluation of high-resolution soil moisture from merged model and earth observation data in the Great Britain. *Remote Sensing of Environment, 264*, 112610.

Pereira, L. S., Allen, R. G., Smith, M., & Raes, D. (2015). Crop evapotranspiration estimation with FAO56: Past and future. *Agricultural Water Management, 147*, 4–20. https://doi.org/10.1016/j.agwat.2014.07.031

Peters, R. T., Desta, K. G., & Nelson, L. (2013). *Practical use of soil moisture sensors and their data for irrigation scheduling*. Washington State University.

Petropoulos, G., Carlson, T. N., Wooster, M. J., & Islam, S. (2009). A review of T-s/VI remote sensing based methods for the retrieval of land surface energy fluxes and soil surface moisture. *Progress in Physical Geography, 33*, 224–250.

Pôças, I., Calera, A., Campos, I., & Cunha, M. (2020). Remote sensing for estimating and mapping single and basal crop coefficients: A review on spectral vegetation indices approaches. *Agricultural Water Management, 233*, 106081. https://doi.org/10.1016/j.agwat.2020.106081

Prost, G. L. (2001). *Remote sensing for geologists: A guide to image interpretation* (2nd ed.). Gordon and Breach. (2001).

Ragab, R., & Prudhomme, C. (2002). Sw—Soil and water: Climate change and water resources management in arid and semi-arid regions: Prospective and challenges for the 21st century. *Biosystems Engineering, 81*(1), 3–34.

Rani, A., Kumar, N., Kumar, J., & Sinha, N. K. (2022). Machine learning for soil moisture assessment. In *Deep learning for sustainable agriculture* (pp. 143–168). Academic Press.

Robinson, D. A., Campbell, C. S., Hopmans, J. W., Hornbuckle, B. K., Jones, S. B., Knight, R., et al. (2008). Soil moisture measurement for ecological and hydrological watershed-scale observatories: A review. *Vadose Zone Journal, 7*(1), 358–389.

Sabaghy, S., Walker, J. P., Renzullo, L. J., & Jackson, T. J. (2018). Spatially enhanced passive microwave derived soil moisture: Capabilities and opportunities. *Remote Sensing of Environment, 209*, 551–580.

Sánchez-Ruiz, S., Piles, M., Sánchez, N., Martínez-Fernández, J., Mercè, V.-l., Camps, & Adriano. (2014). Combining SMOS with visible and near/shortwave/thermal infrared satellite data for high resolution soil moisture estimates. *Journal of Hydrology, 516*, 273–283.

Sandells, M. J., Ian, J., Davenport, & Gurney, R. J. (2008). Passive L-band microwave soil moisture retrieval error arising from topography in otherwise uniform scenes. *Advances in Water Resources, 31*, 1433–1443.

Santos, W. J. R., Silva, B. M., Oliveira, G. C., Volpato, M. M. L., Lima, J. M., Curi, N., & Marques, J. J. (2014). Soil moisture in the root zone and its relation to plant vigor assessed by remote sensing at management scale. *Geoderma, 221*, 91–95.

Schepers, A. R., Shanahan, J. F., Liebig, M. A., Schepers, J. S., Johnson, S. H., & Luchiari, A. (2004). Appropriateness of management zones for characterizing spatial variability of soil properties and irrigated corn yields across years. *Agronomy Journal, 96*, 195–203.

Scudiero, E., Teatini, P., Manoli, G., Braga, F., Skaggs, T., & Morari, F. (2018). Workflow to establish time-specific zones in precision agriculture by spatiotemporal integration of plant and soil sensing data. *Agronomy, 8*, 253. https://doi.org/10.3390/agronomy8110253

Seyar, M. H., & Ahamed, T. (2023). Development of an IoT-based precision irrigation system for tomato production from indoor seedling germination to outdoor field production. *Applied Sciences, 13*(9), 5556.

Seyar, M. H., Kahandage, P. D., & Ahamed, T. (2023). An IoT-based precision irrigation system to optimize plant water requirements for indoor and outdoor farming systems. In *IoT and AI in agriculture: Self-sufficiency in food production to achieve society 5.0 and SDG's globally* (pp. 47–69). Springer Nature Singapore.

Simonneaux, V., Lepage, M., Helson, D., Metral, J., Thomas, S., Duchemin, B., Cherkaoui, M., Kharrou, H., Berjami, B., & Chehbouni, A. (2009). Estimation spatialisée de l'Evapotranspiration des cultures irriguées par télédétection. Application à la gestion de l'Irrigation dans la plaine du Haouz (Marrakech, Maroc). *Sécheresse, 20*(1), 123–130.

Singh, G., Das, N. N., Panda, R. K., Colliander, A., Jackson, T. J., Mohanty, B. P., Entekhabi, D., & Yueh, S. H. (2019). Validation of SMAP soil moisture products using ground-based observations for the paddy dominated tropical region of India. *IEEE T. Geosci. Remote, 57*, 8479–8491.

Soulis, K. X., Elmaloglou, S., & Dercas, N. (2015). Investigating the effects of soil moisture sensors positioning and accuracy on soil moisture based drip irrigation scheduling systems. *Agricultural Water Management, 148*, 258–268.

Tagesson, T., Horion, S., Nieto, H., Fornies, V. Z., González, G. M., Bulgin, C. E., et al. (2018). Disaggregation of SMOS soil moisture over West Africa using the temperature and vegetation dryness index based on SEVIRI land surface parameters. *Remote Sensing of Environment, 206*, 424–441.

Thompson, R., M. Gallardo, L. Valdez, & M. Fernández. (2007). "Using plant water status to define threshold values for irrigation management of vegetable crops using soil moisture sensors." Agricultural Water Management 88 (1): 147–158. https://doi.org/10.1016/j.agwat.2006.10.007.

Tilman, D., & Clark, M. (2015). Food, agriculture & the environment: Can we feed the world & save the earth? *Daedalus, 144*(4), 8–23. https://doi.org/10.1162/DAED_a_00350

Torres-Rua, A. F., Ticlavilca, A. M., Bachour, R., & McKee, M. (2016). Estimation of surface soil moisture in irrigated lands by assimilation of landsat vegetation indices, surface energy balance products, and relevance vector machines. *Water, 8*(4), 167.

Tuller, M., Babaeian, E., Jones, S. B., Montzka, C., Vereecken, H., & Sadeghi, M. (2019). The paramount societal impact of soil moisture. *Eos, 100*, 1.

Tuller, M., Or, D., & Hillel, D. (2004). Retention of water in soil and the soil water characteristic curve. *Encyclopedia of Soils in the Environment, 4*, 278–289.

Ulbay, F. T., Dobson, M. C., & Brunfeldt, D. R. (1983). Improvement of moisture estimation accuracy of vegetation-covered soil by combined active/passive microwave remote sensing. *IEEE Transactions on Geoscience and Remote Sensing, GE-21*(3), 300–307.

Walker, J. P., & Houser, P. R. (2001). A methodology for initializing soil moisture in a global climate model: Assimilation of near-surface soil moisture observations. *Journal of Geophysical Research, 106*(D11), 11761–11774.

Walker, J. P., Troch, P. A., Mancini, M., Willgoose, G. R., & Kalma, J. D. (1997). Profile soil moisture estimation using the modified IEM. *Geoscience and Remote Sensing, 3*, 1263–1265.

Wang, L., & Qu, J. J. (2009). Satellite remote sensing applications for surface soil moisture monitoring: A review. *Frontiers of Earth Science in China, 3*(2), 237–247.

Wang, L., Qu, J. J., & Hao, X. (2008). Forest fire detection using the normalized multiband drought index (NMDI) with satellite measurements. *Agricultural and Forest Meteorology, 148*(11), 1767–1776.

World Bank. (2022). Water in Agriculture.

Zhan, X., Fang, L., Liu, J., Hain, C., Yin, J., Schull, M., et al. (2017). Fusing microwave and optical satellite observations for high resolution soil moisture data products. In *Geoscience and remote sensing symposium (IGARSS), 2017 IEEE international* (pp. 2519–2522). IEEE.

Zhao, W., Sánchez, N., Lu, H., & Li, A. (2018). A spatial downscaling approach for the SMAP passive surface soil moisture product using random forest regression. *Journal of Hydrology, 563*, 1009–1024.

Chapter 19
AI-Based IoT Greenhouse Control System for Environmental Parameters

Abstract The environmental parameters of traditional greenhouse which need to be controlled continuously by farmers are not convenient and precise. In this study, an AI-based IoT greenhouse control system for environmental parameters was developed to solve the disadvantages of the traditional greenhouse system. IoT technology was used to help greenhouses connect to the internet that users could monitor greenhouses remotely and conveniently. AI technology was used to detect plant (leaf lettuce) growth and control the greenhouse environmental parameters (soil moisture, light intensity, humidity) automatically. In terms of plant detection, this study used a nonanchor-based object detection model, CenterNet, and anchor-based object detection, YOLOv3 model to detect the growth stage of leaf lettuce, and then recommend a suitable environmental parameter for the corresponding plants. In this study, the growth stage of lettuce was divided into four stages. The results show the mAPs of CenterNet were 1.0, 0.98, 1.0, and 1.0 from growth stage 1 to growth stage 4. The mAPs of YOLOv3 were 0.43, 0.75, 0.85, and 0.99 from growth stage 1 to growth stage 4. Therefore, the performance of CenterNet was better than YOLOv3. In terms of environmental parameters control, this study compared the normal control, typical PID algorithm, and fuzzy PID control algorithm to control current environmental parameters to the optimum environmental parameters. The results show fuzzy PID control algorithm had the lowest overshoot and highest robustness.

Keywords AI-based IoT greenhouse control system · Environmental parameters control · Detection of leaf lettuce growth stage · CenterNet · YOLOv3 · PID control algorithm · Fuzzy PID control algorithm

19.1 Introduction

The arable land area and natural resources worldwide are significantly decreasing due to urbanization and industrial transformation. How to use the limited land effectively and improve agriculture production has become an important issue in the world. Hence, the adoption of greenhouse production is one of the important alternatives to solve the problem (Yang et al., 2021).

© The Author(s), under exclusive license to Springer Nature Singapore Pte Ltd. 2024

T. Ahamed, *IoT and AI in Agriculture*,
https://doi.org/10.1007/978-981-97-1263-2_19

Traditionally, most of the greenhouses are located far from cities and need to be managed by farmers physically. These traditional greenhouses have two major disadvantages. Farmers have to go to their greenhouses to work and manage their crops. It is very inconvenient, especially during the pandemic of Coronavirus. Additionally, the environmental parameters of a greenhouse should be monitored and controlled continuously by farmers with agricultural experience, which is prone to human error, may not be precise, and costs the labor force. To solve the above disadvantages, there is a need for an automatic and smart system that can manage the greenhouse environment parameters precisely. For controlling the greenhouse environment, several methods and control techniques including predictive control, fuzzy logic, and Internet of Things (IoT)-based systems have been developed.

Agricultural greenhouse is an important technical means of livelihood projects all over the world. The digital management and operation of the greenhouse have become an urgent problem (Zhao Hua-fei & Jian, 2019). Therefore, IoT-based agricultural greenhouses have been designed by engineers and researchers as it has become a big important role in agriculture recently. The aim of the IoT application is to connect anything through the internet that can be accessible from anywhere (Vishwakarma et al., 2019). Ruishi et al. (2021) designed an agricultural greenhouse management platform based on IoT and Spring, SpringMVC, and MyBatis (SSM) architecture. These research integrated big data technologies with IoT to improve the management efficiency of greenhouses. However, they only focused on monitoring the situation in the greenhouse through IoT without proposing a fusion of Artificial Intelligence (AI) and control algorithms to effectively control the environment in the greenhouse and object detection for monitoring growth stages.

Object detection has been significantly improved with the help of deep learning (Girshick et al., 2014). In the current era, there are two popular object detection series: the anchor-based detection model and the nonanchor-based detection model. The anchor-based flowchart starts with setting a large number of anchors on an image. For example, You Only Look Once (YOLO) is an anchor-based object detection model. If an object is in an anchor, this anchor is used to detect the object, which is not conducive to the bounding box classification tasks (Redmon et al., 2016). Nonanchor-based flowchart does not rely on the anchors first. For example, CenterNet is a keypoint-based object detection model. The flowchart of CenterNet places points on an image first. If an object is at a point, this point is used to detect the object (Duan et al., 2019).

Several studies have utilized object detection models for plant detection. Kavitha and Savarimuthu (2021) explored the potential of computer vision-based object detection methods for early plant disease detection. They compared different anchor-based object detection models YOLOv4, EfficientDet, and Scaled-YOLOv4 for plant disease detection. The results showed Scaled-YOLOv4 model is the most suitable object detection model. Sudha et al. (2022) used deep learning Faster Region Convolutional Neural Network (RCNN) method to detect fruit for autonomous harvesting system using IoT Technology, in which the mean average precision of fruit was 0.869.

These studies showed that deep learning is suitable for plant detection in different fields. However, there is a lack of systematic comparison between the anchor-based object detection model and the nonanchor-based object detection model for plant detection.

In terms of the greenhouse environmental control system. The greenhouse system is an ill-defined, nonlinear, and time-varying controlled object that makes it difficult to get a specific mathematical model of the controlled object. This is because the environment of the greenhouse system is very complex and has a strong lag effect. Environmental control information needs to change with the growth of plants and sometimes there are also external interference (Alaviyan et al., 2020). Therefore, the normal control method is not suitable for greenhouse environmental parameters control. Abdulrhman (2000) developed greenhouse climate control using a proportional integral derivative (PID) and fuzzy logic with optimization. The research compared various control algorithms through simulation experiments and proposed the use of an improved fuzzy control algorithm to control the environment in the greenhouse, which can get better results. Although the control algorithms for greenhouse parameters have been studied in this research, however, there are no relevant management measures for the different growth stages of plants. Moreover, in some cases, simulation results are difficult to apply to actual complex greenhouse systems.

To address the shortcomings in the control system for greenhouse environmental parameters, a system based on IoT and AI to monitor plant growth and control the environmental parameters of the greenhouse based on the plant growing stages has been proposed in this research. The IoT technology was used to help farmers to monitor their greenhouses remotely and conveniently. The AI technology, on the other hand, was used to detect plant growth and control environmental parameters. In this study, the CenterNet detection model was used to detect the growing stage of the plants and then recommended suitable environmental parameters for corresponding plants. Additionally, this study also used a fuzzy PID control algorithm to control current environmental parameters to match with the optimum parameters.

Monitoring greenhouses and managing plant growth, especially for the greenhouses that are located far from cities have become a challenge and time-consuming for most of the producers. Therefore, in this study, we have developed a greenhouse control system by integrating IoT, AI detection, and AI control functions which is robust, convenient, and easy to use. The system can control the environmental parameters of greenhouses accurately according to the growth stage of plants, greatly reduce the labor cost, and improve the utilization rate of resources. The control algorithm and object detection model were compared systematically, and the best detection model and fuzzy PID algorithm were chosen to deploy in the system.

The main objective of the study is to develop an AI-based IoT control system for greenhouse environmental parameters. In this study, leaf lettuce was chosen as the research plant. The system was developed to detect the growth stage of the leaf lettuce and provided a control environmental parameter of the greenhouse based on the corresponding growing stages.

19.2 Materials and Methods

19.2.1 IoT-Based Greenhouse System

Nowadays, IoT technology has been widely used in agricultural greenhouses. IoT technology is used to upload the environmental parameters, plant growth conditions, and control actuator working conditions in the greenhouse to the cloud platform through different communication means and protocols. Users can use mobile phones or web pages to remotely monitor the situation and control the actuator in the greenhouse.

IoT system is mainly divided into two subsystems, embedded system and cloud system. The embedded system is deployed in the greenhouse, which is generally composed of main controllers, communication nodes, sensors, control actuators, and other peripherals. Therefore, an embedded system is the thing of IoT. Cloud system is the Internet of IoT, which is used to transfer data, store data, and interact with users. Cloud systems are different from general real servers. Cloud systems are provided by some network operators, which enable users to deploy their own network systems quickly and conveniently without buying the servers.

Connecting the embedded system to the cloud system is also the key to IoT technology. Developers can use a variety of communication means to connect an embedded system to the network such as through Universal Serial Bus (USB), serial communication, Wi-Fi, Bluetooth, 4G/5G, and Narrowband Internet of Things (NB IoT) (Sharma & Gondhi, 2018). Developers can also use various communication protocols to interact the embedded system with the cloud system by using Hyper Text Transfer Protocol (HTTP), Message Queuing Telemetry Transport (MQTT) protocol, and others. The communication means and protocols mainly depend on the actual requirements. At present, MQTT is the main communication protocol for IoT, but the communication means depend on developers and actual requirements. In this study, Wi-Fi and MQTT were used to connect the embedded system to the cloud system.

MQTT is an asynchronous communication message protocol based on the Transmission Control Protocol (TCP) / Internet Protocol (IP) stack (Fig. 19.1). It is a lightweight information transmission protocol based on publishing and subscribing (Eridani et al., 2019). Therefore, MQTT needs a message middleware to achieve the publish and subscribe functions. In this study, the middleware was the Alibaba cloud platform. It can be expanded in an unreliable network environment and is suitable for scenarios with limited device hardware storage space or network

Fig. 19.1 Working principle of MQTT protocol

bandwidth. Using the MQTT protocol, message senders and receivers are not limited by time and space. Hence, the MQTT protocol is currently the main communication protocol for IoT devices (Tantitharanukul et al., 2017).

19.2.2 YOLOv3 Object Detection Model

YOLOv3 is the third version of the YOLO series of object detection algorithms. It is an anchor-based object detection model. The principle working of YOLOv3 is started by setting a large number of anchors on the image, and the network adjusts the anchors to obtain the prediction bounding boxes of objects. The anchors greatly improve the detection precision of the network, but the precision can be limited by the size of objects and the detection speed also limits by lots of anchors (Liu et al., 2020).

For each input image, YOLOv3 adjusted the image to 416 * 416 * 3. Then, predicted the output of three different scales to detect objects of different sizes where 13 * 13 scale was for big objects, 26 * 26 scale was for medium objects, and 52 * 52 scale was for small objects. Therefore, the 13 * 13 scale was used for the big objects. The backbone of YOLOv3 is Darknet-53 (Redmon & Farhadi, 2018). Darknet-53 is mainly composed of Conv2D Block and Residual Block. The architecture of YOLOv3 is shown in Fig. 19.2.

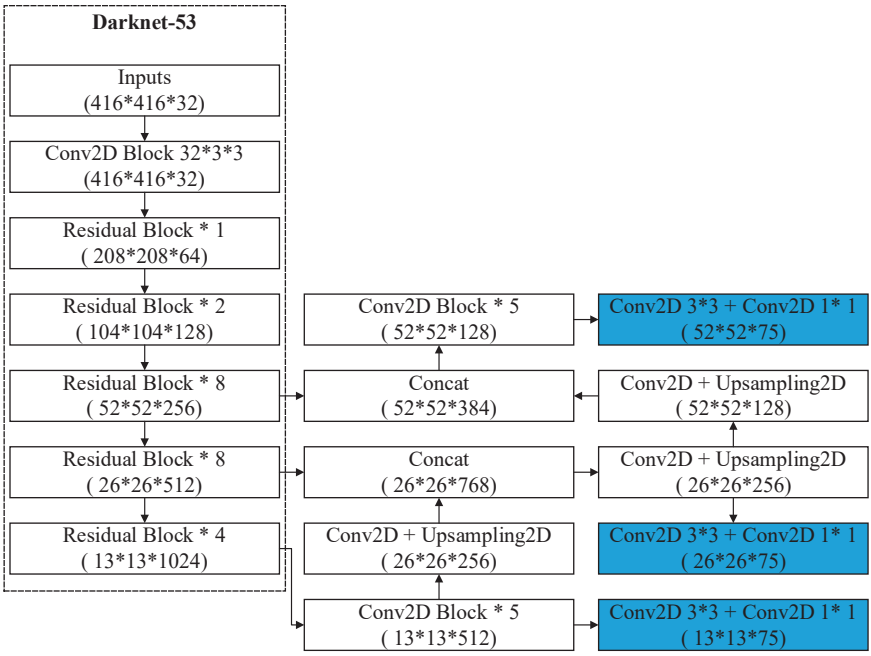

Fig. 19.2 Architecture of YOLOv3

Conv2D block is a convolutional block, which is the smallest component in the YOLOv3 network structure (Fig. 19.3). Conv2D block consists of three network layers: Conv layer, batch normalization layer, and Leaky ReLU layer.

The Conv layer is a convolution layer. The input image is processed with multiple different convolution kernels to obtain different response feature maps.

The Batch Normalization layer (BN) is used after the convolution layer and before the activation function. The main operation step of the BN layer is to calculate the mean value and variance of all batch data, and then divide the difference between pixel value and mean value by variance for normalization. At the same time, the offset factor and scale change factor are added to control the normalized value. The factor value is learned by the neural network during training.

The Leaky Rectified Linear Units (Leaky ReLU) function (Glorot et al., 2011), (Eq. 19.1) is a variation of the Rectified Linear Units (ReLU) function (Maas et al., 2013), (Eq. 19.2). They are widely used as activation functions in neural networks. In Leaky Relu, the negative axis retains a very small constant leak, so that when the input information is less than 0, the information is not completely lost and is retained accordingly. ReLU function and Leaky ReLU function are shown in Fig. 19.4.

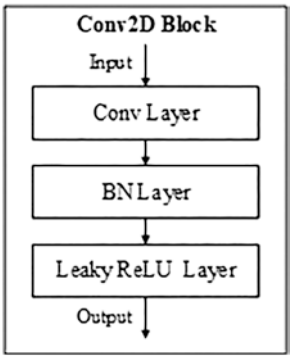

Fig. 19.3 Architecture of Conv2D block

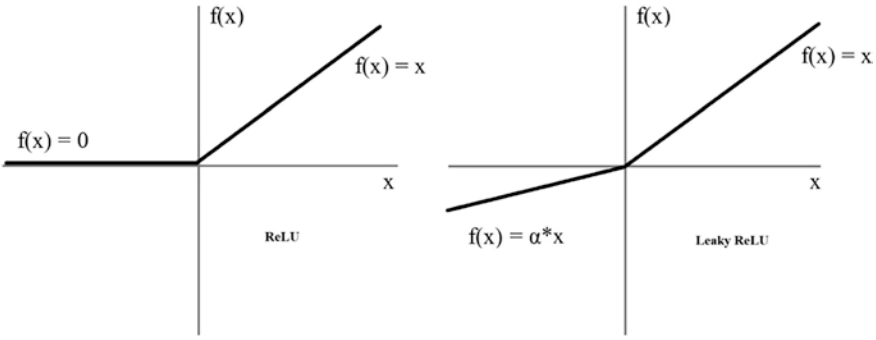

Fig. 19.4 ReLU function and Leaky ReLU function

$$f(x)=\begin{cases} x, & x \geq 0 \\ 0, & x < 0 \end{cases} \tag{19.1}$$

$$f(x)=\begin{cases} x, & x \geq 0 \\ ax, & x < 0 \end{cases} \tag{19.2}$$

The residual block (Fig. 19.5) directly skips multiple layers of data input from a certain layer of the first few layers and adds it to the input part of the subsequent data layer. It means that the content of the following feature layer partially contributed in a linear way by a layer in front of it (He et al., 2016).

After the Darknet-53 network, YOLOv3 built a Feature Pyramid Network (FPN) for the obtained feature layers, and then made classification prediction and regression prediction. Finally, three feature layers had output through FPN. The shapes of the output layers were (13, 13, 75), (26, 26, 75), and (52, 52, 75). The last dimension was 75 because the images were based on the VOC dataset. It had 20 classes. YOLOv3 had three anchors for each feature point of each feature layer, so the number of channels in the predicted result was 3*25. If the COCO dataset is used, then the datasets become 80 classes. The final dimension should be 255 = 3*85. The shapes of the three feature layers are (13, 13, 255), (26, 26, 255), and (52, 52, 255).

Each output feature layer divides the entire image into grids corresponding to its length and width. For example, the feature layer of (13,13, 255) divides the entire image into 13×13 grids; Then, multiple anchors are created from each grid center. These anchors are preset by the network. The prediction results of the network judged whether these anchors contain objects and the types of objects. The prediction results can be as follows: (13, 13, 3, 85), 26, 26, 3, 85), (52, 52, 3, 85). Among them, 85 can be divided into 4 + 1 + 80, of which 4 represents the adjustment parameters of the anchors (x offset, y offset, width, height). 1 represents whether the anchor contains objects, and 80 represents the type of the prior frame. Since there are 80 types of cocoa, there are 80 here.

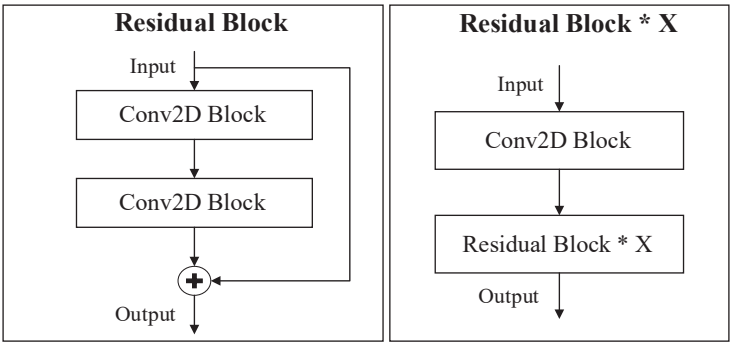

Fig. 19.5 Architecture of residual block

However, the predicted results are not the positions of the final bounding boxes on the image. The results should be decoded. The decoding process of YOLOv3 is divided into two steps: First, each grid point is added with its corresponding coordinate offset. The result is the center of the bounding box. Then, the width and height of the bounding box are calculated by combining the anchor with the height and width from the prediction results. In this way, the position of the whole bounding box can be obtained.

After the decoding process, final prediction results are obtained, and score sorting and nonmaximum inhibition screening shall be carried out. Finally, bounding boxes are drawn on the original image.

19.2.3 CenterNet Object Detection Model

CenterNet is a nonanchor-based object detection model. First, CenterNet sets many points on the image, and the network adjusts the points to obtain the center points of objects and prediction bounding boxes. The network structure of CenterNet is much simpler than YOLOv3, but the performance is better than YOLOv3. Especially in the detection of small objects. There are many kinds of backbone networks that can be used by CenterNet. Generally, Hourglass Network or ResNet50 is used as the backbone network. Since the number of Hourglass Network parameters used by CenterNet are too large, therefore, RestNet50 was used as the backbone feature extraction network in this study (Fig. 19.6).

ResNet50 has two basic blocks, called Conv Block and Identity Block respectively. The input and output dimensions of Conv Block are different, so Conv Block cannot be concatenated consecutively. Its role is to change the dimensions of the network. Identity Block has the same input dimension and output dimension, which can be concatenated to deepen the network. The Architecture of the conv block and identity block is shown in Fig. 19.7.

The shape of the last feature layer of ResNet50 is 16*16*2048. For this feature layer, CenterNet uses three times of deconvolution for upsampling to get higher resolution output. To save computation, the output channels of the three deconvolutions are 256, 128, and 64 respectively. Each deconvolution doubles the height and width of the feature layer. Therefore, after three times of deconvolution, the height and width of the feature layer turns 8 times the original. Finally, CenterNet obtained a 128*128*64 effective feature layer (high-resolution feature map), and the final prediction results can be obtained by using this effective feature layer.

This feature layer is equivalent to dividing the whole image into 128*128 regions. Each region has a feature point. If the center of an object falls in this region, the object detects by this feature point. If the center of an object falls in this area, the object is detected by the feature point at the upper left corner of this area. Finally, CenterNet uses this feature layer to do three convolutions to get results.

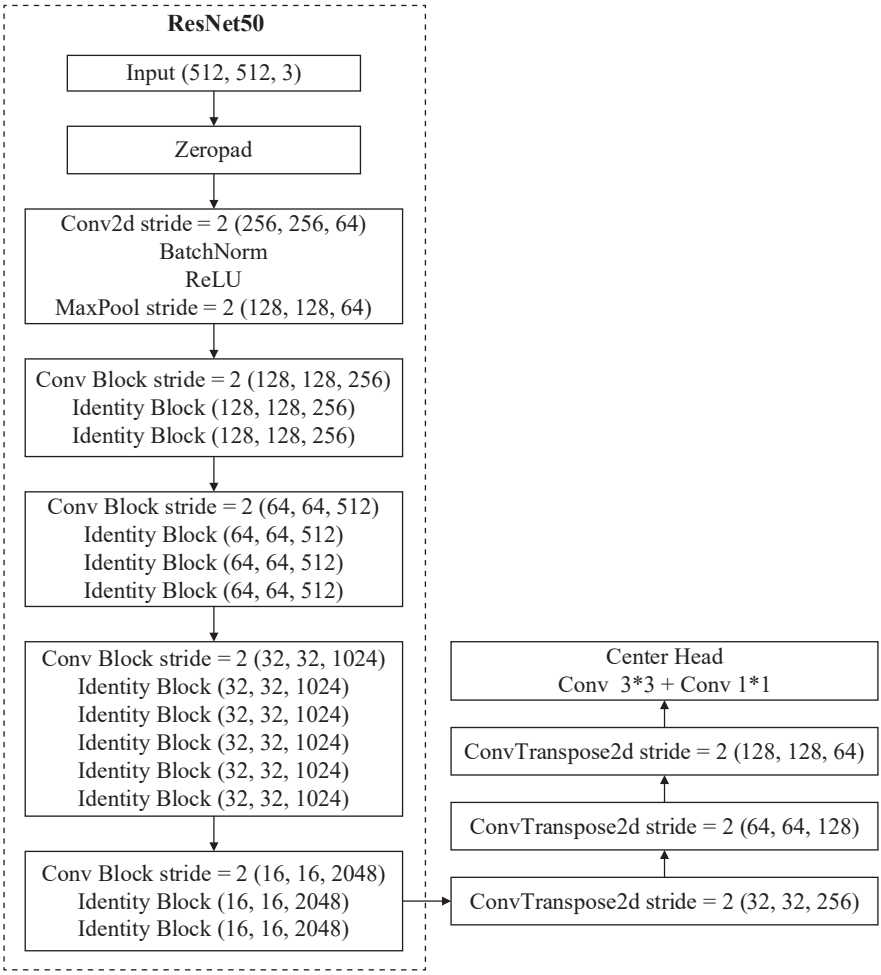

Fig. 19.6 Architecture of CenterNet

Then after the decoding process. The final prediction results can be obtained, and score sorting and nonmaximum inhibition screening shall be carried out. Finally, draw bounding boxes on the original image.

19.2.4 Evaluation Metrics for Object Detection Model

The task of object detection is to find out all the objects of interest in the image and determine their position, size, and type. Since it is necessary to evaluate the quality of the detection model, several common evaluation indicators such as Intersection

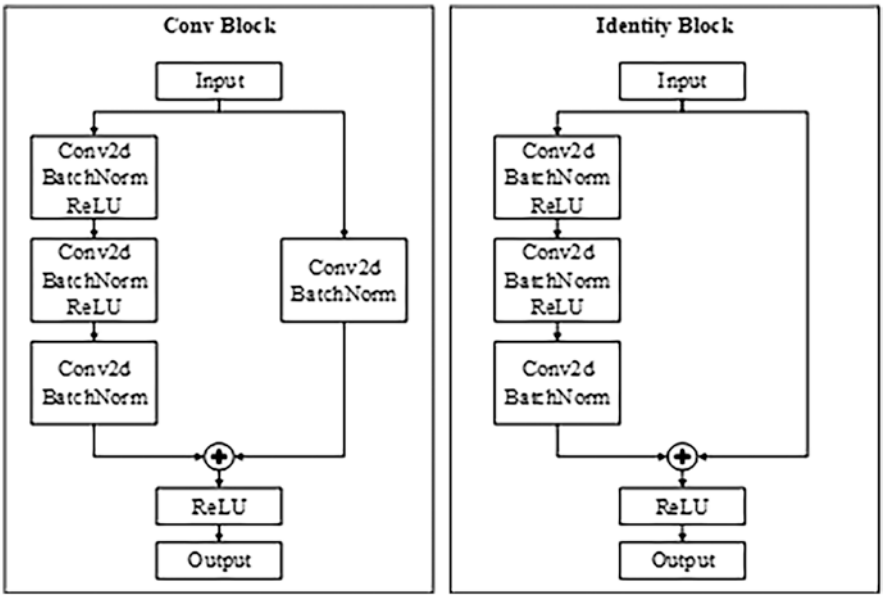

Fig. 19.7 Architecture of conv block and identity block

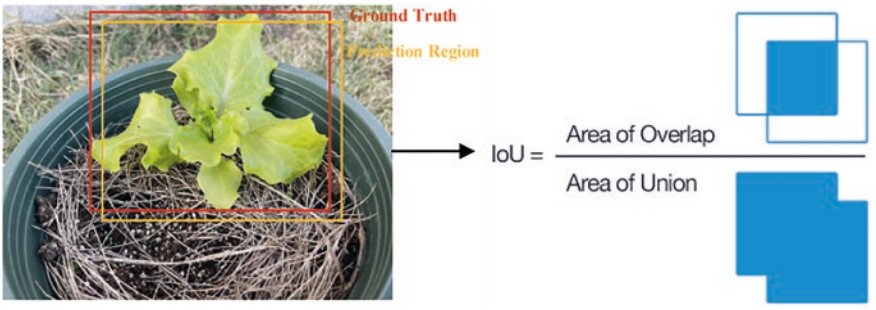

Fig. 19.8 Schematic diagram of IoU definition

over Union (IoU), Precision, Recall, F-score, Average Precision (AP), and mean average Precision (mAP) were selected in this study.

IoU is a number that quantifies the degree of overlap between two boxes (Fig. 19.8). In the case of object detection and segmentation, IoU evaluates the overlap of the ground truth and prediction region. Generally, if IoU ≥ 0.5, the prediction result is acceptable.

Precision and recall are two important indicators to evaluate object detection models. Precision is defined as how many of the samples predicted to be positive are true positive samples, which is based on prediction results. Precision reflects the model's ability to distinguish negative samples. The higher the precision, the stronger the model's ability to distinguish negative samples. The definition of recall is

how many true positive examples in the sample are predicted correctly, which is based on samples. Recall reflects the model's ability to identify positive samples. The higher the recall, the stronger the model's ability to identify positive samples. F-score, also called F1 score, is a weighted average of precision rate and recall rate. F-score is a combination of the two. The higher the F-score, the more robust the model. The general definition of the average precision is the area under the precision-recall curve. mAP is the average of AP. The equations for precision, recall, F-score, AP, and mAP are shown below.

$$\text{precision} = \frac{TP}{TP + FP} \tag{19.3}$$

$$\text{recall} = \frac{TP}{TP + FN} \tag{19.4}$$

$$F_1 = \frac{2}{\frac{1}{\text{recall}} + \frac{1}{\text{precision}}} \tag{19.5}$$

$$\text{TP} = \text{True Positive}, \text{FP} = \text{Flase Positive}, \text{FN} = \text{False Negative} \tag{19.6}$$

$$AP = \int_{r=0}^{1} p(r)\,dr \tag{19.7}$$

$$p(r) = \text{precision} \quad \text{recall curve} \tag{19.8}$$

$$mAP = \frac{\sum_{i-1}^{k} AP_i}{k} \tag{19.9}$$

$$AP_{\text{i}} = \text{the AP of class i}, k = \text{the number of classes} \tag{19.10}$$

19.2.5 *Fuzzy PID Control Algorithm*

The proportional Integral Derivative (PID) feedback control algorithm is widely used in industrial process control systems because of its simple structure and robust performance (Heidari & Khodadadi, 2017). The typical PID algorithm formulas are shown in Eqs. 19.11 and 19.12.

$$u(t) = K_p e(t) + K_i \int_0^t e(t)\,dt + K_d \frac{de(t)}{dt} \tag{19.11}$$

$$e(t) = r(t) - y(t) \tag{19.12}$$

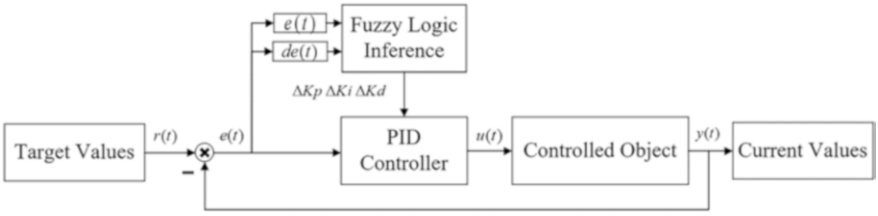

Fig. 19.9 Architecture of fuzzy PID controller

In a greenhouse, the environmental parameters change over time (t). r(t) is the target environmental parameter. y(t) is the current environmental parameter from sensors. Therefore e(t) is a system error. u(t) is a linear combination of system error in proportion, integral, and differential. Which means the power of the control actuator. K_p, K_i, K_d are the gains of each part.

If the PID control algorithm is required to have good performance, the key is to set the appropriate K_p, K_i, K_d parameters. If the controlled object has a specific mathematical model, it is easy to calculate each parameter by mathematical analysis. However, the greenhouse system is an ill-defined, nonlinear and time-varying controlled object and it is hard to get the specific mathematical model of the controlled object.

The fuzzy PID control algorithm imitates the experience of an expert controlling the system, instead of relying on the specific mathematical model of the controlled object. It can realize self-tuning of PID parameters with the change of controlled objects based on a knowledge base that contains membership functions and fuzzy logistic rules. Therefore, this study used a fuzzy PID control algorithm to control the environmental parameters in the greenhouse (Fig. 19.9).

The input of fuzzy PID is system error e(t), the change rate of system error de(t). These are all specific figures that represent the conditions of a controlled object. In a fuzzy interface, the specific figures are changed into linguistic variables and corresponding degrees of membership functions. The inference engine selects the optimal control rules by using the linguistic variables and corresponding membership degrees from the knowledge base and then gets the fuzzy values of K_p, K_i, and K_d. Finally output the specific figures of K_p, K_i, and K_d by the fuzzy interface.

19.3 Results

19.3.1 System Architecture

The overall structure of the control system for the greenhouse was divided into three subsystems (Fig. 19.10):

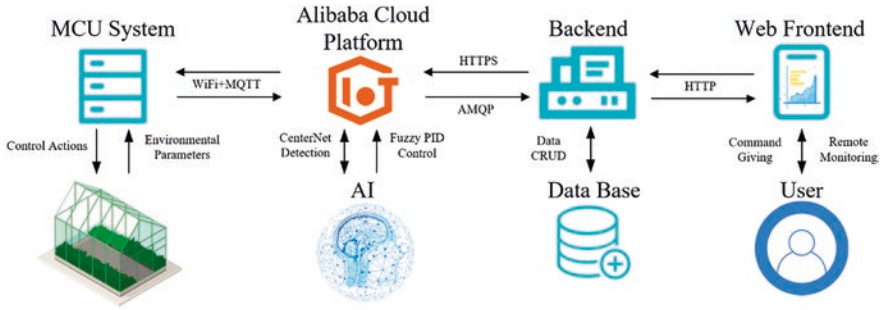

Fig. 19.10 Architecture of the AI-IoT-based environmental parameter control system

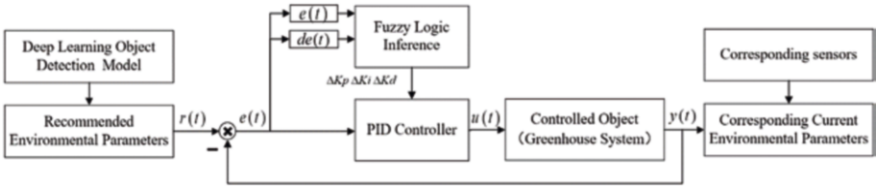

Fig. 19.11 Architecture of AI control system

Embedded System: The embedded system is the thing of IoT and was deployed in the greenhouse. It consisted of a main controller (STM32L475VE), a Wi-Fi module, sensors module (humidity, moisture, light intensity, and temperature), and a control actuator module (water pump, LED light, fan, humidifier).

Cloud System: The cloud system is the internet of IoT. It includes cloud platform, backend system, and front-end system. The cloud platform was used to transform data and connect to other systems. The back-end system was used to store data from the cloud platform and front-end system and respond data to front-end system and cloud platform. The front-end system was used to show data to users on a website.

AI System: The AI system was used to detect the growth stage of leaf lettuce and control the environmental parameters of the greenhouse. In the detection system, this study compared CenterNet and YOLOv3. In a control system, this study compared normal control, traditional PID control, and fuzzy PID control (Fig. 19.11).

19.3.1.1 Embedded System Design

The embedded system was composed of a main controller, communication module, sensor module, control actuator module, and other peripherals. STM32L475VET6 was the main controller of the embedded system. ATK-ESP8266 Wi-Fi module was

the communication module, which was used to connect the embedded system to the cloud system, and the network application layer transport protocol was MQTT. The sensors module consisted of a temperature and humidity sensor (AHT10), light intensity sensor (BH1750FVI), and soil moisture sensor (FC-28), which was used to collect environmental parameters in the greenhouse. The controller actuator module consisted of a water pump, LED light, fan, and humidifier, which was used to control environmental parameters in the greenhouse.

AHT10 is the temperature and humidity sensor that was used in this research. The sensor is based on the Inter-Integrated Circuit (IIC) communication protocol. BH1750FVI is a light intensity sensor used for the system and is also based on the IIC communication protocol. It is possible to detect a wide range at high resolution and the resolution has three different modes. FC-28 is the moisture sensor used in the system and is based on Analog to Digital Converter (ADC). FC-28 sensor has two probes, which are based on resistance. When the soil moisture changes, the resistance of the probes changes, and the data acquisition circuit outputs different analog voltages. The control module system had four control actuators: a water pump, an LED lamp, a fan, and a humidifier. The system used the L298N motor drive module and STM32 chips to output the Pulse Width Modulation (PWM) wave to control the power of the control actuators.

19.3.2 Monitoring Web Pages of IoT System

The IoT monitoring pages were mainly composed of two pages: the greenhouse environment parameter monitoring page and the greenhouse AI live broadcast page (Fig. 19.12). On the environmental parameters page, the user can monitor the real-time greenhouse parameters remotely. The plant's growth progress can be monitored from the live stream page.

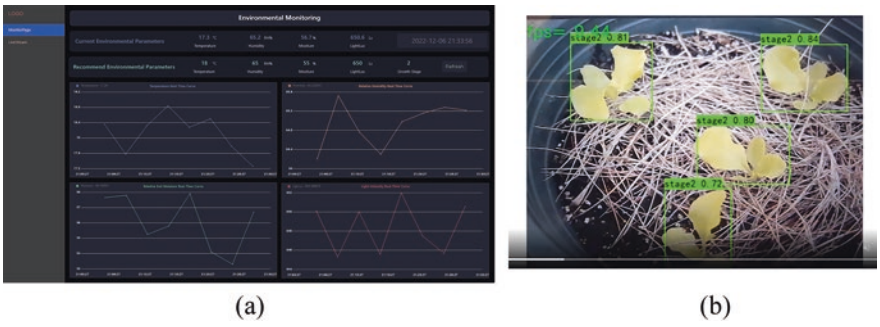

Fig. 19.12 Web pages of AI-based IoT greenhouse system (**a**) greenhouse environment parameter monitoring page and (**b**) the greenhouse AI live broadcast page

19.3.3 Object Detection Experiment Results

19.3.3.1 Object Detection System Design

In this study, 600 lettuce images were collected from October 8 to December 9, 2021. According to the size of the lettuces, the images were divided into four different growth stages for model training purposes. CenterNet and YOLOv3 were trained for 100 epochs, and the epoch with the smallest loss was deployed in the system as the final model. The training loss of YOLOv3 and CenterNet is shown in Fig. 19.13 respectively.

19.3.3.2 Images Results of Growth Stage Detection

This study used an anchor-based object detection YOLOv3 model and a nonanchor-based object detection CenterNet model to detect the growth stage of leaf lettuce. The user can also determine the recommended environmental parameters according to the AI growth stage detection system. Figures 19.14 and 19.15 show the detection images from YOLOv3 and CenterNet model in a soil system respectively. The research also deployed the object detection system to the hydroponics system to test whether the object detection system could correctly detect the growth stage of lettuce in the hydroponics system. The experiment in a hydroponics system was conducted for two weeks, and only growth stage 1 was detected. Figure 19.16 shows the detection images from the YOLOv3 and CenterNet model in the hydroponics system respectively.

The obtained results, show that YOLOv3 had difficulties detecting lettuce in growth stages 1 and 3. The detection accuracy in growth stages 2 and 4 is also relatively low. On the other hand, CenterNet can detect almost all the leaf lettuces corresponding to all growth stages, and the accuracy was higher than YOLOv3.

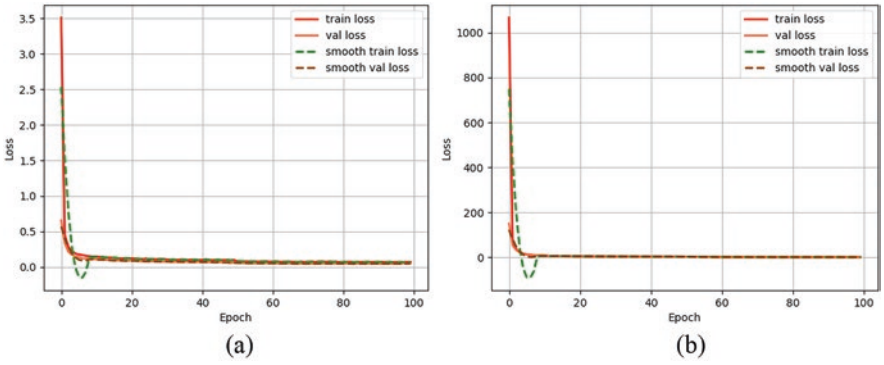

Fig. 19.13 Training loss of (**a**) YOLOv3, (**b**) CenterNet for 100 epochs

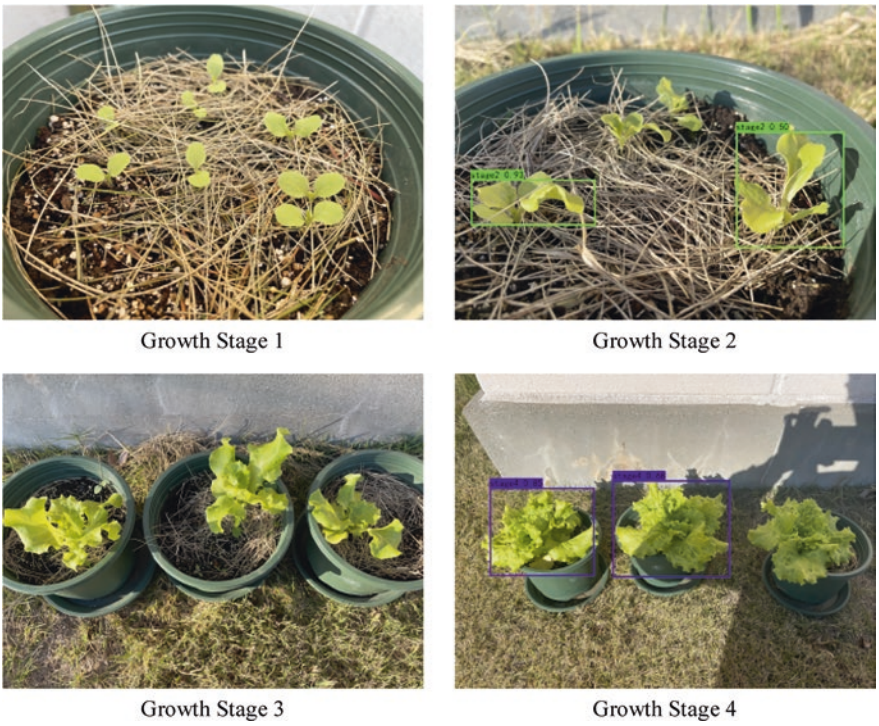

Fig. 19.14 Growth stage detection images of YOLOv3 in the soil system

19.3.3.3 Performance Comparison

Figures 19.17, 19.18, 19.19 and 19.20 show F1 curves of CenterNet and YOLOv3 in detection of different growth stages for leaf lettuce. The results show when the threshold is 0.5, the F1 of CenterNet is better than YOLOv3 in the detection of all growth stages.

Figures 19.21, 19.22, 19.23, 19.24 and 19.25 show the AP and mAP curves of CenterNet and YOLOv3 in the detection of different growth stages for leaf lettuce. The results show the mAPs of CenterNet were 1.0, 0.98, 1.0, and 1.0 from growth stage 1 to growth stage 4. The mAPs of YOLOv3 were 0.43, 0.75, 0.85, and 0.99 from growth stage 1 to growth stage 4. The results indicate that the mAP of CenterNet was better than YOLOv3 in the detection of all growth stages, even in the detection of small objects.

In conclusion, the detection performance of YOLOv3 and CenterNet for the lettuce growth stage was analyzed based on Precision, Recall, F1, AP, and mAP. The results show that the nonanchor-based CenterNet model performed better than the anchor-based YOLOv3 model in terms of leaf lettuce growth stage detection from the above indicators.

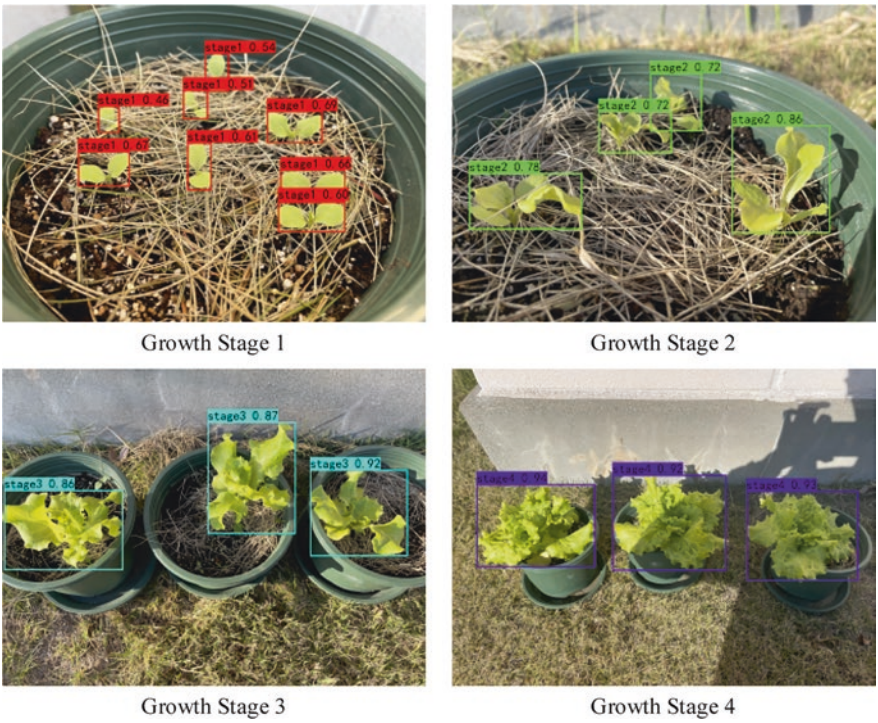

Fig. 19.15 Growth stage detection images of CenterNet in the soil system

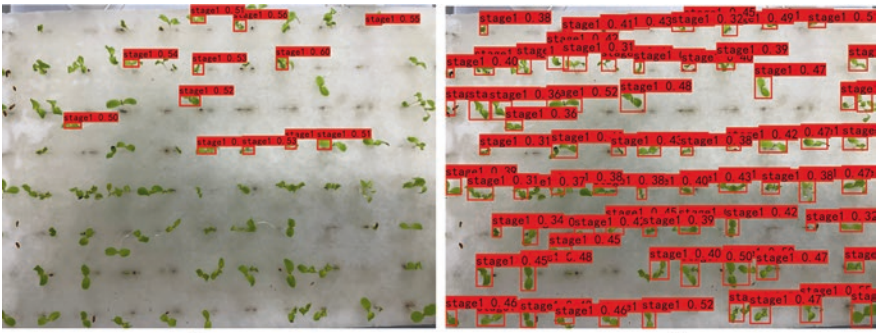

Fig. 19.16 Growth stage detection images of (**a**) YOLOv3, (**b**) CenterNet in hydroponics system

19.3.4 Control Experiment Results

19.3.4.1 Humidity Control Experiment Results

Figure 19.26 shows the error changes in humidity control experiments. Figure 19.27 shows K_p, K_i, K_d parameters change of humidity fuzzy PID control experiment.

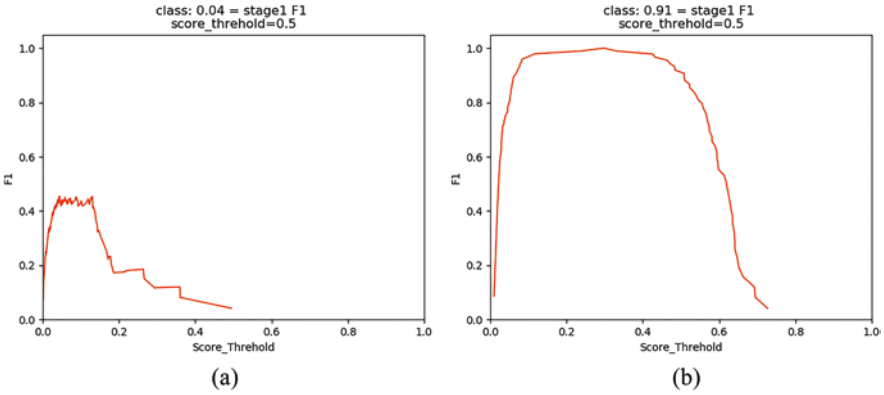

Fig. 19.17 F1 curve of (**a**) YOLOv3, (**b**) CenterNet for growth stage 1 detection

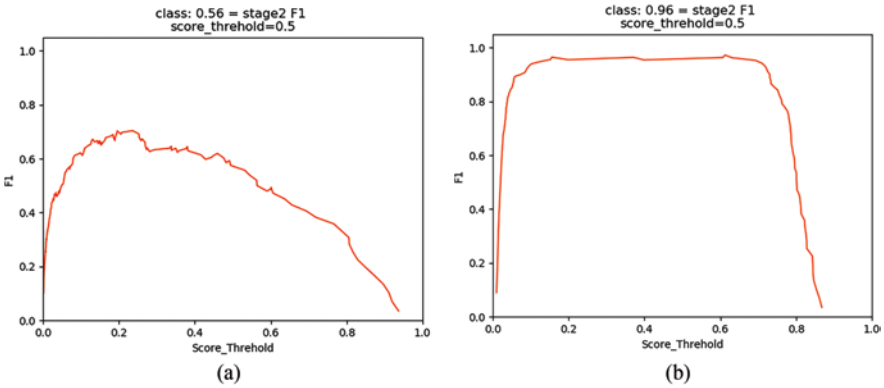

Fig. 19.18 F1 curve of (**a**) YOLOv3, (**b**) CenterNet for growth stage 2 detection

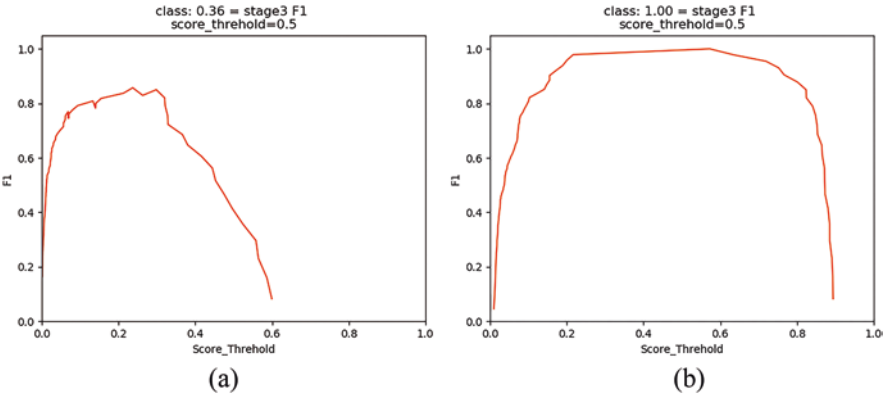

Fig. 19.19 F1 curve of (**a**) YOLOv3, (**b**) CenterNet for growth stage 3 detection

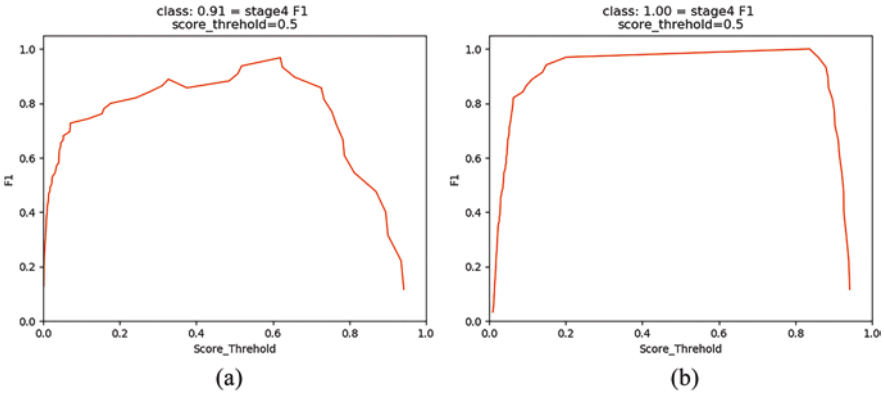

Fig. 19.20 F1 curve of (**a**) YOLOv3, (**b**) CenterNet for growth stage 4 detection

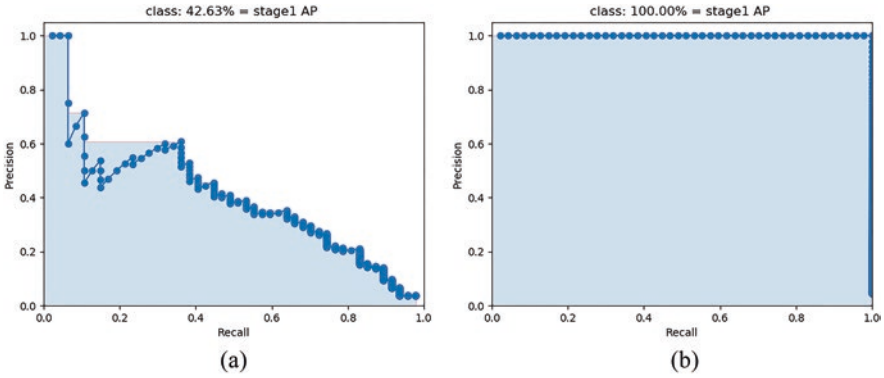

Fig. 19.21 AP curve of (**a**) YOLOv3, (**b**) CenterNet for growth stage 1 detection

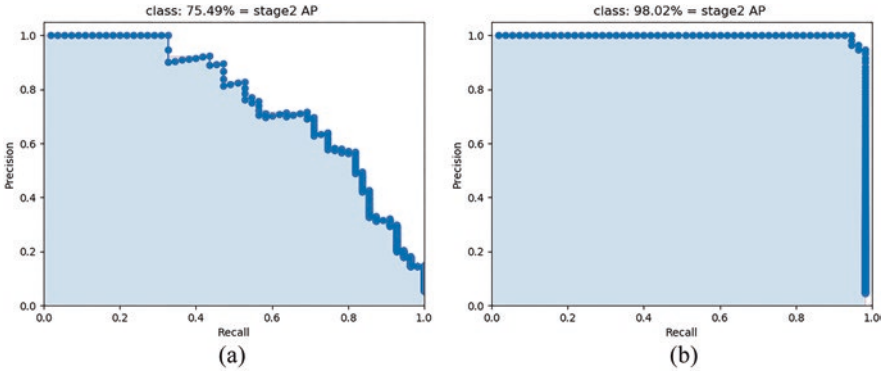

Fig. 19.22 AP curve of (a) YOLOv3, (b) CenterNet for growth stage 2 detection

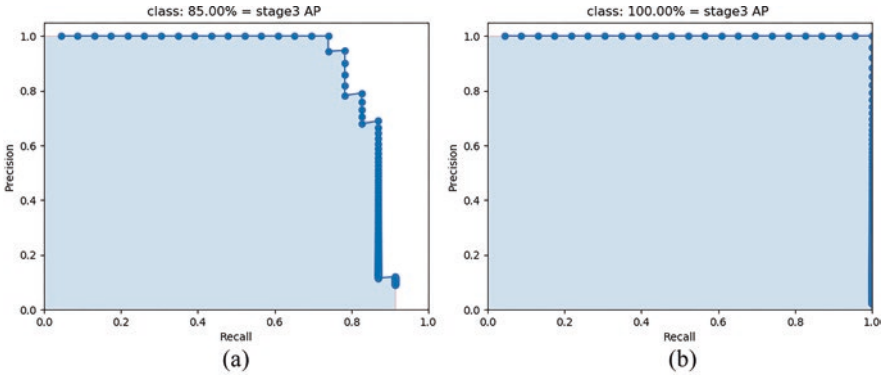

Fig. 19.23 AP curve of (**a**) YOLOv3, (**b**) CenterNet for growth stage 3 detection

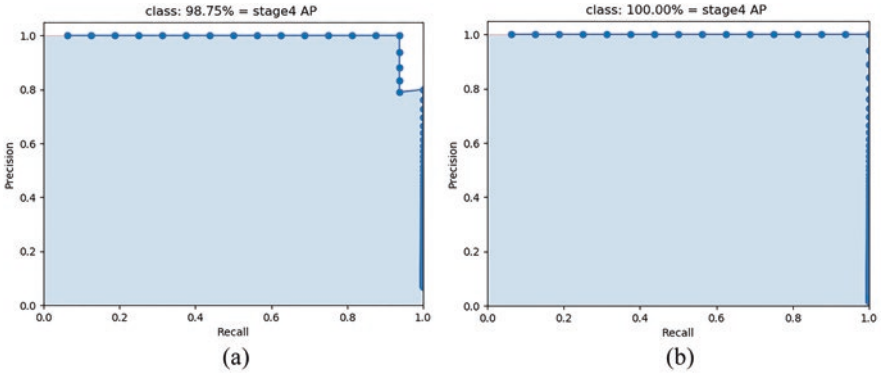

Fig. 19.24 AP curve of (**a**) YOLOv3, (**b**) CenterNet for growth stage 4 detection

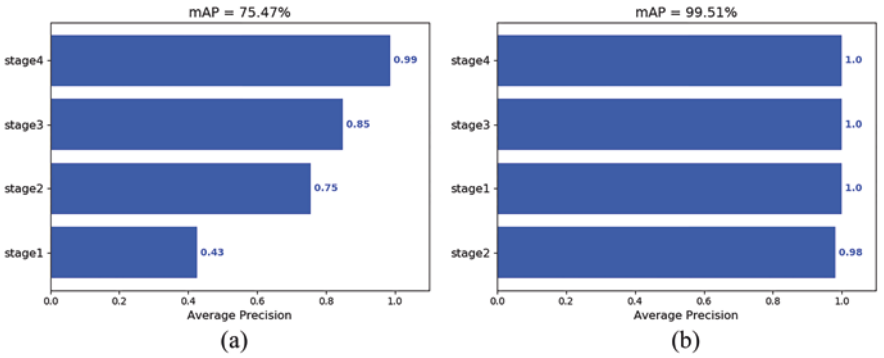

Fig. 19.25 mAP of (**a**) YOLOv3, (**b**) CenterNet for growth stage detection

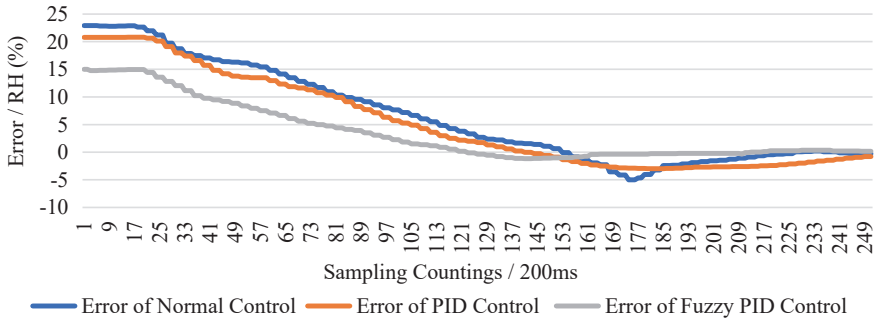

Fig. 19.26 Error change of humidity control experiments

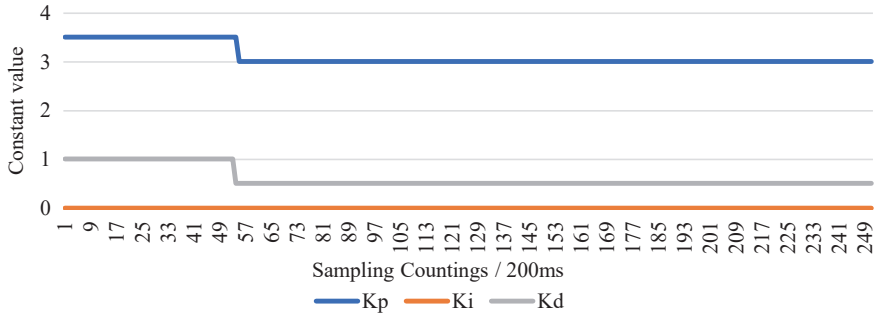

Fig. 19.27 K_p, K_i, K_d parameters change of humidity in fuzzy PID control experiment

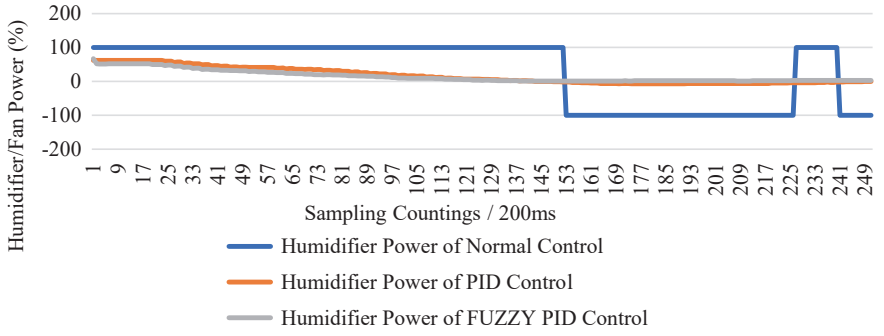

Fig. 19.28 Humidifier/fan power change of humidity automatic control experiments

Figure 19.28 shows the humidifier/fan power change of humidity control experiments. Table 19.1 shows the parameters of the controller in the humidity control experiments. In the experiments, the target humidity was to control the current humidity to 65% RH. The results show that the fuzzy PID controller had the minimum overshoot. In a steady state, the fuzzy PID had the minimum error oscillation.

Table 19.1 Parameters of controller in humidity control experiments

Parameters of control experiment	Values
Target humidity	65% RH
Initial K_p	3
Initial K_i	0.001
Initial K_d	1
Offset of ΔK_p in fuzzy controller	0
Offset of ΔK_i in fuzzy controller	0
Offset of ΔK_d in fuzzy controller	0
Boost of ΔK_p in fuzzy controller	0.5
Boost of ΔK_i in fuzzy controller	0.001
Boost of ΔK_d in fuzzy controller	0.5
Boost of domain in fuzzy controller	50
Offset of domain in fuzzy controller	0

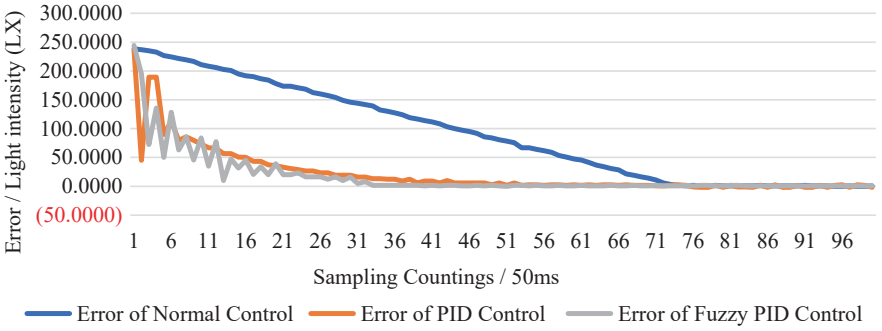

Fig. 19.29 Error change of light intensity control experiments

Therefore, the fuzzy PID controller had the highest robustness in humidity control experiments.

19.3.4.2 Light Intensity Control Experiment Results

Figure 19.29 shows error changes in light intensity control experiments. Figure 19.30 shows Kp, Ki, and Kd parameters change of light intensity fuzzy PID control experiment. Figure 19.31 shows LED light power change of light intensity control experiments. Table 19.2 shows the parameters of the controller in the light intensity control experiments. In this experiment, the target light intensity remained at 600 lx. The results show that all the controllers had very small overshoots. In a steady state, all the controllers had very small error oscillation. However, the fuzzy controller was the fastest one to reach the steady state. Although all controllers had good robustness, in terms of control speed, the fuzzy controller was still the best controller in light intensity control experiments.

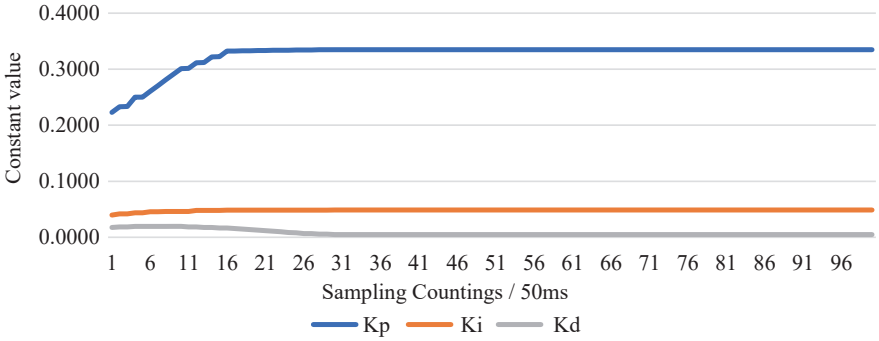

Fig. 19.30 K_p, K_i, K_d parameters change of light intensity in fuzzy PID control experiment

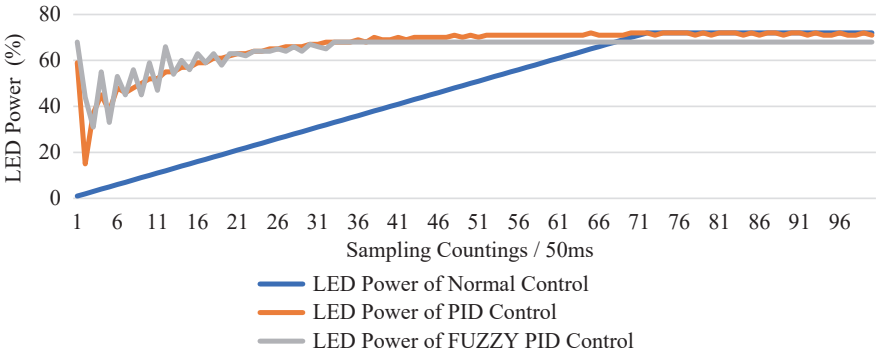

Fig. 19.31 LED light power change of light intensity control experiments

Table 19.2 Parameters of controller in light intensity control experiments

Parameters of control experiment	Values
Tagert light intensity	600 lx
Initial *Kp*	0.2
Initial *Ki*	0.035
Initial *Kd*	0.015
Offset of Δ*Kp* in fuzzy controller	0
Offset of Δ*Ki* in fuzzy controller	0
Offset of Δ*Kd* in fuzzy controller	0
Boost of Δ*Kp* in fuzzy controller	0.01
Boost of Δ*Ki* in fuzzy controller	0.002
Boost of Δ*Kd* in fuzzy controller	0.001
Boost of domain in fuzzy controller	250
Offset of domain in fuzzy controller	0

19.3.4.3 Soil Moisture Control Experiment Results

Figure 19.32 shows error changes of soil moisture control experiments. Figure 19.33 shows the Kp, Ki, and Kd parameters change of soil moisture fuzzy PID control experiment. Figure 19.34 shows the water pump power change of soil moisture control experiments. Table 19.3 shows the parameters of the controller in the soil moisture control experiments. The target was to control the current soil moisture to 65% in the experiments. The results show that the fuzzy PID controller has the minimum overshoot. In a steady state, the fuzzy PID had the minimum error oscillation. Therefore, the fuzzy PID controller had the highest robustness in soil moisture control experiments.

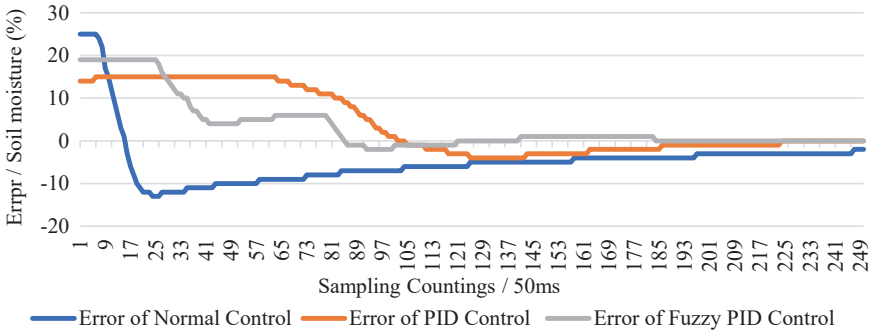

Fig. 19.32 Error change of soil moisture control experiments

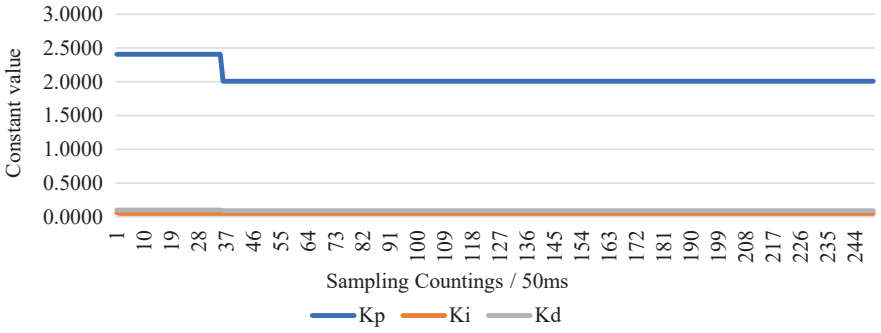

Fig. 19.33 Kp, Ki, Kd parameters change of soil moisture of fuzzy PID control experiment

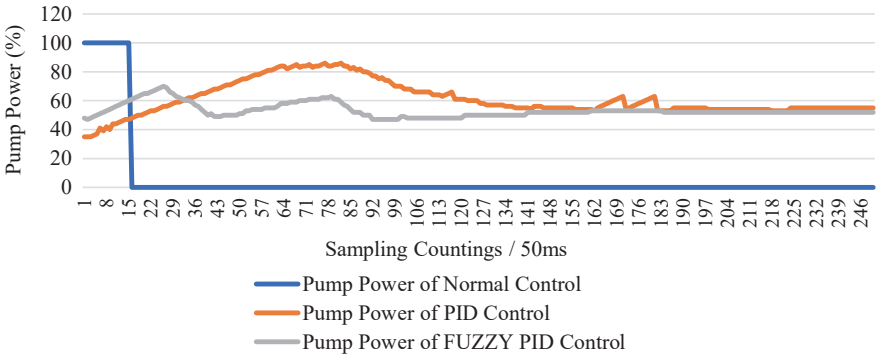

Fig. 19.34 Water pump power change of soil moisture control experiments

Table 19.3 Parameters of controller in soil moisture control experiments

Parameters of control experiment	Values
Tagert soil moisture	65%
Initial *Kp*	3
Initial *Ki*	0.001
Initial *Kd*	1
Offset of Δ*Kp* in fuzzy controller	0
Offset of Δ*Ki* in fuzzy controller	0
Offset of Δ*Kd* in fuzzy controller	0
Boost of Δ*Kp* in fuzzy controller	0.5
Boost of Δ*Ki* in fuzzy controller	0.001
Boost of Δ*Kd* in fuzzy controller	0.5
Boost of domain in fuzzy controller	50
Offset of domain in fuzzy controller	0

19.4 Conclusions

In this study, an AI-based IoT greenhouse control system for environmental parameters was built by the author. IoT was used to connect the greenhouse to the internet so that users could monitor the greenhouse remotely and conveniently. AI was used to detect the plant's growth stage and control the greenhouse environmental parameters. In terms of plant detection, this study used a nonanchor-based object detection CenterNet model and anchor-based object detection YOLOv3 model to detect the growth stage of leaf lettuce and then recommended suitable environmental parameters to the corresponding plant's growth stage. In this study, the growth stage of lettuce was divided into four stages. The results show the mAPs of CenterNet were 1.0, 0.98, 1.0, and 1.0 from growth stage 1 to growth stage 4. The mAPs of YOLOv3 were 0.43, 0.75, 0.85, and 0.99 from growth stage 1 to growth stage 4. Therefore, the performance of CenterNet was better than YOLOv3. In terms of environmental parameters control, this study compared the performance of normal control, typical

PID control algorithm, and fuzzy PID control algorithm to control current environmental parameters to the recommended environmental parameters. The results show fuzzy PID control algorithm had the lowest overshoot and highest robustness.

However, this developed AI-based IoT greenhouse system is limited only to detecting the growth stage of leaf lettuce which was determined by the user. The system was also limited only to control light intensity, soil moisture, and humidity of the greenhouse. Therefore, this system can be improved from the following aspects in the future: (i) Collect images of different kinds of plants to train the model so that AI can detect other kinds of plants. (ii) Add more control rules, sensors, and control actuators so that the embedded system can control other kinds of environmental parameters. (iii) Cooperate with agricultural experts to set appropriate growth stages and corresponding environmental parameters for plants.

References

Abdulrhman, U. (2000). *Using proportional integral derivative and fuzzy logic with optimization for greenhouse climate control*. University of Idaho.

Alaviyan, Y. M., Aghaseyedabdollah, M. S., & Yazdizade, A. (2020). Design and manufacture of a smart greenhouse with supervisory control of environmental parameters using fuzzy inference controller. In *2020 6th Iranian Conference on Signal Processing and Intelligent Systems (ICSPIS)* (pp. 1–6). ICSPIS. https://doi.org/10.1109/ICSPIS51611.2020.9349619

Duan, K., Bai, S., Xie, L., Qi, H., Huang, Q., & Tian, Q. (2019). CenterNet: Keypoint triplets for object detection. In *2019 IEEE/CVF International Conference on Computer Vision (ICCV)* (pp. 6568–6577). IEEE. https://doi.org/10.1109/ICCV.2019.00667

Eridani, D., Martono, K. T., & Hanifah, A. A. (2019). MQTT performance as a message protocol in an IoT based chili crops greenhouse prototyping. In *2019 4th International Conference on Information Technology, Information Systems and Electrical Engineering (ICITISEE)* (pp. 184–189). ICITISEE. https://doi.org/10.1109/ICITISEE48480.2019.9003975

Girshick, R., Donahue, J., Darrell, T., & Malik, J. (2014). Rich feature hierarchies for accurate object detection and semantic segmentation. In *Proceedings of the IEEE conference on computer vision and pattern recognition* (pp. 580–587). IEEE.

Glorot, X., Bordes, A., & Bengio, Y. (2011). Deep sparse rectifier neural networks. In *Proceedings of the fourteenth international conference on artificial intelligence and statistics*. JMLR Workshop and Conference Proceedings.

He, K., et al. (2016). Deep residual learning for image recognition. In *Proceedings of the IEEE conference on computer vision and pattern recognition*. IEEE. https://doi.org/10.48550/arXiv.1512.03385

Heidari, M., & Khodadadi, H. (2017). Climate control of an agricultural greenhouse by using Fuzzy logic self-tuning PID approach. In *2017 23rd International Conference on Automation and Computing (ICAC)* (pp. 1–6). https://doi.org/10.23919/IConAC.2017.8082074

Kavitha, L. R., & Savarimuthu, N. (2021). Investigation on object detection models for plant disease detection framework. In *2021 IEEE 6th international conference on computing, Communication and Automation (ICCCA)* (pp. 214–218). ICCCA. https://doi.org/10.1109/ICCCA52192.2021.9666441

Liu, S., Zhou, H., Li, C., & Wang, S. (2020). Analysis of anchor-based and anchor-free object detection methods based on deep learning. In *IEEE International Conference on Mechatronics and Automation (ICMA)* (pp. 1058–1065). IEEE. https://doi.org/10.1109/ICMA49215.2020.9233610

Maas, A. L., Hannun, A. Y., & Andrew, Y. N. (2013). Rectifier nonlinearities improve neural network acoustic models. *Proc icml, 30*(1), 3.

Redmon, J., Divvala, S., Girshick, R., & Farhadi, A. (2016). You only look once: Unified, real-time object detection. In *IEEE Conference on Computer Vision and Pattern Recognition (CVPR)* (pp. 779–788). CVPR. https://doi.org/10.1109/CVPR.2016.91

Redmon, J., & Farhadi, A.. (2018). "*Yolov3: An incremental improvement*." arXiv preprint arXiv:1804.02767.

Ruishi, L., Yuhang, S., Xiaojia, Z., & Miao, X. (2021). The agricultural greenhouse management platform based on IoT and SSM architecture. In *International Conference on Machine Learning and Intelligent Systems Engineering (MLISE)* (pp. 335–338). MLISE. https://doi.org/10.1109/MLISE54096.2021.00070

Sharma, C., & Gondhi, N. K. (2018). Communication protocol stack for constrained IoT systems. In *2018 3rd International Conference On Internet of Things: Smart Innovation and Usages (IoT-SIU)* (pp. 1–6). IoT-SIU. https://doi.org/10.1109/IoT-SIU.2018.8519904

Sudha, C., JaganMohan, K., & Arulaalan, M. (2022). Real time Riped fruit detection using faster R-CNN deep neural network models. In *International Conference on Smart Technologies and Systems for Next Generation Computing (ICSTSN)* (pp. 1–4). ICSTSN. https://doi.org/10.1109/ICSTSN53084.2022.9761356

Tantitharanukul, N., Osathanunkul, K., Hantrakul, K., Pramokchon, P., & Khoenkaw, P. (2017). MQTT-topics management system for sharing of open data. In *2017 International Conference on Digital Arts, Media and Technology (ICDAMT)* (pp. 62–65). ICDAMT. https://doi.org/10.1109/ICDAMT.2017.7904935

Vishwakarma, S. K., Upadhyaya, P., Kumari, B., & Mishra, A. K. (2019). Smart energy efficient home automation system using IoT. In *2019 4th international conference on internet of things: Smart Innovation and usages (IoT-SIU)* (pp. 1–4). IoT-SIU. https://doi.org/10.1109/IoT-SIU.2019.8777607

Yang, J., Xu, Z., & Sun, Q. (2021). Research and design of greenhouse environment monitoring system based on NB-IoT. In *2021 33rd Chinese Control and Decision Conference (CCDC)* (pp. 5641–5646). CCDC. https://doi.org/10.1109/CCDC52312.2021.9601377

Zhao Hua-fei, X. U., & Jian, Z. N. (2019). Design of Agricultural Internet of things server system based on Netty. *Modern Agricultural Science and Technology, 9*, 254–255.

Chapter 20
Enhancement of Cottage Mushroom Cultivation in Tropical and Subtropical Regions with IoT and AI Applications

Abstract Commercial mushroom cultivation at the cottage level is a popular form of self-employment in rural areas of many tropical and subtropical countries. Although large-scale mushroom production is adequately mechanized and advanced, cottage-level cultivation has received insufficient attention. As living organisms are involved, continuous and careful human attention is imperative in mushroom cultivation to ensure optimal living conditions and superior output. Furthermore, many stages in the production process are carried out manually, resulting in high production costs, subpar sanitation, and, ultimately, an inability to sustain the enterprise. Human involvement can have detrimental effects in various aspects of mushroom cultivation, can be reduced through suitable mechanization and automation, along with the application of artificial intelligence (AI), and IoT technologies. Substrate preparation and filling transparent polythene bags are among the most labor-intensive activities of oyster mushroom cultivation. When sawdust is used as the main ingredient of the substrate, the separation of the finer particles through sieving and use in the mixture will improve the growth of mycelium by promoting the decomposition. Therefore, an integrated continuous operating system with sawdust sieving, ingredient mixing, and mixture filling into polythene bags was introduced to improve productivity by reducing time and labor. The actual capacities of sieving, mixing, and filling machines were 200 kg/h, 300 kg/h, and 81 bags/h, respectively. Sterilization of the prepared substrate is crucial to avoid the growth of uneconomical fungi available in raw material. The centralized steam sterilization system is possible to develop with automation and IoT technology to increase its performance and reduce human involvement. The new system can maintain the required conditions accurately throughout the process. As the total duration of the process is more than 4 h, operation and monitoring with IoT allow farmers to engage in other activities. Maintaining the optimum environmental conditions during the different growth stages of mushrooms is essential to achieve the maximum possible yield by avoiding disease and stress conditions. The integration of IoT technology facilitates continuous real-time monitoring of conditions within the mushroom shed and allows for remote operation of controlling systems. This capability reduces the need for frequent entry into the shed, thereby minimizing the risk of contamination. Moreover, the development of an AI system for the

© The Author(s), under exclusive license to Springer Nature Singapore Pte Ltd. 2024

T. Ahamed, *IoT and AI in Agriculture*,
https://doi.org/10.1007/978-981-97-1263-2_20

accurate detection of the optimal harvesting stage and the implementation of mechanical harvesting processes can further reduce human involvement. In conclusion, the strategic deployment of mechanization, automation, artificial intelligence, and IoT technologies can effectively enhance productivity and efficiency at the cottage-level mushroom industry.

Keywords Artificial intelligence · Automation · IoT · Mechanization · Mushroom cultivation

20.1 Introduction

Addressing the food demand of the growing global population is one of the most challenging problems because the availability of cultivable land is decreasing due to acquiring it for residential and infrastructure purposes. Therefore, there is a growing focus on developing high-yield crops with low costs, short duration crops, and minimum area crops to address this issue. Edible mushrooms, which are the reproductive structures of multicellular fungi, offer a particularly promising food supplement with high productivity and impressive medicinal and nutritional benefits. Although there are more than 74,000 identified mushroom species (Chang & Miles, 2004), only about 2000 species are edible, and 20 species out of them are widely cultivated commercially (Aida et al., 2009). Naturally grown mushrooms have been a part of the human diet for centuries, and efforts have been focused on developing it as an industry due to the rapidly growing demand.

The artificial cultivation of mushrooms represents a profitable agricultural industry that involves various types of fungi, especially for consumption, medicinal and industrial purposes. It is highly popular as a cottage industry in many tropical and subtropical countries, as the prevailing environment of these regions is favorable for mushroom cultivation. However, when cultivating mushrooms in tropical and subtropical regions, several key factors, such as choosing the right mushroom species and growing medium, favorably controlling the temperature, light, and humidity levels, and frequent monitoring and controlling of pests and diseases should be paramount concern. The *Pleurotus* species, or oyster mushrooms, are ideal for commercial cultivation in temperate and subtropical climates and can be grown economically using a variety of substrates, including sawdust, rice straw, crop residues, bagasse, chopped paper, cardboard, and vegetable waste (Sanjel et al., 2021; Shrestha et al., 2021). With a nutrient content of 30–40% protein and 50–60% carbohydrate, as well as speedy preparation times and low technological demands, oyster mushrooms are cultivated worldwide, particularly in Asia, Europe, and Africa (Mandeel et al., 2005).

The artificial cultivation process of mushrooms involves several steps, such as spawn preparation, substrate preparation, disinfection of substrate, inoculation, incubation, upkeeping, and harvesting. The ways of realizing these steps may differ according to the production scale, substrate, availability of machinery, and

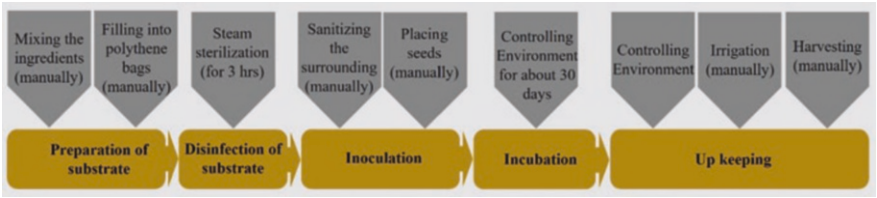

Fig. 20.1 Production process of oyster mushroom at cottage level

labor. As the cottage mushroom cultivation process requires more human involvement, farmers find many difficulties such as more drudgery, high production costs, low sanitation, and inability to keep a continuous production. Figure 20.1 illustrates the production process of *Pleurotus* species (Oyster mushrooms) at the cottage level.

Appropriately mechanizing and automating the labor-intensive tasks in the production process can enhance efficiency and overall productivity by ensuring consistent quality and quantity of mushrooms throughout the year and reducing labor costs. Given the increasing importance of Artificial Intelligence (AI) in the agriculture sector (Abeyrathna et al., 2023), it can be applied in mushroom cultivation to monitor mycelium growth during the incubation period, identify diseases early and accurately, and estimate yields. By utilizing IoT technology, farmers can connect the equipment and machinery used in mushroom cultivation to the internet, thereby reducing contaminations through remote monitoring and operation. It can be applied in mushroom cultivation in monitoring growth of mycelium in incubation period, identifying diseases early and accurately, and estimating yield. Using IoT technology, farmers can connect the equipment and machinery used in mushroom cultivation to the internet so that contaminations can be reduced by remote monitoring and operation. Reducing human involvement improves the sanitation and hygiene of the growing environment, thereby reducing the risk of pest and disease infections (Setiawan et al., 2018).

The aspects emphasized in this chapter include the mechanization of certain labor-intensive tasks, the application of AI for improved management with minimum human involvement, and the use of IoT techniques to reduce the time allocated for care in cottage-level mushroom cultivation in tropical and subtropical countries.

20.2 Oyster Mushroom Production Process at Cottage Level

The mushroom production process involves several unit operations such as spawn production, substrate preparation, substrate disinfection, inoculation, incubation, maintaining, and harvesting. The procedure for each unit operation is determined based on factors such as the type of mushroom, expected production scale, substrate type, technology availability, and environmental conditions. Given that the

cultivation of *Pleurotus* species (Oyster mushroom) on a sawdust substrate is widely practiced at the cottage level, the production process is described accordingly.

Spawn production requires strict hygiene and skill. Spawn is a substance colonized by mushroom mycelium. Disinfected nutrition-rich substrates such as paddy, wheat, rye, and sawdust are commonly used in spawn production. The produced spawns are inoculated into the mushroom substrates to disseminate mushroom mycelium. Although this step is associated with mushroom production, it has gained popularity as a separate business in cottage level.

Substrate preparation is considered the most labor-intensive and time-consuming operation in the entire production process. As the substrate is the material on which the mushrooms grow, it should contain all the necessary nutrients to facilitate the growth of mycelium. Therefore, the primary ingredient should be uniformly and thoroughly mixed with the other ingredients. For example, mix 100 kg of sawdust with 10 kg of rice bran, 2 kg of dolomite, 1 kg of mung bean flour, and 200 g of magnesium sulfate, along with the appropriate amount of water (Wijeratne & Silva, 2012). Mixing is done manually or with some simple tools at the cottage level, which requires a significant amount of time and effort. Once thoroughly blended, the mixture is packed into clear polyethylene bags until they weigh approximately 1 kg. A piece of PVC pipe is used to create a neck at the top of each bag, and a cotton lid is then attached to prepare it for disinfection.

Disinfection of the prepared substrate is the crucial step that demands careful attention to establish the necessary conditions for enhancing the mycelial growth by eliminating pathogenic and competitive microorganisms before introducing the economical fungi (Shrestha et al., 2021). The two techniques used for disinfecting mushroom substrates through heat treatment are pasteurization and sterilization. Pasteurization only partially eliminates harmful microorganisms by exposing the substrate to a temperature of 60 °C for 30 min (Kurtzman Jr, 2010). Sterilization involves heating the substrate to temperatures exceeding 120 °C under a pressure of 151 kPa for 1.5–2.0 h to eliminate nearly all active or dormant pathogens (OGM, 2022). Studies demonstrate that steam sterilization outperforms other sterilization and pasteurization methods for oyster mushroom cultivation (Shrestha et al., 2021).

Inoculation is performed when the substrate reaches room temperature after the disinfection process. In this process, oyster mushroom spawn obtained from a reliable supplier or homemade is introduced to the substrate under hygienic conditions and then sealed. The inoculated substrate should be incubated for a few weeks in a dark and humid environment to allow the mycelium to colonize the substrate and begin to produce fruiting bodies.

After the mycelium has sufficiently colonized the substrate, the polythene bags are opened to allow the fruiting bodies to develop. During this period, careful attention should be given to providing the required environmental conditions such as high humidity and cool temperatures for proper fruiting. After a few days of pinhead initiation, harvesting should be done carefully.

20.3 Mechanization and Automation of the Substrate Preparation

Maintaining continuous production is crucial in the artificial cultivation of mushroom as a business. The short lifespan of mushroom and the limited available nutrients in the substrate determine the economic life of a mushroom batch, indicating the need for introducing a new batch. Consequently, to ensure profitability, it is necessary to timely replace the older mushroom batch with a new one by maintaining stocks at different growth stages. Therefore, it is important to allocate sufficient time for preparing new substrate while also giving due attention to the necessary routing maintenance tasks involved in the cultivation. Mechanization and automation of highly labor-intensive activities, like substrate preparation, are important for saving time and reducing human involvement. Preparing the substrate involves several activities, such as sieving the sawdust to extract fine particles, mixing the ingredients thoroughly and uniformly, filling them into polythene bags, and preparing for disinfection. Currently, executing all these tasks manually is costly, but automating them with an appropriate mechanical solution will enhance efficiency by reducing time and cost, minimizing human labor, and improving quality, through continuous operation. Although several mechanical methods for some activities are available, there is not any properly evaluated mechanical solution for all the activities in preparation (Suraweera et al., 2020). Figures 20.2, 20.3, and 20.4 give the technical

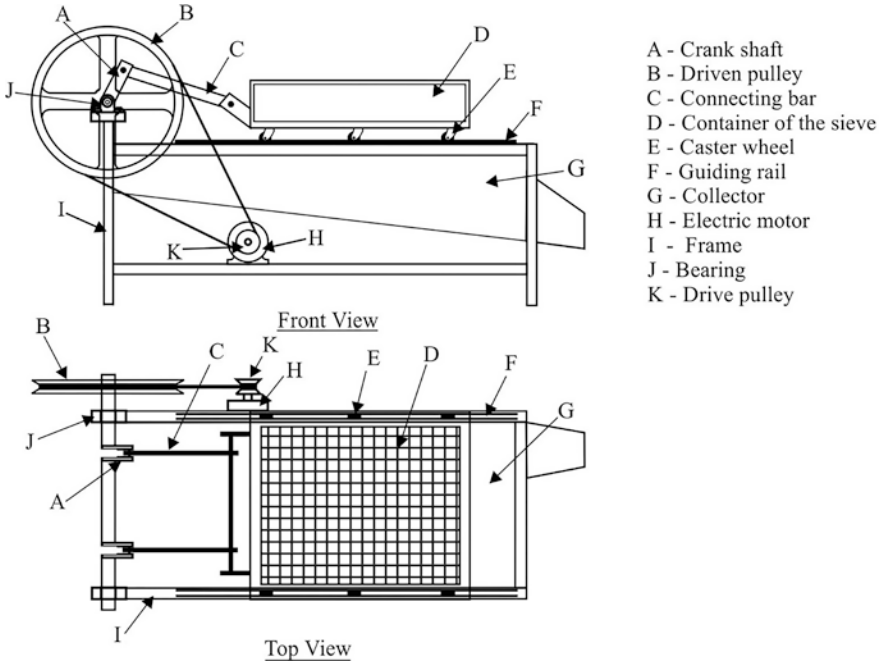

Fig. 20.2 Components and arrangement of the designed sawdust sieving machine

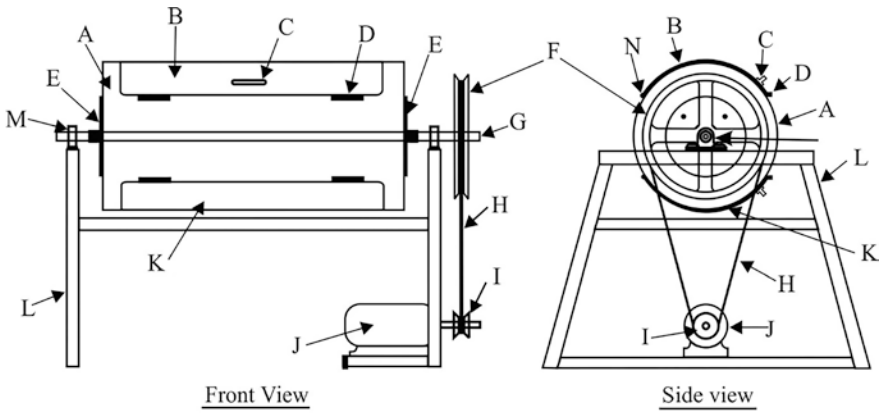

Fig. 20.3 Components and arrangement of the designed ingredient mixing machine

drawings for the sawdust sieving, ingredient mixing, and mixture filling mechanisms, respectively. Figure 20.5 shows the fabricated saw dust sieving machine and Fig. 20.6a shows the fabricated ingredient mixing machine while Fig. 20.6b, c displays the arrangement of the mixing tank. Figure 20.7 shows the fabricated mixture filling machine.

All the proposed machines were developed in the engineering workshop at the Faculty of Agriculture, Rajarata university of Sri Lanka, and were evaluated properly in comparison to the existing manual methods. Materials for components were selected considering their properties. Mild steel was selected for the main frames considering the strength and workability (Kumarasiriwardhana et al., 2020). Stainless steel was chosen for the internal parts of the mixing machine due to its strength, lightness, and corrosion resistance (P. D. Kahandage et al., 2021). Table 20.1 summarizes the important results of the comparison.

According to the results in Table 20.1, a considerable difference can be observed between the mechanical sieving (200 kg/h) with one operator and manual sieving (160 kg/h) with two operators. The results indicated that the machine replaces the labors and lead to time savings. Since, the mechanical sieving method is a continuous process, it takes very less time to refill and unload the residues. But in manual method, after every loading, residues need to be removed, which takes a significant amount of time (Kahandage et al., 2016). Time wastage during the operation of mechanical method is low compared to manual method. Therefore, high efficiency of mechanical sieving can be obtained. A comparison of the results between manual and mechanical mixing is shown in Table 20.2.

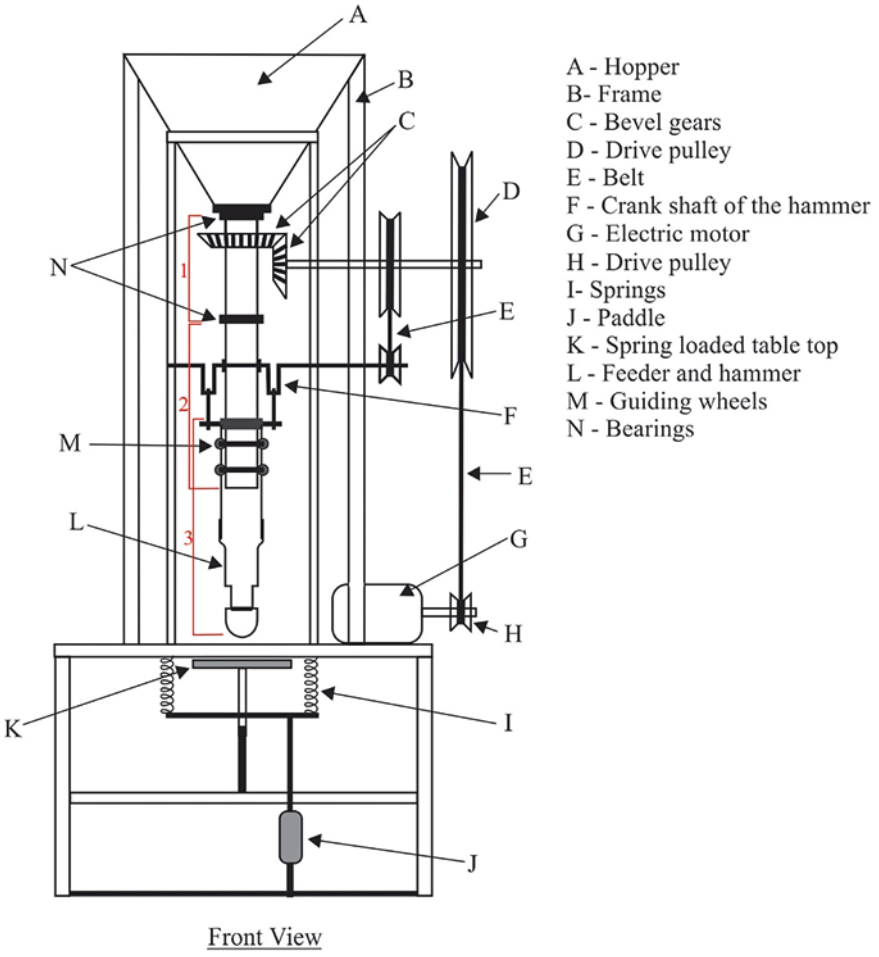

Fig. 20.4 Components and arrangement of the designed mixture filling machine

According to Table 20.2, a considerable difference can be highlighted between the mechanical mixing (300 kg/h) and manual method (160 kg/h) with one operator. In the mechanical method, 20 kg of saw dust with other ingredients must be mixed at least 45 s before adding water. Since, the designed capacity of the mixing container is 25 kg and this mixing procedure is a batch-based, it takes a considerable amount of time to load the materials and unload the mixture when working for an extended period. But, in manual mixture, more than 25 kg of saw dust mixture can be prepared without wasting time for loading and unloading. Therefore, if the machine's mixing capacity is very high, the efficiency is somewhat low compared to the manual method. Therefore, continuous operation of the machine with automation will improve the efficiency of the machine with the highest working

Fig. 20.5 Fabricated sawdust sieving machine

Fig. 20.6 Mechanical mixing unit, (**a**) fabricated mixing machine, (**b**) main door and sliding doors of the tank, (**c**) internal arrangement of the mixing tank

capacity. Table 20.3 provides a comparison between mechanical and manual filling of substrate mixture.

Due to its continuous operational mode, the mechanical filling method has an actual capacity of 81 bags/h, making it significantly more efficient than the manual method.

Fig. 20.7 Fabricated mixture filling machine

Table 20.2 Comparison of mechanical and manual mixing

	Mechanical sieving	Manual sieving
Theoretical capacity	480 kg/h	250 kg/h
Actual capacity	300 kg/h	160 kg/h
Efficiency	62.5%	64%

Table 20.1 Comparison of mechanical and manual sieving

	Mechanical sieving	Manual sieving
Theoretical capacity	228 kg/h	200 kg/h
Actual capacity	200 kg/h	160 kg/h
Efficiency	88%	80%

Table 20.3 Comparison of mechanical and manual filling

	Mechanical sieving	Manual sieving
Theoretical capacity	97 bags/h	44 bags/h
Actual capacity	81 bags/h	32 bags/h
Efficiency	83%	72%

Fig. 20.8 Connection of all the machines for continuous operation

20.3.1 Enabling Seamless Continuity by Integrating the Three Operations

Integrating the three operations is challenging due to the varying actual capacities of the machines involved. In particular, the sieving mechanism has a nearly twofold capacity compared to the mixing machine. Additionally, the capacity of the mixing machine is 3.3 times higher than that of the filling machine, assuming an average filled grow bag weighs an average of 0.85 kg. Doubling the capacity of the mixing machine and connecting seven filling machines to the existing sieving machine enables seamless integration of all systems. To operate the entire system continuously, a suitable feeding mechanism such as a bucket elevator, should be connected to the sieving machine with an appropriate feeding rate. Figure 20.8 shows the connection of existing designs for continuous operation.

20.4 Application of IoT Technology in Disinfection of Substrate

Sterilization with saturated steam using simple apparatus made with steel barrels is widely practiced at the cottage level. These sterilization systems can see in two types such as conventional steam sterilization systems and centralized steam sterilization systems. The conventional system consists of a steel barrel with a lid and a biomass burner. The lower portion of the steel barrel is used as the steam generating unit, while the upper portion is used for sterilization of grow bags. A wooden frame is placed inside the barrel to arrange grow bags above the steam generating unit. In a centralized system, a small separate steel barrel is used for steam generation, and 2–4 barrels connected laterally to the steam generating unit are used for the sterilization of grow bags. Burners in both systems utilize biomass sources, such as sawdust, rice husk, and wood fuel, as heat sources. The operation and working principles of both the conventional system and a centralized system are illustrated by Fig. 20.9.

The variations of the thermodynamic parameters inside sterilization units of conventional system and centralized system with different number of sterilization units are summarized in Table 20.4. Figure 20.10 gives a comparison of sterilization systems with important parameters.

Due to its superior performance in commercial-level applications, the centralized system with four units was selected for technological integration with IoT. Figure 20.11 shows the arrangement of all the components in an automated centralized steam sterilization system with IoT technology.

In the new sterilization system, biomass (rice husk/ sawdust) is supplied to the burner in a controlled manner with the assistance of a rotating screw conveyor. Choosing rice husk as biomass for heat generation can contribute to the mitigation of global warming by enabling the absorption of released carbon by the upcoming (Bardant et al., 2021; Kahandage et al., 2023; Setiawan et al., 2019). The screw conveyor is connected to the biomass bin and powered by an electrical motor. Air supply for the combustion process is accomplished by an electric blower and the conveyor directs the provided biomass to the burner through the airflow. The air fuel ratio can be adjusted by controlling the speeds of the motor and electric blower. The steam generating unit and all the sterilization units are equipped with temperature and pressure sensors to measure and report the real-time values of the system. The controller receives the measured parameters and stores them in the IoT cloud platform using Wi-Fi connectivity to enable remote monitoring. Simultaneously, the controller compares all the temperature and pressure values with the required levels and determines the operational speeds of the conveyor and the blower to control the heat supply to maintain the desired values.

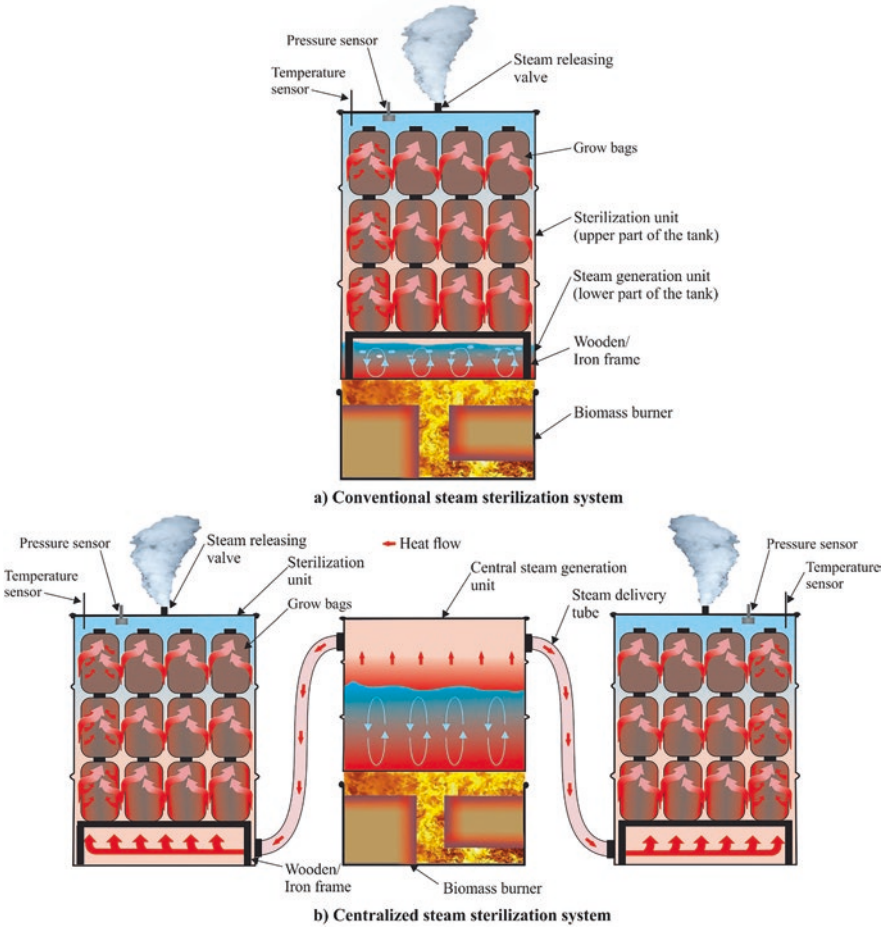

Fig. 20.9 Components and operation: (**a**) Conventional steam sterilization system, (**b**) centralized steam sterilization system

Table 20.4 Variation in some thermodynamic properties in conventional and centralized systems

Parameter	Conventional system (60 kg)	Centralized system		
		with 2 units (120 kg)	with 3 units (180 kg)	with 4 units (240 kg)
Max. Steam temperature (°C)	104.17	103.00	102.50	102.33
Absolute steam pressure (kPa)	118	113	111	111
Time to reach max. Temp. (mins.)	89.00	108.66	129.00	142.67
Enthalpy of steam (kJ kg^{-1})	2682.31	2680.37	2679.58	2679.18

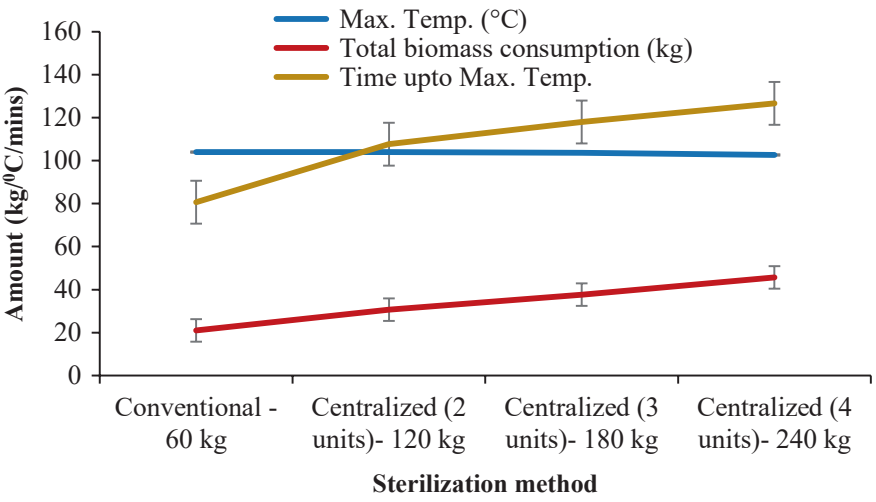

Fig. 20.10 Comparison of conventional steam sterilization and centralized sterilization with different number of units

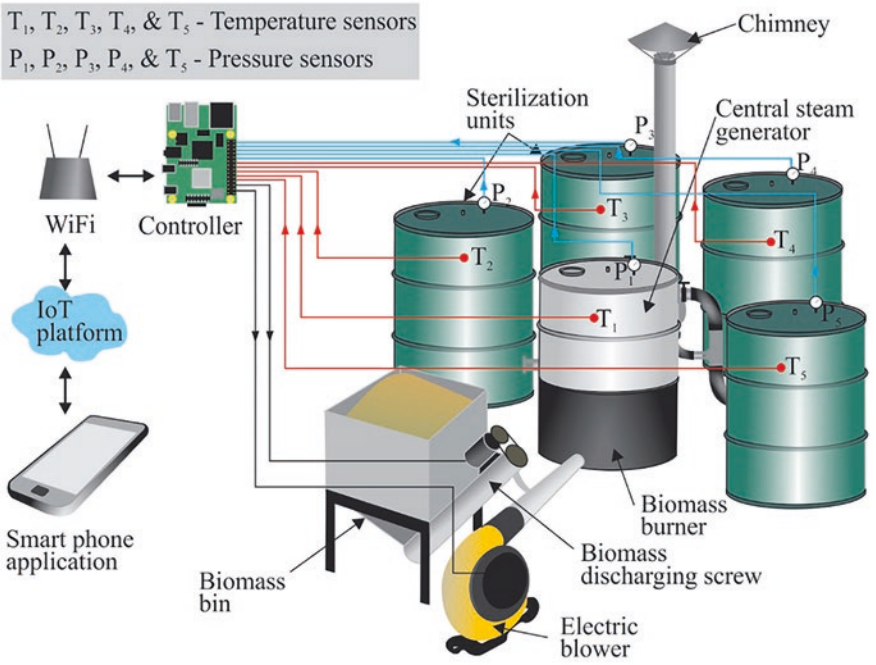

Fig. 20.11 Application of automation and IoT to the centralized steam sterilization system with four units

20.4.1 Controlling the Biomass Supply to the Burner

The frequency of the AC voltage supplied to the motor is changed to control its speed using a variable frequency drive (VFD). The relationship between the frequency of the voltage and the speed of an AC motor is given by the following equation:

$$V = (120 \times F) / P$$

where V is the speed of the motor in revolutions per minute (RPM), F is the frequency of the AC voltage supplied (Hz), and P is the number of poles in the motor.

In the first step, the VFD converts the incoming AC voltage to a DC voltage. Then variable frequency AC voltage is created using an inverter to supply to the motor. Changing the output of the inverter can control the frequency of the AC voltage. Figure 20.12 illustrates the decision process of the automation system.

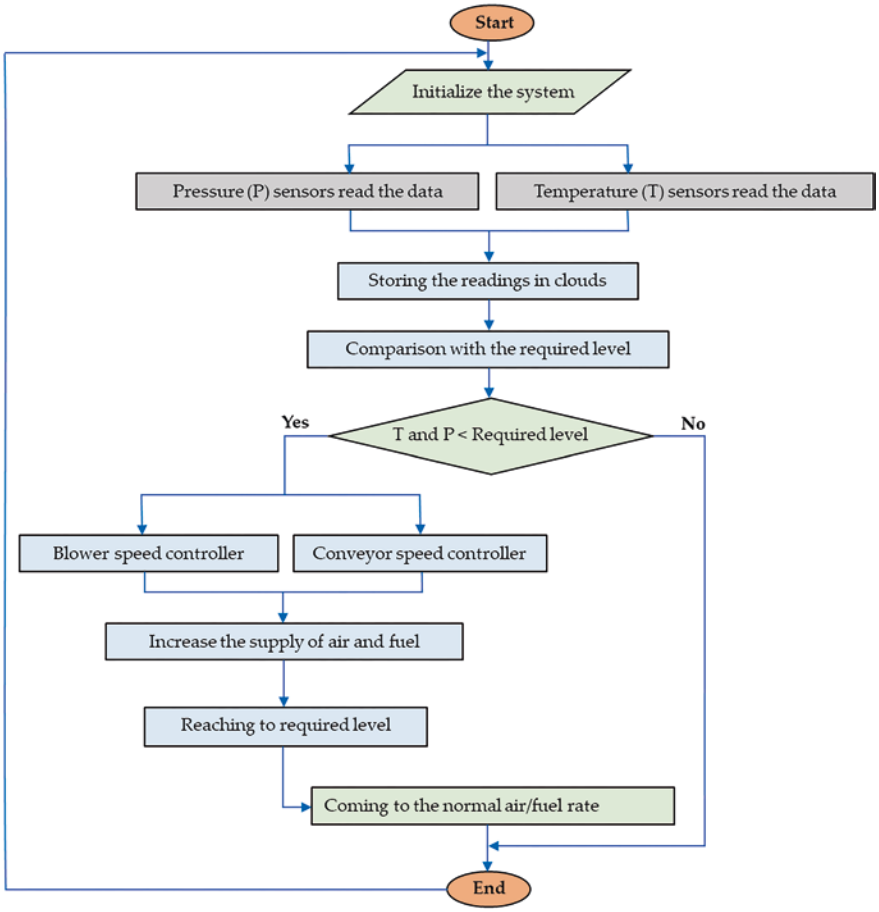

Fig. 20.12 Block diagram of the decision process of the automation

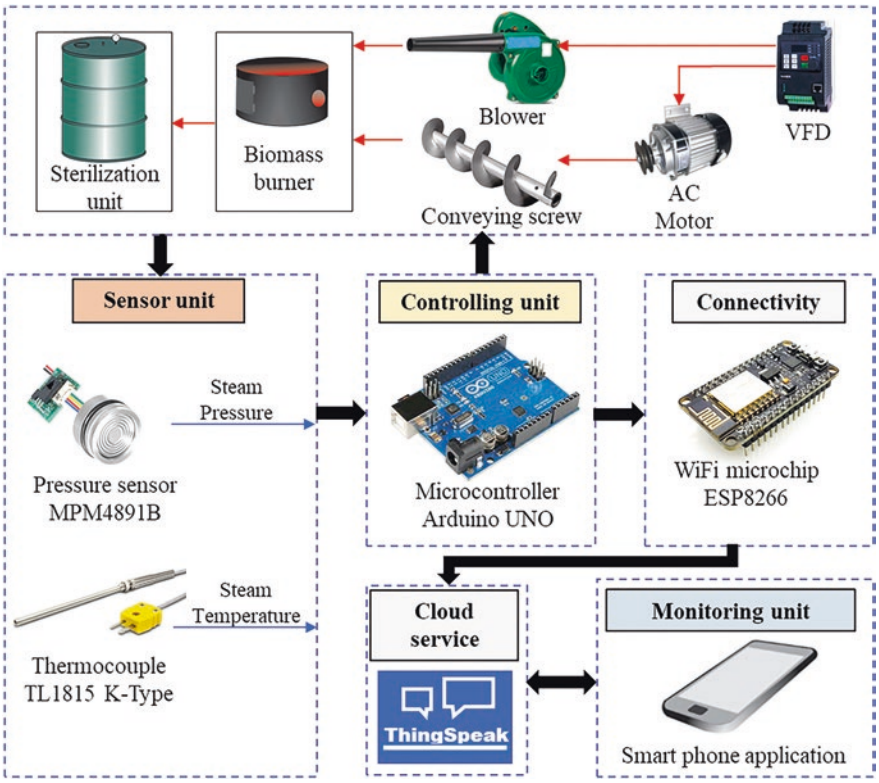

Fig. 20.13 Arrangement of the components in the IoT system

The recommended temperature and pressure for better sterilization of mushroom substrates are 120 °C and 151 kPa (OGM, 2022). Therefore, the required levels of temperature and pressure have been set as 120 °C and 151 kPa, respectively. Figure 20.13 shows the arrangements of the components in the IoT system and the sterilization system.

Arduino Uno microcontroller was selected as the controller of the system and for enabling cloud service connectivity, an ESP8266 Wi-Fi microchip was incorporated. The MPM4891B pressure sensor and TL1815 K-type thermal sensor were chosen due to their ability to measure values in the preferred range. As a popular choice in the field of IoT, ThingSpeak cloud service was selected for this project.

20.5 Controlling the Environment in a Mushroom House/Shed

Monitoring and accurately maintaining favorable environmental conditions are crucial for successful spawn growth in mushroom cultivation. The parameters that should be carefully monitored include temperature, humidity, ventilation,

Table 20.5 Favorable environmental conditions for different growth stages of oyster mushroom

Growth stage	Duration (days)	Temperature (°F)	RH (%)	CO_2 (ppm)	Light
Incubation	10–14	78–84	90–100	20,000	Total darkness
Pinhead initiation	7–14	55–60	95	>600	Natural light
Cropping and harvesting	5–7	60–64	85–92	>600	Natural light

light, CO_2 concentration, and air purity (Sihombing et al., 2018). The temperature of the substrate can be managed by controlling the surrounding air temperature, and heating and cooling equipment can be helpful in extreme climates. Proper ventilation and air circulation can be achieved with a well-ventilated room. Humidity must be maintained between 90 and 100% to prevent evaporation from the substrate, and steam humidifiers or cold-water misters can be used for humidification. Care must be taken with steam to avoid raising the substrate temperature above ideal ranges. During spawn run, carbon dioxide levels of 10,000–15,000 ppm are considered beneficial, as mushroom mycelium has been shown to absorb CO_2. Proper air circulation is important to avoid CO_2 buildup at the bottom of the room. The suitable environmental conditions for different growth stages of Oyster mushroom (Pleurotus species) are given in Table 20.5.

During the incubation period, inoculated substrates in polythene bags are placed in a separate room because the required conditions for incubation are entirely different from those in other stages. After incubation, the polythene bags are opened by removing the upper part of the bag and placed horizontally on racks in the mushroom shed. Figure 20.14 displays the arrangement of a commercial-level mushroom shed.

20.5.1 Controlling the Temperature and Humidity of a Mushroom House with IoT

Temperature and humidity in mushroom houses are controlled with exhaust fans and mist blowers. During extreme climate conditions, these fans and blowers may need to be operated manually to maintain the temperature and humidity inside the house. Figure 20.15 illustrates the decision-making process of the operation of exhaust fans and mist blowers with IoT technology.

In tropical countries, maintaining a low temperature inside the mushroom shed is one of the most challenging tasks. Therefore, integrated approaches should be practiced accurately to overcome the heat stresses. The proposed design includes exhaust fans for air circulation, mist blowers to increase humidity, and a roof installed

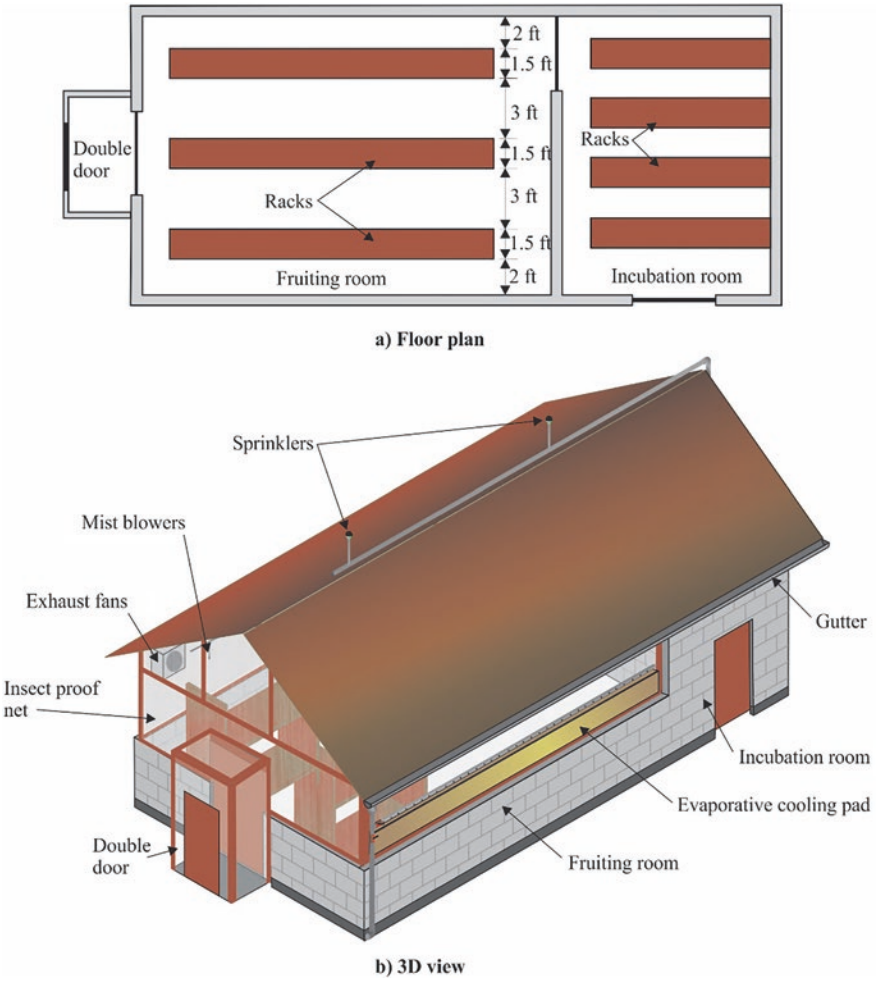

Fig. 20.14 Arrangement of a commercial-level mushroom shed. (**a**) Floor plan, (**b**) 3D view

sprinkler system to cool the roof top. The system is integrated with IoT for remote monitoring and operation. Real-time sensors read the temperature and humidity inside and determine the necessary operations. If the temperature is higher than desired and humidity is lower than desired, the exhaust fans, mist blowers, and sprinklers start operating simultaneously. The water collected from the sprinklers is directed to the evaporative cooling pad to increase the moisture of the incoming air. When the temperature and humidity reach to the desired value, operation of fans, blowers, and sprinklers will be stopped.

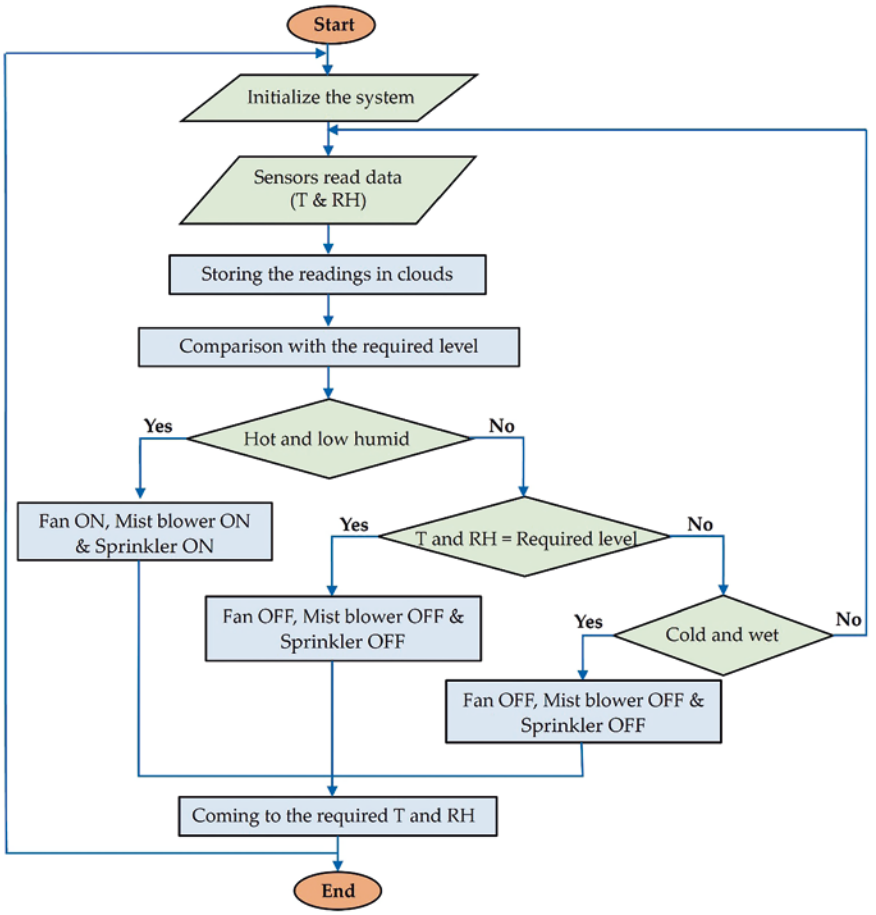

Fig. 20.15 Block diagram of the decision-making process of temperature and humidity controlling in a mushroom house

20.6 Conclusion

In conclusion, although cottage-level mushroom cultivation is a popular self-employment option in rural areas of many tropical and subtropical countries, it is highly labor-intensive and inefficient due to the higher involvement of human labor throughout the production process. This study suggests that the integration of mechanization, automation, artificial intelligence, and IoT technologies can reduce the cost of production, improve the quality of the output, and reduce human involvement, making the cottage-level mushroom industry more efficient and profitable. The study has developed an integrated continuous operating system for sawdust sieving, ingredient mixing, and mixture filling into polythene bags, a centralized steam sterilization system with IoT, and IoT-based environmental controlling

system for mushroom sheds. Additionally, continuous real-time monitoring of environmental conditions in the mushroom shed using IoT technology is expected to yield better results by preventing disease and stress conditions. These advances can promote the cottage-level mushroom industry and improve the income level of rural communities in developing countries.

References

Abeyrathna, R. M. R. D., Nakaguchi, V. M., Minn, A., & Ahamed, T. (2023). Recognition and counting of apples in a dynamic state using a 3D camera and deep learning algorithms for robotic harvesting systems. *Sensors, 23*(8), 3810. https://doi.org/10.3390/s23083810

Aida, F. M. N. A., Shuhaimi, M., Yazid, M., & Maaruf, A. G. (2009). Mushroom as a potential source of prebiotics: A review. *Trends in Food Science and Technology, 20*(11–12), 567–575. https://doi.org/10.1016/j.tifs.2009.07.007

Bardant, T. B., Setiawan, A. A. R., Haq, M. S., Prasetia, H., Mastur, A. I., Harianto, S., Putra, A. S., Sulaswatty, A., Wiloso, E. I., & Noguchi, R. (2021). Simulation of gamboeng tea product manufacturing process and their role in reducing environmental impact. *Management and Production Engineering Review, 12*(2), 86–97. https://doi.org/10.24425/mper.2021.137681

Chang, S. T., & Miles, P. G. (2004). Mushrooms: Cultivation, nutritional value, medicinal effect, and environmental impact. *Economic Botany, 59*(3), 310. https://doi.org/10.1663/0013-0001(2005)059[0310:dfabre]2.0.co;2

Kahandage, P., Rupasinghe, C., Weerasooriya, G. V. T. V., & Alwis, P. (2016). Mechanization of growing media preparation and poly bags filling in oyster mushroom (Pleurotus ostreatus) cultivation! In *International symposium on agriculture and environment* (pp. 215–217). University of Ruhuna, Sri Lanka.

Kahandage, P. D., Piyathissa, S. D. S., Ariesca, R., Namgay, I. R., Kosgollegedara, E. J., & Noguchi, R. (2023). Comparative analysis of Paddy harvesting systems toward low-carbon mechanization in the future : A case study in Sri Lanka. *PRO, 11*(6), 1851.

Kahandage, P. D., Weerasooriya, G. V. T. V., Ranasinghe, V. P., Kosgollegedara, E. J., & Piyathissa, S. D. S. (2021). Design, development and performance evaluation of a seed Paddy cleaning machine. *Sri Lankan Journal of Agriculture and Ecosystems, 3*(2), 41. https://doi.org/10.4038/sljae.v3i2.78

Kumarasiriwardhana, C. A., Kahandage, P. D., & Weerasooriya, G. V. T. V. (2020). Design, fabrication and evaluation of solar and biomass hybrid dryer with trackable solar collector. *Sri Lankan Journal of Agriculture and Ecosystems, 2*(2), 164–182. https://doi.org/10.4038/sljae.v2i2.45

Kurtzman, R. H., Jr. (2010). Pasteurization of mushroom substrate and other solids. *Environment Science And Technology, 4*(December), 936–941.

Mandeel, Q. A., Al-Laith, A. A., & Mohamed, S. A. (2005). Cultivation of oyster mushrooms (Pleurotus spp.) on various lignocellulosic wastes. *World Journal of Microbiology and Biotechnology, 21*(4), 601–607. https://doi.org/10.1007/s11274-004-3494-4

OGM. (2022). *Ultimate guide to sterilising mushroom substrate*. Retrieved February 4, 2023, from https://mycobio.co.nz/ultimate-guide-to-sterilising-mushroom-substrate/

Sanjel, P., Shrestha, R. K., & Shrestha, J. (2021). Yield performance of oyster mushroom (Pleurotus ostreatus) on different substrates. *Journal of Agriculture and Natural Resources, 4*(1), 291–300. https://doi.org/10.3126/janr.v4i1.33370

Setiawan, A. A. R., Sulaswatty, A., Haq, M. S., Utomo, T. H. A., Randy, A., Arutanti, O., & Haryono, A. (2019). A study on ecolabeling and life cycle assessment for food products in Indonesia: Potential application to improve the competitiveness of the tea industry. *IOP Conference Series: Earth and Environmental Science, 277*(1), 012026. https://doi.org/10.1088/1755-1315/277/1/012026

Setiawan, A. A., Rahman, S., & A., Meliana, Y., & Haryono, A. (2018). Innovation readiness assessment toward research commercialization: Case of surfactants for food processing. *International Journal of Innovation, 6*(2), 180–193. https://doi.org/10.5585/iji.v6i2.291

Shrestha, S., Bhattarai, S., Shrestha, R. K., & Shrestha, J. (2021). Effect of different substrate sterilization methods on performance of oyster mushroom (Pleurotus ostreatus). *Agraarteadus, 32*(1), 127–132. https://doi.org/10.15159/jas.21.03

Sihombing, P., Astuti, T. P., & Herriyance, & Sitompul, D. (2018). Microcontroller based automatic temperature control for oyster mushroom plants. *Journal of Physics: Conference Series, 978*(1), 012031. https://doi.org/10.1088/1742-6596/978/1/012031

Suraweera, R., Kahandage, P. D., Kosgollegedara, E. J., & Dissanayake, D. (2020). A review of mechanization and automation of mushroom. In *Annual Reseach symposium* (p. 15). Faculty of Agriculture, Rajarata University of Sri Lanka.

Wijeratne, M., & Silva, N. D. (2012). *Mushroom production as an enterprise*. Neat Graphics, YMBA building, Rahula Rd. Matara.

Chapter 21
Approaches for Improving Fruit Detection and Gripping Mechanisms in Orchard Robotic Fruit Harvesting

Abstract Harvesting robots provide a promising solution to overcome the challenges of manual harvesting in fruit orchards, which is usually the most time-consuming and laborious part of the orchard fruit production process. Despite the technological advancements in robotic harvesting, real-world applications are hindered by field-level limitations. This chapter first analyzes the major challenges in field-level harvesting robotic applications concerning the detection power of the robotic vision system and robotic arm manipulation and then proposes corresponding state-of-the-art developments to overcome these challenges. The key challenges encountered include (1) occlusion caused by leaves, fruit clusters, branches, and other plant parts, which reduces both the detection ability of the robotic vision system and the operational capacity of the robotic gripper, and (2) day–night light variation (uneven lighting), wind, and reflections or shadows that limit the detection ability of the vision system. There are two types of approaches to robotic fruit harvesting. On the one hand, developments in horticulture have compelled the use of simpler harvesting robots due to the simpler fruit architecture in contemporary fruit orchards than in conventional orchards. On the other hand, recent developments in electronics and computational capacity can make the task of robotic operations easier, especially in orchard fruit picking. Recently developed vision systems are reliable and accurate in localizing target fruits. Within this context, the application of simple linear and rotational manipulations in orchard fruit harvesting robots has become increasingly important as an alternative to existing complex harvesting robots.

Keywords Robotic harvesting · Fruit picking · Uneven lighting · Horticultural approach · Robotic arm configurations · Occlusion

© The Author(s), under exclusive license to Springer Nature Singapore Pte Ltd. 2024

T. Ahamed, *IoT and AI in Agriculture*,
https://doi.org/10.1007/978-981-97-1263-2_21

21.1 Introduction

Orchard fruit production is one of the key subsectors of agriculture. Agricultural operations are mostly complex and labor intensive, and orchard fruit production is no exception. The ever-growing global demand for orchard fruit crops has necessitated an improvement in the sector's production and productivity. Thus, improvement of orchard productivity has always been at the forefront of the sector's concerns. Harvesting is the most costly, time-consuming, and laborious part of the orchard fruit production process. Since a high fruit demand leads to a large amount of fruit production during the harvesting stage, harvest scheduling should be optimized to increase production efficiency, among many other reasons that should be considered. The profit of fruit harvesting depends on the optimal utilization of resources and how much those resources can increase the operation efficiency. In this context, robotics developed for harvesting provide a promising solution for the scarcity of high-volume seasonal labor and the rising cost of labor.

In recent decades, mechanization has enhanced agricultural productivity due to the development of robotics and automation. The introduction of agricultural robots has improved the quality of freshly harvested products, reduced production costs, eased manual labor, and most importantly, helped address labor shortages in orchards. However, as harvesting robots should be able to work in varied and uncertain environments with no predefined structure, in contrast to their industrial counterparts that perform repetitive, defined, and fixed tasks, automation in crop cultivation has been limited. According to estimates, automation still performs 15% of harvesting in the field of horticulture, and 50% crop shortages have been recorded when most of the harvesting is carried out manually (Ceres et al., 1998). Given the limitations of robotic harvesting in open field conditions in many cases, orchard fruit growers have turned to mechanical harvesters, which carry out harvesting by shaking either branches or whole trees using different mechanisms. Mechanical fruit harvesters can be used for bulk harvesting, resulting in the harvest of the entire crop from the trees or branches, including pest-and disease-infected fruits and unevenly matured fruits. The fruits are collected in a large cover placed at the bottom. When fruits fall from trees, they can hit the branches, other fruits, and mechanical parts of the shaking machine, degrading their postharvest lifetime and quality. Although mechanically harvested fruits are suitable for fruit juice production, problems may arise when these fruits are sold in the fresh market, leading to substantial postharvest losses (Kahandage et al., 2021). At the same time, sorting and grading mechanically harvested samples may require more time and labor than manual harvesting in some situations. Moreover, bulk harvesting leads to excessive damage to fruits and leaves, as well as branches in some cases, by the mechanical parts, and this is of concern for growers (Moseleya et al., 2012).

By considering the drawbacks of mechanical fruit harvesting as well as the practical limitations of robotic fruit harvesting, scientists are now on the path to address these issues by breeding new fruit varieties. Selective harvesting is one of the key challenges in both mechanical and robotic fruit harvesting. Within the crop sector,

the crops that ripen uniformly in the field (i.e., wheat, corn, potatoes, etc.) allow efficient mass harvesting of the crop at a single point in time by large machines. In contrast, high-value crops such as orchard crops (i.e., apples, pears, grapes) ripen heterogeneously and require selective harvesting of only ripe fruits. In bulk harvesting, the maturity of the fruits can vary considerably, as less mature and overmature fruits are inevitably harvested collectively (Saunders, 2005). Most importantly, harvesting should be done without damage to the fruit to ensure that it has a long and high-quality postharvest life so that it can be directly sent to the fresh market, where customers prefer to buy fruit at a higher selling price. Selective harvesting has turned out to be difficult to automate and is often performed by human labor. However, recently developed orchard fruit varieties have paved the way for automation, as these varieties have both morphological and physiological characteristics that can be properly manipulated to achieve the desired orchard fruit architecture (i.e., the new varieties can produce fewer fruit clusters, which facilitate selective robotic harvesting). Moreover, farmers who are more concerned about harvesting and demand high-quality output yield can cultivate fruits inside greenhouses. This has paved the way for popularizing robotic applications, as these controlled environments do not present some of the difficulties encountered by robotics in open fields, as the color, position, shape, and size of the fruits can be precisely controlled based on environmental conditions in the greenhouse (Bac et al., 2014). Farmers who cultivate highly valued orchard crops such as berries, kiwi, tomatoes, grapes, apples, pears, citrus, peaches, plums, and figs have already taken the initiative to apply automation techniques for management.

Fruit plants can be categorized into three groups based on their growth habits, namely, bushes or shrubs, vines, and trees. These three types have different tree architectures. Vines require physical support for growing, whereas trees and bushes can support themselves. Each variety of these fruit plants has different morphological characteristics; therefore, horticulturists have developed different tree training methods for these plants. There are different fruit orchard architectures for different fruit types. However, the simpler the orchard architecture is, the easier it is to apply robotic harvesting. The most challenging key robotic operations in conventional orchard systems with complex canopy structures are detecting and tracing fruits with a robotic vision system and performing less obstructing movements with the robotic arm to reach the fruits. Newly developed fruit wall architectural structures and trees are genetically and physically trained to have fewer leaves and avoid fruit clustering, enabling machine vision to pick up target locations easily and at the same time facilitating the gripping mechanism.

Even with this newly developed fruit tree architecture, there are still some limitations to robotic harvesting and detection, as well as localization of fruits in particular. One such difficulty is occlusions created by plant parts and other obstacles, which hinder the detection ability of the robotic vision system. Usually, robotic fruit harvesters are followed by mechanical harvesters with high computational power based on sensors with links to actuators. The harvesting robots should identify the target fruits based on detection, which is supported by convolutional neural networks (CNNs). Detection is followed by the localization of the

detected fruits. Many factors affect the use of a trained CNN. However, after localization, the robotic arms can obtain the coordinates of the harvestable fruits. The geometry of the canopy and branches plays a critical role at this stage in determining whether the target locations can easily be reached, depending on several factors. Moreover, because collisions with branches, fruit clusters, and leaves; shaking due to wind; and variation in light affect the detection accuracy, some of the fruit remains unrecognized by the vision system. Even when fruits are detected, the robotic arm may be unable to reach the target locations due to the presence of obstacles (Grift et al., 2008). This makes operating the gripping mechanism more difficult.

Therefore, the objective of this chapter is to analyze the major challenges in field-level harvesting robotic applications concerning the detection power of the robotic vision system and robotic arm manipulation in detail and to propose corresponding state-of-the-art developments to overcome these challenges.

21.2 Occlusions Caused by Plant Parts and Challenges for Robotic Operations

21.2.1 Challenges for the Vision System

The main tasks of the vision system of a harvesting robot include detection, localization, and harvesting of the fruits. Usually, CNNs in vision systems are programmed to precisely detect and localize fruits for harvesting. In fruit orchards, compactly arranged leaves, branches, and immature fruits are not rare, and such objects create difficulties in accurately localizing and approaching harvestable fruits. When a fruit is covered with plant parts (i.e., leaves, branches, other fruits) and/or supporting structures of the tree architecture (Fig. 21.1), the vision system may fail to detect and localize the fruit accurately. In other words, the localization

Fig. 21.1 Apple detection (YOLOv7): (**a**) apples covered with leaves, (**b**) apples covered with branches, (**c**) apples covered with supporting poles

Fig. 21.2 Localization of detected apples in the presence of leaf occlusion

coordinates cannot be obtained accurately. In some instances, illumination may worsen the situation because the appearance of fruits differs in different light conditions. Thus, occlusion is the quintessential challenge that hinders the ability of the vision system to perform such tasks precisely. Therefore, to successfully implement detection and localization of fruits with a vision system, there should be either no occlusion or few occlusions.

The vision system can reach and identify a fruit even if it is covered with a plant part. However, the problem is that when an obstruction occurs, it is difficult to obtain the exact coordinates of the fruit due to poor coverage. The coordinates of the position of the fruit, usually the XYZ coordinates, are obtained by the 3D camera. The detection model gives the X and Y coordinates based on the frame reference, and the Z value can be obtained from the central point of the bounding box. When there is occlusion, the obtained Z-axis value is not accurate (Fig. 21.2). However, it is noteworthy that the coordinates may change not only due to leaf occlusion but also due to wind. This inaccurate Z value will then lead to a series of miscalculations. The distance value calculated from this depth value will generate a false reading. Usually, RGBD cameras are used for the localization of target objects. As shown in Fig. 21.3, the final output of the Realsense D455 3D camera is generated based on the separate RGB streams and depth streams, which are then merged into one image. Therefore, with inaccurate coordinates, the final output produced by the camera is erroneous, and thus, the fruits may not be detected and localized precisely.

21.2.2 Challenges for Robotic Arm Manipulation

Occlusion of plant parts may pose challenges not only for the vision system in detecting and localizing the fruits but also for the movement of the robotic arm. In some instances, even after localizing a fruit, the robotic arm may not be able to approach the fruit due to occlusion. Figure 21.4 exhibits different approaching angles of the robotic arm when occlusion is present. Some apples are occluded by branches and supporting poles, and the others can be reached from one side. The approaching angle of the camera and gripper depends on the robotic arm configuration. Usually, robotic arms are customized based on the targeted fruit type and the canopy structure/orientation.

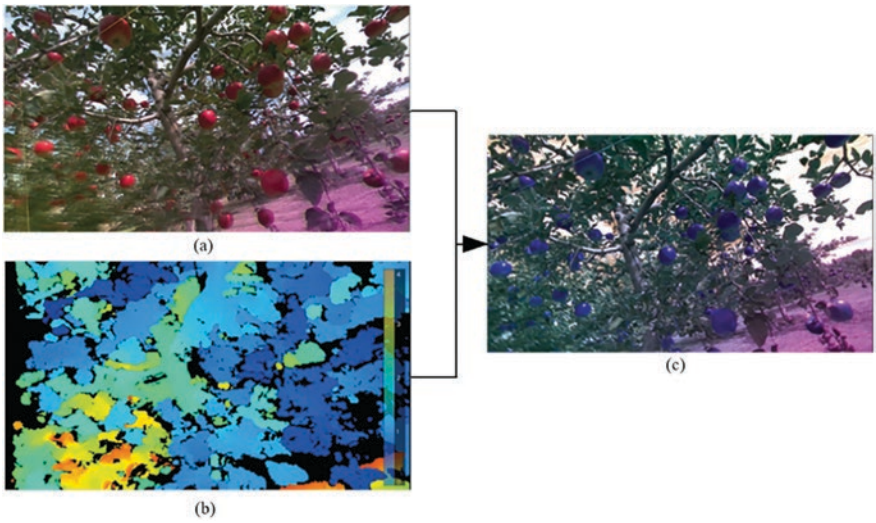

Fig. 21.3 Detection of apples based on an RGBD Realsense D455 camera: (**a**) RGB image, (**b**) depth image, (**c**) combined RGB and depth images

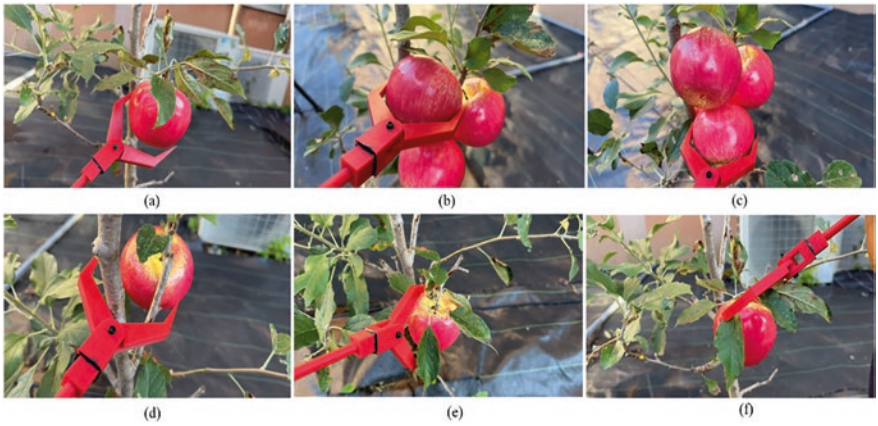

Fig. 21.4 Approaching the target fruits from only one side, (**a**) approaching a single apple with the correct gripping position, (**b**–**c**) approaching fruit clusters, (**d**) branch occlusion, and (**e**, **f**) approaching the fruit from different angles, where obstruction from leaves causes leaf damage

The leaf occlusion percentage is highly correlated with the detecting angle of the 3D camera and the location of the detecting sensor. To capture the relationship between the detecting angle and the leaf occlusion percentage, an experimental setup was designed, as shown in Fig. 21.5. The 3D camera can move up and down at constant speed, and the whole system can move parallel to the apple tree rows.

Figure 21.6 shows leaf occlusions based on the detection angle of the camera when the camera moves vertically and horizontally. Based on the horizontal and

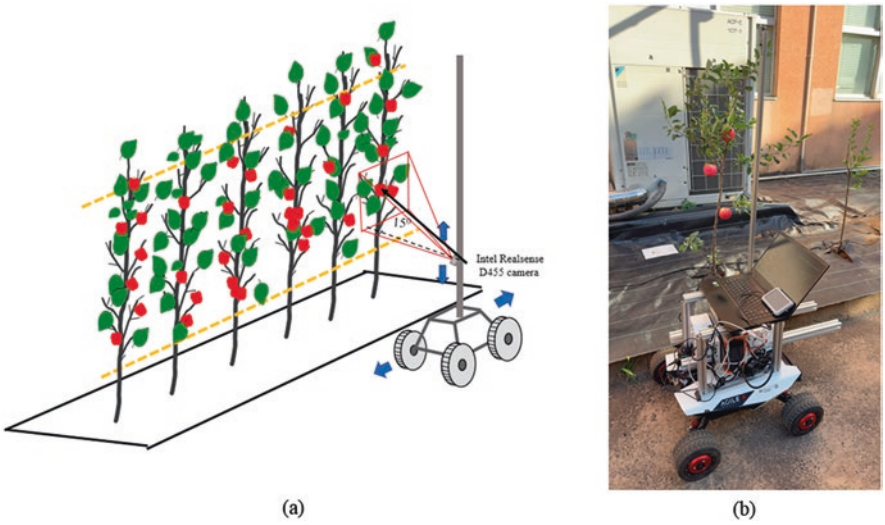

Fig. 21.5 (**a**) Experimental setup for the detection of apples. (**b**) Data collection setup with the help of the AGILE-X robot

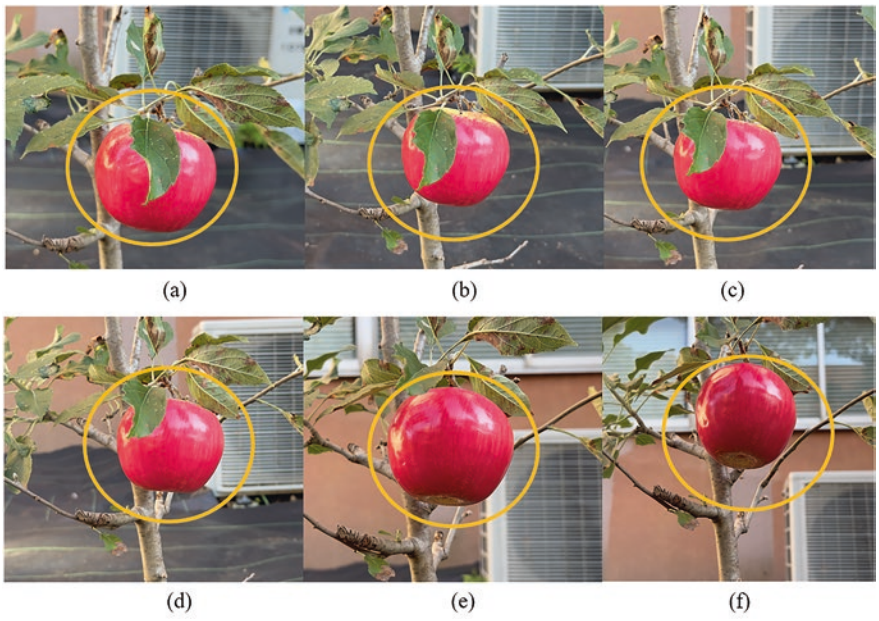

Fig. 21.6 Occlusions by leaves and localization with an appropriate detection angle of the camera. The vision system can avoid occlusion based on the detection position. (**a**–**c**) Camera moving horizontally from left to right. (**d**–**f**) Camera moving vertically (top to bottom)

vertical movement of the camera, the system can determine an appropriate direction to avoid leaf, branch, and fruit cluster occlusion to isolate a single fruit for robotic harvesting.

However, after localization, detaching the fruits from the stem depends on the gripping tool performance as well as the approaching angle of the manipulator. The fruits are bound to the tree stem having an abscission layer that gets soft when fruits ripen, this is the easiest place to separate fruits from the attaching branch. If the gripper can apply force to the abscission layer, the fruit can be easily detached from the branch. Figure 21.7 shows the abscission layer of an apple. Most grippers cannot grip the target fruit from all directions, and some grippers are only made to grip fruits from the side or from the bottom and the stem. In the case of round fruits such as oranges, there is a high possibility of approaching from different directions. Approaching to apply force to the abscission layer is the easiest way of harvesting without damaging the other parts of the plant. However, applying parallel or perpendicular forces to the abscission layer is not always easy because of the orientation of the fruit in the canopy. Therefore, achieving the correct location and proper orientation of the gripper is a challenging task.

The gripping mechanism attached to the robotic arm needs to move close to the orchard canopy, which requires a mobile platform that is either manual or autonomous. The navigation of autonomous mobile platforms is based on RTK-GNSS since a direct GPS link cannot be made because of orchard canopy obstruction. Although RTK-GNSS is more accurate with a ground base station, many errors can occur. One proven method for addressing error is to use 3D cameras and LiDAR-based navigation with the help of CNNs. Moreover, the identification of obstacles is important while the robotic system is navigating through orchard rows; fallen branches, laborers, vehicles, etc., are obstacles that can suddenly appear.

Fig. 21.7 The point at which the gripper should apply force to detach apples: (a) abscission layer (thin-walled parenchyma cells)

While the mobile platform autonomously moves near the orchard canopy, the robotic arm should move the gripper to detach the fruits detected by the vision systems one by one. Another challenge is to avoid the metal poles, cables, scaffolds, and trellises used for orchard fruit training. If fruits appear near such cables and poles, the gripper will be unable to reach or grip the target fruit correctly, causing damage to either the gripper or the fruit during harvest, which is an additional problem. However, these structures provide support and elevation for the fruits and canopy, as well as ventilation and better lighting, while achieving a consistent distribution of fruits. Figure 21.8 shows a pear orchard and obstructions from canopy training structures and cables.

Different fruits need different kinds of gripping mechanisms; in the case of pears, as indicated in Fig. 21.9, the robotic arm should be oriented upward to pick the hanging fruits. The method of bringing the harvested fruits from the gripper to the collecting bucket depends on the exocarp strength; if the exocarp is strong enough to withstand the forces applied to bring the fruit down, the postharvest quality lasts longer. For example, many robotic applications use a spiral connecting a horse from a gripper to a collecting bucket, and some of the applications use a conveyor mechanism to bring the fruits down slowly.

Moreover, the vision system works to detect and localize the gripper so it can grip the fruit in the correct position. As indicated in Fig. 21.10, to harvest an apple, there are few possibilities for a given gripper to approach the apple (a to d); in the e and f positions, the gripper can grip the apple but cannot rotate, as it would hit the branch.

The third challenge is to address the flexible characteristics of the gripping mechanism so that it can vary appropriately with fruit size and shape. Computer

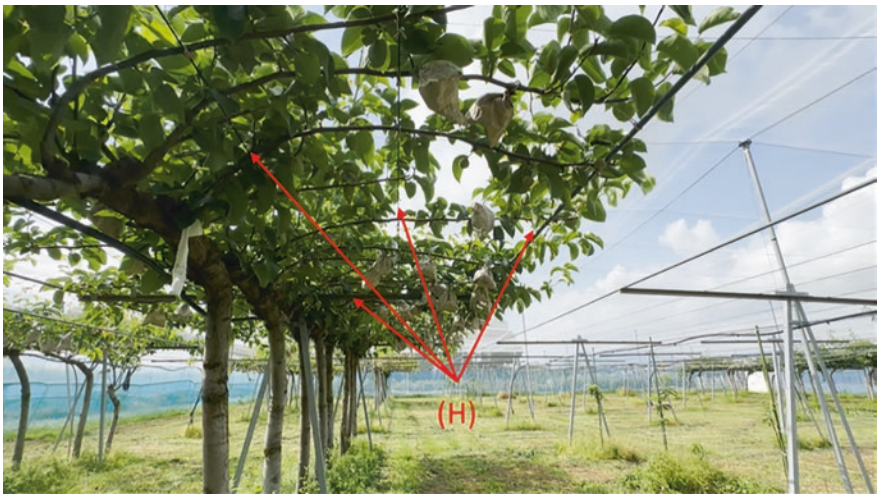

Fig. 21.8 Pear orchard obstructed by canopy training poles and cables for gipping pears; (H) locations of cables and poles

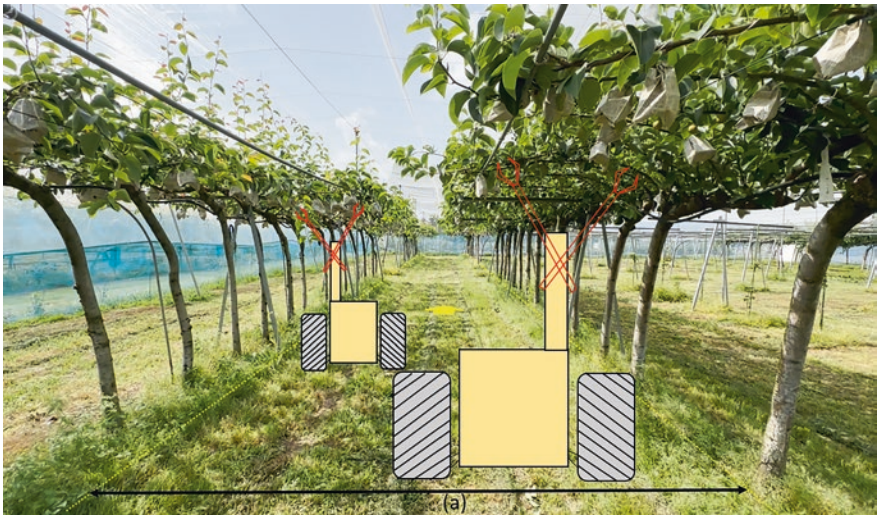

Fig. 21.9 Pear orchard with a single-curtain and double-curtain orchard training system (pear fruit orientation)

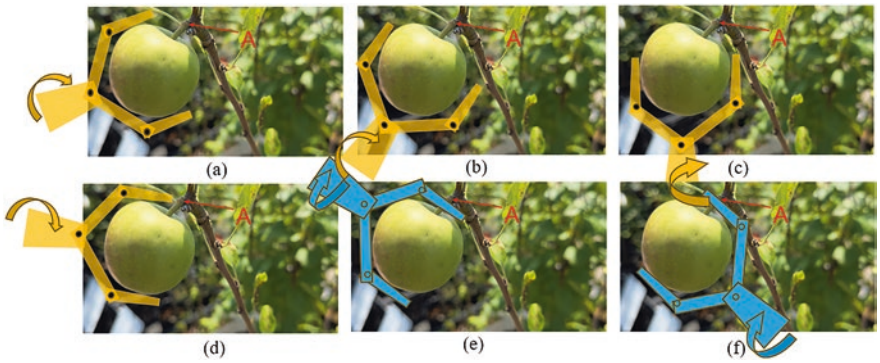

Fig. 21.10 (**a**–**d**) Different possible orientations of the end-effector without occlusions. (**e**–**f**) Occlusions by branches affect the proposed gripping mechanism

vision combined with machine learning and robotic programming helps overcome many automation problems in orchard environments. The challenge is to determine the target locations despite occlusions. The identification of target fruit is performed by the vision system, which normally consists of cameras, and the manipulation of the robotic arm in 3D space requires forward and backward kinematics. In determining forward and inverse motions for controlling the robotic arm end-effector to reach the target locations, trigonometry and calculus expressions are used for trajectory planning.

21.3 Light Variation, Wind, Shadows, and Vision System Challenges

The use of 3D cameras is common for detecting target locations, followed by robotic manipulation. Variations in the lighting conditions tend to result in missed target fruit. When there are shadows, the 3D camera accuracy decreases in determining the geometry of the detected target. Fruit shadows, silhouette spots on leaves, and different patterns of shapes created by leaves lead to false detections. Additionally, the movement of the detected targets due to wind and leaf occlusion created by wind may further worsen the situation. Most of the deep learning models that are used for the detection of fruits are trained using a dataset that covers different periods of the daytime. However, variation in light tends to create errors in open field conditions. When there are sudden environmental changes, there is a higher chance of missing the target fruit. Because natural light variation causes coordinate defects, recent developments have incorporated artificial lighting in detection by vision systems. Under artificial lighting, there are minimal shadows and reflection changes. The recent development of 3D cameras and detection CNNs also plays a critical role in terms of detection improvement.

Red-green-blue-depth (RGBD) cameras are used for detecting and localizing the target fruit based on fruit properties (i.e., color, texture, and shape) with the help of deep learning or with traditional machine learning methods. This is the most accurate, robust, and efficient method for detection and localization. However, RGB cameras are highly sensitive to illumination changes, which makes it challenging to conduct outdoor robotic manipulations (Gongal et al., 2015). For instance, when the surrounding environment and the fruit look the same, it will make the detection task complex. Therefore, initiatives have been taken to develop CNNs by integrating more than one feature (i.e., color and shape) to address this challenge. Multiple feature-based detection systems have fused color and shape features, followed by K-means classification to extract regions of interest (Kang et al., 2022). This method can be applied to increase efficiency in different conditions, such as (a) uneven illumination conditions, (b) fruits that have similar colors to the background, and (c) targets partially occluded by leaves and branches (Tang et al., 2020). A combination of sensors can reduce the error of locating the geometric positions of the detected fruits (Kuznetsova et al., 2020). Another solution is to use thermal sensors to record the temperature information of the canopies and target fruits. Fruits can absorb more heat than leaves and branches; fruits also emit more heat. More importantly, these properties can be used to distinguish fruit and canopy of the same color. Moreover, a key point-based method was introduced for stem length control and stem retention to overcome depth image degradation (Zheng et al., 2021). Some examples of modified detection techniques are listed in Table 21.1. The use of deep neural networks facilitates the detection of target locations after training with image datasets related to target fruits.

Table 21.1 Examples of fruit detection techniques

Detection method	Principle of detection	Features	Application
Color-based detection	Based on the pixels in the image	Uses RGB, LCD, CIE L*a*b; detection depends on lighting conditions	Red apple detection; 95% accuracy Wei et al. (2014)
Fruit texture-based detection	Texture-based	Easy to identify fruits if they are covered with leaves, branches or fruit clusters	Apple detection; 90% accuracy Zhao et al. (2005)
Fruit shape-based detection	Based on geometric shapes, Hough transformation/Canny operator (Canny, 1986; Illingworth & Kittler, 1988)	The effect of the lighting level is lower; can be modified to identify hidden fruits and perform high-speed detection (Xie et al., 2010)	Citrus, apples, tomatoes (spherical fruits) Color and perimeter shape—90% accurate peach detection Hetal et al. (2011); 90% accurate orange detection Hannan et al. (2009)
Detection based on deep neural networks	R-CNN (Girshick et al., 2014), fast R-CNN (Girshick, 2015), faster R-CNN (Ren et al., 2017), mask R-CNN (He et al., 2017), YOLO (Redmon et al., 2016)	Detection based on trained object data	90% accurate detection of kiwi fruit (VGG16) Liu et al. (2020) Mango, almonds, and apples

In the RGBD camera, the most important factor is the depth stream for accurate localization. The depth calculation is performed based on structured light methods and time-of-flight (ToF). In the structured light technique, infrared light is emitted in a pattern, and the level of distortion is calculated to obtain the depth values by comparing the information returned to the receiver. ToF sensors emit infrared light pulses and measure the distances to the target fruits (Gongal et al., 2015). The performance of RGBD cameras decreases, resulting in low-quality depth values, when the camera is used at close scanning distances and under sudden light variations, including effects caused by wind and shadows (Zheng et al., 2021). To perform the depth value calculation, two sensors can be fused, and based on triangulation, the depth can be calculated through a LiDAR sensor, which is robust and performs well with light variation. The harvesting robots run after obtaining the 3D positions of the detected fruits, based on forward and backward kinematics. Usually, if there is an error in the 3D coordinates, this cannot be compensated by the gripper. Calculating the sequence of movements to reach the detected fruits based on the depth values and obtaining the shortest path to the selected targets is called the traveling salesman problem (TSP) (Arkin & Hassin, 1994); many different algorithms have been developed for this problem based on manipulator properties.

21.4 Recent Trends of Harvesting Robots

Recognition and localization are the first two steps of robotic harvesting before deploying the robotic manipulator. Different types of convolutional neural networks have been developed and trained with target fruit images to accomplish these tasks. However, the developed robotic systems still struggle to identify fruits occluded by leaves, fruits that have color variations, and fruits with the same color as the background, for example, green apples, as well as different-colored leaves detected as fruits (Kuznetsova et al., 2020). Light variation, affecting the robotic arm's vision system and resulting in 3D coordinate errors, is one of the main challenges, in addition to occlusion due to leaf branches and fruit clusters, even in developed novel orchard architectures. During the last few decades, enormous improvements in CNNs, 3D cameras, and electronics have created a path for novel robotic developments. With the help of horticultural experts, complex orchard structures have been made simpler to allow easy access to fruits. As indicated in Table 21.2, novel robotic applications have recently been applied for fruit harvesting, and some of them have mechanisms to overcome occlusions.

Harvesting robots need CNNs to understand the complex dynamic environmental information needed to reach the target fruits. Insufficient dexterity of manipulators and grippers tends to result in missed target fruits even though they can be reached easily. To understand the real conditions more deeply, some software has been developed to simulate real conditions, which can be applied before uploading the program into the robotic arm to determine strategies for trajectory planning and obstacle avoidance beforehand. As an example, new three-dimensional (3D)

Table 21.2 Recently developed robotic applications

Type of fruit harvester	Novel approach
Dual-arm tomato harvester Ling et al. (2019)	Picks multiple tomatoes simultaneously based on a binocular vision sensor (Bumblebee2, point Grey, Vancouver, Canada) (detection algorithm integrated with AdaBoost classifier—96% detection at 10 fps, less than 10 mm position error; vacuum-cup grasping mechanism with wide-range cutting). This achieves a success rate of 87.5% and a cycle time less than 30 s
Dual-arm greenhouse eggplant harvesting robot Sepúlveda et al. (2020)	The robotic arms are anthropomorphic, supported by a vector machine (SVM) classifier-based algorithm. Collaborative behavior is used to avoid occlusions to mimic complex human harvesting behavior. One arm is used to push the leaves away and the other for picking fruits, with a success rate of 91.67% and a 26 s/fruit average operational cycle time
Strawberry-harvesting robot Xiong et al. (2020)	Strawberry-picking robot operating inside polytunnels. An obstacle-separation algorithm is used to harvest strawberry clusters. The algorithm can identify surrounding leaves and push them away. To avoid light variation, an improved vision system is used based on color modeling against the intensity of light. The harvesting success rate is 75–100%; for the one-arm mode, the operational time is 6.1 s, and for the dual-arm mode, it is 4.6 s
Kiwi-harvesting robot Mu et al. (2020)	A gripper with two bionic fingers (equipped with fiber sensors and pressure sensors) bends the fruit from the stem for harvesting, with a harvesting time of 4–5 s and a successful picking rate of 94.2%
Four-arm kiwi-picking robots Williams et al. (2020)	As an improvement to the previous robotic version, four robotic arms perform Cartesian linear motions based on a CNN with the integration of a blob analysis algorithm to perform large-scale operations. The gripping mechanism was uniquely developed for picking. The harvester can harvest 86% of reachable fruits and 55.8% of all fruits and has a cycle time of 2.78 s/fruit
Dual-arm apple-harvesting robot Li et al. (2021)	Markov game framework-based multitask deep learning is used to develop a global fruit map to operate multiple arms to achieve high efficiency. The vision system reduces the median locating error by 44.43%, and the average cycle time is reduced by 33.3% based on the proposed task planning algorithm, compared to the heuristic-based algorithm. The harvesting success rate is 71.28–80.45%, and the cycle time is 5.8–6.7 s

software has been developed to make this process easy, and it can be integrated with virtual reality. A grape cluster-picking method and corresponding simulation were performed based on a virtual grip and cut model for grape harvesting, and the results show that the average deviation of the fruit falling ratio and average swing angle were 8.71% and 6.09%, respectively (Liu et al., 2019).

21.4.1 Kinematic Examples for Basic Robotic Arm Design

As discussed in the above sections, when half of a fruit is covered with leaves or branches, localization is difficult, so a camera is needed to look from different sides or angles for complete localization. When the fruit is localized at a different angle, trajectory planning is needed, and the calculations are based on the location (home position) of the robotic arm. If the robotic arm reads the camera coordinates in two stages, at the beginning and halfway to the target, the joint trajectories can be recalculated to perform trajectory planning again with additional information on the occluded fruits at full scale to avoid collisions.

Manipulator configurations are more important for achieving the desired task, and most of the manipulator's design for a specific task depends on the task requirements. However, there are current robotic manipulators with open-source configuration parameters, as indicated in Fig. 21.11.

Generally, manipulator joints are linear (prismatic) or rotary (revolute), and the reachable workspace depends on the degree of freedom (DOF). To reach every arbitrary orientation, the manipulator needs six degrees of freedom; some manipulators that have more than six links are known as kinematically redundant manipulators. The term kinematics defines the manipulator motion without considering the torques and forces involved in a given motion; basically, the kinematics are a geometric description. The forward kinematics define or describe the end-effector frame relative to the base frame (ground frame) as a function of joint angles. The inverse kinematics define the specific location of a space based on position and orientation and the location of a space relative to the base for movement to that location.

Robotic harvesting manipulators have different DOF structures, some of which are specially designed for a certain fruit type and canopy architecture. After localization based on camera coordinates, some fruits need to be neglected because they are outside of the manipulator workspace. Figure 21.12 shows the basic principles of moving a manipulator forward and backward.

A prioritization program is needed after detection and localization to generate a smooth sequence of operations. The forward and inverse kinematics are used to

Fig. 21.11 Basic manipulator configuration parameters

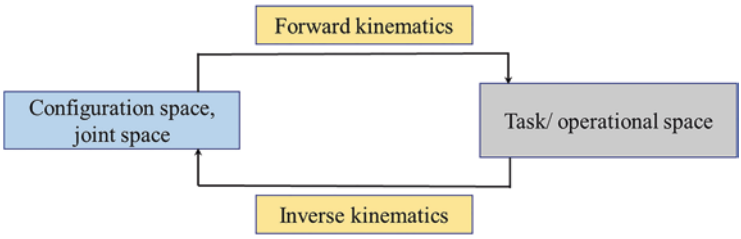

Fig. 21.12 Basic manipulator configuration parameters

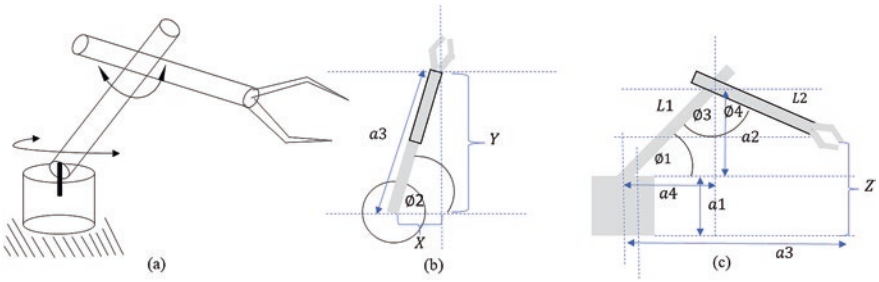

Fig. 21.13 (**a**) Manipulator configuration, (**b**) top view of the manipulator, and X and Y displacements of the gripper in space. (**a**) Side view of the Z displacement of the manipulator gripper in space

identify the manipulator's moving angles and distances based on target locations followed by dynamics. The robotic manipulators are electrically, pneumatically, or hydraulically powered, and the cartesian manipulators (prismatic joints) use these three methods, whereas most revolute joint-only manipulators are powered electrically. Figure 21.13 shows the basic calculation of forward kinematics via trigonometry to determine point coordinates in the working space for robotic manipulation.

Example calculations are given that determine the gripper X, Y, and Z positions in space via trigonometry (forward kinematics).

$$L1 = L2 = 400\,\text{mm}$$

$$a1 = 100\,\text{mm}$$

$$\varnothing 1 = 30^\circ$$

$$\varnothing 2 = 60°$$

$$\varnothing 5 = \left(\varnothing 3 + \varnothing 4\right) = 130°$$

$$\varnothing 3 = 180° - \varnothing 1 - 90° = 60°,\ \varnothing 4 = \left(\varnothing 5 - \varnothing 3\right) = 70°$$

$$\sin 30° = \frac{a2}{400}$$

$$\cos 70° = \frac{a5}{400}$$

$$a3 = a4 + a5$$

$$\cos 30° = \frac{a4}{400}$$

$$\sin 70° = \frac{a5}{400}$$

$$\cos 60° = \frac{X}{722.28}$$

$$\sin 60° = \frac{Y}{722.28}$$

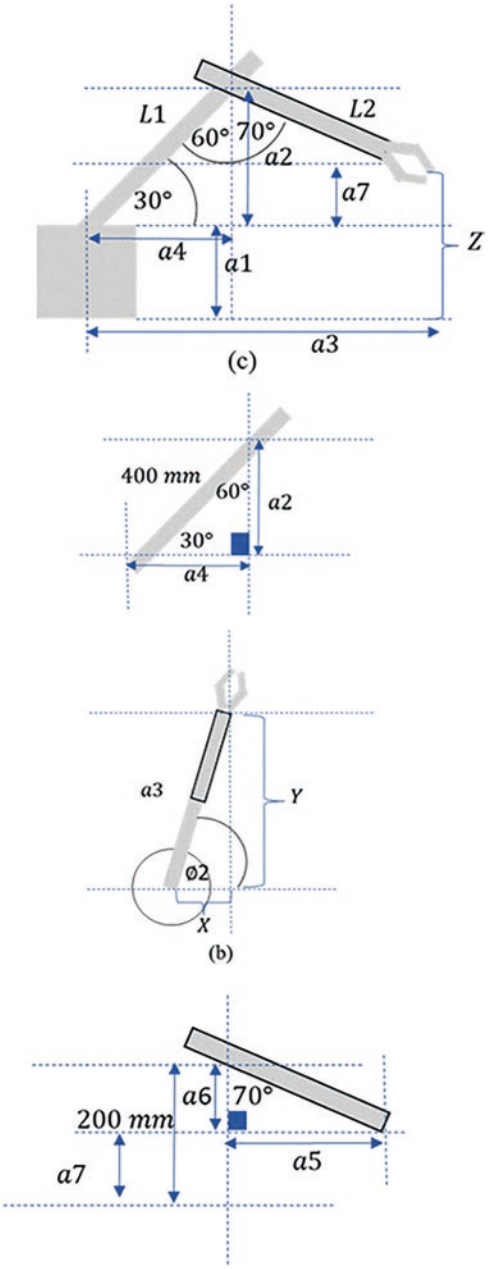

According to the given example, the gripper location is X = 362.14 mm, Y = 625.51 mm, and Z = 163.2 mm in space, and the inverse kinematics can be used to return the gripper to the home position. Keeping these equations inside the program, the gripper path can be calculated when the X, Y, and Z coordinates are given

by the camera. If an occlusion is in the middle of a pathway, an additional sensor is needed. Since most cameras have a minimum distance limitation (the Realsense D455 minimum accurate distance is 0.4 m), once the manipulator reaches the target, additional sensors are needed to find an obstacle-avoiding path. Two-step forward kinematic calculations can be performed to avoid occlusion when gripping the target fruit. If the robotic arm's second kinematic calculations exceed the working space of the robotic arm, the initial position of the arm needs to be changed by moving the autonomous vehicle that carries the robotic arm. Figure 21.14 shows the different basic robotic arm configurations based on possible fruit harvesting techniques.

Articulated manipulators are similar to the human hand. Based on the required task and operational area, these manipulators can be modified to avoid obstacles when picking the target fruit.

The accuracy and repeatability of manipulators are important for finding the target location in space and the home position when returning. Closed-loop servo or stepper motor-operated robots can track the position easily, while open-loop actuators need feedback sensors (position encoders) for tracking the position. In terms of avoiding occlusions, knowing the current position of the robotic arm is important for changing the moving path when the manipulator finds an obstacle on the path to the target location.

Moreover, the accuracy of harvesting robots is important, as many errors can be caused because of stuck grippers due to collisions with branches and fruit clusters;

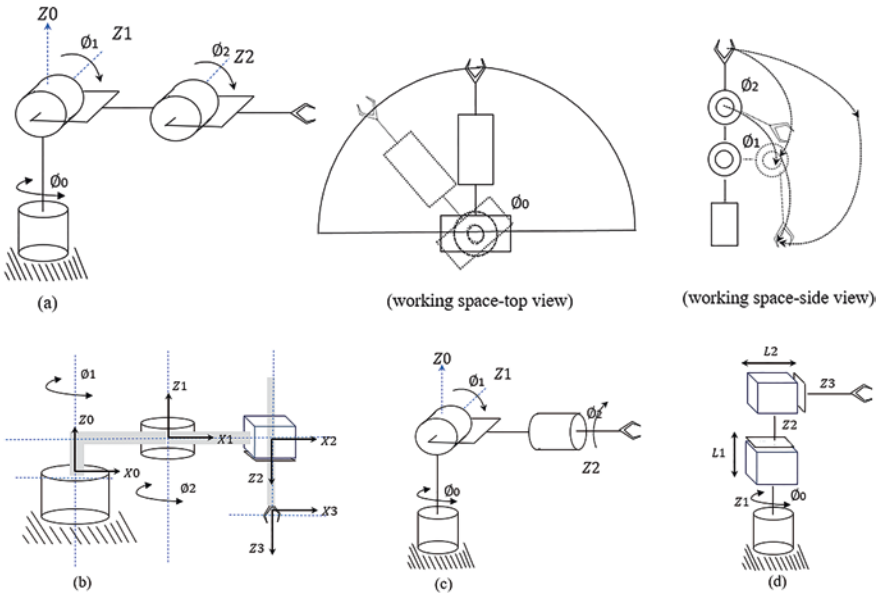

Fig. 21.14 (**a**) Articulated manipulator—RRR, (**b**, **c**) robot with two revolute joints and one prismatic joint—RRP, (**d**) cylindrical manipulator—RPP

dealing with fruit clusters is always challenging. Internal factors such as computational errors, gear backlash, and static and dynamic effects from joints also cause some errors. The rotational axis (revolute joint) is difficult to control because of the accumulation of errors due to kinematic and dynamic coupling. Most recently developed robots, as indicated in Table 21.2, have a linear-motion (prismatic) axis that performs Cartesian manipulations, which results in greater accuracy and success. Thus, the revolute joints occupy a smaller working space than the prismatic joints. Moreover, in terms of avoiding obstacles, revolute joint manipulators are capable of maneuvering around and creating a wider range of access to the target. Most harvesting robots are custom-made with different degrees of freedom.

In addition to kinematics, Jacobian metrics are important in terms of achieving high efficiency; they describe the relationship between the joint velocities and Cartesian velocities (linear and angular) of the end-effector, as well as static forces, joint forces, torques, and the Cartesian forces acting on the gripper. Understanding and applying motion planning is important for the gripper to avoid obstacles and reach the target without colliding with other objects. Force control is essential with acceleration and deceleration of motion. The gripper that contacts the fruit is very important in achieving the objective of robotic harvesting, which is to harvest fruit without any bruising effects. The end-effector or the gripper plays a critical role in avoiding occlusions, and the gripper/end-effector shape is key. The working space inside the canopy is limited, and mobility and manipulation depend on the gripper design, which can vary with different fruit shapes and characteristics.

21.5 Discussion

Replacing manual labor with machines is always challenging. The existing computational electronics and hardware are addressing this challenge to a certain degree with the help of CNNs, aiming to replace some of the high-skill tasks in the agricultural sector, particularly in orchard fruit harvesting. Maintaining quality and productivity at a high level is the main task of fruit production farmers, which has been handled by autonomous robotic systems developed in the past few years.

Harvesting robotics are complex and require understanding complex canopy structures to find fruit using complex trajectory planning. However, plant researchers have understood the necessity of a simple orchard architectural structure, rather than waiting until complex human-like robots are developed for harvesting, which would not be practically applicable. The developed raw novel canopy architectures for tree orchards provide a clear path for robotic systems to reach the target fruits easily, and most genetically improved fruit varieties produce single fruits rather than fruit clusters. Moreover, the development and growth rates are very similar among the fruits so that they ripen during the same period of the harvesting season.

Complex robotic arms are now replacing simple linear-joint robotic arms with fewer DOFs, which are designed with task-specific fruit gripping mechanisms. Moreover, the development of RGBD cameras and LiDAR devices, with different

principles and technologies, improves the detection of target fruit types and accurate localization.

Occlusions of fruits by branches, leaves, and fruit clusters cause errors in the localization coordinates after detection based on a CNN. These occlusions can be avoided based on the vision systems' mobility and robotic arms' working space dynamics. As indicated in this chapter, looking at fruits from different directions is a key strategy; compressed air can be used to move obscuring leaves, and harvesting at night is a strategy to avoid shade and light variations with flashlight systems. However, daytime localization and detection with a flashlight system can reduce the light variation and shadow effect to higher levels.

The ability to avoid bruising effects due to mechanical damage and bring the harvested fruits safely to the storage box with the gripper is basically determined by the robotic manipulator and the gripper's mechanical properties. When there are obstacles, to avoid forward kinematics and safely bring back the end-effector or the gripper to a fruit storage box, inverse kinematics needs to be developed based on several practical experiments. Trajectory planning followed by motion planning needs to be developed based on many considerations in field conditions.

21.6 Conclusion

Based on the context discussed above, it is evident that the newly developed fruit orchard architecture has diverted robotic development requirements more toward the simplest applications. The developed RGBD cameras can identify target fruits from different angles to avoid occlusions caused by leaves, branches, and fruit clusters. Variation in light and shadows can be avoided based on flashlights to a certain extent, and nighttime harvesting under a flashlight can be another way forward. Sensor fusion can be used to determine occlusion levels, and developed algorithms can be used to develop forward kinematics and trajectory planning to avoid occlusions and increase the efficiency of robotic fruit harvesting. Linear robotic arms or robotic arms with a smaller number of revolute joints (i.e., robotic arms with fewer DOFs) are the most convenient types. The fast development of different types of CNNs in fruit orchard detection can make these simple robots into more sophisticated versions that can perform a given task more efficiently and precisely than a complex fruit harvesting robot.

Acknowledgments The authors greatly appreciate the financial assistance provided by the MEXT scholarship and the Japan Leader Empowerment Program (JLEP) for the first author during the doctoral program that led to compiling this chapter.

References

Arkin, E. M., & Hassin, R. (1994). Approximation algorithms for the geometric covering salesman problem. *Discrete Applied Mathematics, 55*(3), 197–218.

Bac, C. W., van Henten, E. J., Hemming, J., & Edan, Y. (2014). Harvesting robots for high-value crops: State-of-the-art review and challenges ahead. *Journal of Field Robotics, 31*(6), 888–911.

Canny, J. F. (1986). A computational approach to edge detection. *IEEE Transactions on Pattern Analysis and Machine Intelligence PAMI, 8*(6), 679–698.

Ceres, R., et al. (1998). Design and implementation of an aided fruit-harvesting robot (Agribot). *Industrial Robot, 25*, 337–346.

Girshick, R. (2015). *Fast R-CNN* (pp. 1440–1448). IEEE.

Girshick, R., Donahue, J., Darrell, T., & Malik, J. (2014). *Rich feature hierarchies for accurate object detection and semantic segmentation* (pp. 580–587). IEEE.

Gongal, A., et al. (2015). Sensors and systems for fruit detection and localization: A review. *Computers and Electronics in Agriculture, 116*, 8–19.

Grift, T., Zhang, Q., Kondo, N., & Ting, K. C. (2008). A review of automation and robotics for the bio-industry. *Journal of Biomechatronic Engineering, 1*(1), 37–54.

Hannan, M. W., Burks, T. F., & Bulanon, D. M. (2009). A machine vision algorithm combining adaptive segmentation and shape analysis for orange fruit detection. *Agricultural Engineering International: the CIGR Ejournal, 11*, 1–17.

He, K., Gkioxari, G., Dollár, P., & Girshick, R. (2017). *Mask R-CNN* (pp. 2980–2988). IEEE.

Hetal, N. R., Jain, R., & Joshi, M. (2011). Fruit detection using improved multiple features based algorithm. *International Journal of Computer Applications, 13*, 1–5.

Illingworth, J., & Kittler, J. (1988). A survey of the hough transform. *Computer Vision, Graphics, and Image Processing, 44*(1), 87–116.

Kahandage, P. D., Hettiarachchi, S. W., Weerasooriya, G. V. T. V., Kosgollegedara, E. J., & Piyathissa, S. D. S. (2021). Design, development, and performance evaluation of a mechanical device for harvesting pineapple. *International Journal of Trend in Scientific Research and Development (IJTSRD), 5*(4), 1109–1116.

Kang, H., Wang, X., & Chen, C. (2022). Accurate fruit localization using high-resolution LiDAR-camera fusion and instance segmentation. *Computers and Electronics in Agriculture, 203*, 107450.

Kuznetsova, A., Maleva, T., & Soloviev, V. (2020). Using YOLOv3 algorithm with pre-and post-processing for apple detection in fruit-harvesting robot. *Agronomy, 10*(7), 1016. https://doi.org/10.3390/agronomy10071016

Li, T., Qiu, Q., & Zhao, C. (2021). Task planning of multi-arm harvesting robots for high-density dwarf orchards. *Nongye Gongcheng Xuebao/Transactions of the Chinese Society of Agricultural Engineering, 37*(2), 1–10.

Ling, X., et al. (2019). Dual-arm cooperation and implementation for robotic harvesting tomato using binocular vision. *Robotics and Autonomous Systems, 114*(C), 134–143.

Liu, J., Yuan, Y., Gao, Y., & Tang, S. (2019). Virtual model of grip-and-cut picking for simulation of vibration and falling of grape clusters. *Transactions of the ASABE (American Society of Agricultural and Biological Engineers), 62*(3), 603–614.

Liu, Z., et al. (2020). Improved *kiwifruit* detection using pre-trained VGG16 with RGB and NIR information fusion. *IEEE Access, 8*, 2327–2336.

Moseleya, K. R., House, L. A., & Roka, F. (2012). Adoption of mechanical harvesting for sweet Orange trees in Florida: Addressing grower concerns on long-term impacts. *International Food and Agribusiness Management Review, 15*(2), 83–98.

Mu, L., et al. (2020). Design and simulation of an integrated end-effector for picking kiwifruit by robot. *Information Processing in Agriculture, 7*(1), 58–71.

Redmon, J., Divvala, S., Girshick, R., & Farhadi, A. (2016). *You only look once: Unified, Real-time object detection*. IEEE.

Ren, S., He, K., Girshick, R., & Sun, J. (2017). Faster R-CNN: Towards real-time object detection with region proposal networks. *IEEE Transactions on Pattern Analysis and Machine Intelligence, 39*(6), 1137–1149.

Saunders, S. (2005) *Follow the Food.* Retrived July, 10 2023, from https://www.bbc.com/future/bespoke/follow-the-food/the-robots-that-can-pick-kiwifruit.html

Sepúlveda, D., et al. (2020). Robotic Aubergine harvesting using dual-arm manipulation. *IEEE Access, 8*, 121889–121904.

Tang, Y., et al. (2020). Recognition and localization methods for vision-based fruit picking robots: A review. *Frontiers in Plant Sciences, 11*, 510. PMID: 32508853; PMCID: PMC7250149.

Wei, X., et al. (2014). Automatic method of fruit object extraction under complex agricultural background for vision system of fruit picking robot. *Optik, 125*(19), 5684–5689.

Williams, H., et al. (2020). Improvements to and large-scale evaluation of a robotic kiwifruit harvester. *Journal of Field Robotics, 37*(2), 187–201.

Xie, Z., Ji, C., Guo, X., & Ren, S. (2010). An object detection method for quasi-circular fruits based on improved Hough transform. *Nongye Gongcheng Xuebao/Transactions of the Chinese Society of Agricultural Engineering, 26*(7), 157–162.

Xiong, Y., Ge, Y., Grimstad, L., & From, P. J. (2020). An autonomous strawberry-harvesting robot: Design, development, integration, and field evaluation. *Journal of Field Robotics, 37*(2), 202–224.

Zhao, J., Tow, J., & Katupitiya, J. (2005). *On-tree fruit recognition using texture properties and color data* (pp. 263–268). IEEE.

Zheng, C., et al. (2021). A mango picking vision algorithm on instance segmentation and key point detection from RGB images in an open orchard. *Biosystems Engineering, 206*, 32–54.

Chapter 22
Smart Automation for End-Effectors in the Development of Horticultural Robots

Abstract Horticultural robots equipped with intelligent automation and advanced end-effectors bring many benefits to the horticultural sector. Integrating intelligent automation into the design of end-effectors increases productivity, accuracy, flexibility, and adaptability. This chapter discusses end-effectors commonly used in horticulture and analyzes their specific application requirements. Subsequently, the vital role played by sensing and perception technologies in end-effector automation is described. Then, the differences between different actuation technologies in terms of speed, force, and volume are compared in terms of actuation and control mechanisms. In addition, the applications of deep learning algorithms to end-effectors are discussed. Finally, a case study demonstrated the design of a three-finger flexible gripper for orchard operations. The proposed gripper was simple, stable, flexible, low-cost, and suitable for a wide range of fruits, potential to provide a solution for orchard harvesting. Overall, horticultural robots with advanced end-effectors and smart automation have the significant potential to increase productivity, reduce labor costs, and promote precision agricultural practices.

Keywords End-effector · Smart automation · Horticultural robot · Sensing technology · Deep learning

22.1 Introduction

Horticultural robots are advanced technological systems designed to automate various tasks involved in plant cultivation, maintenance, and harvesting (Ahn et al., 2018). One key component of horticultural robots is the end-effector. The end-effector refers to the device or tool attached to the robot's arm or manipulator, responsible for interacting with the plants and their environment (Davidson et al., 2020) (Fig. 22.1).

There are various types of end-effectors employed in horticulture, each catering to a specific application. The use of end-effectors brings numerous benefits to the

© The Author(s), under exclusive license to Springer Nature Singapore Pte Ltd. 2024

T. Ahamed, *IoT and AI in Agriculture*,
https://doi.org/10.1007/978-981-97-1263-2_22

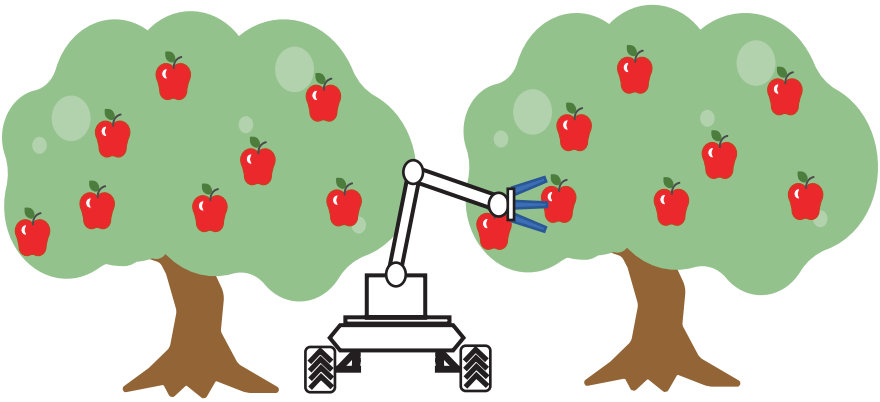

Fig. 22.1 Application of harvesting robot equipped with the end-effector in the orchard

field of horticulture (Feng, 2021). Firstly, end-effectors enhance productivity and efficiency. Robots equipped with appropriate end-effectors can work tirelessly and consistently, thereby increasing the speed and accuracy of various horticultural tasks. Secondly, end-effectors contribute to precision and accuracy. Horticultural robots can perform delicate operations with high precision by employing specialized end-effectors. Moreover, end-effectors enable increased flexibility and adaptability. As horticultural tasks can vary significantly depending on plant types, growth stages, and environmental conditions, robots equipped with interchangeable end-effectors can easily switch between different tasks. This adaptability enhances the versatility of horticultural robots and enables them to handle diverse cultivation requirements efficiently. Additionally, end-effectors contribute to labor reduction and cost savings. By automating labor-intensive tasks, horticultural robots equipped with appropriate end-effectors can reduce the dependency on human workers (Vrochidou et al., 2022). This can address labor shortages, lower labor costs, and allow skilled labor to be allocated to more complex or specialized tasks. Consequently, farmers and growers can achieve significant cost savings while maintaining productivity levels.

With the rise of automation and smart technologies, the design and development of end-effectors have undergone significant advancements. Smart automation in end-effector design and development offers enhanced precision and efficiency in robotic operations (Xie et al., 2022). By incorporating sensors, artificial intelligence, and advanced control systems, end-effectors can gather real-time data and adjust their actions accordingly. This enables them to adapt to change conditions, optimize grip strength, and perform tasks with utmost accuracy. Another significant advantage of smart automation in the end-effector is its increased versatility and adaptability. Traditional end-effectors are often designed for specific tasks and lack the flexibility to handle diverse operations. However, by incorporating smart automation, end-effectors can be equipped with interchangeable tools or adaptive features (Hua et al., 2019) (Fig. 22.2).

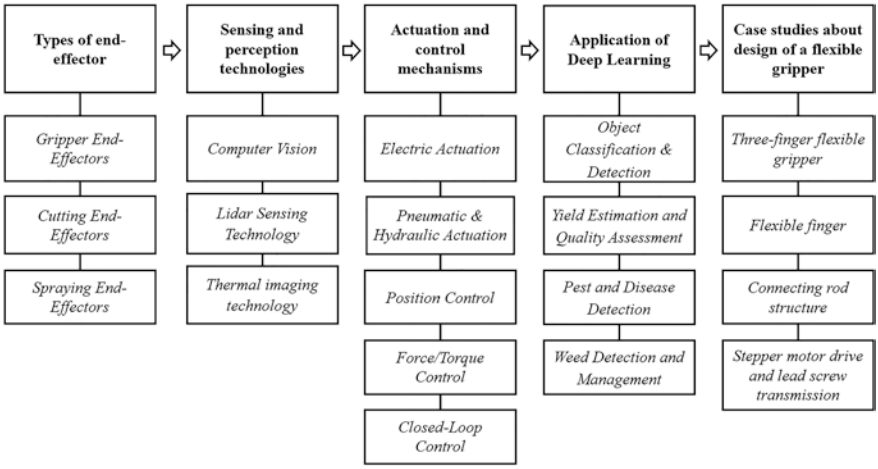

Fig. 22.2 Main contents of this chapter to propose a flexible gripper for fruit harvesting in orchard

In recent years, the integration of smart automation into the end-effectors for horticultural robots has gained significant importance. This chapter explores the significance of smart automation for end-effectors in the development of horticultural robots. It is mainly divided into the following sections: The first section describes the types of end-effectors commonly used in horticulture. The second section focuses on the sensing and perception technologies for end-effector automation. The third section describes the actuation and control mechanisms for smart end-effectors. The fourth section outlines applications of deep learning for end-effector automation in horticultural robots. Finally, the fifth section reports some of the case studies about the design of a three-finger flexible gripper for orchard.

22.2 Types of End-Effectors for Automation in Horticulture

Due to the different shapes, sizes, weights, materials, and surface states of the plants being operated, the end-effectors of horticultural robots are diverse. According to different uses, end-effectors can be divided into gripper end-effectors, cutting end-effectors, and spraying end-effectors, as shown in Fig. 22.3.

22.2.1 Gripper End-Effectors

Gripper end-effectors are widely employed for tasks such as harvesting fruits and picking flowers (Tinoco et al., 2021). These end-effectors come in different forms to accommodate various object structures and sizes. Grippers utilize flexible fingers or

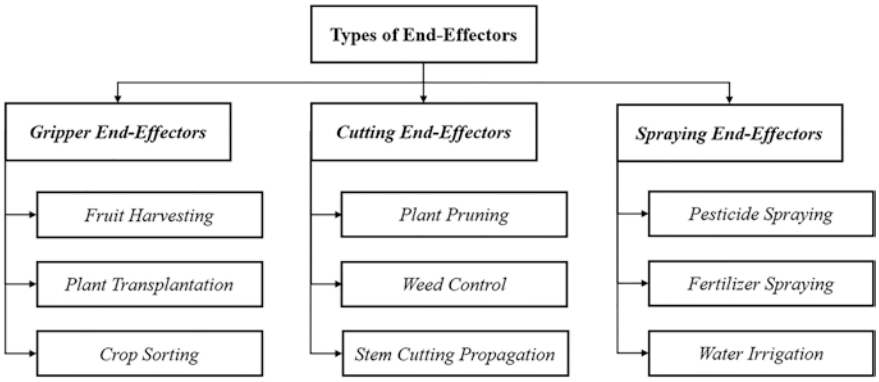

Fig. 22.3 Types of end-effectors for different applications

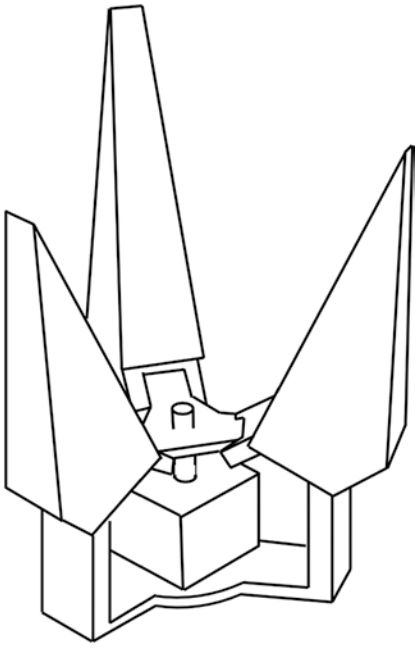

Fig. 22.4 A gripper end-effector with three fingers

suction cups to grasp objects securely. Flexible fingers rely on the flexible deformation during the blessing process to wrap the object, while the suction cups use the negative pressure generated by the air pump to stably absorb the object. Gripper end-effectors provide the necessary flexibility to handle fragile plants without causing damage (Fig. 22.4).

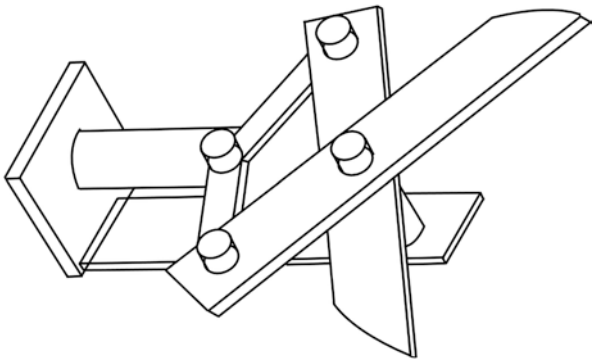

Fig. 22.5 A cutting end-effector in the shape of a scissor

22.2.2 Cutting End-Effectors

Cutting end-effectors are specifically designed to trim leaves, branches, or flowers with precision (Zahid et al., 2021). These end-effectors often employ blades or scissor-like mechanisms to achieve cutting actions. Cutting end-effectors enables uniform and clean cuts, promoting plant health and growth. By automating cutting tasks, horticultural robots equipped with cutting end-effectors reduce labor requirements and ensure consistent results, particularly in large-scale horticultural operations (Fig. 22.5).

22.2.3 Spraying End-Effectors

Spraying end-effectors are essential for precise and targeted application of substances such as fertilizers, pesticides, or herbicides (Meshram et al., 2022). These end-effectors utilize nozzles or sprayers to deliver the required substances in specific quantities and areas. By employing spraying end-effectors, horticultural robots can accurately apply chemicals, minimizing waste, and potential harm to the environment. These end-effectors enable efficient and controlled crop management, allowing for selective treatment and reducing the risk of overuse or underuse of chemicals (Fig. 22.6).

In the field of horticulture, gripper end-effectors facilitate efficient harvesting and picking operations, cutting end-effectors ensure precise and uniform trimming, spraying end-effectors enable targeted chemical application, and sensing end-effectors provide valuable data for informed decision-making. The integration of these various types of end-effectors into horticultural robots improves efficiency, reduces labor costs, and promotes sustainable crop management. As technology continues to advance, further developments in end-effector design and functionality are expected.

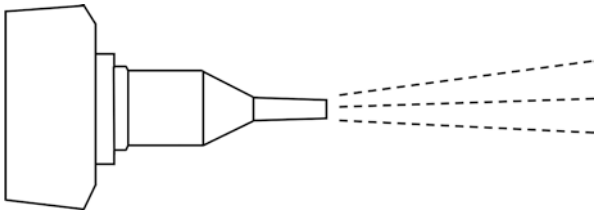

Fig. 22.6 A spraying end-effector basic design

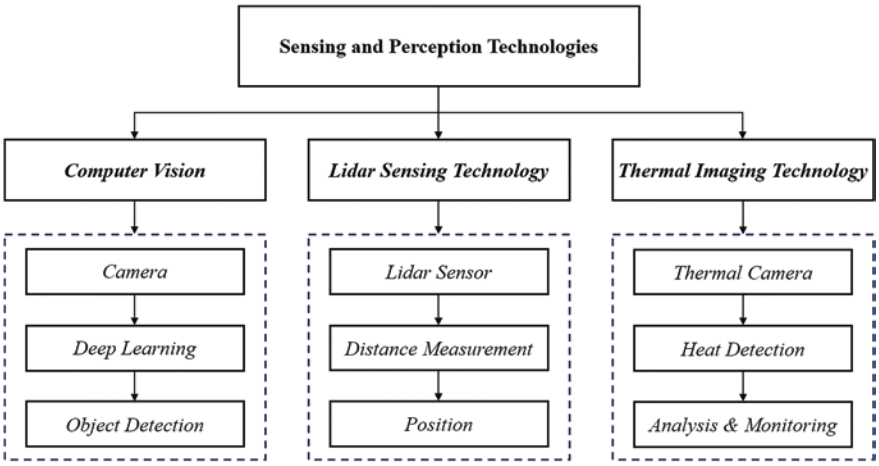

Fig. 22.7 Processes of various sensing and perception technologies

22.3 Sensing and Perception Technologies for End-Effector Automation in Horticulture

Sensing and perception technologies play a crucial role in end-effector automation, enabling robots to gather data about the environment and make informed decisions. Next, we will explore the various sensing and perception technologies used in end-effector automation for horticulture and their impact on improving efficiency, precision, and overall productivity in the field (Fig. 22.7).

22.3.1 Computer Vision

Computer vision is a key technology utilized in horticultural robots to analyze visual data and understand the surrounding environment (Tian et al., 2020). By integrating cameras and image processing algorithms, robots can identify plants,

fruits, or specific features, such as ripeness or disease symptoms. Computer vision enables robots to perform tasks like fruit or flower recognition, quality assessment, and selective harvesting. This technology enhances the efficiency of horticultural processes by enabling targeted actions and reducing waste (Fig. 22.8).

The camera is usually fixed on the end-effector and can also be installed on other parts of the horticultural robot body. In order to adapt to different distance and field of view requirements, a horticultural robot may be equipped with multiple cameras, for example, a close-range camera is suitable for high-precision recognition of a single target, while a wide-angle camera enables a wider range of target detection. As shown in Fig. 22.9, the camera collects images of apples in the orchard, and by training the object detection model, the robot can distinguish between the apple and the background. Once the camera has completed target recognition, the robot can perform corresponding operations according to preset tasks, such as picking ripe fruits in a targeted manner, detecting and treating diseased plants, or evaluating the quality of fruits.

Fig. 22.8 Intel RealSense Depth Camera is employed to capture images and positions of apples

Fig. 22.9 The 3D camera collects image data for the apple detection model

22.3.2 Lidar Sensing Technology

LiDAR (Light Detection and Ranging) sensors are increasingly employed in horticultural robots to gather spatial data about the surroundings (Debnath et al., 2023). By emitting laser beams and measuring their reflections, LiDAR sensors create detailed maps of the environment, including plants, structures, and obstacles. This technology allows robots to accurately perceive distances, shapes, and sizes of objects in real time. In horticulture, lidar sensing technology can locate the object, and the position information used for subsequent path planning, thereby helping the terminal sensor to realize the operation (Fig. 22.10).

As shown in Fig. 22.11, LiDAR emits high-frequency laser beams that travel at very fast speeds and are reflected back when they intersect with objects of interest. LiDAR is also equipped with a high-performance receiver to capture the laser signal reflected from the target object. The collected LiDAR data are processed and analyzed. These data contain spatial information such as the distance, height, and shape of the target object. In the application of agricultural robots, the data collected by

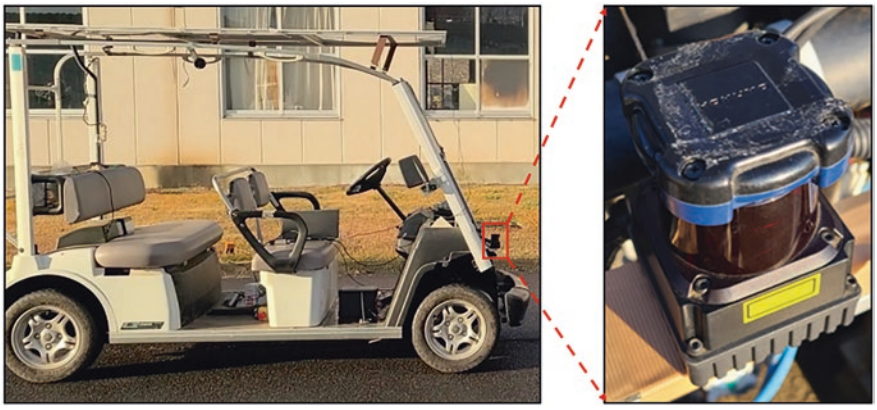

Fig. 22.10 UTM-30LX-EW LiDAR

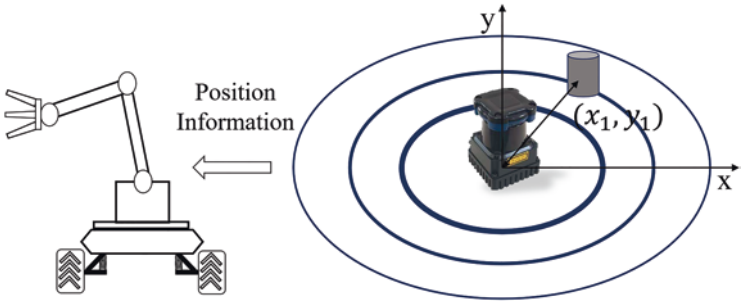

Fig. 22.11 Schematic diagram of LiDAR sending collected position information to a horticultural robot

LiDAR can be used in many aspects: target positioning, path planning, obstacle detection, etc.

22.3.3 Thermal Imaging Technology

Thermal imaging technology, also known as infrared cameras, detects and captures the heat emitted by objects (Ishimwe et al., 2014). In horticulture, thermal cameras are used to assess the temperature variations of plants and their surroundings. By analyzing thermal images, robots can identify thermal anomalies that may indicate stress, disease, or water deficiencies in plants. This technology enables early detection of problems, allowing for targeted interventions. By integrating thermal cameras into horticultural robots, the system can effectively monitor plant health and control the end-effectors to take proactive measures, ensuring optimal growth and yield (Fig. 22.12).

As shown in Fig. 22.13, thermal cameras collect data by sensing and capturing thermal radiation emitted by objects. These cameras use infrared sensors to detect temperature differences on the surfaces of different objects and convert this thermal radiation data into thermal images for visualization. In the application of intelligent end-effectors in gardening robots, the data collected by thermal imaging cameras can be used for the following aspects: object detection, plant health, and monitoring.

Sensing and perception technologies are instrumental in end-effector automation for horticulture, empowering robots to gather data about the environment and make informed decisions. Computer vision, LiDAR sensing technology, and thermal imaging technology all contribute to the efficiency, precision, and productivity of

Fig. 22.12 A thermal camera model FLIR ADK for an orchard robot

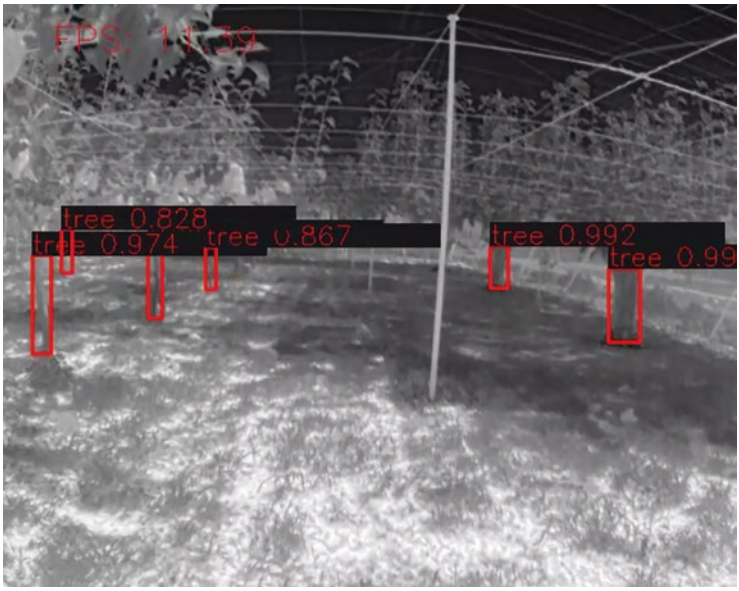

Fig. 22.13 The thermal camera collects thermal images for object detection in the orchard

horticultural processes. By leveraging these technologies, end-effector automation becomes more intelligent and adaptive, allowing for targeted actions. As the field of horticulture continues to automate, the integration of these sensing and perception technologies on the end-effector of horticultural robots has the high potential to promote precision and efficient agricultural practices.

22.4 Actuation and Control Mechanisms for Smart End-Effectors

Smart end-effectors are designed to perform complex tasks with precision and efficiency. To achieve such capabilities, actuation and control mechanisms are essential. This article explores the key aspects of actuation and control mechanisms for end-effectors and their significance in enhancing performance and adaptability (Fig. 22.14).

22.4.1 Actuation Technologies

Actuation technologies are fundamental to the functioning of smart end-effectors (Zaidi et al., 2021). They enable the conversion of control signals into mechanical motion, allowing the end-effector to interact with the environment. Several actuation technologies are commonly employed in smart end-effectors (Table 22.1), including:

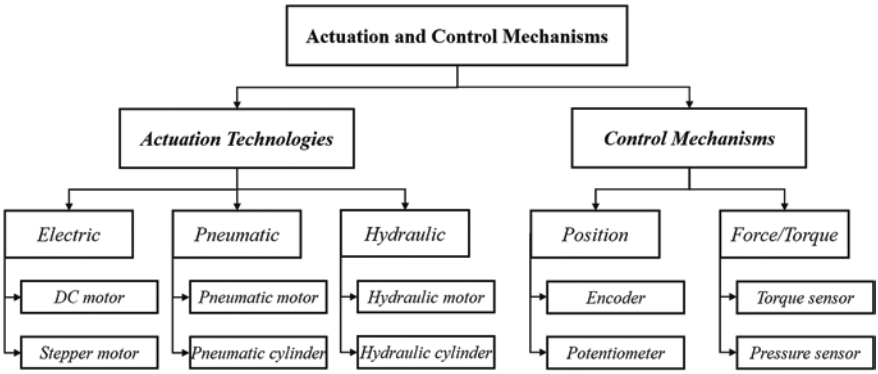

Fig. 22.14 Actuation and control mechanisms for smart end-effectors

Table 22.1 Comparison of end-effectors with different actuation methods

Capabilities	Electric	Pneumatic	Hydraulic
Speed	☆	☆☆☆	☆☆☆
Force	☆	☆☆	☆☆☆
Portability	☆☆☆	☆☆	☆
Environmental adaptability	☆☆☆	☆☆	☆

(a) Electric Actuation: Electric motors provide high precision and controllability, making them suitable for delicate tasks that require accuracy. They can be further classified into direct-drive motors, stepper motors, and servo motors, depending on the specific application requirements. Electric actuation usually does not require special drive equipment and has the advantages of small size and high control precision. However, the execution speed is relatively slow compared with pneumatic and hydraulic actuation.

(b) Pneumatic/Hydraulic Actuation: Pneumatic systems offer higher force capabilities and rapid movement. They are often utilized in applications that require heavy gripping or cutting. These actuation mechanisms are known for their robustness and ability to generate substantial force. Pneumatics and hydraulics generally have greater forces and operating speeds. However, pneumatic and hydraulic usually require separate air pumps and water pumps as air and water sources. They are therefore bulkier and more difficult to install.

22.4.2 Control Mechanisms

Control mechanisms are integral to the precise operation and adaptability of smart end-effectors (Dai et al., 2022). They enable real-time monitoring, feedback, and adjustment of actuation, ensuring optimal performance. Common control mechanisms used in smart end-effectors include:

(a) Position Control: Position control involves accurately controlling the position of the end-effector. Sensors, such as encoders or potentiometers, provide feedback on the end-effector‘s position, enabling precise movements and manipulation. Position control is crucial for applications requiring high accuracy and repeatability.
(b) Force/Torque Control: Force and torque control mechanisms enable smart end-effectors to exert and maintain specific forces or torques during interactions. These control techniques are essential for tasks involving delicate objects, human-robot collaboration, or applications requiring force feedback. Force/torque control enhances safety, improves object handling, and allows for haptic feedback in robotic systems.

Actuation and control methodologies are essential for smart end-effectors, enabling precise manipulation, efficient task execution, and adaptability. By integrating advanced actuation technologies, control approaches, and sensors, smart end-effectors can achieve higher performance, safety, and versatility.

22.5 Applications of Deep Learning for End-Effector Automation in Horticultural Robots

Deep learning, a subset of artificial intelligence, has emerged as a powerful tool in this domain. By leveraging deep learning algorithms, horticultural robots can learn from large datasets, analyze complex visual and sensory information, and make intelligent decisions. This section explores the application of deep learning in end-effector automation for horticultural robots and its potential to enhance efficiency, accuracy, and productivity in the field.

22.5.1 Object Classification and Detection

Deep learning algorithms excel in object classification and detection tasks (Yang & Xu, 2021). In horticultural robots, this capability is crucial for identifying and distinguishing plants, fruits, and other objects of interest. By training neural networks on extensive datasets, robots can accurately recognize and classify various plant species, detect ripe fruits. This enables targeted actions, improving overall efficiency and yield.

22.5.2 Yield Estimation and Quality Assessment

Deep learning models can analyze visual data and estimate crop yield with remarkable accuracy (Dhiman et al., 2022). By processing images or videos of plants, horticultural robots can predict the number and size of fruits, assess their ripeness,

and estimate overall yield. This information helps farmers plan harvest schedules, optimize resource allocation, and ensure timely delivery of high-quality produce to market. Deep learning algorithms also enable robots to assess the quality of harvested products, identifying defects, blemishes, or signs of damage. This enhances the sorting and grading process, ensuring consistent product quality, and reducing waste.

22.5.3 Pest and Disease Detection

Early detection of pests and diseases is crucial for effective plant management. Deep learning algorithms can be trained to recognize specific symptoms or patterns associated with pests, diseases, or nutrient deficiencies (Vasavi et al., 2022). By analyzing images or sensor data, horticultural robots equipped with deep learning capabilities can identify potential issues at an early stage, allowing for targeted interventions and minimizing crop losses. This technology provides farmers with valuable insights for implementing pest control measures, precise application of pesticides, or adjusting nutrient regimes.

22.5.4 Weed Detection and Management

Weed control is a critical aspect of horticulture, as weeds compete with crops for resources and can significantly reduce yields. Deep learning algorithms can be trained to detect and classify different weed species based on visual cues (Hasan et al., 2021). This enables horticultural robots to precisely target and remove weeds, reducing the need for manual labor or excessive herbicide use. By integrating deep learning with robotic weed control systems, farmers can achieve effective and environmentally friendly weed management strategies, optimizing crop growth and minimizing ecological impact.

Deep learning has revolutionized the field of end-effector automation in horticultural robots. It enables robots to perform tasks in a more intelligent way through training with large amounts of data. Whether it's object recognition, yield estimation, pest detection, or weed management, deep learning algorithms empower horticultural robots to make intelligent decisions and execute precise actions.

22.6 Case Studies About Design of a Three-Finger Flexible Gripper for Orchard

Among the above control, perceptions and sensing system, end-effector mechanism still had lack of research and challenges to detect the fruits without damages. Research have concentrated on the actuation and vision system; however gripping

mechanism needs still significant effort to make the orchard more successful. In this regard, this section introduces case studies about the flexible gripper that can be proposed in the development of orchard robots.

22.6.1 The Three-Finger Flexible Gripper

As shown in Fig. 22.15, the three-finger flexible gripper consists of flexible fingers, connecting rod, a screw rod, a stepper motor, and a base. Among them, the stepper motor provides power as a driving device to control the rotation of the screw rod. The screw converts rotary motion into linear motion. The connecting rod and the screw rod are connected by a connecting piece. The linkage converts the linear motion of the lead screw into the rotational motion of the three flexible fingers. Finally, a motion driven by a stepping motor is formed to control the opening and closing of fingers. Since the fingers are made of flexible materials, they would not cause damage to the fruit during the picking process and can adaptively fit the surface of the fruit. Not used for pneumatic grippers, the motor drive does not require a special air source and pneumatic controller. In short, compared with the pneumatic gripper, this electric flexible gripper has the advantages of simple structure, small size, low cost, easy installation, and is suitable for a variety of fruits. However, compared with pneumatic grippers, electric grippers also have disadvantages such as slow speed and small clamping force. In the process of selecting grippers, factors such as fruit types and orchard environment should be fully considered.

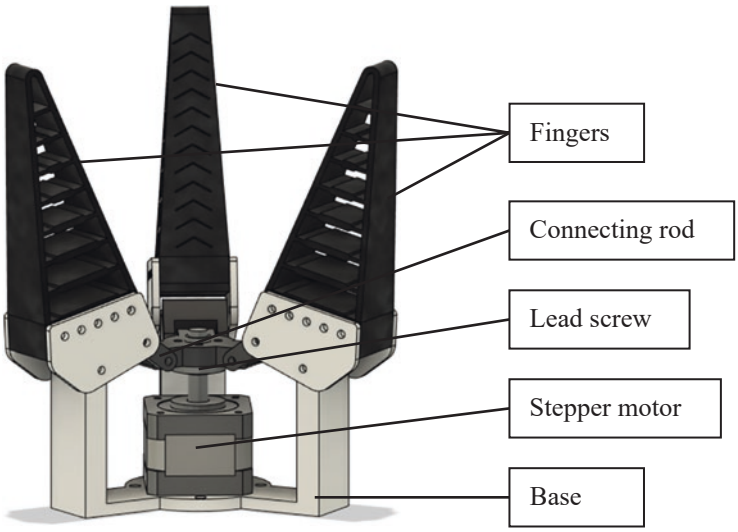

Fig. 22.15 The three-finger flexible gripper

22.6.2 Flexible Finger

As shown in Fig. 22.16, the fingers of the gripper are made of a flexible material TPU (Thermoplastic polyurethanes), which can be made by injection molding or 3D printing. Compared with traditional rigid materials, this material has good flexibility, which does not cause damage to the fruit during the picking process. In terms of the structure of the finger, the fish fin structure is referred to (Xu et al., 2018). If the finger is pushed in one direction, the finger will not bend in the direction of the thrust, but in the opposite direction of the thrust. This phenomenon is called: the "fin ray effect." Compared with other flexible structures, the fin structure can bear a larger load and has better flexibility. After receiving an external force, it can passively wrap the fruit. Due to the characteristics of the flexible fingers adopting the fin structure, the gripper can use many kinds of fruits.

22.6.3 Connecting Rod Structure

As shown in Fig. 22.17, the gripper finger has a connecting rod structure, with a total of three active components in one finger. The movement of the screw can be regarded as a sliding pair, and the others are three rotating pairs, so there are four low pairs in total, and the number of high pairs is 0. According to the DoF (Degrees

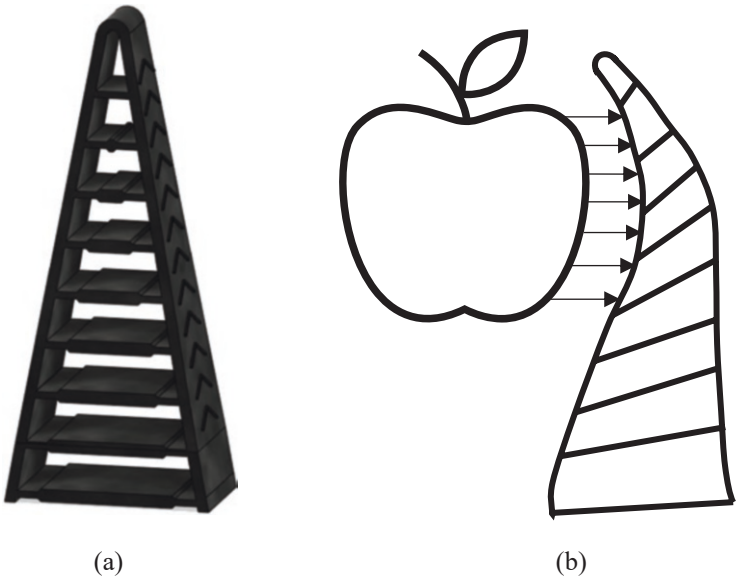

Fig. 22.16 (**a**) The flexible fingers with fin structure, (**b**) deformation of the flexible gripper after stress

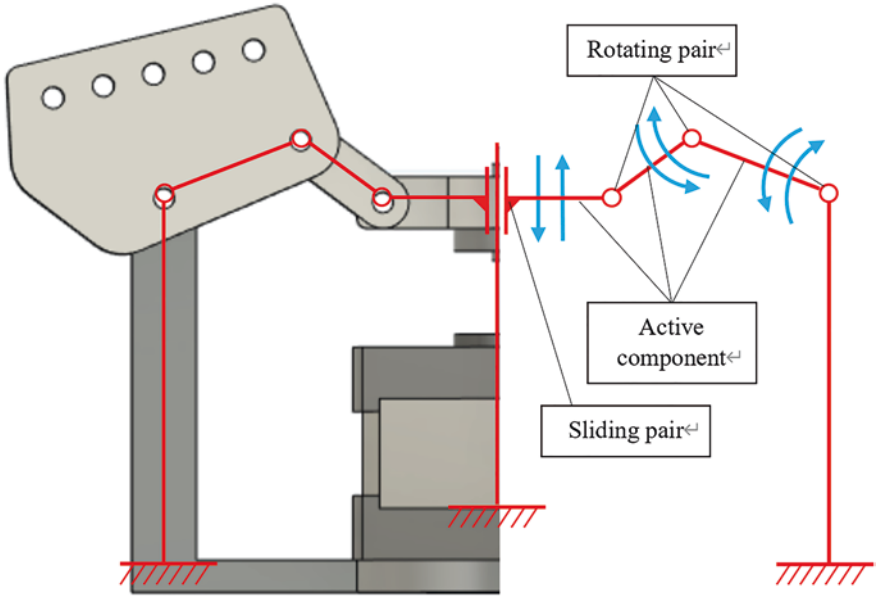

Fig. 22.17 Connecting arm structure of flexible gripper

of Freedom) formula below (Gao et al., 1998), we can calculate that the DOF of a finger is 1.

$$F = 3n - \left(2P_l + P_h\right)$$

where, n is the number of active components, P_l is the number of low secondary constraints, P_h is the number of high secondary constraints, and F is the degree of freedom of the mechanism.

The fingers of the jaws are fixed to one of the movable members for rotational movement. This rotational movement is the tightening movement of the jaws as a whole. With the up and down movement of the screw rod, the fingers tighten and loosen the fruit.

22.6.4 Stepper Motor Drive and Lead Screw Transmission

As shown in Fig. 22.18, the driving device of the flexible gripper can be a 42-stepper motor. Wherein, the shaft output mode of the motor can be a screw rod. The screw converts the rotational motion of the motor shaft into linear motion. Among them, because the lead of the screw rod is small, the small torque can be converted into a large thrust, so the force acting on the surface of the fruit is greater, and the fruit can be better fixed. The thrust of the screw is related to the lead and the torque of the motor, the formula is as follows (Repanich, 2016):

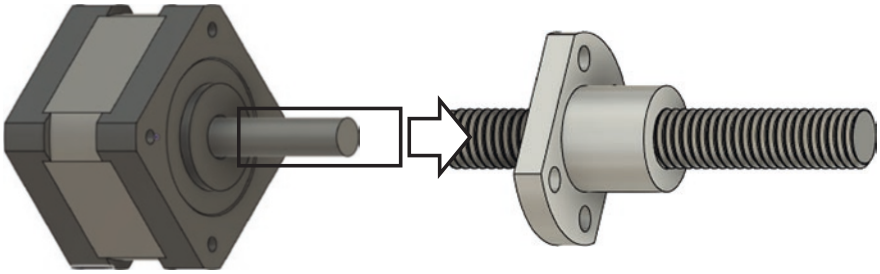

Fig. 22.18 Stepper motor and lead screw

$$F = \frac{2\pi T}{L} \times n$$

where, F is the thrust of the screw, T is the torque of the motor, L is the lead of the screw, and n is the transmission efficiency.

This section introduced a flexible gripper based on the fish fin structure that can be applied to orchard picking operations, which can grab fruits of different shapes within a certain size range. The gripper is composed of three flexible fingers, a stepping motor, and a connecting piece, and the opening and closing of the gripper are realized by driving the stepping motor. TPU can be used as the material to make the jaws flexible enough. The gripper has the advantages of a wide grabbing range, simple structure, stable grabbing, strong wrapping, easy installation, and low cost. Provides a solution for the selection of grippers in an orchard environment.

22.7 Conclusion

Horticultural robots with advanced end-effectors and intelligent automation have the potential to revolutionize the horticultural sector. Incorporating intelligent automation in end-effector design can increase productivity, accuracy, flexibility, and adaptability. This chapter reviewed several types of end-effectors commonly used in horticulture, including gripping end-effector, cutting end-effector, and spraying end-effector. Gripping end-effector enables efficient harvesting and picking operations, cutting end-effector ensures precise and uniform pruning, and spraying end-effector enables targeted chemical applications. This is followed by a list of several sensing and perception technologies, such as computer vision, LIDAR sensing, and thermal imaging, which provide data about the environment and plants. Then, actuation and control mechanisms, including electric, pneumatic, and hydraulic technologies, are compared for end of effectors. In addition, the applications of deep learning algorithms to end-effector are also discussed, including tasks such as object classification, yield estimation, pest detection, and weed management. Finally, a case study demonstrated the design of a three-fingered flexible manipulator for orchard operations, providing a simple, cost-effective potential solution for fruit

picking. In conclusion, horticultural robots with advanced end-effectors and intelligent automation features are expected to revolutionize the horticultural field. By leveraging sensing technologies, advanced control mechanisms, deep learning, and material applications, these robots can increase productivity, precision, and efficiency while reducing labor costs. Therefore, this chapter provided an outlook of the end-effector, including the review of existing technologies and the proposed flexible griper to avoid injuries to fruits and accuracy in gripping to enable precision management of orchard crop.

References

Ahn, H.S., Dayoub, F., Popovic, M., MacDonald, B., Siegwart, R., Sa, I. (2018). *An overview of perception methods for horticultural robots: From pollination to harvest*. https://doi.org/10.48550/arXiv.1807.03124

Dai, Y., Xiang, C., Qu, W., & Zhang, Q. (2022). A review of end-effector research based on compliance control. *Machines, 10*, 100.

Davidson, J., Bhusal, S., Mo, C., Karkee, M., & Zhang, Q. (2020). Robotic manipulation for specialty crop harvesting: A review of manipulator and end-effector technologies. *Global Journel of Agricultural Allied Sciences, 2*, 25–41.

Debnath, S., Paul, M., & Debnath, T. (2023). Applications of LiDAR in agriculture and future research directions. *Journel of Imaging, 9*, 57.

Dhiman, B., Kumar, Y., & Kumar, M. (2022). Fruit quality evaluation using machine learning techniques: Review, motivation and future perspectives. *Multimedia Tools and Applications, 81*, 16255–16277.

Feng, Q. (2021). End-effector technologies. In *Fundamentals of agricultural and field robotics* (pp. 191–212). Springer.

Gao, F., Liu, X., & Gruver, W. A. (1998). Performance evaluation of two-degree-of-freedom planar parallel robots. *Mechanism and Machine Theory, 33*, 661–668.

Hasan, A. M., Sohel, F., Diepeveen, D., Laga, H., & Jones, M. G. (2021). A survey of deep learning techniques for weed detection from images. *Computers and Electronics in Agriculture, 184*, 106067.

Hua, Y., Zhang, N., Yuan, X., Quan, L., Yang, J., Nagasaka, K., & Zhou, X.-G. (2019). Recent advances in intelligent automated fruit harvesting robots. *Open Agricultural Journal, 13*, 101.

Ishimwe, R., Abutaleb, K., Ahmed, F., et al. (2014). Applications of thermal imaging in agriculture—A review. *Advanced Remote Sensing, 3*, 128.

Meshram, A. T., Vanalkar, A. V., Kalambe, K. B., & Badar, A. M. (2022). Pesticide spraying robot for precision agriculture: A categorical literature review and future trends. *Journel of Field Robotics, 39*, 153–171.

Repanich, N. (2016). *Introduction to motor sizing* (pp. 12–13). Deartment of Mechanical and Mechatronic Engineering and Sustainable Manufacturing California State University.

Tian, H., Wang, T., Liu, Y., Qiao, X., & Li, Y. (2020). Computer vision technology in agricultural automation—A review. *Information Processing in Agriculture, 7*, 1–19.

Tinoco, V., Silva, M. F., Santos, F. N., Rocha, L. F., Magalhães, S., & Santos, L. C. (2021). A review of pruning and harvesting manipulators. In *2021 IEEE international conference on autonomous robot systems and competitions (ICARSC)* (pp. 155–160). IEEE.

Vasavi, P., Punitha, A., & Rao, T. V. N. (2022). Crop leaf disease detection and classification using machine learning and deep learning algorithms by visual symptoms: A review. *International Journal of Electrical and Computer Engineering, 12*, 2079.

Vrochidou, E., Tsakalidou, V. N., Kalathas, I., Gkrimpizis, T., Pachidis, T., & Kaburlasos, V. G. (2022). An overview of end effectors in agricultural robotic harvesting systems. *Agriculture, 12*, 1240.

Xie, D., Chen, L., Liu, L., Chen, L., & Wang, H. (2022). Actuators and sensors for application in agricultural robots: A review. *Machines, 10*, 913.

Xu, W., Zhang, H., Zheng, N., & Yuan, H. (2018). Design and experiments of a compliant adaptive grasper based on fish fin structure. In *2018 IEEE international conference on robotics and biomimetics (ROBIO)* (pp. 293–298). IEEE.

Yang, B., & Xu, Y. (2021). Applications of deep-learning approaches in horticultural research: A review. *Horticulture Research, 8*, 123.

Zahid, A., Mahmud, M. S., He, L., Heinemann, P., Choi, D., & Schupp, J. (2021). Technological advancements towards developing a robotic pruner for apple trees: A review. *Computers and Electronics in Agriculture, 189*, 106383.

Zaidi, S., Maselli, M., Laschi, C., & Cianchetti, M. (2021). Actuation technologies for soft robot grippers and manipulators: A review. *Current Robotics Reports, 2*, 355–369.

Chapter 23
Strategic Short Note: Spatially Factorized Spectroscopy—Focusing on a Single Component in a Mixed Sample

Abstract Although nondestructive spectroscopy methods have been applied widely to food measurement, they have an inherent problem in that the spectra acquired from samples contain information on multiple chemical components present in the samples. We propose a novel measurement method: Spatially Factorized Spectroscopy (SFS) to overcome the challenge of separating spectra of the target compounds from the background. We show how this method can be applied to quantification of a specific sugar in a sample consisting of multiple powders.

Nondestructive spectroscopy methods have been applied widely to food measurement. These methods generally are rapid and simple, and they are increasingly being focused on as a green technology since they do not use organic solvents for extraction or produce toxic waste (Pallone et al., 2018; Xu et al., 2023). Furthermore, the evolution of complex mathematical analysis methods such as machine learning and deep learning has allowed the extraction of valuable information from complicated spectra.

However, nondestructive spectroscopic methods have an inherent problem in that the spectrum acquired from a sample contains information on multiple chemical components existent in the sample. This means a calibration model built to estimate the concentration of a certain component needs to be altered if the background spectra (coming from the other components existent in the sample or other contributing factors) are very different. In practice, it is challenging to decide how much difference in the background spectra can be tolerated, and this leads to uncertainties when estimating new samples (Sharma et al., 2013).

While most spectroscopy methods assume that the sample is homogeneous in macroscopic scale and that the spectra acquired reflect the average chemical composition of the target, most food materials are nonuniform when viewed in microscale (Aguilera et al., 2000). For example, emulsions contain oil droplets inside a water phase (or vice versa) and mixtures of powders are nonuniform when viewed in the scale of the powder particles. Therefore, if a spectrum can be measured from a microscopic point on the sample, it can reflect a purer component than a spectrum taken from a larger measurement point.

© The Author(s), under exclusive license to Springer Nature Singapore Pte Ltd. 2024

T. Ahamed, *IoT and AI in Agriculture*,
https://doi.org/10.1007/978-981-97-1263-2_23

Here, we propose a novel measurement method: Spatially Factorized Spectroscopy (SFS), in which multiple point measurement in microscopic scale is used to separate spectra of the target components with background spectra. A simple set of samples consisting of a mixture of different sugars is used to demonstrate the effectiveness of the method.

The sample set used in this demonstration was composed of mixtures of white powders, with glucose as the target compound, as shown in Table 23.1. The powders were mixed thoroughly and compressed into tablets for measurement. As can be understood from the composition, the background constituents of the calibration and test datasets are very different.

A typical partial least squares regression (PLSR) model fails miserably with this set of data since the model can only learn from the variability within the calibration dataset. Figure 23.1 shows the performance of a PLSR model built from Raman spectroscopy measurements of the tablets. A single spectrum was measured for each sample and the calibration model was built with three latent variables. As can be

Table 23.1 Composition [%] of calibration and test samples (n = 3)

	Target	Background			
	Glucose	Galactose	Fructose	Lactose	$CaCO_3$
Calibration 1	75.0	12.5	12.5		
Calibration 2	50.0	25.0	25.0		
Calibration 3	33.3	33.3	33.3		
Test 1	75.0			12.5	12.5
Test 2	50.0			50.0	0.0
Test 3	33.3			33.3	33.3
Test 4	25.0			0.0	75.0
Test 5	0.0			50.0	50.0

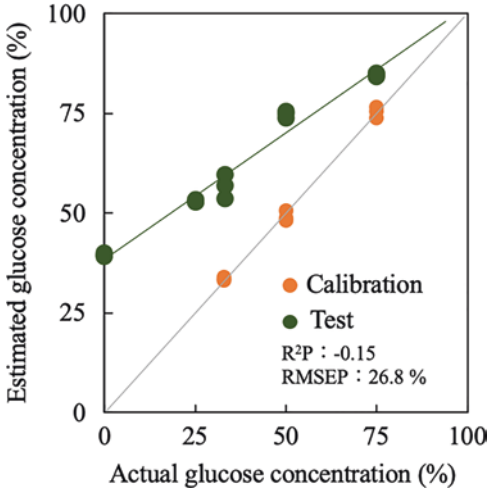

Fig. 23.1 Performance of PLSR model

observed from Fig. 23.1, the calibration dataset can estimate the glucose concentration in the calibration data very well, but highly overestimates the glucose concentration in the test data. This is because the PLSR model learns from the mixed spectra and cannot separate information on the target compound (glucose) and information on the other compounds.

To overcome this problem, there is a need to separate the mixed spectra into the pure spectra of the components in the mixture. SFS was performed with the following steps: (1) The surface of the tablet was measured with a Raman spectrometer coupled with a microscope system. The laser light source was focused to give a spot size of 4 μm and 200 points were measured per sample. Three samples were measured for each composition shown in Table 23.1. (2) After preprocessing the Raman spectra for baseline removal and normalization, nonnegative matrix factorization (NMF) was performed (Berry et al., 2007) to decompose the spectra ($\boldsymbol{X} \in R^{m \times n}$) into the linear product of $\boldsymbol{W} \in R^{m \times k}$ and $\boldsymbol{H} \in R^{k \times n}$. Here, m is the number of spectra (approximately 600), k is the number of components (3), and n is the number of wavelengths. The matrix $\boldsymbol{H}$ contains the "pure spectra" and $\boldsymbol{W}$ holds the weights of each spectrum for every measurement point. (3) The weights corresponding to the spectrum of glucose were averaged for each sample and this average value was calibrated against the actual glucose content (33.3, 50.0, and 75.0% for the calibration samples). (4) The test datasets were decomposed with NMF in a similar manner, and the glucose content for each sample was calculated using the calibration line created with the calibration dataset.

Figure 23.2 shows the results of this approach, where both calibration and test datasets were first decomposed into their pure components, and only the information related to the target compound (glucose) was used to create the regression model. This decomposition was possible because the input data ($\boldsymbol{X}$) already contained spectra that were almost "pure." The measurement of small points (approximately 4 μm in diameter) allowed the acquisition of spectra corresponding to single

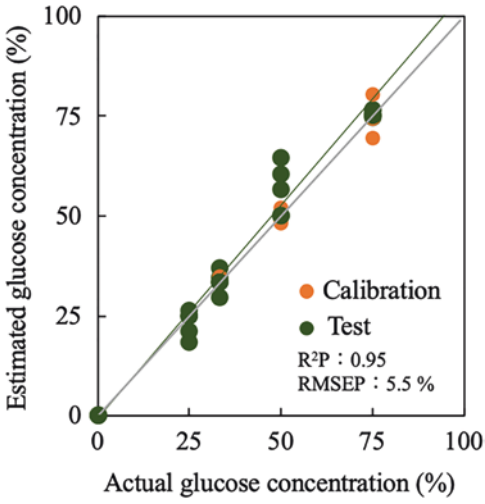

Fig. 23.2 Performance of SFS model

particles of glucose, fructose, etc., and this led to an accurate decomposition of the input data.

Although this preliminary study focused on relatively simple mixtures of food components, it can be developed to measure more complex foods and agricultural products as well as pharmaceuticals. With more complex materials, it may not be possible to acquire spectra of pure constituents, even when a high spatial resolution is used. However, many decomposition methods that allow the estimation of the "pure spectra" have been developed in the field of remote sensing (Bioucas-Dias et al., 2012) and these may be applicable to micrometer-scale imaging, leading to efficient separation of information. Overall, the combination of micrometer-scale hyperspectral imaging and advanced decomposition methods is expected to lead to a new dimension to nondestructive analysis.

References

Aguilera, J. M., Stanley, D. W., & Baker, K. M. (2000). New dimensions in microstructure of food products. *Trends in Food Science & Technology, 11*(1), 3–9. https://doi.org/10.1016/s0924-2244(00)00034-0

Berry, M. W., Browne, M., Langville, A. N., Pauca, V. P., & Plemmons, R. J. (2007). Algorithms and applications for approximate nonnegative matrix factorization. *Computational Statistics & Data Analysis, 52*(1), 155–173. https://doi.org/10.1016/j.csda.2006.11.006

Bioucas-Dias, J. M., Plaza, A., Dobigeon, N., Parente, M., Du, Q., Gader, P., & Chanussot, J. (2012). Hyperspectral Unmixing overview: Geometrical, statistical, and sparse regression-based approaches. *IEEE Journal of Selected Topics in Applied Earth Observations and Remote Sensing, 5*(2), 354–379. https://doi.org/10.1109/JSTARS.2012.2194696

Pallone, J. A. L., Caramês, E. T., & d. S., & Alamar, P. D. (2018). Green analytical chemistry applied in food analysis: Alternative techniques. *Current Opinion in Food Science, 22*, 115–121. https://doi.org/10.1016/j.cofs.2018.01.009

Sharma, S., Goodarzi, M., Wynants, L., Ramon, H., & Saeys, W. (2013). Efficient use of pure component and interferent spectra in multivariate calibration. *Analytica Chimica Acta, 778*, 15–23. https://doi.org/10.1016/j.aca.2013.03.045

Xu, Y., Zhang, J., & Wang, Y. (2023). Recent trends of multi-source and non-destructive information for quality authentication of herbs and spices. *Food Chemistry, 398*, 133939. https://doi.org/10.1016/j.foodchem.2022.133939

Chapter 24
Strategic Short Note: Reviving Local Resources for Healthier Foods in Indonesia

24.1 Introduction

Indonesia has been categorized as a mega biodiversity country in the world, comprising with more than 16,000 islands, providing a great variety of edible food sources. There are at least 77 types of carbohydrate sources, 26 legumes, 389 fruits, 228 vegetables, and 110 types of spices and seasonings that can be found in Indonesia (MAFSA, 2020). Indonesian local fruits include 266 indigenous fruits and 62 species of them are cultivated (Uji, 2007). There are 208 native cultivars of mango (Fitmawati & Purwoko, 2010), and 200 local cultivars of banana (Musaceae) (Poerba et al., 2016), and many other fruits with a wide range of colors indicating different composition of nutrients, especially carotenoids, one of the most essential pigments responsible for the color of fruits (Ranganath et al., 2018).

In Indonesia, the agriculture industry contributes nearly 14% of the country's GDP (Gross Domestic Product), and almost 29% of the Indonesian workforce is in the agricultural sector (World Bank, 2022). Despite the high diversity found in Indonesia's agroecological systems, currently, most of the agricultural production has shifted from food crops toward high-value and commercial commodities, such as rice, maize, soybean, chili, and shallot, which have significant roles in fulfilling Indonesian's food demands and contribute to the inflation of food items (Ruslan, 2021). This shift reduces the range of food available on the market, leaving hundreds of edible and nutritious species untapped.

A study conducted on 2785 rural households covering a period between 2000 and 2015 showed a positive relationship between production diversity and household dietary diversity, as well as between market access and household dietary diversity (Mehraban & Ickowtz, 2021). The study reported that an overall decline in dietary diversity was mostly driven by the decreased consumption of nutritious food groups, i.e., fruits, vegetables, legumes, and fish. Interestingly, the consumption of instant noodles in Indonesia has increased from 13.27 in 2021 to 14.26 billion servings in 2022 (World Instant Noodles Association, 2023), has made the country one

© The Author(s), under exclusive license to Springer Nature Singapore Pte Ltd. 2024

T. Ahamed, *IoT and AI in Agriculture*,
https://doi.org/10.1007/978-981-97-1263-2_24

of the world's largest importers of wheat with 10.29 million tons in 2020 based on the data from the Food and Agriculture Organization (FAO). There are specific food groups that have increased in percentage over the period that are also nutrient-rich, such as dairy, eggs, and meat. However, they are also associated with future cardiovascular risk in a population that is experiencing a rapid rise in heart diseases (Vermeulen et al., 2019).

Over the last two decades, Indonesia's undernourishment has significantly declined (from 17% of the population in 1999 to 8.3% in 2017). Child stunting and wasting, however, remain stubbornly high at 21.6% and 7.7%, respectively, based on the Nutrition Status Survey Results Indonesia (SSGI) 2022 (BKPK, 2022). There is a widespread problem of poor diet quality in Indonesia, resulting in micronutrient deficiencies, especially in vitamin A, vitamin D, iron, and zinc (Ernawati et al., 2021). While Indonesia is undergoing a nutrition transition marked by a shift away from complex carbohydrates, fruits, legumes, and vegetables in favor of simple carbohydrates, fats, and meats (Vermeulen et al., 2019). Such a transition is associated with a rise of overweight and obesity, along with noncommunicable diseases (Popkin et al., 2020), and even more vulnerable to COVID-19 infection (Rossi et al., 2022).

24.2 Repositioning Local Food Resources

What are the challenges for Indonesia in the future? In short, if our food statistics are correct, the main challenge in ensuring food security is not only production. The government should also focus on improving food distribution and access with the support of data and technology, in addition to the development of food production based on advanced research. Especially the local food resources need to be revived. The momentum of the COVID-19 pandemic provides an opportunity for Indonesia to recampaign a diverse solution to ensure the food system's sustainability. In addition to local carbohydrate sources, local fruit and vegetable sources of vitamins and minerals must be integrated into the food system. Often the question that emerges is, do local food resources have competitiveness and potential as a source of nutrition.

In the recent 5 years, our research group has focused on Indonesia's native and endemic fruits. We evaluated the carotenoid composition in the fruit of *Pandanus conoideus* Lam., an indigenous *Pandanus* plant of the Papua Islands and widely spreads in Maluku, Papua Indonesia, and Papua New Guinea. The fruit is formed by a deep red color of the integrated compounds, called syncarp (86–110 cm of length and 30–35 cm of girth), with a right-triangular cylindrical shape and consists of many single fruits, called drupe (1.0–1.5 cm of length). The fruit extract contains oil as the main component, and the deep red color is used for food colors and medicine for various diseases by the Papuan. The main red color constituent group in carotenoids—namely capsanthin and capsorubin—has a much higher content, which is 92% compared to red chili, which is only 62% (Heriyanto et al., 2021). We also

evaluated the provitamin A carotenoid composition of the Agung Semeru banana (*Musa paradisiaca* L. AAB plantain), cultivated only in East Java, especially in the Lumajang regency. The characteristic of this plantain includes the color of its pseudostem (light red), the number of suckers per cluster (only 1–2 suckers per cluster), the size of the fingers (33–36 cm long and 19 cm around), the number of hands per bunch (only 1–2 hands per bunch), and a weight of ~10–20 kg/bunch. Compared to the Cavendish variety, which is consumed worldwide, the Agung Semeru banana had vitamin A activity that was 40–90 times higher, depending on the stage of ripening, with the highest level of vitamin A activity at 457.33 ± 5.18 μg retinol activity equivalents (RAE)/100 g dw (Chandra et al., 2020).

Food diversification has become one of the food crisis intervention strategies supported by FAO. It is possible to develop further many of Indonesia's native and endemic plants that are adapted to local ecosystems through research and investment. In the example above, the food-producing plants are culturally familiar to the farmers, which makes supporting their development in the agroforestry system beneficial to their livelihoods, food security, and nutrition. Featuring more than 16,000 islands and 1300 ethnic groups, Indonesia's food system offers not only rice culture but also a variety of cultures and practices pertaining to food. Indonesia is learning to consider holistically food, nutrition, and the environment that pays attention to biodiversity and diversity of local food-producing plants.

References

Badan Kebijakan Pembangunan Kesehatan (BKPK). (2022). *Buku Saku Hasil Studi Status Gizi Indonesia*. [Internet]. Kementerian Kesehatan RI. Available https://www.badankebijakan.kemkes.go.id/laporan-hasil-survei/. Cited 19 Aug 2023

Chandra, R. D., Siswanti, C. A., Prihastyanti, M. N. U., Heriyanto, L. L., & Brotosudarmo, T. H. P. (2020). Evaluating provitamin a carotenoids and polar metabolite composition during the ripening stages of the Agung Semeru banana (*Musa paradisiaca* L. AAB). *International Journal of Food Science, 2020*, 8503923.

Ernawati, F., Syauqy, A., Arifin, A. Y., Soekatri, M. Y. E., & Sandjaja, S. (2021). Micronutrient deficiencies and stunting were associated with socioeconomic status in Indonesian children aged 6–59 months. *Nutrients, 13*(6), 1802.

Fitmawati, H. A., & Purwoko, B. A. (2010). Diversity of Indonesian mango (*Mangifera indica*) cultivars based on morphological and rapd markers. *SABRAO Journal of Breeding and Genetics, 42*(2), 84–95.

Heriyanto, G. I. A., Fujii, R., Maoka, T., Shioi, Y., Kameubun, K. M. B., Limantara, L., & Brotosudarmo, T. H. P. (2021). Carotenoid composition in buah merah (*Pandanus conoideus* Lam.), an indigenous red fruit of the Papua Islands. *Journal of Food Composition and Analysis, 96*, 103722.

Mehraban, N., & Ickowtz, A. (2021). Dietary diversity of rural Indonesian households declines over time with agricultural production diversity even as incomes rise. *Global Food Security, 28*, 100502.

Ministry of Agriculture's food security agency (MAFSA). (2020). *Roadmap diversifikasi pangan lokal sumber karbohidrat non beras 2020–2024*. Ministry of Agriculture's Food Security Agency. Available https://badanpangan.go.id/storage/app/media/Bahan%202020/Roadmap%20Diversifikasi%20Pangan%202020-2024.pdf. Cited 19 Aug 2023.

Poerba, Y. S., Martanti, D., Herlina, H. T., & Witjaksono. (2016). *Koleksi Kebun Plasma Nutfah Pisang Pusat Penelitian Biologi-LIPI*. Lembaga Ilmu Pengetahuan Indonesia.

Popkin, B. M., Corvalan, C., & Grummer-Strawn, L. M. (2020). Dynamics of the double burden of malnutrition and the changing nutrition reality. *Lancet, 395*(10217), 65–74.

Ranganath, K. G., Shivashankara, K. S., Roy, T. K., et al. (2018). Profiling of anthocyanins and carotenoids in fruit peel of different colored mango cultivars. *Journal of Food Science and Technology, 55*(11), 4566–4577.

Rossi, A. P., Muollo, V., Dalla Valle, Z., et al. (2022). The role of obesity, body composition, and nutrition in COVID-19 pandemia: A narrative review. *Nutrients, 14*(17), 3493.

Ruslan, K. (2021). *Food and horticulture crop productivity in Indonesia* (Policy Paper No. 37). [Internet]. Center for Indonesian Policy Studies. Available https://www.cips-indonesia.org/publications/food-and-horticulture-crop-productivity-in-indonesia. Cited 19 Aug 2023.

Uji, T. (2007). Species diversity of indigenous fruits in Indonesia and its potential. *Biodiversitas, 8*(2), 157–167.

Vermeulen, S., Wellesley, L., Airey, S., Singh, S., Agustina, R., Izwardy, D., & Saminarsih, D. (2019). *Healthy diets from sustainable production*. [Internet]. The Royal Institute of International Affairs. Available https://www.chathamhouse.org/sites/default/files/2020-12/2019-01-24-healthy-diets-sustainable-production.pdf. Cited 19 Aug 2023.

World Bank. (2022). *The World Bank supports Indonesia's agriculture sector to become more resilient and inclusive*. Press Release. [Internet]. Available https://www.worldbank.org/en/news/press-release/2022/09/09/the-world-bank-supports-indonesia-agriculture-sector-to-become-more-resilient-and-inclusive. Cited 19 Aug 2023.

World Instant Noodles Association. (2023). *Demand rankings*. [Internet]. Available https://instant-noodles.org/en/noodles/demand/table/. Cited 19 Aug 2023.

Chapter 25
Development of IoT-Based Platform for Biomass Utilization Toward Low-Carbon Economic Society: Case of Oil Palm Residue

Abstract The global effort to mitigate the climate change effect leads to the transformation of society toward a low-carbon economy. Biomass residue has been marked to have a potential contribution to this society and is increasingly considered for its utilization to substitute fossil fuels. Biomass residue has potential applications for various valorization purposes, such as fertilizer, ethanol, and electricity. The use of information technology such as IoT has been recognized for accelerating the effort on biomass utilization. This study proposes an IoT-based platform to evaluate the potential biomass utilization from oil palm residue in Indonesia. The proposal is based on the currently underdeveloped prototype for oil palm residue utilization, to be integrated with other available tools. The platform is proposed by considering the theoretical conversion of biomass by considering their nutrient content (NPK), cellulose-hemicellulose-lignin content, and calorific value. The theoretical conversion refers to available literature that can be modified later by a user based on field or laboratory data. It is expected that by using the platform, stakeholders such as farmers, industrial practitioners, and policymakers can perform a simulation to explore the best potential utilization of biomass to help reduce environmental impact in the future.

Keywords Biomass residue · Oil palm · IoT platform · Fertilizer · Ethanol · Electricity

25.1 Introduction

25.1.1 Trend on IoT and Application for Agriculture

The history of the Internet of Things (IoT) can be dated back to some elements that construct the concepts, such as the emergence of interconnected smart devices in 1982 utilized by Coca-Cola vending machines in Pennsylvania, U.S. (Kumar et al., 2021). John Romkey in 1990 introduced the first Internet "device" in the form of a toaster that could be turned on and off via the Internet, while Steve Mann designed

© The Author(s), under exclusive license to Springer Nature Singapore Pte Ltd. 2024

T. Ahamed, *IoT and AI in Agriculture*,
https://doi.org/10.1007/978-981-97-1263-2_25

WearCam in 1994, with near-real-time performance utilizing a 64-processor machine (Suresh et al., 2014). Kevin Ashton from the Massachusetts Institute of Technology was generally regarded as the founder of IoT in 1999, which characterized IoT by radio-frequency identification (RFID) to allow computers to connect to the transceivers in various gadgets (Kumar et al., 2021).

IoT technology can be defined as a link between humans, computers, and things (Suresh et al., 2014). The fundamental characteristics of IoT cover connectivity, things, data, communication, intelligence, action, and ecosystem (Kumar et al., 2021). IoT has been evolving with the advancement of devices and technology such as sensors, RFID, Wi-Fi, barcode, QR codes, Bluetooth, etc. It has been implemented in wider sectors of industry such as automotive, transportation, telecommunication, health care, logistics, agriculture, smart city, etc.

In the agriculture sector, the traditional farming system was characterized by the use of intensive labor, manual measurement of land and plant quality, and susceptibility to weather occurrence. Accordingly, there are some severe occurrences of agricultural losses that have been reported due to climate change impact, such as pests and diseases affecting the productivity drop and mitigation cost (Maraveas & Bartzanas, 2021). The use of artificial intelligence (AI) elevates the overall agriculture production through utilization of real-time analysis and machinery automation (Hamidon et al., 2023).

25.1.2 Potential of Agriculture Residue Utilization to Replace Fossil Fuel

According to the World Energy Outlook published by the International Energy Agency (IEA) in 2023, around 80% of total global energy demand is still dominated by fossil fuels, which comprises oil, coal, and gas (IEA, 2023). The IEA projected some scenarios for future demand and predicted that total energy demand will still increase in the next few years and expected to decrease by 2030. Meanwhile, the renewable energy portion is expected to make more contributions in the future, as illustrated in Fig. 25.1.

Fossil fuels have been identified to cause some environmental issues when they are burned. A large number of green gases such as carbon dioxide and nitrogen oxides will be released into the air. Carbon dioxide traps heat in the atmosphere affecting global warming by increasing temperatures. Nitrogen oxides contribute to the formation of smog and acid rain. Governments from many countries signed up to the Paris Agreement in 2015, committing to reduce carbon emissions. As a legally binding international treaty on climate change, it was adopted by 196 Parties at the UN Climate Change Conference (COP21) in Paris, France, on 12 December 2015 and entered into force on 4 November 2016 (UNFCC, 2018). Its overarching goal is to hold the increase in the global average temperature to well below 2 °C above preindustrial levels. However, a recent report by the UN Environment Program shows that globally, the amount of coal, oil, and gas produced is over twice as

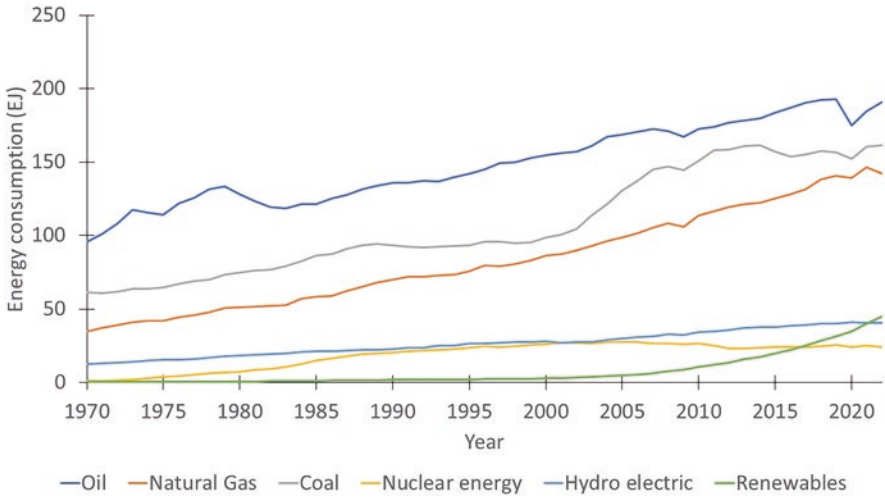

Fig. 25.1 Global energy consumption in the last 30 years, created based on Statistical Review of World Energy Data (Energy Institute, 2023)

targeted by 2030 (Clientearth, 2022), thus, more actions are required to halt the worsening trend.

As part of climate actions, the United Nations considers renewable energy derived from natural sources that are replenished at a higher rate than they are consumed. Among the sources of renewable energy, biomass is also included as it has lower environmental impacts compared to fossil fuels (United Nations, 2020). Biomass can be sourced from crops or trees, residues from agriculture and forestry, and various organic waste streams. Biomass is a clean, renewable energy source. Its initial energy comes from the sun, and plants or algae biomass can regrow in a relatively short amount of time. If trees and crops are sustainably cultivated, they can offset carbon emissions by respiration. In some bioenergy processes, the amount of carbon that is reabsorbed even exceeds the carbon emissions that are released during fuel processing or usage (Turgeon & Morse, 2023).

Biomass can be applied as biofuels to replace fossil fuels, such as ethanol as a gasoline substitute and combusted in power plants as coal substitution. As a low-carbon substitute for fossil fuels, biofuels are being promoted as a way to lessen greenhouse gas (GHG) emissions and the associated climate change impact (Jeswani et al., 2020). In the past, ethanol was produced primarily from food sources such as corn and sugarcane, but many countries such as the USA, Brazil, and India have been investigating alternative sources from nonfood cellulose materials. In the future, it is predicted that biofuels will be produced increasingly from crop residues (e.g., corn cobs, stalks), forestry residues (e.g., forest thinning, wood byproducts), energy crops (e.g., switchgrass, miscanthus), sorted municipal wastes, and algae (U.S. Department of Energy, 2015). Biomass has been utilized in Indonesia, particularly as an alternative source for cofiring. Total electricity generation by power

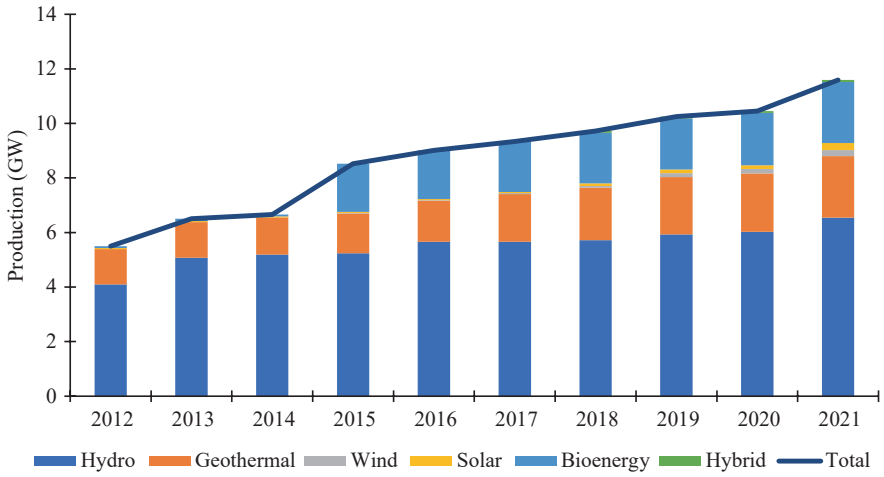

Fig. 25.2 Renewable energy source for electricity generation. (Source: National Energy Council of Indonesia, 2022)

plants in Indonesia is approximately 75 GW, of which nearly half is combusted from coal, followed by gas for 28% and renewable sources for 15% (National Energy Council of Indonesia, 2022). Among six type of renewable sources, biomass contribution was around 18% in 2012 and increased yearly as illustrated in Fig. 25.2.

The current mass cultivation and production of oil palm to feed the international market has been expanding, reaching 28.36 million ha around the globe (FAO, 2020), thus, resulting in abundant availability of biomass residue. This residue, if piles up on the ground, may emit emissions, such as 7 $tCO_2eq\ ha^{-2}\ y^{-1}$ from palm oil mill effluent (Taylor et al., 2014) or 230 kg $CO_2eq.t^{-1}$ empty fruit bunch or EFB (Krishnan et al., 2017). With increasing awareness and practice for sustainable production, there is also a rising concern about utilizing biomass to reduce GHG emissions.

Among research to evaluate the potential utilization of biomass, three sectors of implementation have been intensively studied globally, i.e., composting, electricity, and bioethanol. These sectors are considered important to substitute current widely used products based on depleting fossil feedstock such as synthetic fertilizer, coal-based power plants, and gasoline. The technology process of these sectors has been inventoried in many prior studies, as well potential environmental reduction for substituting current products has also been accessed. Furthermore, there is a need to transform this research into more practical user-friendly information, to help relevant stakeholders in utilizing the biomass.

25.1.3 Existing IoT Platform for Oil Palm Production System

Some software for oil palm has been developed to support sustainable practices, such as for daily data transactions by tracing the flow process of oil palm from the plantation, transportation, production, and distribution, or imaging-based detection. However, there are still a few tools that accommodate the potential impact calculation of the products. GHG calculation platform, as developed by Indonesia Sustainable Palm Oil (ISPO), and PalmGHG, used by Roundtable on Sustainable Palm Oil (RSPO), are among the initiatives to calculate the environmental aspect of oil palm production system, which mainly focused on main products such as CPO, PKO, PKE (Bessou et al., 2014). Theses tools have not considered biomass residue utilization yet, which will be specifically addressed in this study to help in reducing global warming. Table 25.1 lists further the available tools relevant to oil palm production.

The position of various tools as previously described in Table 25.1 can be illustrated in Fig. 25.3. Generally, the scope of these tools can be classified into the tools that focus on the main production system and the tools that exploit the utilization of biomass residue. This main production system is marked with an orange line-dot in the figure while extending the biomass residue process is in the blue line-dot scope. Most existing tools are focused on the main production system, while the tool prototype being developed in this study attempts to utilize the biomass residue.

Table 25.1 Existing IoT platform in oil palm production system

IoT platform	Developer	Description	Source
PalmSim	Wageningen University	Estimate potential growth and yield of oil palm	Hoffmann et al. (2015)
eCognition Oil Palm	Trimble Geospatial	Analyze aerial data and identify oil palm trees	Trimble Geospatial (2019)
PalmGHG	Roundtable on Sustainable Palm Oil (RSPO)	Calculate the environmental aspect of the oil palm production system	Bessou et al. (2014)
GHGCalculator	Indonesia Sustainable Palm Oil (ISPO)	Calculate the environmental aspect of the oil palm production system	Gan Lian and Cap (2016)
Oil Palm Management Program (OMP)	Agrisoft System Indonesia	Provide information on agricultural parameters such as production yield, fertilizer, climate data, budget, etc.	Agrisoft System Indonesia (2014)
OWL Plantation System	Origin Wiracipta Lestari	Integrated production flow planning covering plantation, production, and distribution	Origin Wiracipta Lestari (2011)
Oil Palm Biomass Utilization and GWP Estimator (OPBUGE)	The authors of this study	Explore the potential biomass residue availability to substitute the fossil fuel and estimate the environmental impact	Prototype in this study

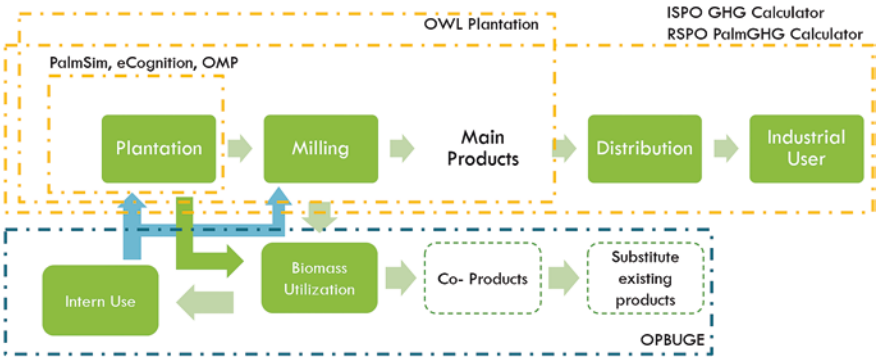

Fig. 25.3 Position of various tools in the supply chain system of oil palm production

The scope of the main production system covers products such as crude palm oil, palm kernel oil, and their downstream process. Among these tools, some are focused on one specific area such as plantation only, by analyzing the characteristics of plant, area, fertilizer, image detection, etc. Other tools extend the scope, comprising from plantation to milling, distribution, and industrial users. These tools typically list the mass flow of products, evaluate the cost, and analyze the environmental impact.

Aside from the main products, the oil palm also generates biomass residue. This residue can be utilized further by converting it to more valuable products, to replace fossil fuel. If this residue can be commercially produced at an economic scale, it can be treated as the coproduct of the oil palm system.

25.2 Methods for Developing the Prototype

Relevant stakeholders or users of the tool should be defined first to clarify to whom the program will be intended and how the interface should be developed accordingly. After that, the theoretical formula for calculation and data inventory will be constructed. The tool was then tested and validated and finally, the simplified user manual was added. Figure 25.4 illustrates further the methods.

The proposed tool works as follows. The biomass consists of an empty fruit bunch, kernel shell, mesocarp fiber, frond, trunk, and POME. Starting with the number of available biomasses based on the input plantation area, the quantity of possible generated products, i.e., compost, electricity, and bioethanol, will be calculated. The obtained product then substitutes the currently available product (fertilizer, coal-based power plant, and gasoline) with a certain amount of equivalent. Finally, the potential environmental impact will be estimated, by considering emissions of the conversion process as well as avoided emissions from substituted products and utilized biomass.

The tool will be developed based on the theoretical conversion of biomass by considering their nutrition content of nitrogen, phosphor, and Kalium (NPK), cellulose-hemicellulose-lignin content, and calorific value, which can be

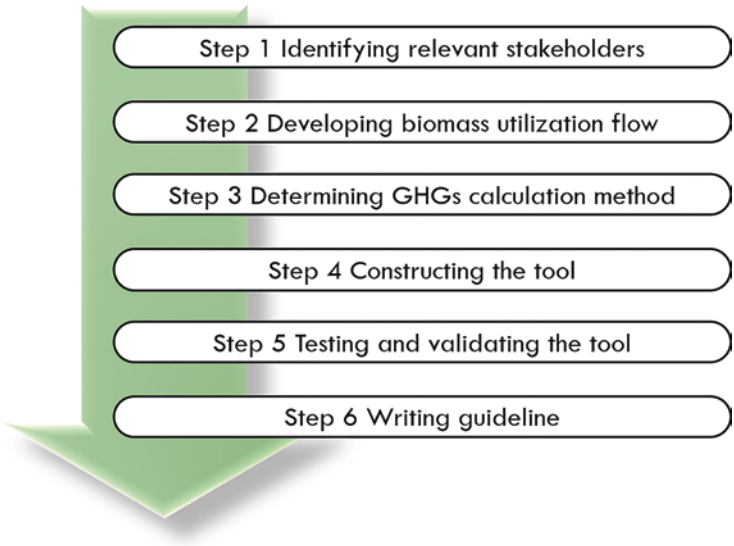

Fig. 25.4 Method for developing the tool

modified later by the user based on field or laboratory data. NPK content is essential to compare the amount of synthetic fertilizer substituted by oil palm residue-based fertilizer. For instance, if 1 kg synthetic fertilizer available in the market has 10% N, while 1 kg oil palm residue-based fertilizer mixed from trunk and POME has 5% N, it means that 2 kg of oil palm residue-based fertilizer is required to replace the same amount of synthetic fertilizer. The same approach is also applicable to estimate the equivalent amount of ethanol needed to replace gasoline, based on the calorific value of both fuels. Similarly, the required oil palm residue as converted to pellets is also calculated based on equivalent energy to replace coal.

25.2.1 Identifying Relevant Stakeholders

IoT platform for biomass utilization involves stakeholders from various backgrounds such as suppliers, plant factories, consumers, government, IT developers, etc. Stakeholders who can utilize the platform in general can be classified into (i) general users, (ii) specialized users, (iii) administrators, and (iv) super administrators. The role/authority and required competency for each user type can be summarized in Table 25.2.

Table 25.2 Relevant stakeholders as classified by user type, role, and required competency

User type	Role/authority	Required competency
General user	Read the result	Common reader
	Input limited parameter	Basic knowledge of the process
Specialized user	Modify the background inventory data	Technical knowledge of the process
	Change the reference source	Assess other databases or references
Administrator	Assign user type account and its role	Authorized permission from respective stakeholders
	Maintain the administration process of the system such as user registration, system hosting, big data storage, etc.	Administration background to maintain the system
Super administrator	Edit the programming language of the overall system	Ability in information system technology
	Modify the structure flow of the process	Understanding the technical knowledge of the process

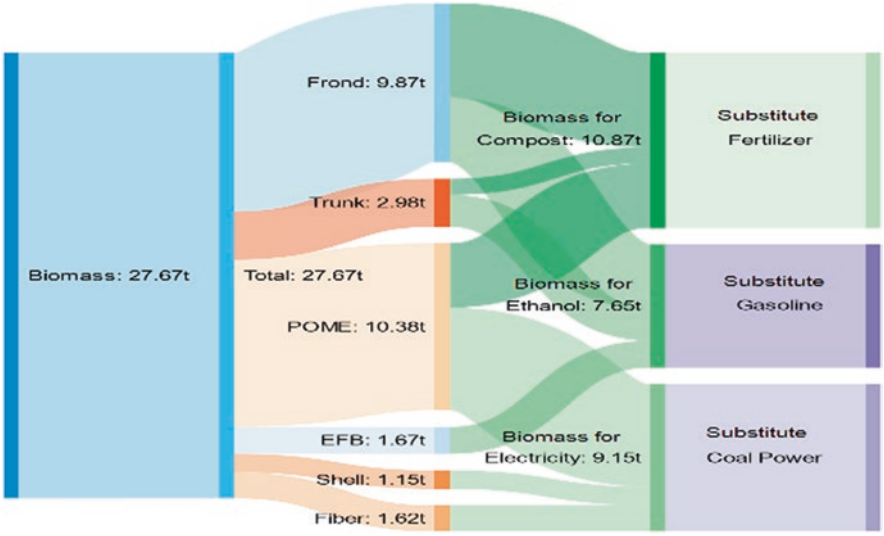

Fig. 25.5 Biomass utilization flow of oil palm using Sankeymatic diagram

25.2.2 Developing Biomass Utilization Flow

The utilization of biomass depends on the intended use by the stakeholder, and the value can be inputted in the foreground tool. The biomass utilization flow is constructed by accommodating nutrient content (NPK) for fertilizer, cellulose-hemicellulose-lignin content for ethanol, and calorific value for power plant

combustion. This nutrient content is taken out from available literature, where the sources are listed in the program.

An example of biomass utilization flow can be illustrated in Fig. 25.5. In this example, the total available biomass residues is 27.67 t, comprising frond, trunk, palm oil mill effluent (POME), empty fruit bunch (EFB), kernel shell, and fiber. Each type of biomass residue then can be converted to substitute fossil-based products such as synthetic fertilizer, gasoline, and coal-based power plants. Users need to specify further the amount of the residue to be allocated for each type of substituted product. For instance, frond is allocated almost equally to substitute synthetic fertilizer and gasoline, while EFB is entirely converted to ethanol for gasoline reduction.

Although allocating the biomass seems simple, in the actual case it can become a difficult and complex decision, as the user needs to have sufficient information about the current stock of residue, the nutrient and energy content of residue, the demand for each of substituted product, the available technology conversion, the potential economic benefit, potential environmental impact reduction, and relevant regulation by government, etc. For such purposes, the IoT system can provide significant support in decision-making. The system, which connects to many stakeholders, will provide up-to-date information in a systematic, simultaneous, and dynamic way.

25.2.3 Identifying GHG Calculation Methods

Biomass residue, as a waste of the oil palm product system, is assumed to be free of burden as the starting point of the calculation. It means that all environmental impacts from the upstream process (during plantation and production) are already allocated to main products, hence, no more impact is assigned to the residue. However, if this biomass is left or abandoned on the ground, it will naturally release gas due to the decaying process. Therefore, utilizing the residue will avoid decay emission, and the amount of avoided emission is credited from the calculation.

Utilizing the biomass residue requires a conversion process into organic fertilizer, ethanol, or pellets. This conversion process requires raw materials and energy with their emission factors. In addition, the conversion process at the plant may also release emissions. The sum of raw material and conversion process is counted as production emission in the formula.

Finally, the obtained oil palm residue-based product is used to substitute fossil-based products such as synthetic fertilizer, gasoline, and coal. Substituting these fossil products can avoid the emissions due to the production process and implementation (combustion) process for these products. Oil palm residue-based products when implemented or combusted at vehicle or power plant also release GHG emission. However, this emission is typically not accounted for due to the carbon neutrality of biomass (Baral, 2014). Therefore, only avoided emissions from substituted products are subtracted from the formula. The above description can be

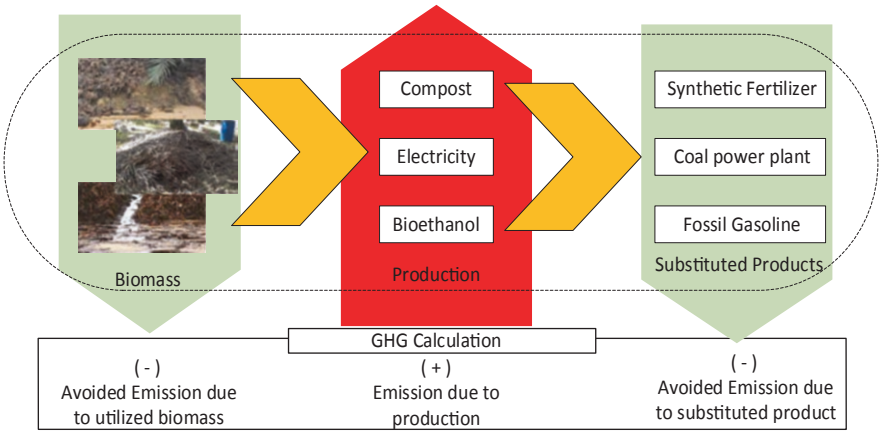

Fig. 25.6 GHG calculation of biomass conversion

illustrated further in Fig. 25.6, where the formula for GHG emission was calculated as follows.

$$\mathrm{GHG} = -\mathrm{Ab} + \mathrm{C} - \mathrm{Ap} \tag{25.1}$$

where

Ab: Emission (avoided decay) if the biomass is utilized (not left on the ground)
C: Emission (production) from converting biomass into a product
Ap: Emission (avoided substitution) from the existing product substituted by biomass-based converted product

25.2.4 Constructing the Tool

The tool in general can be classified into three frames, namely introduction, foreground, and background. Each frame has designated contents and relevant users (Fig. 25.7).

The tool is constructed by accommodating some characteristics such as:

- Simplicity: Flow diagram illustrated in simple figure.
- Portable program: No installation is required to run the prototype.
- Compact: All necessary information is displayed on one page to allow wider comprehension of the system under study.
- Light resource: Approximately 2 MB is required for the permanent memory drive (ROM) and only requires small capacity of temporary memory (RAM).
- User orientation: Allow user to easily modify the parameter.

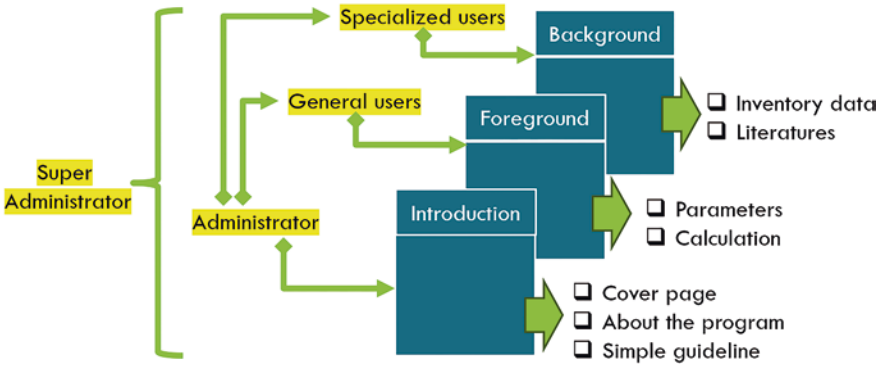

Fig. 25.7 Framework for constructing the tool

Fig. 25.8 Cover page of the tool prototype

The tool prototype can be illustrated in Fig. 25.8 for the cover and Fig. 25.9 for the main content. The cover describes the name of the tool, i.e., oil palm biomass utilization and global warming potential (GWP) estimator abbreviated as OPBUGE.

The foreground page was constructed in a systematic flow so that the user can easily fill in the tool. The flow starts from the upper left side of the page, where the user can fill the area of oil palm plantation or CPO production. After the button "Calculate Biomass Yield" is clicked, the program will estimate the amount of biomass residue for each type. In the next step, users need to define the amount of biomass residue used for internal purposes such as for being combusted at the milling boiler or mulched in the plantation. This internal amount will be deducted from the total biomass available for utilization. Consecutively, users input the intended

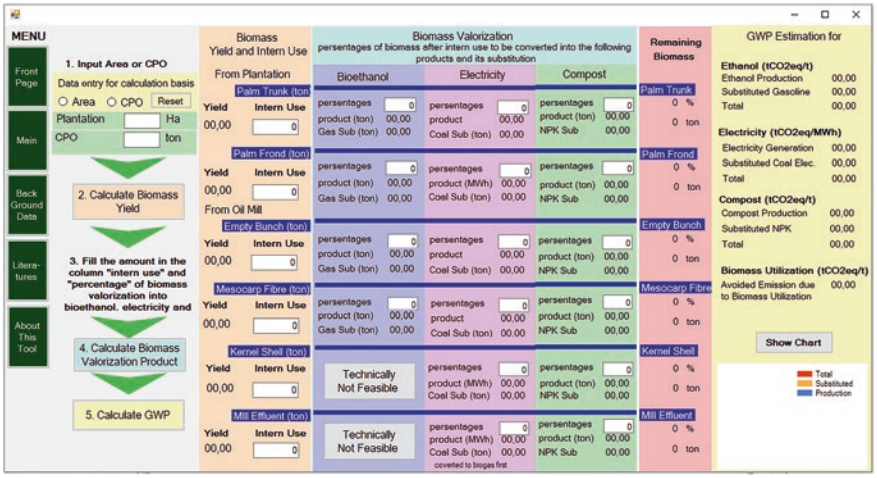

Fig. 25.9 Foreground page of the tool prototype

proportion of biomass utilized for bioethanol, electricity, and compost. The total proportion of biomass is not necessarily sum up to 100%, due to some constraints such as demand, price, technological conversion, etc. This remaining biomass will be calculated automatically as residue, which is assumed to have decay emission due to being abandoned on the ground. Therefore, in case all conversion is economically feasible, it is preferred to utilize all biomass for fossil fuel substitution to avoid decay.

After all blank fields in the third step are filled out, the user can click the button "Calculate Biomass Valorization Product." This button executes the estimated amount of biomass conversion to other possible products. For instance, oil palm trunk is calculated to generate the amount of bioethanol product and how much this ethanol can substitute gasoline based on energy content comparison for both fuels.

25.2.5 Testing and Validation

Testing was performed to identify whether the program had already worked without error. It is performed by using the debug function in the programming software. In addition, the tool is also tested by inputting the number and clicking the button to see if there are any errors. There are some approaches to handle the potential errors, such as:

- A step-by-step instruction is provided to avoid incorrect input.
- The reset button is provided to allow the user to reentry the incorrect number.
- In case incorrect input is still detected by the system, the tool will send a notification and offer a choice to return or close the program.

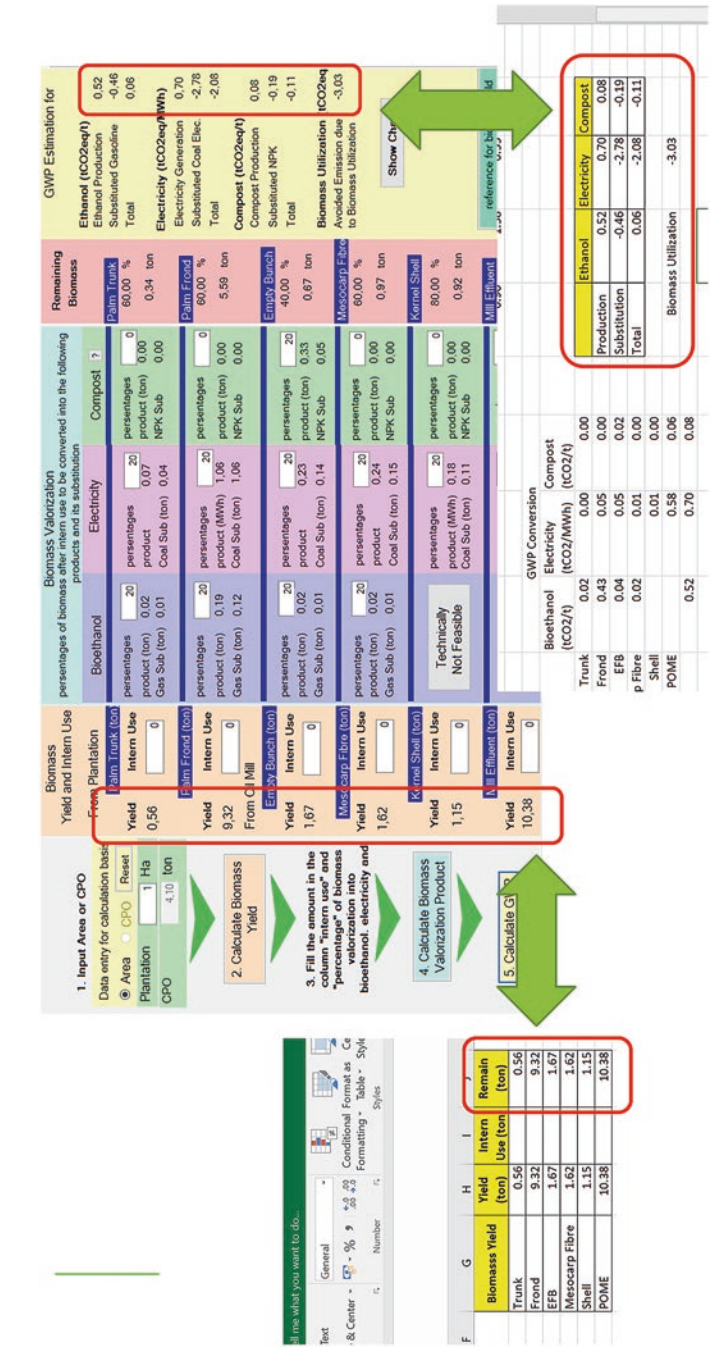

Fig. 25.10 Verification of the tool with the manual spreadsheet

Validation was conducted to ensure that the calculation result from the tool is not different from the manual calculation by using the spreadsheet. The same numerical case is deployed for both the tool and spreadsheet and the calculation results are then compared side by side as depicted in Fig. 25.10.

25.2.6 Writing Guideline

General guidelines were provided to assist users in entering and modifying data. The manual is written in the form of simple instructions directly inside the tool, such as in the "Main" and "About" sections. A step-by-step guideline is provided in the "Main" section, to allow the user to fill in directly while reading the instruction. In addition, more information is also provided in the "About" section to specify the general requirement of the computer operation system for running the tool optimally and how the tool and calculation method work.

25.3 Integrating the Tool Toward IoT Platform of Low-Carbon Economic Society

The prototype above can be developed further into an integrated IoT platform along with other available tools. This prototype serves as the backbone for the IoT platform, which can be enhanced further by considering the relevant practices of the stakeholders. For instance, at the oil palm plantation, the platform can be integrated with the existing production platform, added to the inventory counting and decay

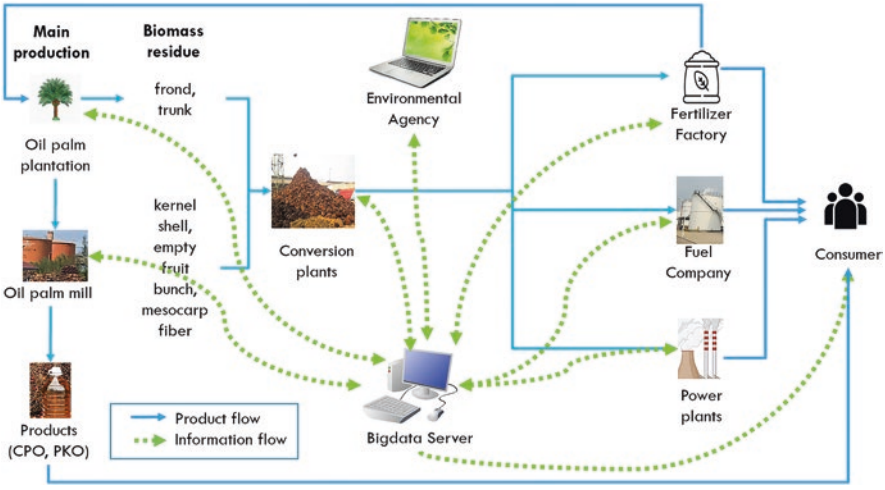

Fig. 25.11 Proposed IoT platform for oil palm residue utilization

Table 25.3 Information interaction between stakeholders and database servers

Stakeholder	Function	Delivered information	Acquired information
Oil palm plantation	Tree planting and harvesting to yield fresh fruit bunch (FFB)	Amount of residue, demand of fertilizer, production capacity, biomass selling price, environmental performance report	Demand for biomass residue, capacity of biomass conversion plants, biomass purchasing price, fertilizer availability and price, government regulation
Oil palm mill	Process fresh fruit bunch to crude palm oil and palm kernel oil	Amount of residue, production capacity, biomass selling price, environmental performance report	Demand for biomass residue, capacity of biomass conversion plants, biomass purchasing price, government regulation
Conversion plants	Convert the biomass residue into valuable products such as organic fertilizer, ethanol, or pellet	Production capacity, purchasing price of biomass, biofuel selling price, environmental performance report	Demand for biofuel, amount of biomass residue, biomass selling price, purchasing price of biofuel, government regulation
Fertilizer factory	Produce fertilizer by gradually replacing the synthetic fertilizer from biomass residue	Production capacity, fertilizer selling price, environmental performance report	Demand for fertilizer, consumer willingness to pay, government regulation
Fuel company	Blending fossil fuel with biomass-based fuel	Production capacity, biofuel selling price, environmental performance report	Demand for biofuel, consumer willingness to pay, government regulation
Power plants	Cofiring coal along with biomass and gradually increasing the proportion of biomass	Electricity production capacity, purchasing price of biomass, environmental performance report	Biomass availability, biomass selling price, consumer willingness to pay, government regulation
Environmental agency	Implement the biomass utilization policy to achieve the target of global warming reduction	Government regulation, carbon price instrument	Environmental performance report, biofuel demand, biofuel price, biomass residue availability, etc.
Consumers	Use biomass-based products to gradually substitute fossil-based product	Product demand, consumer willingness to pay, consumer preference on the environmental performance of product	Availability of biofuel, selling price of biofuel, environmental performance report, government regulation

emission measurement from the biomass residue. At the conversion plants, the platform can be adjusted to accommodate the production process data and emissions conversion (Kahandage et al., 2023). For the substituted products, the platform covers the emission measurement of fossil fuel and biofuel. The government, typically represented by an environmental agency, uses the platform to evaluate the environmental performance of the relevant industry so that it can provide tax or incentives. Finally, the consumer as an end user requires the platform to simply check the environmental impact reduction of the biomass fuel. Consumers, in particular from downstream industries that use fertilizer, fuel, or electricity, need the environmental impact data to calculate the impact of their product. This can be a critical requirement for the competitive advantages of the industry, especially if they want to sell the product to other countries that obligate the environmental report of the product.

Figure 25.11 depicts the product flow and information flow between stakeholders. The product flows can be delivered consecutively from oil palm plantations to consumers, while the information flows are controlled through a centralized big data server. This big data contains a database connecting to all relevant stakeholders and provides the required information. The detailed information flow between each stakeholder and database servers is described in Table 25.3.

25.4 The Role of AI in Biomass Utilization Platform

The utilization of AI has been long incorporated in precision agriculture to explore farming practices in an optimized manner. Some data such as weather conditions, soil composition, and crop performance are steadily updated by AI algorithms to assist in decision-making for arranging appropriate irrigation, fertilization, and pesticide application (Seyar et al., 2023).

In the biomass utilization platform, the role of AI can be extended further. Some of the potential utilizations are listed below:

1. Geographical Information System (GIS) has been widely used in the palm oil industry. The geospatial data may be collected, analyzed, visualized, and managed with the help of GIS technology. There have been some studies using the GIS to assess land suitability, as well as yield prediction and monitoring in the agricultural sector, in particular oil palm commodity. Concerning the IoT, integrating AI with GIS will help in mapping the availability of biomass residues, particularly in oil palm plantations. AI can predict the amount of biomass residue based on the plantation area and productivity. AI can estimate the potential production of biomass residue, by calculating the quantity of biomass residue per oil palm tree in a hectare of land multiplied by area (ha). In addition, the calculation also considers the productivity of oil palm trees, which is affected by many factors such as soil fertility, diseases, and age. The oil palm tree has been known to have an economic life span of around 25 years, whereas productivity increases when it reaches its maturity stage.

2. Based on the initial calculation of available biomass residue, AI can help in estimating how much the biomass residue should be returned to the ground to maintain soil fertility and how much it can be processed for other purposes such as bioenergy. This practice is essential to reduce the requirement of chemical fertilizer to mitigate the cost and environmental impact.
3. AI that has been connected to the database of oil palm plantations can provide the life cycle inventory dataset about the input and output for growing, maintaining, and harvesting the tree and their mechanical instruments (Kahandage et al., 2021). The data such as the amount of water, fertilizer, pesticides, emission, etc. are used for life cycle impact assessment and can be allocated further into biomass residue along with the potential economic value of this biomass.
4. AI integrated with the database system of oil palm mill provides the dataset for the production of crude palm oil and palm kernel oil from fresh fruit bunch. This system lists input and output covering electricity, chemicals, water, and waste such as empty fruit bunch, fiber, and palm oil mill effluent (POME).
5. AI can also be developed further by incorporating bioenergy production in conversion plants such as pellet plants and ethanol plants. In these plants, datasets of input and output are also listed, to contribute to calculating the environmental impact in aggregate. In this stage, AI can provide recommendations on how to utilize biomass residue, based on the capacity of the conversion plant and potential impact reduction.
6. After the bioenergy product is obtained from the conversion plant, AI can be deployed in the targeted substitution of fossil fuel plants. For instance, ethanol is targeted to blend with gasoline at a certain rate in a petrol factory. Petrol factory can provide information on dataset inventory during the blending process. This data can provide the amount of environmental impact reduction, which is in proportion to the amount of substituted fossil fuel.
7. In the end-user sector, AI can help the consumer of bioenergy to determine the environmental product performance. This is very important, particularly for the downstream industry. If the environmental impact of electricity decreases due to biomass use, for instance, it will also reduce the environmental impact of the industry that consumes the electricity.
8. Finally, AI can also help the government to monitor the overall environmental impact performance in the bioenergy sector and agriculture sectors, based on the data provided by relevant stakeholders. The government can device more poli-

Table 25.4 Component of IoT platform and estimated cost

Component	Description	Estimated cost range (thousand US $)
Hardware	Computer set, printer, wireless network, camera, sensor, communication devices	5–40
Software	Application program to allow end users to read, modify, and input the data	5–30
Services	Installation, training, and certification	5–25
Maintenance	Update, repair, reinstall	5–25 per year

cies such as carbon tax, carbon trade, and carbon incentives to stimulate more impact reduction in the country.

25.5 Estimating the Cost and Potential Benefits

Simplicity is a fundamental requirement to make the platform assessed and implemented widely (Evdokimov et al., 2019). It also affects the price and potential benefits of using the platform. If the system becomes complex, the cost will also expand, and in some situations, expand unexpectedly. However, the cost also corresponds with the scale of the platform. Large-scale platforms that involve many stakeholders require more resources and escalate the budget.

IoT cost can vary between $30,000 and $50,000 where hardware can contribute up to 70–80% of the total budget (Klubnikin, 2022). In the case of oil palm, the price also depends on the land areas, production capacity, and location. For instance, an oil palm plantation of less than 5000 ha with a mill production may cost approximately $163,000 in Indonesia or $230,000 overseas (Origin Wiracipta Lestari, 2011). This cost may be adjusted further by installing additional features.

There are some components to be considered for estimating the cost of IoT platform as listed in Table 25.4. Hardware such as computer sets, printers, and wireless network instruments are critically required as the backbone of the platform. Other hardware such as cameras, sensors, and communication devices are possibly equally important for field data observation, recording, and collection from plantation, transportation, biomass conversion plants, and substituted fossil fuel plants. The camera can be used to monitor the inventory at the storage, while a sensor can be deployed to measure the temperature to spot any possible fire hazard at stockpiles (Temp-pro, 2022).

In addition to economic profit from selling the product, the benefit of utilizing the biomass residue comes from the environmental impact reduction, due to the avoided decay of biomass if left on the ground and the avoided impact from fossil fuel as substituted by biomass. This benefit can be extended further if a carbon economic value is applied. A company has potential additional income if they can trade their carbon savings to other companies which need to lessen their impact to comply with the maximum cap value set by the regulation. A company also has potential economic savings if it can reduce its impact to avoid the carbon tax.

The utilization of IoT has the potential benefit of helping the decision-makers in the industry to determine how they will utilize the biomass. IoT can also help the government in regulating policies such as carbon prices to achieve national targets in global warming mitigation. Finally, IoT has also benefited consumers as the end users since they can view the estimated fuel emissions as they consume.

The cost can be minimized further by collaborating with an open platform, free or low-cost software available in the coding developer community such as GitHub, GitLab, Bitbucket, Sourceforge, Apache Allura, Gitea, etc. Some of this community may also provide hosting support with cloud storage for software development. The

available software covers the functions such as crop and climate resource, nutrition and fertilization, irrigation, soil and planting management, and production machinery and equipment management (dos Santos et al., 2023).

25.6 Conclusion

As the production of palm oil is expanding, the utilization of biomass is important to help mitigate global warming. As the existing utilization of IoT is mostly focused on the main product of oil palm, the utilization of IoT for biomass residue becomes equally important. This chapter has explored the potential utilization of IoT for biomass utilization, by using a case example of an oil palm GHG tool prototype.

The developed prototype can calculate the biomass availability based on the total CPO production or area inputted. It can also calculate the biomass-based product, substituted products, and estimated GWP. Further research can be conducted to integrate the prototype with other tools and extend the tool by including more features. A detailed cost also needs to be specified further to assess the potential applicability and profit at the economic scale of implementation.

References

Agrisoft System Indonesia. (2014). *Oil palm management program*. http://www.agrisoft-systems.com/products/omp/. Accessed 21 June 2023.

Baral, A. (2014). *Demystifying the carbon neutrality of biomass* (pp. 4–7). International Council on Clean Transportation.

Bessou, C., Chase, L. D. C., Henson, I. E., Abdul-Manan, A. F. N., Canals L, M. I., Agus, F., Sharma, M., & Chin, M. (2014). Pilot application of PalmGHG, the Roundtable on Sustainable Palm Oil greenhouse gas calculator for oil palm products. *Journal of Cleaner Production, 73*, 136–145. https://doi.org/10.1016/j.jclepro.2013.12.008

Clientearth. (2022). *Fossil fuels and climate change: The facts*. https://www.clientearth.org/latest/latest-updates/stories/fossilfuels-and-climate-change-the-facts/.

dos Santos, R. P., Fachada, N., Beko, M., & Leithardt, V. R. Q. (2023). A rapid review on the use of free and open source technologies and software applied to precision agriculture practices. *Journal of Sensor and Actuator Networks, 12*. https://doi.org/10.3390/jsan12020028

Energy Institute. (2023). *Statistical Review of World Energy*. https://www.energyinst.org/statistical-review.

Evdokimov, I. V., Alalwan, A. R. J., Tsarev, R. Y., Yamskikh, T. N., Tsareva, O. A., & Pupkov, A. N. (2019). A cost estimation approach for IoT projects. *Journal of Physics Conference Series, 1176*, 042083.

FAO. (2020). *Oil palm plantation area by country*. http://www.fao.org/faostat/en/#data/QC

Gan Lian, T., & Cap, H. (2016). RSPO PalmGHG, ISCC and ISPO GHG calculator—A comparative analysis. *Planter, 92*, 379–399.

Hamidon, M. H., Seyar, M. H., Kahandage, P. D., Nakaguchi, V. M., Minn, A., Jiang, A., Abeyrathna, R. M. R. D., & Ahamed, T. (2023). IoT × AI: Introducing agricultural innova-

tion for global food production. In *IoT and AI in agriculture* (pp. 1–20). Springer. https://doi.org/10.1007/978-981-19-8113-5_1

Hoffmann, Donough, Oberthur, Vera, Wijk, Lim, Asmono, Samosir, Lubis, Moses, & Whitbread. (2015). Benchmarking yield for sustainable intensification of oil palm production in Indonesia using PALMSIM.pdf. *Plant Kuala Lumpur, 91*, 81–96.

IEA. (2023). World Energy Outlook 2023: Executive Summary. https://www.iea.org/reports/world-energy-outlook-2023/executive-summary. Accessed 6 Apr 2024.

Jeswani, H. K., Chilvers, A., & Azapagic, A. (2020). Environmental sustainability of biofuels: A review: Environmental sustainability of biofuels. *Proceedings of the Royal Society A: Mathematical and Physical Science Engineering, 476*, 20200351. https://doi.org/10.1098/rspa.2020.0351

Kahandage, P. D., Hettiarachchi, S. W., Weerasooriya, G. V. T. V., Kosgollegedara, E. J., & Piyathissa, S. D. S. (2021). Design, development, and performance evaluation of a mechanical device for harvesting pineapple. *International Journal of Trend in Scientific Research and Development, 5*, 1109–1116.

Kahandage, P. D., Seyar, M. H., Noguchi, R., & Ahamed, T. (2023). Purification of agricultural polluted water using solar distillation and hot water producing with continuous monitoring based on IoT. In *IoT and AI in agriculture* (pp. 75–96). Springer. https://doi.org/10.1007/978-981-19-8113-5_6

Klubnikin, A. (2022). *How much does IoT cost?* https://itrexgroup.com/blog/how-much-iot-cost-factors-challenges/. Accessed 27 June 2023.

Krishnan, Y., Bong, C. P. C., Azman, N. F., Zakaria, Z., Othman, N., Abdullah, N., Ho, C. S., Lee, C. T., Hansen, S. B., & Hara, H. (2017). Co-composting of palm empty fruit bunch and palm oil mill effluent: Microbial diversity and potential mitigation of greenhouse gas emission. *Journal of Cleaner Production, 146*, 94–100. https://doi.org/10.1016/j.jclepro.2016.08.118

Kumar, M. S., Rachel, S., & Kaviselvan, M. V. (2021). Machine learning-based industrial Internet of Things. In *Applied learning algorithms for intelligent IoT* (p. 123). Routledge.

Maraveas, C., & Bartzanas, T. (2021). Application of Internet of Things (IoT) for optimized greenhouse environments. *Agricultural Engineering, 3*, 954–970. https://doi.org/10.3390/agriengineering3040060

National Energy Council of Indonesia. (2022). *Indonesia energy outlook 2022.*

Origin Wiracipta Lestari. (2011). *OWL plantation system*. http://web.owl-plantation.com:8080/index.php. Accessed 21 June 2023.

Seyar, M. H., Kahandage, P. D., & Ahamed, T. (2023). An IoT-based precision irrigation system to optimize plant water requirements for indoor and outdoor farming systems. In *IoT and AI in agriculture* (pp. 47–69). Springer. https://doi.org/10.1007/978-981-19-8113-5_4

Suresh, J. P., Daniel, V., Parthasarathy, V., & Aswathy, R. H. (2014). A state of the art review on the Internet of Things (IoT). In *2014 International conference on science engineering and management research (ICSEMR)* (pp. 1–8).

Taylor, P. G., Bilinski, T. M., Fancher, H. R. F., Cleveland, C. C., Nemergut, D. R., Weintraub, S. R., Wieder, W. R., & Townsend, A. R. (2014). Palm oil wastewater methane emissions and bioenergy potential. *Nature Climate Change, 4*, 151–152. https://doi.org/10.1038/nclimate2154

Temp-pro. (2022). *How Temp-pro's temperature sensors help biomass projects*. https://temp-pro.com/2022/04/29/temperature-sensors-biomass-projects/. Accessed 28 June 2023.

Trimble Geospatial. (2019). *eCognition oil palm*. https://geospatial.trimble.com/products-and-solutions/trimble-ecognition-oil-palm-solution

Turgeon, A., & Morse, E. (2023). *Biomass energy*. https://education.nationalgeographic.org/resource/biomass-energy/. Accessed 25 Apr 2023.

U.S. Department of Energy. (2015). *Biomass basics: The facts about bioenergy.*

UNFCC. (2018). *The Paris agreement: What is the Paris agreement*? https://unfccc.int/process-and-meetings/the-paris-agreement. Accessed 24 Apr 2023.

United Nations. (2020). *What is renewable energy*? https://www.un.org/en/climatechange/what-is-renewable-energy?gclid=CjwKCAjw0ZiiBhBKEiwA4PT9z0SXmVKYyUhig6wKXdFs80TxBNkrksgQJR-0Uw25yY8YkDBqCUXsWxoCwYwQAvD_BwE. Accessed 25 Apr 2023.

Chapter 26
A Web-Based IoT Monitoring and Service System for Agricultural Applications

Abstract Many agriculture industries in Malaysia are small and have a low adoption level of modern information technologies and automation, which restricts data analysis and its use. The traditional data collection method implemented in current farming practices is hardly integrated, and the data could not be analyzed promptly. This research presents an integrated approach to track and trace overall agricultural production through a web-based IoT monitoring application. Two experiment setups were conducted in this work. One is a customized-developed IoT system prototype at the Tenth College (K10) of Universiti Putra Malaysia, and another is an IoT-equipped weather station at the College of Bioresources, National Ilan University Taiwan. The data collected from these two study areas were displayed in a web dashboard with interactive functions using a Python web analytics framework called Dash. It visualizes the collected real-time environmental data through the Dash platform, including humidity, temperature, soil moisture content, wind rate, and rainfall parameters. The web dashboard can be updated dynamically and loaded onto any type of web server. The web applications showed an average overall performance score in Google PageSpeed Insights and Google Lighthouse in terms of speed, connectivity, and accessibility. The statistical analysis of the T-test showed no significant difference ($P > 0.05$) in performance for the web applications developed for both IoT systems.

Keywords Web application · IoT system · Phyton, dashboard visualization, smart farming

26.1 Introduction

Many agriculture production industries in Malaysia do not have an information system that could help farmers make reasonable, prompt decisions. The low degree of automation and labor-intensive agricultural work has slowed down data integration within the production system and restricts data utilization and analysis. Many of Malaysia's small-scale farmers rely on paper records for their daily

© The Author(s), under exclusive license to Springer Nature Singapore Pte Ltd. 2024

T. Ahamed, *IoT and AI in Agriculture*,
https://doi.org/10.1007/978-981-97-1263-2_26

production information and manage them in traditional spreadsheet software (Kannan et al., 2017). Moreover, the conventional data collection method implemented in current farming practices could not be promptly integrated for rapid data analysis. Thus, farmers cannot supervise the farm production processes efficiently in real time.

Recently, Wireless Sensor Network (WSN) has been widely used in many areas, especially for rapid and real-time data collection. A WSN describes numerous sensor nodes that could communicate wirelessly to detect, monitor, and analyze environmental conditions (Matin & Islam, 2012). An environmental monitoring system controls and monitors ecological parameters such as humidity, temperature, and rainfall. However, without appropriate processing, the sensors' raw data can be meaningless, hardly interpreted, and offer little value to farmers (Bhawana et al., 2010). On the other hand, by analyzing the data in a graphical form, data visualization could provide context, and meaning and allow data aggregation with other data sources for more efficient data utilization (Li, 2020). The development of computational techniques and digital technology facilitates data visualization to process extensive data in real time.

With the increasing adoption of WSNs, data visualization has become a key component in sensor networks. A low-cost and user-friendly web-based application is needed to help farmers share and analyze the collected data to enhance data utilization for production efficiency. The main objective of this study was to demonstrate the development of a web application for easy visualization of farm data. In this chapter, a web application is developed to visualize the data from the IoT systems that allows the farmer to track and access the information for more efficient agricultural management.

26.2 Materials and Methods

The developed system is based on open-source tools using a programming language, software, and hardware that is low-cost, effective, and simple to install. Despite many web programming languages such as HTML, Java, JavaScript, and C++, Python provides the most practical web programming language because of its easy-to-use, readable, and asynchronous wide coding approaches, which are often used in machine learning and AI for advanced analytics. The most powerful web-based graphing and analytics library within Python is called Plotly. In the Plotly framework, a dashboard visualization framework called "Dash" was developed to provide practical solutions to analytics application development without learning JavaScript, HTML, and other web technologies. A recent study by Wei et al. (2018) showed that a web browser using Plotly's Dash web framework to display interactive real-time data in WSN was developed without mastering advanced programming techniques. Thus, a web-based monitoring system using Plotly's Dash web framework is developed in this study to visualize the raw data

into a user-friendly interface. The IoT system architecture consists of four layers: perception layer, transport layer, processing layer, and application layer (Fig. 26.1). The perception layer is the physical layer, which has sensors for sensing and gathering information about the field environment. The transport layer transfers the sensor data from the perception layer to the processing layer and vice versa through Wi-Fi network. The application layer is responsible for delivering application specific services to the user, in this case the farm information to the farm managers. The developed web dashboard application was then evaluated using Google Lighthouse and PageSpeed Insights for web performance assessment.

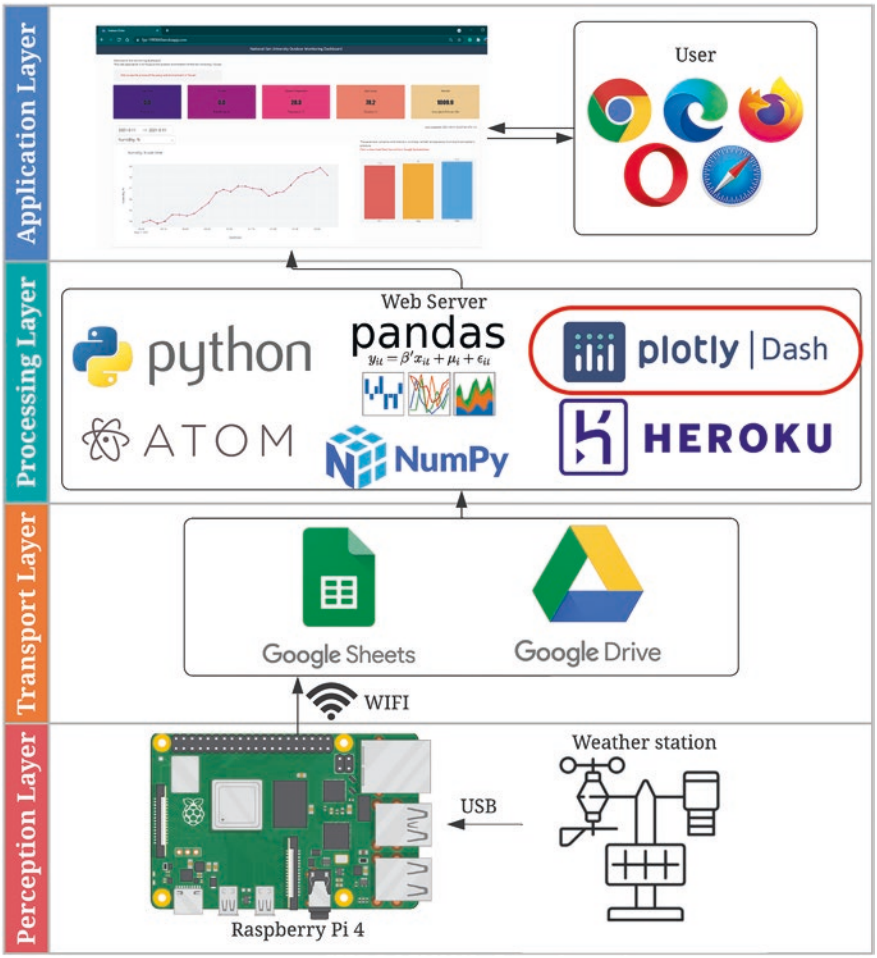

Fig. 26.1 The web-based IoT monitoring system architecture

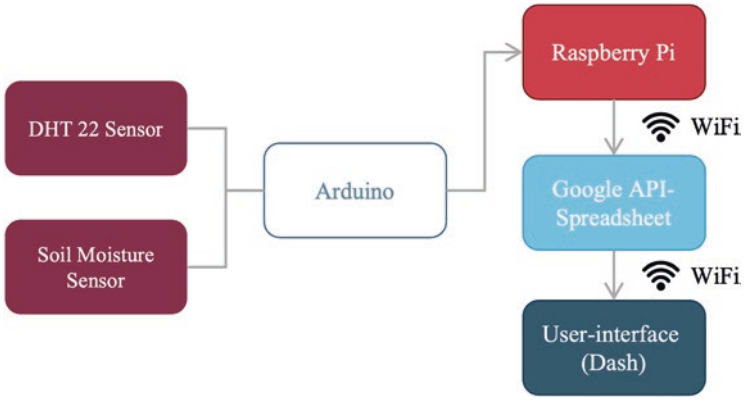

Fig. 26.2 The web-based IoT monitoring system consists of a temperature and humidity sensor (DHT22), and a soil moisture sensor connected to an Arduino microcontroller interfaced with a Raspberry Pi Wi-Fi module

26.2.1 Web-Based IoT Monitoring System

Custom-developed IoT sensor nodes to measure environmental parameters such as temperature, humidity, and soil moisture were developed as the physical layer of the IoT system (Fig. 26.2). The sensor nodes were connected to a microcontroller, which was interfaced with a Wi-Fi module. The microcontroller collects the environmental parameters from the sensors and sends the serial data to the Wi-Fi module. A cloud server on the internet fetches and stores the real-time data collected by the sensors using a Google API spreadsheet. Then, this data was interfaced with the user on a web application using the Dash visualization platform.

26.3 Hardware Configuration for Sensor Node for an IoT System Prototype in Universiti Putra Malaysia (UPM)

The hardware components used to set up the sensor node consist of a temperature and humidity sensor (DHT22), a capacitive soil moisture sensor V1.2, an Arduino UNO Rev 3 microcontroller, and a Raspberry Pi 4 (Fig. 26.3). The temperature, humidity, and soil moisture data were measured, while the heat index parameter was calculated using the DHT library's built-in heat index function. The Arduino UNO collected the analog data from the sensors and converted it to digital measurements, which were transmitted serially to the Raspberry Pi's Wi-Fi module. The Raspberry Pi 4 served as a network interface, enabling wireless communication. It received serial data from Arduino and uploaded it to Google Spreadsheet through wireless networking onboard.

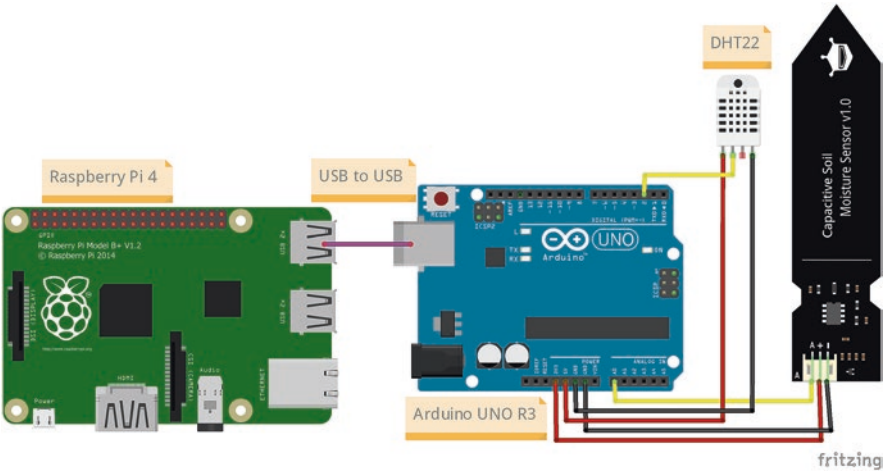

Fig. 26.3 Assembly circuit of the sensor node for the IoT system

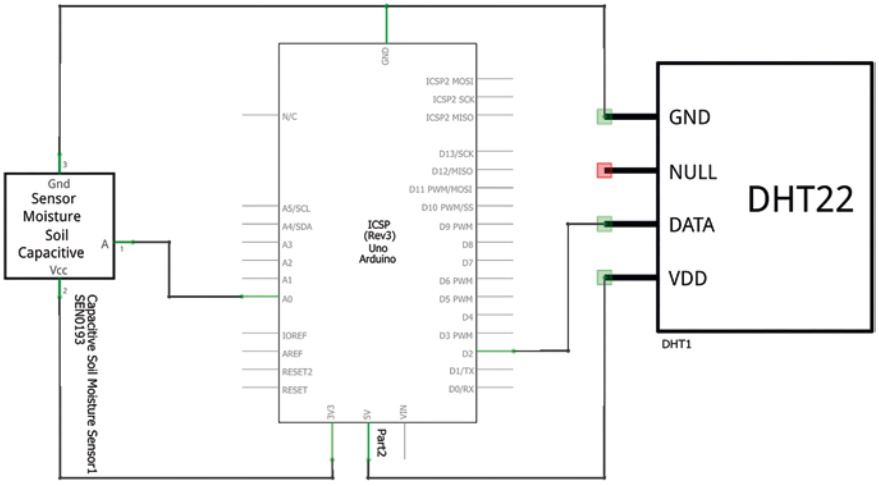

Fig. 26.4 Schematic diagram of the assembly circuit for temperature and humidity (DHT22), and soil moisture sensor to the Arduino microcontroller

The Arduino UNO and Raspberry Pi 4 are connected via a USB port for data transmission. The connection circuit diagram is shown in Fig. 26.4. The DHT22 sensor is connected to the digital pin 2 of the Arduino, while the capacitive soil moisture sensor is connected to analog pin A0. The sensors' GND and VCC are connected to the corresponding GND, 3.3, and 5 V pins.

The Raspberry Pi programming algorithm (Fig. 26.5) is responsible for reading the data collected by the Arduino and uploading it to the Google Spreadsheet. The serial communication method is deployed to transmit data from Arduino to the Raspberry Pi.

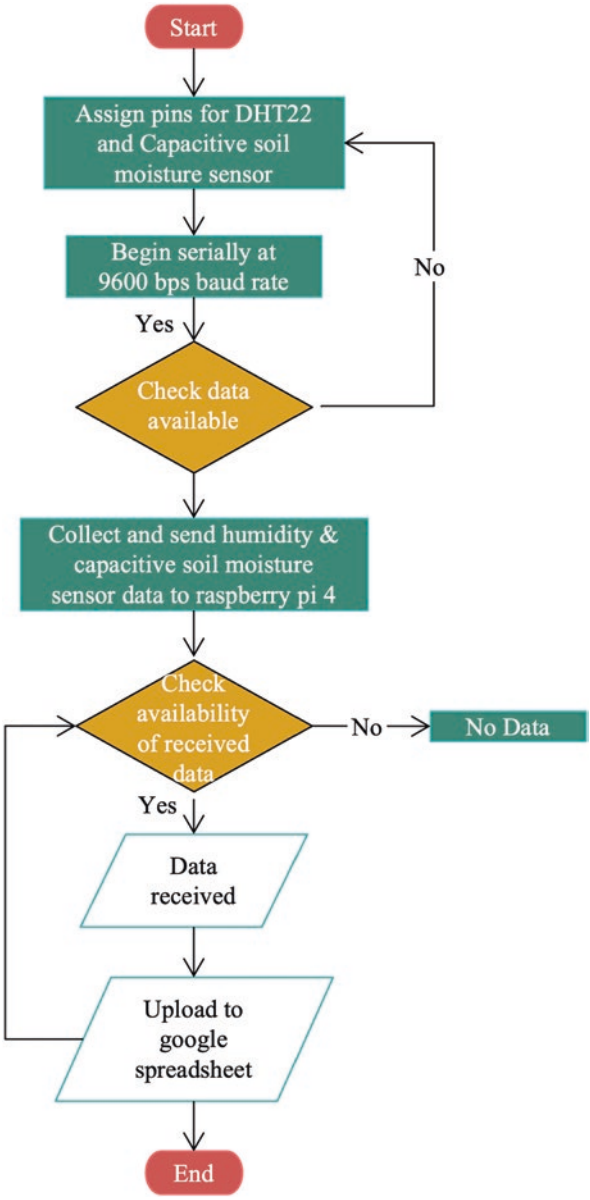

Fig. 26.5 Programming flowchart to read the data from the sensor using Arduino microcontroller and transmit to the Raspberry Pi

26.4 Dash Plotly Framework Design

The web-based application in this project was built using the Dash (Plotly Technologies Inc., 2015) visualization framework, which utilizes Python as a programming language. Dash is a powerful library for data visualization that integrates

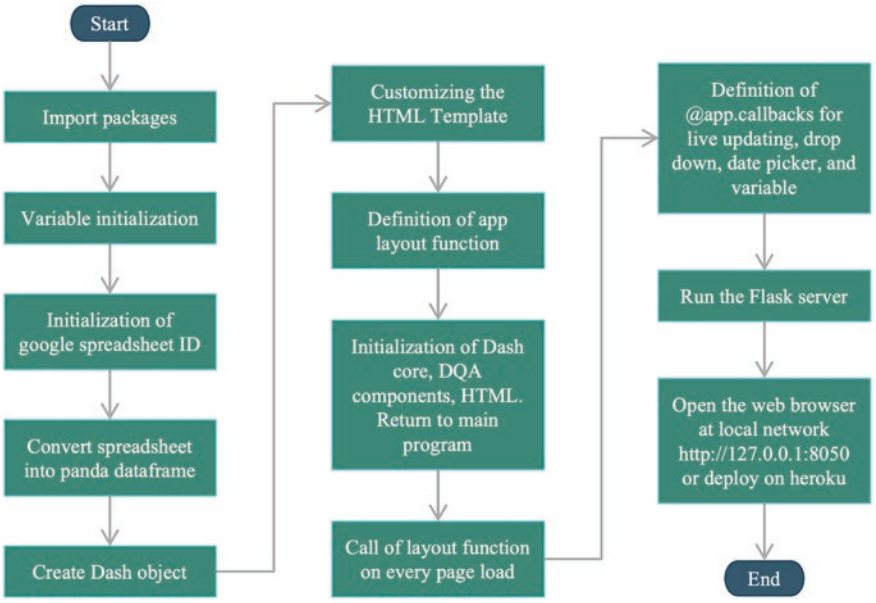

Fig. 26.6 Process flow to develop the web application

Flask as a back-end server and React (Facebook In., 2020) as a front-end JavaScript framework. There are two main parts in the Dash application framework, which are the dash layout and the interactive dash components. The dash layout determines the design of the application and the arrangement of the interactive elements that affect the appearance of the web applications. In contrast, the interactive elements describe the interactivity of the application. Various dash objects such as date picker, graphs, dropdown, and texts were created and organized using an HTML template. The dashboard updates at a predefined interval of time, and it waits for the callback events on the predefined interval. A flowchart in Fig. 26.6 presents the logic behind the development of the web application.

26.4.1 Dash Layout

Dash provides two distinct component libraries to make up the dash components, which are dash-html-components and dash-core-components libraries. The dash-html components contain an HTML tag for every component, mirroring the process of building a website layout, such as html.H1 for the header of the webpage. The dash-core components offer higher-level, interactive components such as sliders, dropdowns, and text inputs generated with JavaScript, HTML, and CSS through the React.js library. The Dash documentation is comprehensive, covering various usage patterns in-depth; it could create complex applications.

26.4.2 Interactive Dash Components

After developing the dash layout, the interactions between the components are mapped out. The Dash callback's function allows reading input values in the dash layout and computes the output value. The callback function is triggered when there's a change in the input value.

26.4.3 Launch of the Dash Application

The Dash applications are rendered in the web browser and run on localhost:8050 locally on the user's device at default. The Dash web application was deployed in Heroku (Salesforce.com Inc., 2007) to create HTML links for access from different devices that would allow other devices to access it.

26.5 Web-Based Dashboard Deployment and Experiment Setup

There are two study locations for the experimental setup of this work, which is the Tenth College (K10) of UPM using the custom-developed IoT system prototype, and the College of Bioresources, National Ilan University (NIU), Taiwan using an IoT-equipped weather station. The first stage of the experiment focuses on measuring and collecting environmental data using the IoT system prototype in UPM. In the second stage, a cloud server is established to receive and store data from the sensors. Finally, the third stage involves replicating the same process for the weather station in Taiwan and deploying it to the web browser that could visualize the data from both experiment locations.

26.5.1 Soil Moisture, Humidity, and Temperature Measurement Test in the Tenth College (K10), UPM

The developed IoT monitoring system was tested in an indoor gardening project at K10, UPM (Fig. 26.7). The plant chosen for the project was a Philodendron Burle Marx, which was planted on a regular soil pot and watered with filtered water every 2 days. The soil moisture sensor was positioned at a depth of 6 cm and a distance of 2.5 cm from the plant. Then, the temperature and humidity

Fig. 26.7 IoT system prototype and the indoor gardening environment in the Tenth College (K10), UPM

sensors were placed near the pot to measure the air temperature and surrounding humidity. Data were recorded at minute intervals and pushed to a cloud server for 20 weeks. A web application that was developed for this system is named K10 Web App.

26.5.2 Outdoor Environmental Measurement in Taiwan

The second data source to build up the Dash visualization scheme is collected from the College of Bioresources, National Ilan University, Taiwan (Fig. 26.8). The weather station (Fig. 26.9) is used to collect data on temperature, wind rate, rainfall, humidity, and atmospheric pressure. To retrieve this data, a Raspberry Pi is connected to the weather station through USB. The Raspberry Pi then uploads the collected data to the Google Spreadsheet through the name of the application developed for this IoT weather station called NIU Web App.

Fig. 26.8 The red pin icon on the google map shows the location of the weather station at National Ilan University, Taiwan

Fig. 26.9 The weather station at National Ilan University, Taiwan

26.6 Assessment of Web-Based IoT Platform

The performance and accessibility of the two web applications were evaluated using Google Lighthouse and PageSpeed Insights (Google, 2021). The scores range from 0 to 100, with a score of 90 or above considered good, scores between 50 and 90

indicating room for improvement, and scores below 50 indicating poor performance. The evaluation was conducted every 3 h, which is 9 am, 12 pm, 3 pm, 6 pm, 9 pm, and 12 am for 3 days, resulting in a total of 18 Google Lighthouse scores, and 18 PageSpeed Insights scores for each web application. The evaluation was conducted using Malaysia Wi-Fi and Taiwan Wi-Fi connections. The Wi-Fi download and upload speed test results for Taiwan's internet connection are 80 and 20 Mbps. The Wi-Fi download and upload speed test results for UPM Wi-Fi are 35 and 10 Mbps, respectively.

In Google Lighthouse, the accessibility evaluation focuses on compliance with web accessibility best practices, ensuring elements like alt tags on images and accessible versions of buttons are impaired to navigate the website. Best practices describe the web page's security, use of HTTPS, absence of errors, and image attributes. Lastly, the Search Engine Optimization (SEO) reports the list of SEO best practices such as the presence of metatags, crawlability of links, and the index of the age, which could improve the quality and quantity of the website traffic to the web app from the search engine. The performance score measures the website's loading speed across different categories, including metrics, opportunities, and diagnostics. There are two broad categories of metrics: timing metrics and other metrics, which show the page features that may impact the application speed. Timing metrics analyze the speed at various stages of the loading process, from early to middle to end.

26.6.1 Web Application's Overall Performance

The overall performance of the web applications was assessed by calculating the mean scores of the 18 Google Lighthouse scores and 18 PageSpeed Insights scores for each application. Statistical analysis using T-test or ANOVA was used to compare the means of (1) the performance scores under different types of internet connections, and (2) the Google Lighthouse and PageSpeed Insights performance based on different time zones.

26.6.1.1 The Performance Scores Under Different Types of Internet Connections

The T-test was conducted to compare the performance of the web applications based on the Google Lighthouse and PageSpeed Insights scores. An F-test needs to be done before the T-test to determine if the sample has an equal or unequal variance. The null hypothesis of the F-test is that there is no significant difference in the variance between two types of internet connection when p is greater than 0.05, and the F-test result falls within the critical F-value range. The null hypothesis for the T-test is that there is no significant difference in performance scores between Google Lighthouse and PageSpeed Insights with different types of internet connection when the T-test result is within the T-critical value.

26.6.1.2 The Google Lighthouse and PageSpeed Insights Performance Is Based on Different Time Zones

To determine the variability between the Google Lighthouse and PageSpeed Insights performance scores based on the different times, an ANOVA is used to compare the means of more than two groups, which are 9 am, 12 pm, 3 pm, 6 pm, 9 pm, 12 am. Single-factor ANOVA was used to analyze variation in the performance's relationship based on different times as there is only one factor, either Google Lighthouse or PageSpeed Insights evaluation. The null hypothesis in ANOVA is when the statistic value is lower than the F critical value.

26.7 Results and Discussion

The Dash Visualization scheme for this study can be employed on web browsers such as Firefox, Google Chrome, or Internet Explorer by deploying the web applications on Heroku. The web browser will pull and convert data to Pandas DataFrame from Google Spreadsheet.

26.7.1 The Overall Performance of the Web Applications

The K10 Web App (Fig. 26.10) is a web application dashboard that provides real-time data visualization of soil moisture, humidity, temperature, and heat index. It retrieves data from Google Spreadsheets based on the predefined intervals, and it waits for the callback events on the predefined interval. As default, the dashboard that was developed can only be accessed by local devices at http://127.0.0.1:8050/, but to allow access from other devices, it is deployed on the Heroku application with the address room-199364.herokuapp.com.

The dashboard components (Fig. 26.11) feature the value and the scale of the obtained data. The values are processed and filtered based on the optimal ranges defined by the Food and Agriculture Organization (FAO) for crop water requirements (Doorenbos & Pruitt, 1997). The ideal temperature and humidity are 16–30 °C, and 40–70%, respectively. The K10 web application categorizes temperature as "hot" if it exceeds 30 °C, and "cold" if it is below 16 °C. Similarly, humidity (h) is classified as highly humid ($h > 70\%$), medium humid (40–69%), and dry ($h < 39\%$). The soil that is used in the pot (Fig. 26.7) is black, a type of clayey soil. Northeast Region Certified Adviser (NRCCA, 2010) stated the saturation of clayey soil is 60%, field capacity is at 50%, management allowable depletion is at 40%, and the permanent wilting point is 30%. Thus, the soil moisture condition (mc) is labeled as wet soil ($mc > 60\%$), moist soil (41–60%), dry soil (20–40%), and extremely dry soil ($mc < 20\%$). The computed heat index (hi) was compared with the chart value developed by the National Oceanic and Atmospheric

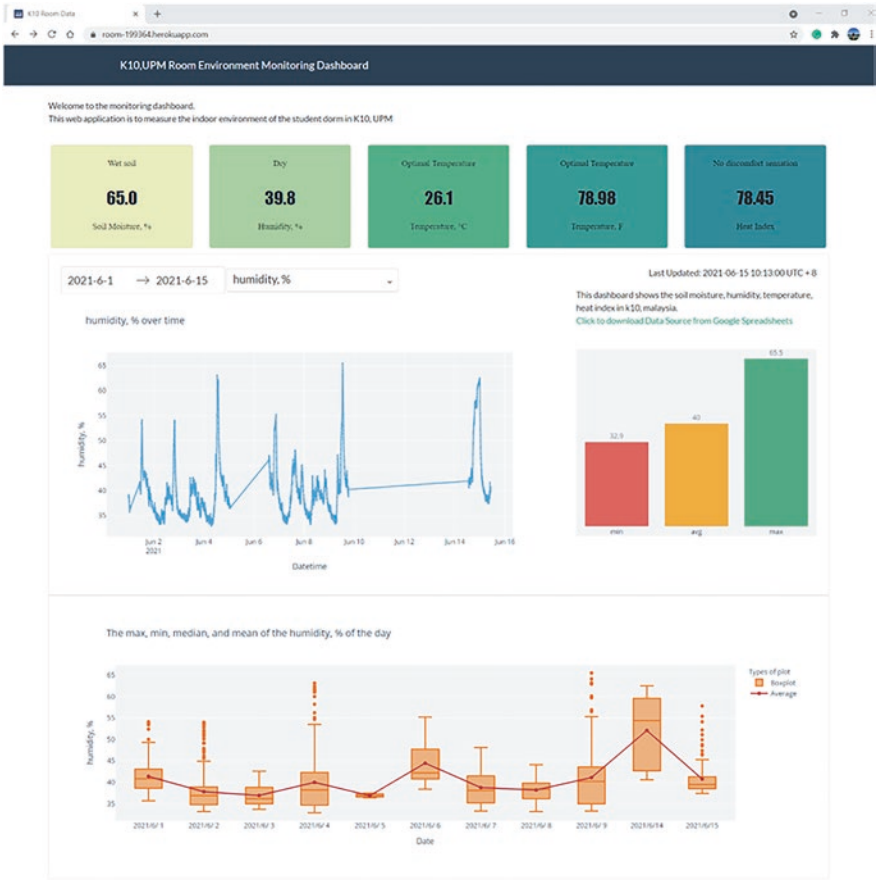

Fig. 26.10 Web application layout developed for soil moisture, temperature, humidity, and heat index measurements in the Tenth College (K10), UPM

Fig. 26.11 Live data components displayed on the web application dashboard on 15th June 2021 at 10.13 am

Administration's National Weather Service (National Weather Service, 2020) to estimate the severity of heat stress in the plant. The filtered value assesses the severity of heat stress on plants, labeled as no discomfort sensation (hi < 80 F), warm sensation (80–89 F), hot sensation (90–104 F), and very hot sensation (hi > 105 F). Therefore, the K10 IoT system effectively presents the data and conditions for informed decision-making.

The web application, graphs, and text value of a component utilize the Dash interactivity function to be updated through the callbacks function (Fig. 26.12). The user can select a specific period of interest using the date picker and variable components, which dynamically update the graph accordingly. The callback function takes about 2–4 s to update the Dash components in the web application.

The web application allows the user to select a specific date and variable from a dropdown menu (Fig. 26.13), which in turn modifies the scatter plot. The scatter plot (Fig. 26.14) provides insights into the patterns and fluctuations of the indoor environmental parameters over the past few weeks. Despite some irregular patterns on 5th June, and from 10th June to 14th June due to technical issues with the Raspberry Pi, Dash plotly still successfully captures newly updated data from the Google Spreadsheet. However, more data are still required to facilitate a more comprehensive comparison over time.

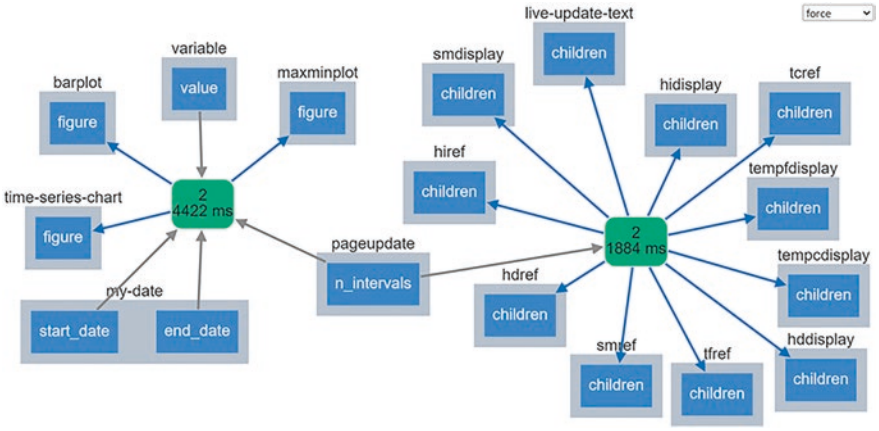

Fig. 26.12 The callbacks relation between each component

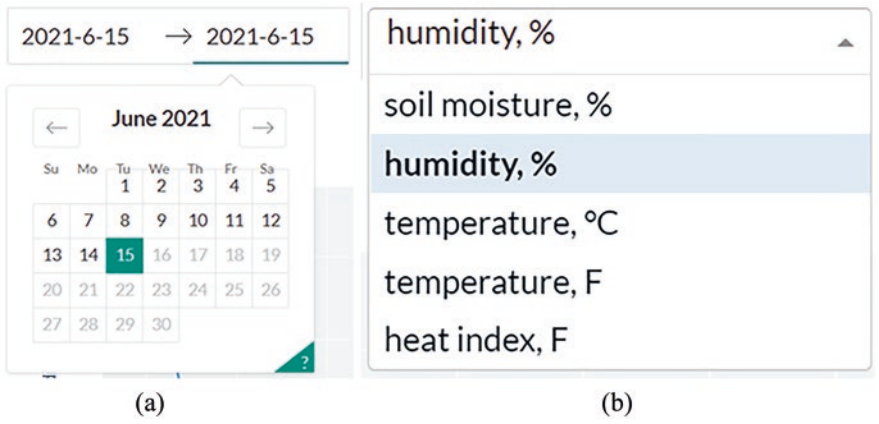

Fig. 26.13 (**a**) Date picker in Dash plotly, (**b**) dropdown component

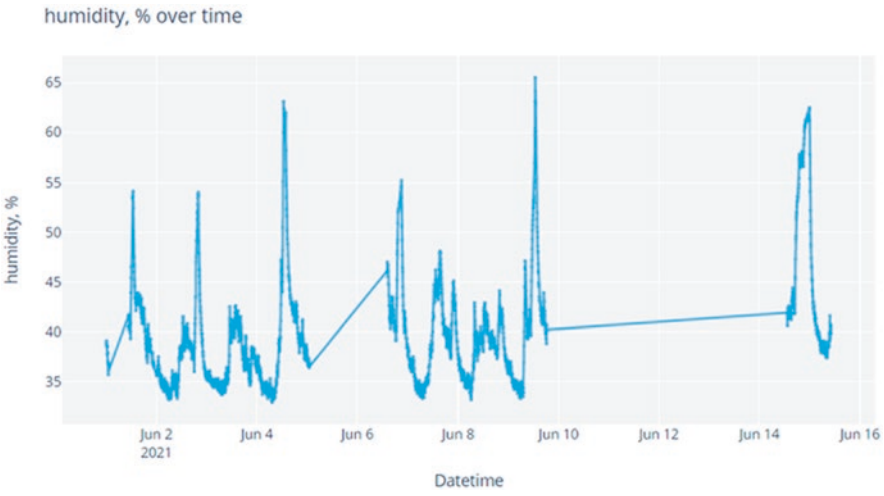

Fig. 26.14 Scatter plot of percentage humidity at K10 experimental setup for selected dates from 1st June–16th June

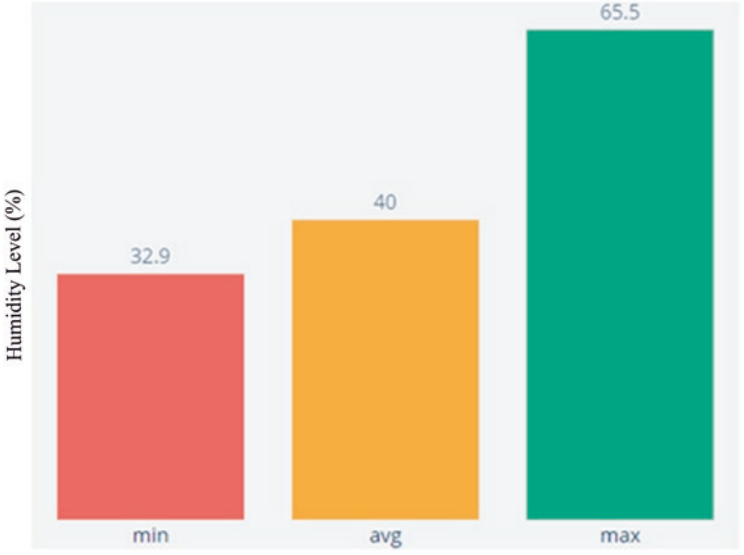

Fig. 26.15 Bar plot visualizes the minimum, average, and maximum humidity level for the selected date (1st June–16th June)

The bar plots (Fig. 26.15) in the web application will dynamically adjust according to the selected date and variable parameter, visualizing the selected data's minimum, average, and maximum values.

The box plot and the line graph are the last components of the K10 Web App. The box plot (Fig. 26.16) is a standardized method to display data distribution based on

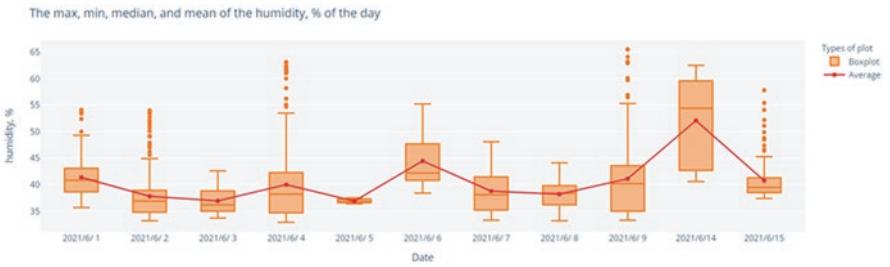

Fig. 26.16 Box plot and line graph for the daily humidity over the selected date (1st June to 16th June)

the minimum, first quartile, median, third quartile, and maximum collected data. The box plot method provides the ability to compare multiple datasets side-by-side and provides insights into central tendency, skewness, dispersion, and extremes. The line graph complements the box plots by displaying the daily average data over time and enhancing the understanding of the parameter changes over time. However, more data are needed to gain a better interpretation to determine the patterns over time.

26.7.2 Web Application for National Ilan University, Taiwan's Weather Station

The NIU Web App (Fig. 26.17) is a web application dashboard designed for the weather station at National Ilan University, Taiwan to visualize the wind rate, rainfall, temperature, humidity, and atmospheric pressure that are extracted from the Google Spreadsheet. The dashboard is updated every minute, and it waits for the callback events on the predefined interval. Similar to the K10 Web App for UPM's IoT system, the NIU Web App is deployed on the Heroku application platform.

The values and scales of the obtained data are presented (Fig. 26.18). The reference of the status data is slightly different compared to the K10 Web App, due to various parameters and climatic conditions. The temperature and humidity values obtained from the weather station in Taiwan are processed and filtered based on the general levels of climatic variables stated by FAO (FAO, 1977). The basic Beaufort scale is calm wind when it is at 0 scale until hurricane force during the scale of 1, in which the wind rate ranges from 0.1 to 32.6 m/s. However, due to the typhoon in Taiwan, the extended Beaufort scale (Northeast Region Certified Crop Adviser (NRCCA), 2010; Raspberry Pi Foundation, 2021; Salesforce Inc, 2021; Skybrary, 2020; Trillionz, 2020), which is above 32.7 m/s, was applied as a wind rate scale reference for this web application (Skybrary, 2020). Rainfall rates (r) are classified according to the references from the Central Weather Bureau whereas, Light rain ($r < 10$ mm/h), Moderate rain (10–25 mm/h), Heavy rain (25–200 mm/h), and

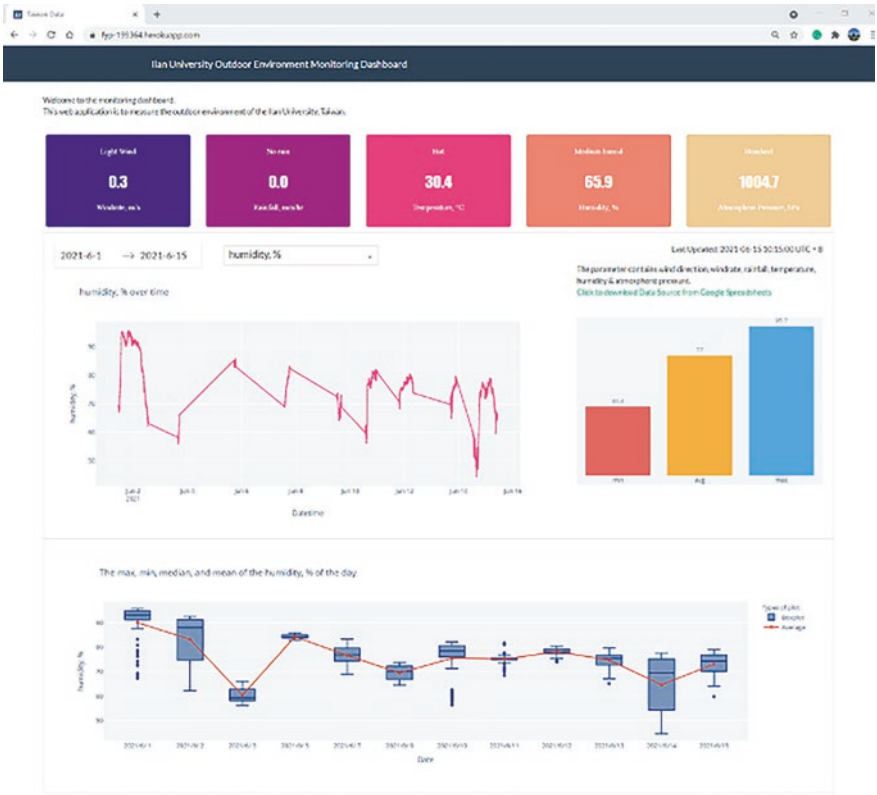

Fig. 26.17 Web application layout developed for wind rate, rainfall, temperature, humidity, and atmospheric pressure read from the weather station installed at National Ilan University, Taiwan

Fig. 26.18 Live data components on NIU Web App dashboard on 15th June 2021, 10.15 am

Extraordinary rainstorm (r > 200 mm/h) (Central Weather Bureau, 2021). Based on the Central Weather Bureau in Taiwan, the range of atmospheric pressure within the range of 1000–1030 hPa is considered normal based on the standards.

The update of web applications, graphs, and text value components are dynamically updated through the dash interactivity callback's function (Fig. 26.19). The date picker (Fig. 26.20a) allows the users to select their desired period within the range of available data. The dropdown component (Fig. 26.20b) is based on the parameters provided by the National Ilan University, which are wind rate, rainfall, temperature, humidity, and atmospheric pressure.

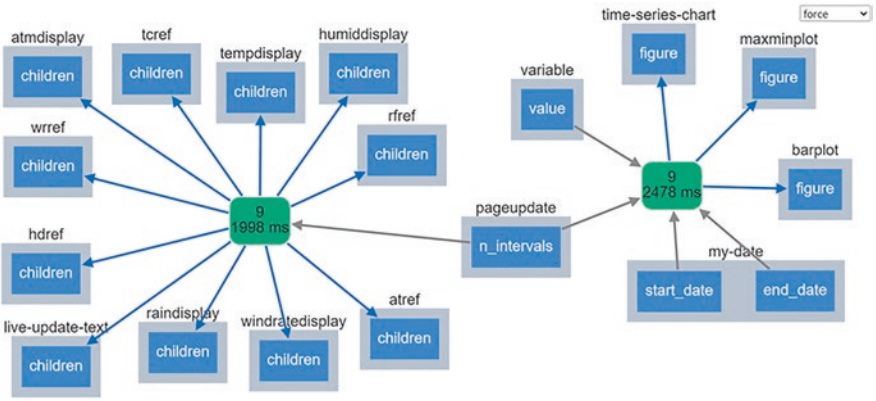

Fig. 26.19 The callbacks relation between components for the NIU Web App

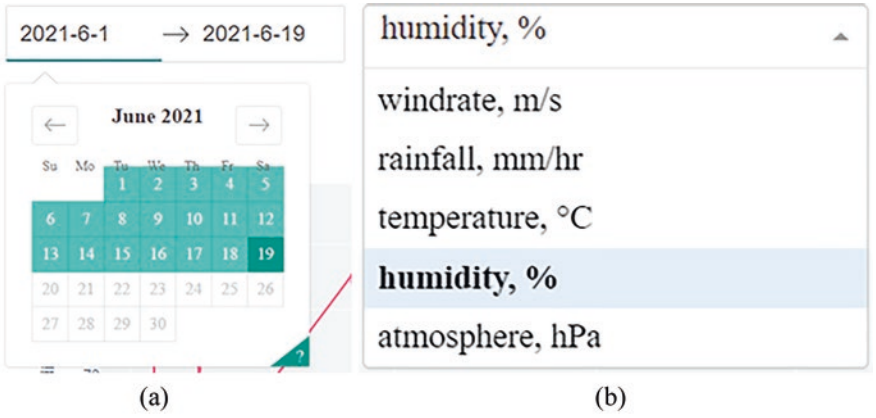

Fig. 26.20 (**a**) Date picker, (**b**) dropdown component for NIU Web App

The scatter plots (Fig. 26.21) lack sufficient information due to a significant amount of missing data. This is because Taiwan implemented a voluntary quarantine during that period, resulting in reduced usage of the laboratory and missing data points. Despite the missing data, Dash plotly connects the available data points to create a continuous line graph. Thus, it is believed that a consistent data source is needed to provide a clearer perspective and patterns of the graphs.

Next, a bar plot in Fig. 26.22 provides an overview of the data distribution of the selected parameter and allows for easy comparison of the minimum, average, and maximum values within the specified period from the date picker.

The last component of the Taiwan Web App is the box plot and line graph (Fig. 26.23). The data distribution is based on the minimum, first quartile, median, third quartile, and maximum collected data with the box plot. Meanwhile, the line graph represents the average daily humidity. However, the box plot and line graph

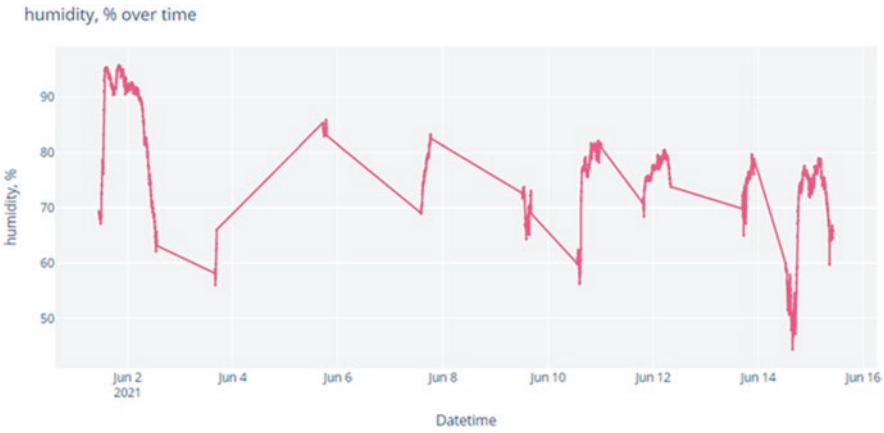

Fig. 26.21 Scatter plot for the selected date (1st June–16th June) for percentage humidity

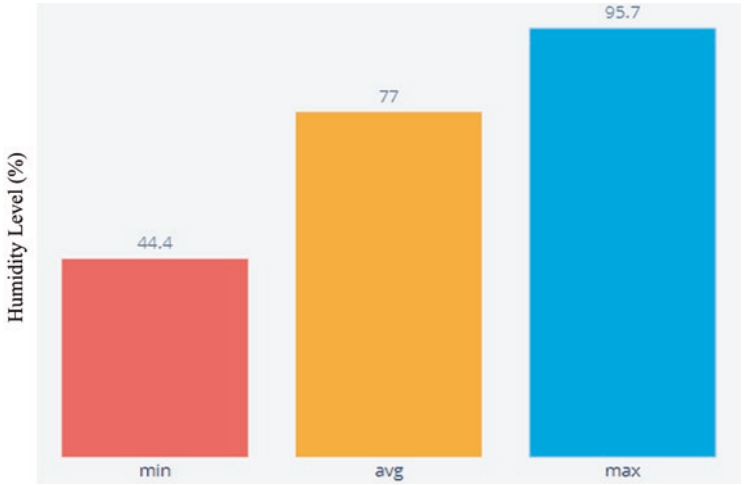

Fig. 26.22 Bar plot visualizes the minimum, average, and maximum humidity level for the selected date (1st June–16th June)

Fig. 26.23 Box plot and line graph visualize the average, mean, median, first quartile, and third quartile daily humidity over the interested time zone (1st June to 16th June)

may not accurately reflect the complete information due to the missing data points. Thus, ensuring complete and reliable data is crucial to obtaining meaningful insights for farmers to make reasonable decisions.

26.7.2.1 Overall Performance of the Web Applications

The performance of the web applications in both experimental setups was assessed using Google Lighthouse and PageSpeed Insights scores, which were generated every 3 h for three consecutive days. A total of 144 scores were obtained for both tools over the 3-day assessment with different internet connections. The evaluated results are reported in Table 26.1 to compare the performance score based on various internet speeds.

The results indicate the Google Lighthouse performance score fluctuates due to inherent variability in web and network technologies. The PageSpeed Insights performance tends to change as it takes into account field data collected over time from anonymous users using different devices and network conditions. The change in timing between visits will affect the PageSpeed Insights scores.

The Google Lighthouse performance of the K10 Web App and NIU Web App is relatively average, with scores of 59.2 and 60.1 respectively. One of the reasons that drag the web application's performance is the limited processing resources with a free Heroku account, which only offers 512 MB RAM dynos sizes to run the web application (Heroku DEV Centre, 2021). Also, the applications running on free dynos will experience sleep mode after 30 min of inactivity, resulting in longer load times as the application needs to be reactivated (Trillionz, 2020).

Table 26.2 presents the Google Lighthouse results for both web applications, providing insights into their performance, accessibility, best practices, and search engine optimization (SEO). Although the accessibility, best practices, and SEO metrics are identical for both applications due to their shared design concept, dash

Table 26.1 Google Lighthouse and PageSpeed Insights average score based on Taiwan (80Mbps Wi-Fi speed test) and Malaysia (30 Mbps Wi-Fi speed test) internet connection

Web dashboard applications	Analyze based on Malaysia Internet		Analyze based on Taiwan Internet	
	Lighthouse score	PageSpeed Insights score	Lighthouse score	PageSpeed Insights score
K10 Web App	59.2	58.7	59.1	60.9
NIU Web App	60.1	61.0	62.8	62.8

Table 26.2 Google Lighthouse score an average performance, accessibility, best practices, and search engine optimization

	K10 Web App	NIU Web App
Performance	59	60
Accessibility	77	77
Best practices	93	93
SEO	70	70

layout, and elements, the performance scores differ. By analyzing the failing indicators highlighted in the Google Lighthouse report, it is possible to identify areas and develop plans for improvement to enhance the performance of these applications.

The slow loading of the application can be attributed to factors such as the length of chains required for a page load and the presence of unnecessary resources such as JavaScript. The large async-plotly.js loaded in a dash app are the significant problems causing the application's slow down. Despite the lack of official documentation from Dash plotly addressing this issue, some creators have created a solution by downloading bundles from external links and attaching them to the Dash application or utilizing external CDN. However, implementing these solutions requires advanced programming skills to reduce the size of the async-plotly.js file.

26.7.2.2 The T-Test of Web Application Performance Based on Internet Connection

The F-test results for the Google Lighthouse scores and PageSpeed Insights scores of both the NIU Web App and K10 Web App are 1.0447 and 1.0688, respectively. Tables 26.3 and 26.4 present the F-test result of the Google Lighthouse and PageSpeed Insights scores based on Malaysia and Taiwan internet connection for the NIU Web App. Thus, the null hypothesis for the Google Lighthouse and PageSpeed Insights evaluation for the NIU Web App is accepted as there are no

Table 26.3 F-test two-sample for variances (Google Lighthouse evaluation for NIU Web App)

	Malaysia line	Taiwan line
Mean	60.11	62.78
Variance	9.16	8.77
Observations	18.00	18.00
Ddf	17.00	17.00
F	1.04	
P(F <= f) one-tail	0.46	
F critical one-tail	2.27	
P two-tailed	0.93	

Table 26.4 F-test two-sample for variances (PageSpeed Insights evaluation for NIU Web App)

	Malaysia line	Taiwan line
Mean	61.00	62.83
Variance	19.65	18.38
Observations	18.00	18.00
df	17.00	17.00
F	1.07	
P(F <= f) one-tail	0.45	
F Critical one-tail	2.27	
P two-tailed	0.89	

Table 26.5 Results of T-test for the Google Lighthouse and PageSpeed Insights performance score based on Malaysia and Taiwan internet connection for two web applications

NIU Web App		K10 Web App	
Lighthouse score in Malaysia vs. Taiwan line	PageSpeed Insights score in Malaysia vs. Taiwan line	Lighthouse score in Malaysia vs. Taiwan line	PageSpeed Insights score in Malaysia vs. Taiwan line
0.0115	0.2158	0.8656	0.0751
Critical T-value: ±2.1098			

significant differences in the variance of Google Lighthouse and PageSpeed Insights scores between the two types of internet connections. The F-test is repeated for the K10 Web App. A similar result was found where the F-test result for the Google Lighthouse scores and PageSpeed Insights based on the Malaysia and Taiwan internet connection for the K10 Web App has the same result, which is 1.102. Therefore, the null hypothesis for the Google Lighthouse and PageSpeed Insights evaluation for the K10 Web App is accepted as the critical F is larger than the F-test result. This implies that the performance scores obtained from Google Lighthouse and PageSpeed Insights are consistent across the different types of internet connections as there is no significant variation in scores between the two types of internet connections.

In conclusion, the F-test results show that the null hypothesis is accepted as there are no significant differences in the variance of performance scores between the two applications. Both the P two-tailed results are higher than 0.05, and the F critical is higher than the F value. Thus, it can be concluded that a two-sample equal variance T-test should be done for this assessment.

Table 26.5 presents the Google Lighthouse and PageSpeed Insights performance scores on both applications based on different types of internet connections. To conclude, there are no significant differences between the performance scores of Google Lighthouse and PageSpeed Insights with varying types of internet connection as the T-test result is within the t-critical value.

26.7.2.3 The Comparison Between Google Lighthouse and PageSpeed Insights Performance Based on Different Time Zones

The F statistics for the NIU Web App Google Lighthouse and PageSpeed Insights scores are 0.7864 and 0.9966, respectively. These F statistic values are lower than the critical F value of 3.1059. Tables 26.6 and 26.7 show the ANOVA table results generated by Excel for Google Lighthouse and PageSpeed Insights performance scores based on different time sessions using the Malaysia internet connection for the NIU Web App. The fluctuation in Google Lighthouse performance scores can be attributed to the inherent variability in web and network technologies. At the same time, the change in timing between visits affects the PageSpeed Insights scores as it uses real-world field data from various devices and network conditions. Hence, it can be concluded there are no significant means differences for the Google

Table 26.6 Single-factor ANOVA result for NIU Web App's Google Lighthouse performance score for different time

Summary						
Groups	Count	Sum	Average	Variance	S. deviation	
9 am	3	183	61.00	0	0	
12 pm	3	184	61.33	2.33	1.53	
3 pm	3	185	61.67	20.33	4.51	
6 pm	3	176	58.67	1.33	1.15	
9 pm	3	173	57.67	4.33	2.08	
12 am	3	181	60.33	30.33	5.51	
ANOVA						
Source of variation	SS	df	MS	F	P-value	F crit
Between groups	38.44	5	7.69	0.79	0.58	3.11
Within groups	117.33	12	9.78			
Total	155.78	17				

Table 26.7 Single-factor ANOVA result for NIU Web App's PageSpeed Insights performance score using Malaysia internet connection for different time

Summary						
Groups	Count	Sum	Average	Variance	S. deviation	
9 am	3	184	61.33	57.33	7.57	
12 pm	3	174	58.00	3.00	1.73	
3 pm	3	174	58.00	3.00	1.73	
6 pm	3	184	61.33	14.33	3.79	
9 pm	3	190	63.33	12.33	3.51	
12 am	3	192	64.00	28.00	5.29	
ANOVA						
Source of variation	SS	df	MS	F	P-value	F crit
Between groups	98	5	19.60	0.99	0.46	3.11
Within groups	236	12	19.67			
Total	334	17				

Lighthouse score between the time sessions using the Malaysia internet connection for the NIU Web App.

Table 26.8 shows the F statistics value for the Google Lighthouse (L) and PageSpeed Insights (P) scores for the NIU Web App and K10 Web App based on the different internet connections for the six-time period using ANOVA.

Based on the assessment conducted, there is no significant difference between the different times at the 0.05 level of significance, 9 am, 12 pm, 3 pm, 6 pm, 9 pm, and 12 am, since all the F ratios are smaller than the F critical. Thus, the web application has almost identical Google Lighthouse and PageSpeed Insights performance based on different internet connections in the interested period. Thus, it can be concluded that the web applications' performances are not affected by the internet connection or the time. It can only be improved by the method mentioned in 3.2.1,

Table 26.8 F ratio for Google Lighthouse and PageSpeed Insights performance based on a different internet connection for 9 am, 12 pm, 3 pm, 6 pm, 9 pm, and 12 am

NIU Web App				K10 Web App			
Malaysia line		Taiwan line		Malaysia line		Taiwan line	
L	P	L	P	L	P	L	P
0.7864	0.9966	1.8944	2.0421	1.2746	1.7694	0.4421	0.2182
F critical: ±3.1059							

where the unnecessary files should be removed to reduce the loading time for the web applications.

26.7.3 Impact of the WebBased IoT Monitoring and Service System for Agricultural Applications to Society, Safety, and Health

The presented visualization method in this study provides interactive charts that enable farm managers to gain detailed insights and make better decisions. Each interactive element facilitates a large volume of data and allows the farm manager to extract information easily. The IoT system is mounted with multiple sensors to provide the information on current growth status and the development of crops in the field through various plant conditions and parameters such as soil moisture, rainfall, and wind rate during the growing season. For example, real-time soil moisture data allow farm managers to optimize irrigation practices and improve water use efficiency. Excessive irrigation of plants will reduce the yield of plants. It also impacts water quality by causing soil erosion, transporting chemicals such as nutrients, herbicides, and pesticides or decreasing the amount of water flowing into streams and rivers resulting in a lower groundwater table. It is believed that the public water supply can be contaminated with chemicals if there is a runoff of chemicals toward the water bodies. By monitoring the real-time soil moisture through the visualized graphs on the web-based IoT monitoring and service system, they can accurately assess the crop needs and apply the appropriate amount of water, avoiding water quality issues and reducing waste. Also, farm managers can predict future soil and environmental conditions, facilitating better planning and decision-making. In short, the use of agricultural data helps the farm manager to understand the trends and expand their perspective on agricultural statistical systems.

26.8 Conclusions

Two Dash Plotly applications were successfully developed to visualize and analyze the collected data from National Ilan University, Taiwan and Tenth College (K10), UPM. These applications enable farm managers to identify the environmental

patterns, and maximum, average, and minimum values over a specific period through graphical visualizations. The insights gained from the visualizations help the farm managers to understand the rainfall patterns, water cycles, and make appropriate decisions for optimal plant growth. Dash Plotly's flexibility and customization options allow for personalized and tailored dashboards, showcasing the power of Python programming. The interactive dashboard allows the user to have a better understanding of the data. Also, web applications can be accessed locally and publicly over the internet. However, both applications received an average score in Google Lighthouse and PageSpeed Insights due to the performance issues caused by the large size of the unused plotly.js bundle. Hence, a document on this issue should be released from the official Dash plotly in the future to reduce the unused JavaScript and decrease the bytes consumed by network activity to speed up the page loading.

Future improvements include enhancing the website's esthetics and rendering it for mobile screens to offer a responsive dashboard for mobile users, reducing unused JavaScript, and minimizing junk files for faster loading times. Moreover, additional visualizations such as future trends, more parameters, and in-depth analytics can be incorporated to provide more valuable information to farmers. Finally, using a more consistent data source can provide more intensive information to farm managers.

Funding This study was supported by the Putra Grant scheme (Ref. No.: UPM/800–3/3/1/GPB/2019/9671500) awarded by Universiti Putra Malaysia.

Conflicts of Interest The authors declare no conflict of interest.

References

Bhawana, P., Dwivedi, A. K., & Vyas, O. P. (2010). Data visualization tools for WSNs: a glimpse. *International Journal of Computers and Applications, 2*(1), 14. https://doi.org/10.5120/617-868

Central Weather Bureau. (2021). *Analysis of weather forecast*. Retrieved June 22, 2021, from https://www.cwb.gov.tw/V8/C/W/analysis.html

Doorenbos, J., & Pruitt, W. O. (1997). *Guidelines for predicting crop water requirements*. http://www.fao.org/3/f2430e/f2430e.pdf

Facebook In. (2020). *React*. Retrieved June 21, 2021, from https://react.dev/

Heroku DEV Center. (2021). *Limits | Heroku Dev center*. Retrieved June 22, 2021, from https://devcenter.heroku.com/articles/limits

Kannan, P., Hana Basaruddin, N., Hashim, K., et al. (2017). Monitoring and reporting of oil palm fresh fruit bunch (FFB) transactions among independent smallholders and dealers: an analysis of a case study in Selangor, Malaysia. *Oil Palm Industry Economic Journal, 17*(2).

Li, Q. (2020). Overview of data visualization. In *Embodying data* (pp. 17–47). Springer. https://doi.org/10.1007/978-981-15-5069-0_2

Matin, M., & Islam, M. (2012). Overview of wireless sensor network. In *Wireless sensor networks—technology and protocols* (pp. 1–22). INTECH. https://doi.org/10.5772/49376

National Weather Service. (2020). *Heat index calculation*. https://www.wpc.ncep.noaa.gov/html/heatindex.shtml

Northeast Region Certified Crop Adviser (NRCCA). (2010). *Soil hydrology AEM*. https://nrcca.cals.cornell.edu/soil/CA2/CA0212.1-3.php

Plotly Technologies Inc. (2015). *Collaborative data science*. Plotly Technologies Inc.. Retrieved from https://plot.ly

Raspberry Pi Foundation. (2021). *Raspberry Pi 4 (Model B)*. Retrieved June 22, 2021, from https://www.raspberrypi.com/products/raspberry-pi-4-model-b/specifications/

Salesforce Inc. (2021). *Heroku*. Retrieved June 22, 2021, from https://www.heroku.com/

Skybrary. (2020). *Beaufort wind force scale*. Retrieved June 22, 2021, from https://www.skybrary.aero/index.php/Beaufort_wind_force_scale

Trillionz, E. (2020). *Your Heroku app is slow to load because of this*. Retrieved June 22, 2021, from https://dev.to/elijahtrillionz/your-heroku-app-is-slow-to-load-because-of-this-4lep

Chapter 27
Strategic Short Note: Application of Smart Machine Vision in Aquaculture and Animal Husbandry

Abstract As the global population approaches 9.7 billion by 2050, the demand for protein sources intensifies. Aquaculture and animal husbandry products accounted for approximately 40% of the global average protein intake. Aquaculture and animal husbandry are labor-intensive. Although automation has been applied to these two fields, manual patrols are still required to monitor the conditions of the economic animals to be raised. This article delves into the role of smart machine vision as a replacement to manual monitoring of animals in these two fields. By integrating advanced technologies like deep neural networks, machine vision facilitates automatic monitoring of animal conditions, thereby reducing reliance on manual labor. This technology encompasses video acquisition, model training, database management, and real-time analysis. Pioneering applications in observing chicken behaviors, monitoring sow and piglet interactions, and assessing shrimp appetite illustrate the profound impact of smart machine vision. These advancements promise improved animal survival rates and appropriate feed amounts. This article underscores the growing importance of smart machine vision as a critical area for ongoing research and development.

Keywords Artificial intelligence · Convolutional neural networks · Deep learning · Images and videos

27.1 Introduction

Proteins are essential for human health, aiding in cell structure, enzymes, and immunity. Aquaculture and animal husbandry products accounted for approximately 40% of the global average protein intake in 2019 (OECD and FAO, 2021). Given the United Nations' projection that the global population will reach 9.7 billion by 2050 (UNDESA, 2022), the anticipated rise in protein demand is evident. However, aquaculture and animal husbandry are labor-intensive. Due to the lack of

© The Author(s), under exclusive license to Springer Nature Singapore Pte Ltd. 2024

T. Ahamed, *IoT and AI in Agriculture*,
https://doi.org/10.1007/978-981-97-1263-2_27

proportional rewards, fewer people are willing to enter these two fields. Therefore, solutions are required to produce enough proteins to feed the global population in the context of a labor shortage.

Automation is the fundamental solution to alleviate the issues of labor shortage in aquaculture and animal husbandry. Machines, equipment, and facilities have been developed for automatic animal care, such as feeders, cooling systems, manure scrapers, etc. However, the conditions of the animals to be raised in aquaculture and animal husbandry still require attention. Conventionally, farmers conduct routine patrols to ensure the health and welfare of their livestock. These patrols are time-consuming. Automatic solutions to replace manual patrols are needed.

Recent advances in smart machine vision make it possible to observe animal conditions automatically. Smart machine vision approaches can recognize and analyze the behavioral patterns, postures, body conditions, and physiological characteristics of animals; thus, the reliance on human observations can be reduced. Also, smart machine vision can work 24/7 in almost real-time. Necessary actions can be taken when needed, thereby reducing production loss of economical animals and benefiting both animal farmers and aquaculture professionals.

In this chapter, basic concepts of smart machine vision are introduced. Several applications of smart machine vision in aquaculture and animal husbandry are included. These studies illustrate how smart machine vision can be used to assist farmers and aquaculture professionals in resolving the aforementioned problems.

27.2 Overview of Smart Machine Vision in Aquaculture and Animal Husbandry

Typical machine vision applications consist of four main components: (1) video acquisition, (2) model training and implementation, (3) database management, (4) resulting and analyzing (Fig. 27.1; Chang et al., 2023). The objects to observe in

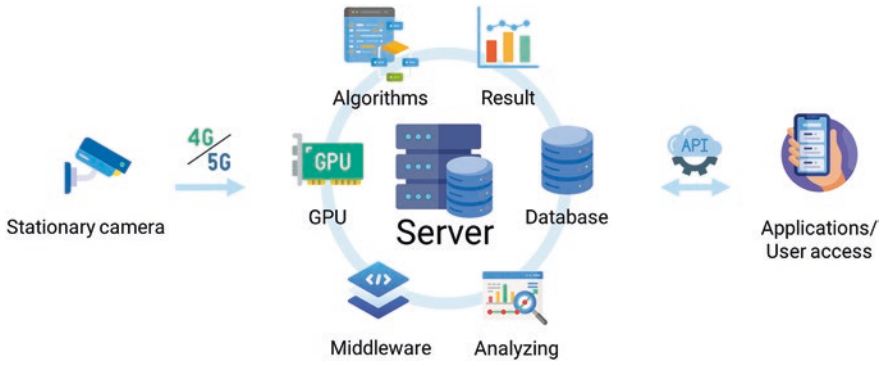

Fig. 27.1 The flow of smart machine vision

aquaculture and animal husbandry are usually animals. Thus, stationary cameras are used to acquire videos of the animal to observe. The acquired videos are transmitted to cloud servers through 4G or 5G internet. Nowadays deep neural network (DNN) models (e.g., convolutional neural networks and transformers by Sze et al., 2017) are commonly used for various purposes (e.g., classification, localization and classification, segmentation, etc.) in machine vision because of their outstanding performance. However, training and implementing DNN models requires strong computation power. Thus, cloud servers for training DNN models are usually equipped with graphical processing units for accelerating model training and implementation (Fig. 27.1). The outcomes from trained DNN models are usually analyzed and visualized on the cloud servers too. Another essential component of a cloud server is database. Database makes it possible to store the data (i.e., the acquired videos and their corresponding ground-truth labels) used for model training efficiently. The last essential component of smart machine vision is user access. User access establishes a bridge between the trained DNN models, model inputs, and end users (Fig. 27.1). It also provides the function for end users to contribute new data.

27.3 Examples of Smart Machine Vision in Aquaculture and Animal Husbandry

Chickens play a significant role in animal husbandry. In 2020, poultry meat accounted for approximately 40% of global meat production (FAO, 2021). Although broilers dominate the market, certain native chicken varieties (e.g., red feather native chickens) are popular in certain countries (i.e., Taiwan) because the meat quality of these native chicken varieties fits the cooking styles of these countries. Native chickens are usually more active than broilers and have longer breeding periods, making the farming of native chickens more costly. In the farming of native chickens, farmers usually understand the health status of the chickens by observing their activity levels, dispersions, and open-beak behaviors. However, manual observation is labor-intensive and time-consuming. Moreover, manual observation can be subjective and is not continuous. Thus, in recent years, machine vision has started to be applied to the chicken industry for observing the behaviors of chickens. Chang et al. (2022) oversaw chicken activities, targeting at heat stress levels, using YOLOv4-tiny. Chen et al. (2023) autonomously tracked and quantified vital behavior indicators of chickens (movement and dispersion) using YOLOv7-tiny and moving average models.

Pork accounts for a major proportion of meat consumption worldwide. Even though pig farming has been renovated in the past years, there still exists several areas that can be improved. Particularly, reducing the mortality rate of preweaning piglets is one of the issues that remains to be worked on. Knowing the lactation-related behaviors of sows and their own piglets is the key to reducing the mortality of preweaning piglets (Gasco et al., 2013). Conventionally, these behaviors were

observed by pig farmers. However, naked-eye observation is subjective and is not continuous. Thus, in recent years, machine vision has started to be applied to the pig industry for observing the behaviors of sows and piglets. Zheng et al. (2018) identified five postures, daily activity levels, and posture change frequencies of sows using Faster R-CNN and depth images. Gan et al. (2021) detected and tracked piglets simultaneously using a customized approach. Ho et al. (2021) recognized the lactating frequencies of sows, tracked individual piglets, and quantified their movements in videos.

Shrimp plays an essential role in aquaculture. Recent estimates indicated that the global shrimp market size was approximately US$ 56.49 billion in 2022, and it was projected to escalate to US$ 74.84 billion by 2028 (BlueWeave Consulting, 2022). In shrimp farming, feed takes account for approximately 40% of the overall cost. Shrimp appetite varies based on the ambient conditions. Accurate shrimp appetite estimation is thus the key to optimize shrimp growth and farming cost. Conventionally shrimp appetite was observed manually using feeding trays and baits. However, manual approaches can be subjective. In addition, feeding trays may hurt shrimp. In recent years, machine vision approaches were proposed to observe shrimp directly in water. Lee and Kuo (2022) used a UNet model with underwater imaging system to analyze shrimp appetite through residual feed variations. Lai et al. (2022) utilized YOLOv4-tiny and image processing techniques with underwater imaging system to measure shrimp lengths.

27.4 Conclusion

As the global population continues to surge, the demand for protein sources is escalating rapidly. Smart machine vision can be a critical key to the problem of labor shortage in agriculture and animal husbandry. Smart machine vision promises increased production and cost reduction by observing animal conditions automatically and in almost real-time. The approach improves food security while using less labor. Smart machine vision is a key area that attracts many researchers in recent years. The trend will continue in the following years as well.

References

BlueWeave Consulting. (2022). *Global Shrimp Market to grow at a CAGR of 10.4% during 2022–2028*. BlueWeave Consulting. https://www.blueweaveconsulting.com/report/global-shrimp-market/report-sample

Chang, K. R., Shih, F. P., Hsieh, M. K., Hsieh, K. W., & Kuo, Y. F. (2022). Analyzing chicken activity level under heat stress condition using deep convolutional neural networks. In *2022 ASABE annual international meeting* (p. 1). American Society of Agricultural and Biological Engineers.

Chang, K. R., Ma, T. H., & Kuo, Y. F. (2023). Strategic short note: Application of smart machine vision in agriculture, forestry, fishery, and animal husbandry. In T. Ahamed (Ed.), *IoT and AI in agriculture self-sufciency in food production to achieve society 5.0 and SDG's globally* (p. 128). Springer.

Chen, B. L., Cheng, T. H., Huang, Y. C., Hsieh, Y. L., Hsu, H. C., Lu, C. Y., et al. (2023). Developing an automatic warning system for anomalous chicken dispersion and movement using deep learning and machine learning. *Poultry Science, 102*(12), 103040.

FAO. (2021). *Gateway to poultry production and products*. FAO of the United Nations. https://www.fao.org/poultry-production-products/production/en/

Gan, H., Ou, M., Zhao, F., Xu, C., Li, S., Chen, C., & Xue, Y. (2021). Automated piglet tracking using a single convolutional neural network. *Biosystems Engineering, 205*, 48–63.

Gasco, J., Holbrook, T. J., Patel, A., Smith, A., Paulson, D., Muns, A., et al. (2013). Neurosurgery simulation in residency training: Feasibility, cost, and educational benefit. *Neurosurgery, 73*, S39–S45.

Ho, K. Y., Tsai, Y. J., & Kuo, Y. F. (2021). Automatic monitoring of lactation frequency of sows and movement quantification of newborn piglets in farrowing houses using convolutional neural networks. *Computers and Electronics in Agriculture, 189*, 106376.

Lai, P. C., Lin, H. Y., Lin, J. Y., Hsu, H. C., Chu, Y. N., Liou, C. H., & Kuo, Y. F. (2022). Automatic measuring shrimp body length using cnn and an underwater imaging system. *Biosystems Engineering, 221*, 224–235.

Lee, C. C., & Kuo, Y. F. (2022). Automatically estimating shrimp feed residue using CNN and an underwater imaging system. In *International symposium on machinery and mechatronics for agriculture and biosystems engineering*. ISMAB.

OECD & FAO. (2021). *OECD-FAO agricultural outlook 2021–2030*. Organisation for Economic Co-operation and Development. https://doi.org/10.1787/19428846-en

Sze, V., Chen, Y. H., Yang, T. J., & Emer, J. S. (2017). Efficient processing of deep neural networks: A tutorial and survey. *Proceedings of the IEEE, 105*(12), 2295–2329.

UNDESA. (2022). *Revision of world population prospects*. UNDESA Population Division. https://population.un.org/wpp/

Zheng, C., Zhu, X., Yang, X., Wang, L., Tu, S., & Xue, Y. (2018). Automatic recognition of lactating sow postures from depth images by deep learning detector. *Computers and Electronics in Agriculture, 147*, 51–63.

Chapter 28
Deep Learning Algorithms for Postharvest Quality Assessment: A New Sensing Methodology for Quail Eggs Freshness Estimation and Shelf-Life Revalidation

Abstract The Shelf-Life of Eggs is complex to determine since it is dependent on several parameters, including freshness. Available techniques to estimate the degradation of albumen and enlargement of the air cell are either destructive or not suitable for high-throughput applications. The aim of this research was to introduce a new approach to evaluate the air cell of quail eggs for freshness assessment as a fast, noninvasive, and nondestructive method. A new methodology was proposed by using a thermal microcamera and deep learning object detection algorithms. In this work, computer vision-based models were produced, referred to as "You Only Look Once" version 5, 7 (YOLOv5, YOLOv7) and EfficientDet. We tested the models in a new dataset composed of 60 eggs that were kept for 15 days after the labeled expiration label date. The validation of our methodology was performed by measuring the air cell area highlighted in the thermal images at the pixel level; thus, we compared the difference in the weight of eggs between the first day of storage and after 10 days under accelerated aging conditions. The statistical significance showed that the two variables (air cell and weight) were negatively correlated ($R^2 = 0.676$). The deep learning models could predict freshness with F1 scores of 0.86, 0.90, and 0.86 for the YOLO (v5, v7), and EfficientDet models, respectively. The new methodology for freshness assessment demonstrated that the best model reclassified 38.33% of our testing dataset. Therefore, those expired eggs could have their expiration date extended for another 2 weeks from the original label date.

Keywords Freshness assessment · Quail Eggs · Deep Learning · YOLOv7 · Nondestructive analysis

28.1 Introduction

The agricultural supply chain has been passing through a digital transformation over the last few years by absorbing elements from industry 4.0 (Rotz et al., 2019). Innovations linked to sensor technology, telecommunications, robotics, the Internet of Things (IoT), and artificial intelligence (AI) are being applied to management

© The Author(s), under exclusive license to Springer Nature Singapore Pte Ltd. 2024

T. Ahamed, *IoT and AI in Agriculture*,
https://doi.org/10.1007/978-981-97-1263-2_28

automation and real-time data-driven intervention. In addition, these revolutions toward enhancing the production of food, fibers, and energy are expected to provide solutions for the contention of wastes and the mitigation of environmental pollutants (Benyam et al., 2021). Novel practices for agri-food industries introducing computational methods combined with smart devices are allowing new alternatives to assess the quality of farming products and traceability. Hence, with the recent release of 5th generation telecommunications networks (5G), for the very first time, rural areas can obtain access to fast internet connections, which may support farmers and decision-makers in the adoption of best practices and mediation just in time.

In the field of computer sciences, AI is a cutting-edge technology from recent decades with the potential to disrupt society in the coming years. Deep neural networks (DNNs) are the workhorse of AI that have been leading solutions to nonlinear and multidimensional problems, such as image processing, natural language processing, and speech recognition. In addition, a combination of big data, faster algorithms, and powerful processing units are considered to be mainly responsible for bringing the deep learning (DL) approach to the spotlight, and DL is currently considered the state of the art in human-centered AI systems.

In the meantime, the greatest efforts have been focused on computer vision to address image classification, object detection, segmentation, and localization. Faster algorithms have been improved continuously to reach high confidence and speed by employing convolutional neural networks (CNNs) on the backbone of those algorithms. Currently, the state-of-the-art object detection algorithms are based on the You Only Look Once (YOLO) (Redmon et al., 2016). A series of improvements on this deep learning algorithm have achieved fast inference on edge devices, including smartphones, low-end computers, and cloud processing platforms (Wang et al., 2022). YOLO is classified as a one-stage detector algorithm (Alexey et al., 2020), the same class as RetinaNet (Lin et al., 2017b) and SSD (Liu et al., 2016); however, the architecture is anchor-based and inherited from two-stage detectors, such as the R-CNN family (Girshick et al., 2014), Fast R-CNN (Girshick & Fast, 2015), and Faster R-CNN (Ren et al., 2015).

YOLO was introduced in 2015 (Redmon et al., 2016); the breakthrough of this object detection algorithm was its ability to predict classes and localize coordinates in images (bounding boxes) by using a single CNN, which makes the inference faster and real-time applications become possible. The basic idea behind YOLO architecture was to look at the entire image (or frame) all at once, then divide it into a grid $S \times S$, after which, the localization of an object is treated as a regression problem instead of a traditional classification problem. When the center of an object falls into a specific grid, that grid becomes responsible for detecting the object (Zhao et al., 2019).

Since its release, YOLO has evolved into a series, also known as versions. The first three versions of YOLO were released by Redmon et al. (2016), Redmon and Farhadi (2017), Redmon and Farhadi (2018), respectively, and the fourth version (YOLOv4) by Alexey et al. (2020); this last one was reported to overperform the previous version (YOLOv3) by 12% in speed and 10% for accuracy, and then became one of the most used real-time solution object detection algorithms.

Over time, the upgraded versions have stepped-up the tradeoff between speed and accuracy of detections, and besides that, from the version 5 (referred to as YOLOv5), the YOLO algorithms have incorporated user-friendly characteristics, including less complex framework, training efficiency, and portability of models among diverse inference platforms (Jiang et al., 2022). Computer vision systems based on the YOLO series have been reported for solutions related to detecting fruits in orchards using YOLOv3 (Lawal, 2021), YOLOv4 (Gai et al., 2021), and YOLOv5 (Kuznetsova et al., 2021), leaf diseases detections (Qi et al., 2022), defects assessment on fruits (Fan et al., 2022), and pest detection (Chen et al., 2022).

Furthermore, for other agricultural purposes, computer vision systems based on deep learning object detection algorithms show enormous potential, which includes self-driving vehicles (Gupta et al., 2021; Li et al., 2019), robotics (Karaoguz & Jensfelt, 2019), and object tracking (Zhang et al., 2021). However, most of the utilization of vision systems has been concerned with in-farm operations aiming to supply labor shortages and quality of operations; few implementations are given to reduce waste at the shelf level as a priority target.

Egg quality is a complex task to be assessed because it involves diverse parameters, such as size, weight, color, eggshell defects, spoilage, bacterial infection, and freshness (which can be considered the major criteria for quality (Karoui et al., 2006)).

The freshness domain is explained as an objective attribute that represents biochemical and physical variables that are sensory (Schmilovitch et al., 2002). The lack of fresh characteristics occurs principally due to aging effects that start to compromise egg quality immediately after oviposition. The loss of water and CO2 through shell pores reduces the weight of eggs (Romanoff & Romanoff, 1949) and increases the pH (Burley, 1989), respectively, liquefying the albumen and yolk, and therefore facilitating osmotic exchange between them (Brasil et al., 2022). These factors can be intensified by environmental conditions, especially temperature and humidity (Stadelman et al., 2017), during the storage period.

Several methods to evaluate the freshness of eggs have been reported, including destructive analysis, such as the Haugh unit (HU) (Haugh, 1937), the pH of the albumen (Dong et al., 2017), the yolk index (YI) (Jiang et al., 2018), and the air cell size (Kumbár et al., 2015). Nondestructive techniques mainly involve NIR/Raman spectroscopy (Giunchi et al., 2008; Liu et al., 2020), odor sensors (Dutta et al., 2003; Liu et al., 2010; Xiang et al., 2019), electrical conductivity (Tsarenko & Karaseva, 1986), ultrasound (Aboonajmi et al., 2014), and candling (Cattaneo et al., 1997). However, most of these techniques are not robust for real-time applications, and the nondestructive analysis techniques are not even suitable due to issues regarding equipment cost, intraclass variations related to shell color (specific calibration is required) and thickness, and environmental parameters, such as illumination, temperature, and humidity (Harnsoongnoen & Jaroensuk, 2021). A recent study used a pulse phase thermography approach with neural networks and was able to estimate the aging of hen eggs according to the approximation of the air cell size and obtained a high degree correlation ($R^2 > 0.95$) (Quattrocchi et al., 2022), which demonstrates the potential of high-throughput application of thermal imaging and heuristic algorithms.

All over the world, different countries have adopted distinct metrics for freshness standards. The European Union (EU), for instance, adopted air cell size as a parameter to evaluate the freshness of avian eggs (EC. Commission Regulation No. 2295, 2003), while in Brazil, the standard is HU (Brasil, MAPA, 1990). Therefore, the aim of this work was to develop a fast and accurate method using a computer vision model based on deep learning algorithms for air cell detection as a fast and nondestructive method to classify nonfresh quail eggs using a thermal microcamera. Our hypothesis was that the loss in egg weight, as determined by the air cell increase, can be detected by thermal cameras due to gas transmission through the eggshell; thus, a machine vision system could be carried out by detecting this feature in a quick and nondestructive way. In this study, we dealt with deep learning object detection algorithms to assess the shelf-life quality of quail eggs toward freshness by classification of radiometric images from a thermal camera according to the new proposed methodology.

28.2 Materials and Methods

28.2.1 Experimental Environment

For this study, we used Japanese quail eggs (Coturnix japonica) collected from local grocery stores. The label expiration date was considered the reference for the end point of freshness. The experiments were conducted in the Bioproduction and Machinery laboratory, University of Tsukuba, Japan, during the middle of the summer season, in which the average range daily temperature was 24–32 °C. The methodology was developed in two phases: first, air cell assessment by pixel measurement; second, deep learning object detection for automatic classification of nonfresh eggs using thermal images.

28.2.2 Thermal Imaging

A FLIR® (Teledyne FLIR LLC, Wilsonville, OR, USA) Model VUE™ 336, 6.8 mm, thermal camera with a sensor resolution of 336 × 256 pixels, and a spectral band range of 7.5–13.5 μm, size 2.26″ (5.74 cm) × 1.75″ (4.44 cm), was used to collect radiometric images from the quail eggs. Thermal cameras can produce images by interpreting the intensity of infrared (IR) radiance emitted from the target when interacting with the environment. Therefore, the images result from atmospheric transmission, IR reflection, and the emission wavelength from the target (Nakaguchi & Ahamed, 2022). In this regard, three variables are determinant to acquire information of objects: the size, distance of targets, and the angle from the camera.

The main point when using thermal cameras relies on the fact of no-light dependency compared to optical cameras. Thermal cameras are specifically used for night

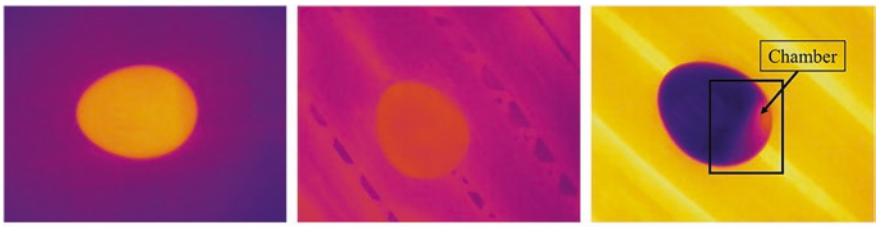

Fig. 28.1 (**a**) Thermal image of an egg at room temperature. (**b**) Warmed egg at 37 °C. (**c**) Thermal picture from a cold egg at 17 °C while room temperature was 28 °C

vision problems and body temperature measurements. However, limitations are found due to low resolution and high cost compared to conventional cameras. In addition, thermal cameras provide relative temperatures, and absolute measurements can be reached after data processing or calibration procedures for specific purposes.

In this study, we used a thermal microcamera to collect egg images. By random exploration of the thermal camera, we found that radiometric images collected from cold eggs could highlight a "chamber" on the large base of the eggs, as we knew that the air cell is located in the same position. We investigated the possibility of assessing the freshness according to the size of this feature, which could be a reference to the air cell in proportion to the aging effects on eggs (Fig. 28.1). When the eggs are colder than room temperature, the chamber is highlighted (Fig. 28.1c).

We collected images inside an automatic incubator machine (no brand) to avoid direct atmospheric interference on the eggs. The incubator was warmed to 38 °C to enhance the temperature contrast between the environment and the cold eggs and was rewarmed after every 20 egg images. The room temperature was constant at 27 °C during the data collection period. We kept the eggs inside the incubator by picking them up by their equator region. The thermal camera was placed above the target in an up-view position ±10 cm from the eggs (Fig. 28.2). The thermal camera was controlled with a SHARP® smartphone (Sharp Corporation, Sakai, Osaka, Japan), AQUOS™ sense4 basic Model A003SH with an ANDROID™ version 11 operating system connected to the camera by Bluetooth technology. The software used was FLIR® UAS™ 2 version 2.2.4.

28.2.3 Dataset Collection

We collected 390 quail eggs from local grocery stores at random. However, eight eggs were found to be cracked; therefore, the remaining 382 eggs were used for the experiments. The eggs were divided into three groups:

The first group was composed of 174 eggs stored for 60 days continuously inside a conventional refrigerator under a minimum cold temperature of 17 °C and a

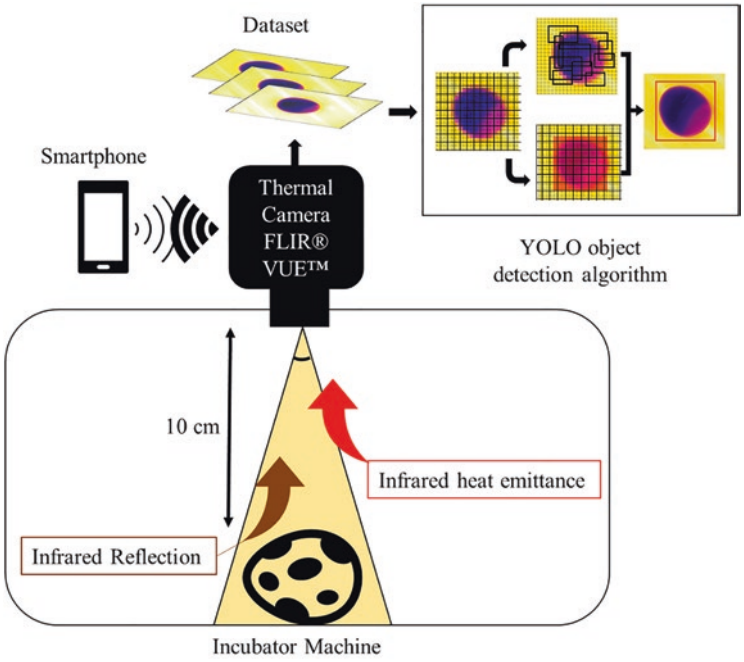

Fig. 28.2 A schematic representation of the methodology proposed to collect thermal images from quail eggs

relative humidity of 45%. On the 30th, 50th, and 60th days, the eggs were removed from the refrigerator for image sampling (thermal pictures acquired). After the 30th day of storage, we assumed that no eggs would be fresh at all; to make sure, data were collected on the 50th day and on the 60th day. In addition, by collecting samples at three time points, we could obtain more representative data over long storage periods. This dataset was used to train vision-based object detection algorithms.

The second group was formed of 148 eggs, and this group was used to assess the air cell size. Air cells increase due to aging effects, and there is a loss in egg weight due to that; therefore, these measures could be correlated.

The third group had 60 eggs that were used for testing the prediction model. This group was stored under the same conditions as group 1 and evaluated 15 days after the expiration date. To assess the air cells in this group, we boiled the eggs and visually confirmed the air cell size by cutting the eggs longitudinally.

28.2.4 Air Cell Assessment Methodology

To correlate the air cell enlargement with the loss in egg weight, an experiment was performed with eggs from group 2. Basically, we scaled fresh eggs immediately after purchase (1st day) and after a 10-day storage period under accelerated aging

conditions (the eggs were kept at room temperature in summer conditions, where the average temperature of the room was 27 °C and humidity of 60%, such conditions can speed up the dehydration of eggs).

The 148 eggs from group 2 were all numbered and scaled on a digital semi-precise scale (0.001 g precision, no brand). In addition, the long axis (Y) size was measured with a digital caliper (0.01 mm precision). Figure 28.3 shows the procedures.

The measurements of the representative air cell on the pictures were performed manually by contouring the feature highlighted on the large base of the eggs. We used the open-source software ImageJ (64 bits, version 1.8.0) developed by Wayne Rasband and contributors from the National Institutes of Health in the United States (Rasband, 1997). The software could provide a conversion between real measurements and the length of pixels, according to a known real distance. Figure 28.4 shows the workflow procedure. First, the real distance was converted into a pixel length. Next, according to the scale (pixel/mm), the contoured area was calculated by the software.

We determined the pixel distance between two points by means of three-line distances (three points A-B) to reduce the error and the subjectivity of pixel length conversion.

The Pearson correlation (Eq. (28.1)) was adopted to calculate the relationship between weight and air cell size variation during the accelerated aging period.

$$r = \frac{\sum(x_i - \bar{x})(y_i - \bar{y})}{\sqrt{\sum(x_i - \bar{x})2\sum(y_i - \bar{y})2}} \tag{28.1}$$

(a) (b)

Fig. 28.3 (**a**) Digital semi-precise scale. (**b**) Digital caliper measurement of the longitudinal axis

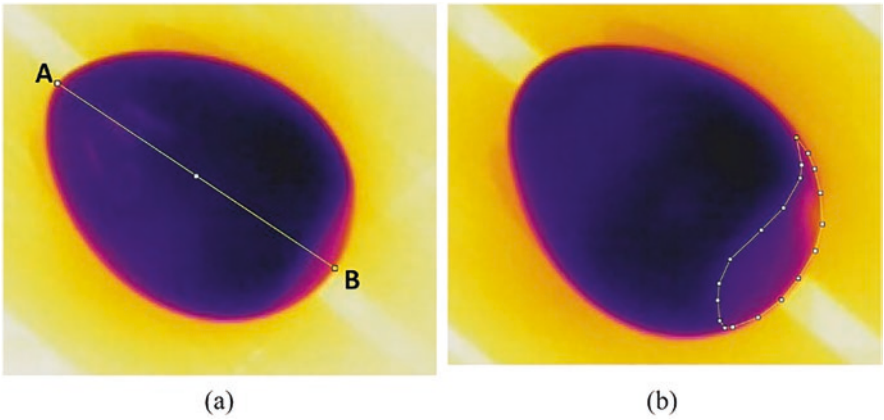

Fig. 28.4 (**a**) The calibration process was performed by scaling the known distance from point "A" to point "B." (**b**) The area was determined by calculating the number of pixels under the delimited contour in relation to the known distance defined in (a)

where r is the coefficient of correlation, x_i and y_i are the x and y variable samples (area and weight), respectively, and $\bar{x}$and $\bar{y}$ are the mean values of the x-y sample variables.

28.2.5 Deep Learning-Based Object Detection Algorithms

In the field of machine learning (ML) techniques, deep learning (DL) uses deep neural networks to deal with nonlinear problems involving big data to create predictive models. In recent years, compared to traditional ML, such as logistic regression, support vector machine, and other methods, DL has been faster and more accurate when performing under multidimensional data (Ahmad & Rahimi, 2022), for instance, image classification, segmentation, and localization.

The complexity of DL algorithms makes us think of it as a combination of "black boxes" where the entire process is difficult to visualize in a simple way. However, YOLO is a DL object detection algorithm that uses a single convolutional neural network (CNN) to localize the object of interest inside the image and classifies the object as a regression problem.

In our problems, the training dataset was fed into YOLO (v5 and v7). The algorithm then looked at every image at once and then divided each image into grids of same size. For example, if our input size was 416 × 416, each cell of the grid had 32 × 32 pixels. Thus, when a high probability of the center point of the eggs with a large air cell was located, that grid was addressed to the prediction of the "not-fresh" class. The YOLO algorithm simplified architecture workflow can be seen in Fig. 28.2.

Since its release, YOLO has achieved many series, including YOLOv5 (Ultralytics, 2021), YOLOv6 (Meituan, 2022), and YOLOv7 (Wang et al., 2022), which includes modifications made by the community of developers and companies to improve the speed and accuracy of the original project YOLO. The first four versions of YOLO were released based on the Darknet framework and form the fifth version it uses the PyTorch framework, which is based on a Python ecosystem, one of the most used programing languages worldwide (Paszke et al., 2019), especially in the data science field.

A few elements were modified from YOLOv4 to YOLOv5, including the modified bottom-up and top-down layers in the new feature pyramid network (FPN) (Lin et al., 2017a, b) inside the path aggregation network (PANet) (Liu et al., 2018) on the neck of the algorithm. Another modification was the loss function; the fifth version uses binary cross entropy with the logit loss function (Upesh & Hossein, 2022).

It is important to note that the YOLO family has been improving the tradeoff accuracy–speed by adding and modifying the parameters of its basic architecture. YOLOv7 has improved the efficiency over the previous versions when comparing the mAP on the MS COCO (Microsoft Common Objects in Context) dataset, which is the far most used reference dataset to train localization models. This new version contains several adjustments that makes the training process and the inference more accurate for object detection problems such as data augmentations (bag of freebies), multiple learning rate schedulers for model scalability, and samplers carry on data loader workers.

As an updated version, YOLOv7 introduces a new approach to improve the feature extraction at the CNN level, the extended efficient layer aggregation networks (E-ELAN), which focuses on the problem of gradient saturation over the training process when scaling models (network size and number of hyperparameters). E-ELAN employs expansion, rearranging, and integration cardinality to attain the capacity for incessantly enhancing the network's learning capability without compromising the initial gradient trajectory. In the computational block, E-ELAN solely modifies the structure while keeping the transition layer architecture completely unaltered. The approach of E-ELAN involves utilizing group convolution to enlarge the channel and cardinality of computational blocks. These new additions make the training process and feature extraction more efficient, therefore the model can be scaled to low-end devices with less trade-off.

In this work, we trained YOLOv5, YOLOv7, and EfficientDet object detection architectures to predict nonfresh eggs after the expiration date and to revalidate the label date of the remaining eggs. The overall architecture of the deep learning algorithms is shown in Fig. 28.5.

The backbone of the algorithm represents the CNN type, which is responsible for feature extraction (edges, shapes, color differences) and the creation of the feature map by using convolutional operations. The neck is the feature aggregator network; it collected those features from the backbone and put them together as bottom-up and top-down features to the head, which was the final step to predict the nonfresh egg position on the image or frame. This last part was responsible for plotting the bounding boxes around the class and labeling the image with its name. Table 28.1

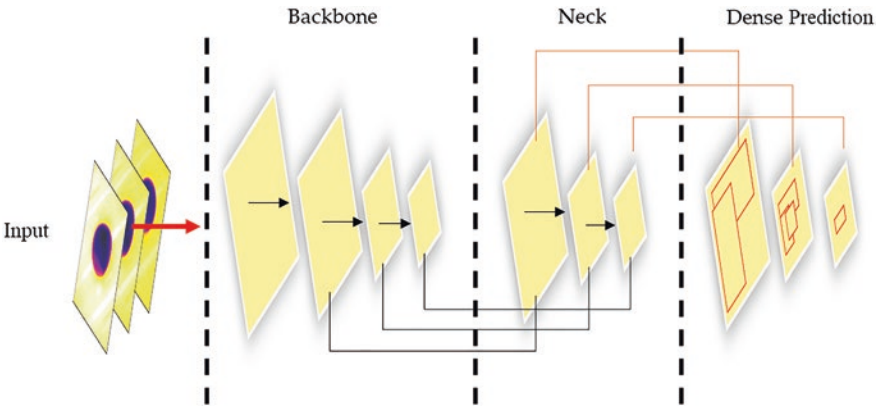

Fig. 28.5 One-stage detectors YOLO, and EfficientDet basic architecture for the thermal imagery-based datasets

Table 28.1 YOLOv5, YOLOv7, and EfficientDet deep learning object detection algorithms basic architecture comparison

Model	Backbone	Neck	Head	Loss function	Training framework
YOLOv5	CSPDarknet53	PANet Modified FPN	YOLO layer	Binary cross entropy and logits function	PyTorch
YOLOv7	E-ELAN	CSPSPP + (ELAN, E-ELAN) PAN	YOLOR	Binary cross entropy	PyTorch
EfficientDet	EfficientNet	BiFPN	Box prediction net	Focal loss	TensorFlow

shows a comparison between the object detection models and its basic architecture employed in this study.

EfficientDet was released by Google Research, LLC (Tan et al., 2020a). The main point of this algorithm is the light model, high accuracy, and multiscalability, which focus on efficiency when detecting small objects and the speed of detections aiming at low-end devices. EfficientDet uses the EfficientNet convolutional neural network on the backbone to extract the features related to the egg shape, color, and borders of air cells with maximum efficiency in terms of computation costs. The bidirectional feature pyramid network (BiFPN) on the neck part is an aggregator similar to PANnet for feature fusion except for some skipped connections between the pyramid network from the backbone, which also contributes to increasing the detection efficiency of our thermal features related to eggs. Finally, the box prediction network on the head is responsible for labeling the predicted class.

28.2.5.1 Data Labeling

The first group (174 eggs) was used to train the YOLO and EfficientDet algorithms, and the total data were 522 (from the 30th, 50th, and 60th days). We considered that after 30 days of storage, all eggs would not be fresh at all. Therefore, the model of nonfresh eggs could be well-represented according to this dataset. The 522 images were enlarged by augmentation techniques to extend the generalization and to better extract features during training. We adopted spatial, pixel, and cutmix augmentation techniques.

Spatial augmentation was performed by applying free rotation to the eggs. Pixel augmentation was performed due to monochrome transformation (black and white), and the cutmix was made manually by mounting 100 images in the composition of images (Fig. 28.6) from the other two thermal conditions described in Fig. 28.1a, b. Note that YOLOv4 has the mosaic, and the cutmix augmentation techniques already included in the backbone and detector parts of the algorithm as a "bag of freebies." Nevertheless, considering that we had only one object per image, when mounting similar objects that did not belong to our class of interest, we could have an honest model to detect difficult objects with more confidence.

28.2.5.2 Training Parameters

The total training dataset composed of 3610 images was split into two groups in a proportion of 70:30; thus, 2527 images were used for training, and 1083 were used for validation.

To train YOLO object detection, the data were labeled according to YOLO format using a self-designed program that could give the bounding box and label coordinates x, y, height, and width (Fig. 28.7). On the other hand, to train EfficientDet, the images were labeled using the open-source software LabelIMG, which gives bounding box coordinates in PASCAL VOC XML format.

To train the models, we used different frameworks. YOLOv5 and YOLOv7 are based on PyTorch, and EfficientDet is onboard TensorFlow.

EfficientDet was trained on a personal computer running Windows® 10™ 64 bits, with an Intel® Xeon™ E5-1607 processor, 32 GB of RAM, a NVIDIA® GTX 1650™ 4 GB GPU, Python version 3.8.5, CUDA 10.1, cuDNN 7.6.5, OpenCV 4.4.0., Tensor-Flow 2.3.1, and TensorFlow-GPU 2.3.1. We trained YOLOv5 and YOLOv7 in Google, LLC, Collab cloud environment with PyTorch 1.11.0 + cu102 and a 16 GB GPU Tesla T4.

Some hyperparameter values were different, such as the batch size and number of iterations (Table 28.2), as a consequence of different frameworks. However, as our intention was to evaluate only the detection accuracy, training performance was not considered in this study.

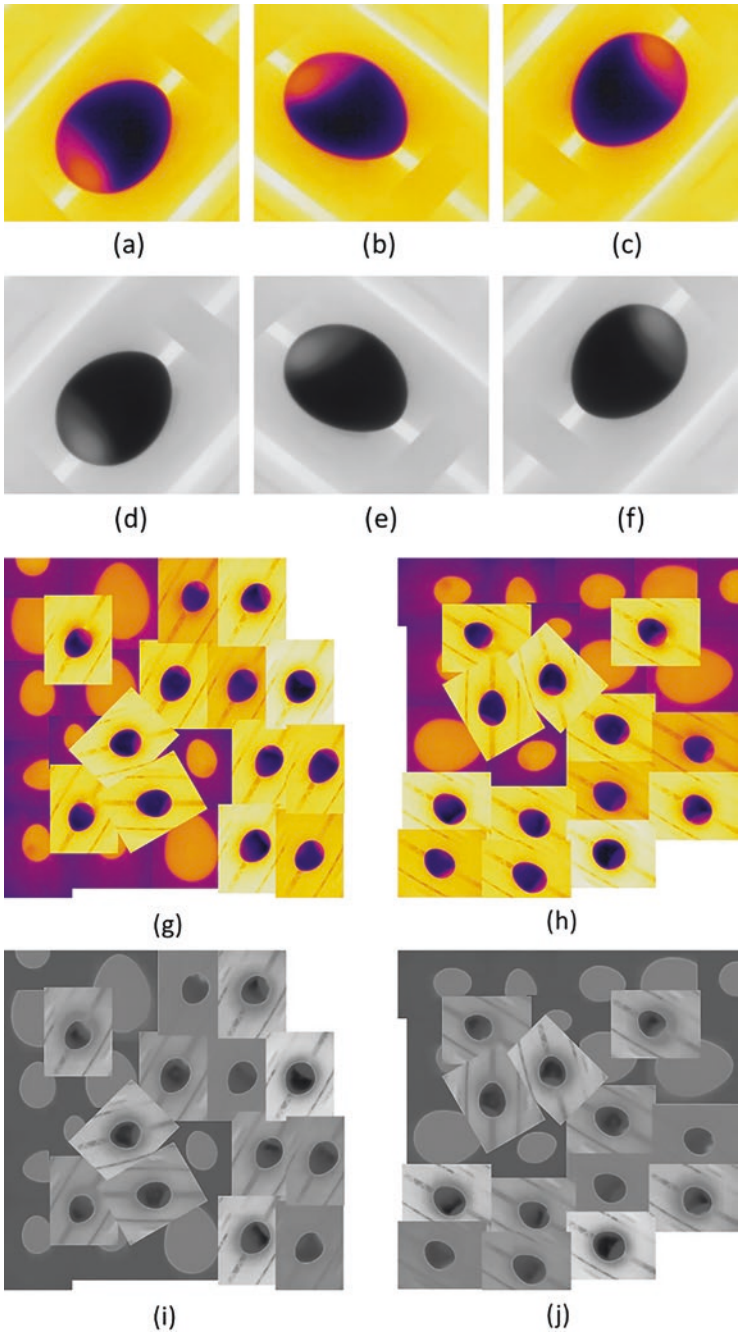

Fig. 28.6 (**a**) Original image. (**b**, **c**) Free rotations applied to the original image. (**d**–**f**) Monochrome transformation for pixel augmentation. (**g**) Cutmix original. (**h**) Cutmix + free rotation. (**i**, **j**) Cutmix + monochrome transformation + free rotation

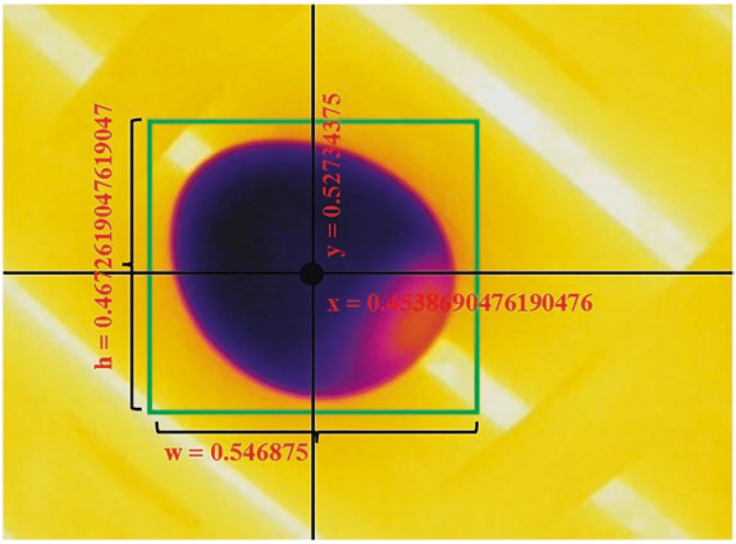

Fig. 28.7 Image labeling for YOLO format. The coordinates x and y represent the position of the center point of the object in relation to the figure in pixels. H and W are the sizes of the bounding boxes in pixels

Table 28.2 Training parameters for each object detection algorithm used in this work

Algorithm	Batch size	Input size	Momentum	Number of iterations
YOLOv5	16	640 × 640	0.937	30 epochs
YOLOv7	16	640 × 640	0.937	30 epochs
EfficientDet	4	512 × 512	0.899	30,000 steps

28.2.5.3 Evaluation Metrics

To validate the models and compare the results, we adopted the common metrics accepted and recognized by deep learning developers and the academy: the precision (P) is defined as the proportion of true-positive (TP) detections in relation to false-positive (FP) detections (Eq. (28.2)), the recall (R) is TP in relation to false-negative (FN) detections (Eq. (28.3)), and the F1 score (Eq. (28.4)) indicates the balance between precision and recall and is a good metric to compare the efficacy between models. The average precision (AP, Eq. (28.5)) and mAP@0.5 (Eq. (28.6)) are metrics adopted to evaluate the trained parameters of the models adopted by the PASCAL VOC challenge (Everingham et al., 2009).

$$P = \frac{TP}{TP + FP} \tag{28.2}$$

$$R = \frac{TP}{TP + FN} \tag{28.3}$$

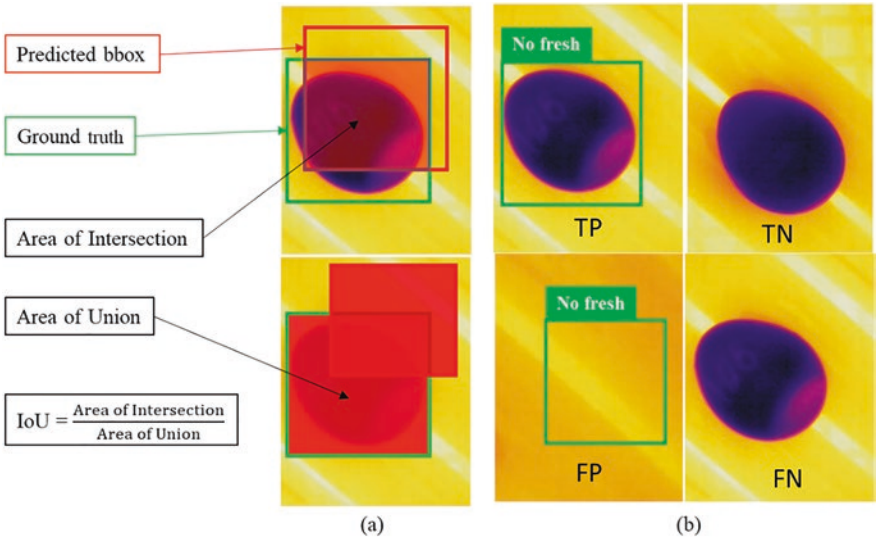

Fig. 28.8 (**a**) IoU demonstrates the relation between the area of intersection and the area of union. (**b**) TP represents correct object detection, TN represents the correct object nondetection, FP is a false detection, and FN is a false negative, representing the case when the object should have been detected but was not

$$\text{F1 score} = \frac{2PR}{P+R} \tag{28.4}$$

$$AP = \frac{1}{11}\sum_{R_i} PR_i \tag{28.5}$$

$$mAP = \frac{1}{N}\sum_{i=1}^{N} AP_i \tag{28.6}$$

It is important to note that concepts of true and false detections are determined according to the prediction bounding boxes (bbox) in relation to the reference label bbox, called the ground truth. The trueness is determined by setting the intersection over union (IoU), which calls for the proportion of a prediction in relation to the reference. Usually, the IoU is defined to be greater than 50% on the training setup (Fig. 28.8).

28.3 Results

28.3.1 Correlation Test

The thermal camera interprets the intensity of the infrared wavelength transmitted through the atmosphere. Cold eggs show different features according to the eggshell thickness and the conditions of the egg content, which may vary according to the

storage conditions and their chemical properties. We observed that the air cell of eggs was visible when the egg temperature contrasted room temperature; some examples of thermal images from eggs are shown in Fig. 28.9.

The size of the air cell was measured according to the methodology described in Sect. 28.2.4. The results were tabulated in Microsoft® Excel™ version 2209, and the statistics were calculated for the correlation test (Table 28.3). The variation in the air cell size occurred from the 1st day to the 10th day (Fig. 28.10); all eggs were affected by aging with no exceptions, as we could observe the weight loss. However, some eggs were affected more than others, which is probably related to the composition of the eggshell that could provide resistance to the loss of water and gases.

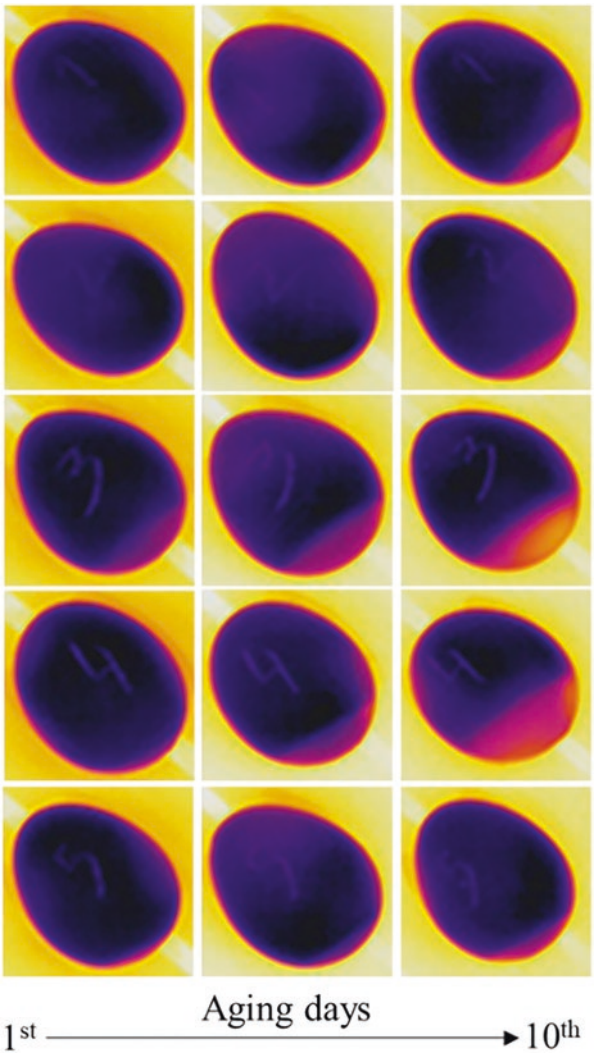

Fig. 28.9 The aging effects on eggs after 10 days of storage under accelerated aging conditions of 28 °C and 60% humidity

Table 28.3 Data exploration analysis for weight and air cell size of stored eggs

Metric	Height (mm)	1st day pixel length	10th day pixel length	Chamber area 1st day	Chamber area 10th day	Weight (g) 1st day	Weight (g) 10th day
Average	30.993	147.678	141.122	40.464	93.763	9.902	9.282
SD	1.306	16.963	18.897	32.071	59.454	0.930	0.968

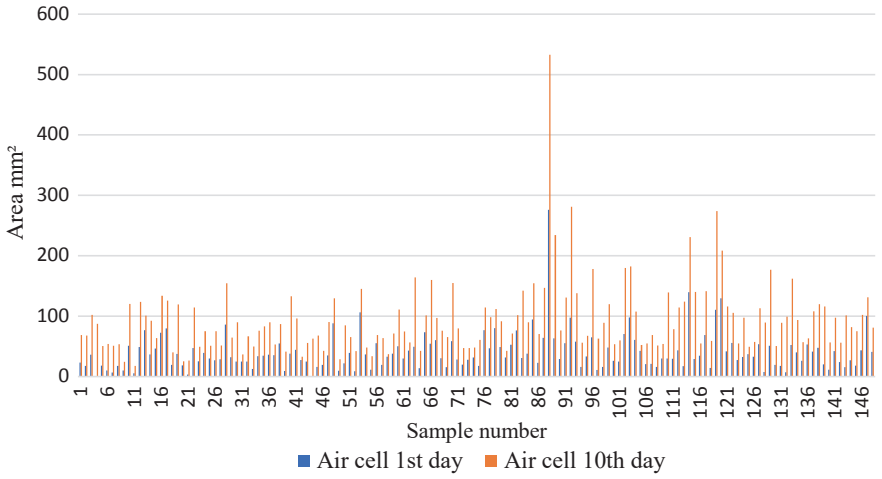

Fig. 28.10 The variation in the air cell size for each egg between the 1st day of storage and the 10th day under accelerated degradation conditions

Table 28.4 Statistical analysis for the Pearson correlation between the weight and air cell size

Weight difference (mean)	Pixel area difference (mean)	n observations	Degrees of freedom (n − 2)	T-statistic	Coefficient (r)	*p* Value
−0.620	53.300	148	146	17.47713	−0.82256	1.3×10^{-37}

The height was the real distance measured with a digital caliper, and the pixel length was the corresponding height distance in pixels provided by ImageJ software. We collected the pixel length for the 1st day and for the 10th day to ensure that any minimum modification on the position of eggs in relation to the camera did not interfere with the representative height in the images. The air cell area was determined by the program according to the reference length (pixel/mm) obtained from previous measurements.

The statistics show that the difference in the weight [(weight 10th day) − (weight 1st day)] and the pixel area [(pixel area at 10th day) − (pixel area at 1st day)] was correlated by a Pearson's test (Table 28.4).

The p value was very close to 0, which means we could reject the null hypothesis regarding the loss of weight which was not related to the enlargement of air cell size (Table 28.4). The alternative hypothesis was accepted in this case; in other words, a

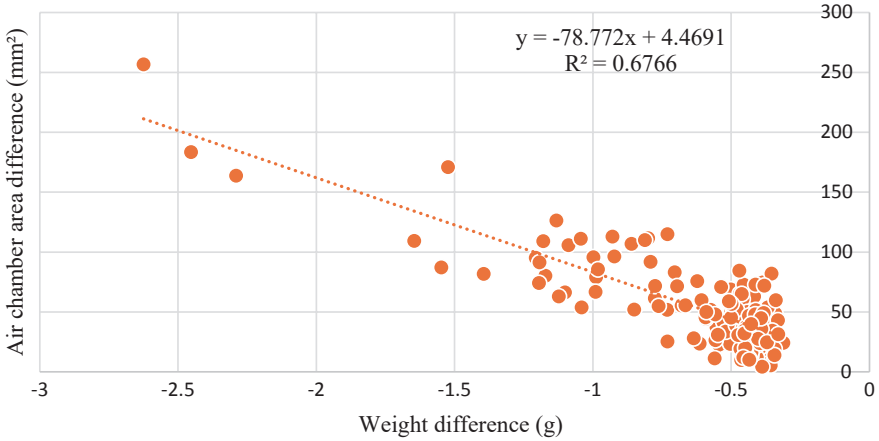

Fig. 28.11 Correlation test for weight difference and air cell area

change in the weight could explain the variation in the air cell size, and the chance of that occurring by chance was close to zero.

The difference in weight and size was plotted in the graph (Fig. 28.11). The average weight difference was 0.620 g over 10 days, which represents 6.26% of the average weight of fresh eggs. Quail eggs have different colors and pigmentation, making the detection of cracks and small fissures difficult to identify by human eyes. Some eggs that lost more weight than others may have been damaged at a location that was not identified before the experiment.

The graph shows that there was a negative correlation between the weight and size of air cells, with $R^2 = 0.6766$. Hence, a negative correlation was observed, and an inverse relation between the two variables was found, which means that when the variable weight decreased, the air cell size increased.

In addition to the statistical analysis, a visual assessment of the air cell features was provided from boiled eggs and corresponding thermal images. We noticed that the highlighted area on the thermal images corresponds to the cavity in the photo (Fig. 28.12). The thermal images that did not show air cell features from the radiometric picture also did not show orifices in the boiled egg.

28.3.2 Computer Vision Model Prediction

28.3.2.1 Training Results

As mentioned in Sect. 28.2.5.2, YOLOv5 was trained in the PyTorch framework in the Google LLC Colab environment for approximately 1 h. The evaluation of PyTorch models is given in the Tensorboard™ application (Fig. 28.13); such a tool was also used for the evaluation of EfficientDet. Different from the Darknet framework, the Tensorboard data report was more detailed and easier to understand.

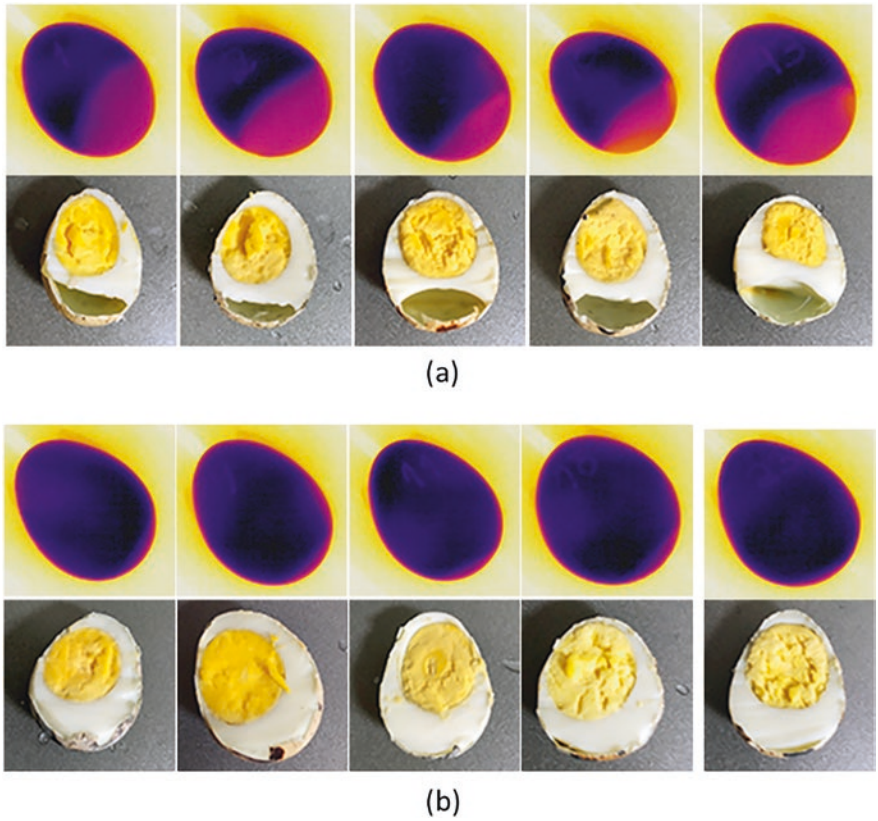

Fig. 28.12 Egg assessment by boiling eggs and the corresponding thermal picture. (**a**) Nonfresh eggs present a large air cell. (**b**) Still fresh eggs show no chamber or reduced size compared to nonfresh eggs

YOLOv5 was trained for 30 epochs. However, when looking at the evaluation graphs, it was observed that after 25 epochs of training, the object loss reached a satisfactory value as a learning parameter, which was close to the minimum accuracy cost of the model as a supervised learning algorithm. In addition, when compared to the metric precision, the mAP could be considered stable after 25 epochs, with minimum improvements from visual analysis. Therefore, the model was trained more than enough epochs to reach the best results for the model. YOLOv7 was also trained on the cloud-based framework Google Collab. The training results are shown in Fig. 28.14.

Our third model, despite being part of the one-stage detector class, had a different architecture compared to the YOLO models. A notable difference was observed in the standard network size, which was higher (512 × 512), and was accomplished for the efficient detection of small objects for the purpose of scalable models.

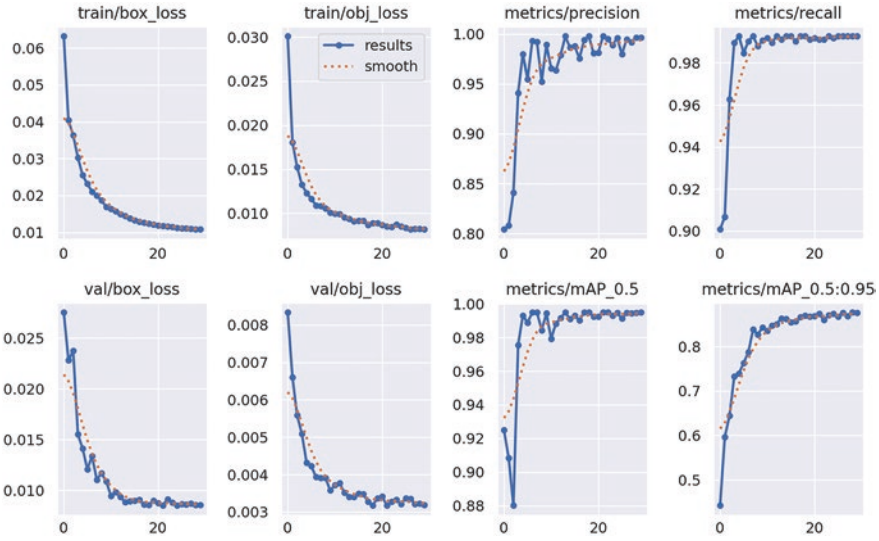

Fig. 28.13 Training results from YOLOv5

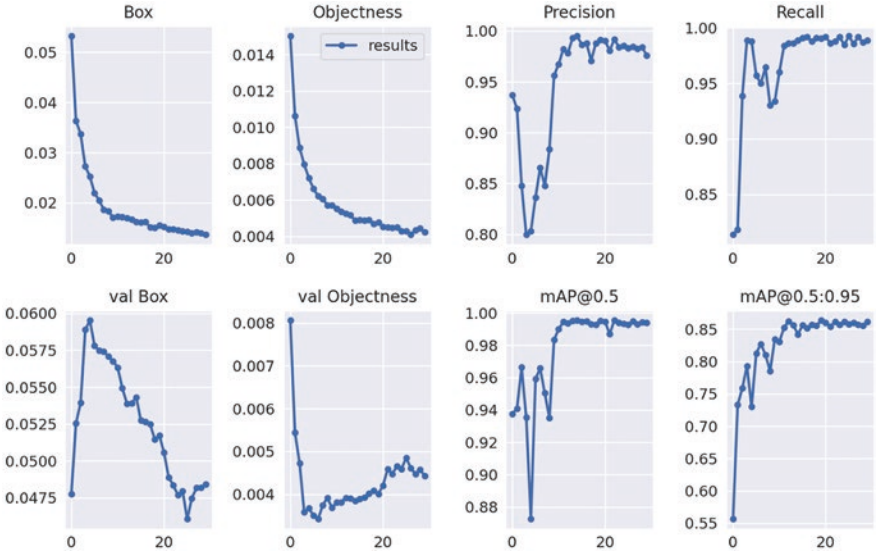

Fig. 28.14 YOLOv7 training results after 30 epochs

The training total loss (Fig. 28.15) did not reduce considerably after 6000 steps, which means the training could be shorter than 30,000 steps, repeating the same results from the previous models (YOLOv5 and YOLOv7).

The precision and accuracy of each model (YOLOv5, YOLOv7, and EfficientDet) were not compromised by the training steps, and all models were trained for more

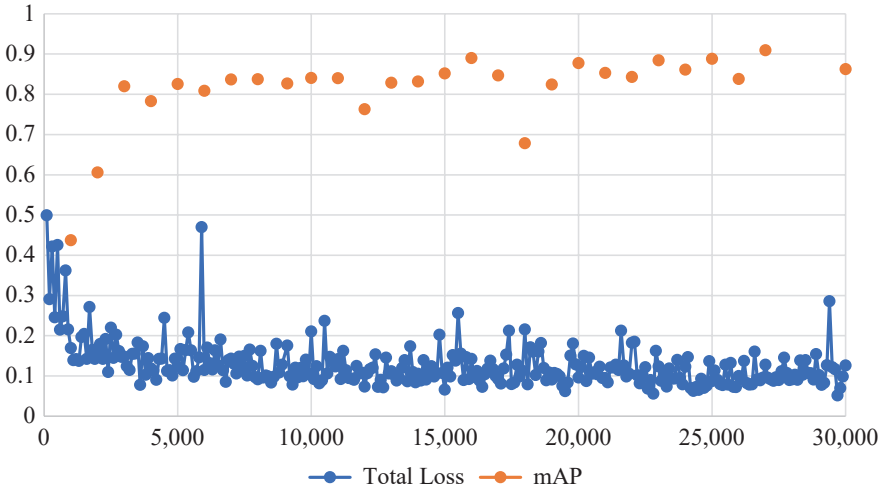

Fig. 28.15 Training progress of EfficientDet during 30,000 steps and the mAP@0.50

Table 28.5 Evaluation of object detection models for IoU 0.5

Model	Precision (P)	Recall (R)	F1 score	mAP@0.50
YOLOv5	0.99	0.99	0.99	99.5%
YOLOv7	0.97	0.98	0.97	99.4%
EfficientDet	0.95	0.73	0.82	95.0%

time than was necessary to achieve mAP stability, which was the main parameter to evaluate the accuracy of the models (Table 28.5).

To test the models, the testing samples were grouped with all 60 quail eggs. The assessment of the results was performed by calculating the metrics of Eqs. (28.2)–(28.4) as given in Sect. 28.2.5.3. The accuracy assessment of the thermal images was made by boiling the eggs and cutting the longitudinal axis manually (Fig. 28.12). The eggs with no or minimum air cells were considered fresh, the original image (Fig. 28.16a) was used to test the YOLOv5, YOLOv7, and EfficientDet object detection models (Fig. 28.16b–d).

The accuracy assessment of the eggs (longitudinal cutting of boiled eggs represented in the Fig. 28.12) corresponded to the "correct answers" of a supervised learning algorithm and served as the main reference parameter for the calculation of the metrics' precision, recall, and F1 score. In our dataset, 22 eggs were found to be still fresh, which corresponded to the true-negative (TN) detections (eggs that must not be detected as "nonfresh eggs").

In Fig. 28.16a, we referred to the original testing image where the eggs were kept in numerical order from 1 to 60 (from top left to bottom right) to test the object detection models' accuracy on it. In Fig. 28.16b–d, each bounding box (bbox) showed its detection score on the top right of the bbox under 25% threshold for all models.

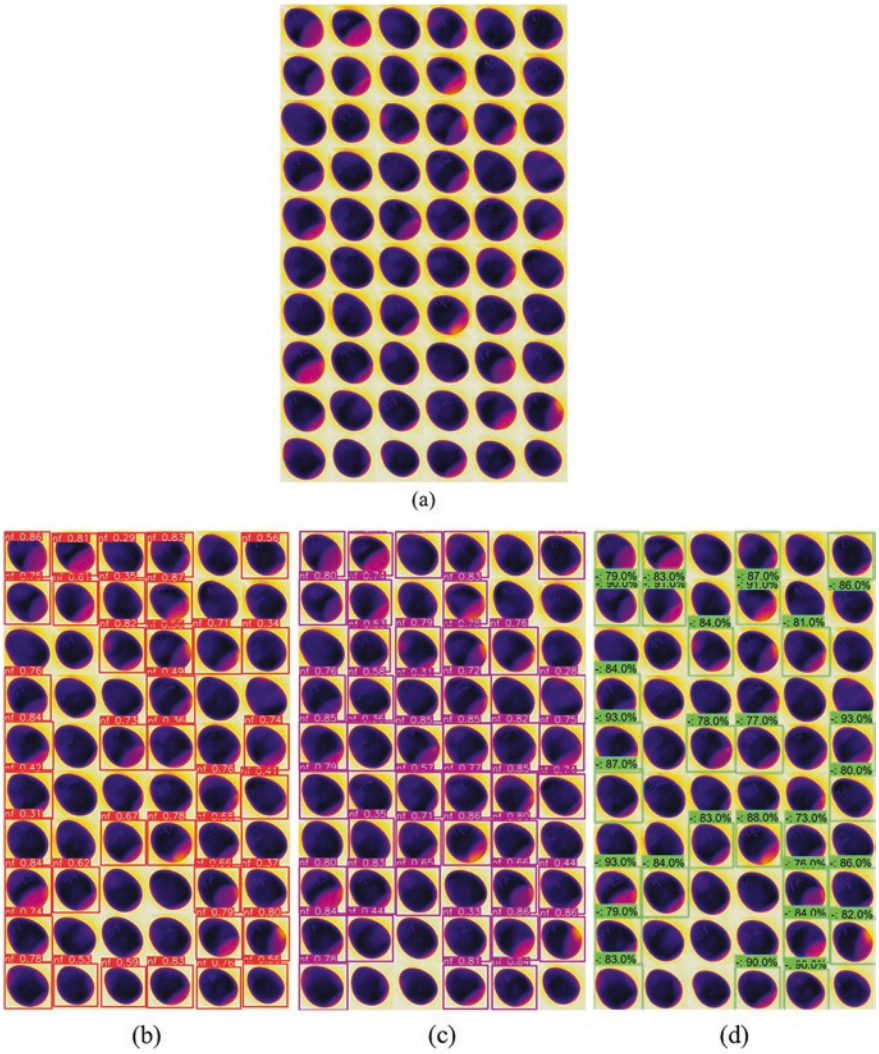

Fig. 28.16 (**a**) The original images of 60 eggs were used to test the deep learning object detection models. (**b**–**d**) YOLOv5, YOLOv7, and EfficientDet models applied to the original testing dataset

EfficientDet testing results are shown in Fig. 28.16d. The minimum confidence score was 0.73 (73%), that was the best result compared to the other two models regarding the confidence score of the bbox. However, it was expected for the scalable model (designed to detect objects from low to high resolution images) and did not affect the final purpose of our investigation, which was based on the accuracy of nonfresh egg detection only.

The output predictions of the testing dataset (Table 28.6) were organized, and the metric calculations were computed.

Table 28.6 Testing dataset metrics for accuracy performance evaluation

Model	Total bbox	True-positive (TP)	True-negative (TN)	False-positive (FP)	False-negative (FN)
YOLOv5	39	33	22	6	5
YOLOv7	44	37	22	7	1
EfficientDet	29	29	22	0	9

Table 28.7 Testing dataset accuracy evaluation with no threshold for YOLOv4 and threshold 0.5 for YOLOv5 and EfficientDet

Model	Precision (P)	Recall (R)	F1 score
YOLOv5	0.85	0.87	0.86
YOLOv7	0.84	0.97	0.90
EfficientDet	1	0.76	0.86

The total bbox in Table 28.6 is the total number of detections for each model employed in this study; the true positive stands for the amount of bboxes that correspond to nonfresh egg detections, in this case all bboxes for all models were correctly assigned to the class nonfresh; the true negatives were those eggs that must not be detected as they correspond to still fresh eggs. The false-positive column calls for still fresh eggs wrongly classified as nonfresh eggs (no eggs were falsely classified for all three models); and, finally, the false-negative column stands for the number of eggs that were supposed to be detected as nonfresh but were not. According to Table 28.5, we could calculate the precision, recall, and F1 score (Table 28.7).

From the testing dataset, the precision metric (Eq. 28.2) for all three models was 1% or 100% for the EfficientDet model, which means that all detections were correctly assigned for the class not fresh. YOLOv5 and YOLOv7 were less precise, which means the models included in detections still fresh eggs as the nonfresh class. The metric recall (Eq. 28.3) described the relation between the correct detections (TP) and undetected eggs that should be detected (FN). The recall was higher for YOLOv7; in this case, we said that this model was responsible for detecting a greater quantity of nonfresh eggs properly (fewer false-negative detections). For the F1 score (Eq. 28.4), this metric stood as the balance for precision and recall and could be understood as an equivalent metric for the mAP. As we did not label the testing dataset, the mAP could not be estimated in the frameworks; in this case, the F1 score was responsible for informing on which model performed better. YOLOv7 outperformed the other two (Fig. 28.17), as well as the validation dataset.

28.3.2.2 Revalidation of the Expiration Date

From the results of the DL prediction, we could calculate the revalidation proportion of the eggs 15 days after the labeled expiration date (Table 28.8). The revalidation was done considering the difference of total detections (total bbox) as "not

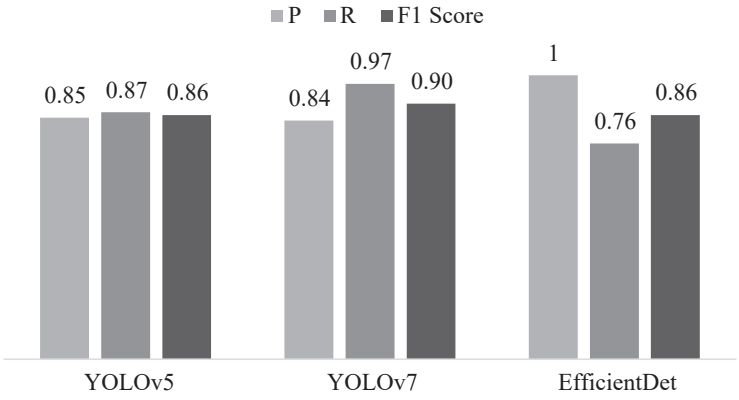

Fig. 28.17 Results from the calculation of metrics to evaluate the testing dataset

Table 28.8 Revalidation amount according to DL object detection algorithms

Model	Total eggs	Not fresh (bbox)	DL fresh (TN + FN)	True-negative (TN)	DL revalidation	True revalidation	Revalidation error
YOLOv5	60	39	27	22	45.00%	36.67%	8.33%
YOLOv7	60	44	23	22	38.33%	36.67%	1.67%
EfficientDet	60	29	31	22	51.67%	36.67%	15.00%

fresh" (YOLOv4, YOLOv5, and EfficientDet) from the total amount of eggs (60). Therefore, the deep learning (DL) revalidation was given by {(TN + FN)/Total eggs] × 100}, and the true revalidation was defined as [(TN/Total eggs) × 100]. The revalidation error was determined by [(DL revalidation − True Revalidation)].

28.4 Discussion

In this work, we used a thermal camera and proposed a new methodology to detect the freshness of eggs according to the air cell size. Thermal cameras can interpret the intensity of infrared wavelengths transmitted through the atmosphere. Hence, considering that CO2 is heavier than atmospheric air (at the same temperature and pressure), when contrasting distinct temperatures of cold eggs and warm room temperature, the CO2, and the composition of other gases in the air cell produce a spectral signature transmitted from the eggs that can be detected by the radiometric sensors of the thermal cameras. We called this method the "thermal imaging contrast technique." When using this method, the identification of the air cell was easy, fast, and approachable to identify stale and not fresh eggs. Therefore, this method can be used in real time for high-throughput applications at the industrial level, especially when combined with deep learning object detection algorithms in automated systems, as demonstrated in this work.

During this study, the pH of the albumen or the yolk was not measured during the storage period. However, the literature shows that for hen eggs, the pH of the albumen may increase slightly more than the yolk pH (Tan et al., 2020a, b), and this modification can be reduced under controlled atmospheric systems by injecting CO2 into the storage room (Reijrink et al., 2010). Additional factors can also contribute to potentializing the chemical transformations of the albumen and yolk, such as genotype, quail feed composition, diseases, age of parental flock, and environmental conditions.

Methods able to perform real time and nondestructive analysis can contribute to the development of quail industry farming and the postharvesting process to keep the quality and safety for the consumers. In this study, it was noticed that some eggs from the same groups were less fresh than others. From this observation, we can presume that eggs collected from the same quail may vary in eggshell composition, such as thickness and hardness.

In the correlation test, we observed that the standard deviation of real measurements and the pixel measurements were very different in magnitude because the pixel measurements were relative to the manual line tracing on marked points, which means that the line traced between two points may change the length of pixels when connecting the line to the top and bottom points of the eggs. Nevertheless, we traced a line three times and used the mean to define our pixel length; consequently, the error was reduced for our measurements.

For the second part of our study, by using deep learning object detection, the prediction of not fresh quail eggs with high accuracy was possible. When comparing the three models, the best results were obtained from YOLOv7, followed by YOLOv5 and EfficientDet. Deep learning-based models for image recognition and localization are being upgraded continuously as the demand for applications for this tool increases in many sectors of our daily lives.

The comparison between deep learning algorithms has demonstrated that improvements on object detection algorithms can reduce the error of reclassification of nonfresh eggs. However, as thermal cameras have low resolution, further improvements on thermal sensing can also enhance the efficiency and accuracy of deep learning-based computer vision systems; therefore, the tradeoff between equipment and algorithms should be considered as a drawback.

While training the deep learning models, some parameters can influence the speed and accuracy of the model, and the most important parameter is the network size. The network size of YOLOv5 and YOLOv7 was set to 640 × 640 pixels because these models use the same architecture; however, the batch size was different due to the dependence on hardware resources, especially processing power (GPU). For EfficientDet, the minimum network size was 512 × 512 due to the scalable feature architecture, and the batch size was reliable for TensorFlow™ processing. It is important to note that different network sizes can produce different results, therefore a full comparison among models and various pretrained models is relevant when selecting the best model to implement the developed system.

28.5 Conclusions

The air cell is one of the most important parameters to qualify the freshness of eggs. The thermal camera was able to interpret the infrared wavelength intensities transmitted through the atmosphere from the eggshell pores and then, by the contrast technique, highlight the portion where the gases were accumulated on the large base of the eggs as a consequence of the storage period. As the aging process affects the size of the air cell, the lack of freshness was correlated with the air cell size ($R^2 = 0.676$). The combination of thermal camera imagery and deep learning object detection algorithms could identify nonfresh quail eggs with high accuracy; besides that, our investigation has demonstrated their potential to compose automatic systems for freshness assessment at industry and civil levels. We tested our model on the eggs after the expiration date, the YOLOv5, YOLOv7, and EfficientDet models could detect nonfresh eggs with an F1 score of 0.86, 0.90, and 0.86, respectively. The best model (YOLOv7) demonstrated that 38.33% of eggs could have their labeled date extended at least 15 days, with an error rate of 1.67%. YOLOv5 and EfficientDet showed reclassification proportions of 45.00% and 51.67% and an error rate of 8.33% and 15%, respectively.

The developed methodology was reported as a fast and nondestructive way to assess the freshness of quail eggs according to the detection of air cell size; the methodology itself can be extended for industrial applications, supermarkets, and restaurants to relabel eggs for extended consumption periods and minimize the postharvest poultry production losses.

The main limitation of the methodology developed is regarding how long the expiry date could be extended for. In this regard, further studies should be addressed including the assessment of eggshell thickness for prediction of ideal shelf-life of quail eggs and other avian eggs as well.

Acknowledgments The authors would like to appreciate the Open Access Publishers Land from MDPI to have their policy to support the authors for reusing of the published article. In this regard, we would like to extend our gratitude to Sensors Journal for publishing this article (Victor Massaki Nakaguchi and Tofael Ahamed. Fast and Nondestructive Quail Egg Freshness Assessment Using a Thermal Camera and Deep Learning-Based Air Cell Detection Algorithms for the Revalidation of the Expiration Date of Eggs. Sensors 2022, 22, 7703. https://doi.org/10.3390/s22207703). Some modifications have been made in this book chapter to add new analysis for comparison of DLs.

Conflicts of InterestThe authors declare no conflicts of interest.

References

Aboonajmi, M., Setarehdan, S., Akram, A., Nishizu, T., & Kondo, N. (2014). Prediction of poultry egg freshness using ultrasound. *International Journal of Food Properties, 17*, 1889–1899.

Ahmad, H. M., & Rahimi, A. (2022). Deep learning methods for object detection in smart manufacturing: A survey. *Journal of Manufacturing Systems, 64*, 181–196. https://doi.org/10.1016/j.jmsy.2022.06.011

Alexey, B., Wang, C.-Y., & Liao, H.-Y. M. (2020). Yolov4: Optimal speed and accuracy of object detection. *arXiv*. arXiv:2004.10934.

Benyam, A. A., Soma, T., & Fraser, E. (2021). Digital agricultural technologies for food loss and waste prevention and reduction: Global trends, adoption opportunities and barriers. *Journal of Cleaner Production, 323*, 129099. https://doi.org/10.1016/j.jclepro.2021.129099

BRASIL Ministério da Agricultura, Pecuária e Abastecimento. (1990). *Portaria n° 1, de 21 de Fevereiro de*. BRASIL Ministério da Agricultura, Pecuária e Abastecimento. Available https://www.gov.br/agricultura/pt-br/assuntos/inspecao/produtos-animal/empresario/arquivos/Portaria11990ovos.pdf/view. Accessed 17 July 2022.

Brasil, Y. L., Cruz-Tirado, J., & Barbin, D. F. (2022). Fast online estimation of quail eggs freshness using portable NIR spectrometer and machine learning. *Food Control, 131*, 108418. https://doi.org/10.1016/j.foodcont.2021.108418

Burley, R. W. (1989). The albumen: Chemistry. In *The avian egg: Chemistry and biology* (pp. 65–128). Wiley-Interscience.

Cattaneo, P., Balzaretti, C., Quaglia, F., & Di Giancamillo, M. (1997). Valutazione della freschezza delle uova in guscio con metodi chimici e fisici. *Ing Aliment Conserve Anim, 13*, 9–20.

Chen, C., Liang, Y., Zhou, l., Tang, X., & Dai, M. (2022). An automatic inspection system for pest detection in granaries using YOLOv4. *Computers and Electronics in Agriculture, 201*, 107302. https://doi.org/10.1016/j.compag.2022.107302

Dong, X., Dong, J., Peng, Y., & Tang, X. (2017). Comparative study of albumen pH and whole egg pH for the evaluation of egg freshness. *Spectroscopy Letters, 50*, 463–469.

Dutta, R., Hines, E. L., Gardner, J. W., Udrea, D. D., & Boilot, P. (2003). Non-destructive egg freshness determination; an electronic nose-based approach. *Measurement Science and Technology, 14*, 190–198.

EC. Commission Regulation No. 2295/2003 of December 2003 Introducing detailed rules for implementing Council Regulation (EEC) No 1907/90 on certain marketing standards for eggs (Official Journal of the European Union L 340 of December 2003). EC.

Everingham, M., Van Gool, L., Williams, C. K. I., Winn, J., & Zisserman, A. (2009). The Pascal Visual Object Classes (VOC) challenge. *International Journal of Computer Vision, 88*, 303–338.

Fan, S., Liang, X., Huang, W., Zhang, V. J., Pang, Q., He, X., Li, L., & Zhang, C. (2022). Real-time defects detection for apple sorting using NIR cameras with pruning based YOLOV4 network. *Computers and Electronics in Agriculture, 193*, 106715. https://doi.org/10.1016/j.compag.2022.106715

Gai, R., Chen, N., & Yuan, H. (2021). A detection algorithm for cherry fruits based on the improved YOLO-v4 model. *Neural Computing and Applications, 35*, 13895. https://doi.org/10.1007/s00521-021-06029-z

Girshick, R., & Fast, R.-C. N. N. (2015). *Proceedings of the IEEE international conference on computer vision (ICCV)* (pp. 1440–1448). IEEE.

Girshick, R., Donahue, J., Darrell, T., & Malik, J. (2014). Rich feature hierarchies for accurate object detection and semantic segmentation. In *Proceedings of the IEEE conference on computer vision and pattern recognition (CVPR)* (pp. 580–587), Columbus.

Giunchi, A., Berardinelli, A., Ragni, L., Fabbri, A., & Silaghi, F. A. (2008). Non-destructive freshness assessment of shell eggs using FT-NIR spectroscopy. *Journal of Food Engineering, 89*, 142–148. https://doi.org/10.1016/j.jfoodeng.2008.04.013

Gupta, A., Anpalagan, A., Guan, L., & Khwaja, A. S. (2021). Deep learning for object detection and scene perception in self-driving cars: Survey, challenges, and open issues. *Array, 10*, 100057. https://doi.org/10.1016/j.array.2021.100057

Harnsoongnoen, S., & Jaroensuk, N. (2021). The grades and freshness assessment of eggs based on density detection using machine vision and weighing sensor. *Scientific Reports, 11*, 16640. https://doi.org/10.1038/s41598-021-96140-x

Haugh, R. R. (1937). The Haugh unit for measuring egg quality. *U.S. Egg and Poultry Magazine, 43*, 522–555.

Jiang, S., Zhu, T., Jia, D., Yao, J., & Jiang, Y. (2018). Effect of egg freshness on their automatic orientation. *Journal of the Science of Food and Agriculture, 98*, 2642–2650.

Jiang, P., Ergu, D., Liu, F., Cai, Y., & Ma, B. A. (2022). Review of Yolo algorithm developments. *Procedia Computer Science*. ISSN 1877-0509., *199*, 1066–1073. https://doi.org/10.1016/j.procs.2022.01.135

Karaoguz, H., & Jensfelt, P. (2019). Object detection approach for robot grasp detection. In *Proceedings of the IEEE international conference on robotics and automation (ICRA)* (pp. 4953–4959), Montreal.

Karoui, R., Kemps, B., Bamelis, F., De Ketelaere, B., Decuypere, E., & De Baerdemaeker, J. (2006). Methods to evaluate egg freshness in research and industry: A review. *European Food Research and Technology, 222*, 727–732. https://doi.org/10.1007/s00217-005-0145-4

Kumbár, V., Trnka, J., Nedomová, S., & Buchar, J. (2015). On the influence of storage duration on rheological properties of liquid egg products and response of eggs to impact loading–Japanese quail eggs. *Journal of Food Engineering, 166*, 86–94.

Kuznetsova, A., Maleva, T., & Soloviev, V. (2021). YOLOv5 versus YOLOv3 for apple detection. In A. G. Kravets, A. A. Bolshakov, & M. Shcherbakov (Eds.), *Cyber-physical systems: Modelling and intelligent control. Studies in systems, decision and control* (Vol. 338, pp. 349–358). Springer.

Lawal, M. O. (2021). Tomato detection based on modified YOLOv3 framework. *Scientific Reports, 11*, 1447.

Li, B., Ouyang, W., Sheng, L., Zeng, X., & Wang, X. (2019). GS3D: An efficient 3d object detection framework for autonomous driving. In *Proceedings of the IEEE/CVF conference on computer vision and pattern recognition (CVPR)* (pp. 1019–1028), Long Beach

Lin, T. Y., Dollár, P., Girshick, R., He, K., Hariharan, B., & Belongie, S. (2017a). Feature pyramid networks for object detection. In *Proceedings of the IEEE conference on computer vision and pattern recognition* (pp. 2117–2125), Honolulu. Available https://arxiv.org/abs/1612.03144v2. Accessed 12 Aug 2022.

Lin, T.-Y., Goyal, P., Girshick, R., He, K., & Dollar, P. (2017b). Focal loss for dense object detection. In *Proceedings of the IEEE international conference on computer vision (ICCV)* (pp. 2980–2988), Venice.

Liu, M., Pan, L. Q., Tu, K., & Liu, P. (2010). Determination of egg freshness during shelf life with electronic nose. Nongye Gongcheng Xuebao/Trans. *Chin Soc Agric Eng, 26*, 317–321.

Liu, W., Anguelov, D., Erhan, D., Szegedy, C., Reed, S., Fu, C.-Y., & Berg, A. C. (2016). SSD: Single shot multibox detector. In *Proceedings of the European conference on computer vision (ECCV)* (pp. 21–37), Amsterdam.

Liu, S., Qi, L., Qin, H., Shi, J., & Jia, J. (2018). Path aggregation network for instance segmentation. In *Proceedings of the IEEE conference on computer vision and pattern recognition* (pp. 8759–8768), Salt Lake City. Available https://arxiv.org/abs/1803.01534v4. Accessed 13 Aug 2022.

Liu, Y., Ren, X., Yu, H., Cheng, Y., Guo, Y., Yao, W., & Xie, Y. (2020). Non-destructive and online egg freshness assessment from the eggshell based on Raman spectroscopy. *Food Control, 118*, 107426. https://doi.org/10.1016/j.foodcont.2020.107426

Meituan. YOLOv6. (2022). Available https://github.com/meituan/YOLOv6. Accessed 12 Aug 2022

Nakaguchi, V. M., & Ahamed, T. (2022). Development of an early embryo detection methodology for quail eggs using a thermal micro camera and the YOLO deep learning algorithm. *Sensors, 22*, 5820. https://doi.org/10.3390/s22155820

Paszke, A., Gross, S., Massa, F., Lerer, A., Bradbury, J., Chanan, G., Killeen, T., Lin, Z., Gimelshein, N., Antiga, L., et al. (2019). PyTorch: An imperative style, high-performance deep learning library. In *Advances in neural information processing systems 32* (pp. 8024–8035). Curran Associates, Inc.. Available http://papers.neurips.cc/paper/9015-pytorch-an-imperative-style-high-performance-deep-learning-library.pdf. Accessed 12 Aug 2022.

Qi, J., Liu, X., Liu, K., Xu, F., Guo, H., Tian, X., Li, M., Bao, Z., & Li, Y. (2022). An improved YOLOv5 model based on visual attention mechanism: Application to recognition of tomato

virus disease. *Computers and Electronics in Agriculture, 194*, 106780. https://doi.org/10.1016/j.compag.2022.106780

Quattrocchi, A., Freni, F., Montanini, R., Turrisi, S., & Zappa, E. (2022). Development, validation and preliminary experiments of a measuring technique for eggs aging estimation based on pulse phase thermography. *Sensors, 22*, 3496. https://doi.org/10.3390/s22093496

Rasband, W. S. (1997–2018). *ImageJ*, U.S. National Institutes of Health, Bethesda. Available https://imagej.nih.gov/ij/. Accessed 20 July 2022

Redmon, J., & Farhadi, A. (2017). YOLO9000: Better, faster, stronger. In *Proceedings of the IEEE conference on computer vision and pattern recognition*, Honolulu.

Redmon, J., & Farhadi, A. (2018). Yolov3: An incremental improvement. *arXiv*. arXiv: 1804.02767.

Redmon, J., Divvala, S., Girshick, R., & Farhadi, A. (2016). You only look once: Unified, real-time object detection. In *Proceedings of the IEEE/CVF conference on computer vision and pattern recognition (CVPR)* (pp. 779–788), Las Vegas.

Reijrink, I. A. M., van Duijvendijk, L. A. G., Meijerhof, R., Kemp, B., & Brand, H. V. D. (2010). Influence of air composition during egg storage on egg characteristics, embryonic development, hatchability, and chick quality. *Poultry Science, 89*, 1992–2000. https://doi.org/10.3382/ps.2009-00610

Ren, S., He, K., Girshick, R., & Sun, J. (2015). Faster R-CNN: Towards real-time object detection with region proposal networks. In *Proceedings of the advances in neural information processing systems (NIPS)* (pp. 91–99), Montreal.

Romanoff, A. L., & Romanoff, A. J. (1949). Physicochemical properties. In *The avian egg*. Wiley..

Rotz, S., Gravely, E., Mosby, I., Duncan, E., Finnis, E., Horgan, M., LeBlanc, J., Martin, R., Neufeld, H. T., Nixon, A., et al. (2019). Au-tomated pastures and the digital divide: How agricultural technologies are shaping labour and rural communities. *Journal of Rural Studies, 68*, 112–122. https://doi.org/10.1016/j.jrurstud.2019.01.023

Schmilovitch, Z., Hoffman, A., Egozi, H., & Klein, E. (2002). Determination of egg freshness by NNIR spectroscopy. In *Proceeding of the AgEn conference*, Budapest. Paper number 02-AP-023.

Stadelman, W. J., Newkirk, D., & Newby, L. (2017). *Egg science and technology*. CRC Press.

Tan, M., Pang, R., & Le, Q. V. (2020a). EfficientDet: Scalable and efficient object detection. In *Proceedings of the IEEE/CVF conference on computer vision and pattern recognition*, Seattle.

Tan, W., Zhang, Q., Yang, L., Tian, L., Jia, J., Lu, M., Liu, X., & Duan, X. (2020b). Actual time determination of egg freshness: A centroid rate-based approach. *Food Packaging and Shelf Life, 26*, 100574. https://doi.org/10.1016/j.fpsl.2020.100574

Tsarenko, P. P., & Karaseva, Z. H. (1986). Ways of improving egg quality. *Poultry Abstract, 12*, 129.

Ultralytics. YOLOv5. (2021). Available https://github.com/ultralytics/yolov5. Accessed 12 Aug 2022

Upesh, N., & Hossein, E. (2022). Comparing YOLOv3, YOLOv4 and YOLOv5 for autonomous landing spot detection in faulty UAVs. *Sensors, 22*, 464. https://doi.org/10.3390/s22020464

Wang, C.-Y., Bochkovskiy, A., & Liao, H.-Y. M. (2022). YOLOv7: Trainable bag-of-freebies sets new state-of-the-art for real-time object detectors. *arXiv*. arXiv:2207.02696.

Xiang, X., Wang, Y., Yu, Z., Ma, M., Zhu, Z., & Jin, Y. (2019). Non-destructive characterization of egg odor and fertilization status by SPME/GC-MS coupled with electronic nose. *Journal of the Science of Food and Agriculture, 99*, 3264–3275.

Zhang, Y., Sun, P., Jiang, Y., Yu, D., Yuan, Z., Luo, P., Liu, W., & Wang, X. (2021). BYTETrack: Multi-object tracking by associating every detection box. *arXiv*. arXiv:2110.06864.

Zhao, Z.-Q., Zheng, P., Xu, S.-T., & Wu, X. (2019). Object detection with deep learning: A review. *IEEE Transactions on Neural Networks and Learning Systems, 30*, 3212–3232. https://doi.org/10.1109/TNNLS.2018.2876865

Chapter 29
AI × IoT: Increasing Agricultural Productivity of Crops, Orchards, and Livestock Management Using Smart Agricultural Space for Achieving SDGs

Abstract This concluding chapter discusses the development of sensors and sensing technologies within the advancements of the Internet of Things (IoT) and artificial intelligence (AI) to achieve the aims of the sustainable development goals (SDGs) resulting from the outcomes detailed in the previous chapters. Concerning the SDGs, several chapters have also reported on increasing productivity, addressing labor shortages in farming, and optimizing land use planning and water usage in arid lands for climate-smart agriculture. Furthermore, AI × IoT domains in agriculture include robotic research for ultra-labor savings and outdoor and indoor smart farm operations. These four domains can increase agricultural productivity to achieve the SDGs and Society 5.0. Finally, the book's contents concisely highlight the application of machine learning and deep learning from preharvest to postharvest levels for infield and in-house agricultural production systems, intelligent automation in fruit crops, and evaluation of postharvest efficiency for crops, orchards, livestock, aquaculture, and poultry production.

29.1 Introduction

Smart agricultural space and development have been discussed with an emphasis on ultra-saving labor strategies using artificial intelligence (AI)-based technologies to increase productivity and the timeliness of operation to ensure food security. Changing climate conditions necessitate a smart agricultural system that includes both outdoor systems and energy-efficient indoor practices. To address the challenges of energy efficiency, a transboundary approach, as well as AI and big data for bioinformatics, is needed to increase timeliness, supplement labor shortages, and ensure the safety of intangible labor migration systems. Ultimately, these efforts contribute to achieving one of the sustainable development goals (SDGs) to guarantee food production for approximately 9 billion people by 2050 (Society 5.0 and SDG 1 &2). Worldwide labor shortages in the agricultural sectors are increasing due to migration to urban areas, which may offer relatively more lucrative jobs for the younger population. This has caused a high inflow of labor into urban areas.

© The Author(s), under exclusive license to Springer Nature Singapore Pte Ltd. 2024

T. Ahamed, *IoT and AI in Agriculture*,
https://doi.org/10.1007/978-981-97-1263-2_29

29.2 Smart Outdoor Systems for Agricultural Production

A concise description of the current trends in agri-food systems related to automation and agricultural robotics for ultra-saving labor strategies has been provided in this book. Precision agricultural production emphasizes improving the analytical abilities of agricultural operations using AI and IoT and is reported as a future trend in the agricultural sector. Recent deep learning and IoT applications also have potential toward contributing to achieving the SDGs and Society 5.0. The global agricultural product transportation sector has been plagued by a severe shortage of workers. Agricultural production now demands higher requirements for automatic navigation systems whose key technologies are positioning and tracking. One promising application is supervised autonomy in agricultural robots (Fig. 29.1). With the development of computer science in agricultural picking robots, traditional bounding box-based visual recognition algorithms are no longer sufficient to describe the shape of fruits. The performance of different types of region-based Convolutional Neural Networks (R-CNNs) models (Mask R-CNN and Faster R-CNN) and instance segmentation models, such as Mask R-CNN and You Only Look at Coefficients (YOLACT), are introduced in this book. A recognition and

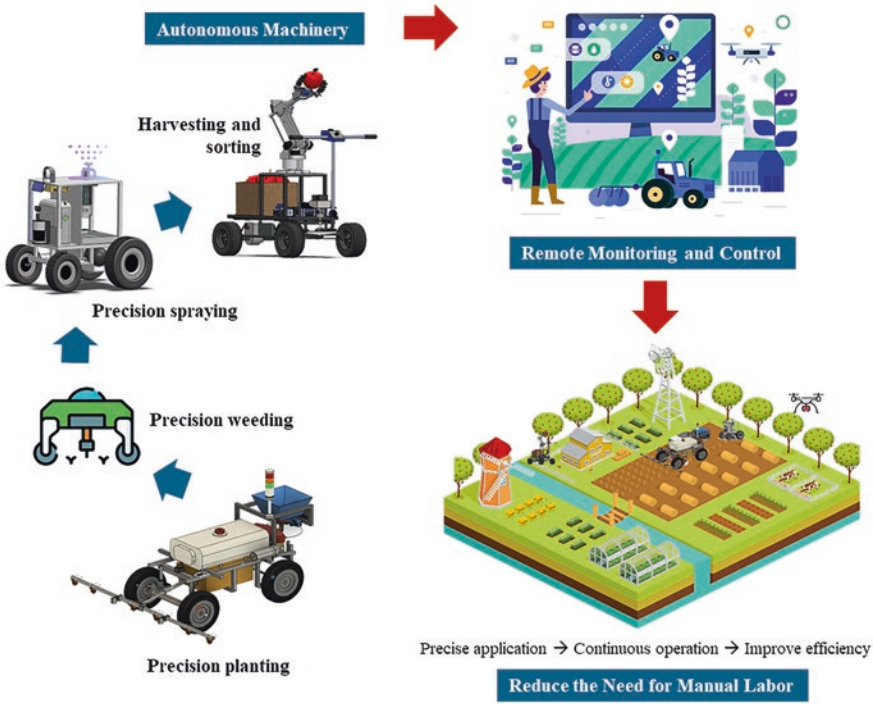

Fig. 29.1 Concepts for reducing infield agricultural labor shortages

localization system for slow and accurate fruit picking are also detailed. Various datasets are applied for object detection models. In orchard crop systems, there are field boundaries, obstacle avoidance, and various extended branches that are required for agricultural automation and autonomous application systems. The field acquisition system and the detection model of the various online dataset systems are evaluated through networking platforms. In addition to discussing robotics applications and various perspectives, this chapter discusses the dataset sizes and their potential for application and performance. It is important to note that pesticide spraying is one of the most important aspects of agricultural work since fruit trees must be sprayed 10–15 times between flowering and harvesting periods. However, this process is very labor-intensive, risky, and time consuming (Fig. 29.2).

Therefore, automatic spraying robots have also been discussed in the context of Light Detection and Ranging (LiDAR) and depth camera applications in orchard environments. One of the most important components of a spraying robot is the navigation system, which enables the robot to work safely and accurately in dense canopy systems, especially in orchards where illumination is a problem. Under low light conditions, especially in orchards, an autonomous driving system for agricultural vehicles faces accuracy challenges. Due to the variety of conditions in fruit orchards, orchard farmers face many challenges. Furthermore, the difficulties associated with the acquisition instability of Real-time Kinematic Positioning-Global Navigation Satellite Systems (RTK-GNSSs) and misrecognition of LiDAR systems in specific environments are also noted. The various sensors widely used in general autonomous driving systems are also detailed. The development of robots for autonomous orchard environments is becoming increasingly important in covering path planning and object detection using depth cameras, LiDARs, and Inertial Measurement Units (IMUs) (Fig. 29.3). It is also necessary to have a navigation system that uses Kalman filters, fuzzy controls, and LiDAR for the transportation of agricultural products.

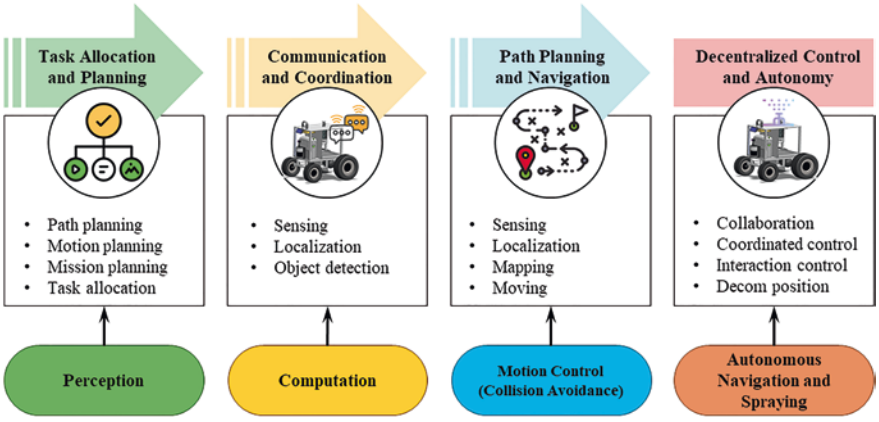

Fig. 29.2 Concepts of autonomous spraying transportation for field work

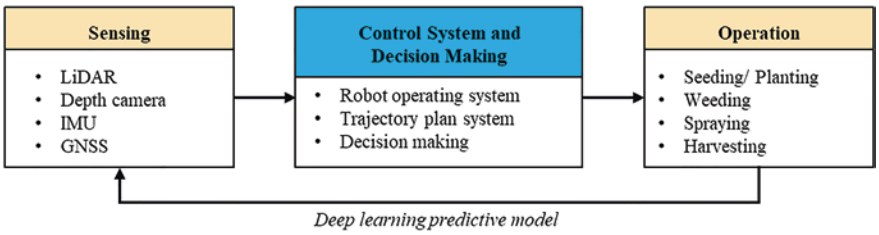

Fig. 29.3 Incorporating deep learning algorithms into sensors for robotic platform development

A 3D camera-based sensing system, which is found to be useful in autonomous driving systems for agricultural orchard vehicles, is described in several chapters. A stereo Simultaneous Localization and Mapping (SLAM) vehicle, which uses a stereo camera for autonomous agriculture, has been developed for indoor use. SLAM combines localization functions with the construction of the surrounding environment. Through pose estimation and sensing, an indoor robot vehicle builds a consistent map of the environment to localize its position. Because GPS and machine vision can be easily influenced by and limited by the environment, LiDAR may be a good candidate for a sensor. Several trials have been conducted on concrete roads and in artificial orchards based on artificial trees to demonstrate the feasibility of the system.

AI can also be utilized to identify and classify drivers' actions to determine dangerous driving behaviors and then provide an early warning signal to ensure safety. Using deep learning algorithms to determine dangerous driving behavior to provide early warning signals can help prevent accidents. Research in this area contributes to developing safer agricultural driving systems.

29.3 Smart Indoor Production Systems

AI and IoT technologies are presented as alternatives to farmer management of greenhouse systems to reduce the labor required and make greenhouse environmental control more precise (e.g., in terms of temperature, humidity, and light intensity) according to lettuce growth stages. The environmental parameters of traditional greenhouses, which need to be constantly controlled, are inconvenient for farmers. Through the use of a Fuzzy proportional-integral-derivative (PID) controller, a new feedback control parameter is introduced, which

significantly improves accuracy in optimizing greenhouse environmental control parameters. Hence, an AI-based IoT greenhouse control system can overcome the limitations of conventional greenhouse management systems. By combining IoT technology with the internet, users can conveniently monitor greenhouses remotely.

Additionally, AI technology can be used to automatically detect plant growth and conditions in indoor farming systems. The applications of deep learning include the identification of leafy diseases and stress conditions, and the assessment of seedling quality in indoor-grown plants (Hamidon & Ahamed, 2022, 2023). The digital transformation of technologies used in horticultural crops is evident, particularly in the early detection of diseases and pest infestations before harvest. Several reviews have provided insights into the development of pest and disease detection models, recommending effective methods for deploying deep learning applications and Convolutional Neural Network (CNN) models for managing horticultural crops (Apacionado & Ahamed, 2023). These designs and systems, as detailed in the review, can be implemented through a cloud platform.

Energy efficiency in indoor plant production is one of the important considerations for bioenergy production using IoT-based information and simulation for energy generation. Using IoT systems is expected to accelerate achieving the target of greenhouse gas (GHG) mitigation. As a result of the insights gained from the system, farm managers can make appropriate decisions to remotely control indoor systems to ensure that green energy is utilized for optimal plant growth. Plant phenotyping is an emerging science that involves quantifying and analyzing plant characteristics to optimize indoor plant growth and monitoring. Phenotyping plays an important role in agricultural decision support. To increase crop quality resilience to climate change, plant phenotyping, such as high-throughput plant phenotyping (HTPP), which focuses on indoor and controlled environments, can be combined with AI to gain insight into the potential and development of nondestructive HTPP phenotyping.

In addition to indoor farming production systems, water management is another key factor that warrants consideration. Sustainable water management is described in the Introduction section of IoT-based smart agriculture. Proper water management, particularly for tomatoes which are sensitive to water, is the key to ensuring sustainable production (Seyar & Ahamed, 2023). Providing plants with an ideal amount of moisture at the right time is crucial for growing healthy seedlings. Using a low-cost sensor coupled with IoT technology could help precisely control the moisture content in the soil and apply water on demand with minimum human intervention (Fig. 29.4).

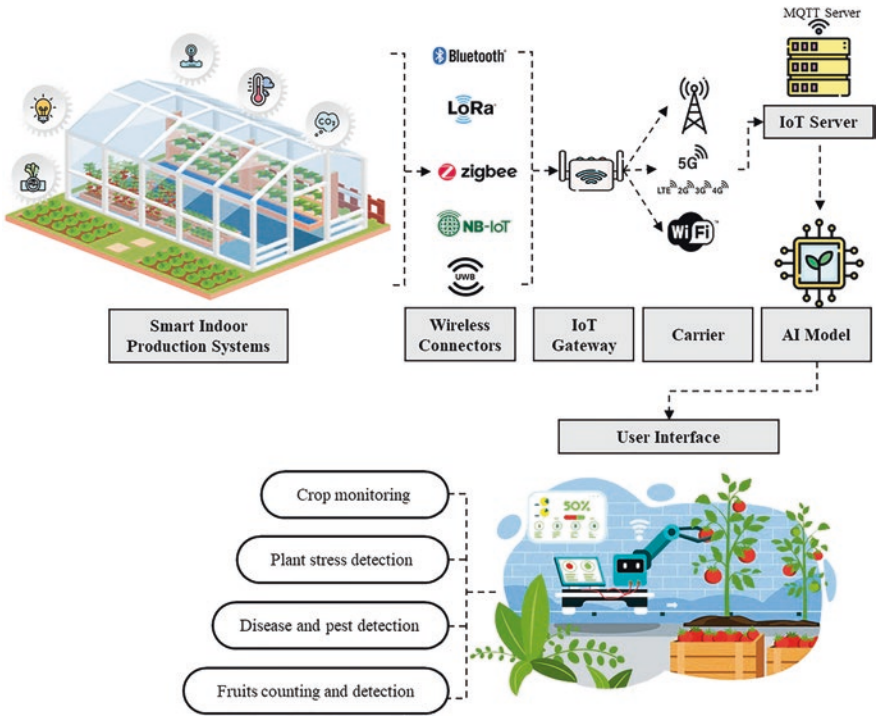

Fig. 29.4 Integration of the IoT and AI for intelligent monitoring and management in indoor farming

29.4 Smart Orchard Management for Increasing Productivity

In intercultural farm operations, spraying and weeding are the most time- and labor-intensive tasks. In complex orchard environments, controlling weeds remains a significant challenge. This book proposes 3D cameras and LiDAR as potential solutions for navigation systems in orchard environments, though some places lack GNSS signal quality due to vegetation or obstacles such as trees or canopies (Jiang & Ahamed, 2023). Sensors are also discussed in terms of their potential uses and drawbacks. In this book, we discuss possible applications for sensors on a vehicle for weed control, particularly for those located within rows, as these weeds can be quite challenging and time-consuming to remove even when using a riding mower or hand grass cutter.

A significant part of precision agriculture is the use of unmanned aerial vehicles (UAVs) to spray pesticides. Despite this, improving pesticide application efficiency and cost performance remains challenging. Replacing skilled orchard laborers with harvesting robots requires advanced research and automation. Newly developed orchard architectures with genetic improvements create pathways for harvesting robots to reduce the complexity of their tasks to several degrees of freedom. This

reduces complex robots' adaptability in terms of cost and sustainability. In terms of detection and localization, harvesting robots face the challenge of being obstructed by leaves, branches, and fruit clusters.

A summary of the understanding and the way forward for avoiding occlusions to increase fruit harvest efficiency in orchards is presented in this book (Abeyrathna et al., 2023). The term "end-effector" refers to a variety of devices used in horticulture, such as grippers, cutting devices, and spraying devices. Electric, pneumatic, and hydraulic actuators and controls enable end-effectors to be precisely controlled and adapted. A number of deep learning algorithms have been applied to end-effector automation, enhancing tasks such as object classification, yield estimation, pest detection, and weed control.

29.5 Smart Management of Poultry and Livestock

Food diversification is a key intervention strategy for addressing food crises that has been supported by the Food and Agriculture Organization (FAO). Both Poultry and animal farming can benefit from smart machine vision technologies coupled with artificial intelligence and the Internet of Things to reduce the need for manual observation. These improvements ultimately contribute to food security. For instance, by deploying cameras, environmental sensors, and IoT devices, real-time data can be analyzed via AI algorithms to monitor poultry behavior, health, and environmental conditions (Fig. 29.5). This enables the automatic detection of anomalies and potential issues, reducing the need for manual observation and enhancing overall operational efficiency. By leveraging AI-driven image recognition and IoT-enabled remote monitoring, poultry farmers can proactively manage their operations, optimize resource utilization, and rapidly respond to emerging challenges, thus

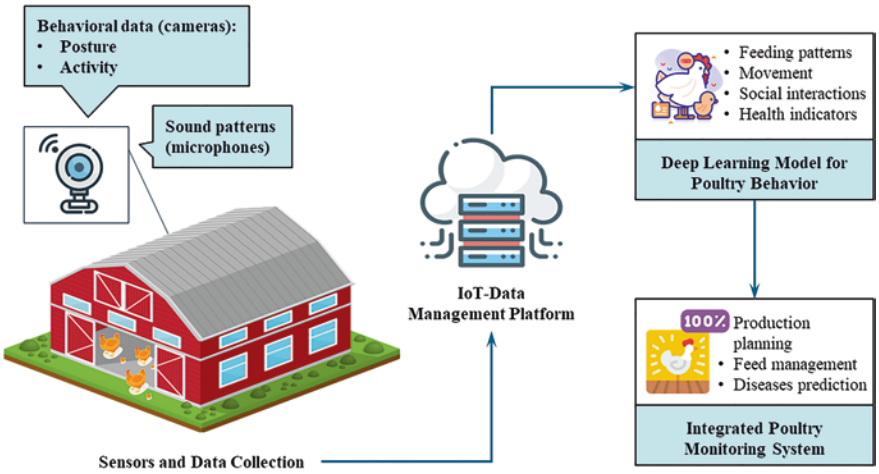

Fig. 29.5 Smart poultry management using AI and the IoT

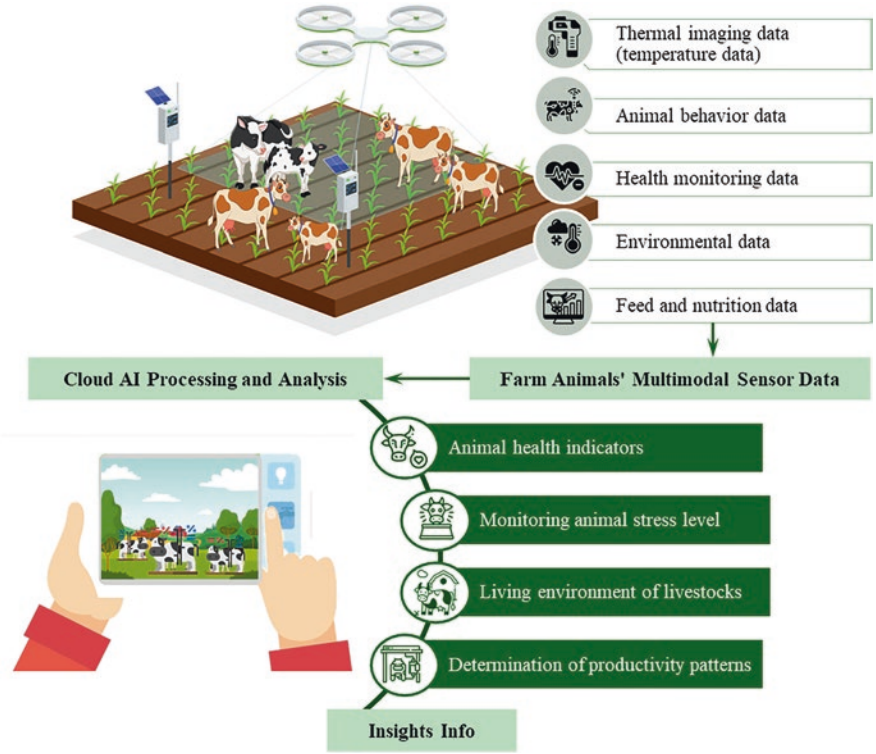

Fig. 29.6 Application of thermal imagery in livestock management

contributing to food security through sustainable and technology-driven poultry farming practices.

Furthermore, by harnessing advanced technologies for precision monitoring, the integration of thermal microcameras and deep learning algorithms plays a pivotal role in enhancing smart husbandry management practices. This innovative technique enables farms to gather nuanced insights into the thermal patterns and health indicators of livestock. By employing deep learning, the system can analyze complex datasets gathered from thermal microcameras, facilitating the auto-detection of temperature variations or signs of distress in animals (Fig. 29.6). This not only enhances the welfare of livestock but also streamlines the decision-making process for farmers.

29.6 Postharvest Management and Nondestructive Quality Measurements

Postharvest food quality control operations are essential for preserving agricultural product quality and shelf life. The complexity of postharvest technology and the

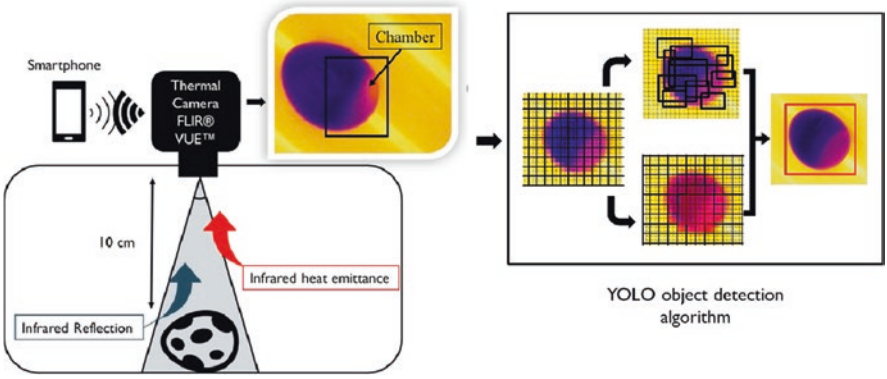

Fig. 29.7 Assessment of quail egg freshness using a thermal microcamera and deep learning

need for expertise in multiple fields make it difficult for companies to manage their operations effectively. Big data schemes emphasize the concept of a centralized data processing unit (CDPU) that integrates AI and data science to improve postharvest operations at the business level. This book provides an overview of the use of AI in food quality detection. AI can detect food quality issues faster and more accurately than traditional methods, allowing for better decision-making and more efficient operations. AI is also able to detect and prevent potential food safety risks. The gaps and future directions require further research to improve the current performance and applicability of AI-based food quality assessment are outlined. Additionally, we mention recent advancements in spectroscopy techniques used in food analysis. Through the exploration of advances in spectroscopic techniques and their integration with chemometric tools, insights are gained regarding possible applications and future directions of these analytical approaches in the food industry.

Building on the exploration of advanced spectroscopic techniques, the integration of a thermal microcamera and deep learning algorithms to develop a novel, noninvasive method for assessing quail egg freshness illustrates a convergence of cutting-edge analytical approaches in the food industry. This synergy highlights the diverse and innovative ways in which technology enhances our ability to monitor and ensure the quality of food products. Using a thermal microcamera and deep learning algorithms, a novel, noninvasive method of assessing quail egg freshness has been developed (Nakaguchi & Ahamed, 2022). By using thermal imaging and calculating a correlation between air cell area and egg weight, the models were able to accurately predict the freshness of eggs (Fig. 29.7). Consumers and the food industry will benefit from this groundbreaking approach. The production of quail faces many challenges in terms of improving efficiency and mitigating ecological imbalances, including water, energy, and physical space waste. With investments in affordable technologies and reliable automation techniques, the sector can further develop. This could contribute to improving the quality and safety of food in the future.

29.7 Conclusion

This chapter covered four main areas: (1) smart outdoor production, (2) smart indoor production systems, (3) smart orchard management for increasing productivity, and (4) nondestructive quality measurements. Applying state-of-the-art technologies as a part of solutions in IoT and AI-based data-driven agriculture, such as autonomous navigation, advanced agricultural systems (e.g., for managing insect infestations), and decreasing agricultural inputs (e.g., water, fertilizer), is essential for ensuring food safety and sustainability. The chapter provided a comprehensive summary of the IoT, machine learning (ML), and AI in the development of intelligent digital farming and smart agriculture, which offers the intended audience a wide range of resources. Furthermore, this chapter discusses the research trends in ML, particularly in relation to deep learning for agricultural platforms. Potential solutions in the context of AI and the IoT for agricultural applications to meet the SDGs in Society 5.0 are recommended throughout this book.

References

Abeyrathna, R. R. D., Nakaguchi, V. M., Minn, A., & Ahamed, T. (2023). Recognition and counting of apples in a dynamic state using a 3D camera and deep learning algorithms for robotic harvesting systems. *Sensors, 23*(8), 3810.

Apacionado, B. V., & Ahamed, T. (2023). Sooty Mold Detection on Citrus Tree Canopy Using Deep Learning Algorithms. *Sensors, 23*(20), 8519. https://doi.org/10.3390/s23208519Hamidon, M. H., & Ahamed, T. (2022). Detection of tip-burn stress on lettuce grown in an indoor environment using deep learning algorithms. *Sensors, 22*(19), 7251.

Hamidon, M. H., & Ahamed, T. (2023). Detection of defective lettuce seedlings grown in an indoor environment under different lighting conditions using deep learning algorithms. *Sensors, 23*(13), 5790.

Jiang, A., & Ahamed, T. (2023). Navigation of an Autonomous Spraying Robot for Orchard Operations Using LiDAR for Tree Trunk Detection. *Sensors, 23*(10), 4808. https://doi.org/10.3390/s23104808

Nakaguchi, V. M., & Ahamed, T. (2022). Fast and non-destructive quail egg freshness assessment using a thermal camera and deep learning-based air cell detection algorithms for the revalidation of the expiration date of eggs. *Sensors, 22*(20), 7703.

Seyar, M. H., & Ahamed, T. (2023). Development of an IoT-based precision irrigation system for tomato production from indoor seedling germination to outdoor field production. *Applied Science, 13*(9), 5556.

Index

A
Adaptations, 10, 30–31, 165, 173, 268, 294
Agricultural driving safety systems, 120
Agricultural mechanization, 26, 34–37, 51, 52
Agricultural navigation, 58, 86, 125
Agricultural products, 5, 60, 76, 77, 271, 396, 482, 483, 488
Agrifood system (AFS), 1–21
Agroecological systems, 397
AI-based IoT greenhouse control system, 301–326
Appropriate solutions, 26–27
Artificial intelligence (AI), 1, 6–8, 12, 17, 19, 20, 26, 27, 38, 42, 43, 48, 58, 101, 124, 126, 151, 156–157, 176, 190, 201, 202, 204, 206, 207, 219, 222, 271–273, 287, 302, 303, 313–315, 325, 326, 331, 346, 374, 384, 402, 416–418, 422, 453, 454, 481, 482, 484–487, 489, 490
Automation, 1, 33, 58, 85, 126, 201, 250, 286, 333, 350, 374, 402, 421, 448, 454, 482

B
Biodiversity, 187, 188, 270, 397, 399
Bioinformatics, 151, 481
Biomass residues, 404–406, 409, 411, 415–419
Biophysical sensitivity, 30–31
Blockchain technologies, 14

C
CenterNet, 207, 209, 302, 303, 308–309, 313, 315–320, 325
Centralized data processing unit (CDPU), 272, 273, 489
Climate change, 2, 3, 160, 183, 190, 197, 200, 201, 211, 222, 267–270, 275, 289, 293, 402, 403, 485
Climate-smart agriculture (CSA), 267, 268, 270
Cloud computing, 196, 271
Coffee leaf rust, 183–197
Controlled environments, 157, 165, 170, 171, 177–179, 208, 351, 485
Convolutional neural network (CNN), 174, 193, 209, 237, 302, 351, 352, 356, 359, 361, 362, 368, 369, 449, 454, 460–462, 482, 485

D
Dashboard visualization, 422
Deep learning (DL), 95, 96, 101, 102, 105, 120, 156, 164, 166, 173–178, 190–197, 207, 209, 210, 215, 216, 218, 235–237, 244, 245, 288, 291, 302, 303, 359, 362, 375, 384–385, 389, 390, 393, 454–456, 460–462, 465, 473–477, 482, 484, 485, 487–490
Detection of leaf lettuce growth stage, 316
Digital innovations, 1–21
Digital technologies, 1, 3, 6, 19, 21, 201–222, 422
Dynamic window approach (DWA), 136, 146

© The Author(s), under exclusive license to Springer Nature Singapore Pte Ltd. 2024

T. Ahamed, *IoT and AI in Agriculture*,
https://doi.org/10.1007/978-981-97-1263-2

E
Electricity, 403, 404, 406, 412, 415–417
End effectors, 216, 358, 363, 368, 369, 373–385, 389, 390, 487
Environmental parameters control, 303, 325
Ethanol, 403, 407–409, 412, 415, 417

F
Fertilizers, 8, 9, 12, 38, 58, 150, 201, 213, 377, 404–409, 415–417, 490
Food diversification, 399, 487
Food measurement, 393
Food production, 1, 3, 4, 10, 155, 398, 481
Food quality, 4, 5, 155–157, 488, 489
Food quality assessments, 156, 157, 489
Food security, 3, 5, 6, 8, 16, 19, 21, 29, 30, 150, 155, 160, 178, 222, 267–270, 398, 399, 450, 481, 487, 488
Freshness assessment, 219, 477
Fruit picking, 215, 389–390, 483
Fuzzy PID control algorithm, 303, 311–312, 326

G
Genomics, 150, 151, 178
Genotypes, 31, 151, 152, 178, 476
Green technology, 393

H
Harvesting, 7–9, 26, 34, 37, 38, 42, 43, 45, 48–52, 59, 124, 125, 160, 178, 187, 201, 203, 208, 214–218, 222, 234, 245, 268, 302, 330–332, 344, 350–352, 356, 361–369, 373–375, 377, 379, 389, 415, 417, 483, 486, 487
Healthy food, 16, 249
High-throughput, 161, 163–173, 178, 179, 455, 475, 485
Horticultural approach, 161, 200–223, 361, 373–390, 487
Horticultural robots, 373–375, 377–382, 384–385, 389, 390
Horticulture, 161, 200–203, 205, 208, 209, 211, 212, 219–223, 350, 373–382, 385, 389, 487

I
Images and videos, 450
Inertial measurement unit (IMU), 59–62, 66–72, 82, 83, 103, 126, 127, 147, 230, 234, 236, 483
Internet of Things (IoT), 1, 4–6, 127, 156, 201, 202, 271, 286, 293, 302, 304, 401, 453, 487
IoT platform, 212, 405–407, 414, 417, 418
IoT systems, 204, 211, 214, 343, 409, 422–425, 428, 429, 433, 436, 444, 485
Irrigation scheduling, 211, 276, 279–291, 293, 294

K
Kalman filters, 61, 69–72, 83, 237, 483

L
Light detection and ranging (LiDAR), 58–62, 68, 72–73, 78–80, 82, 83, 86–92, 94–96, 125, 138, 147, 163, 168–170, 230, 231, 233–245, 361, 368, 380–381, 389, 483, 484, 486
Local food resources, 398–399

M
Mechanization, 33–36, 51–53, 331, 333–339, 346, 350
Mitigation, 10, 30, 31, 268, 269, 289, 339, 402, 418, 454, 485
Mushroom cultivation, 330–332, 343, 346

N
Nondestructive analysis, 396, 455, 476
Nondestructive spectroscopy method, 393

O
Occlusions, 95, 126, 195, 233, 234, 351–359, 361, 362, 367–369, 487
Orchards, 86, 89, 91–96, 125–127, 209, 215, 229–238, 240–245, 250, 350–352, 356–358, 361, 368, 369, 374, 375, 379, 381, 382, 385–390, 455, 483, 484, 486–487, 490

P
Path planning, 36, 44, 61, 62, 73, 74, 83, 86, 88–90, 92, 127, 132, 134–138, 140, 146, 243–245, 380, 381, 483
Phenotypes, 151, 152, 161, 167, 171, 173, 174, 176, 178
PID control algorithm, 312, 326
Plant diseases, 17, 38, 174, 190, 191, 197, 302

Plant morphology, 161–163, 169, 170, 204
Plant phenotyping, 160, 161, 163–179, 485
Plant physiology, 161–163
Plant protection UAV, 250–265
Postharvest, 20, 488–490
Postharvest technologies, 271, 488
Precision agriculture (PA), 1, 5, 16, 19, 21, 26, 27, 41, 42, 44, 47, 48, 52, 126, 178, 201, 202, 265, 268, 283, 416, 486
Production, 3, 26, 29, 38, 58, 85, 124, 157, 160, 183, 200, 250, 269, 275, 301, 330, 350, 397, 402, 421, 448, 454, 482
Production diversity, 397
Proteomics, 150, 151, 178
Pulse width modulation (PWM), 251, 254–260, 262–264, 314

Q
Quail eggs, 456–458, 469, 472, 476, 477, 489

R
Real-time Kinematic Positioning-Global Navigation Satellite Systems (RTK-GNSSs), 86, 483
Remote sensing, 209, 276–283, 286, 289–294, 396
Robotic arm configurations, 353, 367
Robotic harvesting, 37, 216, 350, 351, 356, 361, 363, 368
Robot Operation System (ROS), 60, 61, 66, 68, 72, 73, 82, 105, 133–134, 136

S
Seeding, 9, 42–44
Sensing technologies, 41, 47, 49, 218, 276, 279–281, 286, 380–381, 390
Sensors, 4, 5, 7–11, 13, 19, 26, 36, 38, 41–45, 47–49, 51–53, 59–61, 67–72, 76, 82, 86–88, 94–96, 100, 101, 103, 104, 125, 126, 131, 138, 156, 157, 163, 164, 167, 170–173, 176, 177, 179, 202, 204–207, 209, 211, 212, 214, 218, 222, 230, 231, 233–238, 240, 241, 244, 245, 255, 257, 276–279, 281, 283–286, 289–294, 304, 312–314, 326, 339, 343, 345, 351, 354, 359, 361, 362, 367, 369, 374, 380, 381, 384, 385, 402, 417, 418, 422–426, 428, 429, 444, 453, 455, 456, 475, 477, 483–487
Smart automation, 374, 375
Smart farming, 38, 41, 45, 47–49
Society 5.0, 2–6, 8, 9, 14, 19–21, 481, 482, 490
Soil moisture content (SMC), 214, 276–278, 280, 281, 291
Spatially Factorized Spectroscopy (SFS), 394, 395
Spraying, 9, 47, 86, 124, 202, 229, 250, 375, 483
Spraying uniformity, 250, 251, 258, 262, 263, 265
Sustainable development goal (SDG), 2–6, 8, 9, 14, 16–19, 21, 221–222, 481, 482, 490

T
Technological adaptations, 30–32
3D cameras, 231, 233–245, 353, 354, 356, 359, 361, 379, 486
Tillage, 39–42, 52, 201, 230, 268
Tracking, 26, 42, 58, 59, 61, 62, 74–76, 82, 83, 125, 129, 132, 134–138, 172, 175, 207, 237, 367, 455, 482
Transcriptomics, 150, 178
Transplanting, 44–47
Tree trunk detection, 96

U
Utilizations, 1, 5, 8, 10, 13, 14, 36, 51, 103, 160, 169, 175, 178, 190, 201, 222, 236, 243, 268, 281, 286–288, 294, 303, 350, 402–405, 407–409, 411, 414–419, 421, 422, 455, 487

V
Varietal evaluation, 31
Video classification, 102, 105, 117, 120
Visual-SLAM, 125, 129

W
Web applications, 422, 424, 427–445

Y
YOLOv3, 215, 305–308, 313, 315–320, 325, 454, 455
YOLOv7, 207, 209, 352, 461–463, 465, 470–477